A11100 988151

NAT'L INST OF STANDARDS & TECH R.I.C.

A11100988151

United States-Japan /Wind and seismic ef
QC100 .U57 V560;1980 C.1 NBS-PUB-C 1980

NBS SPECIAL PUBLICATION 560

U.S. DEPARTMENT OF COMMERCE/National Bureau of Standards

National Bureau of Standards
Library, E-01 Admin. Bldg.
OCT 1 198[illegible]

191079

QC
100
.U57

WIND AND SEISMIC EFFECTS

Proceedings of the Tenth Joint UJNR Panel Conference

560
)
2

NATIONAL BUREAU OF STANDARDS

The National Bureau of Standards[1] was established by an act of Congress on March 3, 1901. The Bureau's overall goal is to strengthen and advance the Nation's science and technology and facilitate their effective application for public benefit. To this end, the Bureau conducts research and provides: (1) a basis for the Nation's physical measurement system, (2) scientific and technological services for industry and government, (3) a technical basis for equity in trade, and (4) technical services to promote public safety. The Bureau's technical work is performed by the National Measurement Laboratory, the National Engineering Laboratory, and the Institute for Computer Sciences and Technology.

THE NATIONAL MEASUREMENT LABORATORY provides the national system of physical and chemical and materials measurement; coordinates the system with measurement systems of other nations and furnishes essential services leading to accurate and uniform physical and chemical measurement throughout the Nation's scientific community, industry, and commerce; conducts materials research leading to improved methods of measurement, standards, and data on the properties of materials needed by industry, commerce, educational institutions, and Government; provides advisory and research services to other Government agencies; develops, produces, and distributes Standard Reference Materials; and provides calibration services. The Laboratory consists of the following centers:

Absolute Physical Quantities[2] — Radiation Research — Thermodynamics and Molecular Science — Analytical Chemistry — Materials Science.

THE NATIONAL ENGINEERING LABORATORY provides technology and technical services to the public and private sectors to address national needs and to solve national problems; conducts research in engineering and applied science in support of these efforts; builds and maintains competence in the necessary disciplines required to carry out this research and technical service; develops engineering data and measurement capabilities; provides engineering measurement traceability services; develops test methods and proposes engineering standards and code changes; develops and proposes new engineering practices; and develops and improves mechanisms to transfer results of its research to the ultimate user. The Laboratory consists of the following centers:

Applied Mathematics — Electronics and Electrical Engineering[2] — Mechanical Engineering and Process Technology[2] — Building Technology — Fire Research — Consumer Product Technology — Field Methods.

THE INSTITUTE FOR COMPUTER SCIENCES AND TECHNOLOGY conducts research and provides scientific and technical services to aid Federal agencies in the selection, acquisition, application, and use of computer technology to improve effectiveness and economy in Government operations in accordance with Public Law 89-306 (40 U.S.C. 759), relevant Executive Orders, and other directives; carries out this mission by managing the Federal Information Processing Standards Program, developing Federal ADP standards guidelines, and managing Federal participation in ADP voluntary standardization activities; provides scientific and technological advisory services and assistance to Federal agencies; and provides the technical foundation for computer-related policies of the Federal Government. The Institute consists of the following centers:

Programming Science and Technology — Computer Systems Engineering.

[1]Headquarters and Laboratories at Gaithersburg, MD, unless otherwise noted; mailing address Washington, DC 20234.
[2]Some divisions within the center are located at Boulder, CO 80303.

WIND AND SEISMIC EFFECTS

National Bureau of Standards
Library, E-01 Admin. Bldg.
OCT 2 9 1980
not acc. - circ
QC100
.U57
no.560
1050
c.2

Proceedings of the Tenth Joint
Panel Conference of the U.S.-Japan
Cooperative Program in
Natural Resources

May 23-26, 1978
National Bureau of Standards
Gaithersburg, Maryland

H.S. Lew, Editor

Center for Building Technology
National Engineering Laboratory
National Bureau of Standards
Washington, D.C. 20234

U.S. DEPARTMENT OF COMMERCE, Philip M. Klutznik, Secretary

Luther H. Hodges, Deputy Secretary

Jordan J. Baruch, Assistant Secretary for Productivity, Technology and Innovation

NATIONAL BUREAU OF STANDARDS, Ernest Ambler, Director

Issued October 1980

Library of Congress Catalog Card Number: 79-600134

National Bureau of Standards Special Publication 560
Nat. Bur. Stand. (U.S.), Spec. Publ. 560, 644 pages (Oct. 1980)
CODEN: XNBSAV

U.S. GOVERNMENT PRINTING OFFICE
WASHINGTON: 1980

For sale by the Superintendent of Documents, U.S. Government Printing Office
Washington, D.C. 20402 - Price $11

PREFACE

The Tenth Joint Meeting of the U.S.-Japan Panel on Wind and Seismic Effects was held at the National Bureau of Standards in Gaithersburg, Maryland on May 23-26, 1978. This panel is a part of the U.S.-Japan Cooperative Program in Natural Resources (UJNR). The panel meets annually, alternating between Washington and Tokyo to exchange technical information on the latest research and development activities within governmental agencies of both countries in the area of wind and seismic effects.

These proceedings include the membership list, the formal resolution, the technical papers presented at the joint meeting, and the reports of the task committees.

It should be noted that throughout the proceedings certain commercial equipment, instruments or materials are identified in order to specify adequately experimental procedure. In no case does such identification imply recommendation or endorsemement by the National Bureau of Standards, nor does it imply that the material or equipment identified is necessarily the best for the purpose.

H. S. Lew, Secretary
U.S. Panel on Wind and
Seismic Effects

ABSTRACT

This volume includes thirty eight technical papers presented at the Tenth Joint Meeting of the U.S.-Japan Panel on Wind and Seismic Effects. It also includes the formal resolutions and the reports of the Panel's eight task committees. The subjects covered in the Joint Meeting include: (1) natural wind characterization and extreme wind records, (2) characterization of earthquake ground motions and strong-motion earthquake data, (3) engineering seismology, (4) response of hydraulic and earth structures to seismic forces, (5) structural responses to wind loading, (6) recent developments in seismic design criteria, (7) design and analysis of special structures, (8) damage evaluation, repair and retrofit, (9) earthquake hazard mitigation, and (10) storm surge and tsunami.

Key Words: Accelerograph; codes; design criteria; disaster; earthquakes; ground motion; seismology; standards; structural engineering; storm surge; structural response; wind loads; winds; tsunami.

SI CONVERSION UNITS

In view of the present accepted practice for wind and seismic technology, common units of measurements were used throughout this publication. In recognition of the position of the United States as a signatory to the General Conference on Weights and Measures, which gave official status to the International System of Units (SI) in 1960, the table below is presented to facilitate conversion to SI Units. Readers interested in making further use of the coherent system of SI units are referred to: NBS SP 330, 1972 Edition, The International System of Units; and ASTM E380-76, Standard for Metric Practice.

Table of Conversion Factors to SI Units

	Customary Units	International (SI) UNIT	Conversion Approximate
Length	inch (in)	meter (m)[a]	1 in = 0.0254 m*
	foot (ft)	meter (m)	1 ft = 0.3048 m*
Force	pound (lbf)	newton (N)	1 lbf = 4.48 N
	kilogram (kgf)	newton (N)	1 kgf = 9.807
Pressure	pound per square		
Stress	inch (psi)	newton/meter^2	1 psi = 6895 N/m^2
	kip per square		
	inch (ksi)	newton/meter^2	1 ksi = 5985 x 10^6 N/m^2
Energy	inch-pound (in-lbf)	joule (J)	1 in-lbf = 0.1130 J
	foot-pound (ft-lbf)	joule (J)	1 ft-lbf = 1.3558 J
Torque or Bending Moment	pound-inch	newton-meter (N-m)	1 lbf-in = 0.1130 N-m
	pound-foot (lbf-ft)	newton-meter (N-m)	1 lbf-ft = 1.3558 N-m
Weight	pound (lb)	kilogram (kg)	1 lb = 0.4536 kg
Unit Weight	pound per cubic foot (pcf)	kilogram per cubic meter (kg/m^3)	1 pcf = 16.018 kg/m^3
Velocity	foot per second (ft/sec)	meter per second (m/s)	1 fps = 0.3048 m/s
Acceleration	foot per second per second (ft/sec^2)	meter per second per second (m/s^2)	1 ft/sec^2 = 0.3048 m/s^2

[a] Meter may be subdivided. A centimeter (cm) is 1/100 m and a millimeter (mm) is 1/1000 m.

* Exactly

CONTENTS

	Page
PREFACE	iii
ABSTRACT	iv
SI Conversion Units	v
Program of Joint Meeting	x
List of Members	xvi
Formal Resolutions	xx
TECHNICAL PAPERS	
Natural Wind Characterization and Extreme Wind Records	
1. On the Distribution of Extreme Winds Expected in Japan	1-1
2. Boundary Layer Winds	2-1
3. On the Damage to Buildings In Oki-erabu from the September 1977 Typhoon	3-1
4. Recent Developments in Atmospheric Remote Sensing and Their Implication for Wind Engineering	4-1
5. Extreme Wind Data Base Development at the National Climatic Center	5-1
Characterization of Earthquake Ground Motions and Strong-Motion Earthquake Data	
6. A Strong-Motion Record Information Retrieval System	6-1
7. Integration of Strong-Motion Accelerograms	7-1
8. Some Recent Developments in National and International Seismic Data Exchanges	8-1
9. Report on the International Workshop on Strong-Motion Earthquake Instrument Arrays May 2 - 5, 1978, at Hawaii	9-1
Engineering Seismology	
10. Expectancy of Maximum Earthquake Motions in Japan	10-1
11. Determination of Design Earthquake for the Dynamic Analysis of the Fort Peck Dam	11-1
12. The Izu-Ohshima Kinkai Earthquake of January 1978	12-1
Response of Hydraulic and Earth Structures to Seismic Forces	
13. Empirical and Analytical Methods of Estimating Soil Liquefaction Risk	13-1
14. A Practical Procedure for Assessing Earthquake-Induced Liquefaction of Sandy Deposits	14-1
Structural Response to Wind Loading	
15. Wind-Resistant Design of Cable-Stayed Bridges in Japan	15-1
16. Aerodynamic Stability of Proposed Ohio River Cable-Stayed Bridge	16-1
17. Some Aerodynamic Considerations in the Design of the Ruck-A-Chucky Bridge	17-1
18. A Summary of Wind Tunnel Test Results for the Luling, Louisiana, Cable-Stayed Bridge	18-1
19. A Technique for Measuring Fluctuating Wind Loads on a Tall-Building Model Irrespective of Model Motion	19-1
20. A Study of Building Damage Caused by Wind	20-1

Page

Recent Developments in Seismic Design Criteria

21. Recent Earthquake-Resistant Design Methods for Different Types of Bridge Foundations in Japan 21-1
22. Recent Developments in Seismic Design Codes 22-1
23. Logical Analysis of Seismic Design Provisions 23-1
24. Highlights of California School and Hospital Building Regulations 24-1
25. Summary of Research Projects in the Large-Structures Testing Laboratory from 1967-1977 25-1

Design and Analysis of Special Structures

26. Dynamic Behavior of Rectangular Water Tanks Assembled with Panels 26-1
27. Inelastic Behavior of Non-Bearing Walls in an 11-Story Steel-Reinforced Concrete Frame
Aseismatic Safety of External Surface Finishes and Coatings 27-1

Damage Evaluation, Repair, and Retrofit

28. Seismic Evaluation of Existing Multistory Residential Buildings 28-1
29. Damage to Engineering Structures During the Near Izu-Ohshima Earthquake of January 1978 29-1
30. Repair and Retrofit of Buildings 30-1
31. The Distribution of Property Losses Caused by Historical Earthquakes 31-1

Earthquake Hazard Mitigation, Including Socioeconomic Aspects

32. The Disaster-Resistance of Cities and Their Lifelines 32-1
33. Rescue and Rehabilitation After the Izu-Ohshima Kinkai Earthquake of 1978 33-1
34. National Science Foundation Activity in Earthquake Hazard Mitigation 34-1
35. Rapid Seismic Analysis Procedures for Buildings 35-1
36. US-Southeast Asia Symposium on Engineering for Natural Hazards Protection 36-1

Storm Surge and Tsunami

37. Storm Surge 37-1
38. Operation of the Tsunami Warning System in the Pacific 38-1

Members of Task Committee 39-1

Task Committee Reports

A. Task Committee on Strong-Motion Instrumental Arrays and Data A-1
B. Task Committee on Large-Scale Testing Programs B-1
C. Task Committee on Repairs and Retrofit of Existing Structures C-1
D. Task Committee on Structural Performance Evaluation D-1

Page

E. Task Committee on Land Use Programs for Controlling Natural Hazards Effects E-1
F. Task Committee on Lifeline Systems F-1
G. Task Committee on High Speed Wind Data G-1
H. Task Committee on Soil Behavior and Stability During Earthquakes H-1

TENTH JOINT MEETING

OF

U.S.-JAPAN PANEL ON WIND AND SEISMIC EFFECTS

May 23 - 26, 1978

at the

National Bureau of Standards

TUESDAY - May 23	Lecture Room B
	OPENING SESSION
10:00 A.M.	Call to order by Dr. H. S. Lew, Secretary, U.S. Panel Remarks by Dr. John W. Lyons, Director, National Engineering Laboratory, National Bureau of Standards Remarks by Mr. Kiichiro Nagara, Counselor, Embassy of Japan Remarks by Dr. Edward O. Pfrang, Chairman, U.S. Panel Remarks by Mr. Kazuto Nakazawa, Chairman, Japan Panel
10:30 A.M.	Introduction of U.S. Panel Members by U.S. Chairman and Japan Panel Members by Japanese Chairman
10:45 A.M.	Election of Conference Chairman
10:50 A.M.	Adoption of Agenda
11:00 A.M.	Group Photograph
11:30 A.M.	Lunch - Dining Room C
SESSION I	NATURAL WIND CHARACTERIZATION AND EXTREME WIND RECORDS
	Chairman: Dr. Edward O. Pfrang
1:00 P.M.	On the Distribution of Extreme Winds Expected in Japan - T. Okubo and N. Narita
1:25 P.M.	Boundary Layer Winds - D. A. Haugen
1:50 P.M.	On the Damage to Buildings in Okierabu Island Caused by Typhoon Number 7709 of September 9, 1977 - T. Murota, Y. Ishiyama, S. Fujiwhara, M. Okuda and K. Tsukada
2:10 P.M.	Recent Developments in Atmospheric Remote Sensing and Their Implications for Wind Engineering - W. H. Hooke
2:30 P.M.	Extreme Wind Data Base Developed at the National Climatic Center - M. Changery
2:50 P.M.	Discussion
3:10 P.M.	Break

SESSION II CHARACTERIZATION ON EARTHQUAKE GROUND MOTIONS AND STRONG-MOTION EARTHQUAKE DATA

Chairman: Mr. Kazuto Nakazawa

3:50 P.M.	Strong-Motion Record Information Retrieval System - A. M. Converse and R. B. Matthiesen
4:15 P.M.	Integration of Strong-Motion Accelerograms - S. Iai, E. Kurata, H. Tsuchida and S. Hayashi
4:40 P.M.	Some Recent Developments in National and International Seismic Data Exchange Activities - J. Lander
5:00 P.M.	Development of Dense Strong-Motion Earthquake Instrumentation Arrays - T. Okubo and H. Tsuchida
5:20 P.M.	Discussion
5:30 P.M.	Adjourn

WEDNESDAY - May 24 Lecture Room B, Administration Building

SESSION III ENGINEERING SEISMOLOGY

Chairman: Dr. Edward O. Pfrang

9:00 A.M.	Study on Expectancy of Maximum Earthquake Motions in Japan - M. Watabe and Y. Kitagawa
9:25 A.M.	Determination of Design Earthquake for the Dynamic Analysis of Fort Peck Dam - W. F. Marcuson, III and E. L. Krinitzsky
9:50 A.M.	Analysis of the Izu-Oshima Kinkai Earthquake of January 14, 1978 - M. Tajima, H. Sato, M. Otsuka, K. Sudo and K. Ishibashi
10:10 A.M.	Discussion
10:25 A.M.	Break

SESSION IV RESPONSE OF HYDRAULIC AND EARTH STRUCTURES TO SEISMIC FORCES

Chairman: Mr. Kazuto Nakazawa

10:40 A.M.	Empirical and Analytical Methods of Estimating Soil Liquefaction Risk - R. K. McGuire, F. Tatsuoka, T. Iwasaki and K. Tokida
11:05 A.M.	A Practical Procedure for Assessing Earthquake-Induced Liquefaction of Sandy Deposits - M. Ohashi, T. Iwasaki, F. Tatsuoka and K. Tokida
11:30 A.M.	Discussion
11:40 A.M.	A Presentation on Site Investigation of Dam Failures During the Izu-Oshima Kinkai Earthquake of January 14, 1978 - W. Marcuson, III
12:00 noon	Lunch - Dining Room C

SESSION V STRUCTURAL RESPONSE TO WIND LOADING

Chairman: Dr. Edward O. Pfrang

1:00 P.M. Wind Resistant Design of Cable-Stayed Bridges in Japan - T. Okubo, N. Narita and M. Katsuragi

1:25 P.M. Aerodynamic Stability of Proposed Ohio River Cable-Stayed Bridge - L. R. Cayes

1:50 P.M. Some Aerodynamic Considerations in the Design of the Ruck-A-Chucky Bridge - R. H. Scanlon

2:10 P.M. A Summary of Wind Tunnel Test Results for the Luling, Louisiana, Cable-Stayed Bridge - H. R. Bosch

2:30 P.M. A Technique for Measuring Fluctuating Wind Loads on a Tall Building Model Irrespective of Model Motion - T. Reinhold

2:50 P.M. Discussion

3:15 P.M. Break

3:30 P.M. Task Committee Meetings

a. Task Committee on Strong-Motion Instrumentation Arrays and Data
b. Task Committee on Large-Scale Testing Programs
c. Task Committee on Repairs and Retrofit of Existing Structures
d. Task Committee on Structural Performance Evaluation

5:30 P.M. Adjourn

THURSDAY - May 25 Lecture Room B, Administration Building

SESSION VI RECENT DEVELOPMENTS IN SEISMIC DESIGN CRITERIA

Chairman: Mr. Kazuto Nakazawa

9:00 A.M. Recent Earthquake Resistant Design Methods for Different Types of Foundations in Japan - Y. Shioi, T. Furya, M. Okahara and Y. Mitsuie

9:25 A.M. Recent Developments in Seismic Design Code - R. L. Sharpe

9:50 A.M. Logical Analysis of Seismic Design Provisions - J. Harris

10:10 A.M. Highlights of California School and Hospital Building Regulations - J. F. Meehan

10:30 A.M. Break

10:45 A.M. Summary of Recent Projects Carried Out in the Large-Size Structures Testing Laboratory During the Last Eleven Years - M. Hirosawa, Y. Ishiyama and T. Goto

11:05 A.M. Discussion

11:55 A.M. Inelastic Behavior of Non-Bearing Wall in a 11-Story Steel-Reinforced Concrete Frame and Aseismic Safety of External Surface Finishes and Coatings - M. Watabe, T. Kubota, T. Fukuta, A. Baba and H. Ito

12:15 P.M. Discussion

12:25 P.M. Lunch - Dining Room C

SESSION VIII WIND AND SEISMIC DAMAGE EVALUATION, REPAIR AND RETROFIT OF STRUCTURES

Chairman: Dr. Edward O. Pfrang

1:30 P.M. Seismic Evaluation of Existing Multistory Residential Buildings - G. R. Fuller

1:55 P.M. Damage Features of Engineering Structures Due to the Near Izu-Ohshima Earthquake of January 14, 1978 - K. Nakazawa, T. Iwasaki, K. Kawashima, M. Watabe, H. Yamanouchi and Y. Yamazaki

2:20 P.M. Repair and Retrofit of Buildings in Seismic Areas - R. D. Hanson and J. K. Wight

2:40 P.M. An Evaluation Study on the Distribution of Property Losses Caused by Earthquakes - E. Kuribayashi and T. Tazaki

3:00 P.M. Discussion

3:15 P.M. Break

3:30 P.M. Task Committee Meetings

e. Task Committee on Land Use Programs for Controlling Natural Hazards Effects
f. Task Committee on Disaster Prevention Methods for Lifeline Systems
g. Task Committee on High-Speed Wind Data
h. Task Committee on Soil Behavior and Stability During Earthquakes

5:30 P.M. Adjourn

FRIDAY - May 26 Lecture Room B, Administration Building

SESSION IX EARTHQUAKE HAZARD MITIGATION INCLUDING SOCIOECONOMIC ASPECTS

Chairman: Dr. Edward O. Pfrang

9:00 A.M. Present Status and Problems on Countermeasures to Earthquake Disasters with Emphasis on Disaster-Resistivities of Cities and Their Lifelines - K. Nakazawa and E. Kuribayashi

9:20 A.M. The Investigation on the Rescue and Rehabilitation of the Izu-Ohshima Kinai Earthquake of 1978 - E. Kuribayashi, T. Tazaki and T. Hadate

9:40 A.M. The National Science Foundation Activities on Earthquake Hazard Mitigation - C. Thiel and J. Scalzi

10:00 A.M.	Rapid Seismic Analysis Procedures for Buildings - T. K. Lew, S. K. Takahashi and C. V. Chelapati
10:20 A.M.	U.S. - Southeast Asia Symposium on Engineering for Natural Hazards Protection - A. H-S. Ang
10:40 A.M.	Discussion
11:00 A.M.	Break

SESSION X STORM SURGE AND TSUNAMI

Chairman: Mr. Kazuto Nakazawa

11:15 A.M.	Storm Surge - C. S. Barrientos
11:35 A.M.	Operation of the Tsunami Warning System in the Pacific - M. Spaeth
11:55 A.M.	Discussion
12:05 P.M.	A Presentation on the Teton Dam Failure - J. Dodd
12:30 P.M.	Lunch - Dining Room C

SESSION XI TASK COMMITTEE REPORT

Chairman: Dr. Edward O. Pfrang

Task Committee Reports

1:30 P.M.	a. Task Committee on Strong-Motion Instrumentation Arrays and Data
1:45 P.M.	b. Task Committee on Large-Scale Testing Programs
2:00 P.M.	c. Task Committee on Repair and Retrofit of Existing Structures
2:15 P.M.	d. Task Committee on Structural Performance Evaluation
2:30 P.M.	e. Task Committee on Land Use Programs for Controlling Natural Hazard Effects
2:45 P.M.	f. Task Committee on Disaster Prevention Methods for Lifeline Systems
3:00 P.M.	g. Task Committee on High Speed Wind Data
3:15 P.M.	h. Task Committee on Soil Behavior and Stability During Earthquakes
3:30 P.M.	Break

SESSION XII CLOSING SESSION

Chairman: Dr. Edward O. Pfrang

3:40 P.M.	Adoption of Formal Resolution
	Closing Remarks - Mr. Kazuto Nakazawa and Dr. Edward O. Pfrang
4:10 P.M.	Adjourn

U.S. PANEL ON WIND AND SEISMIC EFFECTS

MEMBERSHIP LIST

MAY 1978

Dr. Edward O. Pfrang
Chairman
Chief, Structures and Materials Division
Center for Building Technology, NEL
National Bureau of Standards
Washington, DC 20234
301-921-2196

Dr. S. T. Algermissen
Office of Earthquake Studies
Denver Federal Center
Branch of Earthquake Tectonics
USGS
Stop 978, Box 25046
Denver, CO 80225
303-234-4014

Dr. Celso Barrientos
Research Meteorologist
NOAA
8060 13th Street
Silver Spring, MD 20910

Mr. Billy Bohannan
Assistant Director
Wood Engineering Research
Forest Products Laboratory, USDA
P.O. Box 5130
Madison, WI 53705
608-257-2211

Dr. Roger D. Borcherdt
Office of Earthquake Studies
Branch of Earthquake Hazards, USGS
345 Middlefield Road
Menlo Park, CA 94025
415-323-8111

Dr. Charles G. Culver
Disaster Research Coordinator
Structures and Materials Division, NEL
National Bureau of Standards
Washington, DC 20234
301-921-2196

Mr. Jerry Dodd
Bureau of Reclamation
P.O. Box 25007
Denver Federal Center
Denver, CO 80225
303-234-3089

Dr. Michael P. Gaus
Division of Problem Focused Research Applications
National Science Foundation
1800 G Street, NW
Washington, DC 20550
202-632-5787

Mr. John J. Healy
Chief, Research and Development Office
Department of the Army
DAEN-RDM
Washington, DC 20314
202-693-7287

Dr. William B. Joyner
Office of Earthquake Studies
Branch of Earthquake Hazards, USGS
345 Middlefield Road
Menlo Park, CA 94025
415-323-8111

Mr. John W. Kaufman
Aerospace Environment Division
ES42-Space Science Laboratory
National Aeronautics and Space Administration
Marshall Space Flight Center, AL 35812
205-453-3104

Mr. James Lander
National Oceanic and Atmospheric Administration
Environmental Data Service
National Geophysical and Solar-Terrestrial Data Center
Boulder, CO 80302

Dr. H. S. Lew
Structures Materials Division
Center for Building Technology
National Bureau of Standards
Washington, DC 20234
301-921-2647

Dr. E. V. Leyendecker
Structures and Materials Division
Center for Building Technology
National Bureau of Standards
Washington, DC 20234
301-921-3471

Dr. Richard D. McConnell
Office of Construction
Veterans Administration
811 Vermont Avenue, NW
Washington, DC 20234
202-389-3103

Dr. William F. Marcuson, III
Research Civil Engineer, WES-SH
Department of the Army
Waterways Experiment Station
Corps of Engineers
P.O. Box 631
Vicksburg, MI 39180

Dr. Richard D. Marshall
Office of the Associate Director for Programs
National Bureau of Standards
Washington, DC 20234
301-921-3132

Dr. R. B. Matthiesen
Chief, Branch of Seismic Engineering
Office of Earthquake Studies, USGS
345 Middlefield Road
Menlo Park, CA 94025
415-333-8111 (FTS 467-2881)

Mr. John F. Meehan
Department of General Services
Office of Architectural Construction
Sacramento, CA 95805

Mr. Howard L. Metcalf
Deputy Director for Construction Standards
and Design
Office of the Assistant Secretary of Defense
(MR&L) Room 3E763
The Pentagon
Washington, DC 20301
202-695-2713

Dr. Thomas D. Potter
Deputy Director
Environmental Data Service, NOAA
3300 Whitehaven Street, NW
Washington, DC 20235
202-634-7319

Dr. John B. Scalzi
Program Manager
Earthquake Hazards Mitigation
National Science Foundation
1800 G Street, NW
Washington, DC 20550

Mr. Charles Scheffey
Director, Office of Research
Federal Highway Administration
Department of Transportation
Washington, DC 20590
202-426-3943

Dr. Warren A. Shaw
Head, Civil Engineering Department
Civil Engineering Laboratory
Naval Construction Battalion Center
Port Hueneme, CA 93043
805-982-5407

Alternates:

Dr. A. Gerald Brady
Physical Scientist
Office of Earthquake Studies, USGS
345 Middlefield Road
Menlo Park, CA 94025
415-323-8111

Dr. James D. Cooper
Structures and Applied Mechanics Division
Federal Highway Administration
Office of Research HRS-11
Washington, DC 20590
202-557-4315

Mr. G. Robert Fuller
Architectural and Engineering Division
Department of Housing and Urban Development
Washington, DC 20411

Dr. Jerry Harbour
Site Safety Research Branch
Office of Site Safety Research Branch
Nuclear Regulatory Commission
Washington, DC 20555
301-427-4370

Dr. Charles T. Thiel
Deputy Director
Division of Advanced Environmental Research
and Technology
National Science Foundation
Washington, DC 20550
202-632-5734

Mr. Drew A. Tiedemann
Bureau of Reclamation
Engineering and Research Center
Denver Federal Center
Denver, CO 80225
303-234-3029

Mr. Robin McGuire
U.S. Department of the Interior
U.S. Geological Survey
Box 25046
Denver Federal Center
Denver, CO 80225
303-234-2874

JAPAN PANEL ON WIND AND SEISMIC EFFECTS

MEMBERSHIP LIST

MAY 1978

Mr. Kazuto Nakazawa, Chairman
Director
Public Works Research Institute
Ministry of Construction
2-28-32, Honkomagome, Bunkuo-ku, Tokyo, 113

Mr. Shigemi Fujiwhara
Head, Typhoon Research Division
Meteorological Research Institute
Meteorological Agency
4-35-8, Koenji Kita, Suginami-ku, Tokyo, 166

Dr. Sadaiku Hattori
Chief, Seismology Section
International Institute of Seismology and Earthquake Engineering (I.I.S.E.E.)
Building Research Institute
Ministry of Construction
3-28-8, Hyakunin-cho, Shinjuku-ku, Tokyo, 160

Dr. Satoshi Hayashi
Director
Port and Harbour Research Institute
Ministry of Transport
3-1-1, Nagase, Yokosuka-shi,
Kanagawa-ken, 239

Mr. Masaya Hirosawa
Chief Researcher
Building Research Institute
Ministry of Construction
5-26-25 Daitakubo, Urawashi, Saitamaken, 336

Mr. Toshio Iwasaki
Chief, Ground Vibration Section
Earthquake Disaster Prevention Division, Chiba Branch
Public Works Reserch Institute
Ministry of Construction
4-12-52, Anagawa, Chiba-shi, Chiba-ken, 280

Mr. Eiichi Kuribayashi
Chief, Earthquake Engineering Section
Earthquake Disaster Prevention Division, Chiba Branch
Public Works Research Institute
Ministry of Construction
4-12-52, Anagawa, Chiba-shi, Chiba-ken, 280

Mr. Tatsuro Murota
Chief, Structure Section
Structure Division
Building Research Institute
Ministry of Construction
3-28-8, Hyakunin-cho, Shinjuku-ku, Tokyo, 160

Dr. Keikichi Naito
Head, Meteorological Satelite Division
Meteorological Research Institute
Japan Meteorological Agency
4-35-8, Koenji Kita, Suginami-ku, Tokyo, 166

Dr. Kiyoshi Nakano
Director
Building Research Institute
Ministry of Construction
3-28-8, Hyakunin-cho, Shinjuku-ku, Tokyo, 160

Mr. Nobuyuki Narita
Chief, Structure Section
Structure and Bridge Division, Chiba Branch
Public Works Research Institute
Ministry of Construction
4-12-52, Anagawa, Chiba-shi, Chiba-ken, 280

Dr. Masamitsu Ohashi
Head, Earthquake Disaster Prevention Division Chiba Branch
Public Works Research Institute
Ministry of Construction
4-12-52, Anagawa, Chiba-shi, Chiba-ken, 280

Mr. Keiichi Ohtani
Chief, Earthquake Engineering Laboratory
National Research Center for Disaster Prevention
Science and Technology Agency
3-1, Tennodai, Sakura-mura, Niihari-gun, Ibaragi-ken, 300-32

Mr. Michio Ohtsuka
Acting Director, International Institute of Seismology and Earthquake Engineering (I.I.S.E.E.)
Building Research Institute
Ministry of Construction
3-28-8, Hyakunin-cho, Shinjuku-ku, Tokyo, 160

Dr. Hiroshi Sato
Chief, Research Division
Crustal Dynamics Department
Geographical Survey Institute
Ministry of Construction
3-24-13, Higashiyama, Meguro-ku, Tokyo, 153

Mr. Kenkichi Sawada
Chief, Soil Dynamics Section
Construction Method and Equipment Division, Chiba Branch
Public Works Research Institute
Ministry of Construction
4-12-52, Aangawa, Chiba-shi, Chiba-ken, 280

Mr. Yukitake Shioi
Head, Foundation Engineering Section
Structure and Bridge Division, Chiba Branch
Public Works Research Institute
Ministry of Construction
4-12-52, Anagawa, Chiba-shi, Chiba-ken, 280

Mr. Akira Suwa
Head, Seismological Laboratory
Meteorological Research Institute
Meteorological Agency
4-35-8, Koenji Kita, Suginami-ku, Tokyo, 166

Mr. Hiroshi Takahashi
Head, Second Research Division
National Research Center for Disaster Prevention
Science and Technology Agency
3-1, Tennadai, Sakura-mura, Niihari-gun, Ibaragi-ken, 300-32

Mr. Hajime Tsuchida
Chief, Earthquake Resistant Structures Laboratory
Structure Division
Port and Harbour Research Institute
Ministry of Transport
3-1-1, Nagase, Yokosuka-shi, Kanagawa-ken, 239

Dr. Makoto Watabe
Head, Structure Division
Building Research Institute
Ministry of Construction
3-28-8, Hyakunin-cho, Shinjuku-ku, Tokyo, 160

Dr. Tadayoshi Okubo, Secretary-General
Head, Planning and Research Administration Division
Public Works Research Institute
Ministry of Construction
2-28-32, Honkomagome, Bunkyo-ku, Tokyo, 113

Secretariat:

Mr. Keisuke Takagi
Chief, Planning Section
Planning and Research Administration Division
Public Works Research Institute
Ministry of Construction
2-28-32, Honkomagome, Bunkyo-ku, Tokyo, 113

RESOLUTIONS OF THE TENTH JOINT MEETING

U.S.-JAPAN PANEL ON WIND AND SEISMIC EFFECTS

U.J.N.R.

May 23 - 26, 1978

In response to the urgent needs expressed by the U.S. Congress in its "Disaster Mitigation Act of 1977" and by Japanese Diet's intention of adopting a similar act within this year, the U.S.-Japan Panel on Wind and Seismic Effects proposes (adopts) the following resolutions for future activities:

1. The Tenth Joint Meeting was an extremely valuable exchange of technical information which was beneficial to both countries. In view of the importance of cooperative programs on the subject of wind and seismic effects, the continuation of Joint Panel Meetings is considered essential.

2. The exchange of technical information, especially revised codes and specification relevant to wind and seismic effects, and the promotion of research programs including exchange of personnel and available equipment should be strengthened.

3. The Panel on Wind and Seismic Effects recognizes the importance of the U.S.-Japan Cooperative Program on Large Scale Testing and it urges early implementation of the program through this Panel.

4. Considerable advancement has been made by various Task Committees. Cooperative research programs should be promoted through the Task Committees.

5. Chairpersons of both sides should encourage broadening the activities to include the topic on tsunami and storm surge.

6. Chairmen of both sides should explore, by correspondence, the feasibility of establishing an additional task committee on wind and earthquake engineering for nuclear facilities construction.

7. Date and location of the Eleventh Joint Meeting of the Panel on Wind and Seismic Effects will be Fall 1979 in Japan. Specific dates and itinerary will be determined by the Japanese Panel with concurrence by the U.S. Panel. Subsequent meetings will be held in May of each year.

1

ON THE DISTRIBUTION OF EXTREME WINDS EXPECTED IN JAPAN

Todayoshi Okubo
Nobuyuki Narita

Public Works Research Institute
Ministry of Construction

On the Distribution of Extreme Winds Expected in Japan

This paper deals with the basic wind speed -- the determination of the expected value of extreme wind, which forms the basis of the design wind speed. Wind speed predictions based on historical data are generally made by using the extreme value theory [1]. Distribution function of yearly maximum ten-minute average wind speed can be fitted by double exponential distribution:

$$F(V) = f(y) = \exp(-\exp(-y))$$
$$y = a(V - b)$$

where F(V), a, and b are the distribution function and constants. R. Saito [2] and E. Kikuchibara [3] have shown that historical wind data at the meteorological observatories satisfy the distribution mentioned above. E. Kikuchibara [4] has also shown that Gringorten's method, in which Hazen's distribution is saved ($F(V) = (2i - 1)/2N$, where N and i denote the number of samples and the order of samples in N respectively), is the best for the estimation.

On the other hand, the multiple regression method has also been used for estimating the expected wind speed at an arbitrary point, in which the topographical factors (altitude, undulation, ratio of land or sea area to surroundings, and so on) are used. R. Satio [5] applied the method to determine expected wind speed every two kilometers between Tokyo and Osaka. The result formed the basis of design wind speeds for railway structures on the New Tokaido Line.

Wind Speed Data

Yearly maximum wind speeds recorded by the meteorological observatories of the Meteorological Agency are the foundation of basic wind speeds. Wind speeds are commonly reported as ten-minute average speed and instantaneous speed. The instantaneous wind speeds are valid for about two seconds depending on the sensitivity of the measuring device.

The wind records were collected from the 163 meteorological observatories. The records were from 1929 to 1975. As the observation method (measuring device, probe height, location, data process regulation, and so on) has been modified during the period, the wind data have been homogonized to give yearly maximum ten-minute speed at a height of ten meters.

The data were checked if they satisfied the Hazen's formula on the double exponential distribution diagram, and the result was as follows:

(number of data)	(fitness)
109 (67%)	better
34 (21%)	good
20 (12%)	not so good

Effects of Statistical Length and Period on Expected Speeds

The wind data at 55 observatories ranging from 1929 to 1975 were classified into four groups according to the statistical length of years as follows:

(I)	47 years	(1929 - 1975)
(II)	33 years	(1943 - 1975)
(III)	21 years	(1955 - 1975)
(IV)	12 years	(1964 - 1975)

The mean and the standard deviation of the ratio of expected wind speeds referring to the specific return period are tabulated in Table 1.

The wind data were also divided into four groups, in which every group had the same statistical period of twelve years:

(I)	12 years	(1964 - 1975)
(II)	12 years	(1954 - 1965)
(III)	12 years	(1944 - 1955)
(VI)	12 years	(1934 - 1945)

Results are given in Table 2. The expected wind speed estimated by the data of the oldest period gives the largest value.

It is desirable for carrying out the multiple regression analysis of topographical factors to select a set of data with the same statistical length and period of years. It is also desirable to select wind data with observation periods as long as possible. Wind data at 101 observatories were selected, which had the statistical period of 33 years (1943 - 1975). Eighty-one data among them were used for deriving the regression equation; the rest (twenty data) were used for checking the equation.

Estimation of Expected Values by Multiple Regression

Definition of topographical factors (X_i):

(1) altitude of anemometer (X_1)
(2) ratio of the sea to the whole area in a specific circle surrounding the point (X_2, X_3 and X_4)
(3) ratio of land to the whole area in a specific circle surrounding the point (X_5,--,X_8)
(4) openess of the surrounding area (X_9,--,X_{12})
(5) undulation of the ground of surrounding area (X_{13},--,X_{16})
(6) slope of the ground (X_{17},--,X_{20})
(7) distance from the point to obstacles (X_{21})
(8) covergence of surrounding area (X_{22},--X_{25})

Relations between expected wind speed and topographical factors were analyzed by multiple regression, in which regression equations were assumed to be linear. Table 3 shows how the multiple correlation coefficients increase as the number of topographical factors increase. The expected wind speed is highly correlated with the openess factor X_{12}, the radius being 40 kilometers.

Table 4 shows the compatibility of the regression equations. The standard deviation by the regression equations (81 points) is nearly equal to that of the checking points (20 points).

Estimation of Expected Values by Modified Method

Estimation errors, i.e., the differences between expected wind speeds from Gringorten's method and those from the multiple regression method, have a regional distribution, and the averaged estimation errors were added to the equations in the modified method. This suffices for the meteorological effects that cannot be expressed by the five topographical factors and constants. Although the standard deviation can be decreased to 1.1 m/s in the case of 81 points (Table 5), this seems lacking in generality, as seen in Table 6.

As the second step, regression equations were derived by the use of 131 stations ranging from 1943 to 1975. The results are given in Tables 7 and 8, in which the standard deviation decreases to 1.1 m/s. The average estimation errors are given in Figures 1 to 3, and the modified regression equations can be written as follows:

$$V_{20} = 30.1+0.0107X_{12}+0.879X_2+0.0126X_1-1.08X_8-0.00669X_{13}+\Delta\overline{V}_{20}$$

$$V_{50} = 34.0+0.00985X_{12}+0.983X_2+0.0137X_1-1.24X_8-0.00790X_{13}+\Delta\overline{V}_{50}$$

$$V_{100} = 37.0+0.00919X_{12}+1.07X_2+0.0145X_1-1.37X_8-0.00883X_{13}+\Delta\overline{V}_{100}$$

where

X_{12}	: R = 40 kilometers	openess
X_2	: R = 3 kiometers	sea
X_1	:	altitude
X_8	: R = 40 kilometers	land
X_{13}	R = 5 kilometers	undulation

Estimation of Expected Wind Speeds at Points Except Observatories

Ninety-seven specific points except meteorological observatories were selected to draw up the contour of expected wind speeds. Figure 4 shows the final distribution map. Similar maps have also been drawn up for the return periods of 20 and 50 years.

The topographical distribution of instantaneous wind speeds has been obtained by using a similar procedure, and Figure 5 shows the map of 100-year expected instantaneous wind speed.

Concluding Remarks

The design wind loads in the present Design Specifications of Bridges in Japan are based on the ten-minute wind speed of 40m/s. However, as seen in Figure 4, the expected wind speed exceeds this specified value in some southern coastal regions on the Pacific Ocean side and in some western coastal regions on the Japan Sea side. For the best bridge designs, the basic wind values representing the region should be used instead.

The authors wish to acknowledge their debt to Dr. A. Masatsuka and Mr. T. Kimura, who prepared the meteorological data.

References

1. Gumbel, E. J., Statistics of Extremes.

2. Saito, R., "Probabilistic Distribution of Strong Wind--Study on High Wind in Japan III," Research Review, 9, No. 7, 1955 (in Japanese).

3. Meteorological Agency, Estimation of Return Period of Strong Wind at the Construction Site of the Proposed Honshu Shikoku Bridges, 1965 (in Japanese).

4. Association for Electrification of Railways, Wind-Strong Wind and Railway Tracks, 1961 (in Japanese).

TABLE 1: VARIATION OF EXPECTED WIND SPEED WITH STATISTICAL LENGTH OF YEARS

return period (yrs)	20			50			100		
ratio	②/①	③/①	④/①	②/①	③/①	④/①	②/①	③/①	④/①
mean	0.97	0.94	0.87	0.97	0.94	0.87	0.97	0.94	0.86
standard deviation	0.057	0.081	0.100	0.063	0.089	0.111	0.067	0.094	0.116

where
(Ⅰ) expected wind speed derived from the data, 1929-1975
(Ⅱ) expected wind speed derived from the data, 1943-1975
(Ⅲ) expected wind speed derived from the data, 1955-1975
(Ⅳ) expected wind speed derived from the data, 1964-1975

TABLE 2: VARIATION OF EXPECTED WIND SPEED WITH STATISTICAL PERIOD OF YEARS

return period (yrs)	20			50			100		
ratio	②/①	③/①	④/①	②/①	③/①	④/①	②/①	③/①	④/①
mean	1.16	1.15	1.21	1.16	1.16	1.22	1.17	1.16	1.23
standard deviation	0.139	0.180	0.194	0.159	0.202	0.216	0.172	0.217	0.232

where
(Ⅰ) expected wind speed derived from the data, 1964-1975
(Ⅱ) expected wind speed derived from the data, 1954-1965
(Ⅲ) expected wind speed derived from the data, 1944-1955
(Ⅳ) expected wind speed derived from the data, 1934-1945

TABLE 3: MULTIPLE CORRELATION COEFFICIENTS

return period	20		50		100	
rank	topographical factor	multiple correlation coefficient	topographical factor	multiple correlation coefficient	topographical factor	multiple correlation coefficient
1	X_{12} (R=40km)	0.629	X_{12} (R=40km)	0.610	X_{12} (R=40km)	0.599
2	X_1	0.661	X_1	0.637	X_2 (R= 3km)	0.627
3	X_3 (R= 5km)	0.721	X_3 (R= 5km)	0.699	X_1	0.679
4	X_{20} (R=20km)	0.732	X_{20} (R=20km)	0.713	X_{19} (R=15km)	0.692
5	X_5 (R=10km)	0.740	X_5 (R=10km)	0.721	X_5 (R=10km)	0.709

TABLE 4: COMPARISON OF ESTIMATION ERRORS

return period	20		50		100	
type	(Ⅰ)	(Ⅱ)	(Ⅰ)	(Ⅱ)	(Ⅰ)	(Ⅱ)
mean (m/s)	0.0	0.5	0.0	0.0	0.0	0.2
standard deviation (m/s)	5.3	5.0	6.1	6.0	6.8	6.7

where
(Ⅰ) data of 81 stations used for determining the multiple regression equations
(Ⅱ) data of 20 stations used for checking the multiple regression equations

TABLE 5: COMPARISON OF ESTIMATION ERROR (81 STATIONS)

return period (yrs)	20		50		100	
type	(Ⅰ)	(Ⅱ)	(Ⅰ)	(Ⅱ)	(Ⅰ)	(Ⅱ)
mean (m/s)	0.0	− 0.1	0.0	− 0.1	0.0	0.1
standard deviation (m/s)	5.3	1.1	6.1	1.1	6.8	1.1

where
(Ⅰ) multiple regression method
(Ⅱ) modified method

TABLE 6: COMPARISON OF ESTIMATION ERRORS (20 CHECK STATIONS)

return period (yrs)	20		50		100	
type	(Ⅰ)	(Ⅱ)	(Ⅰ)	(Ⅱ)	(Ⅰ)	(Ⅱ)
mean (m/s)	0.5	0.6	0.0	− 0.1	0.2	0.5
standard deviation (m/s)	5.0	4.5	6.0	5.2	6.7	5.3

where
(Ⅰ) multiple regression method
(Ⅱ) modified method

TABLE 7: MULTIPLE CORRELATION COEFFICIENTS

return period	20		50		100	
rank	topographical factor	multiple correlation coefficient	topographical factor	multiple correlation coefficient	topographical factor	multiple correlation coefficient
1	X_{12} (R = 40km)	0.599	X_{12} (R = 40km)	0.577	X_{12} (R = 40km)	0.563
2	X_2 (R = 3km)	0.643	X_2 (R = 3km)	0.625	X_2 (R = 3km)	0.614
3	X_1	0.700	X_1	0.674	X_1	0.659
4	X_8 (R = 40km)	0.715	X_8 (R = 40km)	0.690	X_8 (R = 40km)	0.675
5	X_{13} (R = 5km)	0.734	X_{13} (R = 5km)	0.712	X_{13} (R = 5km)	0.699

TABLE 8: COMPARISON OF ESTIMATION ERRORS

return period	20		50		100	
type	(Ⅰ)	(Ⅱ)	(Ⅰ)	(Ⅱ)	(Ⅰ)	(Ⅱ)
mean (m/s)	0.0	- 0.1	0.0	- 0.1	0.0	- 0.1
standard deviation (m/s)	5.2	1.3	6.0	1.2	6.7	1.1

where
(Ⅰ) multiple regression method
(Ⅱ) modified method

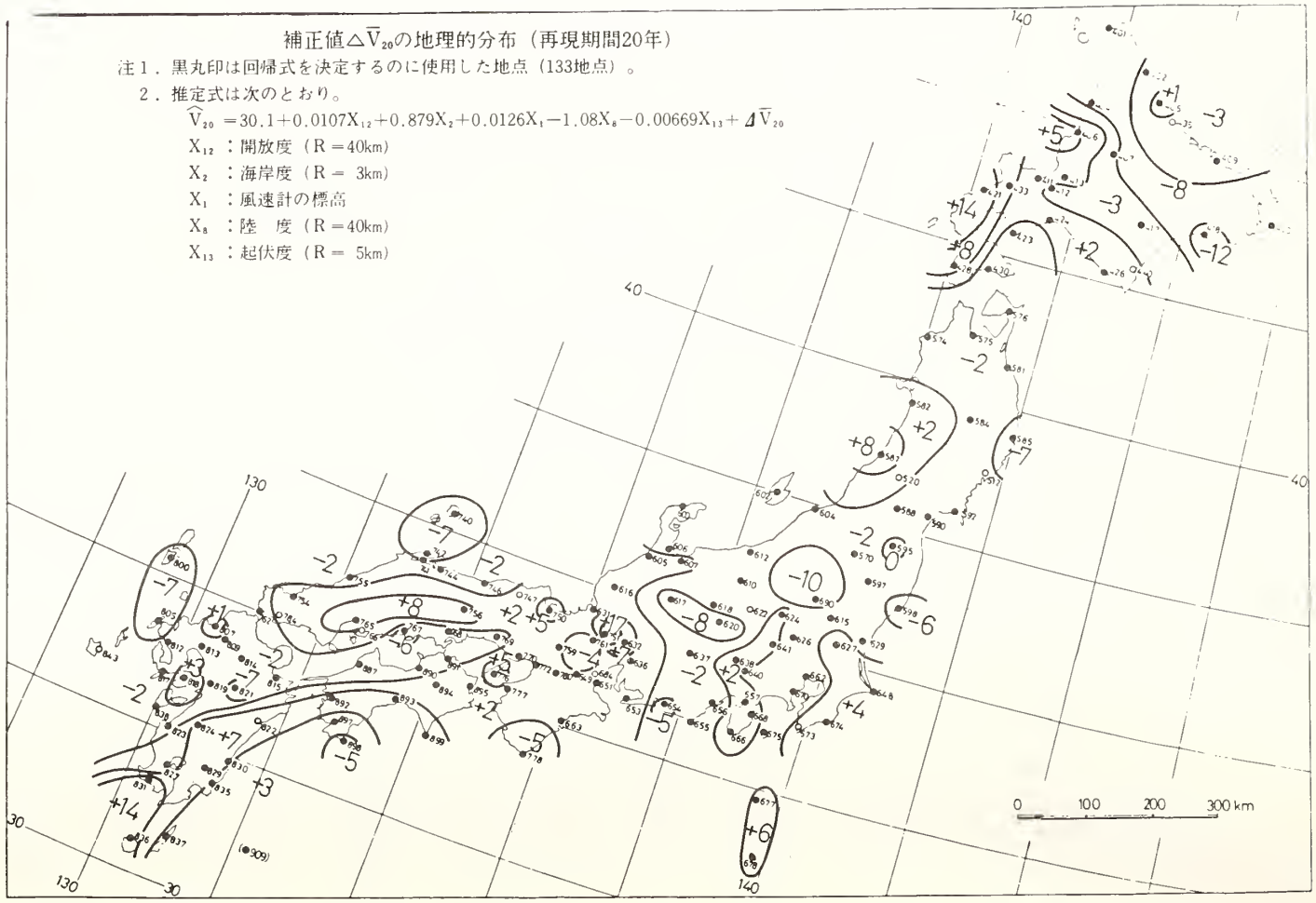

FIGURE 1: TOPOGRAPHICAL DISTRIBUTION OF $\Delta\overline{V}_{20}$

補正値$\triangle\bar{V}_{50}$の地理的分布（再現期間50年）

注１．黒丸印は回帰式を決定するのに使用した地点（133地点）。

２．推定式は次のとおり。

$$\hat{V}_{50} = 34.0 + 0.00985X_{12} + 0.983X_2 + 0.0137X_1 - 1.24X_8 - 0.00790X_{13} + \Delta\bar{V}_{50}$$

X_{12} ：開放度（R＝40km）

X_2 ：海岸度（R＝ 3km）

X_1 ：風速計の標高

X_8 ：陸　度（R＝40km）

X_{13} ：起伏度（R＝ 5km）

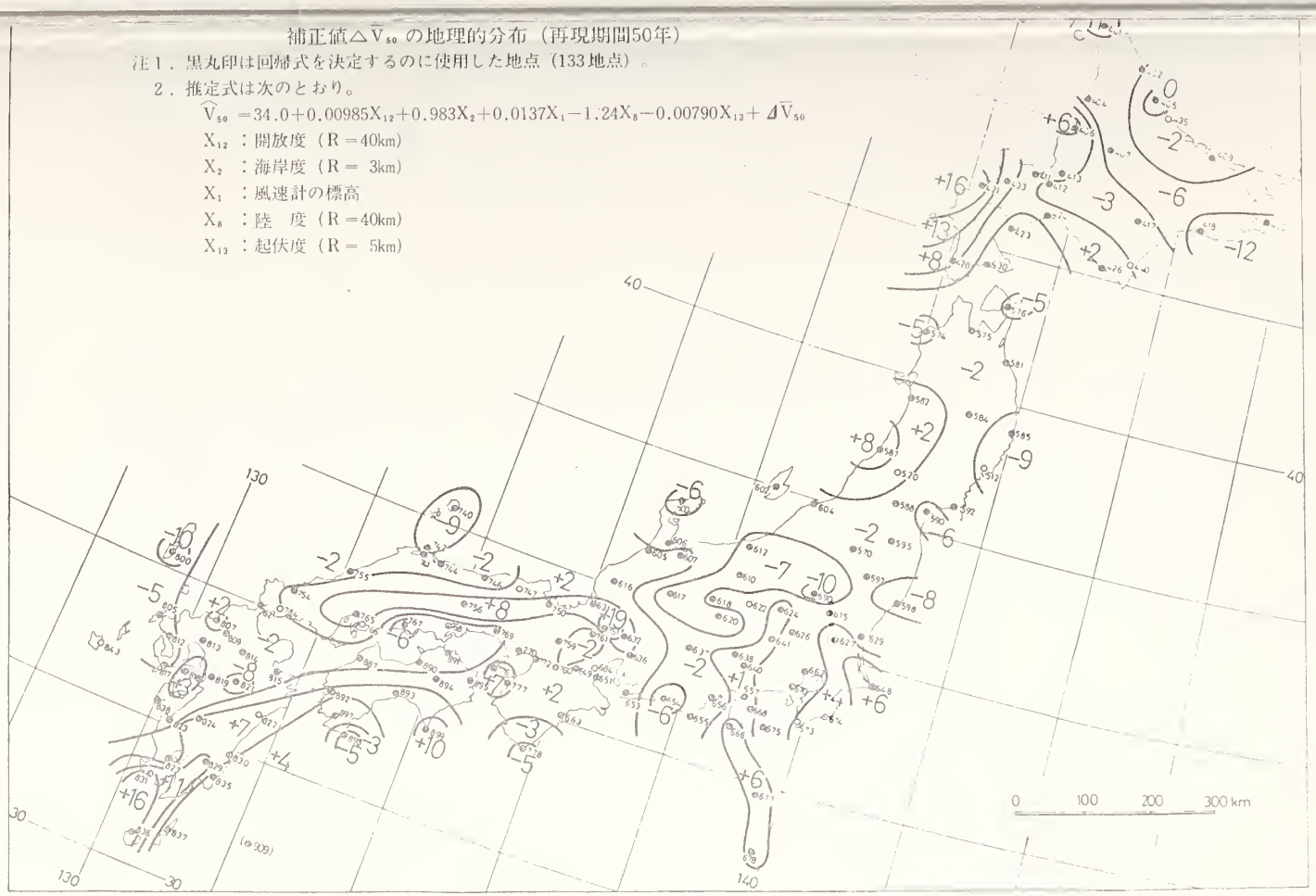

FIGURE 2: TOPOGRAPHICAL DISTRIBUTION OF $\Delta\bar{V}_{50}$

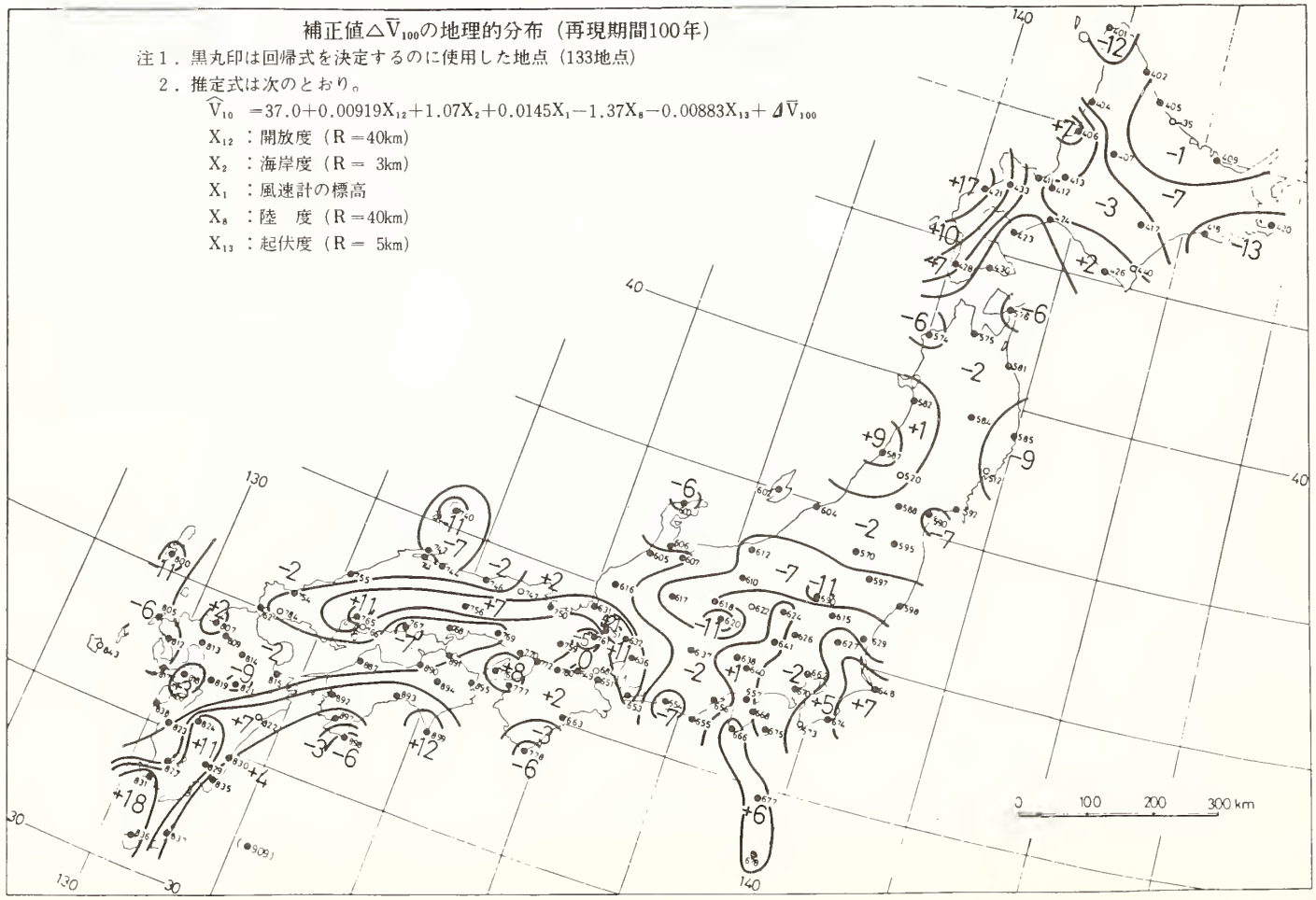

FIGURE 3: TOPOGRAPHICAL DISTRIBUTION OF $\Delta\overline{V}_{100}$

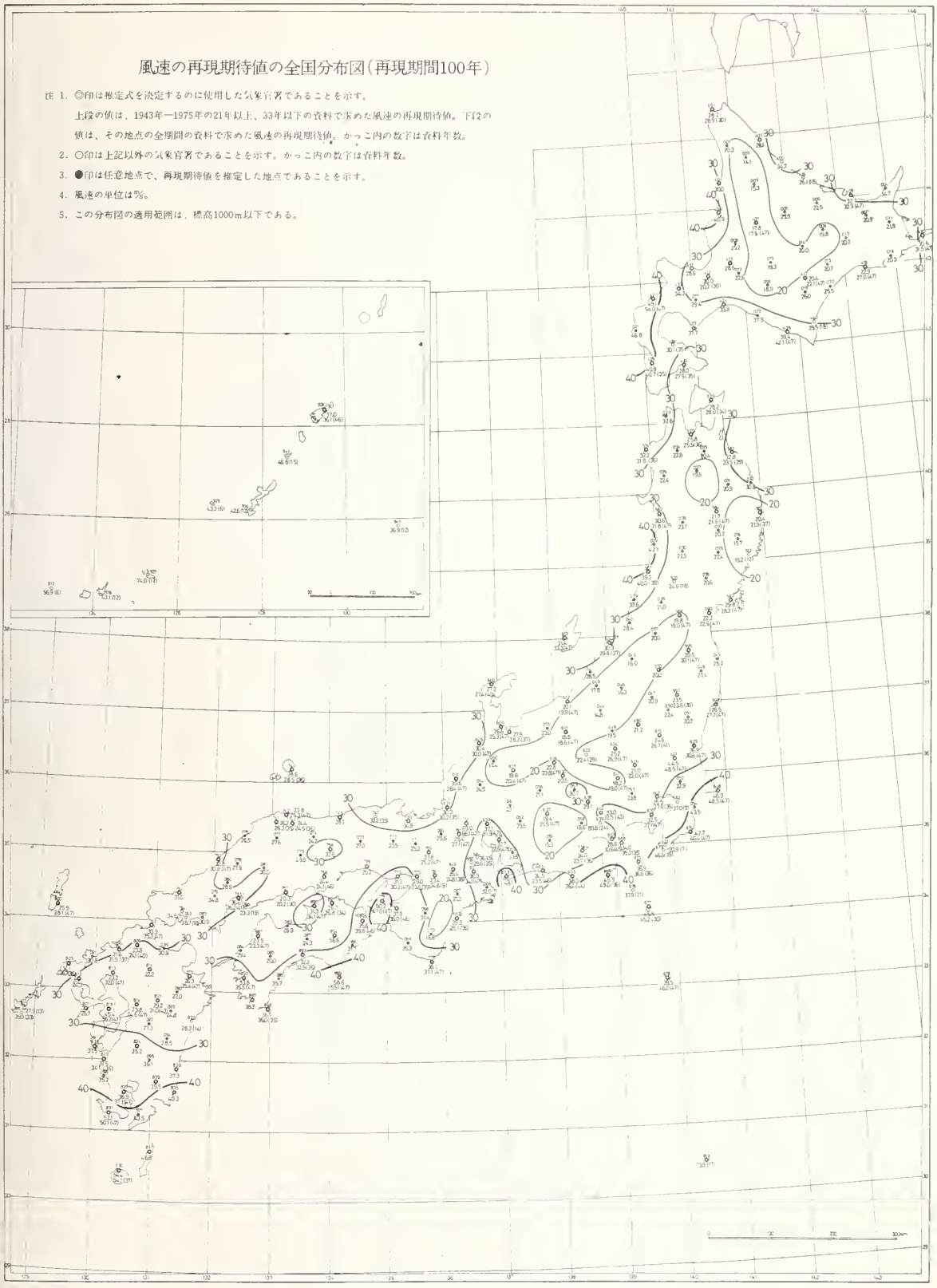

FIGURE 4: DISTRIBUTION OF EXTREME WIND SPEED
(RETURN PERIOD OF 100 YEARS, 10-MIN. AVERAGE)

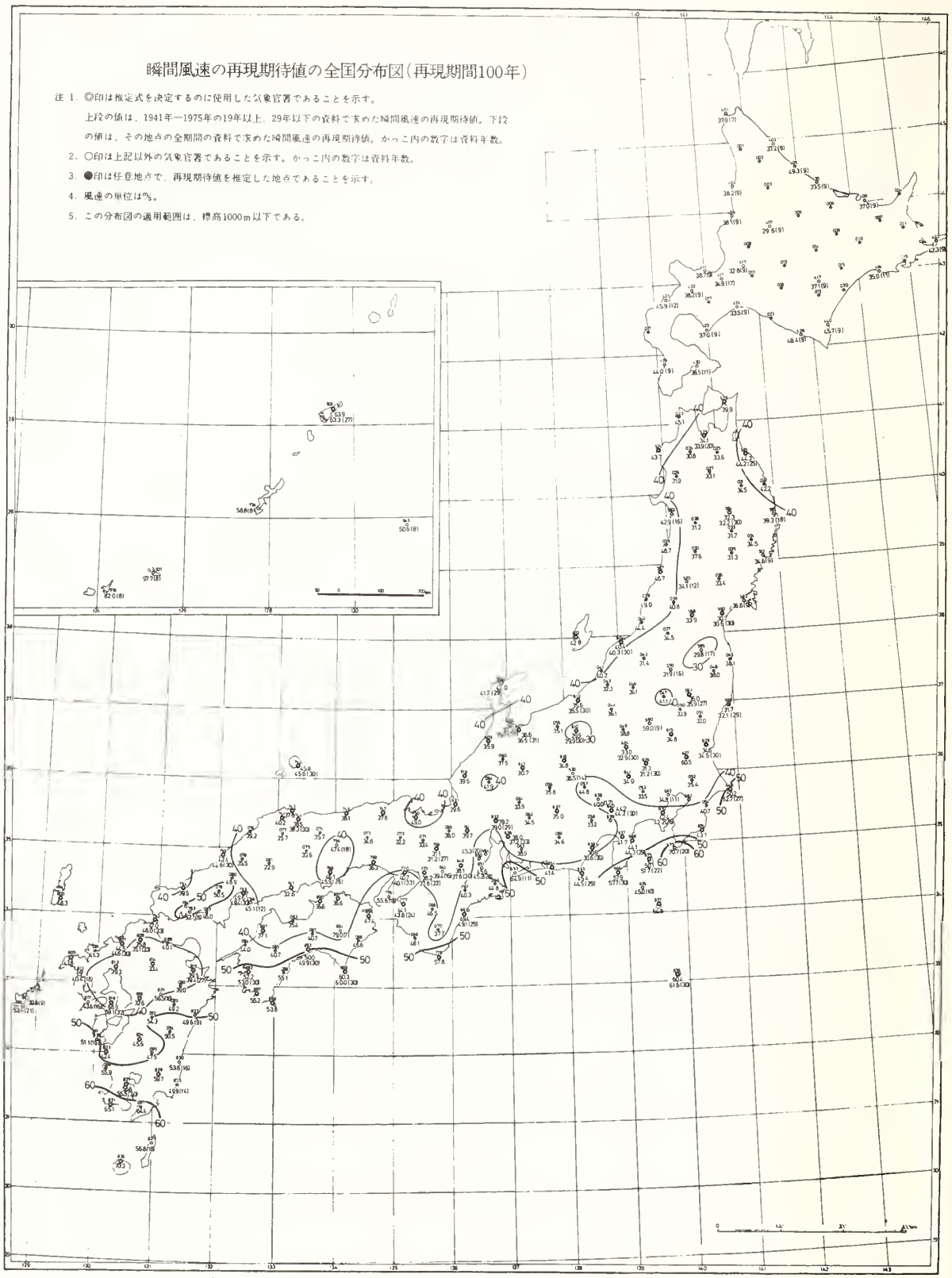

FIGURE 5: DISTRIBUTION OF EXTREME WIND SPEED
(RETURN PERIOD 100 YEARS, INSTANTANEOUS)

2

BOUNDARY LAYER WINDS

Duane A. Haugen

NOAA/ERL/Wave Propagation Laboratory
Boulder, Colorado 80302

Boundary Layer Winds

Introduction

The atmospheric boundary layer has received a great amount of attention by research scientists over the past several decades. Within the last ten years, particularly, the behavior of boundary layer winds over flat, horizontally homogeneous, uncluttered land surfaces has become well known. A large number of empirical laws have been established that describe the height variation of mean wind speed, gustiness ratios, and turbulence scale sizes for these idealized flow conditions. Unfortunately, much of this knowledge can be used only for general guidance in wind engineering problems. Rarely, if ever, does the engineer find the problem located in terrain approximating a flat plane. Furthermore, strong wind conditions are generally of limited interest to boundary layer scientists, but of primary interest to designers and builders of houses, office buildings, and bridges. Indeed, certain types of high winds, viz., tornadoes, thunderstorm wind surges and topographically-generated winds such as chinooks, are considered intermittent, discrete events by the boundary layer scientist and rarely gain his or her attention.

The purpose of this paper is threefold: (a) to outline briefly those results of boundary layer research that seem applicable to wind engineering problems; (b) to emphasize the need for obtaining local wind data sets in generating extreme wind statistics; (c) to draw attention to a few references which might be useful.

Boundary Layer Wind Characteristics

The atmospheric layer of most interest to us is the so-called surface layer. This layer has received the most widespread attention from research meteorologists who find it well-suited as a "laboratory" for testing and developing theories of turbulent flow. As a result, extensive reference material exists on the behavior of surface layer winds. A recent summary article by Panofsky (1973), for example, provides an excellent set of references for further study.

We will restrict our attention to cases in which average wind speeds in the layer exceed roughly 12 m/sec, excluding thunderstorms, tornadoes, and hurricanes. Under these conditions, a fairly simple characterization of the surface layer is possible. The depth of the layer will range between roughly 50 m and 200 m. In general, the stronger the winds, the deeper the layer. The variation of average wind speed with height is given by the so-called log-law,

$$\frac{U_2}{U_1} \cong \frac{\ell n(Z_2/Z_o)}{\ell n(Z_1/Z_2)} \quad ; \quad Z_1, Z_2 >> Z_o \qquad (1)$$

where $\overline{U}_1$ and $\overline{U}_2$ are the average wind speeds at heights Z_1 and Z_2, respectively, and Z_o is the surface roughness parameters. The overbar denotes a time average. The averaging period should be at least 15 minutes, but should not exceed 60 minutes for the law to be most dependable (Wyngaard et al., 1974).

The validity of the log-law is well-established. However, it is often difficult to apply the law because of variations in the surface roughness parameter. Order-of-magnitude estimates of Z_o for three broad categories of surface are given in Table 1. The reader is cautioned that Z_o for any given site might well fall

outside the ranges shown. Furthermore, if the site is not horizontally homogeneous, the appropriate value of Z_o will be a function of wind direction.

TABLE 1. Z_o-values for three general types of surface

Surface	Z_o(m)
Open meadow	0.01 to 0.10
Forests	0.10 to 1.0
Cities	1.0 to 10.0

Another means of specifying wind speed variation with height is the so-called power law.

$$\overline{U}_2 = U_1(Z_2/Z_1)^p \quad ; \quad Z_2 > Z_1 \qquad (2)$$

for which typical values of p are given in Table 2 (Davenport, 1968).

TABLE 2. p-values for three general types of surface

Surface	p
Open meadow	0.14 to 0.2
Forests	0.25 to 0.33
Cities	0.33 to 0.5

As with the log-law, application of the power law depends on knowledge of the local site. There is no way that this can be avoided. It is therefore common practice for the design engineer to choose a wind profile law based largely on personal preference and to specify surface characteristics according to experience and the safety factor judged necessary.

In general, the average wind direction does not vary with height in the surface layer under strong wind conditions. Therefore, it is appropriate to assume no directional change when making first-order estimates of wind loading. The single most important exception to this rule of thumb will be those cases where the structure of interest is in the wake of other structures in which case both wind speed and direction profiles will be strongly dependent on local conditions.

We now briefly consider wind variability or gustiness. By definition, the gust factor is the ratio of the peak wind speed (of a given duration) to the mean wind speed (for a given averaging period). The gust factor may be considered independent of height under strong wind conditions, but its value is highly dependent on

the gust duration and the length of the averaging period (Lettau and Haugen, 1960). The most probable gust factors one should use range from 1.4 to 1.7, whereas maximum gust factors reported range from 1.7 to 2.2 (Sissenwine et al., 1973).

Extreme Wind Statistics

The preceding discussion has not considered discrete phenomena such as severe storms and topographically caused winds. Incorporating extreme wind statistics in engineering design problems is well-established practice. Furthermore, the statistical techniques used for estimating extreme values are also well-tested and widely accepted (Gringorten, 1963; Gumbel, 1958). There is a serious weakness in the application of extreme wind statistics, however, that is frequently overlooked by the practicing engineer. All of the techniques depend on the existence of long years of wind records; the reliability and the statistics increase as the length of record increases. However, many design and/or construction efforts take place in geographical regions where wind records are non-existent and where local wind effects introduce extremes not expected from the closest observing stations. One well-documented example of such anomalous extreme winds is the downslope winds in Boulder, Colorado (Julian and Julian, 1969; Lilly and Zipser, 1972). These winds occur frequently every winter; they often exceed speeds of 95 mph; they cause property damage of roughly $1 million each year (Bergen and Murphy, 1978). Yet it is only in recent years that local building practices have been substantially modified to minimize wind damage to homes and businesses. To my knowledge there are no climatological extreme wind charts that would have accurately predicted such severe wind effects. Instead, local experience was necessary to permit laypersons and engineers alike to appreciate the seriousness of the situation.

Another example of local wind anomalies is the highly-publicized problem with the John Hancock Insurance building in Boston, Massachusetts. Reference material in the open literature is not yet available because of pending lawsuits concerning blame for the wind damage that has occurred. But this skyscraper was constructed in the middle of a large urban area that seemed relatively free of high wind problems. Whatever the resolution of this engineering nightmare, its very occurrence stands as a strong case for obtaining local wind data as a standard operating procedure for all large construction efforts. If traditional wind specification formulas prove to be adequate, all well and good. If not, considerable savings in time and effort will inevitably result.

Wind Threshold Sensor

In closing, it seems appropriate to reference a new wind speed threshold detection device that could be used by the construction industry. Quite frequently designers need only extreme wind statistics to learn of possible wind loading problems either before or after the construction has been completed. A wind threshold sensor designed by Bedard and Fujita (1978) seems ideally suited for this purpose. Its data output consists of time of occurrence and duration of wind speeds above any desired thresold. The device is inexpensive, easy to operate, and reliable. Details of the sensor may be obtained in the referenced article or by direct correspondence with either of the authors. Mr. Bedard is at the Wave Propagation Laboratory, NOAA, Boulder, Colorado; Prof. Fujita is at the University of Chicago, Chicago, Illinois.

References

1. Bedard, Jr., A. J., and Fujita, T. T., 1978: An Omnidirectional, Tilt Insensitive, Wind Speed Thresold Detector, Proc. Fourth Symposium on Meteor. Obs. and Inst., 10-14 April 1978, Am. Meteor. Soc., Boston, Massachusetts.

2. Bergen, W. R., and Murphy, A. H., 1978: Potential Economic and Social Value of Short-range Forecasts of Boulder Wind Storms, Bull. Am. Meteor. Soc., Vol. 59, pp. 29-44.

3. Davenport, A. G., 1968: The Dependence of Wind Load on Meteorological Parameters, Wind Effects of Buildings and Structures, Univ. of Toronto Press, pp. 19-82.

4. Gringorten, I. I., 1963: A Simplified Method of Estimating Extreme Values from Data Samples, J. Appl. Meteor., Vol. 2, pp. 82-89.

5. Gumbel, E. J., 1958: Statistics of Extremes, New York, Columbia Univ. Press, 375 pp.

6. Julian, L. T., and Julian, P. R., 1969: Boulder's Winds, Weatherwise, Vol. 22, pp. 108-112, 126.

7. Lettau, H. H., and Haugen, D. A., 1960: Wind, Handbook of Geophysics, New York, The Macmillan Co., Chapter 5, Section 1.

8. Lilly, D. K., and Zipser, E. J., 1972: The Front Range Wind Storm of 11 January 1972 - a Meterological Narrative, Weatherwise, Vol. 25, pp. 56-63.

9. Panofsky, H. A., 1973: Tower Micrometeorology, Workshop on Micrometeorology, Am. Meteor. Soc., Boston, Massachusetts, pp. 151-176.

10. Sissenwine, N., Tattelman, P., Grantham, D. G., and Gringorten, I. I., 1973: Extreme Wind Speeds, Gustiness, and Variations with Height for ML-STD 210B, AFCRL-TR-73-0560, Air Force Camb. Res. Lab., Hanscom Field, Massachusetts, 72 pp.

11. Wyngaard, J. C., Arya, S. P. S., and Cote, O. R., 1974: Some Aspects of the Structure of Convective Planetary Boundary Layers, J. Atmos. Sci., Vol. 31, pp. 747-754.

3

ON THE DAMAGE TO BUILDINGS IN OKI-ERABU FROM THE SEPTEMBER 1977 TYPHOON

Tatsuo Murota
Yuji Ishiyama

Building Research Institute
Ministry of Construction

and

Shigemi Fujiwhara
Minoru Okuda
Kiyoshi Tsukada

Meteorological Research Institute
Ministry of Transportation

On the Damage to Buildings in Oki-erabu from the September 1977 Typhoon

Typhoon No. 7709 was first detected on September 2, 1977, near the Caroline Islands, moving westward slowly. On September 6, east of Philippine Islands, it turned a NNW direction. At 0900 JST on the 8th, moving to the south-east of Taiwan, it developed into an intensive typhoon with central pressure of 905mb and maximum average wind speed of 55m/s. At 2000 JST on the 9th, it passed about 100 km east of Okinawa toward Oki-erabu Island. Since that time, the typhoon had increased it speed gradually. A little before 2300 JST, it passed Oki-erabu toward East China Sea (see Figure 1). Turning to the west, it moved through the East China Sea and landed near the mouth of the Yangtse River on the morning of the 11th, and shortly declined into a temperate depression.

Mukade (1977) of the Okinawa Meteorological Observatory calculated the detailed typhoon path near Oki-erabu based on radar reports of two stations at Naha and Nase located nearly the same distance from Oki-erabu.

According to him, the typhoon had a circular eye wall 35 km in diameter and the two paths calculated from the two radar reports closely agreed with each other. As a consequence he decided that the typhoon landed near Furusato in the central part of Okierabu and moved in a NNW direction at a speed of 35 km/h as shown by the solid line in Figure 2.

According to weather observations at a few points on the island:

- At Oki-erabu Weather Station, eye phenomenon was not clearly observed but winds calmed down temporarily. The east edge of the eye wall probably passed near the station.

- At the top of Mt. Oyama on the western part of the island, wind direction changed counter-clockwise during the typhoon and a clear eye phenomenon was observed for 25 minutes from 22:30 to 22:55.

- At Wadomari, 6.5 km south-west of Oki-erabu Weather Station, an eye phenomenon was observed.

Summing up, it is inferred that the diameter of clear sky area in the typhoon eye was about 20 km and its center moved on a course more west than that determined by radar observations and also east of Mt. Oyama. A dotted line in Figure 2 shows the inferred path of the typhoon.

The 15 km difference in eye diameter can be explained as follows: calculating radar beam height at Oki-erabu based on the data that height angle of Nase radar was 1 degree during the typhoon observation and distance from Nase to Oki-erabu is about 150 km, the result comes to nearly 4000m. On the other hand, according to rainfall observations at Oki-erabu Weather Station, rather weak rain continued for about 30 minutes while the typhoon eye was passing on the island (see Figure 6). Such a weak rainfall can often be caused by a nimbus lower than 4000m in height. From these it can be assumed that the eye wall diameter would be 35 km. Inside the wall there would be stratocumulus regions about 20 km in diameter surrounding a clear sky area.

Table 1 shows the hourly changes of surface pressure, wind speed, wind direction, and rainfall at Oki-erabu Weather Station during the typhoon. Some of those are illustrated in Figures 3 to 6. The extreme values of meteorological elements observed at the same station during the typhoon passage are listed in Table 2.

Surface pressure continued to fall slowly until 21:20; after that time it fell rapidly. The minimum value of 907.3mb was recorded at 22:50. This is the lowest value that has been observed in Japan.

From 19 to 21 o'clock there were severe winds of around 20m/s in average and more than 30m/s at peak. Then, wind speed increased rapidly; at 22:00 peak gusts exceeded 50m/s. The maximum peak gust of 60.4m/s (wind direction ENE) was recorded at 22:16. At that time a severe gust blew down the wind tower of the station and wind observations were forced to stop. The maximum average wind speed recorded was 39.4m/s (ESE) at 22:10.

A rather heavy rain of 20mm/h occurred at 21:10 at the beginning of the rapid pressure fall, but soon stopped. Another heavy rain with an intensity of about 80mm/h occurred at about 22:00 and continued until 22:30. From 22:30 to 23:00, a weak rain continued. During this period Oki-erabu Weather Station must have been inside of the typhoon eye. At 23:00 a heavy rain with an intensity of 100mm/h rose; it slowed after 20 minutes. During these two intense rainfalls Oki-erabu Weather Station was probably in the eye-wall belt. Based on this, the thickness of eye-wall belt can be estimated at 18 km and 12 km in the forward and backward part of the eye-wall, respectively.

Statistics of Damage

Table 3 shows the statistics of damage in Kagoshima Prefecture announced by prefecture authorities at 8 a.m., September 19. According to this table, no one was killed but as many as 135 persons were injured. The number of buildings damaged amounted to 6290; the corresponding loss forms the major part of the total property loss. Wind damage rather than water damage was the major factor.

Damage to personnel and buildings in every administrative district is shown in Table 4. Note that most of the damage occurred on Oki-erabu, which was on the track of this typhoon. The neighboring islands, Yoron and Tokunoshima, which are situated 25 km east and 40 km west of the typhoon path, respectively, were remarkably free from damage. The high wind zone of this typhoon was confined to the eye-wall belt; these two islands were outside this zone.

In Tables 3 and 4 and also in the later sections, the following are used:

- Major damage: floor areas damaged in a building amount to more than 70% of total floor areas, or repairs amount to more than 50% of the building's current price.
- Moderate damage: 20 to 70% of total floor area damaged, or repairs amount to 20 to 50% of current price.

- Minor damage: less than 20% of total floor area damaged, or repairs amount to less than 20% of current price.

- N_{maj}: number of buildings with major damage.

- N_{mod}: number of buildings with moderate damage.

- N_{min}: number of buildings with minor damage.

- N_t: total number of households in a district

- R_{maj}: rate of the number of households in a district

  $= N_{maj}/N_t$

- R_{mod}: rate of the number of dwellings with major or moderate damage to the total number of household in a district = $(N_{maj} + N_{mod})/N_t$

- R_{min}: rate of the number of dwellings with damage to the total number of households in a district

  $= (N_{maj} + N_{mod} + N_{min})/N_t$

Distribution of Damage to Dwellings in Oki-erabu Island

Oki-erabu Island is a flat coral-island having the topography shown in Figure 7. About 40 villages consisting of a few decades or hundreds of households are loosely distributed there, mainly along the coast.

The statistics of damage to dwellings in those localities are shown in Tables 5 and 6. Damage rates R_{maj} and R_{mod} in the Tables are illustrated in Figures 7 and 8. Note that the damage rate differs remarkably from place to place; R_{maj}, for example, is 44.8% in a western locality and in another locality in the central part of the island it is only 2.0%. This is caused by topography and ground roughness, as follows:

- The higher rate of damage in the eastern part of the island appears to result from its flat farm land with little ground roughness as shown in Photo 1. It was exposed to severe wind throughout the typhoon.

- Some localities southeast of Mt. Koshiyama in the central part of the island suffered severest damage. Those localities are near the top of gentle slopes facing southeast and therefore were exposed to severe winds from ENE-SE-S during the typhoon.

- In a few localities 2 or 3 km west of the area described above, damage was very light. These localities are in a shallow valley open to southeast between Mt. Oyama and Mt. Koshiyama. They were not exposed to strong winds.

- Many localities along the coasts in China-cho suffered heavy damage. These localities are situated on flat gentle slopes of Mt. Oyama. They were exposed to high winds from the sea or parallel to the coast. It also might be that they were exposed to local high winds around conical hills, as observed by Geiger (1950).

Description of Damage to Buildings

Damage to roofs, structural frames, and exterior wall openings of wooden buildings were most frequently observed in our field survey of the island.

Damage to Roofs

Most of the dwellings in Oki-erabu were of wooden frames with corrogated galvanized iron sheet roofing. Usually those sheets are nailed to laths set on bed boards. In some cases, laths are nailed to rafters directly.

The typical feature of damage to the former style of roofs is shown in Photo 2. The latter is shown in Photo 3. In the latter case, secondary damage to ceiling and furnishings was also observed.

As shown in Photo 4 the flying sheet metal can seriously threaten nearby people and buildings.

Tile roofs were less common than sheet metal roofs. When tile roofs had bed boards under them, damage was localized to ridges or eaves; the damaged tile area was generally smaller than damaged sheet metal areas. But on tile roofs without bed boards damage was spread widely. Photos 5 and 6 show examples of damage to tile roofs.

The roof structures of some sheet metal roofs were completely demolished. This damage occurred because roof member connections such as column-beam, beam-post, post-purlin, and purlin-rafter were in most cases short-tennon connections and therefore could not resist to tensile forces generated by the suction pressure on the roof. Photos 7 to 9 show some examples of damage to roof structures.

Total Collapse

The traditional wood framing is a kind of rigid-connection framing consisting of columns and rails. Rigid connections are made by driving wedges into clearances to tennon holes (Photo 10). The efficiency of such structures is said to be uncertain when main members have rotted or the wedging has not been maintained. In recent times, the cross-sectional size of columns and rails has become smaller. It is difficult to expect such a system to have enough strength to resist severe winds. Although diagonal bracings have been installed on many such houses, many of them were inefficient, as shown in Photo 11.

Damage to Exterior Wall Openings

On many houses, strong sliding shutters were used to cover windows. These were definitely effective in protecting glazed openings from wind-generated missiles. Grills were also effective, as shown in Photo 13.

Aluminum sashes have been coming into vogue in Oki-erabu and many of the openings framed by those sashes were observed to have been broken. The absence of shutters in turn lead to broken windows, which then lead to roof loss (Photo 14).

Reinforced Concrete Buildings

Dwellings, hotels, schools, and administrative buildings were of reinforced concrete; they were less than 4 stories. Damage here was confirmed to openings shown in Photo 15. This induced secondary damage to interior furnishings. Most of this damage was caused by wind-generated missiles. Shutters or grills could have prevented this loss.

Steel Buildings

Some factories and roofs of school gymansiums were of steel. Roofings and sidings on these buildings were of slate or galvanized iron sheet. Damage is shown in Photos 16 to 20. It was caused by wind-generated missiles or insufficient strength of finishing material connections to back-up members. The insufficient strength of connections was sometimes caused by the corrosion of steel materials. Note that the damage here was very diffusive. The aim of steel-building design should thus be to prevent initial local failures in some parts of the finishing and to prevent those failures from spreading widely.

Concluding Remarks

The damage seen on Oki-erabu came from winds that are expected more than once per 20 years in that area of the Pacific. Nor were the winds of this typhoon extraordinarily strong. Nevertheless, the wooden-frame construction could not cope sufficiently with today's lighter-weight roofs. The significance of traditional preventives, such as shutters, was forgotten and modernization went on without checking its appropriateness. Since these two complaints about structures can be repeated for many communities, it is important that the lessons of Oki-erabu be remembered.

Acknowledgement

The authors wish to express their thanks to Fukuoka District Meteorological Observatory, Oki-erabu Weather Station, Construction Division of Kagoshima Prefecture, and local administration offices in Oki-erabu for their cooperation in supplying information.

References

1. Geiger, R., The Climate Near the Ground, Harvard Univ. Press, 1950.

2. Kagoshima Local Meteorological Observatory, Abnormal Weather Report About Oki-erabu Tyhpoon, 1977.

3. Okinawa Meteorological Observatory, Okinawa Bulletin, No. 64, 1977.

TABLE 1: HOURLY CHANGES OF METEOROLOGICAL ELEMENTS AT OKI-ERABU WEATHER STATION

Date	Time	Pressure (mb)	Wind dir.	Wind speed (m/s)	Precip-itation (mm)	Weather
Sept.8	03	1003.1	NNE	3.9	0.5	
	06		N E	3.8	0.5	
	09	1003.3	NNE	4.9	0.5	⊕
	12		N E	5.5	-	
	15	1001.0	ENE	5.3	-	◎
	18		NNE	5.1	-	
	21	1000.5	ENE	7.3	1.0	●
	24		E	7.6	6.0	
9	03	996.5	E	6.3	35.0	●
	06		ESE	8.2	1.5	
	09	994.1	SSE	6.6	7.0	◎
	12		ESE	8.8	0.0	
	15	998.3	N E	12.7	0.0	●
	16	986.7	N E	12.6	8.5	●
	17	983.7	ESE	13.6	3.0	●
	18	981.9	N E	19.6	11.0	●
	19	980.1	N E	18.4	5.0	●
	20	976.3	N E	21.4	4.0	●
	21	969.0	ENE	24.0	4.0	●
	22	946.6	ENE	35.6	8.0	●
	23	916.4	-	-	28.0	●
	24	964.7	-	-	53.0	●
10	01	974.8	-	-	0.5	●
	03	984.3	-	-	0.0	●
	05	988.5	-	-	0.0	●

TABLE 2: WEATHER RECORDS OF TYPHOON NO. 7709 AT OKI-ERABU WEATHER STATION

Meteorological elements	Value	Time (JST)
Min. sea-level pressure	907.3mb	2250
Max. wind	ESE 39.4m/s	2210
Max. peak gust	ENE 60.4m/s	2216
Total precipitation	177 mm	1820 (Sept.8)-0510 (Sept.10)
Max. daily precip.	168.0mm	Sept.9
Max. hourly precip.	61.0mm	2220-2320 (Sept.9)

TABLE 3: STATISTICS OF DAMAGE IN KAGOSHIMA PREFECTURE

Items	Number	Loss (1000yen)
1. Personnel damage	135	
seriously injured	15	
slightly injured	120	
2. Buildings	6 290	10 981 150
a.Residential buildings	4 640	9 688 031
major damage	1 348	5 313 930
moderate damage	1 542	2 858 352
minor damage	1 741	1 541 808
flooding over floor	2	561
flooding under floor	7	380
b.Non-residential build.	1 650	1 301 119
major damage	689	773 634
moderate damage	531	338 139
minor damage	430	189 346
3. Hospitals and clinics	5	13 288
4. Crops	15 265ha	1 260 972
5. Livestocks		1 541 911
6. Cultivations	197	374 000
7. Commerce and fisheries		3 303 080
8. Forestries		115 000
9. Public facilities	39	361 500
river banks	20	162 000
sea banks	1	20 000
roads	6	49 000
harbours	12	130 500
10. Education	64	151 034
kinder-gartens	2	14 700
elementary schools	19	24 655
middle schools	10	34 404
high schools	6	27 005
other facilities	27	50 250
11. Electric power facilities		221 567
12. Telephone and telegram facilities		400 000
Total		**18 731 511**

TABLE 4: STATISTICS OF DAMAGE TO PERSONNEL AND BUILDINGS IN ADMINISTRATIVE DISTRICTS OF KAGOSHIMA PREF.

District	No. of house-holds	Person injured	Residential building				Non-residential building							
							Public building				Non-public building			
			N_{maj}	N_{mod}	N_{min}	Total	N_{maj}	N_{mod}	N_{min}	Total	N_{maj}	N_{mod}	N_{min}	Total
Yoron Isl.	1697	2	22	84	167	273		2	4	6	36	15	25	76
Yoron	1697	2	22	84	167	273		2	4	6	36	15	25	76
Oki-erabu Isl.	5309	133	1297	1356	1455	4108	13	7	21	41	596	441	351	1388
China	2778	33	725	691	576	1992	9	4	8	21	359	270	169	798
Wadomari	2531	100	572	665	879	2116	4	3	13	20	237	171	182	590
Tokunoshima Isl.	10619		28	101	113	242		1	1	2	40	61	24	125
Tokunoshima	4748		5	33	7	45		1	1	2	4	6	3	13
Amagi	2618		11	51	50	112					20	37	21	78
Isen	3253		12	17	56	85					16	18		34
Kikaijima Isl.	3616										3	2		5
Kikai	3616										3	2		5
Amami-oshima Isl.	26830		1	1	6	8					1	2	4	7
Nase	14331				1	1					1	1	2	4
Yamato	870													
Uken	1012													
Setouchi	5274													
Sumiyow	825		1	1	5	7						1	2	3
Tatsugow	1863													
Kasari	2655													
Total	48071	135	1348	1542	1741	4631	13	10	26	49	676	521	404	1601

TABLE 5: STATISTICS OF DAMAGE TO DWELLINGS IN WADOMARI-CHO

Locality	No. of house-holds	Popula-tion	N_{maj}	N_{mod}	N_{min}	R_{maj} (%)	R_{mod} (%)	R_{min} (%)
1. Wadomari	540	1666	110	101	150	20.4	39.1	66.9
2. Wa	116	414	17	30	40	14.7	40.5	75.0
3. Tedechina	253	810	31	64	113	12.3	37.5	82.2
4. Kamitedechina	61	219	13	12	21	21.3	41.0	75.4
5. Kibiru	156	504	57	60	59	36.5	75.0	112.8
6. Kunigami	354	1461	124	109	117	35.0	65.8	98.9
7. Nishibaru	87	348	39	20	17	44.8	67.8	87.4
8. Degi	101	327	32	15	23	31.7	46.5	69.3
9. Inobe	31	107	9	7	8	29.0	51.6	77.4
10. Azefu	105	377	22	16	75	21.0	36.2	107.6
11. Neori	69	289	4	19	21	5.8	33.3	63.8
12. Tamashiro	180	589	25	115	45	13.9	77.8	102.8
13. Oshiro	69	232	22	20	11	31.9	60.9	76.8
14. Minagawa	50	132	9	16	28	18.0	50.0	106.0
15. Furusato	65	188	14	7	33	21.5	32.3	83.1
16. Uchijiro	45	152	9	10	10	20.0	42.2	64.4
17. Kamiuchijiro	45	118	6	9	31	12.9	33.3	102.2
18. Goran	35	124	3	6	17	8.6	25.7	74.3
19. Taniyama	26	89	4	0	22	15.4	15.4	100.0
20. Nishi	25	94	3	11	7	12.0	56.0	84.0
21. Nagamine	54	175	9	8	17	16.7	31.5	63.0
22. Sena	64	200	10	10	14	15.6	31.3	53.1
Total	2531	8615	572	665	879	22.6	48.9	86.3

TABLE 6: STATISTICS OF DAMAGE TO DWELLINGS IN CHINA-CHO

Locality	No. of house-holds	Popula-tion	N_{maj}	N_{mod}	N_{min}	R_{maj} (%)	R_{mod} (%)	R_{min} (%)
1. China	358	1075	68	78	40	19.0	40.8	52.0
2. Yakomo	141	450	55	29	21	39.0	59.6	74.5
3. Otsuge	35	87	7	1	12	20.0	22.9	57.1
4. Tokutoki	59	201	17	8	4	28.8	42.4	49.2
5. Sumiyoshi	187	589	48	40	71	25.7	47.1	85.0
6. Masana	124	486	25	48	38	20.2	58.9	89.5
7. Tamina	333	1014	112	132	78	33.6	73.3	96.7
8. Shimoshiro	29	96	5	16	8	17.2	72.4	100.0
9. Kamishiro	58	178	21	6	20	36.2	46.6	81.0
10. Shinjo	77	254	23	23	35	29.9	59.7	105.2
11. Gushiken	43	143	4	1	16	9.3	11.6	48.8
12. Akamine	51	135	1	4	21	2.0	9.8	51.0
13. Saozu	57	173	5	2	19	8.8	12.3	45.6
14. Amata	98	264	15	22	9	15.3	37.8	46.9
15. Kamihirakawa	210	568	42	40	24	20.0	39.0	50.5
16. Shimohirakawa	63	184	14	6	11	22.2	31.7	49.2
17. Yaja	39	125	15	6	15	38.5	53.8	92.3
18. Ashikyora	148	448	29	64	21	19.6	62.8	77.0
19. Kuronuki	82	215	26	11	32	31.7	45.1	84.1
20. Serikaku	278	807	107	89	20	38.5	70.5	77.7
21. Kogome	231	766	86	64	61	37.2	64.9	91.3
22. Oyama	77	77	-	-	-	-	-	-
Total	2778	8335	725	691	576	26.1	51.0	71.7

FIGURE 1: TRACK OF TYPHOON NO. 7709

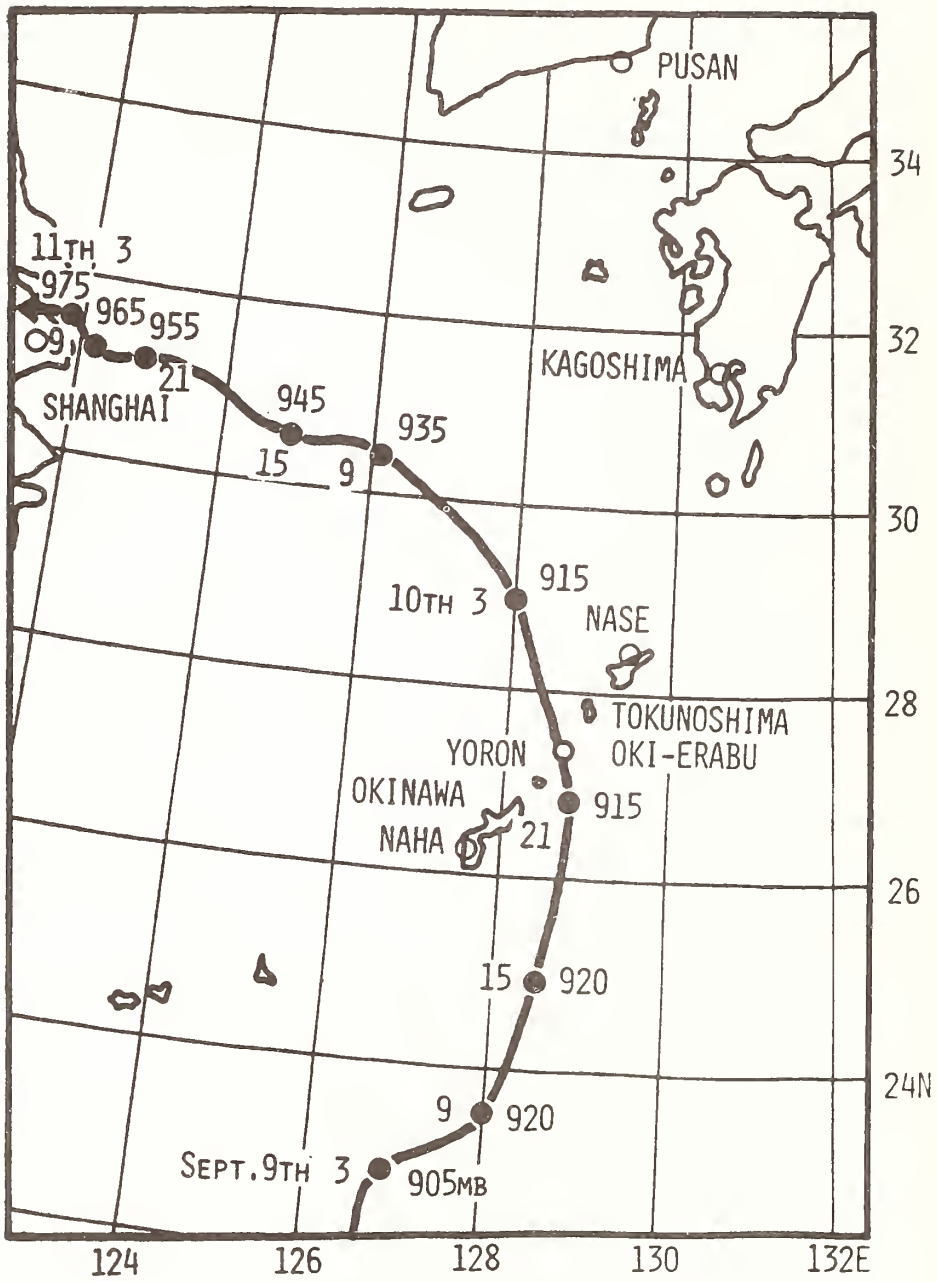

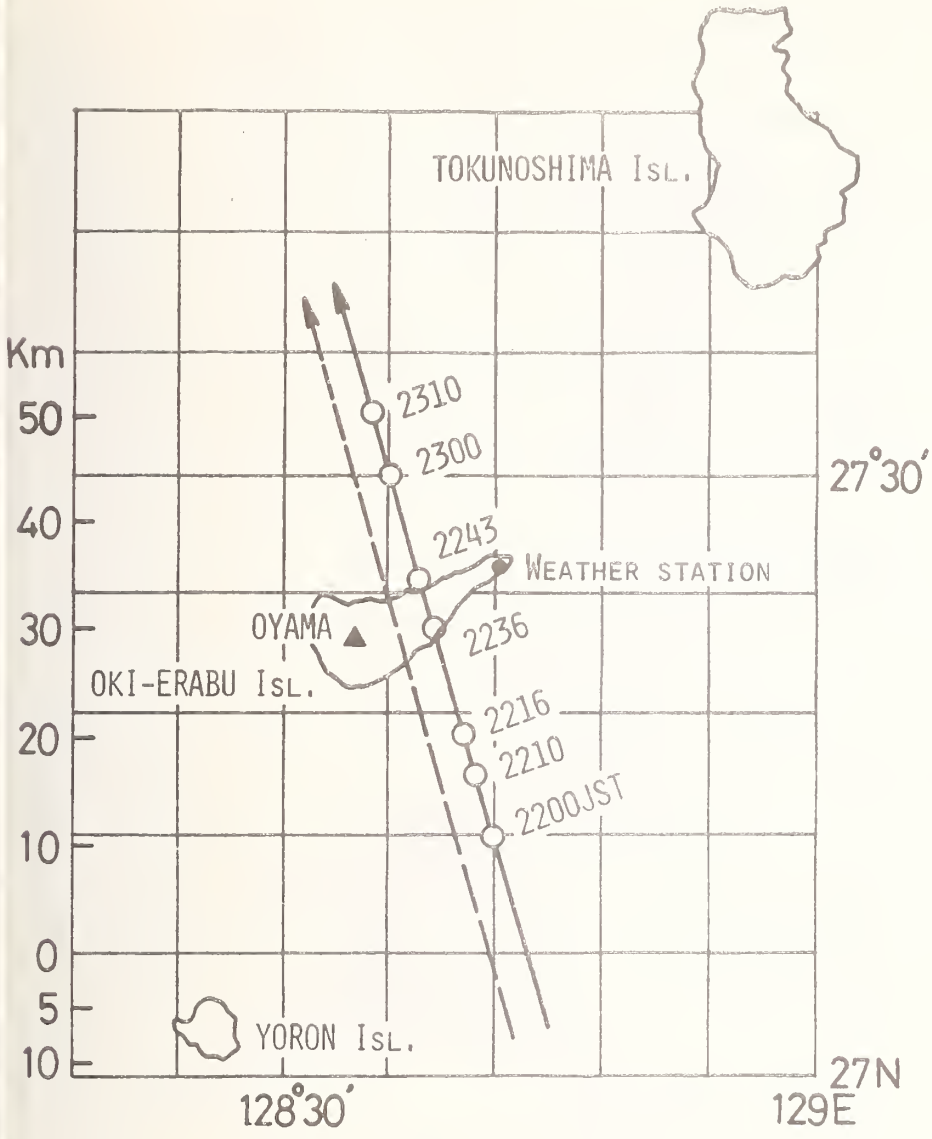

FIGURE 2: DETAILED TRACK OF TYPHOON NO. 7709 NEAR OKI-ERABU ISL. SOLID LINE IS THE TRACK DETERMINED BY RADAR OBSERVATIONS AND DOTTED LINE IS THAT DETERMINED BY WEATHER OBSERVATIONS.

3

FIGURE 3: BAROGRAM AT OKI-ERABU WEATHER STATION

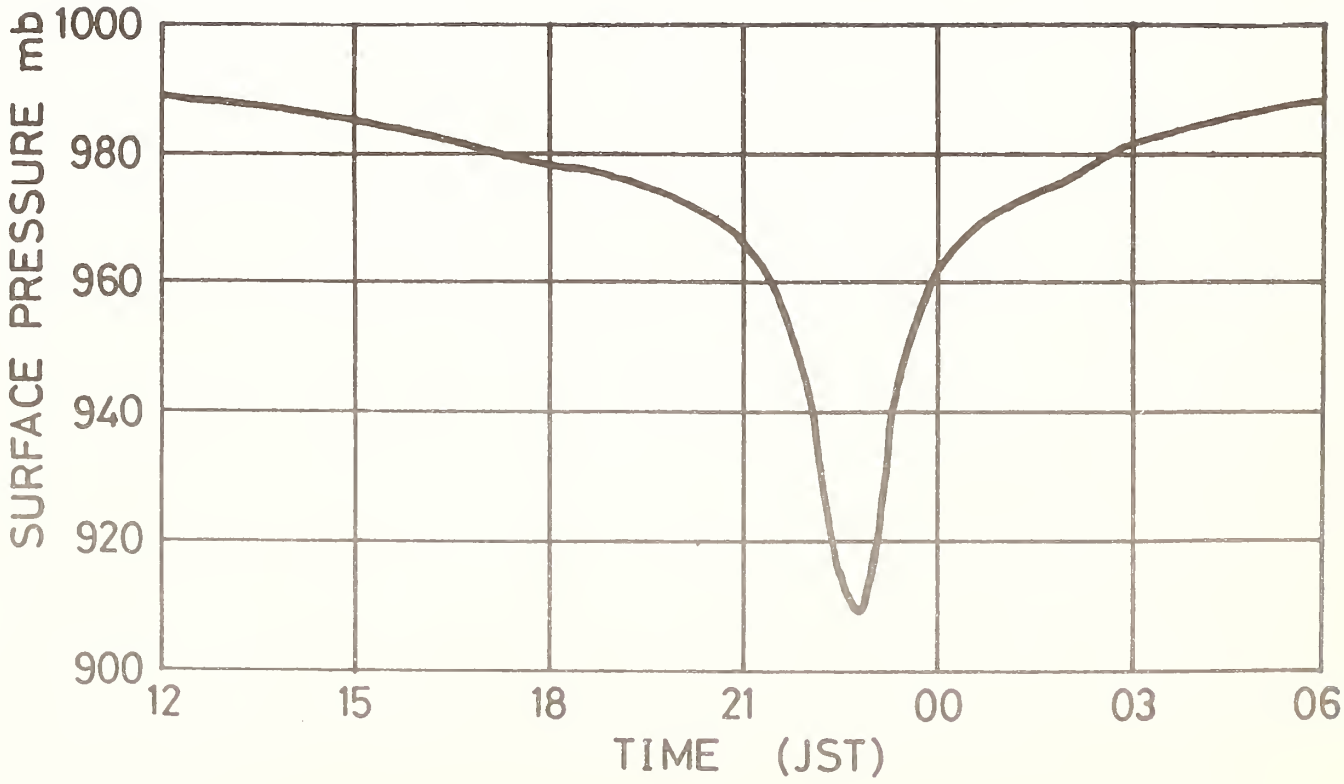

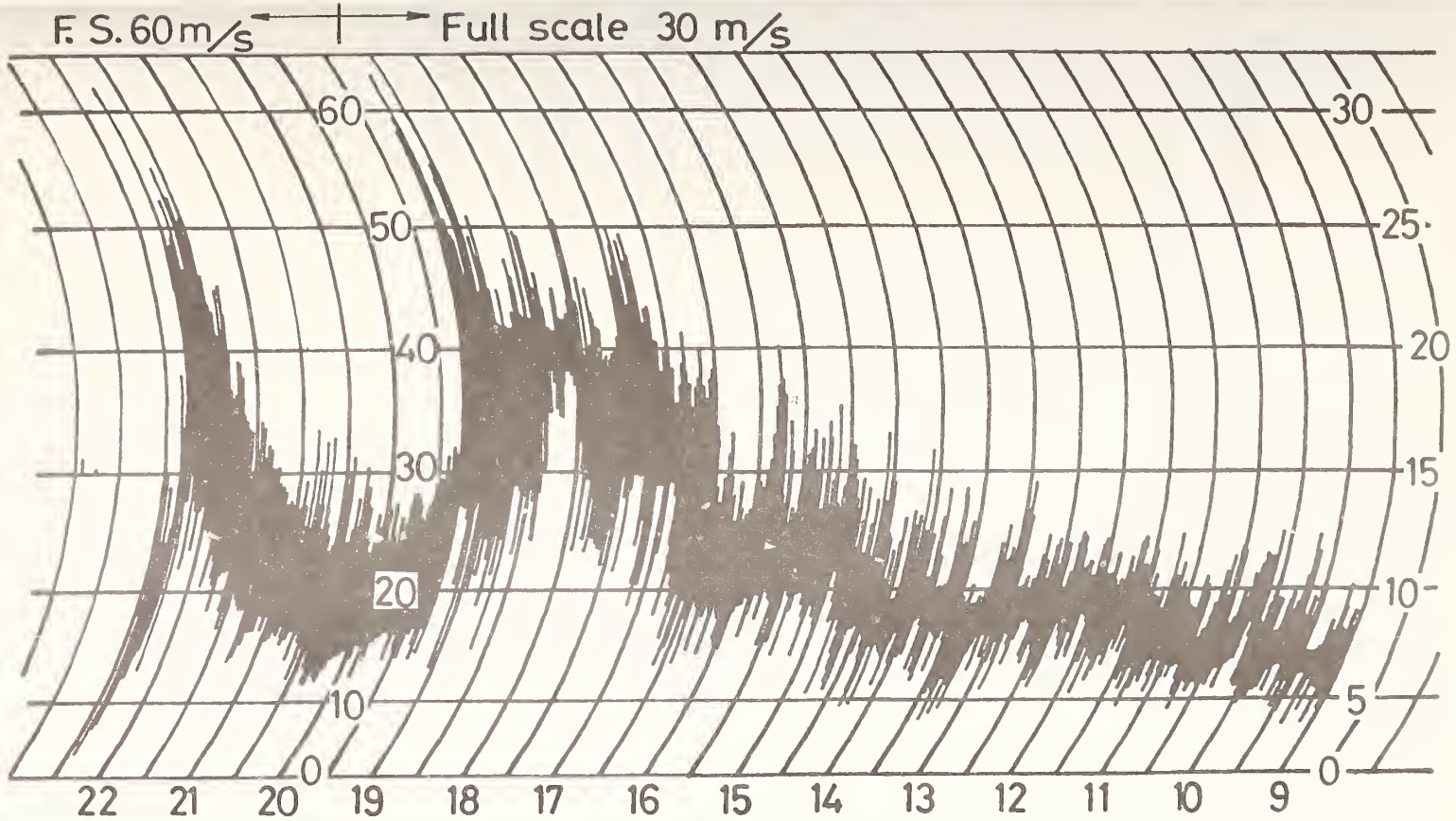

FIGURE 4: ANEMOGRAM (WIND SPEED) AT OKI-ERABU WEATHER STATION

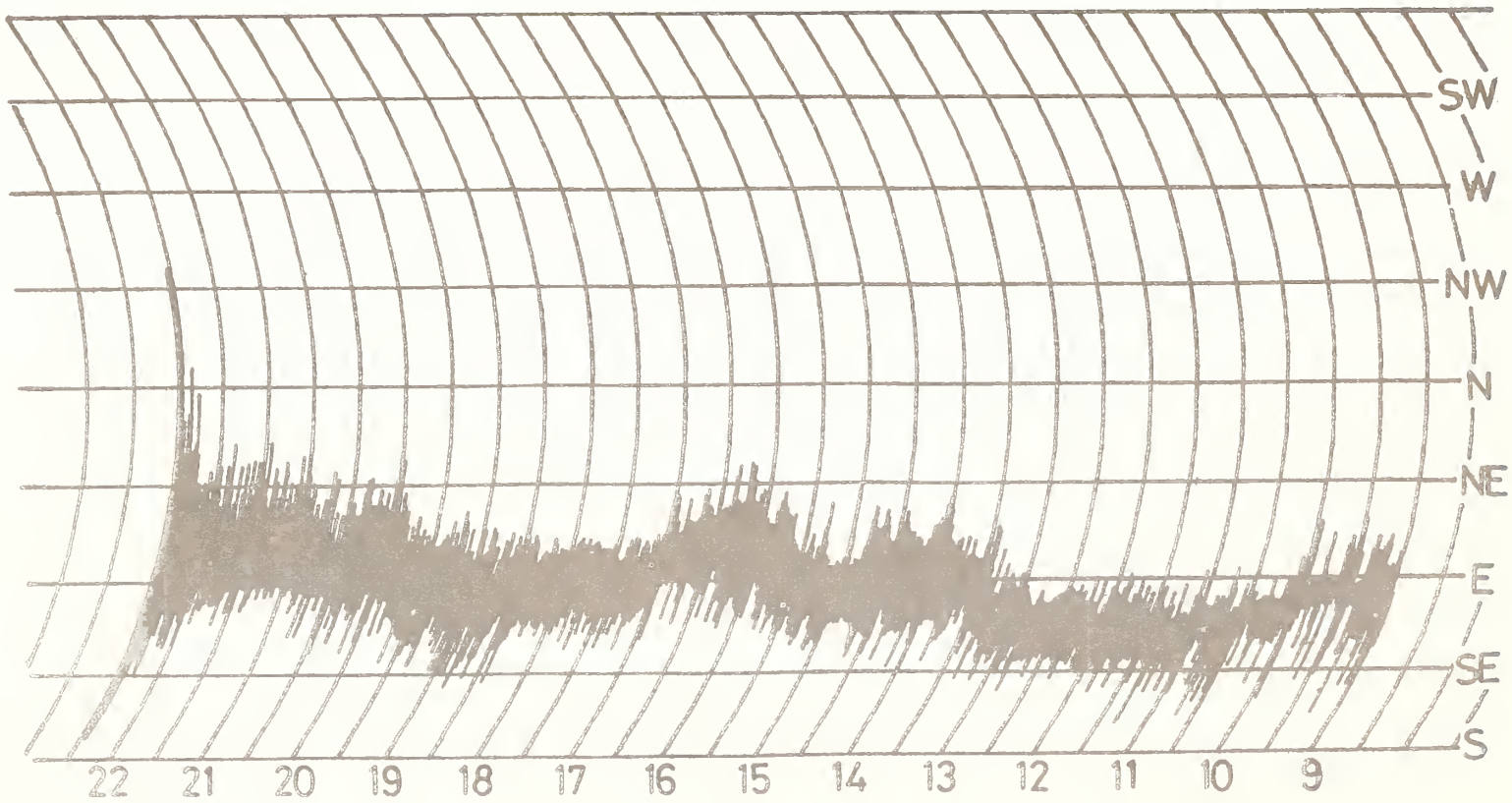

FIGURE 5: ANEMOGRAM (WIND DIRECTION) AT OKI-ERABU WEATHER STATION

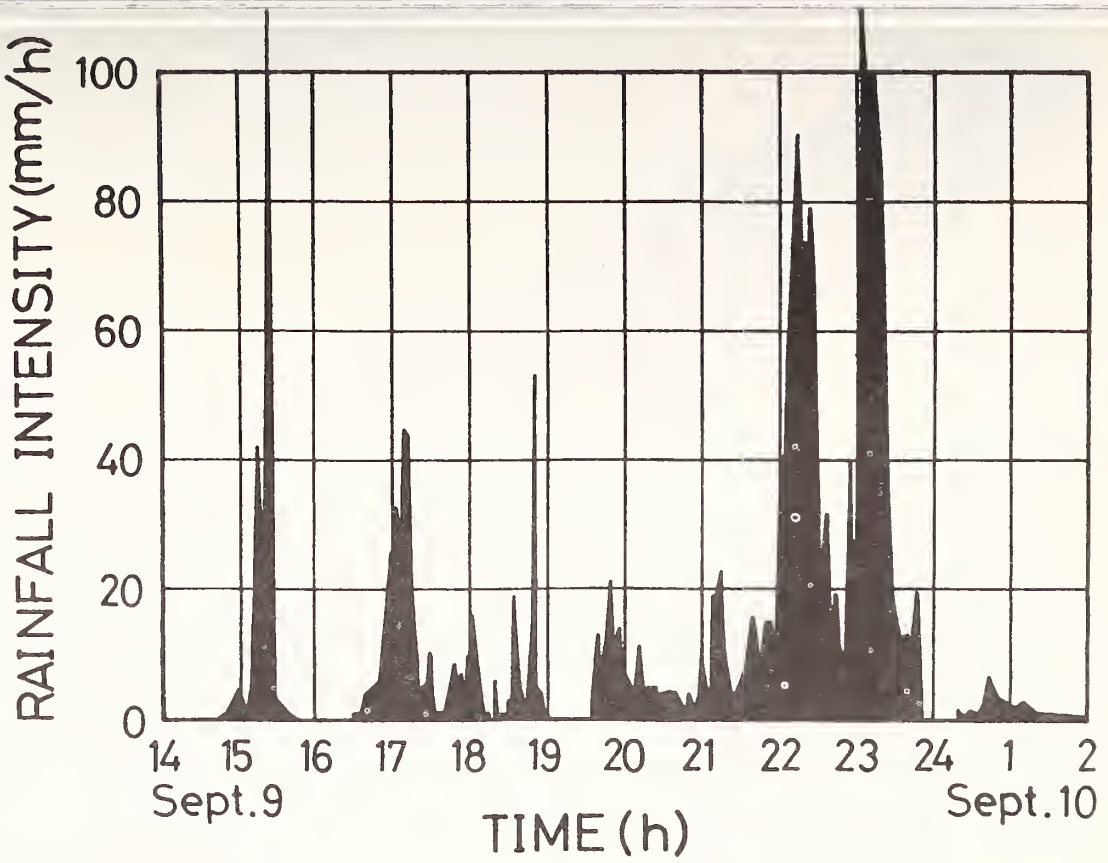

FIGURE 6: TIME CHANGES OF RAINFALL INTENSITY AT OKI-ERABU WEATHER STATION

FIGURE 7: TOPOGRAPHY OF OKI-ERABU ISLAND

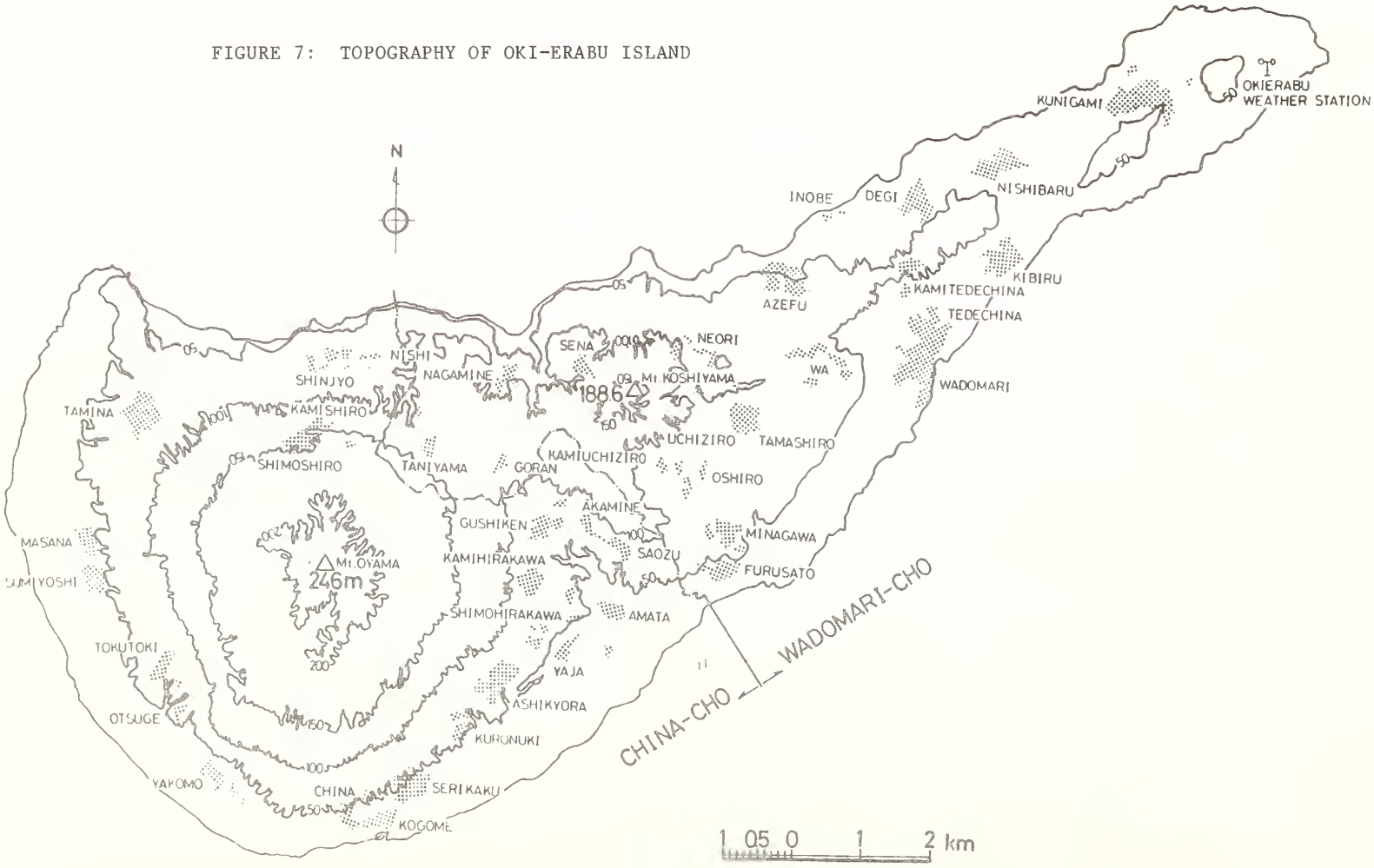

FIGURE 8: DISTRIBUTION OF DWELLING DAMAGE IN OKI-ERABU ISL.
(R_{MAJ} DISTRIBUTION)

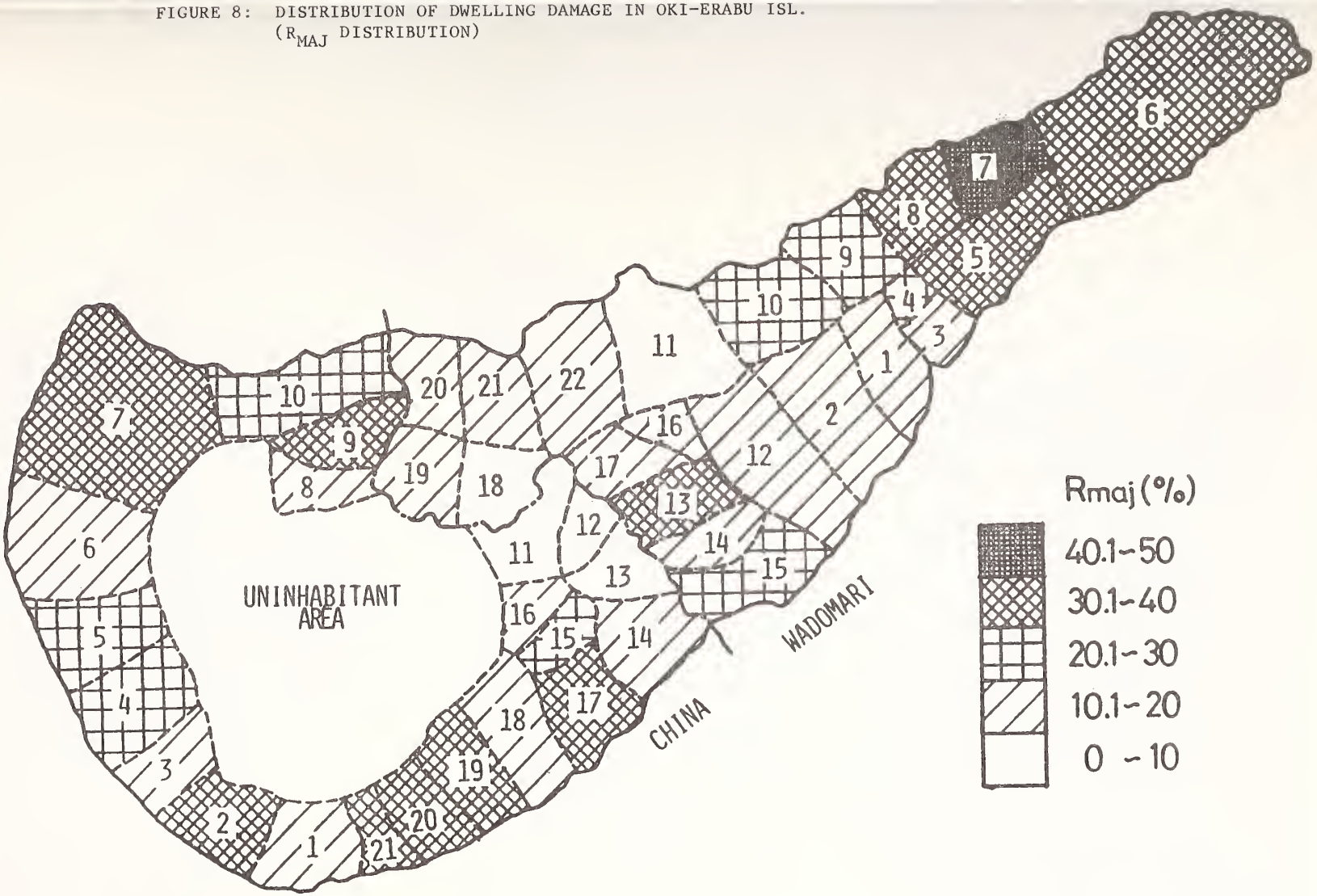

FIGURE 9: DISTRIBUTION OF DWELLING DAMAGE IN OKI-ERABU ISL.
(R_{MOD} DISTRIBUTION)

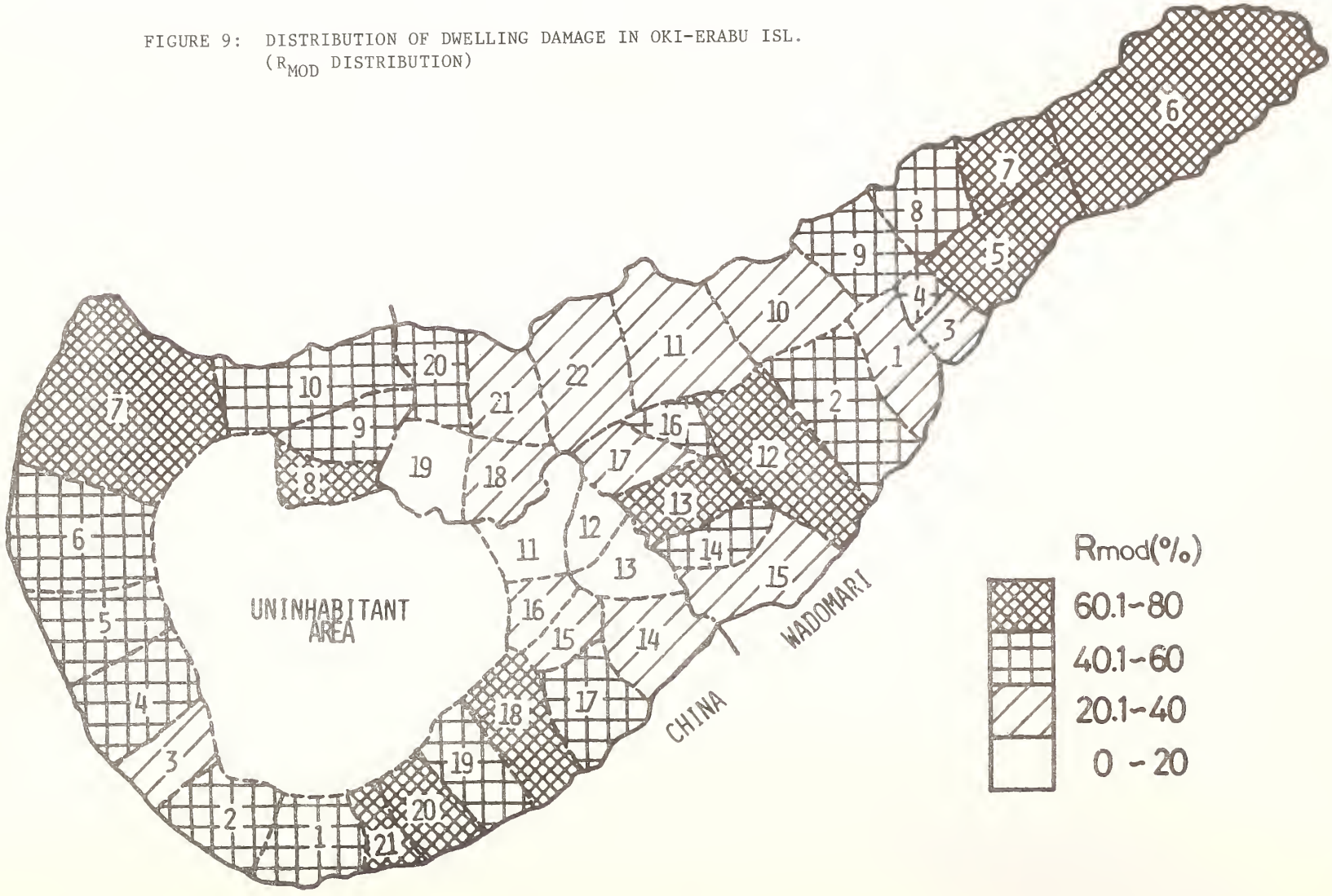

PHOTO 1: LANDSCAPE OF THE EAST PART OF OKI-ERABU ISL.

PHOTO 2: DAMAGE TO SHEET METAL ROOFING WITH BED BOARDS

PHOTO 3: DAMAGE TO SHEET METAL ROOFING WITHOUT BED BOARDS

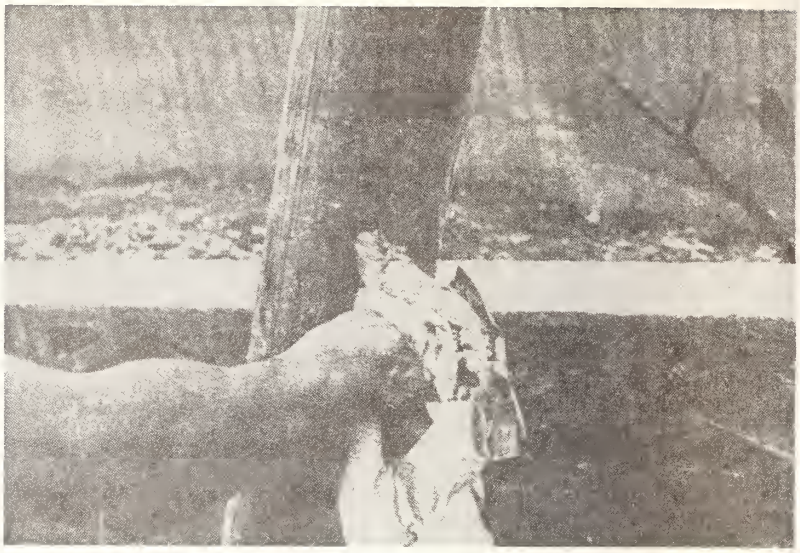

PHOTO 4: SHEET METAL STUCK IN A POLE

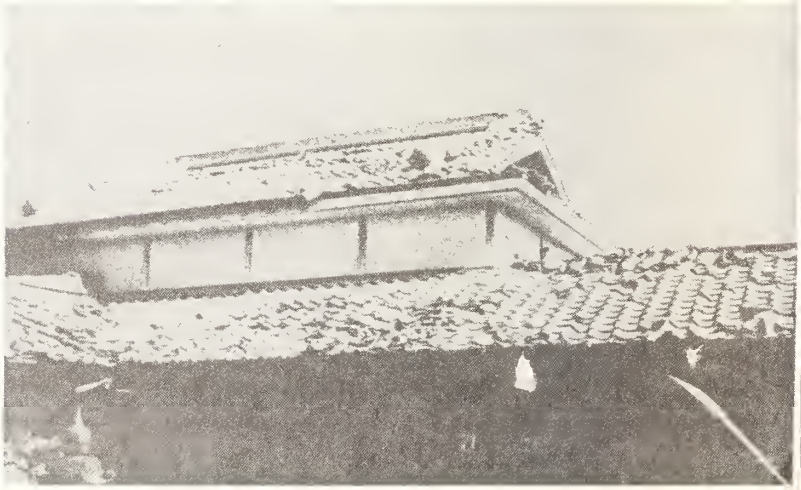

PHOTO 5: DAMAGE TO TILE-ROOFING WITH BED BOARDS

PHOTO 6: DAMAGE TO TILE-ROOFING WITHOUT BED BOARDS

3

PHOTO 7: GABLE ROOF, HALF OF WHICH WAS BLOWN AWAY

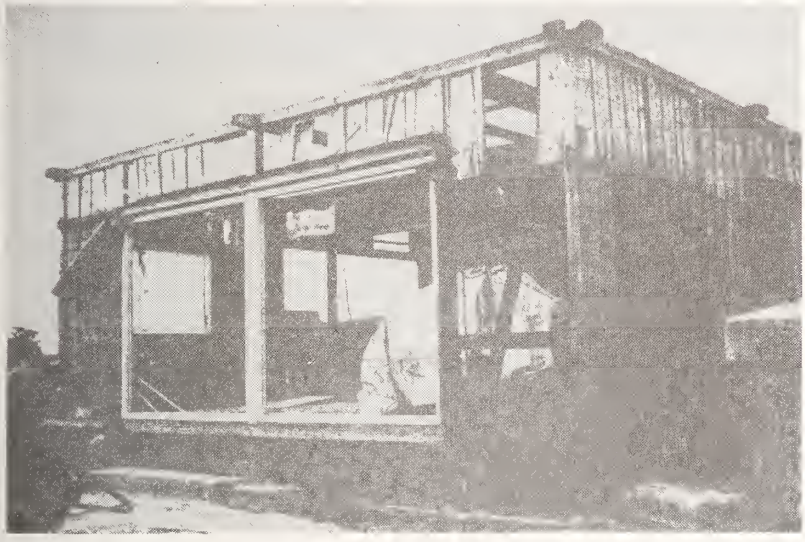

PHOTO 8: DWELLING WHOSE ROOF WAS BLOWN AWAY LEAVING GIRDERS

PHOTO 9: POST OFFICE WHOSE ROOF WAS BLOWN AWAY

PHOTO 10: WEDGE AT COLUMN-RAIL CONNECTION

PHOTO 11: INEFFICIENT DIAGONAL BRACING

PHOTO 12: TOTAL COLLAPSE OF WOODEN DWELLINGS

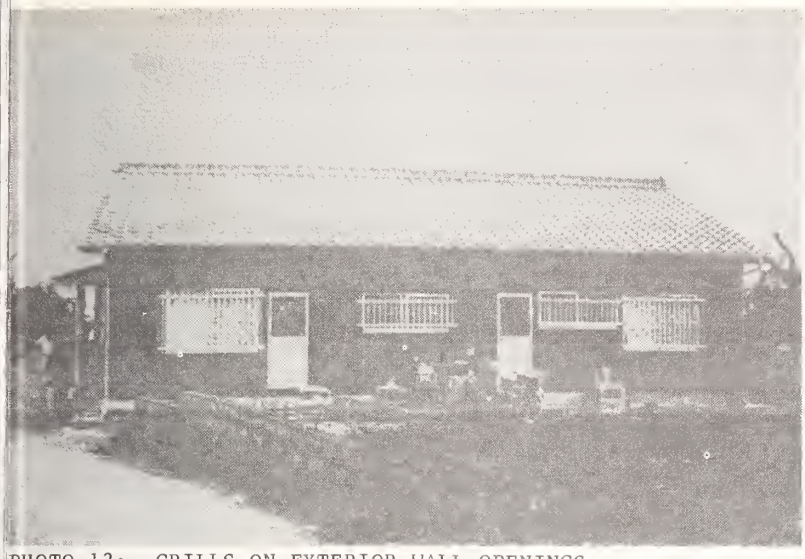

PHOTO 13: GRILLS ON EXTERIOR WALL OPENINGS

PHOTO 14: ROOF DAMAGE INDUCED BY THE BREAK OF EXTERIOR WALL OPENINGS (IN FRONT)

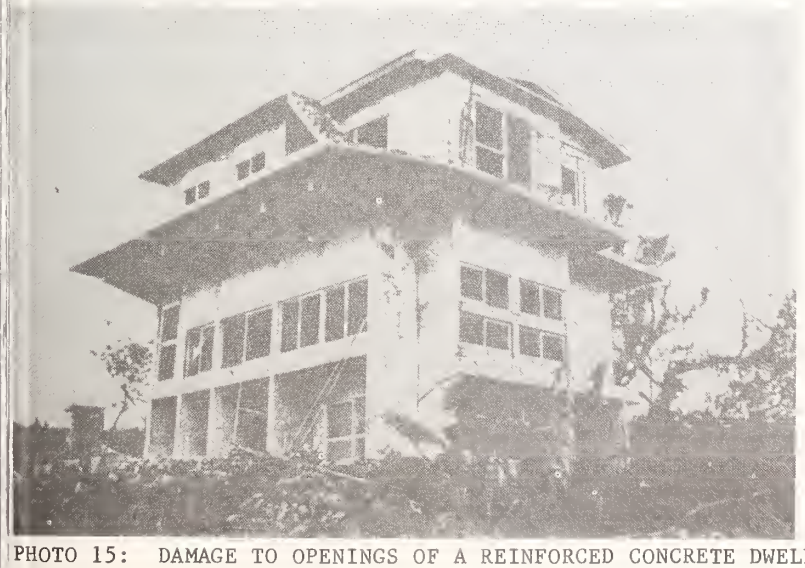

PHOTO 15: DAMAGE TO OPENINGS OF A REINFORCED CONCRETE DWELLING

3

PHOTO 16: DAMAGE TO SHEET METAL SIDING OF A STEEL FRAME FACTORY

PHOTO 17: DAMAGE TO SLATE SIDING OF A STEEL FRAME FACTORY

PHOTO 18: DAMAGE TO SLATE ROOFING OF A STEEL FRAME FACTORY

PHOTO 19: DAMAGE TO SHEET METAL ROOFING OF A GYMNASIUM

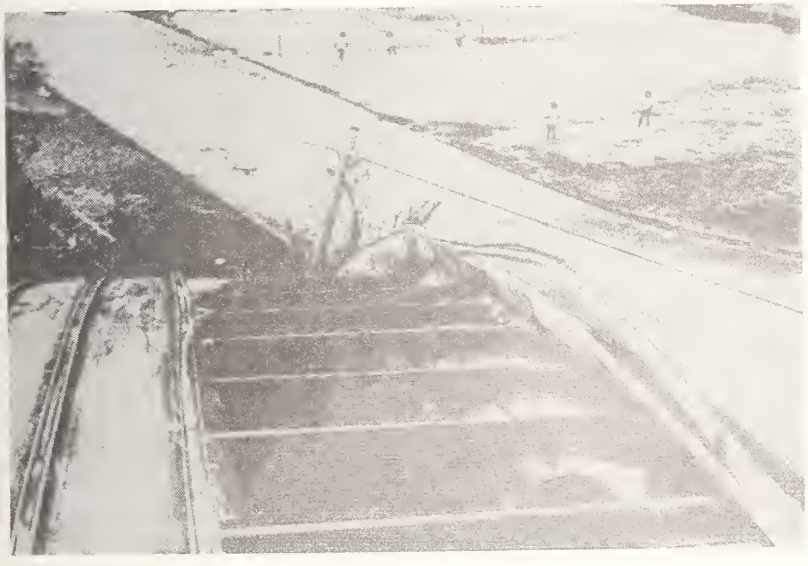

PHOTO 20: CLOSE UP OF GYMNASIUM DAMAGE

4

RECENT DEVELOPMENTS IN ATMOSPHERIC REMOTE SENSING AND THEIR IMPLICATION FOR WIND ENGINEERING

William H. Hooke

Atmospheric Studies Program Area
Wave Propagation Laboratory
Boulder, Colorado

NOTE: FIGURES NOT AVAILABLE FOR THIS PAPER

Recent Developments in Atmospheric Remote Sensing and Their Implications for Wind Engineering

This paper reviews recent progress in developing a most promising source of meteorological observations -- remote-sensing systems that measure the effect of the atmosphere on optical, radio, and acoustic waves. We begin by highlighting several major needs within the wind-engineering community, and then discuss the relative advantages and disadvantages of remote sensing and in-situ approaches to meeting these needs. We find that in general remote-sensing methods offer enormous advantages in area and volume coverage, spatial and temporal resolution, representativeness, technological feasibility, and cost. We then summarize the substantial impact of atmospheric remote-sensing on wind engineering, by identifying and isolating several specific areas of present application, examining each in detail. These areas of application include the development of devices for the study of high winds associated with severe storms, the detection of low-level wind shear at airports, and the transport and diffusion of pollutants. Remote sensors are giving us our first real look at the circulation of air within thunderstorms and hurricanes, even on scales as small as the tornado vortex. Arrays of pressure sensors, lidar, and even modified air-traffic-control radars can provide much information on low-level wind shear in the vicinity of airports. And lidars are now able to track pollution plumes, determine the velocity of the air within the plumes, examine even their chemical composition. Then we look at possible future applications of remote-sensors to wind-engineering problems. These applications include the quantitative study of plume diffusion over irregular terrain and urban areas, the use of remote sensors in wind power-park siting, and the use of lidar to study the influence of high-rise structures on urban airflow. An appendix contains a review of existing remote-sensing capabilities and developments.

Remote-Sensing and In-Situ Approaches to Meeting Wind Engineering Data Requirements

There are many ways we could classify the data requirements of the wind-engineering community. However, for present purposes we shall satisfy overselves by considering wind-engineering data requirements in four categories:

- structural design
- transportation
- pollutant transport and diffusion
- wind power

Structural design is a major concern. In the United States alone, wind damage to buildings and structures amounts to a billion dollars per year; much of this could be prevented were more detailed wind climatologies available to foster improved design practice. Particularly vulnerable are structures whose design extends preexisting technology -- high-rise skyscrapers with glass clading, long cable-stayed bridges, domed and open sports stadia, and high towers. Also economically important because of their large numbers are smaller buildings, such as residential structures, particularly those in high-risk areas (for example, tornado belts and the southern Atlantic and Gulf coastal zones). In addition to problems posed by the need to design structurally sound buildings that won't collapse or be destroyed by high winds, there is also the need to design functionally adequate structures, in which the elevators will continue to operate in high winds, which won't oscillate or sway excessively, and which do not create unacceptably

high street-level winds or snow-drifting in their immediate vicinity. On the other side of the coin, the risks inherent with strong winds lead to over-design of structures such as nuclear power plants, which in some areas must be constructed to withstand a tornado. Because tornado maximum winds and gusts remain ill-defined, reactor design must continue to be correspondingly conservative. This over-design of such expensive structures represents a substantial incremental cost.

Proper structural design requires accurate, reliable data, for long periods of time, on boundary-layer winds. Near-surface winds are relatively well documented, but there is a pressing need for wind and turbulence statistics at heights of 100-1000 m. There is particular interest in data from extreme-wind conditions associated with hurricanes, tornadoes, severe convective storms, downslope winds, and low-level jets. Finally, measurement of these quantities in urban high-rise areas is particularly desirable.

Surface and airborne transportation are quite vulnerable to high winds. For example, the foothills of the Rocky Mountains frequently experience severe downslope winds able to overturn trucks and campers, making it necessary to close the roads to such traffic. Far more serious and widespread, however, is the threat posed to aircraft takeoffs and landings by low-level wind shear. Curiously enough, this hazard can be greater for the most modern jetliners than it is for the smaller, ligther aircraft of general aviation. This is because the latter can respond quickly to changes in air-speed, while the larger aircraft require more time. In some respects, a jetliner landing may more properly be referred to as nearly a controlled crash, with the pilot anticipating future conditions along the glide path at every point in his descent, changing control settings some tens of seconds before those changes are to be in effect. This procedure works satisfactorily when the meteorological conditions prevailing over the airplane glide path are homogeneous and stationary. It is hazardous, however, in the highly-variable and inhomogeneous thunderstorm environment, where gust fronts and thunderstorms downbursts of quite limited extent are difficult to detect. Here the need is for operational systems able to monitor such dangerous phenomena and provide timely warnings to the pilots.

Shipping and boating are also vulnerable to winds, both directly and indirectly, through wind effects on sea state. The trend towards larger and larger ships, while in some respects minimizing such risks through the incorporation of improved design, in other respects enhances the risk, through increases in the size of cargo spills, for instance. Here the need is for accurate information on sea state -- its present state and forecasts for the future, often for periods as long as several days.

Pollutant transport and diffusion pose a whole new set of engineering needs and data requirements. However, here the need is greatest for information pertaining to low-wind conditions, when pollutants do not disperse rapidly but instead build up to dangerous concentrations, and when the effects on the airflow of terrian and buildings, are most pronounced. There is a need for more measurements of winds and turbulence at heights above 100 m, and for more observations of the diffusion of pollutants on a regional scale, particularly in urbanized areas.

Finally, the nation's energy crisis has made wind power a subject of considerable concern. Engineering interest in efficiency must be reconciled with a need for ruggedness, or for an ability to

forecast weather events and to protect a threatened wind generating system (through feathering of propeller blades, for instance). To provide an optimal reconciliation requires more information pertinent to wind siting, including extensive wind and turbulence climatologies for a large number of promising sites. In these cases also, data to substantial heights are needed, in order to accommodate design of the large systems contemplated for operational use.

Underlying all these needs are certain common threads. First, we desire data over extensive regions. To understand the ultimate fate of pollutants in the urban environment or to monitor weather conditions along an entire jetliner glide slope into an airport requires this extensive coverage. Note that we require the information not merely over certain substantial areas, but also over large volumes. For example, since wind speeds increase with height in the boundary layer, the effects of winds on buildings are greatest near the tops of the buildings. Similarly, it is hard to predict pollutant transport and diffusion without knowing the boundary-layer depth ($\sim$1000 m). The critical portion of the aircraft glide slope is between heights of 100 m and 1000 m. Second, within this volume of coverage we are interested in both representativeness and resolution. That is to say, on the one hand we are interested in knowing that our estimates of a certain parameter, e.g., wind speed, or maximum turbulent gust intensity, are representatives or characteristic of the area as a whole, while on the other we need fine spatial and temporal resolution, in order to carry out such tasks as monitoring tornadoes and estimating tornadic winds, or to define the effects of individual buildings and terrain features on pollutant transport and deposition. Third, for engineering purposes we generally require (or at least prefer) site-specific information. It does little good, for example, to estimate the prospects for wind power from the Pali lookout on Oahu by using data from Erie, Colorado. Fourth, and finally, we must often take the measurements without interfering with the medium. A most obvious example concerns airport operations. To place instrumented tall towers in the glide path is no solution.

With these preliminaries, we are now ready to contrast the two basic approaches to measuring wind -- in-situ instrumentation and remote sensors. As its name implies, the former method involves sampling of the medium in the immediate vicinity of the instrument, using some direct effect of the variable in question in order to measure it (for example, the rate at which an airflow turns the cups of an anemometer immersed in it, or the cooling effect of airflow past a hot wire). On the other hand, remote-sensing techniques use the interaction of radio, optical, and acoustic waves with the medium through which they propagate. This interaction depends upon the properties of the medium in a well-defined way. Thus, for example, sound waves propagate through air at a speed that is determined by the local temperature and the local wind velocity. Likewise the Doppler shift introduced into a radio wave by scattering from atmospheric turbulence is proportional to the velocity of the turbulent eddies relative to the radio source. Absorption of an optical wave propagating through a mixture of gases depends upon the composition of the mixture and its density as well as the frequency or color of the incident light.

Passive remote sensors use observed properties of existing radiation of natural origin to draw inferences concerning the medium. For instance, microwave radiometry uses the spectrum of microwave emissions from the clear sky to determine temperature and humidity. Although they are attractive for military purposes, where detection of the sensor itself is a concern, passive sensors

are generally much less desirable than active sensors, which supply their own wave radiation. This added variable gives active sensors the edge in flexibility, improved spatial resolution, and scanning capability.

In general (though not always), because they are typically more complex, remote-sensing systems cost more to make the first measurement than do their in-situ counterpart. However, they offer the major intrinsic advantage that they do not perturb the medium being measured (provided, in the case of the active remote sensors, that we neglect the slight heating of the medium necessarily from any absorption of the probing wave). By contrast, in-situ instruments such as cup anemometers or thermistors necessarily interfere with the flows of interest, and the platforms on which they must be mounted (e.g., towers or aircraft) introduce still more significant obstacles to the flow. Moveover, where remote-sensing equipment really excels is in the cost of incremental measurements, because most such equipment offers a scanning capability which permits rapid sequential interrogation of many measurement cells within large volumes. Thus the cost of remote sensors should be compared more appropriately to the cost of in-situ sensor arrays in aggregate.

Let us now look at the particular advantage of improved spatial and temporal resolution and areal coverage which remote-sensing systems offer, using dual-Doppler radar data on boundary layer winds by way of illustration. Figure 1 shows dual-Doppler radar data on the wind field at a height of 300 m above St. Louis on a summer afternoon during the 1975 METROMEX experiment. The data were taken using chaff dispersed from a light airplane; Doppler shift of the radar echoes yields the wind. The mean wind field has been removed from the data in order to reveal the small-scale structure. Lines of convergence and divergence are evident from the figure, and appear to be associated with an elongated heat island extending from Granite City across the St. Louis central business district (Kropfi and Kohn, 1977, 1978). Although the data are of considerable meteorological interest, we show them here simply to indicate the ability of dual-Doppler radar to provide data with appreciably better than 1-km resolution over an area greater than 100 km^2. An individual anemometer with telemetry and recording system would cost perhaps $1 K if installed on the surface, much less than the $500 K cost of the dual-Dopler radar system. But the array of some 300 anemometers required to reproduce the pattern revealed here would cost $300 K, a figure beginning to approach that of the radars. And if we were to take full advantage of the radar resolution (the equivalent of 10^3 anemometers) the cost of the corresponding anemometer array would be double that of the radars. But the comparison does not end here. The anemometer system described above could give only surface data, whereas the radar data were taken at a height of 300 m. In fact, the radar system provides complete altitude information, up to the top of the boundary layer, as shown in Figure 2, which shows the vertical circulations associated with the horizontal airflow pattern of Figure 1. To provide this information would require four times as many anemometers. And this ignores the major cost -- that of the towers on which the anemometry would have to be mounted. Figuring a cost of $\$10^6$/tower for 300 1000-m towers (an extremely conservative figure) we find a total system cost for the anemometry of $\$300 \times 10^6$, some 600 times the cost of the radar system (a system that doesn't interfere with the airflow or blight the landscape, and which is transportable as well). Note moreover that the radars quite naturally provide data throughout the depth of the mixed layer, because chaff will dispere throughout this volume no matter how deep it happens to be (up to

several km in extreme cases). By contrast, the technology does not exist for constructing towers meeting this more stringent height requirement.

Remote sensors also offer much improved temporal resolution. We might imagine, for example, that rather than put up 300 tall towers, we could deploy 300 radiosondes, which would each provide a single wind profile for the 70-min period shown in Figures 1 and 2. But the cost of radiosonde expendables is some $100/profile, so that the increment cost of one data set represented by Figures 1 and 2 would be $30 K. The incremental cost of the dual-Doppler radar data is orders of magnitude less than this value. Moreover, the data shown represent averages of seventeen such data sets, and to reproduce this by radiosondes would have cost some $500 K. Besides, to acquire a single radiosonde profile through the atmosphere can take up to hour. Both these factors preclude more frequent measurements that would give us a better look at small-scale and short-lived changes in atmospheric conditions on pollutant transport and diffusion, wind gustiness, etc. By contrast, in the dual-Doppler example given above, the entire velocity field can be mapped out every few minutes. The result is a tremendous improvement in the picture available of the time history of such events.

Finally, the deployment of in-situ instruments in necessarily sparse arrays gives rise to questions concerning the extent to which the reported observations accurately reflect conditions over the whole of the area being monitored by each instrument. Instrument siting remains something of a black art, whose precise influence on experimental results is poorly understood. Remote sensors alleviate these difficulties in two ways. First, sensors such as the dual-Doppler radars provide many data points over a large area; in some cases this permits evaluation of the representativeness of various sites. Second, remote-sensing data necessarily represent a line, area, or volume average. In the case of the dual-Doppler radars, for example, each wind vector shown in figures is the spatial average over a second volume some 300 m on a side. Thus the remote sensor acts as a low-pass spatial filter on the data, smoothing out smaller-scale fluctuations, some of which reflect siting problems.

All this might seem to belabour an obvious point. But we are trying to emphasize the fact that remote sensors are not merely making a 10%-20% improvement in our observational capabilities. Rather they make a quantitative difference amounting to orders of magnitude, and they so greatly extend our capability that they imply qualitative changes in our insights into atmospheric behavior and our ways of approaching engineering design. The result is that remote sensors are the instruments of choice, where available, for field experiments, because they provide a look at small-scale, short-lived phenomena, over wide areas, with high reliability.

Remote Sensors Applied to Storm Research

Dual-Doppler radars have also been used to study the circulation in severe convective storms. Such work is easier in the sense that nature supplies the tracer producing the radar echoes; no aircraft dispersal of chaff is required. Figure 3 shows an early result of such a study -- a vertical plane cut through the convective storm. The data reveal a number of the storm circulation features, including the major updrafts and downdrafts, the surface cold-air outflow and gust front preceding the rainshaft itself, and the airflow producing the thunderstorm anvil. A current model of thunderstorm

circulations is included for comparison. Although the present data show only the gross features of the thunderstorm, it should be possible to improve the radar performance to the point where we can examine cloud microstructure and short-lived aspects of cloud dynamics. Radar studies of this type have been a major part of the National Hail Research Experiment (NHRE), which has focused on the dynamics and behavior of hail-producing severe convective storms. Multiple-Doppler radars have also been used at NOAA's National Severe Storms Laboratory (NSSL) to observe and study tornadic storms. In addition to carrying out basic research, NSSL has developed single-radar Doppler approaches to the detection of tornadic meso-cyclones within severe storms, regions that are associated to very high probability with tornado development and maintenance (Lemon et al., 1977; Brown et al., 1978). Figure 4 shows a typical tornado vortex signature (TVS). Although at these ranges of the resolution of the radar is less than that necessary for isolation of the tornado itself, TVS is proving to be a reliable indicator of tornadic activity. NOAA is now considering making such Doppler information operationally available in storm-prone areas.

The Wave Propagation Laboratory (WPL) of NOAA has also developed a frequency-modulated continuous-wave (FM/CW) infrared (IR) Doppler lidar which has been used to measure vortex velocities in dust devils and waterspouts (e.g., Schwiesow and Cupp, 1976; Schwiesow et al., 1977), using truck and light-aircraft platforms. On a stronger aircraft, the instrumentation would be suitable for making profiles of tornadic-vortex velocity. Such data would be of considerable value to those responsible for designing structures (e.g., nuclear reactors, schools) to withstand torando hits. Figure 5 shows a schematic of the approach used to estimate waterspout velocities; Figure 6 shows some of the resulting data.

On a much larger scale, NOAA's highly sophisticated P-3 storm research aircraft uses three radars (nose, belly, and tail) to map hurricane precipitation fields. Attempts are underway to Dopplerize these radars in order to provide data on hurricane wind fields. When completed, these systems should open new horizons in hurricane research.

Remote Sensors Applied to Low-Level Wind-Shear Detection

As mentioned in the introduction, strong shears in low-level winds constitute a major hazard to commercial aircraft takeoffs and landings. Roughly one aircraft disaster per year results from this cause, with an attendant loss on the order of one hundred lives, tens of millions of dollars in property damage, and millions more at stake in the ensuing lawsuits. The first efforts to develop remote-sensing systems for monitoring this hazard focused on low-level wind shear of wind areal extent, associated with frontal passages. For such wind shear it suffices to provide a single vertical profile of the wind speed in the airport vicinity. The Wave Propagation Laboratory developed a prototype system for wind-shear detection at Dulles International Airport which relied primarily on acoustic-sounding Doppler techniques for wind-speed determination. Since the acoustic sounder could not be used in heavy rain, because of noise on the sounder antenna, the Dulles system incorporated a radar unit for making VAD scans and Doppler wind determinations. The resulting hybrid system provided an all-weather capability (Hardesty et al., 1977).

As the work proceeded, however, it became apparent that much of the dangerous low-level wind shear was very localized in nature. For example, a careful analysis of the meteorological causes of the Eastern airlines crash at Kennedy International Airport in June 1975 showed that it resulted from a thunderstorm downburst, perhaps no more than a few km in horizontal dimension (Fujita and Byers, 1977). During such severe-weather events, wind data from single height profiles can no longer be taken as representative of the aircraft glide slope as a whole. What is needed instead is some sort of area coverage or scanning capability. The Wave Propagation Laboratory has developed several approaches to this monitoring needed. The first involves the use of cheap pressure switches to monitor the sharp surface-pressure rise associated with the passage of thunderstorm gust fronts and downbursts. By deploying such instruments in dense arrays, linked by phone lines to a central station, it is possible to monitor the progress of such atmospheric structures as they approach, pass over, and leave the airport area. Figure 7 illustrates this concept. Bedard et al. (1977) and Bedard and Hooke (1978) have described operation of a prototype system used at Dulles International Airport for this purpose. It is worth noting that the pressure switches used are remote-sensors in two senses. First, unlike thermometers or anemometers, pressure sensors measure the integrated mass of the air column above the sensor; as a result, they are less subject to local influences. Second, unlike thermometers or anemometers, pressure sensors can detect gust fronts even when mounted inside buildings. Both features combine with the sensor's mechanical simplicity to make them an ideal choice for gust-front monitoring. A second approach to the problem involves the use of scanning remote-sensors. Chadwick et al. (1976a and b) describe one such technique, based on an extension of FM-CW radar sounding. And recently (Strauch, private communication) WPL has found that the new-generation FAA air-traffic-control radars are sufficiently sensitive to provide clear-air echoes and wind-velocity estimates. Lidar methods have also been considered.

Lidar Studies of Pollutants

This is a rapidly growing discipline, and a difficult one to review completely. Hall (1974) gives a clear exposition. The most commonly used lidar technique is the scatter of pulses from aerosols; work in this area dates back to the early 1960's. Figure 8 shows a time history of plume development monitored by one such pulsed lidar system, shown schematically in Figure 9. As indicated in Section 3, there now exist FM-CW lidar systems for estimating velocity fields within regions of high aerosol density; a number of coherent pulsed lidar systems are also under development for this purpose. One plan includes the possibility of global wind monitoring by satellite in this way. Finally, a variety of techniques, including Raman and differential absorption, are being used to determine quantitatively concentrations of gaseous pollutants such as CO, NO_x, SO_2, and O_3. In the future such devices should offer quantitative diagnostics for air-pollution photochemical studies.

Future Applications of Remote-Sensors to Wind Engineering Problems

4

Remote-sensor application to wind engineering is in its infancy. Many remote-sensing systems have hardly advanced beyond the prototype stage. Still ahead lie the majority of their research applications, to say nothing of long-term operational uses. Moreover, behind these first-generation systems lie even more advanced technology, promising greater spatial and temporal resolution, greater ranges and areal coverage, and providing measurements of

quantities other than wind -- e.g., humidity and temperature. With these will come more powerful, definitive wind-engineering studies.

For example, it should be possible to develop mono-dispersed aerosol generators that could provide artificial plumes for study by lidar systems -- study that could then be quantitative rather than merely qualitative, revealing plume concentrations as well as plume positions. Such systems could then be used to study plume diffusion over irregular terrain, in mountainous regions slated for mineral or energy development, and over urban areas. They would thus provide more reliable environmental impact assessment, both through direct measurement and through enhanced data sets fostering more accurate models.

With their scanning capability and areal coverage, remote sensors are ideally suited for studies of wind power-park siting. The sensors could monitor winds and turbulence in large volumes of a prospective wind power-park. From the data it would be possible to select those specific sites offering the best tradeoff between maximum averaged wind speeds and minimum gustiness.

In another important application, lidar could be used to study the interaction of airflow with high-rise buildings and other man-made structures. Currently, these structures are designed using only data from scale models in wind tunnels. There has never been a major attempt to verify model predictions by comparing the model results with measurements in the field. We do know, however, that the existing approach produces buildings with many design flaws. The failures of glass cladding in Boston's John Hancock building and in the Sears structure in Chicago constitute important although by no means solitary examples. It is now possible in principle, however, to make definitive comparisons between wind-tunnel models and flows observed in the field using high-resolution lidar techniques. In this way it should be possible to develop a new understanding of the relation of wind tunnel flows to those actually obtained, to develop new scalings of wind-tunnel findings that might be more appropriate, and generally to raise user confidence in the modeling procedure.

Far more interesting than these individual efforts, however, in terms of its long-range potential for weather observations and forecasting in general, is the rise of new system concepts of improved local weather prediction. These concepts incorporate recent advances in remote-sensing, mesoscale numerical modeling, data processing, and information dissemination. NOAA is currently examining one such proposal, entitled PROFS (Prototype Regional Observing and Forecasting Service), which calls for exploratory development of such a service in the Denver area and then expansion to a nationwide system, focusing on urban areas. Such systems would attempt to improve local weather services to meet increasingly urgent needs of aviation, agribusiness, the construction industry, and the general public. New system concepts have incorporated a great concern with wind engineering problems, including hazardous-wind forecasts and monitoring, and pollution dispersal. Should such a concept be implemented, it would mean a tremendous increase over the long term in the quality and quantity of routine National Weather Service data available to the wind engineering community.

References

1. Balsley, B. B., Cianos, N., Farley, D .T., and Baron, W. J., "Wind Derived from Radar Measurements in the Arctic Troposphere and Stratosphere," J. Appl. Meteorol., 16, 1235-1239 (1977).

2. Bedard, A. J., Jr., Hooke, W. H., and Beran, D. W., "The Dulles Airport Pressure Jump Detector Array for Gust-Front Detection," Bull. Am. Meteorol. Soc., 58, 920-926 (1977).

3. Bedard, A. J., Jr., and Hooke, W. H., "The Dulles Airport Pressure-Sensor Array for Gust-Front Detection -- System Design and Preliminary Results," Preprint Volume, Fourth Symposium on Meteorological Observations and Instrumentation, Denver, Colorado, American Meteorological Society, Boston, Massachusetts (1978).

4. Benedetti-Michelangeli, G., Congeduti, F., and Fiocco, F., Measurement of Aerosol Motion and Wind Velocity in the Lower Troposphere by Doppler Optical Radar," J. Atmos. Sci., 29, 906-910 (1972).

5. Brown, E. H., "Quantitative Acoustic Measurements of Atmospheric Turbulence," Fourth Symposium on Meteorological Observations and Instrumentation, American Meteorological Society, Boston, Mass. (1978).

6. Brown, E. H., Hall, F. F., Jr., "Advances in Atmospheric Acoustics," Rev. Geophys, Space Res., (1978).

7. Brown, R. A., Lemon, L. R., and Burgess, D. W., "Toronado Detection by Pulsed Doppler Radar," Monthly Weather Rev., 106, 29-38 (1978).

8. Chadwick, R. B., Moran, K. P., Strauch, R. G., Morrison G. E., and Campbell, W. C., "A New Radar for Measuring Winds," Bull. Am. Meteorol. Soci., 57, 1120-1125 (1976a).

9. Chadwick, R. B., Moran, K. P., Strauch, R. G., Morrison, G. E., and Campbell, W. C., "Microwave Radar Wind Measurements in the Clear Air," Radio Sci., 11, 795-802 (1976b)

10. Clark, G. H., Charash, E., and Bendun, E. O. K., "Pattern Recognition Studies in Acoustic Sounding," J. Appl. Meteorol., 16, 1365-1368 (1977).

11. Collis, R. T. H., "Lidar," Adv. Geophys., 13, 113-139 (1969).

12. Cooney, J., "Temperature Profiles from Laser Radar Measurements or Rotational Raman and Elastic Scattering," Fourth Joint Conference on Sensing of Environmental Pollutants, American Chemical Society, Washington, D.C. (1977).

13. Derr, V. E. (Ed.), Remote Sensing of the Troposphere, U.S. Govt. Printing Office (1972).

14. Doviak, R. J., Jobson, C. T., "Mapping Clear Air Winds with Dual-Doppler Radars," Proc. Open International Symposium on EM Wave Propagation and Non-Ionized Media, April 28-May 7, 1977, LaBaule France (URSI).

15. Fiocco, G., Benedetti-Michelangeli, G., Maischberger, K., and Madonna, E., "Measurement of Temperature and Aerosol to Molecule Ratio in the Troposphere by Optical Radar," Nature, 299, 78-79 (1971).

16. Frankel, M. S., and Peterson, A. M., "Remote Temperature Profiling in the Lower Troposphere," Radio Sci., 11, 157-166 (1976).

17. Frankel, M. S., Chang, N. J. F., Sanders, M. J., Jr., "A High-Frequency Radio Acoustic Sounder for Remote Measurement of Atmospheric Winds and Temperature," Bull, Am. Meteorol., Soc. 58, 928-934 (1977).

18. Fujita, T. T., an Byers, H. R., "Spearhead Echo and Downburst in the Crash of an Airliner," Monthly Wea. Rev., 105, 129-146 (1977).

19. Gossard, E. E., Richter, J. H., and Atlas, D., "Internal Waves in the Atmosphere from High-Resolution Radar Measurements," J. Geophys. Res., 75, 3523-3536 (1970).

20. Green, J. L., Warnock, J. M., Winkler, R. H., and VanZandt, T. E., "Studies of Winds in the Upper Troposphere with a Sensitive VHF Radar," Geophys. Res. Letters, 1, 19-21 (1975).

21. Hall, F. F., Jr., "Laser Systems for Monitoring the Environment," Laser Appl., 2, 161-225 (1974).

22. Hardesty, R. M., Mandics, P. A., Beran, D. W., and Strauch, R. G., "The Dulles Airport Acoustic-Microwave Radar Wind and Wind Shear Measuring System," Bull. Am. Meteorol. Soc., 58, 910-918 (1977).

23. Huffaker, R. M., "Laser Doppler Detection Systems for Gas Velocity Measurement," Appl. Optics, 9, 1026 (1970).

24. Huffaker, R. M., "CO_2 Laser Doppler Systems for the Measurement of Atmospheric Winds and Turbulence," Atmospheric Technology, NCAR, p. 71 (1974).

25. Huffaker, R. M., Beran, D. W., and Little, C. G., "Pulsed Coherent Lidar Systems for Airborne and Satellite-Based Wind Field Measurement," Preprints Seventh Conf. on Aerospace and Aeronautical Meteorology and Symposium on Remote Sensing from Satellites, American Meteorological Society, Boston, Mass. (1976).

26. Kaimnal, J. C., and Haugen, D. A., "An Acoustic Doppler Sounder for Measuring Wind Profiles on the Lower Boundary Layer," J. Appl. Meteorol., 16, 1298-1305 (1977).

27. Kaimal, J. C., "NOAA Instrumentation at the Boulder Atmopsheric Observatory," Proc. Fourth AMS Symposium on Meteorological Observations and Instrumentation, Denver, Colorado, April 10-14, 1978 (to be published).

28. Kjelaas, A. G., and Ochs, G. R., "Study of Divergence in the Boundary Layer Using Optical Propagation Techniques," J. Appl. Meteorol., 13, 242-248 (1974).

29. Kropfli, R. A., Kohn, N. M., "Persistent Horizontal Rolls in the Urban Mixing Layer as Revealed by Dual Doppler Radar," Preprints Seventh Conference on Inadvertent and Planned Weather Modification, November 10-13, American Meterological Society, Boston, Mass. (1977).

30. Kropfli, R. A., Kohn, N. M., "Persistent Horizontal Rolls in the Urban Mixed Layer as Revealed by Dual-Doppler Radar," J. Appl. Meteorol., 17, 669-676 (1978).

31. Kunkel, K. E., Eloranta, E. W., and Shipley, S. T., "Lidar Observations of the Convective Boundary Layer," J. Appl. Meteorol., 16, 1306-1311 (1977).

32. Lawrence, R. S., Ochs, G. R., and Clifford, S. F., "Use of Scintillations to Measure Average Wind Across a Light Beam," Appl. Optics, 11, 239-243 (1972).

33. Lemon, L. R., Donaldson, R. J., Jr., Burgess, D. W. and Brown, R. A., "Doppler Radar Application to Severe Thunderstorm Study and Potential Real-Time Warning," Bull. Am. Meteorol. Soc., 58, 1187-1193 (1977).

34. Little, C. G., "Acoustic Methods for the Remote Probing of the Lower Atmospheric," Proc. IEEE, 57, 571-578 (1969).

35. Little, C. G., "Status of Remote Sensing of the Troposphere," Bull. Am. Meteorol, Soc., 53, 936-949 (1972).

36. McAllister, L. G., Pollard, J. R., Mahoney, A. R., and Shaw, P. J. R., "Acoustic Sounding -- A New Approach to the Study of Atmospheric Structure," Proc. IEEE, 57, 579-587 (1969).

37. Noonkester, V. R., Jensen, D. R., Richter, J. H., Viezce, W. and Collis, R. T. H., "Concurrent FM-CW Radar and Lidar Observations of the boundary Layer," J. Appl. Meteorol., 13, 249-256 (1974).

38. Platt, C. M. R., "Lidar Observation of a Mixed-Phase Alto-stratus Cloud," J. Appl. Meteorol., 16, 339-345 (1977).

39. Russell, P. B., and Uthe, E. E., "Sodar Network Measurements of Regional Mixing Depth and Stability Patterns for an Air Quality Model," Proc. Joint Conference on Applications of Air Pollution Meteorology, American Meteorological Society, Boston, Mass. (1977).

40. Schwiesow, R. L., and Cupp, R. E., "Remote Doppler Velocity Measurements of Atmospheric Dust Devil Vortices," Appl. Optics, 15, 1-2 (1976).

41. Schwiesow, R. L., Cupp, R. E., Post, M. J., Abbey, R. F., Jr., and Sinclair, P. C. "Velocity Structures of Waterspouts and Dust Devils as Revealed by Doppler Lidar Measurements," Preprints Tenth Conf. on Severe Local Storms, American Meteorological Society (1977).

42. Strauch, R. G., Derr, V. E., and Cupp, R. E., "Atmospheric Temperature Measurement Using Raman Backscatter," Appl. Optics, 10, 2665-2669 (1971)L

43. Strauch, R. G., Derr, V. E., and Cupp, R. E. "Atmospheric Water Vapour Measurement by Raman Lidar," Remote Sens. Env., 2, 101-108 (1972).

44. Wesely, M. L., "A Comparison of Two Optical Methods for Measuring Line Averages of Thermal Exchanges above Warm Water Surfaces," J. Appl. Meteorol., 15, 1177-1188 (1976).

45. Westwater, E. R., "Improved Determination of Vertical Temperature and Humidity Profiles of the Atmosphere by a Combination of Radiometers and Active Ground-Based Sensors" (Unpublished Manuscript, 1978).

46. Wyngaard, J. C., Kaimal, J. C., Ochs, G. R., Hill, R. J., and Sorenson, D. C., "An Optical Heat Flux Experiment," Proc. Fourth Symposium on Meteorological Observations and Instrumentation American Meteorological Society, Boston, Mass. (1978).

Appendix: Recent Developments in Remote Sensing

It is appropriate to include a partial listing of recent advances in atmopsheric.remote sensing, since the method of presentation used above gives a somewhat fragmented view of the arsenal of techniques now available. In this rapidly evolving field, two of the latest major reviews available (Derr, 1972; Little, 1972) are somewhat out of date. However, our treatment is not by any means exhaustive; we have simply attempted to supply the reader with a sampling of the material available and a few references to direct his first steps.

Acoustic Echo Soundings

Acoustic echo sounding is analogous to radar except that it uses acoustic pulses to interrogate the atmosphere, detecting acoustic energy scattered by atmospheric turbulence. The subject dates back to papers of McAllister et al. (1969) and Little (1969), although even these have antecedents in both western and Russian work. Brown and Hall (1978) have recently reviewed the field thoroughly. From the start, acoustic echo sounding has been used to advantage in visualizing conditions in the atmospheric boundary layer -- studying the development of the convective boundary layer, monitoring inversion height, etc. In recent years, however, interest has turned to the use of acoustic echo sounding as a quantitative tool. One piece of information yielded readily by the frequency shift of the echo returns is the atmospheric wind velocity. The technique has been used for years; a recent system is described by Kaimal and Haugen (1977). Hardesty et al. (1977) describe a quasi-operational system installed at Dulles International Airport to monitor low-level winds and wind shear. More recently, researchers have begun to investigate the potential of acoustic echo sounding for other quantitative information, including height profiles of the turbulence structure function C_T^2 and C_v^2, surface heat flux, surface stress, and Monin-Obukhov length, and rudimentary methods of temperature profiling involving heavy use of similarity theory (Brown, 1978) or phase-coherent techniques (Brown, private communication). Many of these quantities are of fundamental importance to wind engineering design.

Although in many cases acoustic methods for measuring these parameters do not seem as promising as radar or lidar techniques, they are worth pursuing because of the lower cost of acoustic methods. This lower cost is making it practicable to install acoustic echo sounders in large arrays, to determine mesoscale structure in PBL height, for example (Russell and Uthe, 1977). Various pattern recognition schemes are currently under development for use in automated processing of acoustic-sounder facsimile records (Clark et al., 1977; Hall, 1978).

Radio Techniques

The use of pulse Doppler radars in PBL studies has been described at length in the body of the paper. For the most part, the work cited has involved the use of chaff; however some installations, e.g., NOAA's National Severe Storms Laboratory, have demonstrated clear-air pulse dual-Doppler radar capability out to ranges of 40 or 50 km (Doviak and Jobson, 1977). As a rule, the work has

involved the use of two radars to provide two components of the wind directly; the third velocity component has typically been inferred, by assuming incompressibility and using the equation of continuity. However, the use of multiple radars is becoming increasingly frequent, to provide increased area coverage, to provide redundancy and therefore verification of the dual-Doppler approach, and to examine the influence of the lower boundary condition on data recovery. Other research directions are also being pursued in response to the needs of the operational community. Lemon et al. (1977) report use of single Doppler radars for detection of tornado vortex signatures. Strauch (private communication) is currently exploring a variety of single-radar techniques for estimating both horizontal wind components. It has been pointed out recently, by Gal-Chen and by Leise (work in progress) that from the dual-Doppler radar fields and knowledge of the surface boundary conditions it is possible in principle to deduce mesoscale temperature fields from the Doppler radar data. Tests are currently underway to determine whether the approach is practicable. If it is, or if it is true that mesoscale meteorological development is much less sensitive to thermal effects than the initial velocity fields (Anthes, private communication), then radars offer tremendous potential for mesoscale models.

FM-CW radar has been in use for the past decade as a powerful tool for studying the clear-air boundary layer with high resolution (e.g., Gossard et al., 1970). In recent years, however, the utility and flexibility of the technique have been greatly increased by the development of a Doppler capability for determining wind velocities, using a VAD scan (Chadwick et al., 1976a, b).

Another radar advance has been the use of VHF radars for probing the clear troposphere and lower stratosphere (e.g., Green et al., 1975); Balsley et al., 1977, and the references therein). While the technique has not been applied to the problem of lower-tropospheric profiling in any detail, it does appear that it can be (Balsley, private communication) and we can anticipate that it will be in the future.

Optical Techniques

Foremost among the optical techniques is lidar, or laser radar. The most common type is the pulsed lidar, which senses echo returns from aerosol scattering; work in this area dates back to the early 1960's and has been reviewed by Collis (1969) and Hall (1974). Recent papers of interest include a paper comparing FM-CW radar and lidar returns (Noonkester et al., 1974) which shows, as one might expect, that the PBL presents a different characteristic appearance to the two sensors, and a paper describing lidar observations of the convective boundary layer (Kunkel et al., 1977).

As in the case with both the acoustic sounders and the radars, however, lidars offer tremendous potential for quantitative measurement as well. Huffaker (1970, 1974, and the references therein) describes the principles of Doppler lidar velocity determination. Benedetti-Michelangeli et al. (1972) describe preliminary tropospheric wind measurements using lidar. Schwiesow and Cupp (1976) and Schwiesow et al. (1977) have used truck-mounted and airborne infrared CW Doppler lidar to measure atmospheric velocities in dust devils and waterspouts, paving the way for analogous studies to tornado vortices. And in a recent work Huffaker et al. (1976) put forth their concept for satellite-based global wind measurement using pulsed coherent lidar systems.

Lidar also offers some promise for temperature profiling. Fiocco et al. (1971), using molecular thermal broadening of the lidar return, and Strauch et al. (1971), using Raman-scatter lidar estimate of N_2 scale heights, provided early estimates of atmospheric temperatures. In more recent work, Cooney (1977) has used rotational Raman scattering to estimate temperature profiles.

Optical sensing seems to hold the greatest long-term potential for sensing gaseous pollutants, where optical radiation offers in principle a tremendous chemical specificity. Unfortunately however, such spectroscopic effects are often very weak, and, despite its glowing future, optical sensing has only a brief and rudimentary history. The work of Strauch et al. (1972) illustrates the approaches, which include Raman spectroscopy and differential absorption. Some recent work, including that of Swedish and Japanese groups, may be found in the Invited Papers and Conference Abstracts of the Eighth International Laser Radar Conference, held at Drexel University in June 1977 and sponsored by the American Meteorological Society and the Optical Society of America.

Lidar is currently being used to probe cloud microphysical processes. For example, Platt (1977) has used lidar to study phase changes within an altostratus cloud. Derr (private communication) has found recently that cloud glaciation can occur at a much earlier stage in cloud development than previously thought.

Other optical techniques for remote probing include line-of-sight observations of light-beam scintillations which have been used to measure wind (Lawrence et al., 1972), surface convergence (Kjelaas and Ochs, 1974), and surface heat flux (e.g, Weseley, 1976; Wyngaard et al, 1978).

Hybrid Systems

As remote-sensing matures, attention is turning away from the individual technologies themselves, and emphasis is shifting to the development of hybrid systems tailored to particular meteorological tasks. Here we discuss a few of these; however, from recent work such as that of Noonkester et al. (1974) comparing FM-CW radar and lidar returns from the boundary layer, and from recent joint radar and lidar studies of clouds (Derr, private communication), we can expect that much more such research is in the offing.

Microwave radiometry has long been used to retrieve temperature and humidity profiles in the atmosphere from measurements of atmospheric microwave brightness at different frequencies and zenith angles. Recently, Westwater (1978) has shown that should radiometric data be supplemented with data on inversion height then the radiometric inversion techniques can yield much greater resolution of the humidity and temperature variations in the vicinity of the inversion layer itself. Figure A1 shows an example (from a paper study) of the advantages of such a system. Note that since estimates of inversion strength are unnecessary, these supplementary data could readily be supplied by acoustic sounders or FM-CW radar.

Another hybrid technique of considerable novelty is the so-called RASS (Radio-Acoustic Sounding System) approach, which provides temperature profiles by using radiowave pulses to follow an acoustic pulse as it propagates through the atmosphere. In this way it is possible to measure the speed of sound and hence the temperature (Frankel and Peterson, 1976; Frankel et al., 1977).

RASS suffers from the major disadvantage that it is vulnerable to high winds, which advect the acoustic pulse out of the region scanned by the radar. The result is that even with clever engineering a rather formidable array of antennas is required to overcome this difficulty (Priestley, private communication).

FIGURE 1: EDDY WIND FIELD (MEAN WIND FIELD REMOVED) AT 0.3 KM ABOVE GROUND LEVEL ON 28 JULY 1975. WINDS ARE OBTAINED FROM AN AVERAGE OF 17 VOLUME SCANS TAKEN DURING A 70 MINUTE PERIOD ENDING AT 1557 CDT. THE VERTICAL CUTS OF FIGURE 2 LIE AT THE LOCATIONS Y = 2,4,6,8 KM. THE GATEWAY ARCH IS INDICATED BY THE DOT JUST TO THE WEST OF THE MISSISSIPPI RIVER AT THE LOCATION X = 22.6 KM, Y = 8.5 KM KROPFL AND KOHN, 1978).

FIGURE 2: THE VERTICAL CIRCULATION PATTERNS ASSOCIATED WITH THE CIRCULATION OF FIGURE 1 (KROPFI AND KOHN, 1978).

FIGURE 3: WIND FIELD OBSERVED BY DUAL-DOPPLER RADAR IN A THUNDERSTORM, COMPARED WITH A MODEL OF THUNDERSTORM CIRCULATION (VERTICAL PLANE CUT).

FIGURE 4: TORNADIC VORTEX SIGNATURE (STIPPLED AREA) WITHIN A SINGLE-DOPPLER VELOCITY (METERS PER SECOND) FIELD. VELOCITIES ARE RELATIVE TO TVS MOTION. SHORT DASH MARK INDICATES NO DATA, AND DOT INDICATES TORNADO LOCATION. DARK RECTANGLES SHOW RELATIVE RANGE GATE SIZE. RADAR AZIMUTHS AND RANGES ARE INCLUDED (FROM LEMON ET AL., 1977; BROWN ET AL., 1978).

FIGURE 5: A SCHEMATIC REPRESENTATION OF AIRBORNE LIDAR STUDIES OF WATERSPOUTS, INDICATING THE APPROACH USED TO OBTAIN THE DATA OF FIGURE 7.

FIGURE 6: WATERSPOUT VELOCITY PROFILE DEDUCED FROM LIDAR MEASUREMENTS.

FIGURE 7: SCHEMATIC REPRESENTATION OF A SYSTEM FOR DETECTING THUNDERSTORM GUST FRONTS.

FIGURE 8: VERTICAL SLICES OF A COLSTRIP, MONTANA POWER-PLANT PLUME AS MONITORED BY PULSED LIDAR.

FIGURE 9: SCHEMATIC OF THE WPL PULSED-LIDAR SYSTEM FOR AEROSOL STUDIES.

FIGURE A1: TEMPERATURE AND HUMIDITY PROFILES RECOVERED BY RADIOMETRY WITH AND WITHOUT KNOWLEDGE OF INVERSION HEIGHT, COMPARED WITH RADIOSONDE DATA.

NOTE: FIGURES NOT AVAILABLE FOR THIS PAPER

5

EXTREME WIND DATA BASE AT THE NATIONAL CLIMATIC CENTER

Michael Changery

National Climatic Center, NOAA
Department of Commerce

Extreme Wind Data Base Development at the National Climatic Center

esign wind speeds included in currently accepted building codes and tandards are presented in probabilistic terms. A daily extreme ind speed is extracted for a location for as many years as are vailable. This set of observations comprises a population and a requency distribution with the lower bound at zero. From this set f daily values, the series of annual extremes form an extreme value istribution. Statisticians have investigated such distribution nd have found that the limiting distribution can take only three orms regardless of the distribution of the original data. These orms are called Type I, II, and III. Type I is unbound at both nds and Types II and III are bounded by zero, below and above, espectively. Since wind has no strict upper bound, the probability f a known extreme being exceeded exists, although such probability ay be very small. A specified mean recurrence interval corresponds o an expected design wind speed for this location and the associted stresses may not exceed the stress level considered in structural design. Currently, the American National Standard A58.1 pecifies that the 50-year mean recurrence interval (frequently alled the "return period") value is the design wind speed for all tructures excepting those with an unusually high or negligible azard to life. This standard also assumes that the Type II Frechet) distribution best models the behavior of wind extremes.

The national maps (in Standard A58.1) of wind speeds for arious recurrence intervals were obtained by utilizing the Type II istribution and the annual fastest mile speed for approximately 50 locations for an average of 15 to 20 years. In areas subject o the extreme winds of tropical storms, a mixed distribution was sed since tropical storm winds have a different distribution than on-tropical ones.

For a number of reasons, the current design wind standards ave been a source of considerable disagreement among researchers nvestigating design wind and structural wind loading. The first s concern that the fastest mile may not be the most useful extreme o be used in modeling of extreme winds. No readily available lternative set of data exists. Many investigators also believe nat other additional statistical techniques can be employed to ore accurately define the extreme wind environment. No documented et of annual fastest mile speeds used in deriving the standard alues is available. In addition, the period of record used in the tandard covers generally 15 to 20 years -- a period many believe oo short to adequately model the extremes at a location.

The National Climatic Center (NCC), repository for the majority f meteorological data gathered in the United States, is the largest rganization of its kind in the world. In addition to its standard rchival function, the NCC is responsible for extracting and proessing climatological data in a variety of forms for users such as he general public, industry, academia, and other government rganizations.

In response to requests from other agencies, the Center is eveloping additional sets of wind extremes for a greater number of tations and years than currently available. We are also developng documentation on current and historical wind data for the locaions in the Center's archives -- including availability of multiple egister and gust recorder charts (the source of wind extremes), nd instrument height, location, dates of height changes and pertient exposure problems.

5

This paper will present the status of extreme wind data bases the Center is developing for the Department of Energy (DoE), National Bureau of Standards (NBS) and Nuclear Regulatory Commission (NRC). Initially however, a brief discussion of the National Weather Service (NWS) instrumentation and data types is necessary.

NWS Instrumentation

Although various research instruments are available for sampling the wind speed fluctuations at intervals of seconds or fractions of seconds, the standard anemometer of the Weather Service (and its predecessors -- the Weather Bureau and Army Signal Corps) has been the vertical axis rotating cup anemometer. Many modifications were applied to this instrument in an attempt to more accurately record wind speed. The number, shape, and strength of the cups and length of the supporting arms have all been changed. Basically however, these instruments measure wind passage determined by motion applied to a freely rotating mechanism.

Beginning in 1870, the 4-cup (hemispherical) Robinson anemometer was introduced by the Army Signal Corps. This was a contact-type instrument that accumulated wind passage in miles and fractions of miles on a dial. Frequently, this instrument was used with a mechanism which allowed a current to flow at each contact which actuated a light or buzzer. The observer reported wind speed by counting the number of contacts per unit time. A more sophisticated mechanism actuated a pen arm at each contact which recorded each mile of wind passage on a clock-driven drum chart called a single or multiple register.

The 4-cup instrument was used exclusively until 1927 when replaced by a 3-cup anemometer with significantly better accuracy. The 4-cup was known to highly overestimate wind speeds -- particularly the extreme winds. For example, a 100 mph observed speed required a minus 24 mph correction to indicate the true speed. Only the observed speed is entered in the official records and all data before 1928 must be corrected by a table of 4-cup corrections before use. Many investigations early in the century demonstrated the superiority of the 3-cup (hemispherical) anenometer (designated "S" type) and beginning January 1, 1928, the Weather Bureau began using this instrument for official wind measurements. The 4-cup was retained as back-up. Observations made with the 3-cup were also entered uncorrected in the official records on the erroneous assumption that the anemometer ran so close to the true speed that corrections were not necessary. It was later determined that the originally published corrections were in error and hence the published values must also be corrected to true speed before use. Readings from any 4-cup back-up instrument used were corrected to a true speed for entry in the official records. For a few years beginning in 1932 the 4-cup instrument was again the official station instrument, but at most locations the 3-cup was eventually re-adopted for official observations. Most importantly all wind data entered in official records since January 1, 1932 are true speeds with the necessary corrections applied.

Additional investigations at this time demonstrated that cups with "beaded" edges -- produced by rolling the edges outward to form a ring -- ran considerably smoother in a turbulent air-stream than cups with straight edge. Beaded edges were used on 3-cup (semi-conical) small airways contact anemometers (designated "SA") introducted at smaller airports in the 1930's. While beaded cups were found to be advantageous, they were not used on the standard 3-cup ("S") anemometer at major airport stations. However, at

selected locations, a special beaded 4-cup experimental instrument was used in the 1930's and 40's. All instruments mentioned were contact anemometers, although aviation requirements in the 1930's led to the development of contacts for each 1/60th of a mile of wind passage. Thus the number of contacts per minute was converted directly to a mph equivalent.

A second type of instrument employing a different method of recording was introduced during the 1940's at most major airports. This was the direct-reading type (similar to those in operation currently) in which the wind-induced rotation governs the magnitude of electrical current generated by a magneto. The current is linearly related to the true wind speed, which is determined by dial displacement. The direct-reading instrument is frequently connected to a device, called a gust recorder, which provides a continuous record of wind speed. Direct-reading instruments have generally replaced contact-type instruments at all locations except approximately 130 major airport locations which also employ the older-type instrument in recording data on multiple registers.

Types of Wind Measurements

As mentioned in the preceding section, contact-type anemometers accumulated wind passage in miles and fractions in the earlier years, and in 1/60th of miles in the 1930's and 1940's. It is clear that measurement of short-term gusts of wind speed had to await development of the direct-reading anemometer. Early stations measured the wind at 2 or 4 observation times per day. This was done by converting the miles and fractions of wind passage in 5-minutes to a mph equivalent. After the turn of the century, stations began accumulating hourly totals of wind passage on a 24-hour basis. Aviation requirements by the 1920's demand hourly or more frequent measurements determined again by 5-minute measurements made each hour.

At stations equipped with register charts marked by successive passages of miles of wind on a clock-driven drum chart, two measures of wind extremes were made:

(1) Beginning in 1872, any station so equipped determined on a daily basis the greatest number of miles of wind to pass by the instrument in any 5-minute period. This was called the 5-minute maximum speed and was tabulated on a daily basis until ceased by the Weather Bureau of 1957.

(2) Beginning in 1887 and continuing through 1904 and then beginning again in 1912 and continuing through the present, a second type of daily extreme was extracted. Called the "extreme" or fastest mile, this measurement was obtained by determining the shortest time interval between successive marks and converting this to miles per hour. Thus, marks 1-minute apart represents a 60 mph speed; 2-minutes apart -- a 30 mph speed; and 30-seconds apart -- a 120 mph speed. A special graduated scale permitted direct conversion of a "mark spacing" to a mph equivalent.

With introduction of the direct-reading instruments in the 1940's as a standard equipment, the hourly observed winds were obtained by an "eyeball" estimate of the wind for a 1-minute period. Assuming the speed met certain criteria, wind gusts (highest instantaneous speed) observed were included on hourly reports. However, only stations with continuous recording instruments carried a daily peak gust since this gust could occur between

hourly observations and not be seen by the observer. Military sites (Air Force and Navy) were generally equipped by such recorders from the mid-1940's. Natinal Weather Service locations, as a rule, did not have recorders until the late 1960's.

The choice of suitable measurements to be used in extreme value wind analysis is limited to three: 5-minute maximum, fastest mile, and peak gust. As mentioned above a national data base of annual peak gusts must be restricted to the last 10 years excepting military sites - too short to be reliable statistically. It has been assumed that a relatively short burst of extreme winds produces the most dangerous wind load on a structure. An extreme as determined by fastest mile measurement which may be limited to a time frame of 1-minute or less, may be a better parameter to use. In addition, the other available parameter (5-minute maximum) has not been extracted since 1957. For airport locations, at which the contact anemometers have been located since the 1940's, the period of record would be limited to those years prior to 1957 and after the transfer of instrumentation to the airport - again too short a period to be statistically useful. The remainder of this paper discusses the types of extreme wind data base development in which the Center is currently involved.

The NBS Project

The National Bureau of Standards has long been active in investigations of wind load on structures. At their request the NCC is providing additional extreme wind data on a national basis for use in developmental work. The primary purpose of the Center's role in this project is two-fold: (1) To update the set of fastest mile speeds by including the last 10-12 years of data available. As mentioned earlier, the data on which the current Standard is based was restricted to the 15-20 year period prior to the mid 1960's; and (2) To provide a set of 5-minute maximum speeds coincident with the fastest mile.

The original set of fastest-mile data was restricted to airport locations. Neither the period used nor the actual values have been available for use by other reseachers. Therefore, the Center is determining the first full year of fastest mile data at a given airport location and listing all annual values through 1977 or the last year available. It is apparent, unfortunately, that the contact-type anemometer is slowly being phased out as a source of wind data. An additional station is lost to the data base every few years. For each occurrence of the fastest mile, we are also extracting the coincident 5-minute maximum speed. This may or may not be the true annual highest 5-minute maximum. In checking a number of stations for another project, we determined that the annual extreme fastest mile and 5-minute maximum were normally coincident. However, occasionally a fastest mile extreme associated with a short period thunderstorm outflow may have a 5-minute maximum lower than a second episode of sustained strong winds in the same year. We are not providing the true annual value since this would require close analysis of daily charts for approximately 130 locations for the period 1958-1977 -- a very expensive and time consuming proposition. This analysis would be required because 5-minute values were not extraced from charts after 1957.

Two problems have been encountered in this NBS project. We have been consolidating the fastest mile values entered on daily manuscript forms and listed in various publications. Obtaining the coincident 5-minute values after 1957 requires inspection of the register charts for the day of the fastest mile. We have come

cross a number of occurrences where the published fastest mile alue is seriously in error - often by a factor of two. The prob- em is apparently caused by misusing the scale provided for the xtraction of fastest mile data. To conserve space, the scale has een constructed so that four speeds (multiples of one another) an be read in essentially the same location on the scale. It is ery possible for an unskilled observer to misread the scale's rinted speed and report a speed twice the actual. For example, a 0 mph speed requires a mark interval of two minutes and misreading he scale can result in a 60 mph reading. Charts for a given day are nalyzed on station the following day, and the observer could check he extracted value against actual surface observations made at the ame time. Apparently, this is not always done. The erroneous eading is then entered on manuscript and climatological forms used t the NCC as the sources for published data. No quality control rocedures exist for the registered charts and data is not recog- ized as erroneous until a special data requirement, such as this roject, is funded. In cases such as these, we are not providing he published value, but are checking the next highest speed and roviding this value if it appears reasonable.

The second problem encountered is not as serious. It has been tation practice to log the scale value, together with time of ccurrence on the chart for a given day and then apply the necessary nemometer correction before entering the observation on official orms used for published data. Beginning in the late 1960's, we ave found many instances where the speed logged on the chart is he same as entered on the official forms. Either the observer is orrecting the scale value before logging it on the chart or he is ntering uncorrected speeds on the official forms. The differences re minor since most corrections for the 3-cup extracted values are ess than 5 mph. It is not possible to re-analyze the charts for he purpose of obtaining a definitive answer because of the ifficulty in distinguishing (as an example) a 44 mph spacing from 47 mph spacing. We prefer to use, wherever possible, the n-station observer's estimate. Unfortunately, at stations where his has occurred, the problem is not consistent. A few intermedi- te years may have data entered in the "correct" manner. We have hecked with a number of stations and all Weather Service Regional ffices -- all of whom stated that uncorrected values should be ogged on the register chart, although there are no official guide- ines which so dictate. Proceeding under this assumption, we have pplied corrections to the appropriate published uncorrected speeds nd used these unless the corrected value was less than another peed (already corrected) which occurred during the year. We have urnished the available fastest mile and coincident 5-minute speeds o NBS together with the anemometer heights and dates of changes. ncluded are also a number of stations considered as "airports" ue to their location, such as Cape Hatteras, NC, Block Island, RI, orth Head and Tatoosh Islands, WA. Data for these begin early in he century. The entire listing will be published for distribution.

One of the problems in utilizing contact anemometer data is hat the station location changed from an urban city office to a ural airport office 25-30 years ago. The marked change in surface oughness has precluded merging the data for both locations into a ingle set. For a few stations, a considerable period of overlap xisted with registers existing at both city office and airport ocations. For these stations, we are providing not only the vailable annual extremes at both locations, but also the daily xtreme at one location to match the date of the annual extreme at he second if the annuals at both sites did not occur on the same ates. This will enable NBS to investigate possible techniques

for providing a homogeneous set of data for the station's entire period of record.

The last product to be provided will be limited to the period of record for 5 airport stations. Together with the annual fastest mile and associated 5-minute maximum, we will provide a true annual 5-minute maximum. We will also provide the associated 10-minute and true annual 10-minute maximum. To provide the true annual 5- and 10-minute maximum requires detailed analysis of daily charts after 1957 for the 5-minute speed and the period of record for the 10-minute speed. This portion of the project will be restricted to only a few stations to test the validity of providing associated values in lieu of the true annual, and to provide an additional set of measured extremes.

The NRC Project

The Nuclear Regulatory Commission requires detailed wind loading analyses for proposed nuclear power sites -- particularly those along and off the immediate coastline. To provide the largest possible extreme wind data base, the Center is developing a data base for all locations within 10 miles of the Atlantic and Gulf of Mexico coastlines consisting of all fastest mile values for the station's complete period of record. This will be for both city office and airport locations.

In addition to the first-order stations currently in use, we found many additional locations with extracted data -- including city office locations which made observations until 20-30 years ago. The project requires the quality control of available fastest mile data and extraction of data prior to 1887 and between 1905 and 1911 - two periods during which the fastest mile was not extracted on station. We are also extracting data by examining daily traces for those stations with register charts which have never been analyzed. As an example, nearly 70 years of data exist for Delaware Breakwater, DE, which have never been extracted. In addition, 15 to 20 years of data exist for a larger number of Coast Guard sites along the Florida coastline, including the Florida Keys. However, the quality of the charts are, in many cases, less than adequate, with frequent equipment malfunctions and long periods of missing data.

The requirement to analyze charts for annual extremes never extracted has reinforced the conclusion that an accurate estimate of extreme winds becomes very tenuous for the higher wind speeds -- particularly those in association with tropical storms. For example, to determine an 84 mph fastest mile speed requires measuring the spacing between two consecutive marks out of the 6 or 7 which may be marked in a 5-minute space occupying 1/4-inch of chart paper. The overrun problem of the old 4-cup anemometer accentuated the problem at high speeds by registering additional marks in a short spacing -- although the overrun was corrected out. We have found that in most instances, the older register charts are of higher quality than current charts. The oldest charts were originally marked in pencil and these have become very faint with time. However, generally from 1900 through the 1940's, the charts were finely marked by ink and adjacent marks are distinguishable. This instrument quality control presumably was a reflection of the stations' dependence on the chart as the only source of wind data. Currently, the direct-reading instrument is the primary source of wind data, and the quality of register data has suffered. As a result, during severe wind episodes adjacent marks tend to run together and become nearly illegible. We have found a few

historical cases where, because of anticipated very high winds, the station had doubled the speed of the drum, making analysis of the actual extreme significantly easier.

In addition to providing all historical annual fastest mile extremes, the Center is also extracting the coincident 1-, 2- (if available), 5-, 10-, 15-, and 30-minute and 1-, 2-, and 3-hour speeds together with associated directions. This will provide additional sets of wind extremes as well as data from which inter-relationships for various time intervals could be developed. The NRC project is scheduled for completion in late 1978. The final data set will be consolidated and available to all requesters.

The DoE Project

The final project in which the Center is engaged is not directly related to development of actual data sets, but could be very useful to the research community. The Department of Energy requested that the Center publish a concise listing of all stations in its archives with any type of wind data available. Anemometer information was to be included. The listing was designed for those interested in investigating wind power as an alternative source of energy. The publication (to be available within a few weeks) lists all locations with basic wind observations, their location, elevation, approximate number of observations per day, and period of record. Also included were the period with digitized data, multiple register charts, and gust recorders charts. Most important, instrumentation information is provided, such as anenometer height, dates of height changes, exposure location, and exposure problems. The instrument history is of importance in any effort to standardize wind extreme observations to a given height. We have found numerous examples of erroneous anemometer information in published sources. In particular, most sources do not discriminate between contact and direct-reading anemometer and assume similar heights for both if only the direct-reading height is known. This is frequently not the case.

Future Projects

We anticipate two additional developmental projects involving extreme wind data. The Center may analyze additional station-years of data for NBS to determine the accuracy of published values. If numerous examples of inaccurate data exist, we may need to check and correct all the airport extremes.

A second project for the NRC may involve the extraction of annual fastest-mile speeds for the entire historical period of record for all locations east of the Rocky Mountains. This would cover all areas of th U.S. subject to extreme winds excepting the Northwest coastline. If funded, this project would take at least two years to complete.

6

A STRONG-MOTION RECORD INFORMATION RETRIEVAL SYSTEM

A. M. Converse and R. B. Matthiesen

Seismic Engineering Branch
U.S. Geological Survey

A Strong-Motion Record Information Retrieval System

To make information about strong-motion records readily available, the information has been entered into a computerized data-base management system. The system provides ready access to information about strong-motion records, stations, events, and level of data processing and analysis of each record. The system should prove to be of considerable value in the aftermath of a major event as a means of providing immediate information to persons in research, design, operations, and regulation.

The basic organization of the data is illustrated in Figure 1. Of primary importance is the information about the records themselves and the level of processing and analysis that has been performed. Information about the event generating the motion and the stations at which it was recorded are also of major importance. These three elements constitute the major data sets included in the data base. Supplementary data sets include general information about the data base and how to access data, additional information about the stations, and the recorders and transducers. The organizations that own the instruments have additional information about the stations and sites, and archive the original records. The specific information that is included in each data set is indicated in Table 1.

At present, the information included in the data is restricted to that for which the USGS has a primary responsibility. The data sets will be expanded to include information about all strong-motion programs in the U.S. In addition, the computer program will be available to other organizations that operate strong-motion programs in other parts of the world so that information about strong-motion data can be exchanged efficiently.

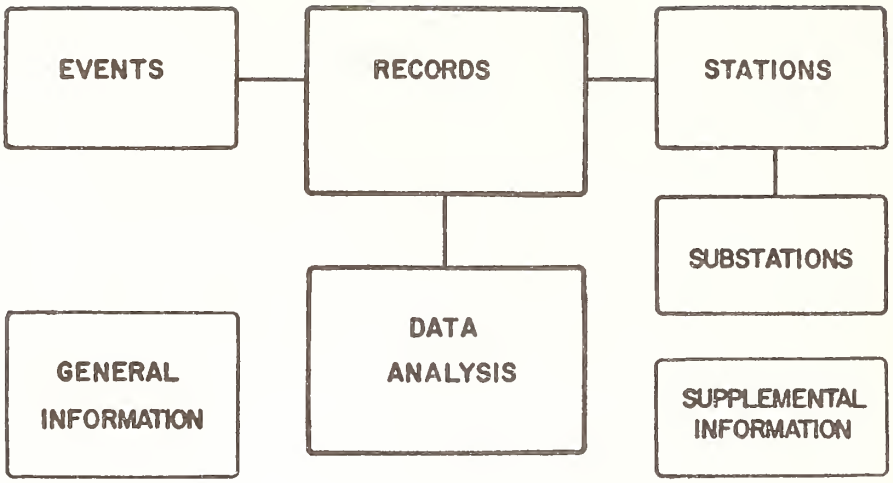

FIGURE 1: STRONG-MOTION DATA ORGANIZATION

TABLE 1: DATA SETS

EVENTS
- event identification (date & suffix)
- time (local or GMT)
- event name
- location: latitude, longitude
- magnitude
- maximum intensity
- references

RECORDS
- event identification
- station number
- substation identification
- transducer level or location
- recorder identification(s)
- s-trigger interval, sec.
- epicentral distance, km.
- intensity at the site
- total length of record
- peak acceleration
- duration >0.1g
- who has the original record
- references

DATA ANALYSES
- who digitized the data
- who has the digitized data
- length of record digitized
- highest stage of analysis
- stage 2 frequency band
- data processing type
- references

STATIONS
- station number
- station name (or street address)
- station location (or city)
- state (or country)
- nearby stations
- references

SUBSTATIONS
- substation identification
- date of installation
- date of removal
- location: latitude, longitude
- geology: class code
- near surface shear wave vel.
- structure: class code, size, short description
- remarks

ARRAYS
- array name
- list of stations and their substations in the array
- remarks

NEARBY STATIONS
- station number
- list of nearby stations
- remarks

RECORDERS
- recorder identification
- owner agency
- date of installation
- date of removal
- remarks

TRANSDUCERS
- transducer serial number
- date of installation
- date of removal
- location: code, short description
- direction of acceleration
- orientation
- trace location on record
- remarks

TRANSDUCER CALIBRATIONS
- calibration date
- sensitivity
- period
- damping
- remarks

RECORDER TYPES
- recorder type code
- descriptions

AGENCIES
- owner-agency code
- remarks about the owner-agency name, address, and contact

7

INTEGRATION OF STRONG-MOTION ACCELEROGRAMS

Susumu Iai
Eiichi Kurata
Hajime Tsuchida

and

Satoshi Hayashi

Port and Harbour Research Institute
Ministry of Transport

Integration of Strong-Motion Accelerograms

Ground displacements have a great influence on structures such as submerged tunnels and pipelines, and also on large-scale structures. Because of the need for ground-displacement records of strong earthquakes, several methods have been proposed for integrating strong-motion accelerograms. Although the methods proposed so far are basically quite similar, the displacements obtained by them are often very different.

An accelerogram always produces some error. Moreover, integration overemphasizes the low-frequency component. Therefore, direct integration of a digitized accelerogram generally produces an abnormal displacement because of low-frequency errors. Therefore, one of the important parts in an integration is the design of an appropriate high-pass filter. The report deals with this problem based on an examination of records accuracy and proposes two new methods for integration of accelerograms.

There are many sources of error in a integrated displacement if the error is defined as difference between a true displacement and an integrated displacement. Some of the errors generated during recording and processing before digitization come from the seismometer itself; some of these errors can be corrected. Although such errors should be examined carefully, the report deals only with the errors generated during the digitization.

Accelerograms examined in the report are those recorded by the ERS accelerographs and those recorded by the SMAC-B_2 accelerographs. The accelerograms were digitized for each kind of record. However, the discussion in this report may be applied to many types of accelerograms and digitizers.

Accelerograms and Digitizers

The ERS accelerograph is composed of three transducers of the moving-coil type and an electromagnetic oscillograph. The frequency characteristics are such that the magnification is maintained at a 90% level in the frequency range 0.18 - 50 Hz. The sensitivity of each accelerograph is adjusted depending on the prevailing seismic activity at the site and other conditions. The sensitivity of the records dealt with later in the report is 10 gal/mm. The recording speed is 4 cm/sec.

The digitizer for making a record from an ERS accelerograph is such that with a cursor an operator traces waveforms on an oscillogram fixed on the table. The sampling intervals along X-axis are 0.1 mm, and the digitization unit has the same values. Length of the record to be digitized without shifting of the oscillogram is 70 cm at the maximum.

The SMAC-B_2 accelerograph is a mechanical one; the natural frequency of the pendulum is 7.14 Hz and its damping is critical. The sensitivity is 12.5 gal/mm and the recording speed is 1 cm/sec. Its digitizer is similar to that used with the ERS accelerograph. The difference is that the digitizer for the SMAC-B_2 accelerograph has a cursor that moves automatically in an incremental manner in 0.1 mm intervals along the X-axis. Digitization units in the Y-axis are 0.008 mm. The maximum length for the digitization is 45 cm. A detailed description of these accelerographs and digitizers is available in a separate report.

7

Accuracy of Digitized Accelerograms

To investigate the accuracy of digitized accelerograms, Fourier spectra of an accelerogram and its errors are studied. The accuracy is specified in terms of ratios between them at individual frequencies. Hereafter, Fourier spectra of an acceleration record will be called SIGNAL (S); Fourier spectra of errors will be called NOISE (N); and the ratio will be called S/N.

There are two kinds of NOISE generated during digitization; one is generated in the process of tracing an acceleration record due to the difference between a recorded line and an actually traced or digitized line. The causes of this difference are parallax, fluctuation of a hand in motion, and errors in the digitizer mechanism and electronics. The other is due to the difference between true zero axis in the record and the base-line located before or after the of tracing. The former will be called digitization errors and the latter will be called base-line location errors.

Digitization Errors

For the examination of digitization errors, accelerograms by the ERS accelerographs were digitized several times by the digitizer described previously. A part of the results of the digitization are shown in Figures 1 and 2. The digitized lengths and the operators are listed in Table 1.

An average of the digitized records is calculated and its Fourier spectra is approximately looked upon as SIGNAL. The difference between the averaged record and each digitized record is calculated and its Fourier spectra is calculated. Then, an average of absolute value of the Fourier spectra is calculated and approximately looked upon as NOISE. Figures 3 and 4 show SIGNAL and NOISE (the figures at the bottom) and their ratio S/N (the figure at the top) in the frequency range up to 1 Hz, where the accuracy is often questionable for integration of acceleration records. S/N in Figure 3 is mostly lower than 1 through the frequency range shown. Increase of SIGNAL with decrease of frequency may be due to the transverse play of the recording paper because in this examination no correction on the transverse play has been applied. By the way, predominant frequencies of SIGNALs are about 10 Hz in both records and S/Ns around this frequency are about 10 in both cases, as shown in Figures 5 and 6.

These results show average characteristics of NOISE and S/N. That is:

- S/N and SIGNAL are similar in the frequency domain. The greater SIGNAL is, the greater S/N is.
- In the frequency range up to 1 Hz, NOISE is almost constant.

These facts imply that digitization errors are approximately white noise. Comparison between Figures 3 and 4 shows the following: NOISE level varies slightly with a digitized accelerogram. However, if we take into consideration the digitizer and the digitization process, it can be expected that this variation will be limited to some specified amount.

These results lead to the following conclusion about digitization errors. Digitization errors are white noise whose level varies with a record to be digitized. The variation is, however, limited.

The average level of NOISE in terms of power spectral density is about 0.05 (gal^2/Hz) in the case of the accelerogram obtained by an ERS-accelerograph whose sensitivity is 10 gal/mm.

With an accelerogram from the SMAC-B_2 accelerograph, a similar examination was carried out. The conclusion was similar to that described above. NOISE level was found to be 0.05 (gal^2/Hz) too.

Base-line Location Errors

If significant part of an accelerogram is longer than the available digitizer table length, it is divided into sections for the digitization. In this case, a base-line is located for each section. Therefore, base-line location errors are piece-wise constant or stepwise errors. Fourier spectra of the errors of this kind are approximately proportional to 1/f, where f is a frequency.

The amount of the step error is approximately equal to the standard deviation of digitization error. In the cases of accelerograms examined previously, the standard deviations were 2.7 gal and 0.8 gal, respectively. This result implies that the amount of the step error is 0-3 gal on an accelerogram from the ERS accelerograph whose sensitivity is 10 gal/mm. In the case of an accelerogram from the SMAC-B_2 accelerograph, the same amount was estimated.

Errors in a Digitized Accelerogram

Here, an equation will be constructed to represent the approximate errors -- digitization errors and baseline location errors -- for the estimation of S/N in a later section.

Digitization error is approximated by white noise whose level is 0.05 (gal^2/Hz), as described previously. An accelerogram to be integrated is corrected with a digitized fixed trace before the integration to eliminate errors due to the transverse play of the recording paper. Since the corrected accelerogram contains digitization errors in the fixed trace, the digitization errors in the corrected accelerogram are approximated by white noise with the level of 0.1 (gal^2/Hz).

On the other hand, power spectra of base-line location errors for each digitization section are expressed as $\frac{1}{T}[a \cdot \sin(2\pi fT)/\pi f]^2$;

where, T (sec) is length of the section and a (gal) is the amount of the step errors. Power spectra of the baseline location errors over total record length may by approximated simply by

$$\frac{1}{2T} \cdot \left(\frac{a}{\pi}\right)^2 \cdot \frac{1}{f^2}.$$

The following equation expresses these errors approximately:

$$E(f) = \left[0.1 + \frac{1}{2T}\left(\frac{a}{\pi}\right)^2 \cdot \frac{1}{f^2}\right] \times 10^{-2} \, p^2 \qquad (1)$$

where, a = 0 ∿ 3 (gal), and

p (gal/mm) is the sensitivity of the ERS accelerograph.

The sensitivity of the SMAC-B_2 accelerograph is 12.5 (gal/min); however, the digitization error of an accelerogram from the SMAC-B_2 accelerograph is almost equal to that from the ERS accelerograph

7

with sensitivity of 10 gal/min. In the case of a record by the SMAC-B_2 accelerograph, the error may be obtained by substituting $p = 10$ into the above equation.

A Relation Among S/N, Frequency Band, and Records

While NOISE, as described previously, becomes higher at low frequencies, SIGNAL (ideally true Fourier spectra of an accelerogram) becomes, for most cases, lower at low frequencies. Therefore, S/N of a digitized record mostly becomes lower at low frequencies. On the other hand, the level of SIGNAL varies with records. Therefore, a degree of the decline of S/N at low frequencies varies with records. In the usual situation where the number of records available is limited, these facts imply the following relation among S/N, frequency band, and records (Figure 7).

- If a frequency band is specified and fixed, S/N maintained in the frequency band varies with records. For each record, the wider the frequency bandwidth is, the lower the S/N ratio is. For a fixed frequency band, the greater the number of records is, the lower is the overall S/N level.

- If a S/N is specified, a frequency band maintaining the S/N varies with records. For each band, the higher the S/N is and the greater the number of records is, the narrower the frequency bandwidth is.

- If an S/N and a frequency band are set, corresponding records are selected. The higher the S/N is and the wider the frequency band is, the smaller the number of corresponding records is.

These three relations are summarized as follows:

- If levels are specified for two items among S/N, frequency band, and records, the level for the rest will be automatically determined. The higher the level of one item is, the smaller the level of the other is, if the level of the rest is fixed. Here, the heights of levels of items denote S/N level, frequency bandwitdth, and number of records respectively.

Design of Filters

Appropriate S/N Frequency Band, and Records

For the Annual Report on Strong-Motion Earthquake Records in Japanese Ports published by the Port and Harbour Research Institute, S/N, frequency band, and records are set as follows:

(1) Records whose maximum horizontal component is greater than 50 gal are integrated. For the vertical component, no limitation is applied.

(2) Two kinds of filters are applied; one maintains a fixed frequency range and the other is expected to maintain constant S/N.

Condition (1) assures some frequency bandwidth and some S/N level and at the same time assures the number of records. Condition (2) meets the desire to use the integrated displacements for a wide range of research.

It should be considered in fixing frequency band that it may usually be required to retain at least 0.1 Hz - 0.3 Hz. However, if width of frequency band is extended excessively, S/N implicity required (say 1.0) cannot be maintained for most records. In connection with fixing S/N, it will be pointed out that there is no clear consensus of required or recommended S/N level among data users. However, if S/N level is fixed to be 10, for example, corresponding frequency band is limited just around the predominant frequency for most of the records, and does not meet the implicitly required (say higher than 0.5 Hz) frequency range. These considerations lead to the conclusion that, in the case of fixing frequency band, appropriate (or expendient) lower boundary is 0.1 - 0.3 Hz, and in the case of fixing S/N, the appropriate S/N level is 2 - 5. Because the upper boundary of the frequency band does not have a great influence on integrated displacements, the report does not treat it. For this matter, a separate report is available.[1]

Sharpness of Roll-Off

To design a high-pass filter, sharpness of roll-off of the filter should be discussed as well as the cut-off frequency.

Three out of the many filters proposed so far are shown in Figures 8(a) through 8(c) as examples of sharpness of roll-off. In the figures, combinations of filters and double integrals $(1/(2\pi f)^2)$ are shown for comparing the influence of the sharpness on integrated displacements. The filter in Figure 8(a) has a stronger effect on artificial predominant components around the cut-off frequency. On the other hand, the filter in Figure 8(c) is too mild to filter some limited frequency band. The sharpness of roll-off of the filter in Figure 8(b) was considered appropriate.

Proposed Filters

A Fixed Filter (which has a fixed cut-off frequency) and Variable Filter (which has a cut-off frequency varying with records) are both proposed in this section. These filters are both being applied to the routine standard processing of the strong-motion accelerograms in the observation network of the Port and Harbour Research Institute.

Fixed Filter

This filter is designed to make it easy to compare the integrated displacements with records observed by the seismographs deployed by the Japan Meteorological Agency (the natural period of horizontal pendulum is 6 sec. and the damping factor is 0.552); see Figure 9.

$$H_1(f) = \frac{1}{1 - \left(\frac{f_0}{f}\right)^2 - 2h\left(\frac{f_0}{f}\right) i} \cdot \frac{1}{\sqrt{1 + \left(\frac{f_1}{f}\right)^2}} \qquad (2)$$

where, $f_0 = 1/6$ (Hz), $h = 0.552$, and $f_1 = 0.1$ (Hz).

Cut-off frequency (3 dB down) of this filter is 0.154 (Hz).

Errors for integrated displacement by this filter, estimated by Equation 1, are 0.01p (cm) to 0.06p (cm) in terms of standard deviation, where p (gal/mm) is the sensitivity of the ERS accelerograph. In the case of an accelerogram from the SMAC-B_2 accelerograph, estimated errors are 0.1 (cm) to 0.6 (cm).

Variable Filter

Variable Filter is defined, with the parameter fc, by the following equation; see Figure 10:

$$H_2(f) = [1 - \exp\{-(\frac{f}{f_c})^2\}]^2 \qquad (3)$$

The cut-off frequency (3 dB down) is 1.36fc (Hz).

The parameter fc varies so as to make σ equal to standard quantity E related to the required S/N, where σ is a quantity to express the low-frequency component level and defined by

$$\sigma^2 = \frac{1}{s}\int_{-\infty}^{\infty} |x(f)|^2 \cdot [1 - \exp\{-(fT)^2\}]^4 \cdot [1 - H_2(f)]^2 df \qquad (4)$$

where, S is length of digitized accelerogram,

T is a minimum length of a section for digitization, and

x(f) is Fourier transform of an acceleration record.

fc is fundamentally determined so as to eliminate some constant amount of the low-frequency components of an accelerogram (Figure 11). Components lower than about 1/T are eliminated for the decision procedure of fc, because, in this frequency range, fluctuation of baseline location errors are considered to be remarkable. The decision procedure is introduced so as to assure some stability against possible fluctuation of NOISE.
The selected values for E are listed below:

E = 0.05 (gal) for a record by the ERS accelerograph whose sensitivity is p(gal/mm),
E = 0.5 (gal) for a record from the SMAC-B_2 accelerograph.

This value E is expected to retain S/N level 2 - 5 in the frequency range higher than the cut-off frequency under the following condition: that is, NOISE is expressed by Equation (1), fc, is about 0.1 - 0.5 Hz, and power spectrum of a digitized record does not extremely vary in the frequency range up to the cut-off frequency.

Specified in terms of standard deviation, expected errors from Equation 1 in the integrated displacement are approximately:

$$5 \times 10^{-4} \cdot p \cdot f_c^{-\frac{3}{2}} \cdot \sqrt{1 + 0.01 \cdot (\frac{30}{T}) \cdot a^2 f_c^{-2}} \text{ (cm)}$$

where, a = 0 - 3 (gal), T (sec) is length of a section for digitization, and p (gal/mm) is the sensitivity of the ERS accelerograph.

In the case of a record from the SMAC-B_2 accelerograph, expected errors are expressed by the same equation with substitution of p = 10.

Comparison of the Filters

The filters proposed so far including the two filters proposed previously in this report are shown in Figure 12. The combination of the filters and double integrals are shown in Figure 13. In the figures, examples of Variable Filters are shown with parameters

fc = 0.07 Hz and fc = Hz. Although Kurihara and Sakurai investigated three cut-off frequencies[3], in the figures, the filter with the lowest one is shown. Figure 14 shows a sample calculation of displacements. In this case, the parameter fc of the variable filter is 0.824 Hz.

Errors in the displacements calculated with filters proposed by the several researchers were estimated by Equation 1. Here records from the SMAC-B_2 accelerograph and digitized by the digitizer described previously are considered. The errors are expressed in terms of standard deviation. The results are as follows:

Fixed Filter	: 0.1 - 0.6 cm
Variable Filter (fc = 0.824 Hz)	: 0.01 cm
Kurihara's Filter [3]	: 0.04 - 1.2 cm
Kurata's Filter [4]	: 0.1 - 0.3 cm
Tanaka's Filter [5]	: 0.3 - 1.2 cm
Trifunac's Filter [6]	: 0.4 - 2.3 cm

It is seen that the error in the calculated displacement with the variable filter is remarkably small in comparison with others. It will be noted, however, that the filter with the smallest error is not necessarily the best filter because the smaller error is a result of narrower frequency range.

Conclusions

The following are concluded about the integration of strong-motion acceleration records:

(1) Errors generated during the digitization process exist in a wide frequency range. They generally become higher as the frequency decreases. The errors depend on each record, but it is considered to be limited to some amount.

(2) S/N, frequency band, and records have the following relation. If levels are specified for two items among them, the level for the other will be automatically determined. The higher the level of one item is, the lower the level of the other is, if the level of the rest is fixed. Here, the heights of levels denote S/N level, frequency bandwidth, and number of records.

(3) For the Annual Report on Strong-Motion Earthquake Records in Japanese Ports published by the Port and Harbour Research Institute, records whose maximum horizontal component is greater than 50 gals are integrated. For these records, two kinds of filters are applied; one maintains a fixed frequency range and the other is expected to maintain constant S/N.

(4) In the case of fixing frequency band of the fixed filter, it is considered that the appropriate lower boundary is 0.1 - 0.3 Hz, and in the case of fixing S/N, appropriate S/N level is 2 - 5.

(5) Sharpness of roll-off of the filter is desired to be neither extremely sharp nor extremely mild.

(6) Two filters have been proposed; one is a Fixed Filter for fixing frequency band and the other is Variable Filter for maintaining S/N.

References

1. Iai, S., Kurata, E., and Tsuchida, H., Digitization and Correction of Strong-Motion Accelerograms, Technical Note of the Port and Harbour Research Institute, No. 286, March, 1978, 56 p. (in Japanese).

2. Kurata, E., Iai, S., and Tsuchida, H., Annual Report on Stong-Motion Earthquake Records in Japanese Ports (1976 and 1977), Technical Note of the Port and Harbour Research Institute, No. 287, March 1978 (in English).

3. Kurihara, C., and Sakurai, A., Integration of Earthquake Acceleration, Journal of Technical Laboratory Central Research, Institute of Electric Power Industry, No. 68077, June 1969 (in Japanese).

4. Trifunac, M. D., Low Frequency Digitization Errors and a New Method for Zero Baseline Correction of Strong-Motion Accelerograms, California Institute of Technology, Report No. EERL 70-07, September 1970.

5. Tanaka, T., Morishita, T., Oosawa, A., and Yoshizawa, S., On the Correction of Records Obtained by Strong-Motion Accelerographs, Proc. of Symposium of Architectural Institute of Japan, October 1972, pp. 411-412 (in Japanese).

6. Tsuchida, H., and Kurata, E., Observation of Earthquake Response of Ground with Horizontal and Vertical Seismometer Arrays, Proc. the Forth Japan Earthquake Engineering Symposium, November 1975, pp. 137 - 144 (in English).

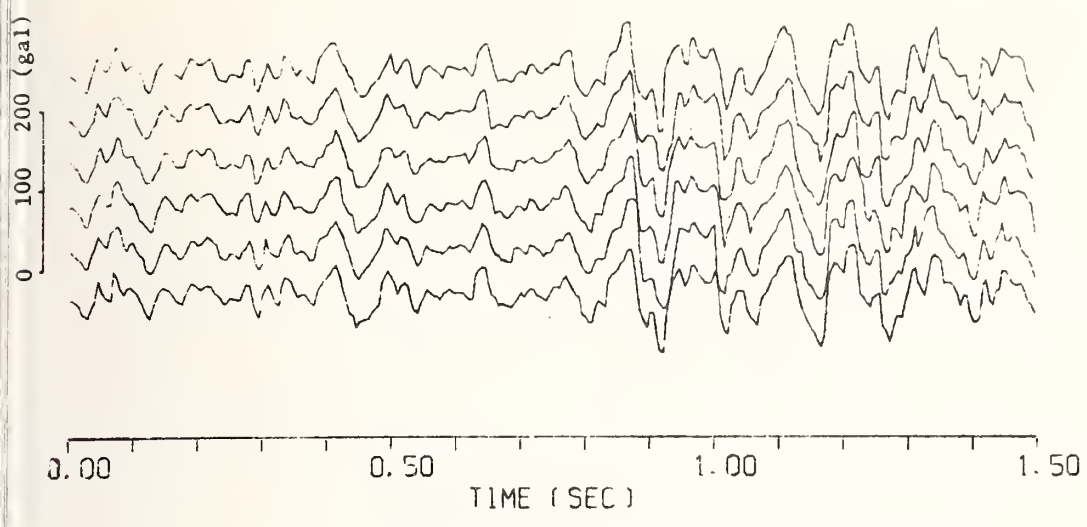

FIGURE 1: A PORTION OF REPEATED DIGITIZATION (M-125 N-S)

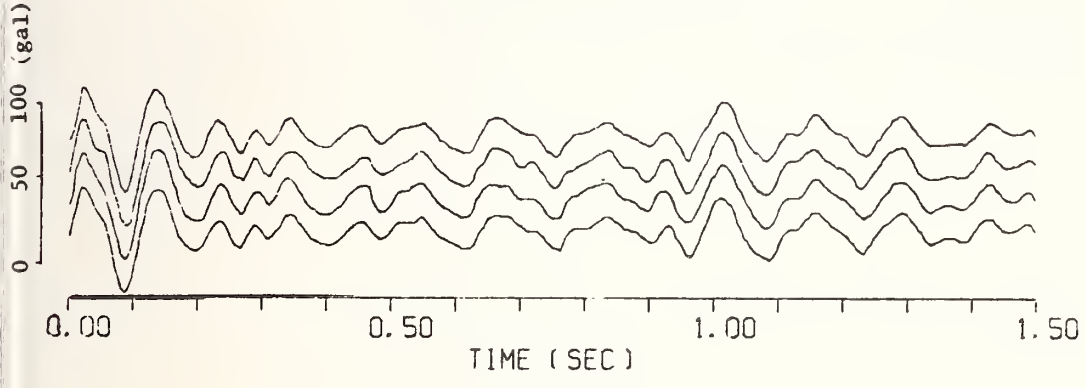

FIGURE 2: A PORTION OF REPEATED DIGITIZATION (M-133 N-S)

TABLE 1: SPECIFICATION OF REPEATED DIGITIZATION

Record Number	Length of Digitized Portion (sec)	Number of Repeated Digitization				Sampling Intervals (sec)
		Total	Operators			
			A	B	C	
M-125 N-S	12.5	6	2	2	2	0.0025
M-133 N-S	10.0	4	2	0	2	0.0025

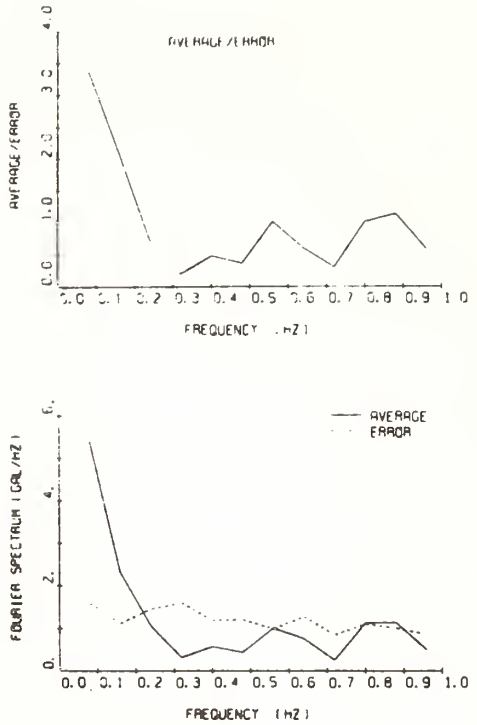

FIGURE 3: ACCURACY OF DIGITIZATION IN LOW FREQUENCIES (M-125 N-S)

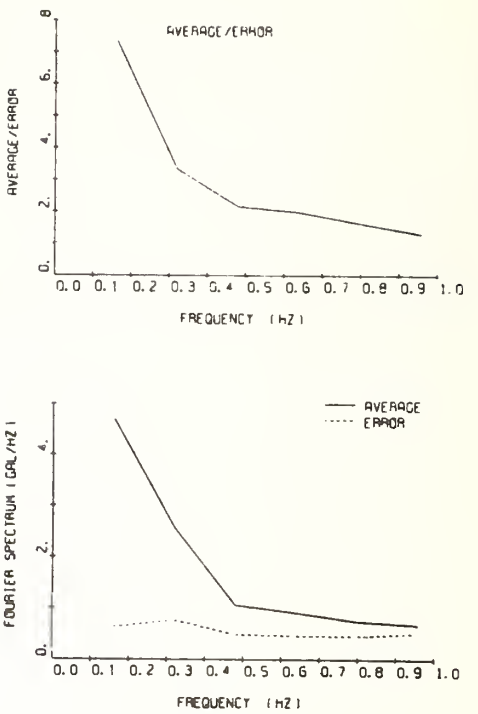

FIGURE 4: ACCURACY OF DIGITIZATION IN LOW FREQUENCIES (M-133 N-S)

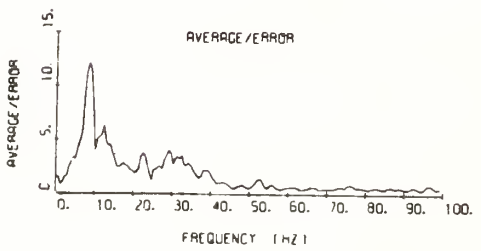

FIGURE 5: ACCURACY OF DIGITIZATION (M-125 N-S)

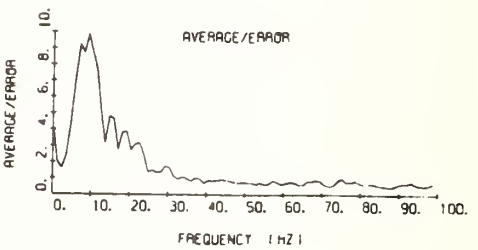

FIGURE 6: ACCURACY OF DIGITIZATION (M-133 N-S)

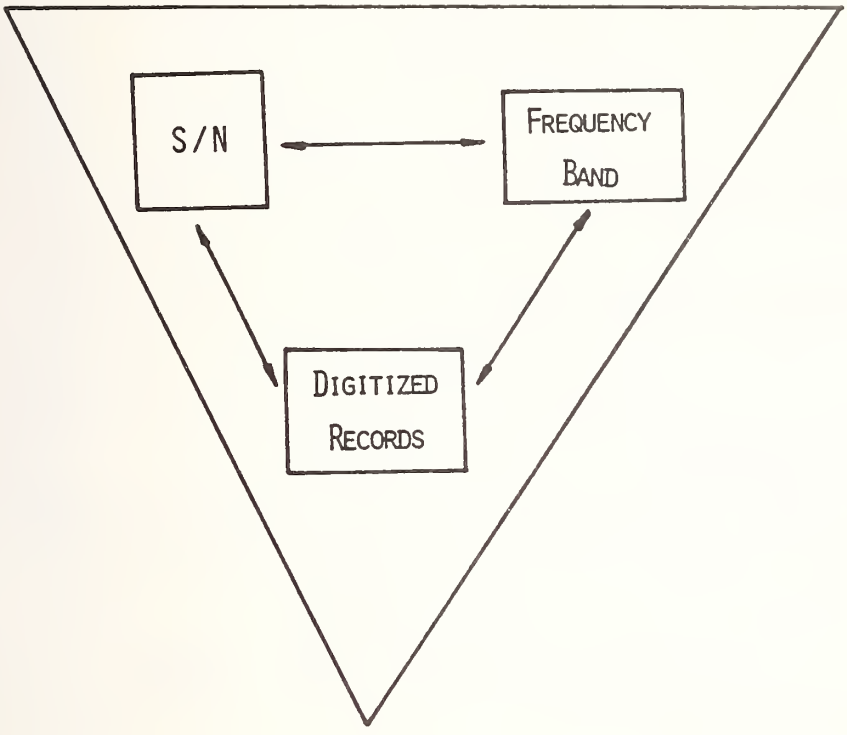

FIGURE 7: RELATION BETWEEN S/N, FREQUENCY BAND, AND DIGITIZED RECORDS

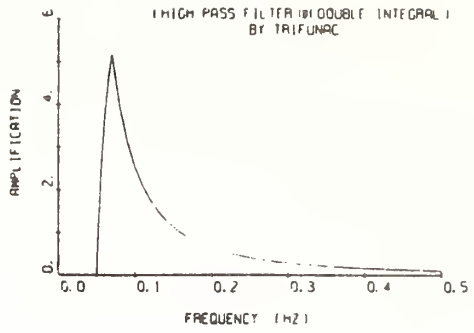

FIGURE 8(a): DOUBLE INTEGRATED FILTER BY TRIFUNAC[4]

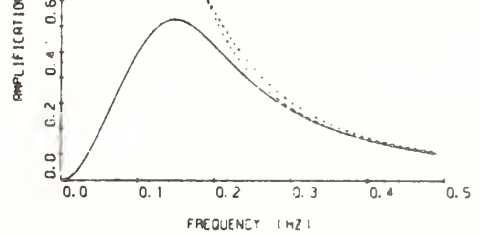

FIGURE 8(b): DOUBLE INTEGRATED FILTER BY KURATA[6]

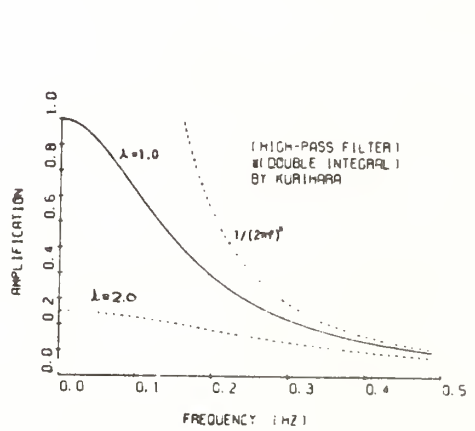

FIGURE 8(c): DOUBLE INTEGRATED FILTER BY KURIHARA[3]

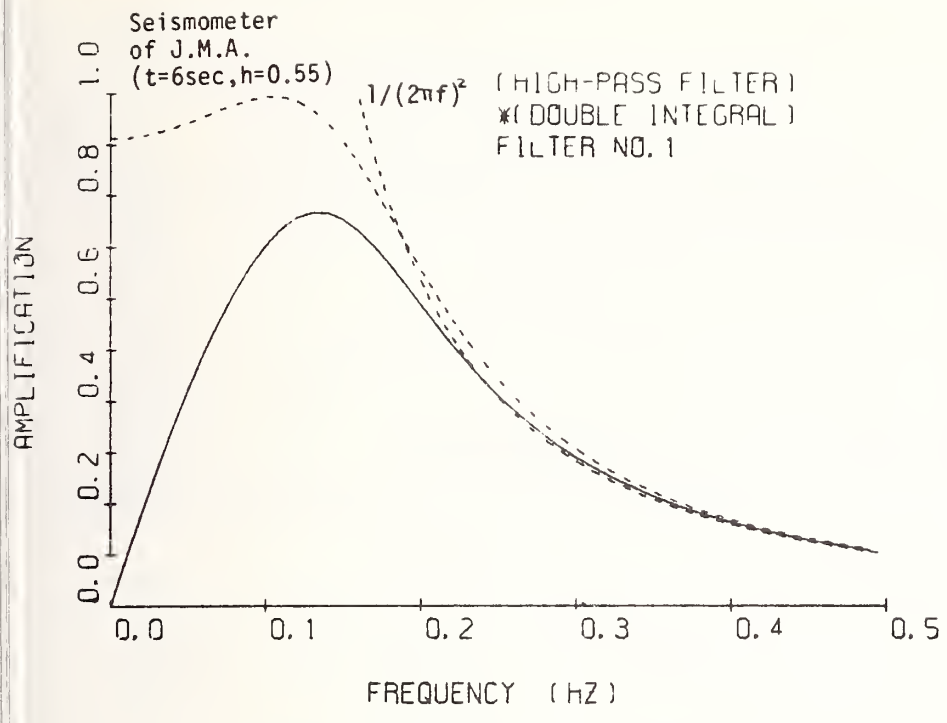

FIGURE 9: FIXED FILTER (DOUBLE INTEGRATED)

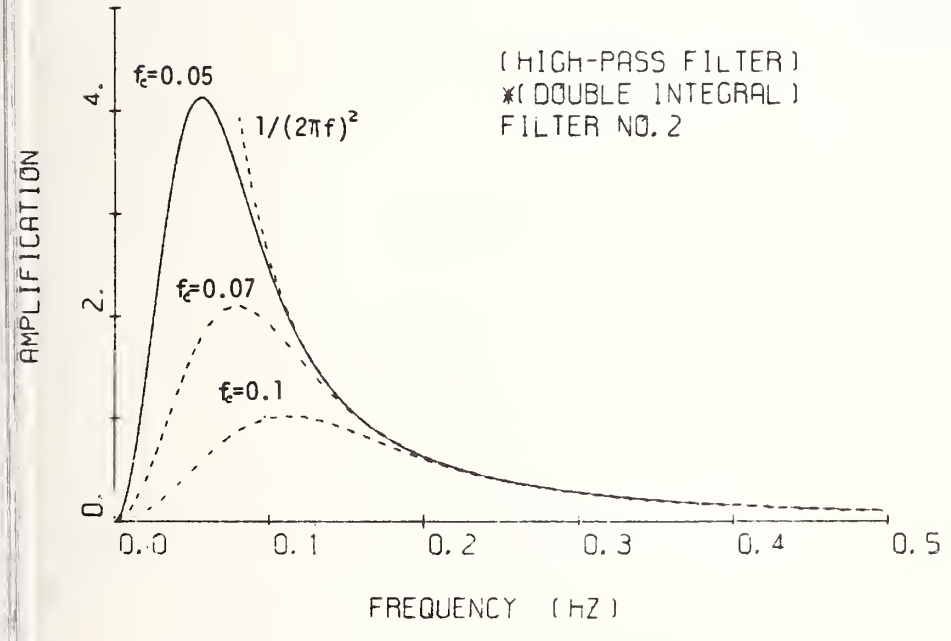

FIGURE 10: VARIABLE FILTER (DOUBLE INTEGRATED)

7

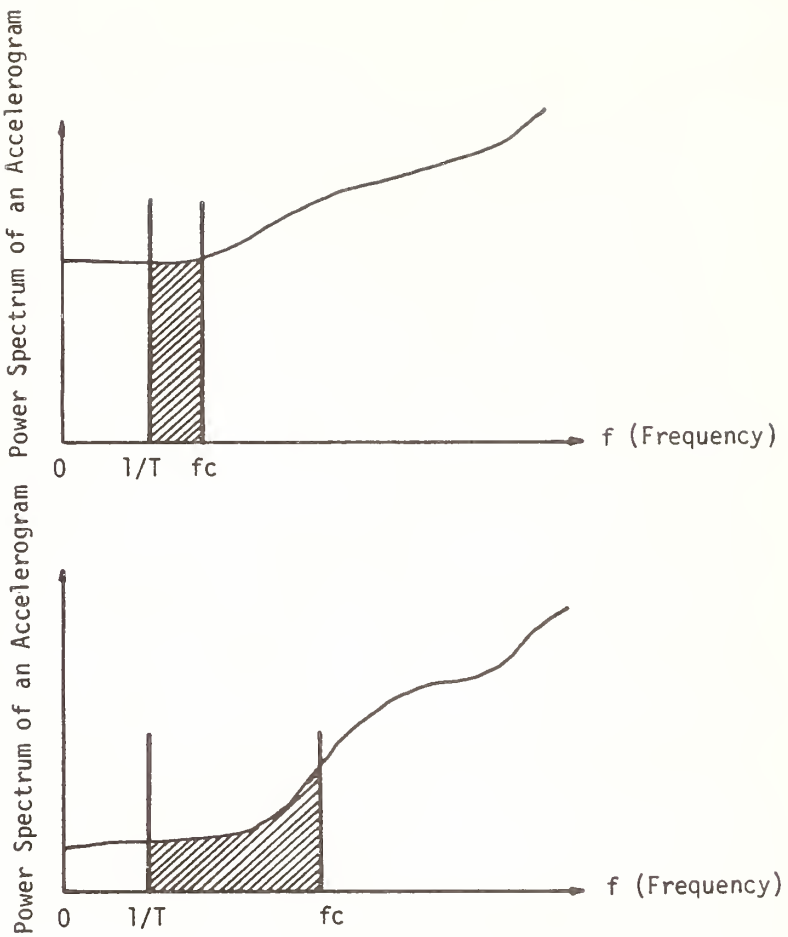

FIGURE 11: SIMPLIFIED ILLUSTRATION OF DECISION PROCEDURE OF FC

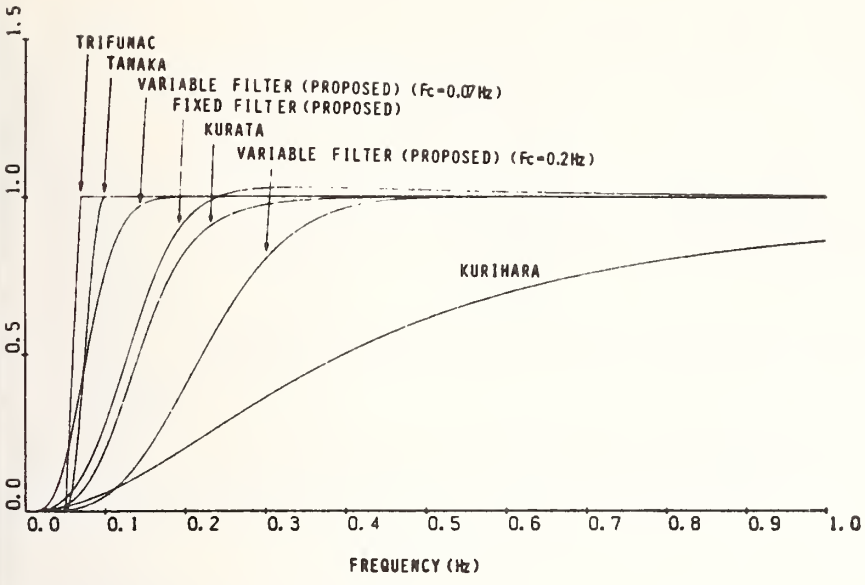

FIGURE 12: COMPARISON OF FILTERS PROPOSED SO FAR

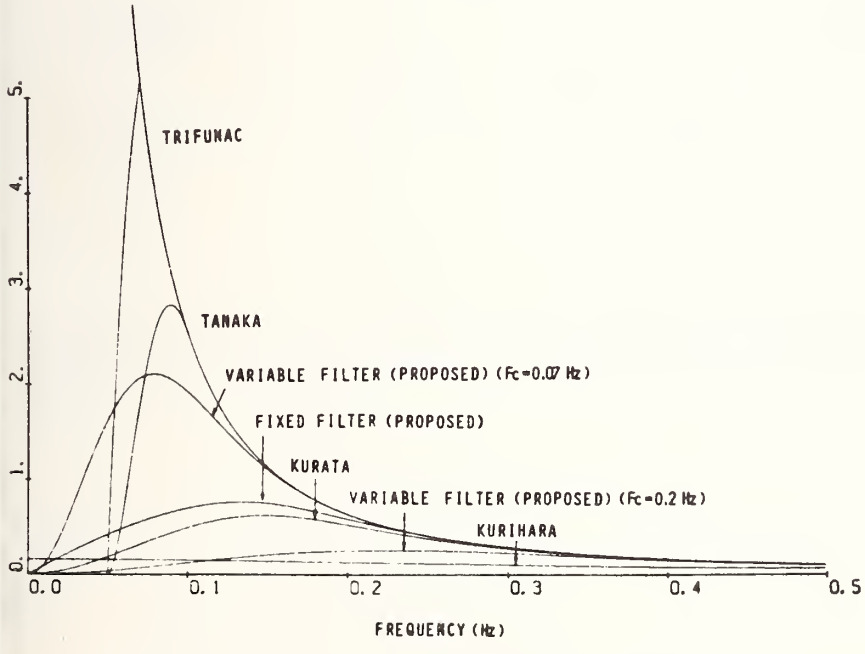

FIGURE 13: COMPARISON OF FILTERS PROPOSED SO FAR (DOUBLE INTEGRATED)

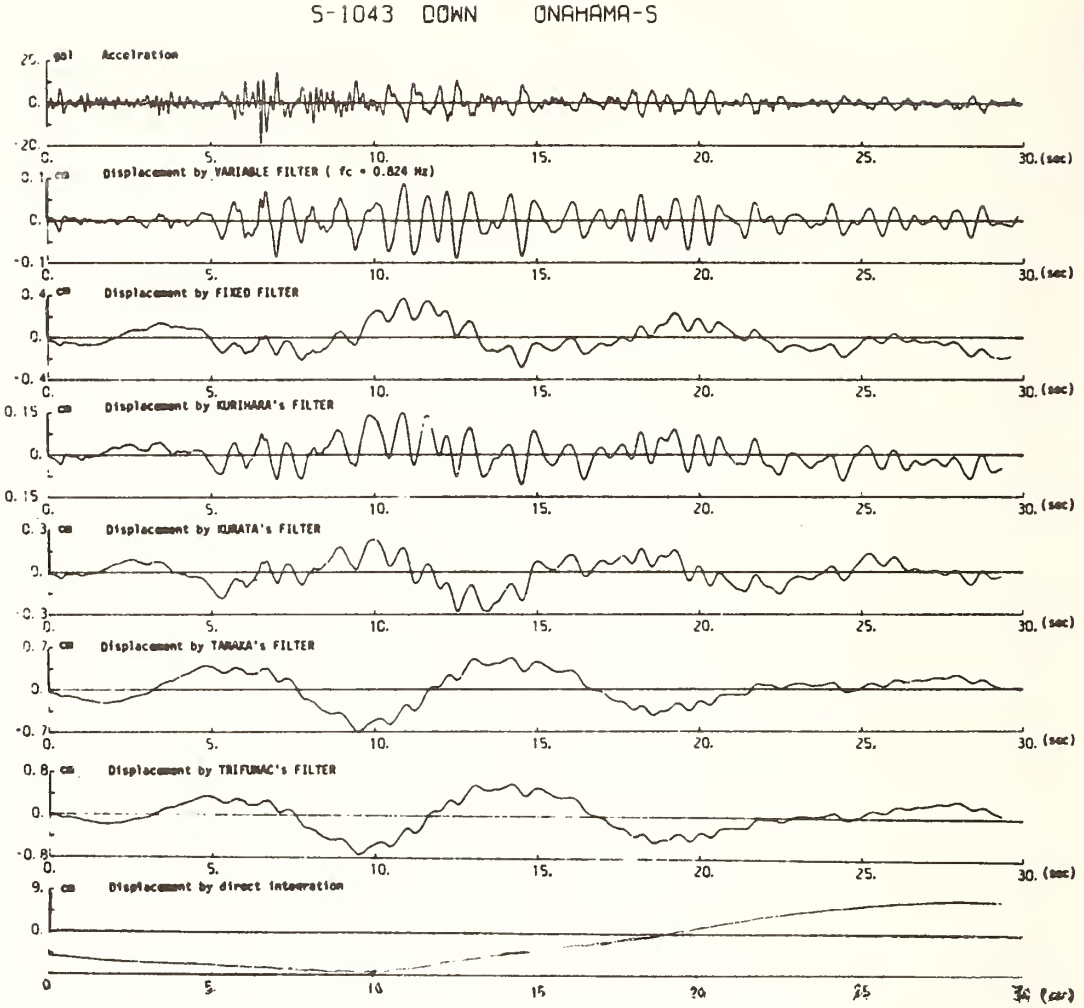

FIGURE 14: AN EXAMPLE CALCULATION OF DISPLACEMENTS BY THE FILTERS PROPOSED SO FAR

8

SOME RECENT DEVELOPMENTS IN NATIONAL AND INTERNATIONAL SEISMIC DATA EXCHANGES

James F. Lander

National Geophysical and Solar-Terrestrial Data Center
Environmental Data Service, NOAA
Department of Commerce

Some Recent Developments in National and International Seismic Data Exchanges

lmost since its beginning, seismology has been an international cience. The fact that stronger earthquakes are recordable at great istances was first observed in 1889 and gave rise to the need to entralize certain data-handling activities internationally. The se of this data has given invaluable insight into the distribution f earthquakes, the properties of the earth's interior, the move- ents of continents, and the cause of earthquake.

Activities in data observations and exchange are expanding and hanging under the pressure of new applied research programs, such s the U.S. Earthquake Hazards Mitigation program, and new oppor- unities are arising in the use of digital technology. This paper riefly reviews some of the trends in seismic data exchange, reports n the status of a number of data-related activities particularly s this involves World Data Center-A and NOAA data activities, and utlines some of the problems to be faced by data centers in the mmediate future.

rends

s an overview, three phases in international data exchanges are onsidered. The first is characterized by the exchange of observed eismic phase data (station bulletins) and graphical or hand- alculations of epicenters. Beginning in 1918 the International eismological Summary (ISS) began to collect and publish seismic eports for numerous stations and to calculate the source of the arthquake. This continued through 1963. It essentially ceased hen ISS was unable to cope with the large quantities of data that egan to become available after World War II. It could not adapt o the use of the digital computer then coming on the scene. The ask was taken over by the International Seismological Centre, hich from the beginning used digitial computers, including com- uter composition of manuscripts. The Bureau Central International e Seismologies was active in the early 1950s and 1960s in compil- ng data on many earthquakes that ISS was unable to include. The unction was no longer needed as the ISC was able to provide full overage. In 1976 the BCIS was terminated and replaced by the egional European-Mediterranean Seismological Center.

The preliminary Determination of Epicenters program also ncreased its activity in the 1950s to provide a fast data service, nd was able to make the switch to computer-processing in the early 960s to meet needs for improved quality and quantity of data.

In 1957 the International Geophysical Year saw the installa- ion of stations in Antarctica and other remote places. It also aw the establishment of the World Data Center system, but the data xchanged were primarily station bulletins. Seismograms were xchanged only by writing to many observatories to borrow original ecords or copies. The records so borrowed were of unknown calibra- ion and in different formats.

The second phase was marked by the installation of the World- ide Standard Seismograph Network beginning in 1961. For the first ime a global network of data in standard form with excellent timing nd known response characteristics was available at a reasonable ost. To date, the master file contains about 5 million records. staggering total of about 70 million copies have been distributed round the world. The benefits to science of this network are eyond calculation.

In 1974 the "Guide to Data Exchange through the World Data Centers" was changed to provide for automatic seismogram exchange for large or high-interest earthquakes. This brought in many more non-standard stations including those from the USSR network. To date, 22 events are included in the exchange and up to 300 stations are included in the program.

Lastly, we are moving into a phase characterized by digitial recording and processing of data. Initially, phase-arrival times were converted to digitial values and large quantities of data could be handled. The resulting digital hypocenters could be plotted automatically on maps.

In 1970, building on earlier experience including LASA, a Long-Period High-Gain network (HGLP) was established with instruments in environmentally controlled containers. An eleven-station network was installed worldwide. The digital recording allowed more sophisticated wave analysis than simple arrival time and amplitude. Soon, however, the higher gains that were possible by recording in bore holes at depths of 100 meters justified a network of Seismic Research Observatories (SRO). Some of the HGLP stations are being modified to have electronic characteristics similar to the SROs. A global network of up to 20 digitally recording gravimeters is being installed to provide information in the ultra low-frequency part of the spectrum. Also it was decided to modify 15 of the WWSSN stations for digital recording. Altogether this constituted a global digitally recording network of about 50 stations. Data from the network will be put on two network data tapes.

Digital recording is also being increasingly used for strong motion recording -- most of the important earlier analog records have been manually digitized and a new worldwide program for digital arrays is being planned. Ocean bottom seismometer recordings are also increasingly being used.

The IASPEI at its Durhan meeting recognized the importance of digital seismology by creating a Commission on Digital Seismology to promote its use and a Working Group on Digital Data Exchange in its Commission on Practice.

WDC-A is compiling an inventory of digital recording seismic stations worldwide and USGS is compiling a manual on the digital stations in the global Digital Seismic Network.

It is clear that the impact of this digital data will be very important for seismology and that the data centers must be prepared to modify their traditional services to provide the new services that will be needed.

This phase is also characterized by the growth of heavily instrumented, often temporary local and regional networks. These present unusual and largely unsolved problems for data archiving.

Current Activities

The historical development outlined above provides a perspective on current activities as is discussed over the next few paragraphs.

Analog Data

Advances in technology have made it possible to use essentially standard microfiche cameras to reproduce copies of seismograms on

108-mm film, 24 images to the chip. They have essentially the same resolution as cameras specially designed for seismogram filming 18 years ago. There will be considerable savings to the users. In July 1978, NGSDC will begin filming data from the WWSSN network in this format.

Historical Microfilming Project

WDC-A is beginning a project to microfilm seismograms from around the world with the support and technical guidance from the USGS. Through the project we hope to save a collection of records from selected stations worldwide for every day and from many stations for selected events. This year will be used for planning and acquiring equipment. Filming will begin next year with some North American data; and foreign participants will be contacted. The program may last five or more years and involve a photography team working with local experts and station directors. A Working Group in IASPEI will give advice to this project.

Digital Data

Of the Global Digital Seismic Network mentioned earlier the IDA data are already being distributed by NGSDC. The SRO digital data are available for use at the data center and I expect that within 3 to 9 months all the data from this station will be available through NGSDC and the World Data Center as network day tapes (two tapes per day) and stacked plots and punched cards. Additional data products may be offered as they become standard requests.

On May 2-5, 1977, there was an International Workshop on Strong-Motion Instrument Arrays in Honolulu sponsored by the (U.S.) National Science Foundation and UNESCO. It was decided to recommed as highest priority the instrumenting of six sites worldwide with an extensive array of strong-motion accelerometers in the hope of recording near-source activity in several kinds of geologic settings. Some instruments will be in bore holes, some centrally and digitally recorded. In all, some 28 sites were recommended for instrumentation. This program promises to be as important to the near field studies as the WWSSN program was to global seismology. We expect to have this data in the World Data Center system.

The need to develop seismic histories has long been felt. Having such information on computer readable files is even more advantageous in that huge files can be searched for events of particular characteristics such as locations, size, depth, etc. In the mid-1960s the Coast and Geodetic Survey started to compile such a computer file. The file now has data from 11 sources including the PDE and ISS and information on nearly 150,000 earthquakes. This file is actively being expanded and will have data from 23 sources by this summer (including the UMA file). We are collaborating with the USGS in this (see Table 1).

Internationally, an even more ambitious project is being proposed. An IASPEI Working Group on Global Digital Data Bases met in Paris in March with UNESCO support to design a definitive Global Seismic Data Base. It was recommended that an activity be attached to the ISC to develop a comprehensive file representing the best possible values. This file would include a substantial amount of pre-instrumental data, some of it several thousand years old. Funding for this project is being sought.

One of the oldest seismic data bases is intensity data. This data form is particularly useful for engineers. It, too, can benefit

from digitization and analysis. We have developed a computer file of about 115,000 felt reports mostly from the U.S. Earthquake periodical (1928-1975). This file has information on the date, location and magnitude of the earthquake, and location and intensity of the community reporting the effect. It allows the listing of felt reports in locations adjacent to sites of interest, construction of maximum reported intensity maps, and analysis of regional variations of intensity and its attenuation with distances. This file is being checked and will be available this fall.

The Modified Mercalli Scale of 1931 consists of 12 steps. Each step is defined by a number of descriptives or elements. Mr. R. J. Brazze, an NGSDC scientist until recently, completed an analysis of how each element behaved with respect to attenuation and found a number of apparently misplaced elements in the scale. His analysis "Re-evaluation of the Modified Mercalli Scale for Earthquakes Using Distance as a Determinant" shows where items not formally in the scale would fit. His study has opened up the way for a quantitative re-evaluation of the MM scale, including using weighting factors, and for computer evaluation of past and future intensity reports.

The World Data Center-A for tsunamis was relocated from Honolulu to Boulder in 1974. It had not been particularly active as part of the International Tsunami Information Center. In the intervening period, a catalog of tsunamis for Alaska and Hawaii were updated and reissued. All of the mareograms showing tsunamis are being microfilmed. We have copied the most recent ten years of U.S. records and will complete the microfilming project in a year for nearly 100 years of records. We are making a collection of photographs of tsunami effects. The present Guide for data exchange in tsunamis lists only a few stations as participating in the exchange. A new Guide is in preparation. WDC-A is in a position to digitize selected tsunami records and to prepare special packages of seismic data including focal mechanisms of interest to tsunami records. The international exchange of data for tsunamis is far less well developed than the seismic data and probably should be improved.

The World Data Center-A has been supportive of various international projects. For the current International Geodynamics Project we are publishing data and information publications such as the Geodynamics International Series and data publications such as the "Summary of Earthquake Focal Mechanism for the Western Pacific -- Indonesian Region" and a World Heat Flow Map. For the U.S. Geodynamics program we are just completing a Directory of U.S. Data Bases that are relevant to the Geodynamics Project. We expect to provide similar or other needed services for the upcoming Crustal Dynamics Program.

Next year there will be a project involving observations of seismic activity on the ocean floor called Project ROSE. Approximately 60 ocean bottom seismometers will be used in an array on the River Fracture zone near the tip of Baja California. The data will be digital and eventually released through the data center system.

Finally, I should mention our guest worker program. Because of the growing size of the data bases and the need to use sophisticated search and retrieval systems it is often useful for scientists to visit the data center and spend more days, weeks, or years in residence. NGSDC supports such visits through a variety of mechanisms and to varying degrees. Scientists in the Solar-Terrestrial Physics part of our data center have availed themselves of this

opportunity to a considerable degree -- particularly Japanese scientists. Dr. Yukutake, a Geomagnetician, spent 6 months with the center last year. Inquiry is invited.

Problems and Opportunities

From the activities described above it is clear that major changes in data services will be made possible because of the new digital environment. Data centers must continue to supply analog and interpreted data to less sophisticated users, be active in proselytizing the new techniques, and must provide advanced services for advanced users. The latter includes expertise in use of computers, remote terminals, interactive graphics, advanced plotters and digitizers, and data base management systems, as well as advances in science.

A second problem area is the expansion of the user base to areas outside classical seismology. The earthquake prediction, energy exploration, geodynamics, and natural hazards programs are examples of new emphasis activities that bring a wide range of user types and related but different data sets such as tilts, gravity, and heat flow mechanisms. There is a growing need for data synthesis for different uses and users.

A third set of problems come from a change in scale of many needs and projects. We find our data bases that are so good in solving global problems are inadequate on the local scale. At present, there are many projects to observe small areas intensely in a variety of ways for a limited period of time. We must discourage the use of global data for local problems. What part of these data may be of use to other and future users? This question has not been examined in detail.

The opportunities are great for providing data worldwide as a resource for science and its applications. The lesson from the past is clear! Keep up or drop out.

TABLE 1: SEISMIC DATA FILES IN HDF - MAY 1978

1. Preliminary Determination of Epicenters 1937-1977
2. United States Earthquakes 1928-1975
3. Gutenberg and Richter "Seismicity of the Earth" 1899-1952
4. Southern California - Cal Tech 1932-1975
5. Northern California - Berkeley 1910-1975
6. Earthquake History of the U.S. 1638-1970
7. Central California Regional Network 1969-1973
8. Coastal and Offshore Earthquakes of the Pacific Northwest 1853-1973
9. Seismicity of the European Area - Karnik 1901-1955
10. International Seismological Summary 1918-1961
11. Bulletin Mensuel ECIS 1950-1961
12. OCSEAP 1973-1977

9

REPORT ON THE INTERNATIONAL WORKSHOP ON STRONG-MOTION EARTHQUAKE INSTRUMENT ARRAYS MAY 2 - 5, 1978, AT HAWAII

Tadayoshi Okubo

Ministry of Construction

and

Hajime Tsuchida

Ministry of Transport

Report on the International Workshop on Strong-Motion Earthquake Instrument Arrays

May 2-5, 1978, at Hawaii

n July 1977, the International Association for Earthquake Engi-
eering (IAEE) appointed a Steering Committee for planning an Inter-
ational Workshop on Strong-Motion Earthquake Instrument Arrays.
ne first meeting of the Steering Committee was held October 17 -
3, 1977, at Caltech and resolved the following:

- Primary Workshop Goal

  The primary goal of the Workshop was to develop a workable plan for the possible future deployment of dense strong-motion earthquake instrument arrays with primary emphasis on ground motion studies.

- Workshop Content

  The major application areas that should be considered are

  - Source Mechanism Studies
  - Wave Propagation Studies (Source to Site)
  - Local Effects

  and the major subject areas of the Workshop are

  - Favorable Array Locations
    - Tectonic environments
    - Site conditions
    - Short-term and long-term rate of data recovery
    - Operating costs over direct instrument related costs
    - Local technical and operating assistance
  - Array Design
    - Number and distribution of arrays
    - Array configurations
      - Number of dimensions
      - Extent
      - Geometry
      - Density
    - Instrumentation
      - Specifications
      - Capital cost
    - Array Construction; technical and economic considerations
      - Site studies
      - Site preparation
      - Equipment installation
    - Array Operation; technical and economic consideration
      - Instrument maintenance
      - Data retrieval, processing, archiving and distribution

9

- Implementation
  - Organization Plan
    - Adequacy of existing organizations
    - Modes of international cooperation
    - Unique contributions of different countries

Because the major subject areas had to intersect with each of the application areas and vice versa, the content of the Workshop was thought of in terms of a type of matrix as indicated in Table 1.

Resolution

After five days, the Workshop published the following resolution:

Resolution of International Workshop on
Strong-Motion
Earthquake Instrument Arrays
May 2-5, 1978
Honolulu, Hawaii

The protection of life and property from the devastating effects of earthquakes is an urgent worldwide problem. An understanding of the nature of strong earthquake motions is of crucial importance in solving this problem. At the present time, however, there is a scarcity of engineering data acquired near the center of destructive earthquakes and existing instrument arrays are inadequate to provide the necessary data. Yet there is a high probability of occurrence of destructive earthquakes in different parts of the world in the next decade. The participants in this international workshop unanimously recommend the earthquake-threatened countries and other concerned countries and organizations make a concerted effort to establish a comprehensive worldwide system of specialized strong-motion earthquake instrument arrays capable of resolving the nature of the earthquake source mechanism, wave propagation, and local site effects. As a first step, the following specific recommendations should be implemented.

- The International Association for Earthquake Engineering in collaboration with the International Association for Seismology and Physics of the Earth's Interior form an International Strong-Motion Arrays Council.

- The earthquake-threatened countries individually and collectively initiate the immediate installation of minimal arrays of 10 strong-motion instruments at least at the 28 worldwide sites identified by this Workshop.

- High priority be given to the design and installation of more elaborate source mechanism, wave propagation, and local effects arrays particularly at the 6 critical sites identified.

- A mobile strong-motion instrument array capable of making source mechanism, wave propagation, and local effects measurements be established and maintained for deployment to sites immediately following the occurrence of a major earthquake for measurements of aftershocks.

TABLE 1: INTERACTION BETWEEN MAJOR SUBJECT AREAS AND APPLICATIONS INDICATING WORKING SUBGROUP ASSIGNMENTS

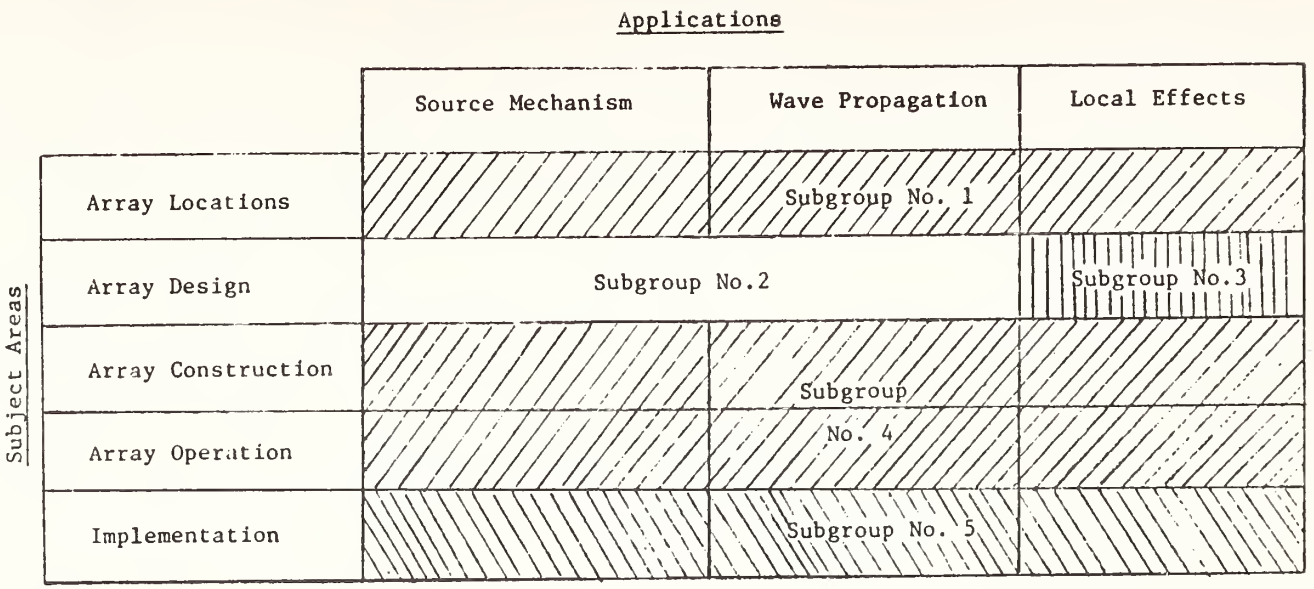

10

EXPECTANCY OF MAXIMUM EARTHQUAKE MOTIONS IN JAPAN

Makoto Watabe
Yoshikazu Kitagawa

Building Research Institute
Ministry of Construction

In the Seismological Bulletin of the Japan Meteorological Agency[2], all the relevant information on earthquakes are reported monthly. The location of the J.M.A. stations and the characteristics of strong motion seismometers used by J.M.A. are shown in Figures 1 and 2. The phase time of P- and S- waves, the maximum displacement amplitude for EW, SN, and UD components, the predominant period of seismic wave, the initial motion for each component, the epicentral distance, and the P-S time are described in List 4 of the J.M.A. Bulletin. These data are transferred to a single card and stored on magnetic tape under the station name.

The data used in this paper are mainly the maximum amplitude and the predominant period for the period of 1967 to 1973. The number of data for each year is shown in Figure 3. In addition, the magnitude reported in the J.M.A. Bulletin (List 3) is determined by Tsuboi's formula, so that we used only the earthquake data with depth $D \leqq 60$m because the earthquake damage to structures is caused by shallow earthquakes with depth $D < 60$ Km. Further, Tsuboi's formula is limited to earthquakes with depth $D \leqq 60$ Km.

Analytical Method

The ground motion in frequency domain (G(jw)) will be generally expressed in the following equation:

$$G(jw) = FS(jw) \cdot EA(jw) \cdot MT(jw) \cdot EC(jw) \cdot ST(jw) \quad (1)$$

where FS(jw) means the spectrum of focal mechanism, EA(jw), MT(jw), and EC(jw) represent the transmission function around the hypocenter, the function in the mantle-rock, and the function of the wave propagation in soil layers. Now equation (1) can be reexpressed as the following equation:

$$G(jw) = FS(jw) \cdot TF(jw) \cdot ST(jw) \quad (2)$$

where TF(jw) means the overall transmission function for the generation of waves at the hypocenter and the propagation of earthquake waves. Then all functions in equation (3) can be combined as follows,

$$G(jw) = FS(jw) \cdot TF(jw) \cdot ST(jw) \quad (3)$$

$$= FS\ (jw) \cdot TF(jw) \cdot ST(jw) \quad (4)$$

The equations (3) and (4) stand for the theoretical seismic records based on the focal mechanism and for the ground motion.

On the other hand, the long period ($10.0 \geqq T \geqq 1.0$ sec.) corresponding to the ground characteristics in a fairly large area is amplified by depth varying from a few hundred meters to 1 to 2 kilometers. The short period ($T \leqq 1.0$ sec.) corresponding to the ground characteristics beneath a structure is affected by depth of soil less than a few hundred meters.[3,4,5]

In this paper, the study is carried out from the viewpoint of equation (4) in the range of long period ($6.0 \geqq T \geqq 2.0$ sec.).

The magnitudes (M) reported in the J.M.A. Bulletin are determined by following Tsuboi's formula.

10

$$M = \frac{1}{2} \log (A_{NS}^2 + A_{EW}^2) + 1.73 \log \Delta - 0.83 \quad (5)$$

where A_{NS}, A_{EW}, and Δ are the maximum displacement (μ) in NS and EW components, and the epicentral distance (km), respectively. When the values of A_{NS} and A_{EW} in equation (5) for a single earthquake are observed at various stations of J.M.A., the mean value of magnitude is reported as the magnitude of the earthquake in Bull. of J.M.A.

From equation (5), the root mean square value (R.M.S.) of the maximum displacement amplitudes in NS and EW components is expressed in the following equation,

$$\sqrt{A_{NS}^2 + A_{EW}^2} = 10^{\beta} \quad (6)$$

where $\beta = M - 1.73 \log \Delta + 0.83$

As mentioned above, since the magnitudes in the Bulletin are the average ones determined by equation (5) from many observation stations, then the value of 10^{β} can be regarded as a standard value of R.M.S. of maximum displacement amplitudes.

Under the assumption that the value of 10^{β} is always regarded as the standard one in the range of long period ($6.0 \geq T \geq 2.0$ sec) reflecting the deep ground characteristics in fairly large area, the following values are calculated at every J.M.A. station,

$$F = \frac{1}{m} \sum_{i=1}^{m} \left[\sqrt{A_{NS}^2(T_i) + A_{EW}^2(T_I)} \; / \; 10^{\beta} \right] \quad (7)$$

$$f = \frac{1}{m} \sum_{i=1}^{m} \left[\sqrt{A_{NS}^2(T_I) + A_{EW}^2(T_i)} - 10^{\beta} \right] \quad (8)$$

or

$$F_{st} = \log | f |$$

where T and m denote the period of the phase giving maximum displacement amplitude and the total number of the earthquake data, respectively. Consequently, the values of F and f (or F^{st}) denote the mean and the variation of the observed values to standard ones at each station of J.M.A.

On the other hand, since the period T being reported has an interval of 0.1 sec in the Bulletin, it is most advisable to vary T. However, the maximum displacement amplitude in NS and EW components are neither always in the same phase nor in the same period. In this study, the concept of the period window ΔT is introduced, such as $\Delta T = T_i \pm 0.2$ sec (in case of J=3), $\Delta T = T_i \pm 0.3$ sec (in case of J=4), and $\Delta T = T_i \pm 0.4$ sec (in case of J=4), where T_i dnotes the medium value of the period window and represents the predominant period of seismic wave.

In addition, the values of F, f (or Fst) with period T_i are smoothed by the weighted mean method.

Regional Distribution of Ground Characteristics

Figures 4 and 5 show the curve of F and F_{st} values calculated by equations (7) and (8) and the number of the earthquake data for the case of J=3, 4, and 5 at Tokyo. Judging from these figures, the number of earthquake data for the case of J=3 and 5 are more than 15 and under 50 in the range of period $T \geqq 4.0$ sec, respectively, and the values of F are little larger than 1.0 and 2.0 - 8.0 in the range of period $T \leqq 3.6$ and period $T \geqq 3.6$, respectively. There is good agreement among the curves of F values vs. period for the case of J=3, 4, and 5 and the characteristics of F and F_{st} values correspond well. Consequently the degree of the "quakability"* is high in the range of fairly long period.

On the other hand, the characteristics of F values look to be more suitable than F_{st} values as the magnification factor of ground characteristics. As a result, the characteristics of F values are mainly dealt with here.

Judging from the characteristics of F value at all stations of J.M.A., the pattern of the characteristics mentioned above is divided into two main classes: (1) there is no great difference among J=3, 4, and 5; (2) there is a remarkable difference among J=3, 4, and 5. In the first case, it means that the earthquake data for all cases are almost identical or enough so not to affect the whole characteristics in number. In the second case, quite new data are introduced by making ΔT larger; these data have a great effect on the characteristics of F values.

Therefore, the criterion for the evaluation in this paper is as follows: the result of J=3 in the first case, and the result of a small J number in the second. Under these criteria, the regional distribution maps of F values corresponding to the period of 1.0, 2.0, 3.0, 4.0, 5.0 sec. are contoured in figures 6(a)-(e). As seen in these figures, the areas where the magnification factor of the ground characteristics is considered to be high are generally as follows: the coast on the Japan sea in the Tohoku district from the Hokkaido district; the southern area of the Kwanto district from the area of the Kinki district; the southwestern area of the Shikoku district from the Kyushu district. However, these are general tendencies only.

Expectancy Based on Seismic Activity and Soil Characteristics

It is fairly difficult to know the detailed underground structure throughout Japan. However, to examine the ground structure down to a fair depth several experiments in the vicinity of Tokyo were carried out by the research groups of Dr. Y. Ohta[3-6] and Dr. E. Shims[7]. The former group analyzed the part regarded as S-wave on the seismographs at Tokyo under the Niigata earthquake (Model 1 and 2) and made their experiment by means of a SH-wave generator and in a deep borehole (Model 5). The latter group made seismic exploration tests in the Tokyo district (Model 3 and 4). These results are shown in Figure 7. As seen in Figure 7, the depth of the base rock with the shear wave velocity V_s = 2 - 3 km/sec is assumed to be 2 - 3 km. Figures 8(a)-(e) show the magnification factor (U_o/U_{in}) of the ground structure mentioned above by means of Haskell's method, assuming the incident wave travels from the base

10

---

* "Quakability" represents the degree of quake to the standard value.

rock. As seen in Figure 8, there is a tendency for the magnification factors in the range of long periods to resemble each other, but to be remarkably different in the range of short periods less than 1.0 sec.

The underground structure, representative of a fairly large area in the Tokyo district, can be geometrically determined. Figures 9 and 10 show the average underground structure in the Tokyo district and the magnification factor, respectively. Under the assumption that the average underground structure shown in Figure 9 is the underground structure at the Tokyo station of J.M.A., the standard ground characteristics shown in Figure 11 are inferred by dividing the magnification factor shown in Figure 10 with the characteristics of F value in Figure 4.

Consequently, the expectancy of the maximum earthquake motion on ground with V_s = 0.6 - 0.8 km/sec in the range of the long period ($6 \geq T \geq 2$ sec.) is represented by the products of three factors: the expectancy of maximum earthquake motion based on seismic activity on the base rock with V_s = 2 - 3 km/sec; the magnification factor of the standard ground characteristics; and the regional "quakability" of the soil layers. However, it should be remembered that the final regional distribution of the expectancy of earthquake motion will be different from that based on the seismic activity. In addition, the effects of ground characteristics just beneath the construction site and the concept of soil profile should also be introduced in future research.

Acknowledgments

This study was partially supported by the New Aseismic Design Method project monitored by Ministry of Construction, Japan[8]. The authors wish to express their thanks to Prof. M. Ozaki, Chiba University, and Dr. S. Hattori, Applied Seismology Division of I.I.S.E.E., for valuable discussion and advice in the course of this research; to Mr. Y. Serizawa and Miss K. Naito, ex-Member of B.R.I., for drawing figures and making fair copies; to Dr. S. Kawamura, Res. Eng. of Taisei Corporation, for his help with a large amount of earthquake data; to Miss M. Ota, Member of I.I.S.E.E., for typing.

References

1. Ozaki, M., Kitagawa, Y., and Hattori, S., "Study on Regional Distribution of Maximum Earthquake Motions in Japan," Ninth Joint Meeting, U.S.A. Japan Panel on Wind and Seismic Effects, UJNR, Tokyo, May 24-27, 1977.

2. The Seismological Bulletin of the Japan Meteorological Agency, 1967-1973.

3. Earthquake Excitation with Soil Classification Comparison of Ground Characteristics up to 10 second Period of Tokyo and Choshi by Low-Sensitivity Displacement Seismometer (in Japanese), Report for Establishment of New Aseismic Design Method, Ministry of construction, Japanese Government, 49-1-2-(2) Ken. Hou. 1, 1975.

4. Earthquake Excitation with Soil Classification -- On Seismic Wave Spectra and Subsurface Structure, Report for Establishment of New Aseismic Design Method (in Japanese), Ministry of Construction, Japanese Government, 50-1-2-(2), Ken Hou. 1, 1976.

5. Earthquake Excitation with Soil Classification -- A Point by Point Evaluation of Amplification Characteristics in Japan on Five Sec. Seismic Motions in Relation to Deep Soil Deposits (in Japanese), Report for Establishment of New Aseismic Design Method, Ministry of Construction, Japanese Government, 51-1-2-(2), Ren. Hou. 1, 1976.

6. Ohta, Y., Goto, N., Shiono, K, Takashashi, T., Yamamizu; F., "Shear Wave Velocities in Deep Soil Deposits -- Measurement in Borehole to the Depth of 3500 Meters at the Iwatsuki" (in Japanese), Proc. of Seismological Inst. of Japan, No. 1, 1977.

7. Shima, E. et al; Experimental Study on Generation and Propagation (in Japanese), Report of Tokyo Prevention Disaster Council, 1975.

8. Earthquake Excitation with Soil Classification -- On the Considerations of Earthquake Danger in and Around Japan (in Japanese), Report for Establishment of New Aseismic Design Method, Ministry of Construction, Japanese Government, 51-1-1-(2), Ken. Hou. 2, 1977.

FIGURE 1: LOCATION OF J.M.A. IN JAPAN.

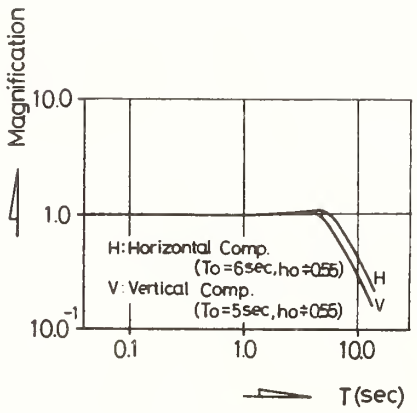

FIGURE 2: CHARACTERISTICS OF SEISMOMETER.

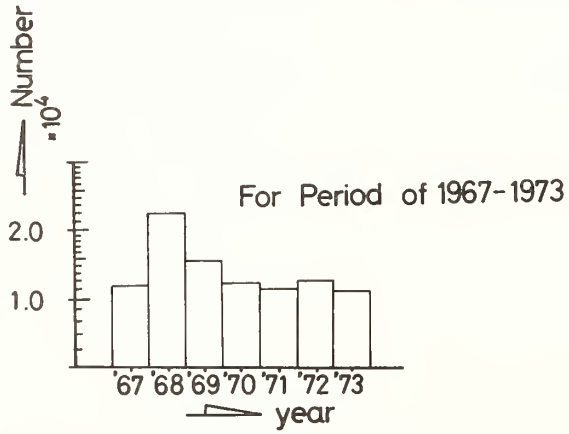

FIGURE 3: EARTHQUAKE DATA IN PERIOD OF 1967 - 1973.

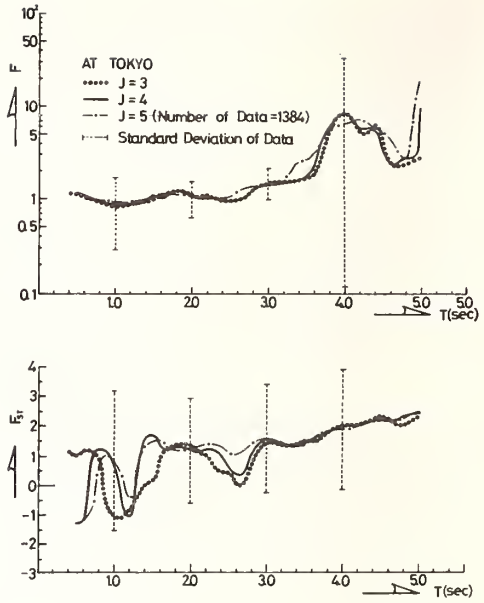

FIGURE 4: CHARACTERISTICS OF F AND F_{st} VALUES AT TOKYO STATION.

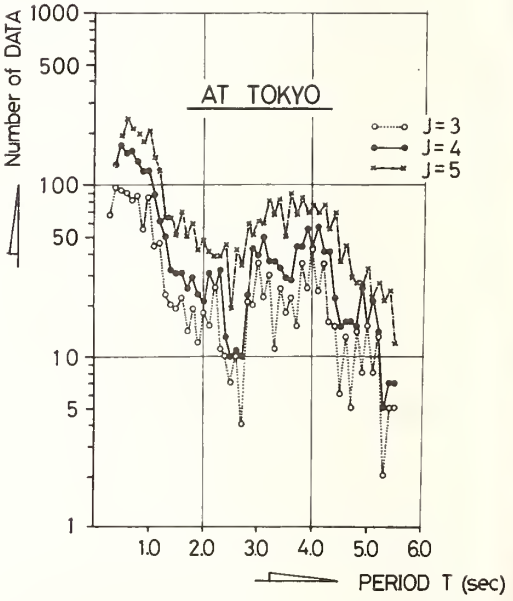

FIGURE 5: NUMBERS OF EARTHQUAKE DATA IN CASE OF J=3, 4, AND 5.

FIGURE 6: REGIONAL DISTRIBUTION OF F VALUES IN PERIODS OF 3.0, 4.0, and 5.0 SECONDS.

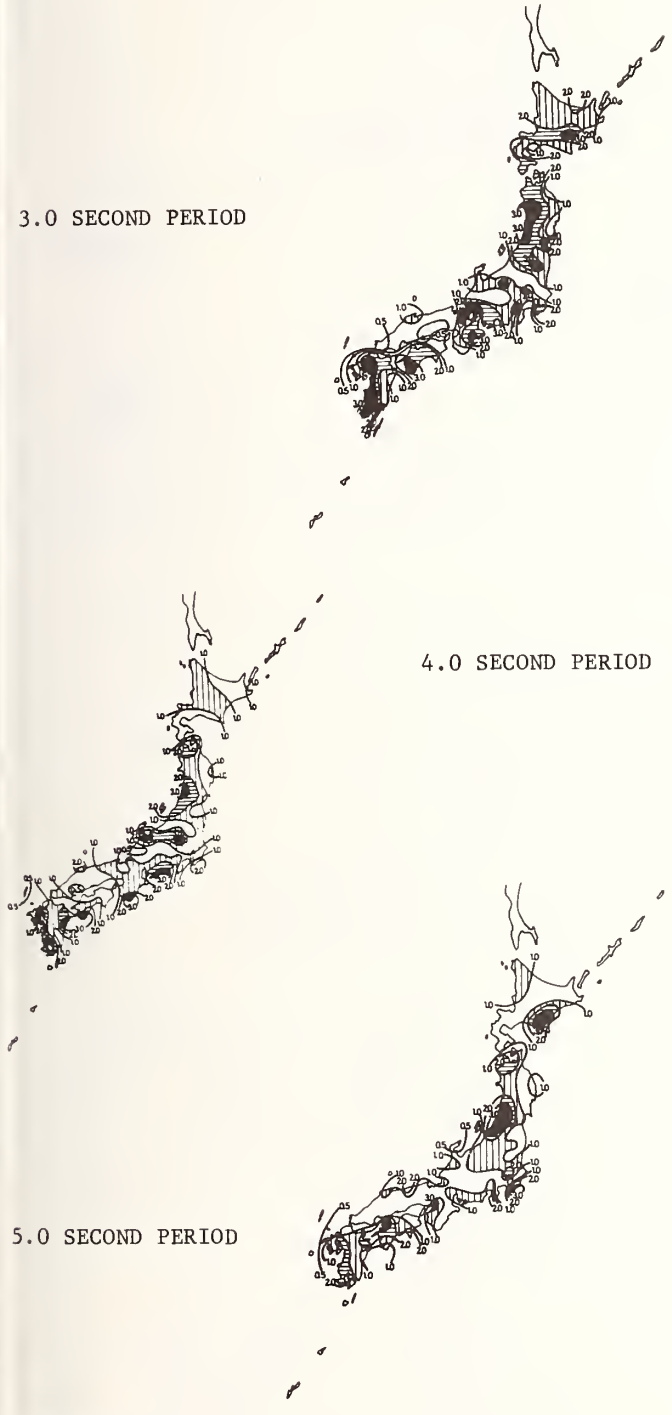

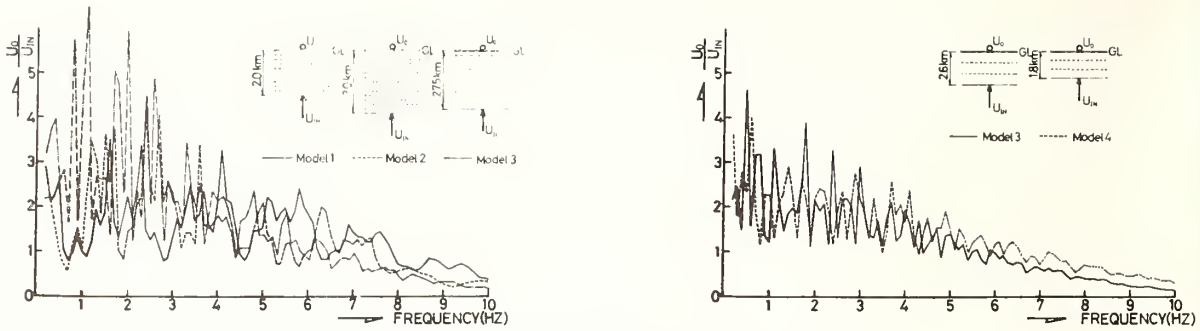

FIGURE 7: PROFILES OF UNDERGROUND STRUCTURES (AFTER DR. OHTA, DR. SHIMA, ET AL.)

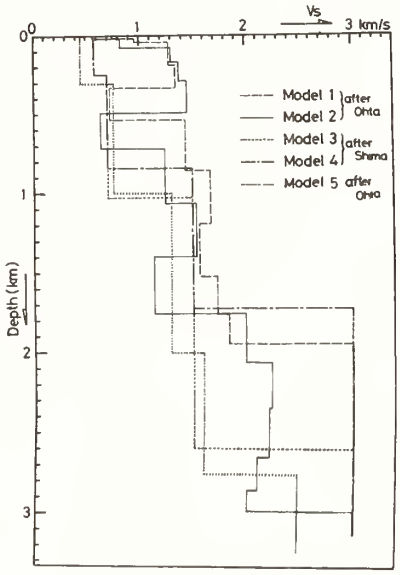

FIGURE 8: MAGNIFICATION FACTORS OF UNDERGROUND CHARACTERISTICS.

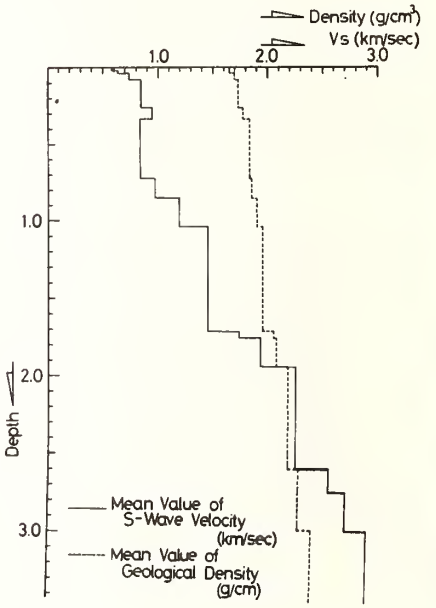

FIGURE 9: PROFILE OF AVERAGE UNDERGROUND STRUCTURE.

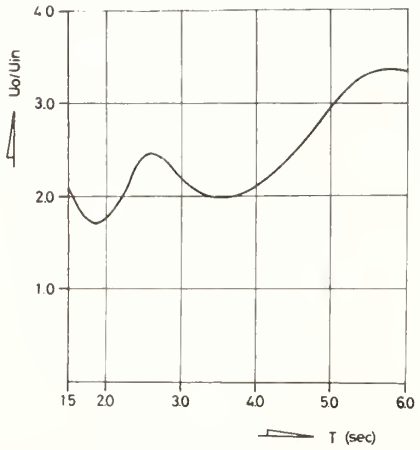

FIGURE 10: MAGNIFICATION FACTOR OF AVERAGE UNDERGROUND STRUCTURE.

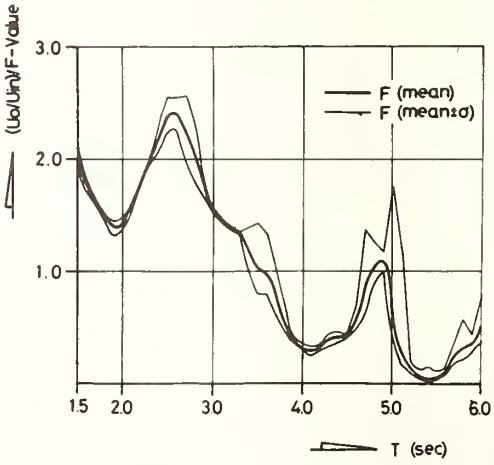

FIGURE 11: STANDARD CHARACTERISTICS OF UNDERGROUND CHARACTERISTICS.

11

DETERMINATION OF DESIGN EARTHQUAKE FOR THE DYNAMIC ANALYSIS OF THE FORT PECK DAM

W. F. Marcuson III and E. L. Krinitzsky

Soils and Pavements Laboratory
Waterways Experiment Station
Vicksburg, Mississippi

Determination of Design Earthquake for the Dynamic Analysis of Fort Deck Dam

Because of the slide in the Lower San Fernando Dam during the San Fernando Earthquake of 9 February 1971, the U.S. Army Corps of Engineers began earthquake studies of its hydraulic-fill structures located in seismically active areas. Fort Peck Dam is a large hydraulic-fill dam in northeast central Montana, on the Missouri River, built during the period from 1933-1940. This paper describes the investigations performed to determine the so-called "design" earthquake used in the dynamic analysis of Fort Deck Dam.

Geological Setting

Fort Peck Dam is on the edge of the Williston basin. The sedimentary section is about 7,500 ft (2,500 m) thick at Fort Peck and about 13,000 ft (4,300 m) thick in the Brockton-Froid area to the southeast. (See Figure 1 for locations.) Strata dip a few tens of feet per mile to the southeast.

The sediments at and near the surface consist of a thin, irregular veneer of glacial deposits that are underlain by thick Cretaceous shales. The shale encountered over much of this area is the Bearpaw Formation, a dark gray clay shale, approximately 1100 ft thick, with bentonite seams. The Cretaceous deposits are underlain by a succession of sandstones, shales, limestones, and dolomites. In some areas, evaporite deposits are found. The section extends to the Cambrian and, in turn, the Cambrian lies disconformably on crystalline basement rock.

Structural features, in addition to that of the Williston basin, are the Bowdoin dome, the Opheim syncline, the Blood Creek syncline, and the Redwater anticline (Figure 1). All of these features, including the Williston basin, date to Paleozoic time. They are essentially gentle features and have not undergone intense tectonism at any time in their history. They have probably been inactive since the Cretaceous.

Normal faults trending from northeast to southwest and downdropped to the southeast are shown in Figure 1 as the Hinsdale, Weldon, and Brockton-Froid faults.

Geological Studies

Since earthquakes are caused by movements along faults, the geologic and seismologic studies centered on the earthquake-generating potentiality of each fault. The study was complicated by uncertainty as to whether Tiger Butte is an active tectonic feature, and the interpretation of linears seen on airborne imagery of the area. Preliminary examinations were made of (1) Earth Resources Technology Satellite (ERTS) imagery, (2) air photography by the Soils Conservation Service (scale 1:20,000), (3) U.S. Geological Survey (USGS) fault studies in the Fort Peck area, (4) Side-Looking Airborne Radar (SLAR) imagery, and (5) aerial reconnaissance and field examination of faults and lineations in the Fort Peck area. Also during this time, inquiries were made to oil companies known to be working in the Fort Peck area to learn if they might provide information on faults from their seismic profiles. Such information was obtained with the stipulation that the sources and certain aspects of the information to kept confidential.

11

Seismological Studies

Concurrent with the geological work, a seismological study of the Fort Peck area was conducted.[1]

The historic earthquake events, both in the Fort Peck environs and in the larger region in which Fort Peck is located, were reviewed. Figure 2 shows the distribution of earthquakes in this region for those events with Modified Mercalli (MM) intensities greater than V. The Canadian Department of Energy and Mines was contacted to obtain what was then unpublished data on the earthquake events in Canada. Contemporary newspaper accounts of the 1909 earthquake that was felt throughout the Fort Peck area were restudied. On the basis of the restudy, the maximum intensity of the 1909 earthquake was downgraded from VIII to VI and its epicenter relocated. A maximum magnitude earthquake of 7.5 was assigned to the zone of active seismicity in western Montana and the ground motions were attenuated to the Fort Peck Dam. Maximum earthquakes for the faults in the Fort Peck area were assigned and their motions attenuated to the dam.

Ground motions in eastern Montana have been monitored by an array of seismometers set up to measure long-distance events such as nuclear explosions in other countries. The Montana array was part of the Large Aperture Seismic Array (LASA) program conducted under the Vela project by the U.S. Air Force. Teledyne Corporation, the contractor for the LASA work, made a limited study of unexamined small events in Montana on the chance that they might identify activity along faults.

In collaboration with Waterways Experiment Station consultants earthquake records were selected and rescaled to provide time histories of ground motion for use in dynamic analyses of the dam.

Seismicity in the Fort Peak Area

Historic seismicity for events greater than intensity V on the MM scale in Montana and adjacent areas is shown in Figure 2 for the period 1852 to 1967. For the eastern half of Montana the period is extended to 1975 since no subsequent events have occurred. It is noteworthy that all of the eastern half of Montana is seismically quiescent. Further, there are no groups of earthquakes observed that might be interpreted to trend into the eastern Montana area. Western Montana, on the other hand, is seismically active along the Rocky Mountain front.

The major event in the Rocky Mountain area of Montana was the Hebgen Lake earthquake of 17 August 1969 which occurred at the upper end of Hebgen Reservoir. It had a magnitude of 7.1 on the Richter scale and an intensity of X on the MM scale.

The seismicity east of the Rocky Mountain front is illustrated in Figure B5 of Reference 1 by all observed events for eastern Montana and the adjacent portion of Canada. The total historic record consists of 14 events of which only two, those of 1909 and 1943, were as great as intensity VI. All others were intensity IV to as little as a possible intensity II.

Of all the earthquakes, only the events of 1956 have an epicenter that plots near a known fault; it is adjacent to the Hinsdale fault. The earthquakes of 1943 and 1946 may be erroneously located and may be relatable to the Brockton-Froid fault, but that is, at best, only a distant possibility.

A more significant possibility is the lineup of earthquakes along a projection to the northeast of the Hinsdale fault. The 1956, 1972, 1968, and 1909 earthquakes appear to trace along an extension of the limited mapped extent of the Hinsdale fault.

The 1909 earthquake appears along the above-mentioned trend because of reinterpretation that was made during this study.

Reevaluation of the 1909 Earthquake

The 1909 earthquake, the strongest in this region, was rated at intensity VIII though very little damage was reported. The earthquake was felt over a large area, approximately 500,000 square miles (1,300,000 square km); its epicenter was located at 50° N and 105° W. Contemporary newspaper accounts were reexamined and on the basis of this information the earthquake was downgraded from intensity VIII to VI and the epicenter moved to the new positio[1]. As a result of the reexamination, the epicenter of the 1909 earthquake lined up with epicenters of the three other earthquakes. The four earthquakes indicated a possible trend of seismic activity that extended from the Hinsdale fault to the northeast and into Canada for approximately 200 miles (320 km). Alternatively, these four earthquakes might be unrelated to a single fault or associated with minor cross faults.

Fault-Plane Solution for the 1972 Earthquake

The 26 July 1972 earthquake, known as the Bengough, Saskatchewan, earthquake, was a minor event with an MM intensity of IV. However, the data were suitable for a fault-plane solution. The interpretation indicated a strike-slip motion on a nearly vertical plane striking approximately N 30° E. These results were later published[2].

The fault strike roughly matches that of the Hinsdale fault and can be used as an evidence for interpreting an extension of the Hinsdale fault or of discontinuous faults that follow this trend.

Microearthquakes

The restudy of the LASA data for 1966 to 1968 located 10 epicenters of microearthquakes.* These microearthquakes had very low orders of magnitude, roughly less than 2 on the Richter scale, and probably are not recordable at all in terms of MM intensity. Locations are shown in Figure 3.

A large group of events not shown in Figure 3 were recorded southeast of the Brockton-Froid fault. These events were found to have been blasts associated with strip mining for coal. A check was also made against oil extraction and water flooding in oil fields; no tremors were associated with these activities. Thus the epicenters in Figure 3 have been closely scrutinized and are believed to be those of very small but valid earthquake events.

The small number of these events suggests that the Fort Peck area is one of very low seismic activity. In central California there would be hundreds to thousands of such events for a comparable area and period of time. Also the events would generally line up to reflect the patterns of traces of active faults. In the Fort Peck area there is nothing comparable. Major fault trends are

* Letter from Teledyne-Geotech to OD, 28 June 1974.

hardly reflected at all by these events. There is one event beyond the southwest end of Hinsdale that might be related to the Hinsdale. Two events occur parallel to the Weldon fault but each is about 15 miles (24 km) away from the fault. Similarly, two events are about 20 to 15 miles (16 to 24 km) from the Brockton-Froid fault.

Thus, none of the microearthquakes are closely associated with any of the faults. There were no microearthquakes relatable to the Tiger Butte feature.

Relation of Earthquakes to Faults

The historical record of earthquakes in the Fort Peck area[1] suggests that:

- The area is one of low seismicity.
- A low level of seismicity appears to be possibly related to the Hinsdale fault and to a trend to the northeast for a total length of about 200 miles (320 km).
- The fault-plane solution for the 1972 earthquake may reflect the trend of the Hinsdale fault but it does not necessarily imply that there is a continuity to this trend.
- No earthquakes have been associated with the Weldon or the Brockton-Froid faults or for the area between them. The 1943 and 1946 earthquakes might have been mislocated and might be relatable to the Brockton-Froid fault, but the possibility is tenuous at best.
- The microearthquake data (Figure 3) do not confirm activity on any of the faults though one event lies along the trend of the Hinsdale fault.

In general, the implication of the earthquake data is that there may be some relationship between seismic activity and the trend of the Hinsdale fault for a distance of 200 miles (320 km). However, there is no certainty of this relationship and the trend may be there without there being any continuity in the faulting. The data suggest that the major structural features exhibit very little earthquake activity.

The area close to the Fort Peck Dam and its reservior shows no evidence of seismic activity.

Geological and Seismological Interpretation of Faults

Following are geological observations on the main structural features of the Fort Peck area that are relatable to earthquake activity. The observations are made with the benefit of the seismological background developed above.

For the faults under study, it must, first, be established that they are deep-seated and have roots in the crystalline basement rocks. Such information is essential to qualify a fault for its capacity to generate earthquakes. In clay shales of the Fort Peck area, faults are generally know to be "rootless," or formed as large slumps during sedimentary deposition. The faults are no longer active and do not act as a source of earthquakes. Second, one must establish whether faults that reach into the basement rocks are active or inactive. To be active, the fault must show

evidence of movement in the recent past,* thus suggesting that it could move in the near future. The geologic evidence suggestive of movements may be of several kinds, and there is no single set of criteria.

Following are discussions of the major faults in the Fort Peck area.

Weldon Fault

Oil company sources confirm that seismic profiles show the Weldon fault has roots in the crystalline basement rocks. The fault is interpreted to have moved more than once during the lower Paleozoic. The fault extends some 40 miles (64 km) farther to the southwest and 9 miles (14.4 km) farther to the northeast than current geologic and tectonic maps indicate. However, seismic profiles did not indicate whether the fault was continuous up to the Brockton-Froid fault. There is a lack of deep subsurface information in eastern Montana because the presence of Devonian evaporite deposits prevents discrimination of the basement in seismic interpretation. There is evidence that solution and collapse in the evaporites are responsible for some faulting in this area. Such faults could not generate damaging earthquakes.

Microseismic data, discussed earlier, suggest that the Weldon fault is either inactive or has a remote possiblility for an extremely low order of activity. Historic seismic records show no earthquakes at this fault.

A study of air and satellite imagery and two reconnaissance flights failed to turn up any field evidence of activity along this fault. It was concluded that this fault is inactive.

Brockton-Froid Fault

The record of historic earthquakes and microearthquakes shows a low order of seismicity in the general area, but the evidence is inconclusive with regard to the relation of seismicity to the fault. None of the events were located on the fault, and it is unlikely that any should have been interpreted as falling on the fault. Even if one or two had been so interpreted the level of activity would still be very low.

Subsurface displacements along this fault were mapped from boring data and oil well records by the USGS in Denver.[3] Also surface maps of the fault area were prepared.[4,5] Indications are that Pleistocene deposits were involved in the faulting and were dropped into the fault zone in many places. This implies that the Brockton-Froid fault was active.

Several linears, or lineations, formed by the Brockton-Froid fault were seen on the airphotos and during the overflights. One linear is a topographic high composed of gravel. This linear was mapped and interpreted to be gravels derived from deposits older than the adjacent till and cut by active faulting.[4,5] This linear runs into sand dunes to the northeast. A boundary of the sand dunes correspond to the linear and to a depression between Froid and Big Muddy Creek.

---

* Reference 1 provides a full review of the evidence and judgments used in classifying fault activity.

During overflight, other linears were observed in the Brockton-Froid area. Figure 4 is a photograph taken under conditions of low-sun angle of traces that extend undisturbed over rolling hills and across several drainage lines. A possible interpretation for these features was that they are the result of faults that have moved very recently.

These linears and the postulated fault traces were examined in the field.

When the linears first seen in the overflights were followed on the ground, they were found to have none of the features associated with fault movements. There were no vertical displacements and no horizontal translations in spurs. Instead, there were only gentle indentations that were traceable over the topography. Old-timers among the Indians living here said that cattle drives took place in this area early in the century and that as many as 80,000 head of cattle were driven yearly along a route that paralleled the Missouri River and was far enough away from it to avoid the bluffs and deep ravines that occur near the river valley. These trails went through valley bottoms and over adjacent spurs and ridges. The trails are covered with colluvium now, but they are still traceable. It was decided by all those persons who made the examinations in the field that the linears such as those in Figure 4 were old cattle trails.

During the field examinations, no evidence could be found for the faults that had been mapped.

The mapped faults are real in the deep subsurface where Jurassic marker beds are shown to be displaced several hundred feet in oil well borings. Surface manifestation of the faults is another matter. A linear ridge of brown chert gravels was found on the surface. These gravels were described as being different in age from lighter colored gravels, called till gravels, that occur irregularly but frequently on topographic highs throughout this area. The brown gravels are called outwash deposits of late Wisconsin age derived from the older Flaxville Formation. The Flaxville Formation outcrops about 50 miles (80 km) distant and contains brown quartzite. The brown color of these gravels was used as a time-stratigraphic designation. Though faults that form the boundaries for these gravels could not be found, the faults might be present. Test trenches would be needed to determine if they were or were not present where they are mapped.

There is reason to question the use of brown color or gravels to interpret age and origin of the gravels. Other hill crests were examined and more brown gravel was found. The brown color could be a secondary effect, resulting from soil-forming processes. In this case, the brown color and soil-forming processes may have contributed to an error in interpretation.

The historic earthquakes are a problem because their epicenters cannot be located with any degree of exactness. Old-timers among the Indians living in the Brockton-Froid area were asked if they knew of ground breakages associated with earthquakes that they could remember from their own experience or oral traditions. They knew of no ground breakage, though some remembered the 1935 and 1943 earthquake events. They could recall no other events from their oral history.

It was concluded that this area is not active on the basis of an absence of Holocene scarps along the mapped faults. However,

the seismic record and the uncertainties in the geological interpretations may allow a very low order of seismicity to be assigned to this area.

Hinsdale Fault

Seismic profiles run by oil companies show that the Hinsdale fault cuts the basement rocks. The fault is not as well understood as the Weldon. It is interpreted to be about 32 miles (51 km) long, extending somewhat farther to the northeast and southwest than previously mapped.

There was no surface evidence of fault activity that could be recognized either along the portion of the Hinsdale fault that had been mapped or along the extended portion to the northeast that is suggested by the lineup of four historic earthquakes.

This fault was interpreted to be inactive by geological criteria. However, the alignment of epicenters observed suggests the possibility of a low order of seismicity.[1]

Tiger Butte Fault

Tiger Butte is a complicated structural feature of small size, a hill about 1 mile (0.62 km) across with steeply dipping beds. It occurs, anomalously, in an area where there is no other structural disturbance. A careful study was made of this feature.* Though there are some uncertainties in proving the conclusion reported, it is believed that the structure resulted from ice thrusting. No evidence was found for deep-seated faults and the structure is considered to be an unlikely source of earthquake.

It has been noted that there is no evidence of seismicity at Tiger Butte.

No evidence of active fault scarps was found. The structure was classified as probably nontectonic in origin. Because there are uncertainties in justifying such a view, in such a small structure, no earthquakes are likely to occur that are greater than Richter magnitude 5.5 to 6.0.

Linears

Linears seen in SLAR imagery were reconnoitered by air and on the ground. One notable linear followed the trend of Bear Creek and projected to the Fort Peck Dam. Its location is shown in Figure 3. This feature was carefully examined on the ground but no ground breakage and no displacement of strata was found anywhere. This linear is nonfault in origin and is inactive as a structural feature.

Selection of Design Earthquakes

Attenuation from the Rocky Mountains

Figure 2 shows the belt of earthquakes in the Rocky Mountains of Western Montana with a center at Helena. A maximum credible

---

* Unpublished report: Tiger Butte Geologic Report, by Kenneth Schulte (1975).

earthquake of body-wave magnitude M_b* = 7.5 at a distance of 250 miles (400 km) from Fort Peck was assigned to this area. The bedrock ground motions attenuated to Fort Peck Dam provided a maximum acceleration of 0.001 g, a value too small for consideration.

Maximum Credible Earthquakes in the Fort Peck Dam

The geological evidence generally is that the major faults in the Fort Peck area are not active though there are some questions in the Brockton-Froid area that are unresolved. The seismological evidence suggests that there is low seismic order activity along the projected Hinsdale trend and there is questionable low order activity along the Weldon-Brockton-Froid trend. Both fault trends are about the same distance from Fort Peck Dam. Tiger Butte is believed to be inactive from both a geological and seismological standpoint. However, since there are some uncertainties in the geological interpretation, and the structure is small, a small possible earthquake hazard was assigned to it.

Floating earthquakes are those that are assumed possible anywhere in an area. All active faults may not be found and the floating earthquake provides for possible oversight. It can be assigned a magnitude based on the area's seismic history. The Fort Peck area has such a low order of seismic activity that the investigation turned up nothing in the vicinity of the dam that would even remotely be considered a geological hazard.[1]

Thus, chiefly on the basis of the seismological evidence, maximum credible earthquakes (the greatest that can reasonably be expected to occur) in the Fort Peck area were assigned as follows:

Fault Zone	Distance from Dam, miles	Distance from Dam, km	Maximum Credible Earthquake
Hinsdale and Weldon-Brockton-Froid	30	48	M_b = 5.8
Tiger Butte	10	48	M_b = 5.5

Selected Design Earthquakes

Time histories for the design earthquakes were produced by rescaling an appropriate existing earthquake record. On the basis of comparability for the sites involved, the Helena record of 1935 was chosen.

---

* The conventional equations that are used to calculate body- and surface-wave magnitude M are of the form

$$M = B + C \log x + \log A/T$$

where

B and C = constants
x = horizontal distance from epicenter to seismograph station
A = displacement amplitude of the body of surface wave
T = period of wave

The most conservative assumption was for a magnitude 5.5 event at Tiger Butte, as no activity has been proven on this structure. Maximum credible earthquakes, peak accelerations, and records taken for rescaling were as follows:

Fault Zone	Peak Accelerations at Fort Peck Dam, g's	Earthquake Record
Hinsdale and Weldon-Brockton-Froid	0.08	Helena (1935)
Tiger Butte	0.2	Helena (1935)

Tiger Butte

Tiger Butte is the most critical event. For this reason, it is the one that was used in the dynamic analysis. Its duration is 10 sec. Figures 5 and 6 show the time histories and reponse spectra, respectively, for the Helena record from which this event was derived.

Acknowledgments

Grateful appreciation is expressed to those colleagues at the Office, Chief of Engineers, the Missouri River Division, the Omaha District, and the Waterways Experiment Station who assisted in this work. In addition, the support of the Omaha District, who funded this project, is gratefully acknowledged.

References

1. Marcuson, W. F., III, and Krinitzsky, E. L., "Dynamic Analysis of Fort Peck Dam," Technical Report S-76-1, March 1976, U.S. Army Engineer Waterways Experiment Station, CE, Vicksburg, Miss.

2. Horner, R. B., Stevens, A. E., and Hasegawa, H. S., "The Bengough, Saskatchewan, Earthquake of July 26, 1972, "Canadian Journal of Earth Science, Vol. 10, 1973, pp. 1805-1821.

3. Colton, R. B., and Bateman, A. F., Jr., "Geologic and Structure Contour Map of the Fort Peck Indian Reservation and Vicinity, Montana," Miscellaneous Geologic Investigations Map I-225, 1956, U.S. Geological Survey, Washington, D.C.

4. Colton, R. B., "Geologic Map of the Brockton Quadrangle, Roosevelt and Richland Counties, Montana," Miscellaneous Geological Investigations Map I-362, U.S. Geological Survey, Washington, D.C.

5. Colton, R. B., "Geologic Map of the Poplar Quadrangle, Roosevelt, Richland, and McCone Counties, Montana," Miscellaneous Geologic Investigations Map I-367, 1963, U.S. Geological Survey, Washington, D.C.

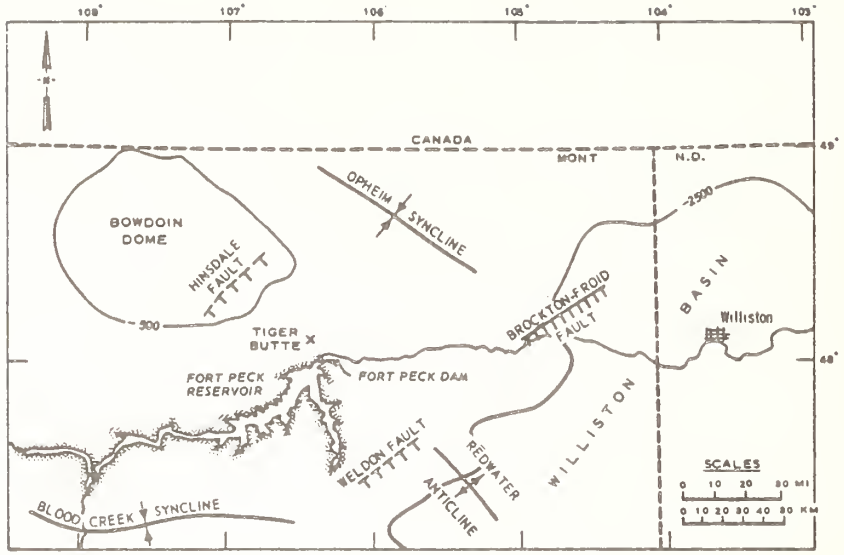

FIGURE 1. GENERAL STRUCTURAL GEOLOGY IN THE FORT PECK AREA

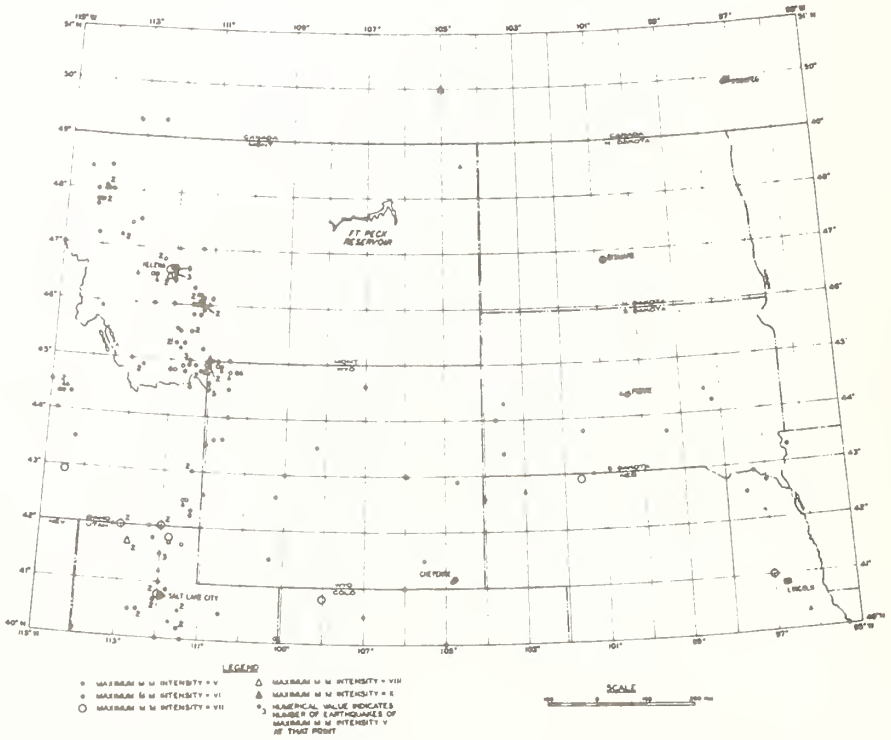

FIGURE 2. EARTHQUAKES OF INTENSITY MM V OR GREATER FROM 1852 to 1975

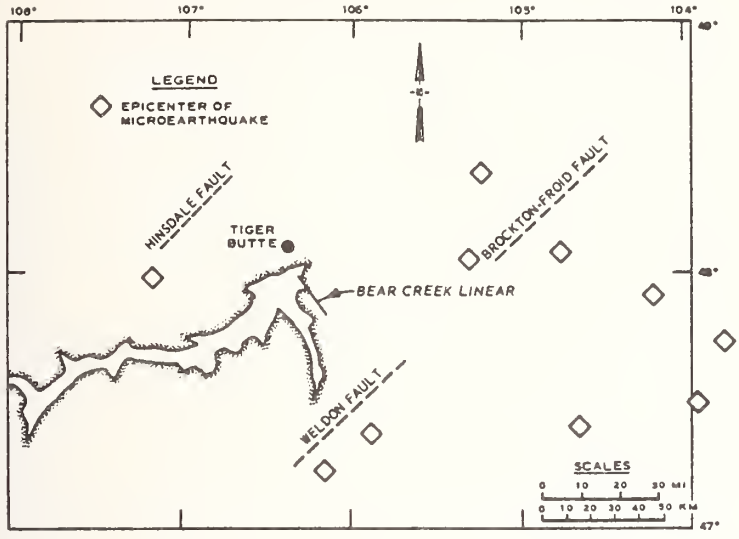

FIGURE 3. EPICENTERS OF MICROEARTHQUAKES RECORDED BY THE LASA ARRAY, 1966-1968 (FROM TELEDYNE-GEOTECH)

FIGURE 4. LINEATIONS THAT CUT ACROSS ROLLING HILLS DRAINAGE LINES IN THE BROCKTON-FROID AREA

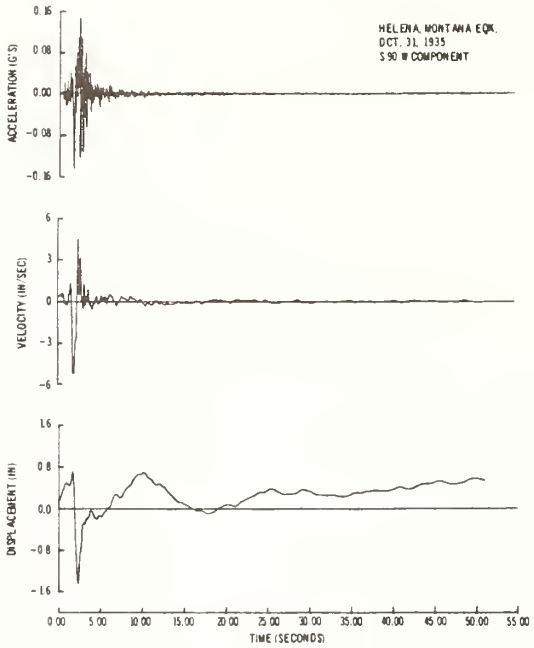

FIGURE 5. THE HELENA EARTHQUAKE RECORD

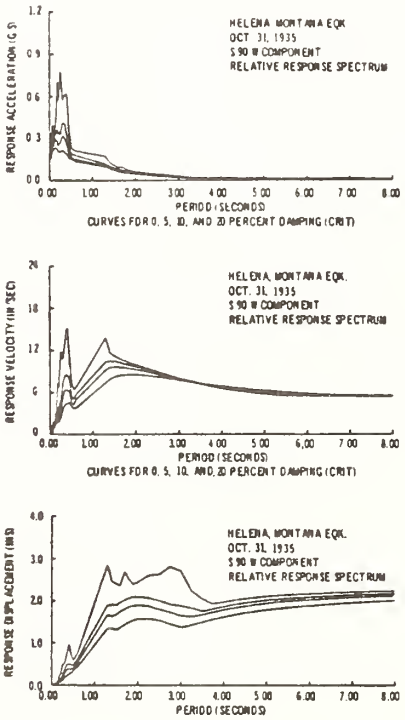

FIGURE 6. RESPONSE SPECTRA FOR THE HELENA RECORD

12

THE IZU-OHSHIMA KINKAI EARTHQUAKE OF JANUARY 1978

Minoru Tajima(*)
Hiroshi Sato(*)
Michio Otsuka(**)
Ken Sudo(**)
Katsuhiko Ishibashi(**)

Geographical Survey Institute(*)
Building Research Institute (**)
Ministry of Construction

The Izu-Ohshima Kinkai Earthquake of January 1978

The Izu-Oshima kinkai earthquake caused severe damage to the Izu peninsula.

The main shock occurred at $03^h\ 24^m$ January 14, 1978, under the ocean bottom between the Izu-Oshima island and the Izu peninsula. The seismic parameters determined by the Japan Meteorological Agency are as follows:

Magnitude:	7.0
Location:	139°15′ E
	34°46′ N
Depth:	3 km

Study of the first P wave recorded by the WWSSN network has shown that in many stations initial kicks are equivocal, which is one of the characteristic features of this earthquake. This makes the determination of the fault plane by use of the P wave push-pull pattern difficult. Thus, the fault generation of the main shocks began with a slow process; its fault plane was of purely the strike-slip type.

Alternatively, use was made of the distribution of polarization angle of S wave read-off from the WWSSN LP seismograms Figure 1). The fault plane solution thus obtained is as follows:

	dip direction	dip angle
a-plane	0.3°	82.8°
b-plane	-91.5°	76.0°

As was suggested by the appearance of initial P wave motions recorded at many stations, the above solution shows that two nodal planes are of the pure strike-slip type directed almost to E-W and N-S directions. This solution is in good harmony with the push-pull distribution obtained from the reading of seismograms from Japanese stations (Figure 2). The slip direction is that of right lateral fault, which is confirmed by visual dislocation amounting to 60 cm at Inatori on the Izu peninsula.

Shock Locations

The characteristic feature through the entire process is the high activity of foreshocks around the epicentral area of the main shock and large aftershock swarms which were activated at the middle part of the Izu peninsula unexpectedly distant from epicenter.

The precise determination of epicenters were made from 35 data provided from stations belonging to Japan Meteorological Agency, Earthquake Research Institute, University of Tokyo, Nagoya University, and the National Research Center for Disaster Prevention. Epicentral distances for the above stations are less than 150 km. The crustal structure assumed for this study is shown in Table 2. Figure 3 and Table 1 show its result. Onset times of P phases are exclusively analyzed and the overall error involved in locating epicenters are estimated to be 2-3 Km. As is shown in Table 1, the location of epicenter of the main shocks is only slightly different from that reported by JMA (No. 4 in Table 1).

The most remarkable fact shown in Table 1 and Figure 3 is that the maximum aftershock (No. 8 in Table 1) with magnitude of 5.8 has

occurred at the central part of Izu peninsula, a location which is unexpectedly distant for the size of the main shock. Moreover, the direction of epicenter of the maximum aftershock seen from location of the main shock indicates a contradictory fact: that is, when speculation is made that rupture has proceeded from the epicenter of the main shock toward the location of the maximum aftershock, the direction of the fault is discordant with this solution. This problem is further discussed in detail later.

Fault Mechanisms

The push-pull distribution is obtained by seismogram reading of the stations used in locating epicenters plus data recorded at the telemetry network stations belonging to Kyoto, Tohoku, and Nagoya Universities (Figure 4).

What is to be noted in comparing mechanism diagrams of fore- and aftershock is that there is a strong contrast between these two. While push-pull distribution for foreshock obtained by superposing two large events is very similar to that of the main shock, that for aftershocks is almost in harmony with that of the Izu-Hanto Oki Earthquake (M = 6.9) which occurred in 1974.

Rupture Process

Figure 5 shows an amplitude-distribution diagram of the long-period Love waves drawn from comparison of seismograms equalized at 90° of the epicentral distance. This pattern is quite concordant with the pattern suggested by the polarization angle of S waves. The seismic moment of this earthquake is estimated to be 9.4×10^{25} dyne cm from study of the focal mechanisms and amplitude distribution of surface waves.

As was described above, the fault plane solution obtained by use of the polarization angle of long period S waves is contradictory with the speculation that rupture of the main shock has proceeded toward the maximum aftershock.

Figure 6 shows the distribution of aftershocks that occurred during half a month after the main shock. Several characteristic features can be pointed out from this figure. Linear trend of distribution of the aftershocks, which stretches toward the west starting from the epicenter of the main shock, is bent sharply near Inatori, which is located at the east coast of Izu peninsula, by the angle of about 23° toward north. This connects the turning point with the location of the epicenter of the maximum aftershock, again with a linear trend.

The distribution of aftershocks shown in Figure 6 suggests the possibility of introducing the hypothesis that the Izu-Oshima kinkai earthquake actually is made up of two events: one having its epicenter as usually assigned and fault azimuth of E-W, and the other having an epicenter somewhere near Inatori and fault proceeding toward Mochikoshi, which is situated 23° northwest from Inatori.

Introduction of the hypothesis of successive occurrence of the two events avoids the necessity of curved growth of the fault. It is not known yet, however, whether the latter earthquake is tectonically independent of the former and was just triggered by it.

It is evident that the latter event is closely related to the heaval of the ground which has been observed locally in Izu ninsula and also the occurrence of Kawazu Earthquake = 5.4 λ=138°57'E, θ=34°47N) in August 1976. However, the pos- bility of the correlation between the occurrence of the former en with these anomalous geophysical activities can not be ruled t.

As for the latter event, the origin time and location is not iquely determined. Judging from the fact that the aftershock o. 5 in Table 1), which took place immediately after the occur- nce of the main shock, is located at the middle part of the Izu ninsula, and that the damage at the east coast of the Izu penin- la is regarded as being caused not long after the main shock, it reasonably inferred that these two events have occurred within short interval of time.

It is to be noted here that the above inferrence brings about new contradictory problem that entails some further explanation. at is, if the assumption is adopted that successive events were volved, it should be reflected in the determination of fault ane through the records of S waves and surface waves. In other rds, the fault-plane solution that is obtained through analysis these waves should be that of the average of the two events. ile, as is described before, the solution is quite concordant th only the former event, it does not fit the latter. This is a zzling problem.

Two possible reasonings are given:

(1) The main shock is related only to the outbreak of the former event, and the latter fault formed gradually with earthquake swarms activated by the first event. This hypothesis reconciles the contradiction that exists between the distribution of aftershocks and that of the amplitudes, but is unsuccessful in explaining the result of the length measurement survey and leveling.

(2) Rise time was very slow and the amount of dislocation was small for the latter event. According to this reasoning, the latter event should have emitted an extremely long period seismic wave. However, it was too small in amplitude to disturb the pattern of amplitude distribution partly because of the frequency window of the observing system and partly because of the smallness of the size of rupture.

As is seen in Figure 8, the expected pattern of ground defor- tion derived from that fault model shown in Figure 7 is in good rmony with that found from the length measurements and leveling rveys (Figures 9 and 12).

Although authors prefer reasoning (2) for the possible mecha- sm of the two events, it should be admitted that it is not mpletely free from weak points. One relates to the question of ether a slow deformation of the ground can give rise to the severe mage that was observed on the east coast of the Izu Peninsula. e answer to this question might be that the damage of this earth- ake was caused mainly by landslides, landslips, and breakage of e ground rather than the seismic wave itself. Does breakage of e ground tend to be accompanied by the long-period deformation of e ground?

In addition to the study of the vibration characteristic, the dynamic response of the ground is also of essential importance not only for earthquake engineering but for seismology.

Land Deformation

Precise leveling and length-measurement surveys were carried out after the earthquake by GSI and other institutes. The results of the surveys have indicated an apparent vertical deformation near Inatori, which suffered the severest damage from the earthquake (Figure 9). At Inatori, visual right lateral dislocation amounting to 60 cm was observed on the ground surface (Figure 10), which is in harmony with the rupture mechanism inferred from study of the seismic waves. A series of fault traces elongate in the direction of NW starting from Inatori. Minor right lateral fault traces have been reported at Neginota, west of Inatori, on the extention of the linear trend of aftershocks.

Since 1975, abnormal upheaval at the north-eastern part of Izu peninsula has drawn the attention of geophysicists. Inatori is located just at the edge of the upheaval, while no significant movement was reported at the center of the activity of the ground deformation.

The horizontal movement of the ground derived from the length measurement survey is in harmony with that expected from the theoretical model (Figures 11 and 12).

According to the result of the length measurement made across Suruga bay on the other hand, no significant change in length was recognized. This implies that the Izu-Oshima Kinkai earthquake gave little direct influence on the strain field of Suruga bay, where a gigantic earthquake is anticipated.

Precursory Phenomena

Abnormal geophysical phenomena such as ground upheaval and high microseismic activity have drawn the attention of geophysicists since 1975 to the middle part of Izu peninsula. Among numerous data of geophysical observation made in connection with the earthquake prediction project, some precursory phenomena can be pointed out.

Professor Mogi of ERI has the opinion that stress accumulation was accelerated by the occurrence of Izu Hanto-Oki earthquake which took place at the southern tip of the Izu peninsula in 1974.

Apart from the detailed explanations, it seems generally plausible to say that the anomalous ground upheaval and high microseismicity resulted from this stress-accumulation process.

It was found out later that the b values of the foreshocks were a significantly small as 0.5-0.6 (Figure 13). JMA issued an earthquake information bulletin at 11^{h} on the 14^{th} of January warning about the possibility that some bigger events might follow. And the main shock occurred at $12^{h}\ 24^{m}$ on that day.

The Borehole volumetric strain meters have been installed at Irozaki and Ajiro and continuous observations have been carried out by JMA. Some unusual change commensed one month before the occurrence of the main shock, and it was amplified several days before (Figure 14).

Significant variation in radon concentration in the ground ater before the main shock is also reported at the middle part of zu peninsula. However, no significant change in the velocity of ave propagation was observed between Izu-Oshima and Izu peninsula efore the occurrence of the main shock.

o.	Date	Origin time	Long.(E)	Lat.(N)	Depth	M	Remarks
1	Jan.14	$09^h36^m14.7^s$	139°18'.2	34°44'.7	5.8km	4.6	Fore-shock
2		09 45 34.0	139 16.3	34 45.8	1.1	4.9	
3		09 47 37.5	139 16.8	34 44.6	7.6	4.9	
4		12 24 38.8	139 14.3	34 44.8	3.4	7.0	Main shock
5		13 42 00.3	138 53.2	34 51.1	1.9	5.1	Aftershock
6	Jan.15	03 46 21.8	138 52.4	34 49.4	3.7	4.9	
7		07 31 47.1	138 52.4	34 50.6	7.1	5.8	
8		07 36 11.0	138 51.9	34 48.3	10.5	5.4	
9	Jan.16	14 28 50.8	138 53.5	34 50.3	15.0	4.7	

TABLE 1: CHRONOLOGY OF SHOCKS

H(km)	V_p(km/sec)
5	5.5
15	6.0
10	6.6
—	7.7

BLE 2: CRUSTAL STRUCTURE USED IN RELOCATION OF HYPOCENTER

12

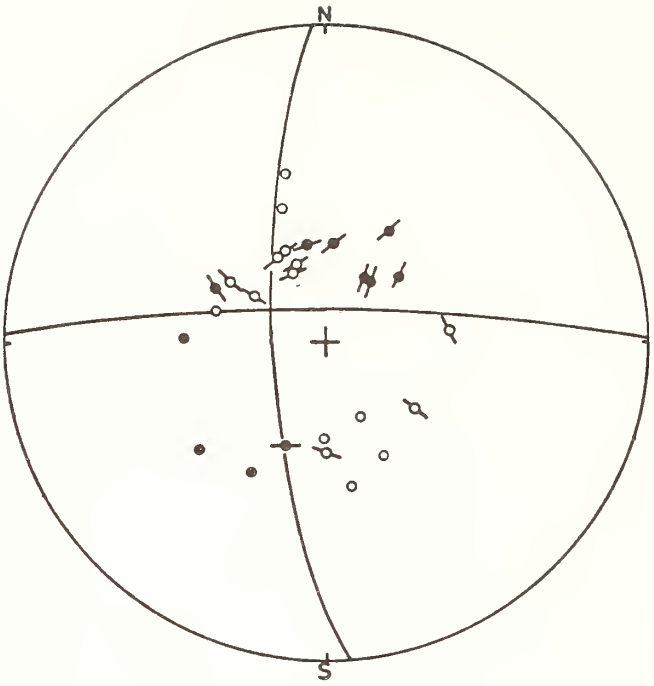

FIGURE 1: POLARIZATION ANGLE OF LONG PERIOD S-WAVE AND PUSH-PULL MOTION OF P-WAVES, SUPPLIED FROM WWSSN-STATIONS

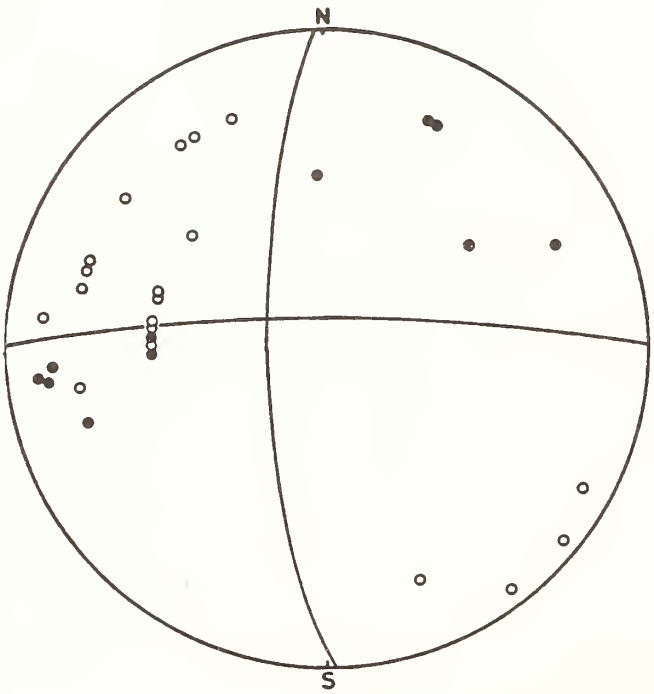

FIGURE 2: DISTRIBUTION OF PUSH-PULL MOTIONS OF P-WAVES IN STATIONS IN JAPAN.

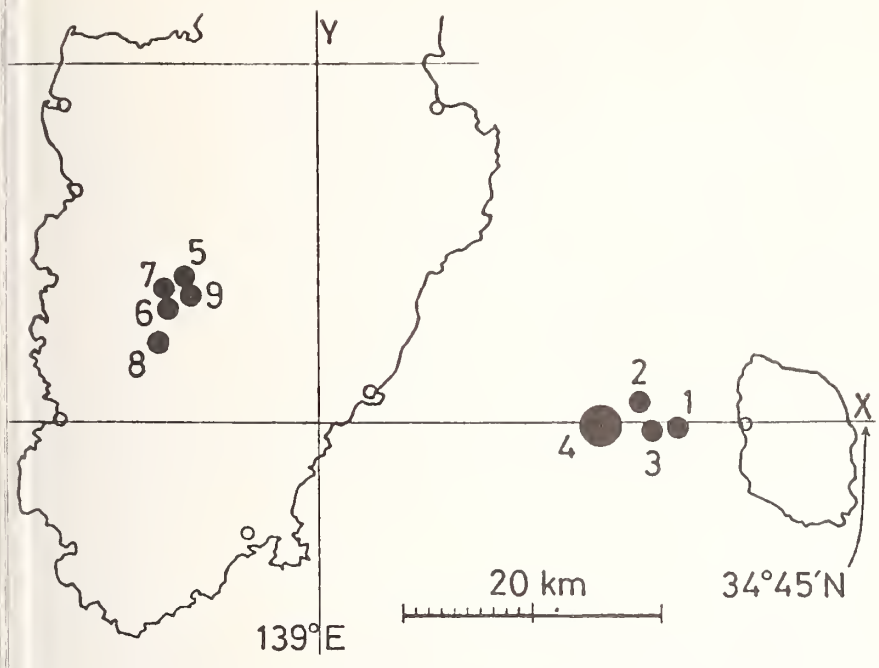

FIGURE 3: EPICENTER OF REMARKABLE SHOCKS. REDETERMINED BY AUTHORS.

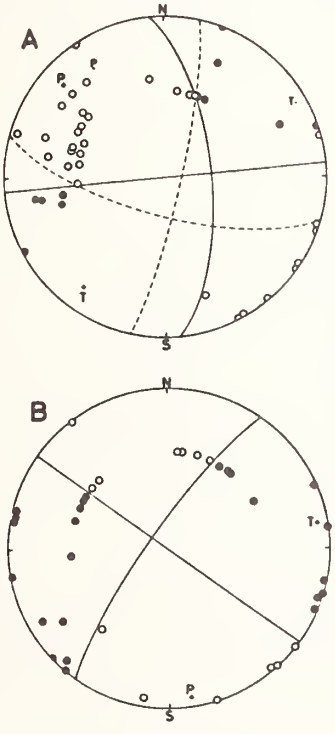

IGURE 4: FAULT PLANE SOLUTIONS FROM P-WAVE FIRST MOTIONS FOR FORE-SHOCKS (NOS. 1 AND 2 IN TABLE 1) (A, COMPOSITE) AND FOR THE LARGEST AFTERSHOCK (NO. 7 IN TABLE 1) (B) OF THE IZU-OSHIMA KINKAI EARTHQUAKE. LOWER FOCAL HEMISPHERES ARE PROJECTED ON EQUAL AREA NETS. SOLID CIRCLES INDICATE COMPRESSION AND OPEN CIRCLES, DILATATION.

12

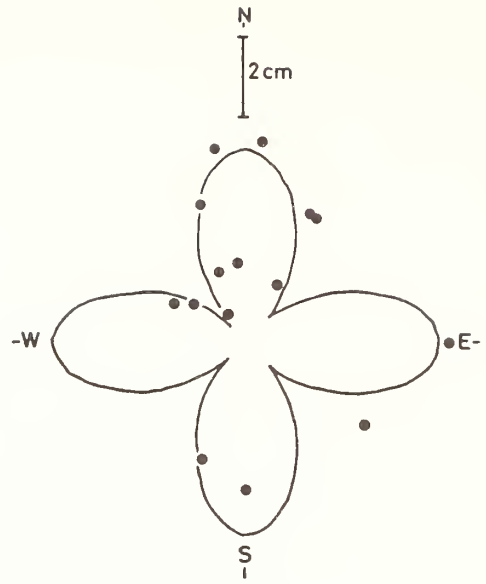

FIGURE 5: RADIATION PATTERN OF LOVE WAVES. SOLID CURVE DENOTES THAT CORRESPONDING TO 1.0×10^{26} DYNE-CM.

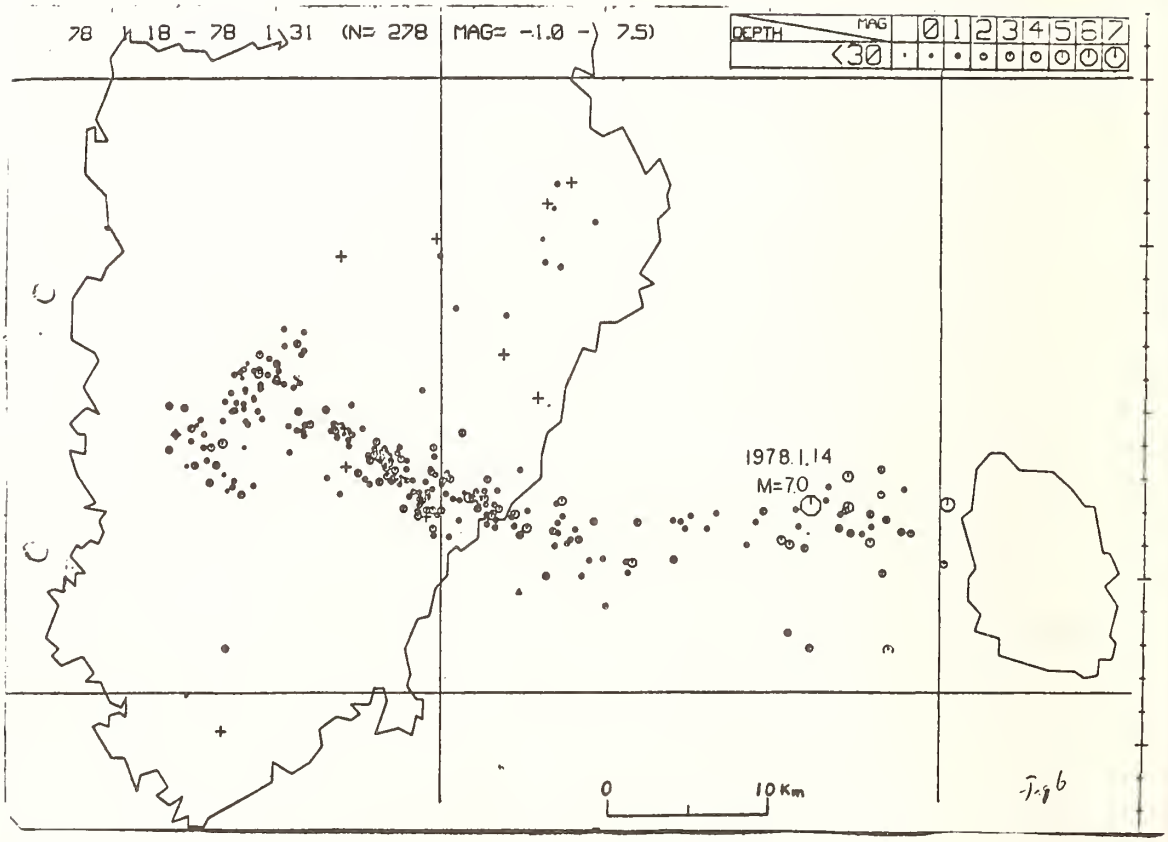

FIGURE 6: AFTERSHOCK DISTRIBUTION DURING THE PERIOD JANUARY 18 - JANUARY 31. LARGE SYMBOL DENOTES EPICENTER OF MAIN SHOCK DETERMINED BY TSUMURA ET AL. (EARTHQUAKE RESEARCH INSTITUTE, TOKYO UNIVERSITY).

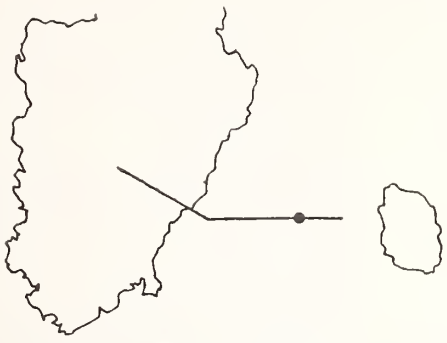

event	L(km)	W(km)	D(m)	τ(sec)	V_R(km/sec)	Type
1st	20	10	1.5	1-2	2.5	Bi-lateral
2nd	17	7	1	1-1	2.0	Uni-lateral

GURE 7: THE 1ST EVENT INITIATES AT THE LOCATION DENOTED BY CLOSED CIRCLE BI-LATERALLY, THAT IS, TO THE EAST, WITH RUPTURE VELOCITY OF 2KM/SEC, DISLOCATION 1M, FAULT LENGTH 7KM AND TO THE WEST, WITH 2.5KM/SEC, 1.5M AND 13KM. THE 2ND EVENT INITIATES AT THE WESTERN END OF THE 1ST EVENT WITH 2KM/SEC, 1M, and 17KM. DIP ANGLE AND DIP DIRECTION OF THIS SHOCK ARE 83° AND N23°E, RESPECTIVELY.

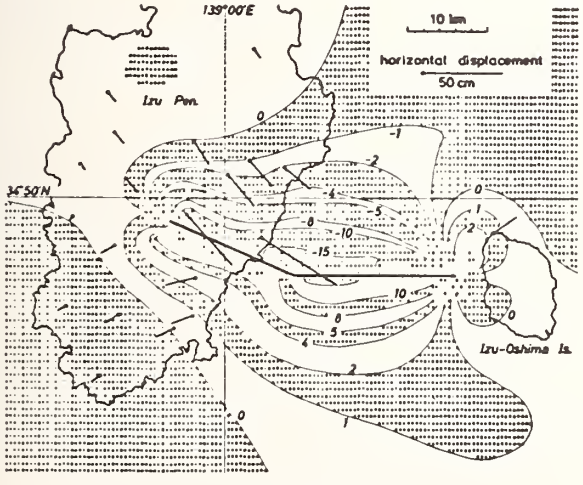

IGURE 8: VERTICAL DISPLACEMENT FIELD (IN CM) AND HORIZONTAL DISPLACEMENTS OF TRIANGULATION POINTS ASSOCIATED WITH THE FAULT MODEL OF THE IZU-OSHIMA KINKAI EARHTQUAKE. AN ASSUMED FAULT TRACE IS INDICATED BY A SOLID LINE.

12

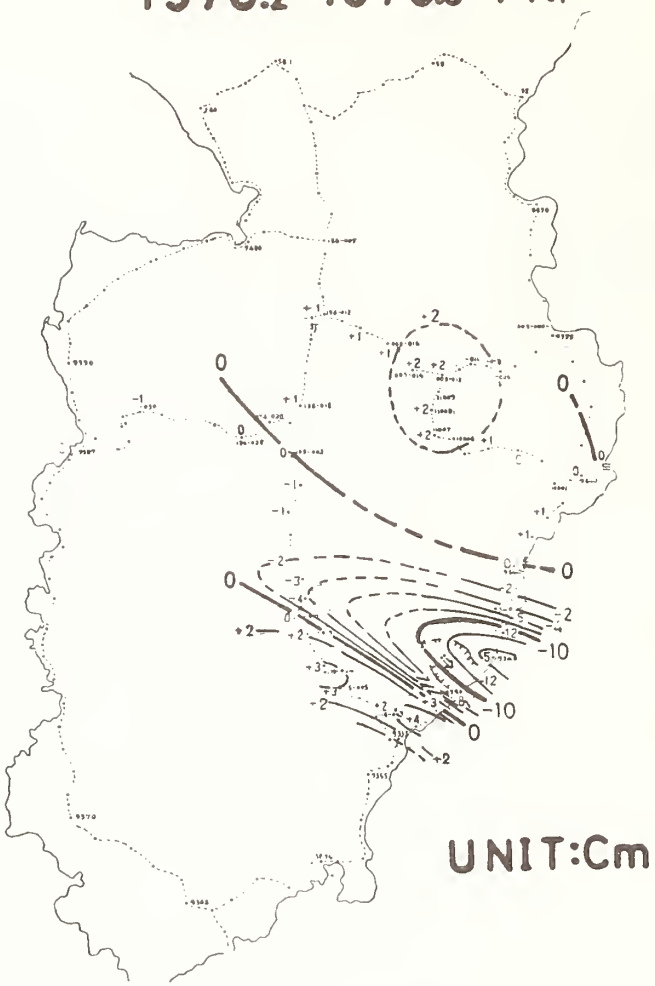

FIGURE 9: VERTICAL MOVEMENT IN THE EAST COAST AREA OF THE IZU PENINSULA BY THE LEVELING SURVEY.

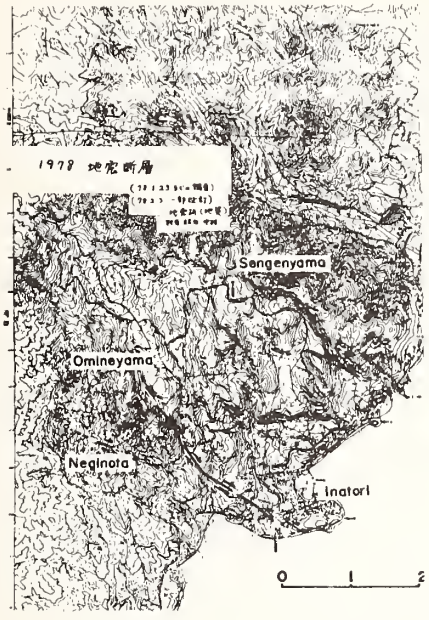

IGURE 10: FAULT TRACES DISCOVERED IN THE EAST COAST AREA OF THE IZU PENINSULA.

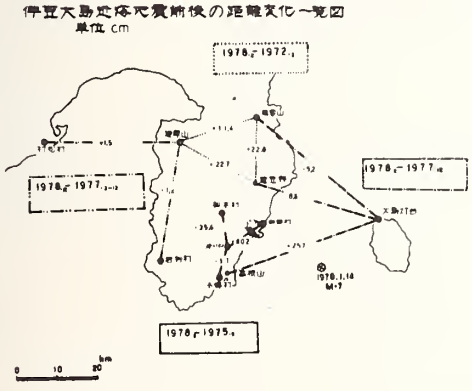

12

'IGURE 11: DISTANCE CHANGES OF THE SIDE LENGTHS.

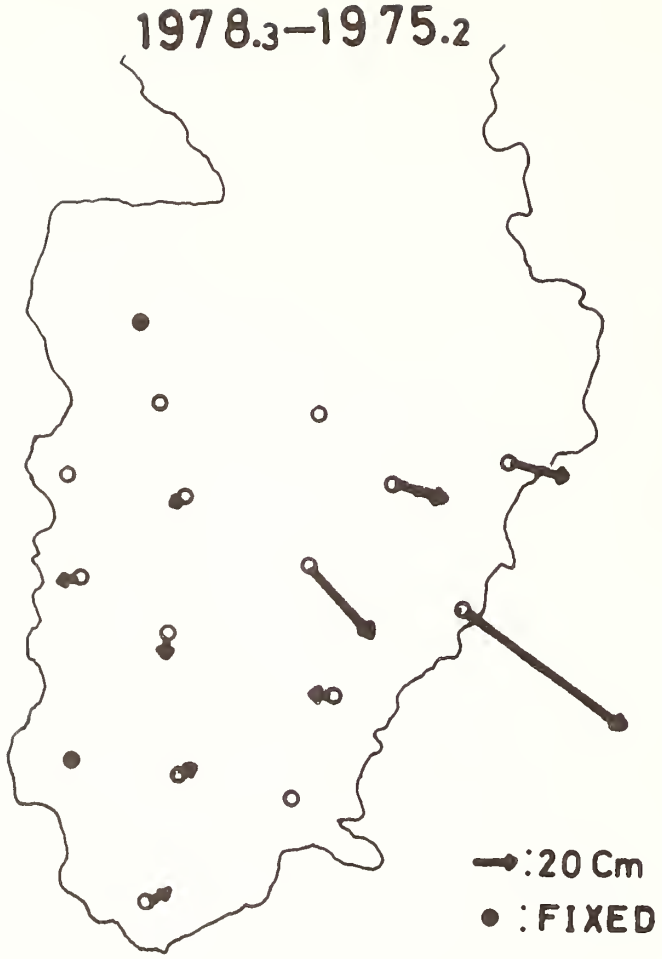

FIGURE 12: HORIZONTAL MOVEMENT OF TRIANGULATION POINTS IN THE IZU PENINSULA.

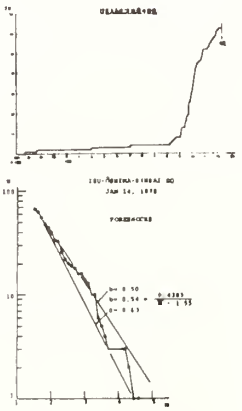

FIGURE 13: FREQUENCY OF FORESHOCKS PRIOR TO THE EARTHQUAKE AND THE B VALUE OF THE GUTENBERG-RICHTER FORMULA.

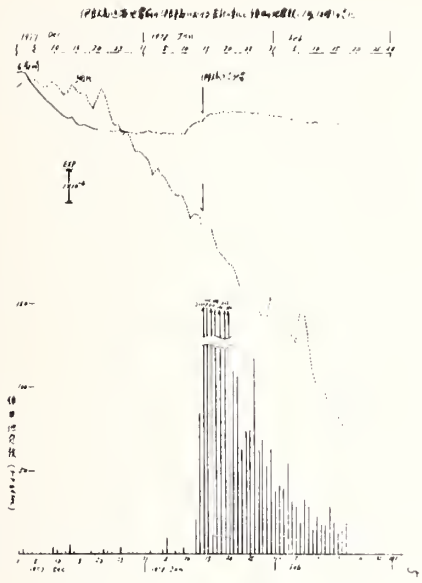

GURE 14: STRAIN CHANGES BY THE BOREHOLE VOLUMETRIC STRAINMETER AT AJIRO AND IROZAKI OBSERVED BEFORE THE EARTHQUAKE (AFTER JMA).

13

EMPIRICAL AND ANALYTICAL METHODS OF ESTIMATING SOIL LIQUEFACTION RISK

R. K. McGuire
U.S. Geological Survey

F. Tatsuoka
University of Tokyo

T. Iwasaki
K. Tokida
Ministry of Construction

Empirical and Analytical Methods of Estimating Soil Liquefaction Risk

The importance of assessing seismically induced liquefaction hazard has been recognized in recent years, primarily as a result of the spectacular liquefaction failures that occurred during the Alaska and Niigata earthquakes of 1964. An additional stimulus for determining liquefaction hazard is the increasing number of structures built or proposed on liquefaction-susceptible deposits. These circumstances have stimulated studies on liquefaction, and many findings have already been reported in this field [Seed, 1976; Yoshimi, 1977; Ohashi et al., 1978].

In assessing soil liquefaction hazard, the principal methods used in the past have been deterministic in nature, involving comparison of soil strength estimated from geotechnical surveys at the site with estimated stresses predicted during a design earthquake. More recently, several probabilistic methods have been proposed. Youd and Perkins [1977] suggested using empirical observations of liquefaction as a function of earthquake size and distance, and geologic classifications of soils, to indicate the liquefaction hazard. Several investigators [Yegian and Whitman, 1977; Ferritto and Forrest, 1977; Crouse et al., 1977] have proposed probabilistic methods that account for uncertainties in the dynamic soil strengths or in the seismically induced shear stresses. However, to date no direct comparison has been made between an empirical method for assessing liquefaction hazard and an analytical method that compares estimated soil strengths and induced shear stresses, for a site where there is available both good geotechnical data and abundant seismicity data.

Such a comparison is the purpose of this study. The site studied is near Tokyo Bay at a location where abundant soil samples have been recovered and analyzed in the laboratory. The historical seismicity in the area is known in some detail for a period of over 1000 years, and observations of liquefaction as a function of earthquake size and distance have been made for a large number of Japanese earthquakes. Thus there is a good opportunity for a direct, detailed comparison of methods of probabilistically assessing seismic liquefaction hazard. This comparison will allow the advantages and disadvantages of the methods to be understood for future applications.

Site Conditions and Seismicity

The site of interest in this study is located near Tokyo Bay (see Figure 1). This location was formerly in Tokyo Bay and was reclaimed about 10 years ago by a pumping method using sandy soils from surrounding seabottoms. At this site, sandy reclaimed deposits with a depth of about 6 m overlie deposits of alluvial origins with a depth of about 4-11 m. Upper parts of the alluvial deposits are sandy and lower parts are clayed. The soil deposits that have high susceptibility of liquefaction are the reclaimed sandy deposits and the alluvial sandy deposits.

13

To define seismicity in the area around Tokyo Bay, the catalog of earthquakes maintained by the Public Works Research Institute, Tokyo, was examined. Figure 2 shows the locations of earthquakes within a 200-km radius of the site of interest (longitude 130°40'E and latitude 35°34'N) for the years 416 to 1977 with magnitudes of 6.5 or greater. The catalog was judged to be complete for these magnitudes from the year to 1977; to expand the data base, a radius of 500 km was considered, and the numbers of events in chosen

magnitude ranges were determined. The slope of a straight line that describes the log number versus magnitude relation is -0.9, which is consistent with the data reported by Ibukiyama et al [1972].

For seismic risk analysis made during this study, a single seismic source, circular in plan and centered at the site of interest with radius 200 km, was used. This is a reasonable representation of the historical seismicity for the purposes of a preliminary assessment of seismic hazard and will not affect the comparison among the methods examined. Based on the historical seismicity over the last 100 years, an activity rate of 11.2 events per year with magnitude 5.0 or greater was used for this circular source. This is consistent with the data reported by Ibukiyama et al [1972]. A maximum-possible magnitude of 8.6 was used, based on the entire historical record.

Emprical Method

The simplest method of evaluating the probability of liquefaction at a site is first to relate past observations of liquefaction to the magnitudes and distances of the earthquakes causing the liquefaction. It then is possible to calculate the probability that an earthquake will occur with sufficient magnitude within a critical distance to induce liquefaction at the site. Such an analysis is extremely simple and does not account for soil strength at the site which might be estimated from subsurface borings or samples. Because relationships between the magnitude of an earthquake and the distance to the farthest liquefied site are made without regard to soil strength (i.e., they include observations of liquefaction at the very weakest sites), the analysis will be conservative for sites with stronger soils. This empirical method is essentially that proposed by Youd and Perkins (1977) for calculating "ground failure opportunity."

A relationship between earthquake magnitude and distance to the farthest liquefied site was available for Japanese earthquakes [Kuribayashi and Tatsuoka, 1975]. The data are shown in Figure 3, along with a lower-bound line and a mean line. The mean line was taken to be the best estimate of the radius within which liquefaction will occur for future shocks; this line was manipulated into the form of a typical attenuation equation:

$$LI = -4.5 + .87\ m - 0.43\ \ln \Delta \qquad (1)$$

where LI is a liquefaction indicator, M is earthquake magnitude, and Δ is epicentral distance in kilometers. A standard computer program [McGuire, 1976] was used to calculate the probability per year that liquefaction would occur (that is that $LI \geq 0$) at the site of interest, using the assumptions on seismicity described above.

Surface Acceleration Method

The second method used to evaluate liquefaction hazard was based on the probability distribution of maximum surface acceleration at the site, which was obtained from a seismic hazard analysis with the assumption described above. From this distribution of surface acceleration, distributions of shear stresses in the soil layers were calculated, and these were convolved with the distributions of soil strengths estimated from soil properties to calculate the probability of liquefaction.

To esimate the maximum earthquake-induced stresses in soil layers from the maximum horizontal acceleration at the surface, the method proposed by Seed and Idress [1971] was used. In this method, the ratio of the horizontal shear stress τ to the vertical effective stress σ_v' in layer i is estimated by

$$(\tau/\sigma_v')_i = a\,(r_d)_i \gamma Z_i/(g\sigma_v') \qquad (2)$$

where a is the surface acceleration, g is the acceleration of gravity, r_d is a depth-varying function that accounts for elasticity of the soil, γ is the the unit weight of the soil, and Z_i is the depth of layer i. The values used for $(r_d)_i$ were determined by analytical methods (McGuire et al, 1978) and were consistent with the values proposed by Seed and Idriss (1971). If the water table is not at the ground surface, equation (2) must be rewritten to reflect the different unit weights of soil in the saturated and unsaturated conditions.

To estimate dynamic soil strength, many laboratory tests were performed on soil samples taken from the site. Details of the sampling methods and tests are explained in McGuire et al (1978). Dynamic triaxial tests were made to determine the dynamic shear strength $R_{\ell 20}$ defined as the stress ratio at 20 loading cycles which causes 3 percent axial strain in single amplitude. Estimation of the in situ dynamic shear strength was then made by applying a number of constants to $R_{\ell 20}$, to correct for laboratory, loading, and soil disturbance effects.

Further investigations involved methods of estimating the dynamic shear strength when less extensive geotechnical data are available, as was the case for most of the soil layers at the site. Consideration of previous work in this field, plus effects observed in comparing estimated strengths with laboratory-determined strengths, led to the following formula for the estimated dynamic shear strength R_E (shear stress divided by effective confining pressure),

$$R_E = 0.0047\, D_r^* + 0.0029\, S \qquad (3)$$

where S is the percentage content of fine soils and D_r^* is relative density estimated by

$$D_r^* = 21\sqrt{N/\sigma_v' + 0.7}$$

(Gibbs and Holtz, 1957). In equation (4), N is the blow count number for the standard penetration test. Estimation of shear strength by equation (3) assumes a linear relationship between strength and estimated density, as do other proposed relationship, but accounts for the effect of fine soil content. This effect is shown in figure (4) which compares laboratory shear strength with estimated relative density. Uncertainty in the soil strength ratio was characterized by a normal distribution with a standard derivation of 0.057 about the value estimated by equation [3].

To calculate the probability of liquefaction, the density function F_R for shear stress ratio $R_i = (\tau/\sigma_v')_i$ in layer i was computed from equation (2) using a risk analysis to obtain the distribution of ground acceleration (this was considered the only random variable on the right side of equation (2)). The probability of no liquefaction in layer i during 1 event can then be expressed as:

$$P[\text{no liquefaction in layer i during 1 event}] = \int P[\text{no liq. in layer i}|r] f_{R_i}(r)dr \quad (5)$$

where the probability in the integrand is calculated from the normal distribution with a mean determined from eq. (3) as described above.

It is commonly assumed in seismic risk analyses that earthquakes conform to a Poisson process in time and that successive events are independent in size and location. Using these assumptions, the probability of no liquefaction in layer i during time t is

$$\begin{aligned} &P[\text{no liq. in layer i during time t}] \\ &= 1 - \exp(vt\, P[\text{no liq., layer i, during 1 event}]) \\ &\approx vt\, P[\text{no liq., layer i, during 1 event}] \end{aligned} \quad (6)$$

where v is the rate of earthquake activity and where the approximation is valid for probabilities less than 0.1.

Often several layers in a soil profile are susceptible to liquefaction, and this is the case at the study site. Consequently, the term "site liquefaction" must be defined in terms of the stresses and strains which occur in the various layers. The most conservative approach is to consider liquefaction in one or more layers to imply site liquefaction. To calculate probabilities consistent with this definition, it is assumed that errors in estimated strengths R_i of layers in the soil profile are uncorrelated; this assumption is justified by examination of errors in shear strengths as a function of depth (McGuire et al., 1978). The probability of no site liquefaction is then

$$P[\text{no site liquefaction}|a] = \Pi_i P[\text{no liq. in layer i}|a] \quad (7)$$

The probability of no site liquefaction in time t can be calculated by an equation analogous to equation (6), substituting the product indicated in equation (7). A similar procedure is used if site liquefaction is defined to be the occurrence of liquefaction in two or more layers, three or more layers, etc.

Results

Using the function described above for the empirical relation between magnitude and farthest distance to liquefaction, and using the seismicity assumptions outlined above, the "Empirical Method" indicates a probability per year of liquefaction of 0.059. This implies that liquefaction will occur, on the average, once every 17 years. Such a liquefaction risk seems high but is consistent with the seismicity assumptions for the area. The risk analysis for acceleration, for instance, indicates that 20 gals or larger (an acceleration generally large enough to cause liquefaction) will occur, on the average, once every 17 years, at the site of interest.

For the "Surface Acceleration Method," six layers were used, each 2 m thick with a mean shear strength determined from soil parameters. Several analyses were done to calculate the probability of liquefaction, using several definitions of "site liquefaction" in terms of "layer liquefaction." (This is defined as the occurrence of a shear stress in a layer greater than the strength.) These results are presented in Figure 5. It is evident that the most conservative criterion for estimating liquefaction risk is to define liquefaction as the occurrence of shear stresses greater

than shear strengths in one or more layers. This may be too conservative a criterion for estimating the effects of liquefaction damage on structures; many structures may be undamaged if only one thin subsurface layer reaches a liquefiable state. If the criterion for liquefaction is that one specific low-strength layer has shear stresses equal to shear strengths, the risk of this phenomenon (0.08 per year) is about equal to the risk that two or more layers liquefy.

Further detailed comparison between the two methods (discussed in McGuire et al., 1978) shows that the empirical method accounts for the liquefaction hazard produced by low amplitude, long duration shaking typically observed long distances from large earthquakes, while the surface acceleration method does not. On the other hand, the surface acceleration method indicates more liquefaction hazard for small earthquakes. When integration is done over all magnitudes, the two methods indicate about the same annual risk, although there are major differences in the methodologies.

It is thought that the estimates of liquefaction probability by both methods are conservative. This results, in the case of the empirical method, because soil strength is not accounted for, so that the analysis is appropriate for sites with only the weakest liquefaction resistance. For both methods the seismicity assumptions appear extremely conservative, especially in light of acceleration and liquefaction experience in the Tokyo area in the past 50 years (recall that the representation of seismicity for the risk analysis used an activity rate and upper-bound magnitude based on the entire historical record; the last 50 years of seismicity indicate a lower activity rate and a smaller upper-bound). Hence it is not thought that the surface acceleration method itself is an inherently conservative method. It is concluded, however, that the surface acceleration method is a viable one for calculating liquefaction hazard. Further research will be done to account for motion duration by this method, both in the seismic loadings and in the soil resistance.

Acknowledgments

This research was conducted at the Public Research Institute, Ministry of Construction, Japan, while the first author was staying at the Institute during the tenure of a Japanese Government Research Award for Foreign Specialists. He expresses his appreciation to the Science and Technology Agency for providing him with the opportunity to study in Japan. He also expresses his appreciation to the staff members at the Public Works Research Institute for their efforts on his behalf as a visiting researcher in the Earthquake Disaster Prevention Division in the Chiba Branch.

References

1. Crouse, C. B., Guzman, R., and Espana, C., (1977). "Probabilistics Evaluation of Liquefaction with the Application to a Site Near a Subduction Zone," Proc. 6th World Conference on Earthquake Engineering, New Delhi, India, Jan., Vol. 6, pp. 34-48.

2. Ferritto, J. M., and Forrest, J. B. (1977). "Siting Structures in Seismic Liquefaction Areas," Proc. 9th International Conference on Soil Mechanics and Foundation Engineering, Tokyo, July, Vol. 2, pp. 225-229.

3. Gibbs, H. J. and Holtz, W. G. (1957). "Research on Determining the Density of Sand by Spoon Penetration Test," Proc. 4th International Conference on Soil Mechanics and Foundation Engineering, London, Vol. 1, pp. 35-39.

4. Ibukiyama, S., Juribayashi, E., and Iwaski, T. (1972). Earthquake Resistibility of Submerged Tunnels," Proc. 4th Joint Meeting, U.S.-Japan Panel on Wind and Seismic Effects, Washington, D.C., May.

5. Kuribayashi, E., and Tatsuoka, F. (1975). "Brief Review of Liquefaction during Earthquakes in Japan," Soils and Foundations, Vol. 15, No. 4, Dec.

6. McGuire, R. K. (1976). "Fortran Computer Program for Seismic Risk Analysis," U. S. Geol. Survey Open-File Report 76-67, 90 pp.

7. McGuire, R. K., Tatsuoka, F., Iwasaki, T., and Tokida, K. (1978). "Probabilistics Procedures for Assessing Soil Liquefaction Potential," Journal of Research, Vol. 19, Public Works Research Inst., Ministry of Construction, Tokyo, March.

8. Ohashi, M., Iwasaki, T., Tatsuoka, F. (1978). "A Simplified Procedure for Assessing Seismic Liquefaction of Silty Sand Deposits," Central American Conference on Earthquake Engineering, San Salvador, El Salvador, Central America.

9. Seed, H. B. (1976). "Evaluation of Soil Liquefaction Effects on Level Ground during Earthquakes," State-of-the-Art, Preprint of ASCE Annual Convention and Exposition on Liquefaction Problems in Geotechnical Engineering, Philadelphia.

10. Seed, H. B., and Idriss, I. M. (1971). "A Simplified Procedure for Evaluating Soil Liquefaction Potential," Journal of the Soil Mechanics and Foundations Division, ASCE, Vol. 97, No. SMA, Sept., pp. 249-274.

11. Yegian, M. K., and Whitman, R. V. (1977). "Soil Liquefaction Analysis Based on Field Observations," Proc. 6th World Conference on Earthquake Engineering, New Delhi, India, Jan., Vol. 7, pp. 25-30.

12. Yoshimi, Y., Richard, F. E., Jr., Prakash, S., Barkan, D. D., and Ilyichev, V. A. (1977). "State-of-the-Art Report of Soil Dynamics and Its Application to Foundation Engineering," Proc. 9th International Conference of Soil Mechanics and Foundation Engineering, Tokyo, June, Vol. 2, pp. 605-650.

13. Youd, T. L., and Perkins, D. M. (1977). "Mapping of Liquefaction Potential Using Probability Concepts," Preprint of ASCE Annual Convention and Exposition, San Francisco, Oct.

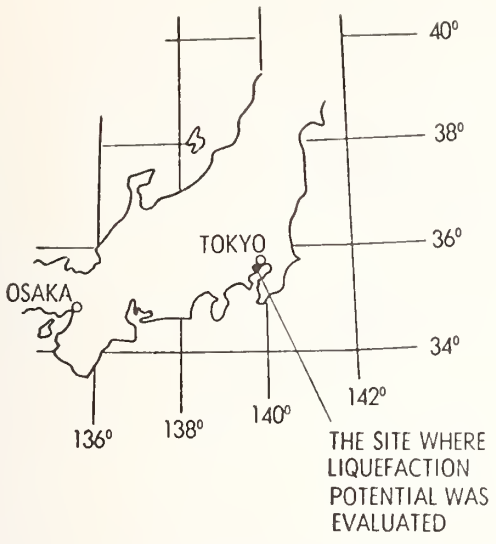

FIGURE 1: LOCATION OF THE SITE WHERE LIQUEFACTION POTENTIAL WAS EVALUATED.

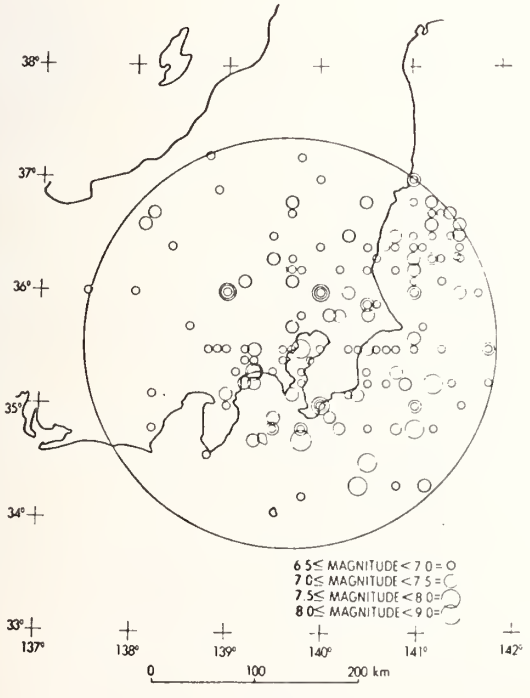

FIGURE 2: OBSERVED SEISMICITY WITHIN 200 KM OF SITE DURING YEARS 416 TO 1977.

13

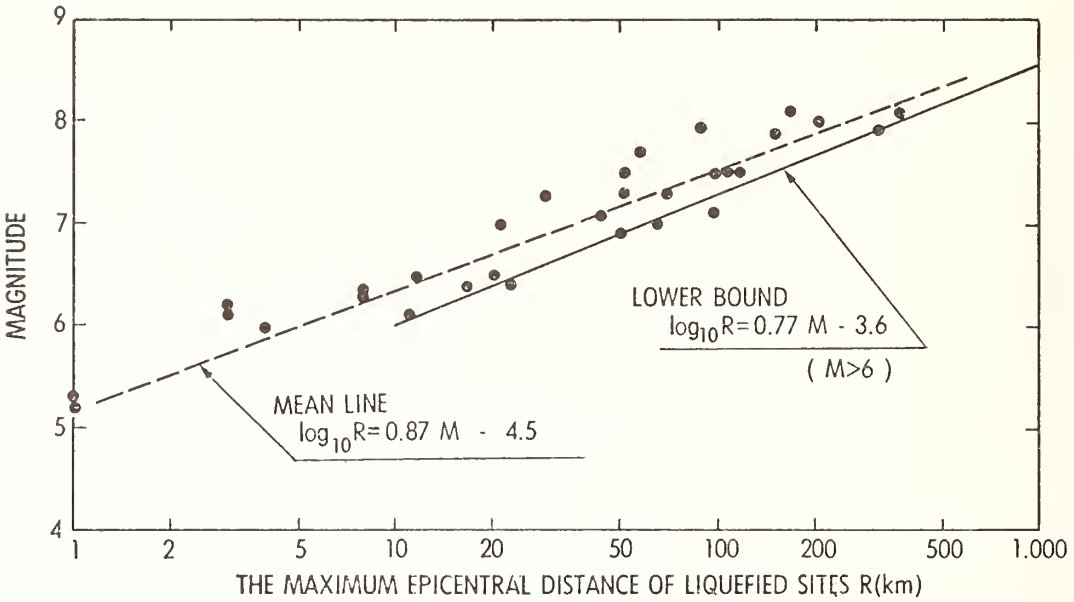

FIGURE 3: RELATIONSHIP BETWEEN FARTHEST DISTANCE TO LIQUEFIED SITES AND MAGNITUDE (AFTER KURIBAYASHI AND TATSUOKA, 1975).

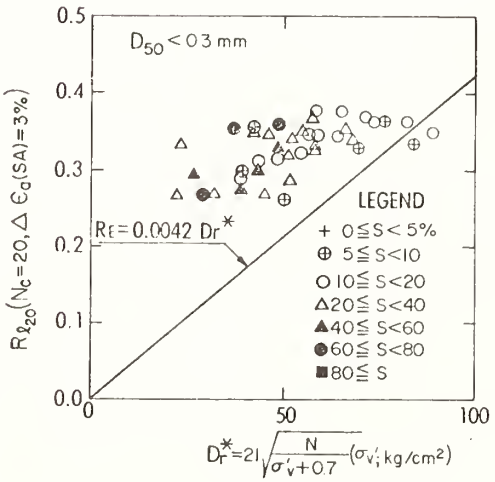

FIGURE 4: COMPARISON OF $R_{\ell 20}$ AND D_R* USING DATA OBTAINED IN THIS INVESTIGATION.

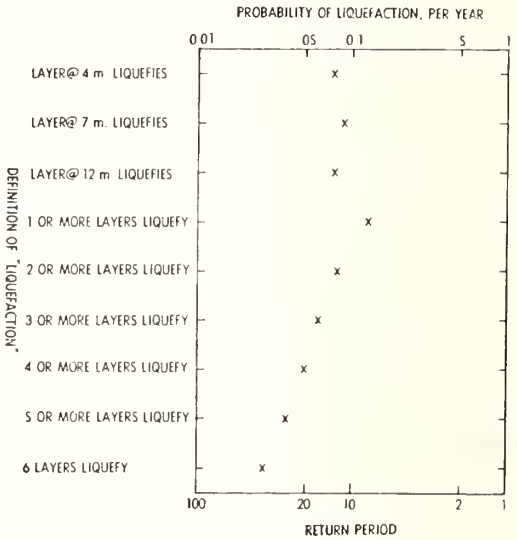

FIGURE 5: PROBABILITY OF SITE LIQUEFACTION USING VARIOUS DEFINITIONS, FOR SURFACE ACCELERATION METHOD.

14

A PRACTICAL PROCEDURE FOR ASSESSING EARTHQUAKE-INDUCED LIQUEFACTION OF SANDY DEPOSITS

Masamitsu Ohashi
Toshio Iwasaki
Fumio Tatsuoka
Ken-ichi Tokida

Public Works Research Institute
Ministry of Construction

A Practical Procedure for Assessing Earthquake-Induced Liquefaction of Sandy Deposits

Many structures were damaged due to severe soil liquefaction and associated ground failures during such major earthquakes as the Niigata earthquake of 1964 and the Alaska earthquake of 1964. During these earthquakes, it also became evident that liquefaction occurred primarily in sandy alluvial deposits and reclaimed lands (Kuribayashi and Tatsuoka, [1975], Kuribayashi, Iwasaki and Tatsuoka, [1977], Youd and Hoose [1977]). Recently, the number of structures constructed or to be constructed in liquefaction-susceptible deposits has been increasing daily. These circumstances have stimulated studies on liquefaction and, at present, many findings have been reported in this field (Seed [1976], Yoshimi et al [1977]). Furthermore, evaluation of liquefaction potential of soil and, if necessary, countermeasures against liquefaction are gradually becoming common in ordinary aseismic design of structures.

In actual practical procedures for evaluation of liquefaction potential of sandy soil deposits, blow counts or N-values by standard penetration tests have been often used. Since a standard penetration test is easy to conduct in situ, it is a common engineering practice in Japan. At present, for most civil engineering designs this test is generally conducted. Therefore, procedures to estimate liquefaction potential with use of N-values are convenient to practical engineers. Figure 1 shows several proposals to evaluate the liquefaction potential of sandy deposits utilizing N-values summarized by (Tsuchida (1975)). Those methods can be called "the critical N-value method." In some of those methods, however, several factors such as ground water level and grain size are not taken into account.

This paper presents a simplified design procedure for evaluating liquefaction potential summarizing the recent research in this field. By this method proposed with the information about (1) ground water level, (2) unit density of soil γt, (3) the standard penetration N-values, and (4) mean grain size D_{50}, the soil liquefaction potential can be easily evaluated.

Outline of the Method Employed

Figure 2 shows schematically the dynamic behavior of a horizontal surface ground during earthquake motions. An element in the surface soil deposit is subjected to cyclic shear stress. In this paper, dynamic loads to soil elements caused by earthquake motions are defined as

$$L = (\tau/\sigma_v')_{max} \qquad (1)$$

in which τ means the maximum amplitude of shear stress in single amplitude and σ_v' is the effective overburden pressure at the static condition (see Figure 2). Corresponding to L, the resistances of soil elements to dynamic loads will be defined as R. The method to evaluate R will be described later. Then, the ability to resist the occurrence of liquefaction of the soil elements can be expressed by

$$F_L = R/L \qquad (2)$$

F_L is the liquefaction resistibility factor. From the special distribution of the value of F_L in the ground concerned, the liquefaction potential can be evaluated. In this method, the effects of seepage of excessive pore pressure caused by cyclic earthquake-induced shear stress are not accounted for. This is because when

14

these effects are included in the analyses, the procedures will become too complicated. A simplified procedure that accounts for the effects of the seepage has to be developed.

Evaluation of Resistance

Figure 3 shows a typical result of undrained cyclic triaxial tests on sand specimens. These were obtained by special sand samplings. The methods of sand sampling employed or referred to in this study are listed in Table 1. These methods can be considered highly advanced ones in Japan. Triaxial specimens were made by cutting the frozen samples which were obtained by the sand samplings.

Undrained cyclic triaxial tests were performed on the specimens isotropically consolidated with the initial effective overburden pressure σ_v'. In Figure 3, the number of cyclic loadings N_c where the double-amplitude axial strain DA becomes 1, 2, 6 or 10 percent or the effective confining pressure becomes zero are plotted against the axial deviator stress σ_{dp} in single-amplitude divided by two times the initial effective confining pressure σ_c'. The detailed procedures of sampling, transporation, sample preparation, triaxial tests or so were described in the previous papers (Ohashi, Iwasaki and Tatsuoka (1977) and Tatsuoka, Iwasaki, Tokida, Yasuda, Hirose, Imai and Kon-no (1978)). In this study, the dynamic shear strength in dynamic triaxial tests is defined as

$$R_1 = (\sigma_{dp}/2_{\sigma c}') \tag{3}$$

which is the stress ratio $(\sigma_{dp}/2_{\sigma c}')$ at the number of loading cycles N_c=20 where the amplitude of axial strain in double-amplitude (DA) becomes 5 to 6 percent. The values of R_1 used in this study were read from figures such as Figure 3. In general, to obtain a value of R_1, three or six specimens obtained from one liner were tested. Of course, the definition of strength as a function of the number of loading cycles and amplitude of axial strain should depend on the purpose of the study; for this research, the definition of Equation (3) was considered adequate. Effects of changes in N_c and in amplitude of axial strain will be considered in future studies. It was found that the difference of R_1 between DA=5 percent and for 6 percent is quite small (3 percent of most) and that R_1 for DA=5 percent and R_1 for DA=6 percent can be considered to be utilized for the same analyses. And in all of the tests referred, the Skempton's B-values were larger than 0.96. Note that except for the values of isotropical confining pressure σ_c' and frequencies of cyclic loading, the dynamic triaxial tests referred in this study were performed by the almost same method using the almost similar apparatus. The other specifications employed are listed in Table 1.

In situ dynamic strength R can be evaluated from R after several corrections as

$$R = C_1 \cdot C_2 \cdot C_3 \cdot C_4 \cdot C_5 \cdot R_\ell \tag{4}$$

Those correction factors C_1 to C_5 are to take into account the random variation in the time history of L, the in situ anisotropic stress condition, the sample disturbance, the densification of samples during sampling and handling, and the effects of the two-dimensional cyclic loading, respectively. These are described in detail in the previous papers (Ohashi, Iwasaki and Tatsuoka (1977), McGuire, Tatsuoka, Iwasaki and Tokida (1978)). It can be considered

that when the in situ coefficient of earth pressure at rest K_o is 0.5,

$$R \fallingdotseq R\ell \tag{5}$$

Note that the value of R or Rℓ depends on the value of DA in equation (3). For this research, the definition of Equation (4) was considered adequate.

In the simplified procedure for liquefaction potential evaluation it is desirable that the value of R can be estimated easily. Actually, it is quite expensive to estimate R using Equations (3), (4) and (5) from the methods described above. Therefore, it has been expected and tried to evaluate R from the N-values, the unit density γt, the ground water level and the grain size distribution of disturbed samples.

In most previous studies, in situ dynamic shear strengths of sands for liquefaction potential analyses were evaluated using relative densities which were in turn estimated from measured N-values and effective overburden pressure σ_v' (Seed and Idriss (1967)). This method is denoted as the A-method in Figure 4. In the A-method, two different equations are utilized, namely (i) the relationship among N, σ_v', relative density Dr and other soil and ground parameters, and (ii) the relationship among undrained cyclic strength, σ_v', Dr and other soil parameters. The most important factor which is firstly evaluated in the A-method is relative density Dr defined as

$$Dr = \frac{e_{max} - e}{e_{max} - e_{min}} \times 100\ (\%) \tag{6}$$

in which e is the estimated in situ void ratio, and e_{max} and e_{min} are the maximum and minimum void ratios of the soil, respectively. In order to estimate in situ dynamic shear strength from values of relative density which have in turn been estimated from measured N-values, it is necessary that the following three points be confirmed.

(1) Relative density can be estimated from measured N-values within the limit of errors allowable for engineering purposes.

(2) The standard methods of measuring the minimum and the maximum densities of sands have been established.

(3) Dynamic shear strength can be estimated from estimated relative densities within the limit of errors allowable for engineering purposes.

To confirm item (1), a number of studies have been performed already. Among them, Meyerhof [1975] proposed the following empirical equation on the basis of laboratory tests using clean sands performed by Gibbs and Holtz (1957):

$$Dr^* = 21 \sqrt{N/(\sigma_v' + 0.7)} \tag{7}$$

in which Dr* is the estimated relative density (as distinguished from measured relative density Dr by Equation (6)) (see Figure 5). Recently Japanese Society of Soil Mechanics and Foundation Engineering conducted sand samplings at Niigata using a reformed Bishop-type sand sampler (JSSMFE [1976], Bishop [1948], Hanzawa and Matsuda [1977]). The liner had an inside diameter of 5.3 cm and a length of 65 cm. The liner was driven into the sand deposit with the position

of the piston fixed. For sampling, the liner was pulled up into the chamber filled with air, causing negative pore pressure and minimizing disturbance to the sample. The methods for estimation of the maximum and minimum void ratios are shown in Table 1. Void ratio determined by this procedure will be denoted as e_F hereafter. Figure 6 shows the comparison between measured relative density Dr and estimated relative density Dr* by Equation (7). As Castro (1975) did, the standard penetration resistances corresponding to undisturbed samples which are referred in this paper were obtained either in adjacent borings at the same boring and the blowcount (N-value) was not considered representative of the undisturbed sample if the soil description or grain size, or both, were different. The sand deposit at Niigata consists of relatively clean medium grain size sand. While a scatter is observed in these figures, the correlation between Dr and Dr* is rather good. And it is evident that Equation (7) becomes quite misleading when the grain size becomes finer. Figure 7 shows the relationship Dr-Dr* and D_{50} from the data of Gibbs and Holtz (1957). Note that Equation (7) was established only on the basis of the data of air-dry and moist coarse sand. It can be seen from Figure 7 that the relative density is underestimated by Equation (7) for fine sand.

Figure 8 shows a summarized relationship between $D_r - D_r^*$ and D_{50} for several sites. The methods of sampling and measurements of e, e_{max} and e_{min} adopted for these sites are listed in Table 1. At site J, a frozen column method was utilized by Yoshimi, Hatanaka and Oh-oka [1977] and Hatanaka [1977]. In this method a large scaled frozen column of sand, around 5 m in length and around 4 cm in diameter, was made in the ground and this was pulled out with a force of 5 tons or more to the ground. Small pieces of frozen specimen were cut from the large frozen column and their void ratios were measured while being kept frozen. It was confirmed by them from other basic experiments that void ratios determined by the method described as above are almost identical to in situ values of void ratio. It is seen in Figure 8 that there is a general trend showing $D_r - D_r^*$ decreases with the increase in D_{50}. Nevertheless, a scatter shown in Figure 8 is too large for Equation (7) to be used in precisely evaluating relative densities of various sands with a large range of D_{50}. Especially for silty sands which include a large amount of fine soils, it is obvious that relative densities are usually underestimated by Equation (7).

As to item (2), the standard method of measuring the values of e_{max} and e_{min} have not been established in Japan so far. Several methods have been proposed by different researchers, and it is well-known that the values for silty sands depend on the method employed significantly. Therefore, it is not possible to determine uniquely the relative density of silty sands in Japan even when samples are given. It can be seen in Table 1 that the values of e_{max} and e_{min} for an identical sand (Toyoura Sand) are different among different methods. This may be one of the reasons which cause a scatter in the data shown in Figure 8.

Finally, as to item (3), it is necessary that the relationship between dynamic shear strength and relative density D_r be established for undisturbed specimens. For reconstituted specimens, Lee and Fitton (1969) and Seed and Idriss (1971) show that there is a variation in dynamic shear strength for an identical relative density with the variation in D_{50}. In this study, available data of undisturbed specimens were utilized to examine whether there is a correlation between dynamic shear strength and D_{50} as follows. Figure 9 is the summary of the realtionship between R_1 and D_r for

undisturbed specimens. It is obvious that there is no correlation among the data. To examine whether the variation in D_{50} is a main cause for a large scatter in the data in Figure 9 or not, a parameter DR_1 was defined as

$$DR_1 = R_1 - 0.0042\ D_r \tag{8}$$

Equation (8) is based on the following equation:

$$R = 0.0042\ D_r \tag{9}$$

This was established on the basis of the test results on reconstituted clean sands by various investigators (Ohashi, Iwasaki and Tatsuoka (1977)). These samples were made by almost the identical method.

Figure 10 shows the relationship between D_{50} and DR_1 for the data shown in Figure 9. It is seen from Figure 20 that there is not a good correlation between DR_1 and D_{50}. From Figures 9 and 10, it is obvious that even if relative density could be estimated precisely, it is still difficult to estimate undrained cyclic triaxial strength from estimated relative density on the basis of the data shown in these figures.

Figure 11 shows the relationship between fine contents and the ratio of R_1 of undisturbed specimens from site A to R_1 of reconstituted specimens which were made from completely disturbed soils obtained from the undisturbed specimens. The reconstituted specimens were made by raining de-aired soil into a mold filled with de-aired water and had equal relative density with that of undisturbed specimens. It is seen from Figure 11 that the differences of R_1 for equal density between undisturbed specimens and reconstituted specimens are considerably large for this case. This has been also reported by Ishihara and Tanaka (1974), Seed, Mori and Chan (1975) and Mulilis, Mori, Seed and Chan (1977). This means that there are some other unknown factors causing a scatter in R_1 and in DR_1. Ladd (1974, 1976) and Mulilis, Chan and Seed (1975) reported that one of these reasons is the fabric of sand. They showed that dynamic shear strength of reconstituted sands are greatly affected by the mode of sample preparation. The variation in dynamic shear strength due to the variation in fabric for the same density may also be possible in in situ dynamic shear strengths, as shown in Figure 11. Therefore, it is evident that relative density is not a unique parameter which determines the dynamic shear strength of sand.

In summary, it is evident that with present knowledge it is extremely difficult to estimate undrained cyclic strength R_1 of various sands by the A-method using standard penetration resistances, σ_v' and other factors within the limit of error allowable for engineering purposes.

The B-method shown in Figure 4 is a more direct method than the A-method as described below. First, it is logical that in situ dynamic shear strength is in general related to several factors such as N-values, overburden effective pressure, σ_v', lateral earth pressure, $\sigma_h' = K_o \sigma_v'$, grading properties and strain or stress histories. As for parameter, K_o, the value of 0.5 may be assumed for all deposits examined in this study. To account for the effects of σ_v' on N-values, Equation (7) was adopted in correlating R_1 with σ_v', N and gradings of sands. However, it should be noted that in these procedures, the value of Dr* does not necessarily mean relative density but represents an in situ parameter of soil conditions.

Figure 12 shows the summary of the correlation where the relationship between R_2 and D_r* is presented. Also shown is the line representing the equation

$$R_1 = 0.0042 D_r^* \quad (10)$$

This can be derived by substituting $D_r = D_r^*$ into Equation (9). The data for $\sigma_r' = 0.5$ to 2.5 kg/cm$_2$ from Castro (1975) are included in Figure 12 in which R_2 for $N_c = 20$, R_{120} were converted from R_1 and $N_c = 10$, R_{110}. Obviously, it is seen from Figure 12 that there is no correlation between R_1 and D_r*. Castro (1975) has reported that the liquefaction of laboratory samples extracted from zones of sand having a high penetration resistance is little better than that of samples extracted from zones of low penetration resistance. He suggested that this is due to a loosening of the dense sand during the sampling process. The data of such dense sands by Castro (1975) are shown by three points D_r* of which are larger than 100. However, it can be assumed that the effects of such loosening may be relatively small for the sand deposits referred in this study. This is because all the specimens referred in this study were extracted from loose or medium sandy deposits which have D_r* less than 100. Furthermore, it should be noted that D_r* or N-values can be largely affected by grain size. This means that a large D_r* or large N-value may be caused by that the zones are gravelly and may not be caused by high density. Therefore, it can be anticipated that there can be a relatively high correlation among R_1, D_r* and parameters which represent grading properties of sands. To find this correlation, a parameter was defined as

$$DR_1^* = R_1 = 0.0042\ D_r^* \quad (11)$$

in which R_1 is measured dynamic strength by Equation (3) and D_r* is measured value by Equation (7). Note that Equation (11) is analogous to Equation (8). Figure 13 shows the relationship between DR_1* and fine material content FC for fine sands D_{50} of which are smaller than 0.3 mm (Ohashi, Iwasaki and Tatsuoka (1977)). It can be seen from Figure 13 that there is a good correlation between DR_1* and FC. The average line can be represented by

$$D_{R_1}^* = 0.0035\ FC \quad (12)$$

in which FC is fine material content in percentage. From Equations (11) and (12),

$$R_1 = 0.0042\ D_r^* + 0.0035\ FC \quad (13)$$

For fine sands D_{50} of which are smaller than 0.3 mm, approximate values of R_1 can be estimated from D_r* and FC using Equation (13). For a wider range of D_{50}, FC is not a good parameter for representing grading properties of sands. The mean diameter D_{50} can be a more general parameter than FC. Figure 14 shows the summary of the relationship between DR_1* and D_{50} from the data available at present. It can be seen from Figure 14 that for a wide range of D_{50}, there is a high correlation between DR_1* an D_{50}. The average line drawn in Figure 14 appears to be a reasonable representation of the relationship between DR_1* and D_{50}. This line was determined to fit the data as well as possible, but not to be too complicated compared with their scatter. Especially for D_{50} larger than 0.6 mm, the constant value of DR_1* was considered appropriate. This average line can be represented by

$$DR_1^* = -0.225 \log_{10} (D_{50}/0.35) \quad \text{for } 0.04 \leq D_{50} \leq 0.6 \text{ mm}$$

nd

$$DR_1^* = -0.05 \quad \text{for } 0.6 \leq D_{50} \leq 1.5 \text{ mm} \qquad (14)$$

rom Equations (11) and (14)

$$R_1 = 0.0042\, D_r^* - 0.225 \log_{10} \left(\frac{D_{50}}{0.35}\right) \quad \text{for } 0.04 < D_{50} < 0.6 \text{ mm}$$

nd

$$R_1 = 0.0042\, D_r^* - 0.05 \quad \text{for } 0.6 < D_{50} < 1.5 \text{ mm} \qquad (15)$$

n which $D_r^* = 21 \sqrt{N/(v' + 0.7)}$.

or D_{50} ranging from 0.04 to 1.5 mm, Equation (15) can be used to stimate approximate dynamic shear strength R_1 using D_r^* and D_{50}. t can be noted that for the same value of D_r^*, R_1 increases with he decrease in D_{50} in Equation (15). This means that if Equation 10) is used to estimate R_1 from D_r^*, R_1 can be underestimated for iner sands. Therefore, it can be pointed out from the facts shown n the above that if liquefaction potential is estimated directly rom N-values without taking into account grading properties of a and, liquefaction potential can be overestimated for finer sands. quation (15), which can be considered to be one of the best ones hich fit the data available at present, has an advantage over the -method as follows. In Equation (15), factors affecting undrained yclic strength such as fabric of sands, static and dynamic stress-train time histories can be considered to have been taken into ccount in a simple manner. This is because these factors also ffect standard penetration resistances in the similar manner to ndrained cyclic strength (Seed (1976)). This makes the B-method onsiderably simpler than the A-method.

valuation of L

he dynamic load L defined by Equation (1) can be estimated from he following equation;

$$L = K_s \frac{\sigma_v}{\sigma_v'} r_d \qquad (16)$$

This is based on the simplified procedure for liquefaction otential evaluation by Seed and Idriss (1971). In Equation (16), $K_s = \alpha_s/g$ in which α_s means the design maximum acceleration on the round surface in gals and g is the acceleration of gravity (980 als), σ_v is the total overburden pressure, σ_v' is the effective verburden pressure and r_d means the reduction factor for dynamic hear stress accounting for the elastic performance of the ground. he most important part in evaluating L is to estimate K_s in quation (16). In general, K_s can be considered to be affected y the magnitude, the frequency characteristics of the input motion t base rock, the response characteristics of the surface soil eposit. Furthermore, the duration of earthquake motion affects he liquefaction potential. Nevertheless, it is rather difficult o evaluate or to establish "the design earthquake motion" for each f numerous construction sites of bridges. On the other hand, in he Specifications for Earthquake Resistant Design of Highway ridges, Japan Road Association 1972, it is specified that the agnitude of earthquake motion is represented by the seismic coeffi-ient K_h. The aseismic design of highway bridges are performed y the static seismic coefficient method. Therefore, it can be onsidered reasonable to introduce such a parameter as K_h into he evaluation of earthquake-induced liquefaction potential for the seismic design of highway bridges. Although additional research

14

is necessary, the value of K_s which is used in Equation (16) can be proposed tentatively as

$$K_s = \frac{3}{4} K_h = \frac{3}{4} \nu_1 \cdot \nu_2 \cdot \nu_3 \cdot K_0 \qquad (17)$$

in which the parmeters K_h, $\nu_1 \cdot \nu_2 \cdot \nu_3$ and K_0 are the ones specified in the Section 4:2 "Design Seismic Coefficient" in the Specifications for Earthquake Resistant Design of Highway Bridges. K_h is the design seismic coefficient for bridges, ν_1 is the zone factor, ν_2 is the ground condition factor, ν_3 is the importance factor and K_o is the standard design seismic coefficient for bridges (K_o=0.2). The value of K_2 is assumed to be 75 percent of K_h which is the seismic coefficient of a bridge, in viewing the results of underground strong-motion observation.

An alternative method to estimate K_s besides Equation (17) can be proposed as

$$K_s = \frac{\alpha_s}{g} = 18.4 \times 10^{0.302M} \times \Delta^{-0.800}/g \qquad (18)$$

in which M is the Richter's magnitude of the design earthquake and Δ is the corresponding epicentral distance of km. Equation (18) can be utilized when the values of M and Δ can be specified for the construction site concerned. Equation (18) was derived from the statistical analysis of the strong motion records measured in Japan (Ohashi, Iwasaki, Wakabayashi and Tokida (1977)).

It is to be noted that the value of σ_v/σ_v' affects L considerably as seen in Equation (16). Figure 15 shows the effects of the ground water level on the value of σ_v/σ_v'. It can be seen in Figure 15 that the value of σ_v/σ_v' decreases with lowering the ground water level and in turn the value of L decreases. This means that to lower the ground water level is quite an effective way to reduce liquefaction potential. It is also noted that the value of γt affects considerably σ_v/σ_v'. It was found that the value of r_d is considerably affected both by the frequency characteristics of input motions and by the rigidity of subsoils. Figures 16 and 17 show the typical results of earthquake response analyses using several earthquake records for an alluvial deposit, and soft alluvial deposit, respectively. These analyses were performed by the computer program "SHAKE" by Seed, et al. (1971). It can be seen in those figures that the value of r_d is, in general, smaller for the input earthquake motion with smaller predominant period T_e and for the subsoils with large natural frequency Tg. It can be also expected that T_e is correlated with the magnitude of earthquake M, the epicentral distance Δ, or so. As a simple correlation among r_d, T_e (or M, Δ), Tg or so is not established yet, it was considered reasonable to estimate r_d for the simplified method from the average relationship as

$$r_d = 1-0.015Z \text{ (Z:depth in meters)} \qquad (19)$$

In some cases, there exists extremely soft deposit of the thickness of 2-4 m whose unit density is around 1.2-1.3 t/m^3 above the liquefaction susceptible sand layer in river beds. In those cases, the value of σ_v/σ_v' at the top of the sand layer becomes extremely high. As it can be expected that the deformability of those extremely soft clay layers are quite large and therefore the value of r_d can be considered very low. Although additional research necessary, it can be considered reasonable to estimate L assuming that those extremely soft clay layers do not contribute to both L and R when r_d is estimated from Equation (19).

Some Case Studies

The liquefaction potentials of several sites in Niigata City were analysed by the method proposed in this paper. In the procedures, it was assumed that $K_s = 0.17$ and $r_d = 1-0.015Z$. This is because the maximum acceleration of the recorded earthquake motion at the ground surface at Niigata was around 170 gals and it was found from response analyses of sand deposits that $r_d = 1-0.015Z$ is reasonable for the sandy deposits in Niigata City. Figures 18 and 19 show the variation of F_L with depth for the sites where no liquefaction phenomena were observed. It can be seen in these figures that the values of F_L are larger than 1.0. Figures 20 and 21 show the variation of F_L with depth for the sites where severe liquefaction phenomean were observed. It can be seen in those figures that F_L is, in general, less than 1.0 for the liquefied zones. The ranges of liquefied zones were estimated from the damage to the pile of a bridge (in the case of Figure 20) or from the comparison of the grading of the spouted sand with those of the soil deposits (in the case of Figure 21). Figure 22 summarizes the results of the analyses of the sites in Niigata city in the $F_L \sim Z$ relationship. The ranges of liquefied zones were estimated from several observations as described above. It can be seen in Figure 22 that the most data points where the values of F_L less than 1.0 are those of liquefied zones and that the most data points where the values of F_L were are larger than 1.0 are those of non-liquefied zones. This tendency is especially noted for a depth shallower than 10 m. From those facts, it can be concluded that, while some modifications are necessary, the simplified method proposed herein can be used for evaluating approximate liquefaction potential.

A Method for Evaluating F_L

It is obvious that the damage of foundations due to soil liquefaction is considerably affected by the severity of liquefaction phenomena at each zone and the depth and the width of liquefie d zones. For this purpose, the damage to foundation structures was compared with the distribution of the estimated values of F_L in the case of the Niigata Earthquake of 1964. It was found that the severe damage to foundation structures was found only when the value of F_L is considerably less than 1.0, say 0.6, and the zone where F_l is considerably less than 1.0 is not thin, say thicker than 5 m. From those observations, the following method can be proposed tentatively for the aseismic calculation of lateral behavior of pile foundations of bridges:

$$\left.\begin{aligned} q_{h\ell} &= C \cdot q_h \\ K_{h\ell} &= C \cdot K_h \end{aligned}\right\} \qquad (20)$$

in which q_h and K_h are the lateral bearing capacity and the lateral spring constant, respectively, which are estimated when neglecting liquefaction phenomena. $q_{h\ell}$ and $K_{h\ell}$ are the lateral bearing capacity and the lateral spring constant accounting for liquefaction phenomena. C is a correction factor accounting for liquefaction phenomena, and is assumed to be given as follows:

$$\begin{aligned} &C = 1.0 \text{ for } F_L \geq 1.0, \\ &C = 2/3 \text{ for } 1.0 \geq F_L > 0.8, \\ &C = 1/3 \text{ for } 0.8 \geq F_L > 0.6, \\ \text{and} \quad &C = 0.0 \text{ for } F_L \leq 0.6 \end{aligned} \qquad (21)$$

Acknowledgments

The principal part of this research project was concluded at the Public Works Research Institute, the Ministry of Construction, while the third author was a staff member at the Ground Vibration Section of the Institute. Extensive in situ soil surveys and dynamic shear tests have been conducted by the Kanto Regional Construction Bureau of Ministry of Construction, Honshu-Shikoku Bridge Authority and Yokohama City. The authors express their cordial appreciation to the staff members concerned.

References

1. Bishop, A. W., (1948). "A New Sampling Tool for Use in Cohesionless Sand below Ground Water Level," Geotechnique, Vol. 11, pp. 125-131.

2. BRI, "Report on Damage to Buildings during Niigata Earthquake," The Building Research Institute, Ministry of Construction, No. 42, 1965.

3. Castro, G. (1975). "Liquefaction and Cyclic Mobility of Saturated Sands," Journal of the Geotechnical Engineering Division, ASCE, Vol. 101, No. GT6, pp. 551-569.

4. Gibbs, H. J. and Holtz, W. G. (1957). "Research on Determining the Density of Sand by Spoon Penetration Test," Proc. 4th International Conference on Soil Mechanics and Foundation Engineering, London, Vol. 1, pp. 35-39.

5. Hanzawa, H., and Matsuda, E. (1977). "Density of Alluvial Sand Deposits Obtained from Sand Sampling," Proc. of Speciality Session No. 2,, 9th ICSMFE, Tokyo, pp. 7-14.

6. Hatanaka, M. (1977). "Fundamental Studies on Undisturbed Sampling of Saturated Sands by Freezing", A Thesis for the Degree of Doctor of Eng., Tokyo, Institute of Technology.

7. Ishihara, K., and Tanaka, Y. (1974). "Liquefaction of Undisturbed Sand includng Fine Content," Proc. 9th Annual Meeting of JSSMFE, pp. 379-382 (in Japanese).

8. Ishihara, K. (1977). "Simple Method of Analysis for Liquefaction of Sand Deposits during Earthquakes," Soils and Foundations, Vol. 17, No. 3, pp. 1-18.

9. Ishihara, K., and Silve, M. L. (1977). "Lager Diameter Sand Sampling to Provide Specimens for Liquefaction Testing, "Proc. Speciality Session, No. 2, 9th ICSMFE, Tokyo, pp. 1-8.

10. Ishizawa, M., Nakagawa, S, and Kurohara, I. (1977). "Liquefaction Test of Undisturbed Samples Containing Fine Content," Proc. the 12th Annual Meeting of JSSMFE, pp. 397-400 (in Japanese).

11. Japanese Society of Soil Mechanics and Foundation Engineering (1976). "Report on Earthquake Damages of Subground Streets and Structures," March (in Japanese).

12. Kolbuszewski, J. J. (1948) "An Experimental Study of the Maximum and Minimum Porosities of Sand," Proc. 2nd ICSMFE, Vol. 11b, pp. 158-165.

Kuribayashi, E., and Tatsuoka, F. (1975). "Brief Review of Liquefaction during Earthquakes in Japan," Soils and Foundations, Vol. 15, No. 4, Dec.

Kuribayashi, E., Iwasaki, T., and Tatsuoka, F. (1977). "A History of Soil Liquefaction in Japan," Proc. 6th World Conference on Earthquake Engineering, New Delhi, India, Jan., Vol. 7, pp. 31-36.

Ladd, R. S. (1974). "Specimen Preparation and Liquefaction of Sands," Journal of GT Div., ASCE, Vol. 100, No. GT10, pp. 1180-1184.

Ladd, R. S. (1976). "Specimen Preparation and Cyclic Stability of Sands," Pre-print of ASCE Annual Convention and Exposition on "Liquefaction Problems in Geotechnical Engineering," pp. 199-226.

Lee, K. L., and Fitton, J. A. (1968). "Factors Affecting Cyclic Loading Strength of Soil," Vibration Effects of Earthquakes on Soils and Foundations, ASTM, STP450, pp. 71-95.

Meyerhof, G. G. (1957). "Discussion of Session 1," Proc. 4th International Conference on Soil Mechanics and Foundation Engineering, London, Vol. 3,

Marcuson III, W. F., Cooper, S. S., and Bieganousky, W. A. (1977). "Laboratory Sampling Study Conducted on Fine Sands," Proc. of Specialty Session, No. 2, 9th ICSMFE, Tokyo, pp. 12-22.

McGuire, R. K., Tatsuoka, F., Iwasaki, T., and Tokida, K. (1978). "Probabilistic Procedures for Assessing Soil Liquefaction Potential," Journal of Research, Public Works Research Institute, Vol. 19, March, 1978.

Mulilis, J. P., Chan, C. K., and Seed, H. B. (1975). "The Effects of Method of Sample Preparation on the Cyclic Stress-Strain Behavior of Sands," EERC-Report No. EERC 75-18, College of Engineering, University of California, Berkeley.

Mulilis, J. P., Mori, K., Seed, H. B., and Chan, C. K. (1977). "Resistance to Liquefaction due to Sustained Pressure," Journal of GT Div., ASCE, Vol. 13, No. GT7, July, pp. 793-797.

Ogura, K., Imai, T., and Suzuki, K. (1978). "Twist-type Sand Sample," Proc. 13th Annual Meeting of JSSMFE (in Japanese).

Ohashi, M., Iwasaki, T., and Tatsuoka, F. (1977). "Studies on Soil Liquefaction Related to Earthquake Resistant Design on Structures," 9th Joint Meeting, U.S.-Japan Panel on Wind and Seismic Effects, U.J.N.R. May.

Ohashi, M., Iwasaki, T., Wakabayashi, S., and Tokida, K. (1977). "Statistical Analysis of Strong-Motion Acceleration Records," 9th Joint Meeting, U.S.-Japan Panel on Wind and Seismic Effects, U.J.N.R. May.

PWRI, "Report on Niigata Earthquake," Report of the Public Work Research Institute, Ministry of Construction, Vol. 125, June, 1965.

27. Saito, A. (1977). "Characteristics of Penetration Resistance of a Reclaimed Sandy Deposit and their Changes through Vibratory Compaction," Soils and Foundations, Proc. of JSSMFE, Vol. 17, No. 4, pp.

28. Seed, H. B., and Idriss, I.M. (1967). "Analysis of Soil Liquefaction: Niigata Earthquake," Journal of SME Div., ASCE, Vol. 93, No. SM3, pp. 83-108.

29. Seed, H. B., Mori, K., and Chan, C. K. (1975). "Influence of Seismic History on Liquefaction of Sands," Journal of GT Div., ASCE, Vol. 102, No. GT4, pp. 257-270.

30. Seed, H. B. (1976). "Evaluation of Soil Liquefaction Effects on Level Ground during Earthquakes," State-of-the-Art Report, Preprint of ASCE Annual Convention and Exposition on Liquefaction Problems in Geotechnical Engineering, Philadelphia.

31. Seed, H. B., and Idriss, I. M. (1971). "A Simplified Procedure for Evaluating Soil Liquefaction Potential," Journal of the Soil Mechanics and Foundations Division, ASCE, Vol. 97, No. SM9, Sept., pp. 249-274.

32. Tanimoto, K., and Iwasaki, T. (1975). "Method of Measurement of Minimum Density of Sand," Proc. 10th Symposium on Soil Mechanics and Foundation Engineering, JSSMFE, pp. 11-14.

33. Tsuchida, H. (1975). "Present State and Problems in Earthquake Resistant Design of Grounds against Liquefaction," Tsuchi-to-kiso, Proc. JSSMFE, Vol. 13, No. 6, pp. 5-10.

34. Yoshimi, Y., and Tohno, I. (1972). "Statistical Significance of the Relative Density," ASTM, Special Technical Publication, No. 523.

35. Yoshimi, Y., Hatanaka, M., and Oh-oka, H. (1977). "A Simple Method for Undisturbed Sand Sampling by Freezing," Proc. of Specialty Session 2, ICSMFE, Tokyo, pp. 23-28.

36. Yoshimi, Y., Richard, F. E., Jr., Prakash, S., Barkan, D. D., and Ilyichev, V. A. (1977). "State-of-the-Art Report of Soil Dynamics and Its Application to Foundation Engineering," Proc. 9th International Conference on Soil Mechanics and Foundation Engineering, Tokyo, June, Vol. 2, pp. 605-650.

37. Yond, T. L., and Hoose, S. N. (1977). "Liquefaction Susceptibility and Geologic Setting," Proc. 6th World Conference on Earthquake Engineering, New Delhi, India, Jan., Vol. 6, pp. 37-42.

TABLE 1. LIST OF SAND SAMPLINGS AND DYNAMIC TRIAXIAL TESTS (see NOTE)

No.	Site	Moist Condition	Sand Sampling	Void Ratio Measurement	e_{min} Measurement	e_{max} Measurement	Dynamic Triaxial Test Condition				Reference
							σ_c' (kg/cm^2)	Frequency (Hz)	DA for Rf(%)	Specimen (ϕcm, hcm)	
1	Artificial in tank, compacted by vibration	Air Dry. Moist. Saturated	-	Direct density determination	Vibrating or hammering container using saturated sand	Lightly pouring dry sand into container	-	-	-	-	Gibbs and Holtz (1957)
2	Site A (in Tokyo, along Tokyo Bay) Alluvial and Reclaimed	Underwater	Reformed Bishop-type sand sampler; the liner is 5.3 cmϕ and 65 cmt *)	e_F; average void ratio in the liner	Tamping mold with air-dry sand**) (0.64)	Lightly pouring air-dry sand into mold**) (0.96)	= σ_v' = 0.2 ∿ 1.15	1.0	6	5ϕ, 10h	This Investigation *) Hanzawa and Mateuda (1976) **) Yoshimi and Tohno (1972)
3	Site B (in Shikoku, along Setonaikai Sea) Alluvial and Reclaimed	Underwater	Twist sand sampler; the liner is 7 cmϕ and 80 cmt	e'_F: estimated average void ratio in the liner	Identical to No. 2		= σ_v' = 0.45 ∿ 1.75	0.5	5	7ϕ, 14h	This Investigation
4	Site C (in Niigata City, along Shinano River) Alluvial and Reclaimed	Underwater	Larg diameter sand sampling; the liner is 20 cmϕ and 100 cmt;	e_0; void ratio of unconsolidated thawed specimen at σ_3 = 0.2 kg/cm^2	Vibrating mold using air-dry sand on shaking table with 1 kg/cm^2 being applied on the top (0.61)	Spooning air-dry sand into mold (0.96)	1.5 (σ_v' = 0.3 ∿ 1.15)	1.0	5	5ϕ, 10h	Ishihara (1976, 1977) Ishihara and Silver (1977)
5	Site D (in Tokyo) Alluvial	Underwater	Identical to No. 4				0.5 (σ_v' = 0.265∿0.610)	1.0	5	5ϕ, 10h	Ishizawa, Nakagawa and Kurohara (1977)
6	Site E (in Yokohama, along Tokyo Bay) Reclaimed	Underwater	Identical to No. 2	-	-	-	= σ_v' = 0.37∿0.77	1.0	6	5ϕ, 10h	This Investigation
7	Site F (in Tokyo, along Tokyo Bay) Alluvial	Underwater	Thin-wall sampling with enough cares	-	-	-	0.5, 1.0 (σ_v' = 0.24∿0.65)	1.0	6	5ϕ, 10h	This Investigation
8	Site G (in Tokyo along Tokyo Bay) Alluvial and Reclaimed	Underwater	Identical to No. 2				= σ_v' = 0.8∿1.14	0.5	6	5ϕ, 10h	This Investigation
9	Site H (Kawagish-cho, Niigata City) Alluvial and Reclaimed	Underwater	Identical to No. 2	e_F	Tamping mold using air-dry sand and applying pressure of 1 kg/cm^2 on the top (0.60)	Average by two method; Kolbuszewski (1948) and Tanimoto (1975) (0.94)	-	-	-	-	JSSMFE (1976)
10	Site I (Oh-gi Shima) Reclaimed	Underwater	Identical to No. 2	e_F	Identical to No. 9		-	-	-	-	Saito (1977)
11	Site J (in Yokohama, along Tokyo Bay) Reclaimed	Underwater	Frozen Column Method; making frozen 5mt, 40 cmϕ large column in ground	Void ratio of frozen specimen	The Yoshimi-and-Tohno method (0.62)	(0.98)	-	-	-	-	Yoshimi, Natsnaka and Oh-oka (1977), Natsnaka (1977)

NOTE: Figures in ( ) represent the maximum and minimum void ratios of Toyoura Sand determined by each method.

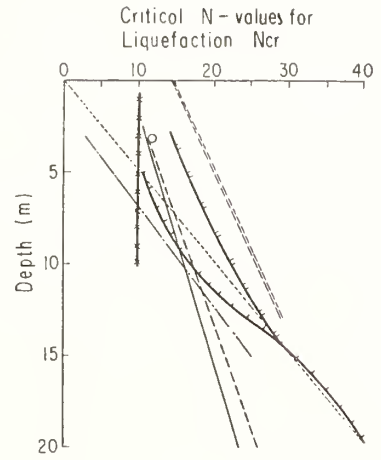

LEGEND

LEGEND

- ------ Design Code for Building Foundotions (the Architectural Institute of Jopon, 1974)
- Specificotion for Eorthquoke Resistont Design of Highwoy Bridges (Jopon Rood Associotion 1972)
- o Design Code for Port ond Horbour Structures (Jopon Port ond Horbour Associotion 1971)
- Koizumi (1965), Kishida (1971)
- Oh-soki (1970), Ishihoro (1973)
- Tonimoto (1971), Seed ond Idriss (1971)

Note ; Ground woter level - 3m ; Moximum occeleration during Eorthquoke ; 200 gols for Tonimoto, Seed ond Idriss ond Design Code for Building Foundotions.

FIGURE 1: CRITICAL N-VALUES FOR LIQUEFACTION POTENTIAL (TSUCHIDA (1975))

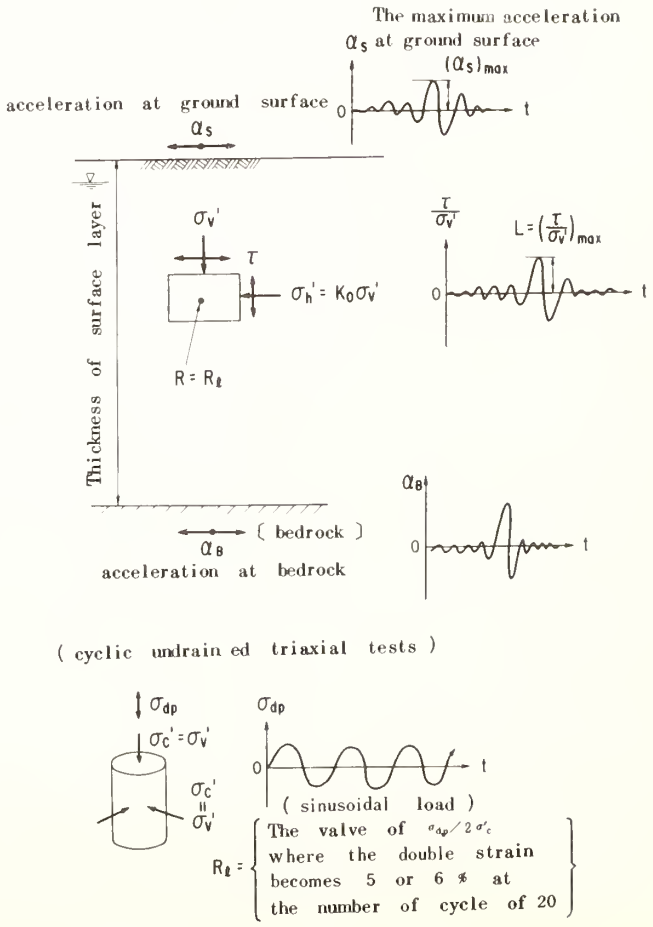

FIGURE 2: DEFINITIONS OF EARTHQUAKE INDUCED STRESS L AND DYNAMIC STRENGTH R

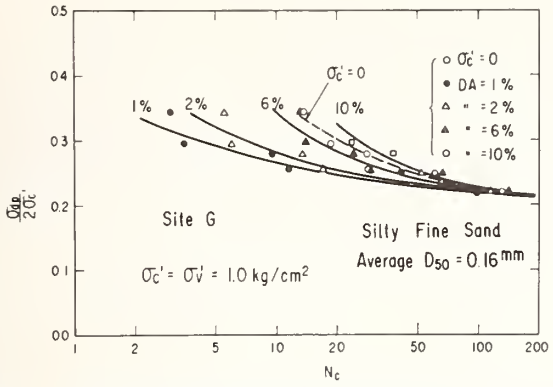

FIGURE 3. TYPICAL TEST RESULT OF DYNAMIC TRIAXIAL TEST ON UNDISTURBED SANDY SPECIMENS FOR SITE G

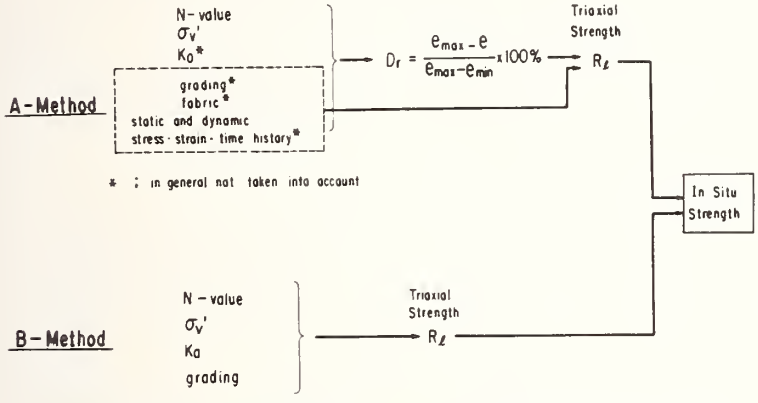

FIGURE 4: COMPARISON BETWEEN A-METHOD AND B-METHOD

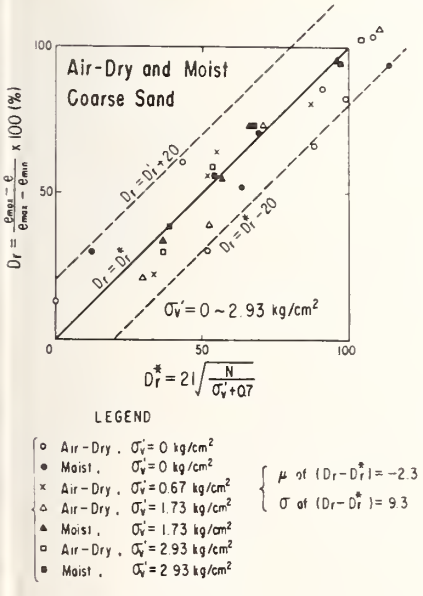

Figure 5: D_r AND D_r* RELATION OF AIR-DRY AND MOIST COARSE SAND

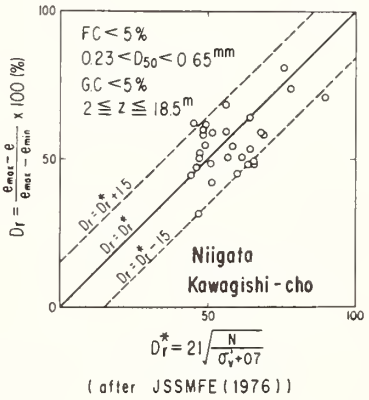

FIGURE 6: D_r AND D_r* RELATION BY THE DATA OF JSSMFE (1976)

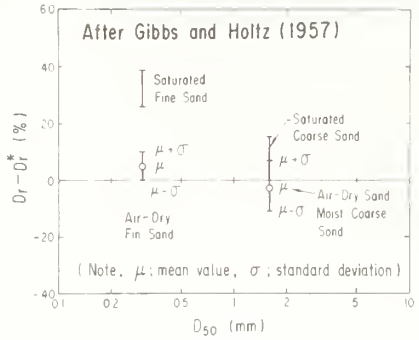

FIGURE 7: D_R-D_R* AND D_{50} RELATION AFTER GIBBS AND HORTZ (1957)

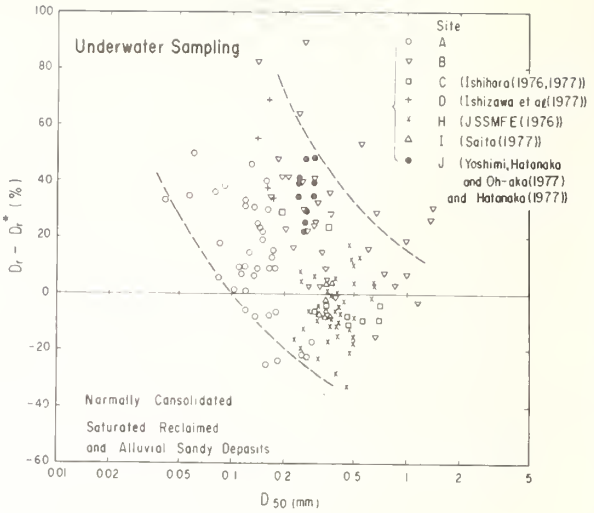

FIGURE 8: D_R-D_R* AND D_{50} RELATION

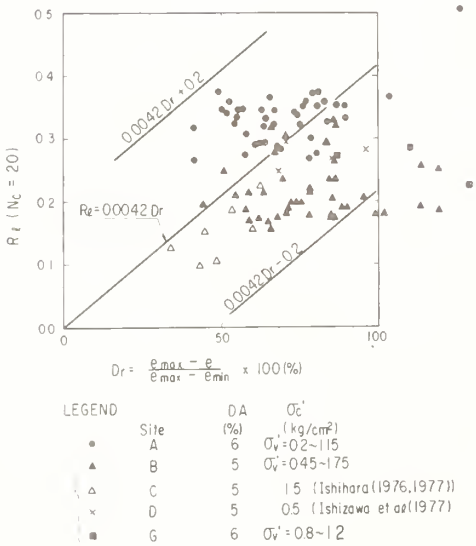

FIGURE 9: R (NC=20) AND D_R RELATION

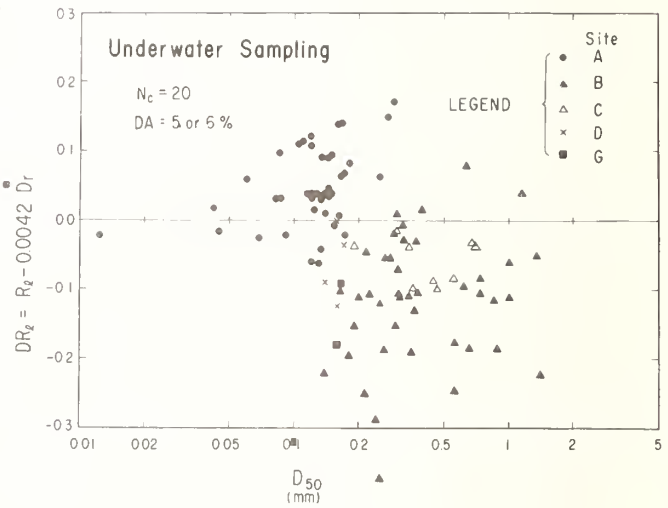

FIGURE 10: DR_ℓ=R_ℓ-0.0042 D_R AND D_{50} RELATION

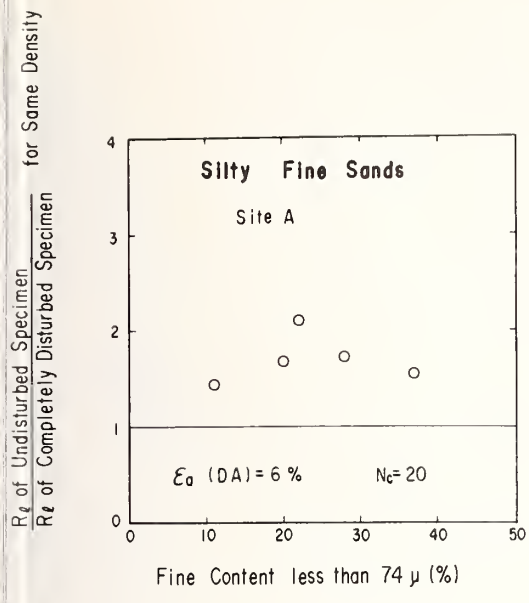

FIGURE 11: COMPARISON OF R_ℓ OF UNDISTURBED SPECIMENS WITH RECONSITUTED SPECIMENS FROM SITE A

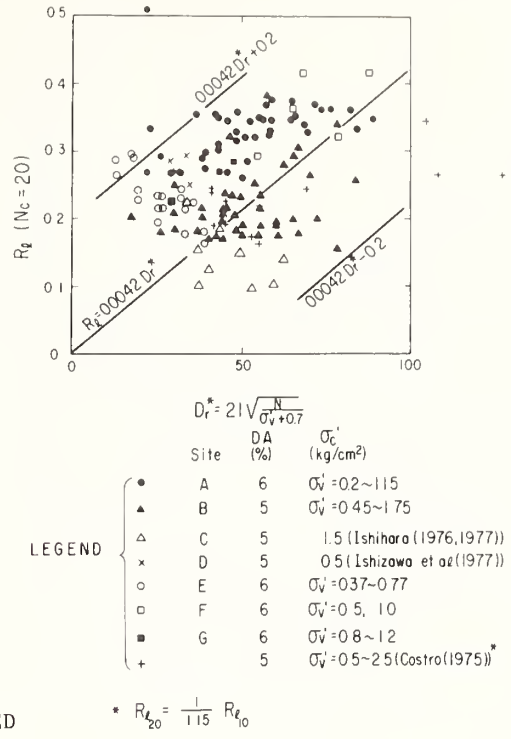

FIGURE 12: R AND D_R* RELATION

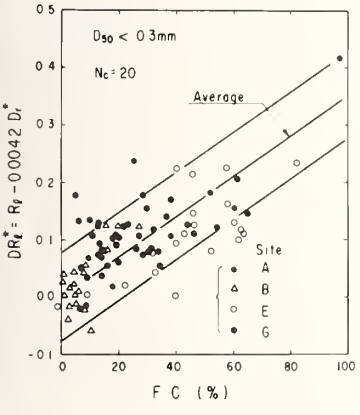

FIGURE 13: DR *=R_ℓ-0.0042 D_R* AND F.C. RELATION

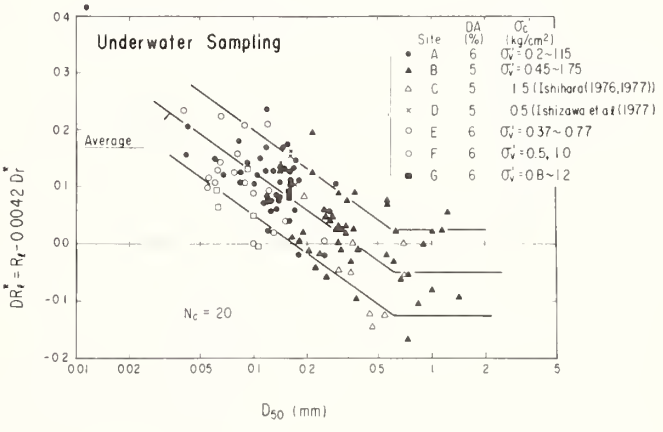

FIGURE 14: DR_ℓ* AND D_R* RELATION

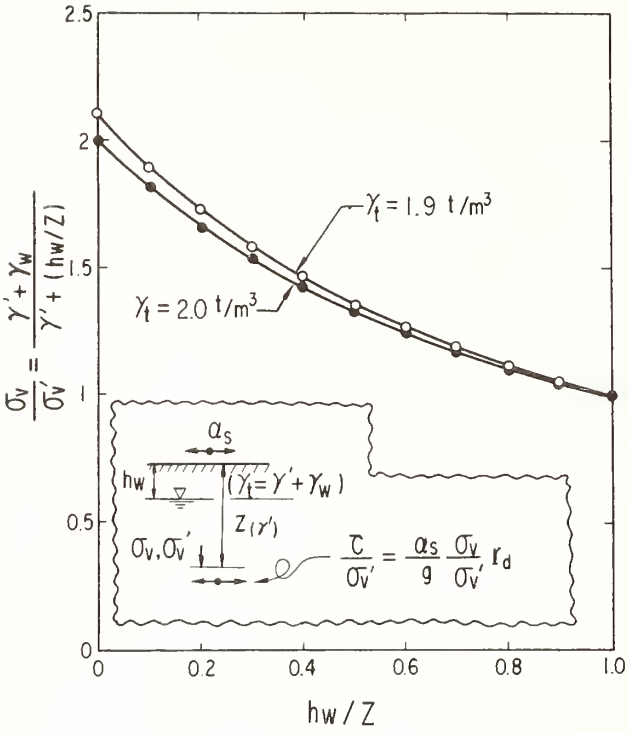

FIGURE 15: EFFECTS OF WATER TO σ_v/σ_v'

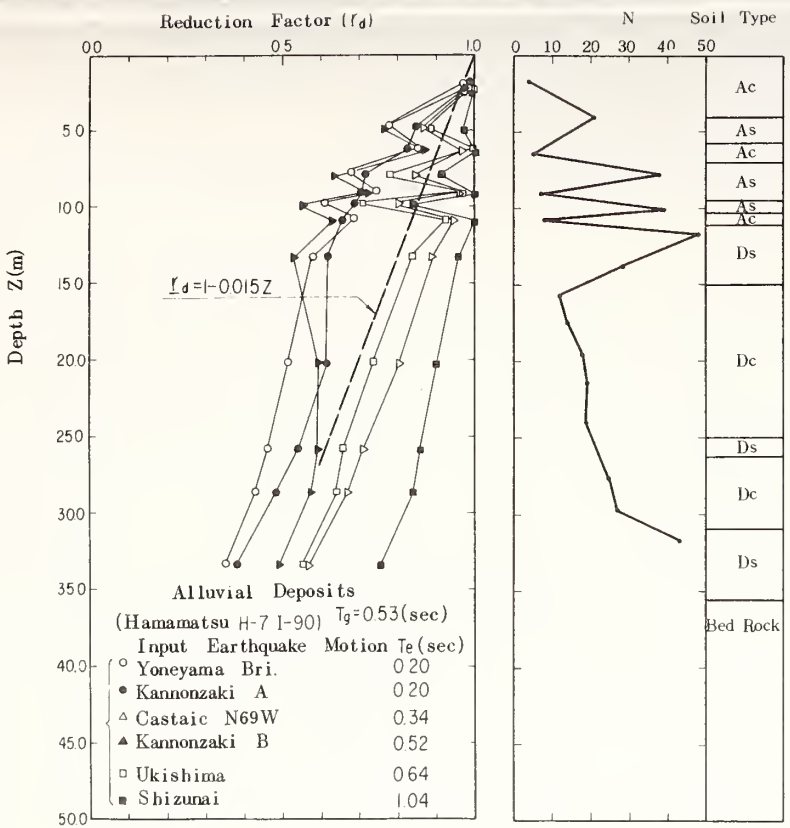

FIGURE 16: REDUCTION FACTOR r_d AT ALLUIVAL DEPOSITS

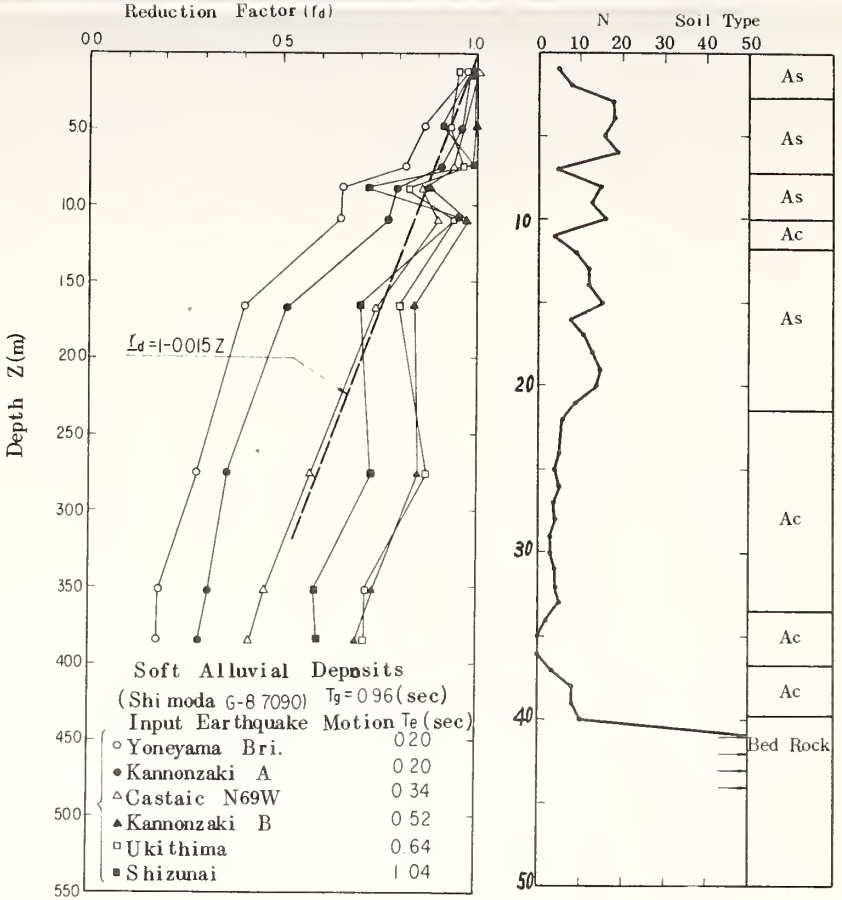

FIGURE 17: REDUCTION FACTOR d AT SOFT ALLUVIAL DEPOSITS

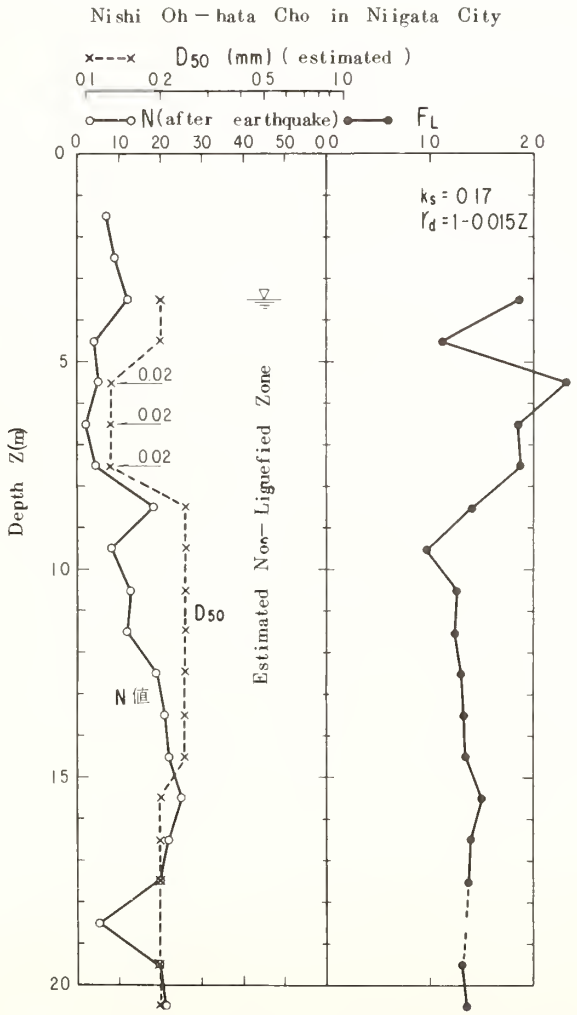

FIGURE 18: RELATIONSHIP BETWEEN F_L AND Z AT THE NON-LIQUEFIED SITE

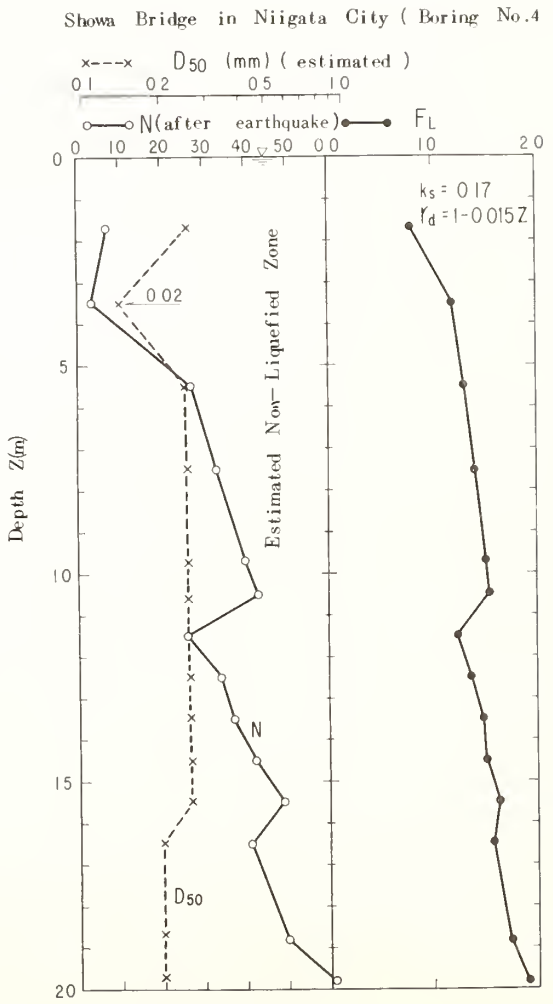

FIGURE 19: RELATIONSHIP BETWEEN F_L AND Z AT THE NON-LIQUEFIED SITE

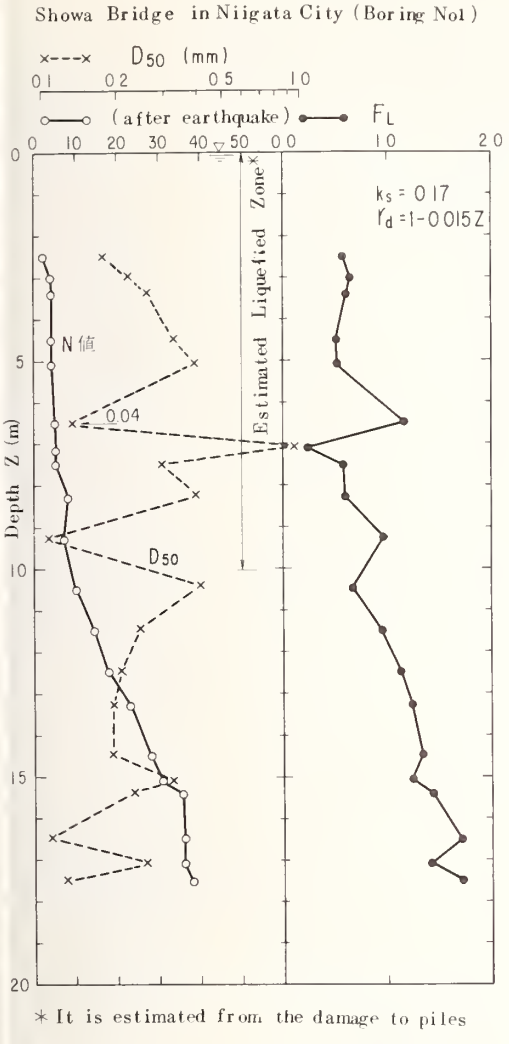

FIGURE 20: RELATIONSHIPS BETWEEN F_L AND Z AT THE LIQUEFIED SITE

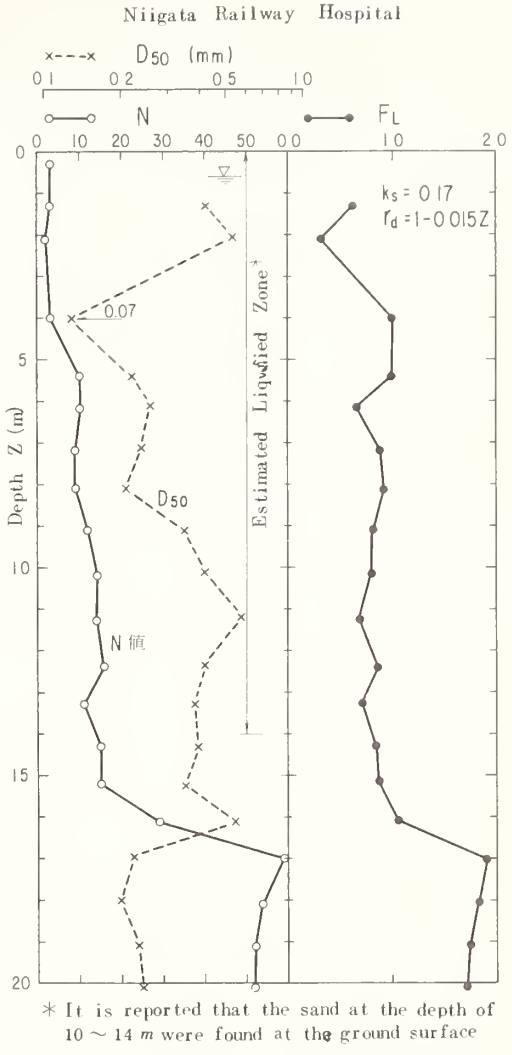

FIGURE 21: RELATIONSHIPS BETWEEN F_L AND Z AT THE LIQUEFIED SITE

14

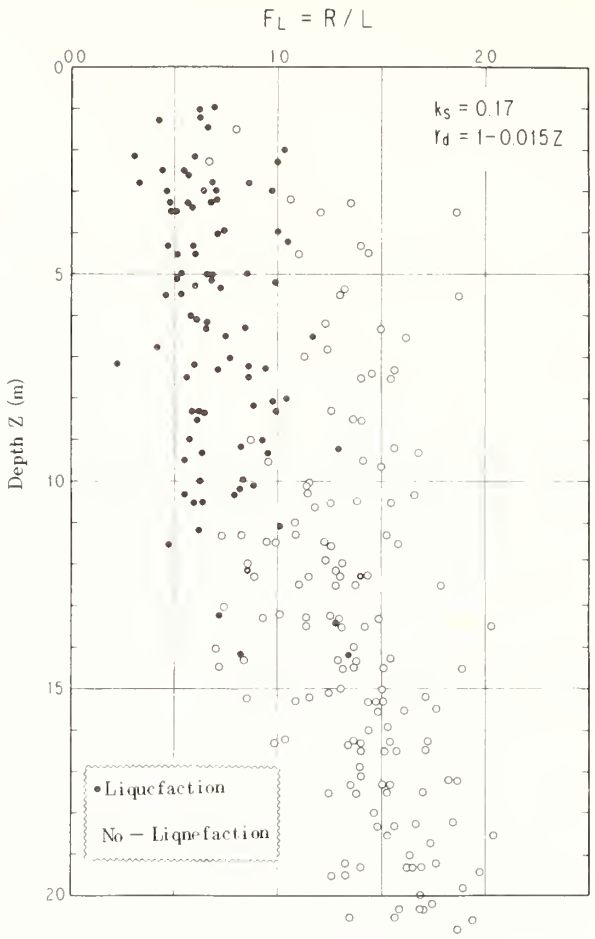

Note) The range of liquefied zone was estimated by the seueral observations.

FIGURE 22: RELATIONSHIP BETWEEN F_L AND LIQUEFACTION PHENOMENON (THE NIIGATA EARTHQUAKE OF 1964)

15

WIND-RESISTANT DESIGN OF CABLE-STAYED BRIDGES IN JAPAN

TadayoshI Okubo
Nobuyuki N. Narita
Masataka M. Katsuragi

Public Works Research Institute
Ministry of Construction

cable-stayed bridge, spanning from about 200 to 400 meters, can
e constructed even at a site with bad soil conditions. Though the
echanical principle of the bridge is different from that of the
spension bridge, both of the bridges are flexible structures.
it with the trend towards lighter and more flexible structures,
oblems of dynamic instability are becoming increasingly prevalent.

The purpose of this paper is to introduce the Japanese approach
solving instability problems. Countermeasures may consist either
removing the cause of the aerodynamic excitation by installing
tachments or of reducing the response to the excitation attachments
of reducing the response to the excitation by increasing the
gidity or damping capacity. In this context field observation
indispensable to supplement the wind-tunnel testing with laminar
ow.

ief Description

Suehiro Bridge

The Suehiro Bridge is a three-span cable-stayed bridge with
e center span of 250 m and the side spans of 110 m. The
idge deck carrying four lane tracks is composed of a trapezoidal
no-box girder with cantilevers on both edges. The dead weight
the girder is 9.3 t/m/br. The fundamental natural frequencies
e 0.483 Hz in vertical bending and 1.817 Hz in torsional oscilla-
on. The construction site is fairly flat and open to the Kii
raits. The prevailing wind direction is nearly perpendicular to
e bridge axis and a strong seasonal wind is expected in winter
igure 2).

Suigo Bridge

The Suigo Bridge is a two-span cable-stayed bridge with a
in span of 178.9 m and a side span of 111.6 m. The bridge
ck carrying four-lane highway tracks and sideways of 2.5 m
de on both sides is composed of a trapezoidal mono-box girder
th cantilevers. The dead weight of the girder is 13.4 t/m/br.
e natural frequencies were calculated as 0.448 Hz in vertical
nding and 1.859 Hz in torsional oscillation (see Figure 4).

nd-Resistant Design Procedure

In the preliminary design, three types of deck girders were
oposed for each bridge:

Suehiro Bridge

Trapezoidal mono-box girder with cantilevers 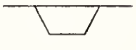

Rectangular twin-box girder with cantilevers 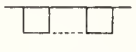

Rectangular mono-box girder with cantilevers 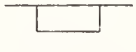

Suigo Bridge

Trapezoidal mono-box girder with cantilevers 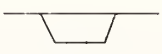

15

Rectangular twin-box girder with cantilevers 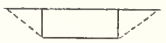

Rectangular mono-box girder

The stability test on these six different configurations of deck girder showed that the trapezoidal mono-box girder with cantilevers had excellent aerodynamic characteristics: no susceptibility was observed in torsional flutter at high wind speed, but vertical bending oscillation was observed at comparatively low wind speeds (around 15m/s for Suehiro Bridge and around 25 m/s for Suigo Bridge) when the wind flow approached the models with a large angle of attack.

This type of oscillation -- vortex induced oscillation -- should either be suppressed to a limited amplitude or be eliminated to avoid discomfort to pedestrains or passengers.

Two types of coutermeasures were proposed: reduce the vibrational response to the excitational by increasing either rigidity or damping capacity of the girder, and reduce the excitation itself by installing special attachments. However, the former measure was abandoned for economic and technical reasons.

The original model of Suehiro Bridge showed instability at 20 m/s ($\alpha \geqq 2$ deg). To suppress the vortex-induced oscillation the handrail openings were closed. But this did not show remarkable improvement. The effect of height of curb (road parapet) was examined in the second test stage, and it was found that the thinner curb improved the stability at $\alpha = 0$ deg. However, it did not work well for larger angle of attack.

Most effective was the installation of a fairing at the top of the handrail as shown in Figure 3. The sharpness of deck edge, which is achieved by installation of triangular fairing or by diminution of curb height, helped the effeciency of the fairing.

The effect of fairing was confirmed not only by a stability test but by non-steady aerodynamic force measurement. Test result is given in Figure 6.

A series of tests were also carried out for the Suigo Bridge. Prior to the construction of the bridge, data on wind inclination was gathered at the construction site. The results of field observation are shown in Figures 8 to 11, from which it can be concluded that the wind inclination varies violently with time in random manner and the average inclination angle decreases rapidly with the increase of average wind speed as well as the average time of wind inclination. It was concluded that no vortex-induced oscillation might occur at the bridge. In Figure 5 the countermeasures for bridge vibration due to wind action are summarized.

Wind Response of Real Bridges

Wind tunnel tests have so far been carried out under laminar flow, but no attemps have been made on turbulent effects. The authors will continue their long-term observation after the completion of the bridges to complete this study (see Figure 1).

Figure 7 introduces the instrumentation array at the Suehiro Bridge, and Figures 12 to 15 show the field observation results. These will be completed in the near future.

References

1. Okubo, T., Narita, N., and Yokoyama, K., "Some Approaches for Improving Wind Stability of Cable Stayed Bridges," Fourth Int. Conf. on Wind Effects on Buildings and Structures, 1975, Heathrow, London.

2. Okubo, T. and Narita, N., "A Comparative Study on Aerodynamic Forces Acting on Cable Stayed Bridge Girders," U. S.-Japan Res. Sem. on Wind Effects on Structures, 1974, Kyoto, Japan.

3. Narita, N., "On the Wind Resistant Design of Cable Stayed Bridges with Solid Girders," February 1978.

- Structural effects
  - static effects
    - wind force
      - distribution of wind pressure
      - total wind loading
    - stability
      - lateral buckling
      - divergence
  - dynamic effects
    - forced oscillation
      - random oscillation
    - self-excited oscillation
      - galloping
      - torsional flutter
      - bending-torsional flutter
      - vortex-induced oscillation
- Functional effects
  - wind stream
    - concentration of wind stream
      - noise
  - dynamic problem
    - vortex-induced oscillation

FIGURE 1. WIND EFFECTS ON BRIDGES

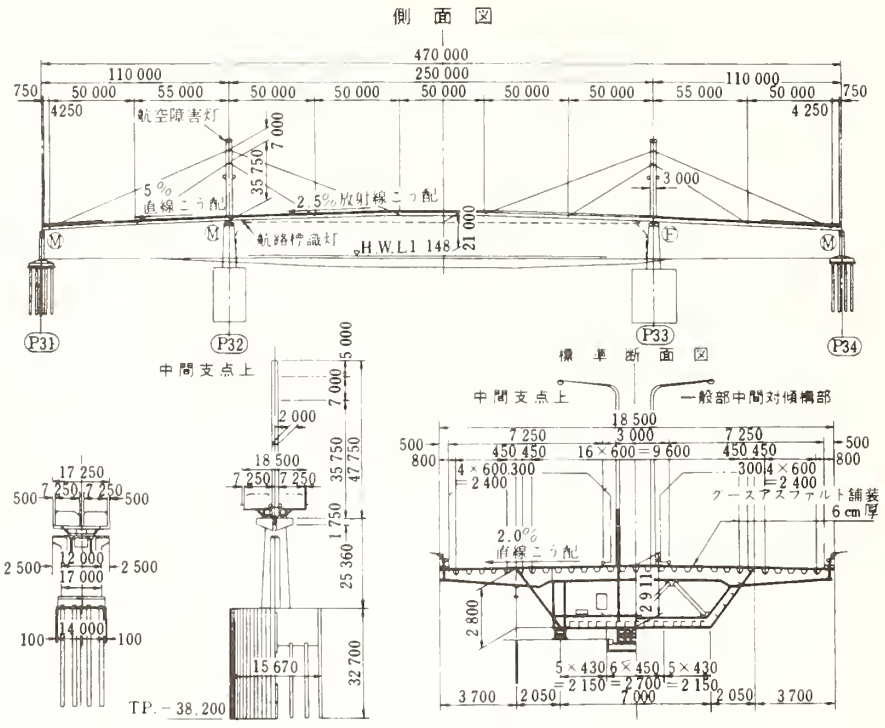

本広大橋一般図

FIGURE 2. GENERAL DRAWING OF SUEHIRO BRIDGE

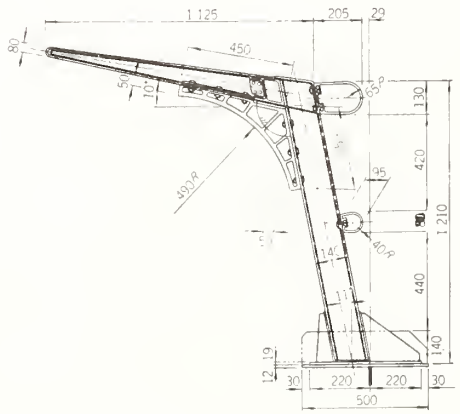

端部流板付高欄

FIGURE 3. HANDRAIL WITH FAIRING

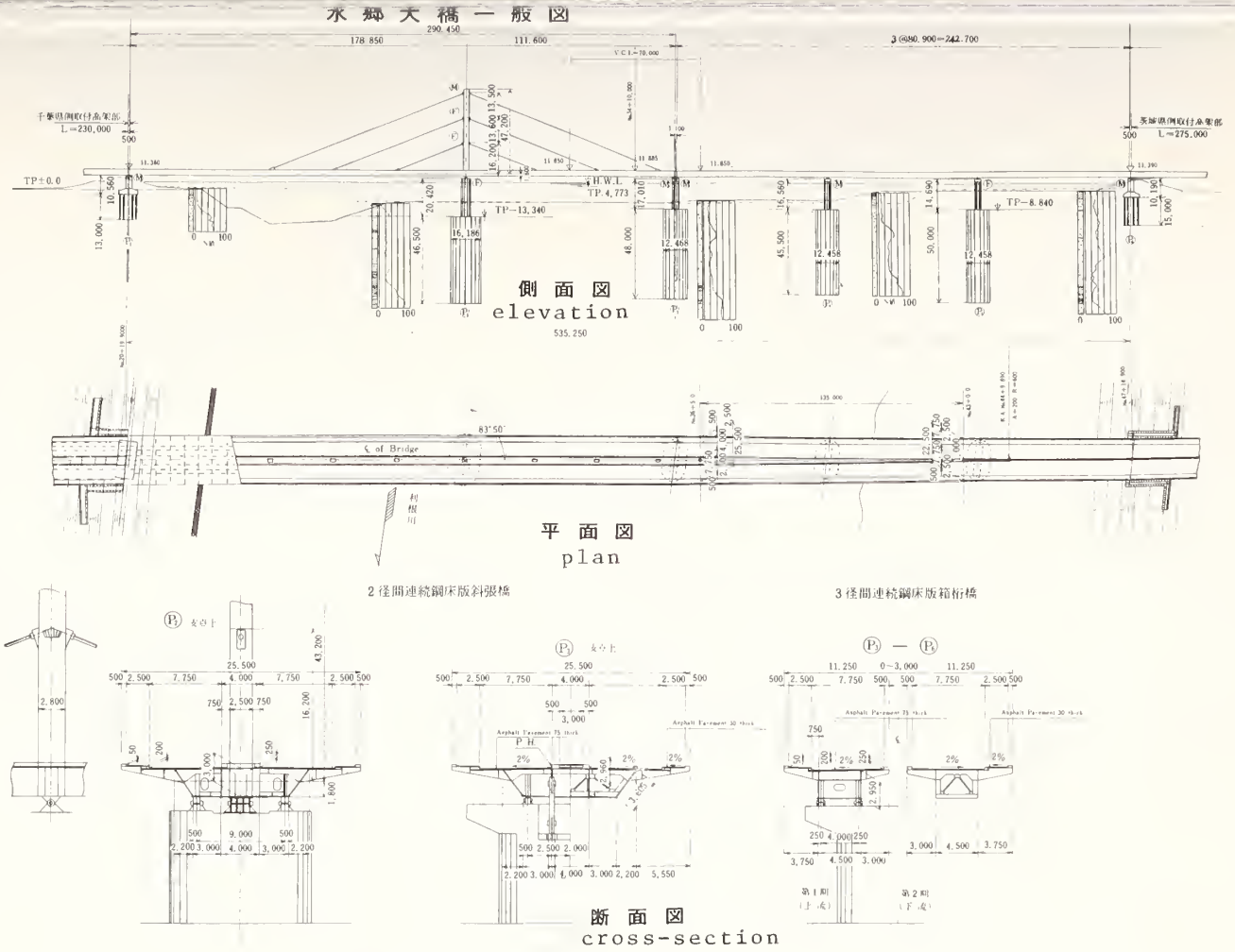

FIGURE 4. GENERAL DRAWING OF SUIGO BRIDGE

15

type	original design	modified design	examples
fairings		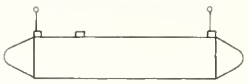	石狩川河口橋 Ishikari Br.
			Long's Creek橋 Long's Creek Br.
flaps	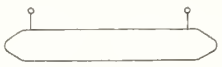		Lillebaelt橋 Lillebaelt Br.
		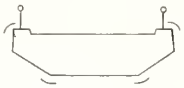	St.Nazaire橋 St. Nazaire Br.
			末広大橋 Suehiro Br.
			かもめ大橋 Kamome Br.
			安治川橋(計画案) Ajigawa Br. (Propcsed)
			永才橋 Eisai Br.
splitters	トラス補剛桁 (truss stiffened)		Severn橋 Severn Br.
			新水郷大橋 Suigo Br.
		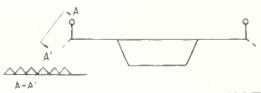	Lower Yarra橋 Lower Yarra Br.
deformations			荒川大橋 Arakawa Br.
		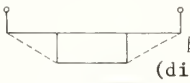 断続的 (discrete)	Strömstein橋 Strömstein Br.
			尾道大橋 Onomichi Br.
			Humber橋 Humber Br.

FIGURE 5. COUNTERMEASURE FOR SUPPRESSING VORTEX-INDUCED OSCILLATION

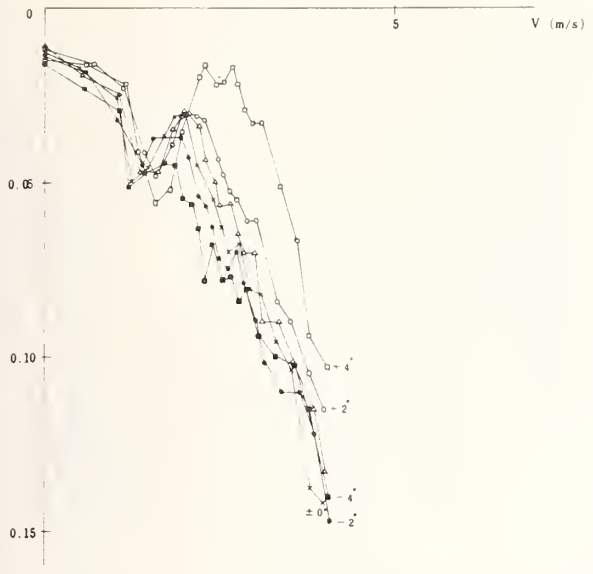

風速－減衰率曲線（端抑流板なし）

FIGURE 6.1. V - δ (WITHOUT FAIRING)

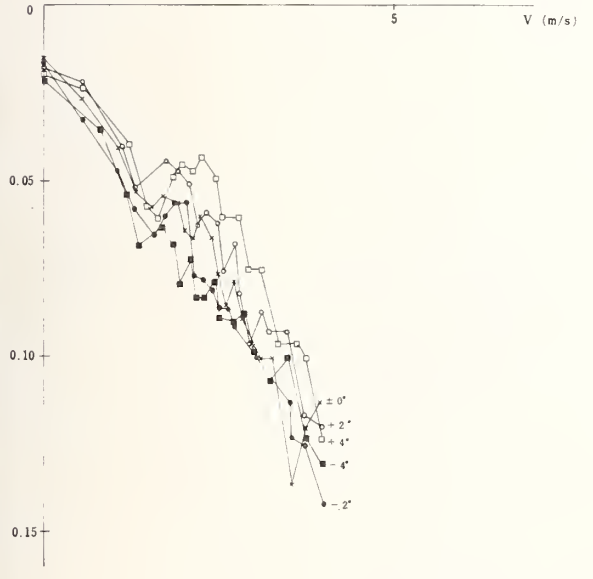

風速－減衰率曲線（端抑流板あり）

FIGURE 6.2. V - δ (WITH FAIRING)

15

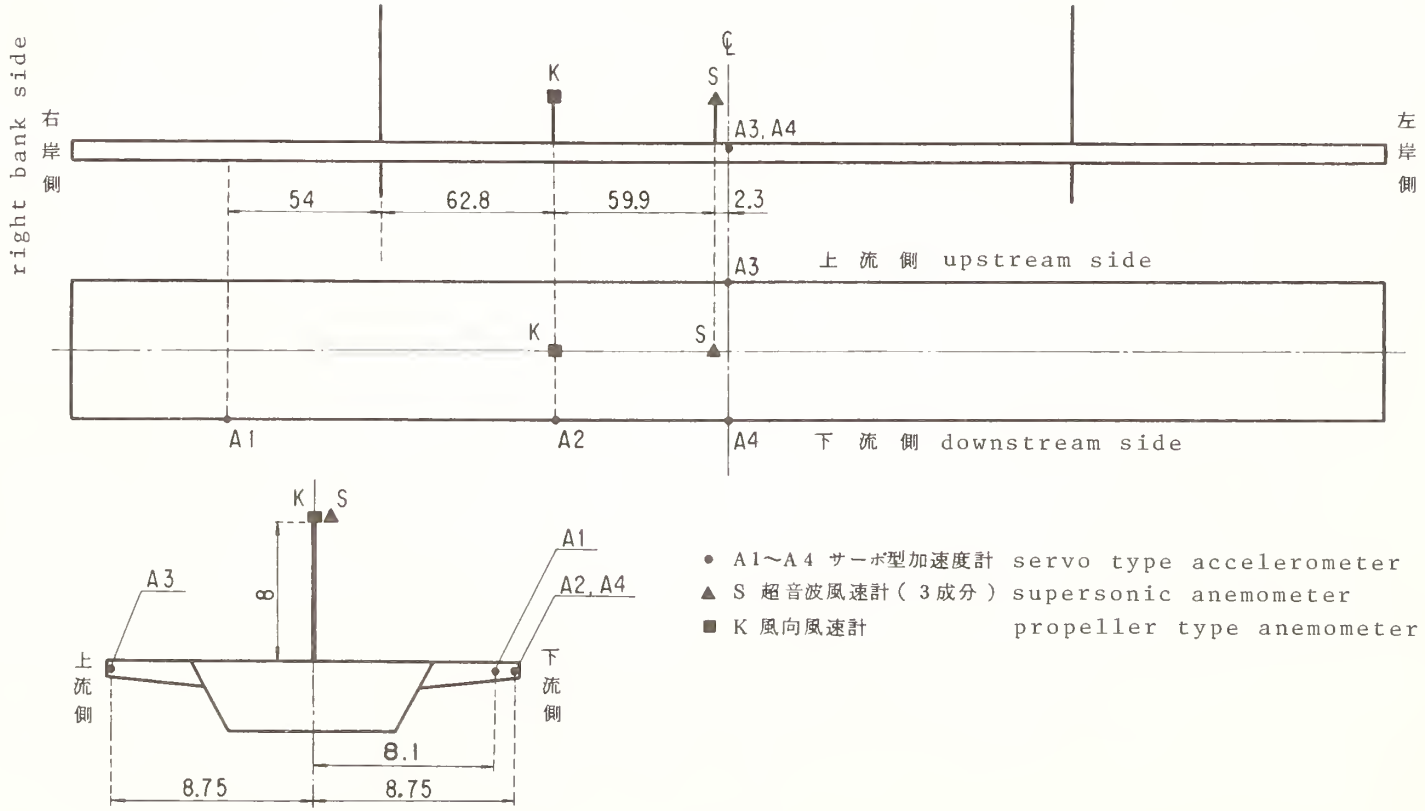

長期観測システム配置図

FIGURE 7. LOCATION OF SIGNAL TRANSDUCERS FOR LONG-TERM OBSERVATION

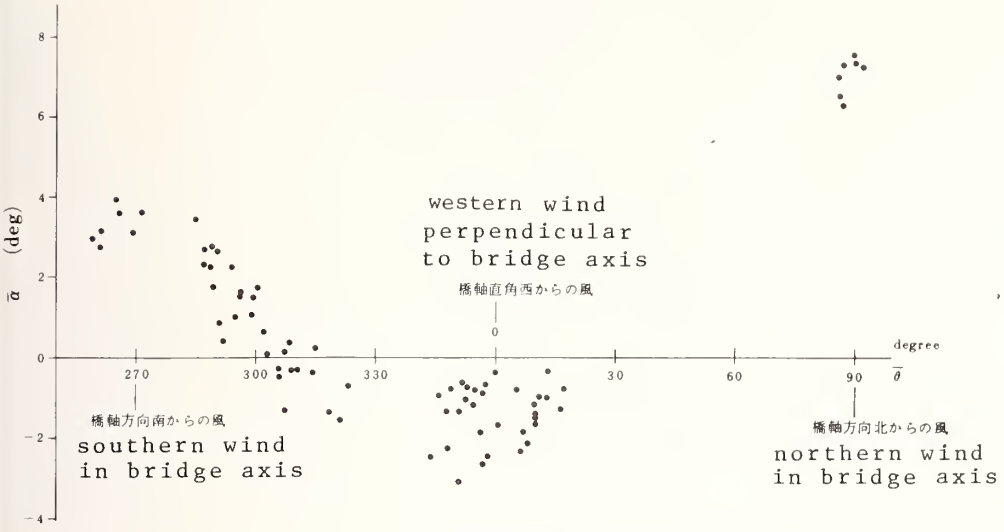

平均水平偏角と平均迎角の関係

FIGURE 8. AVERAGED WIND DIRECTION AND VERTICAL INCIDENTAL ANGLE

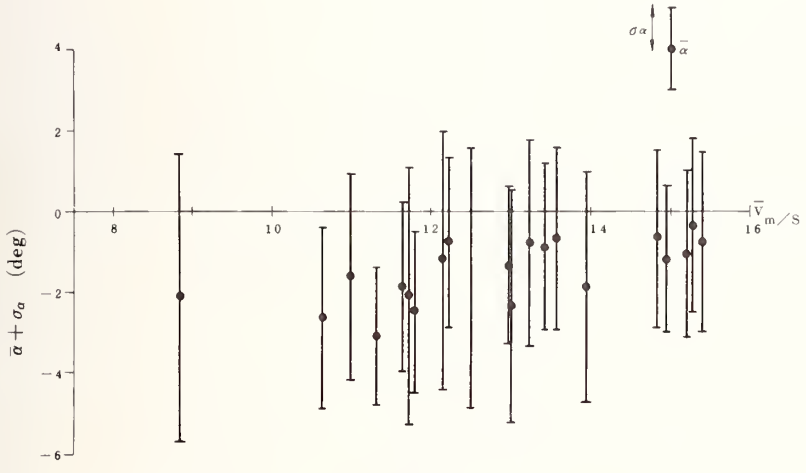

$\bar{V}$ と $\bar{\alpha}$, σ_α の関係　但し $\bar{\theta} = 350° \sim 10°$

FIGURE 9. $\bar{V}$, $\bar{\alpha}$, AND σ_α ($\bar{\theta}$ = 350°~10° DEG.)

15

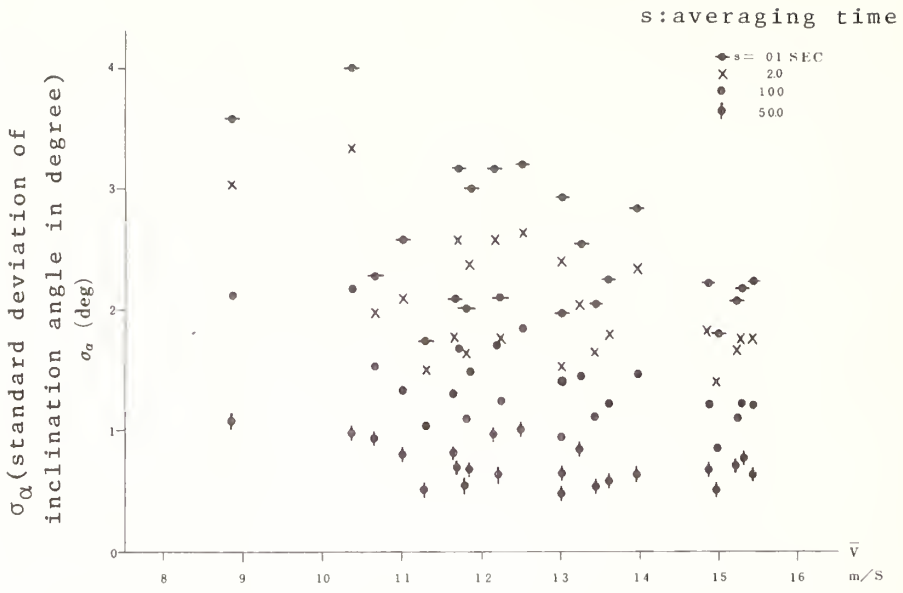

平均主流方向風速($\bar{V}$)と迎角標準偏差(σ_α)と評価時間(s)の関係

FIGURE 10. $\bar{V}$, σ_α , AND S

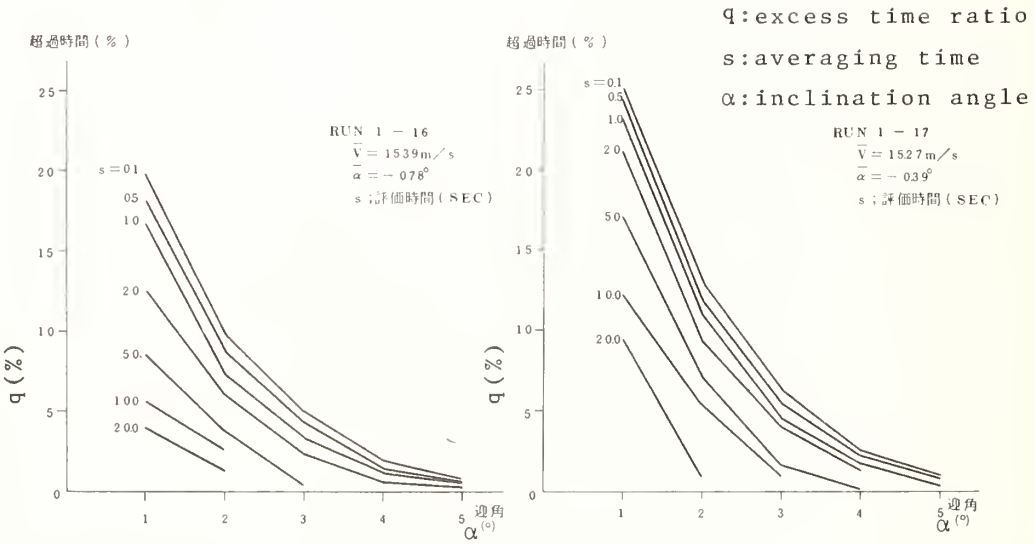

図－4.1 7　評価時間と超過時間の関係

FIGURE 11.　s AND q

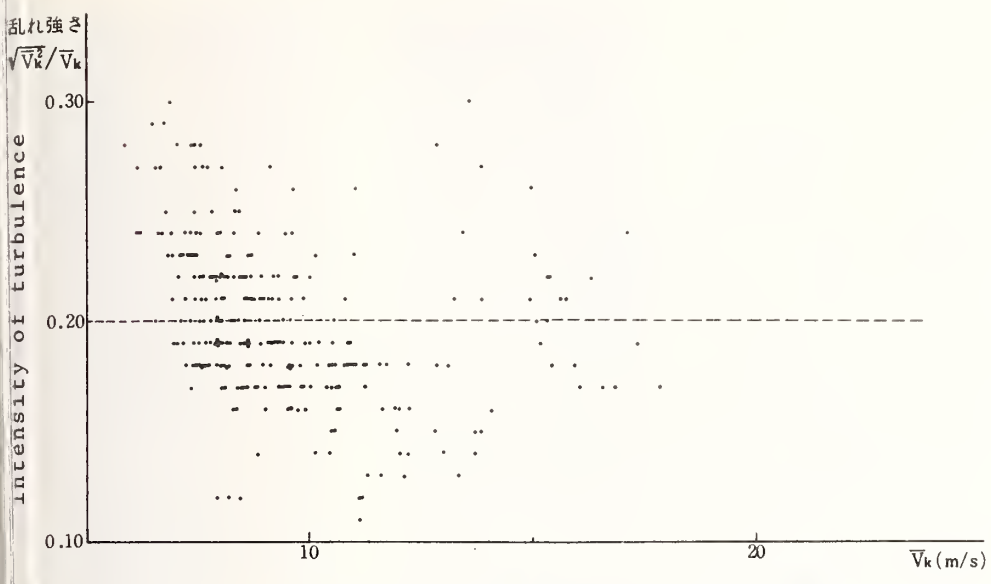

乱れ強さと平均風速の関係（昭和51年度解析）

FIGURE 12. AVERAGE WIND SPEED AND INTENSITY OF TURBULENCE

15

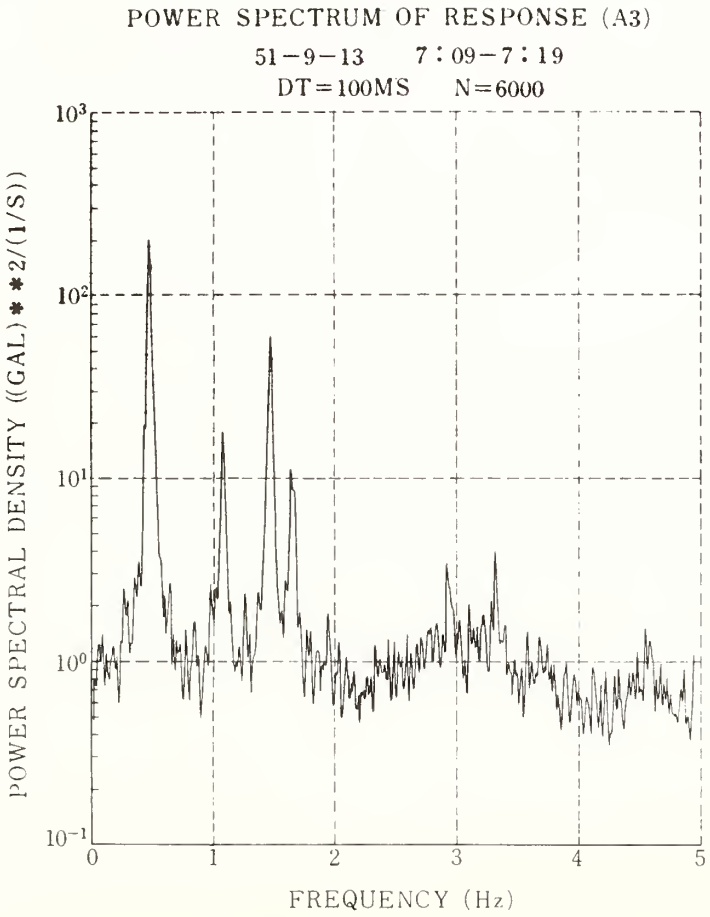

加速度パワースペクトル（メインスパン 1/2 点上流側）

FIGURE 13.1. P.S.D. OF ACCELERATION (MID-POINT OF CENTER SPAN, UPSTREAM SIDE)

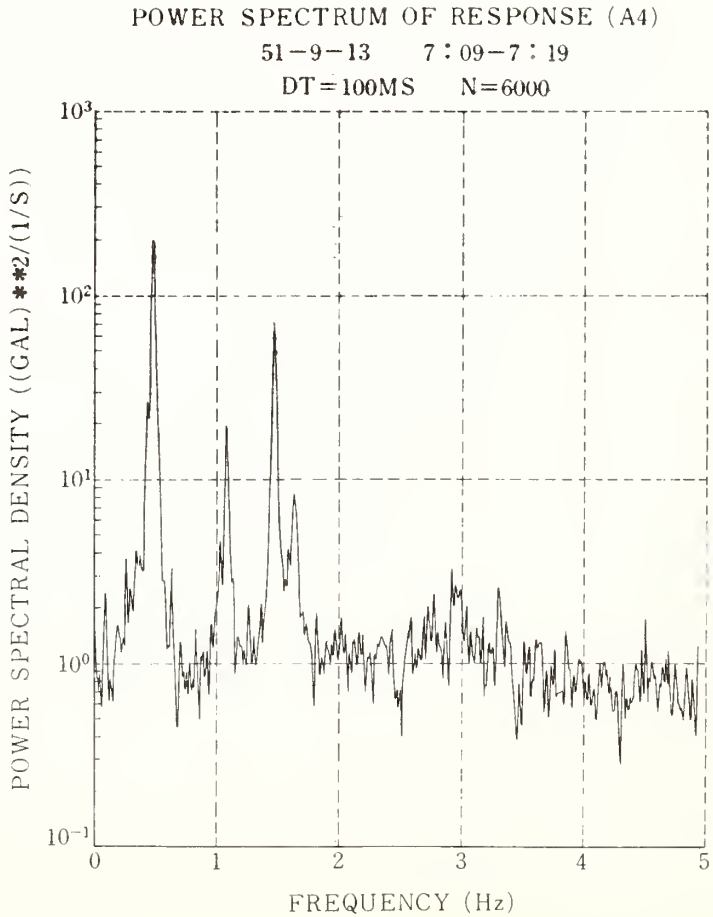

加速度パワースペクトル（メインスパン 1/2 点下流側）

FIGURE 13.2. P.S.D. OF ACCELERATION (MID-POINT OF CENTER SPAN, DOWNSTREAM SIDE)

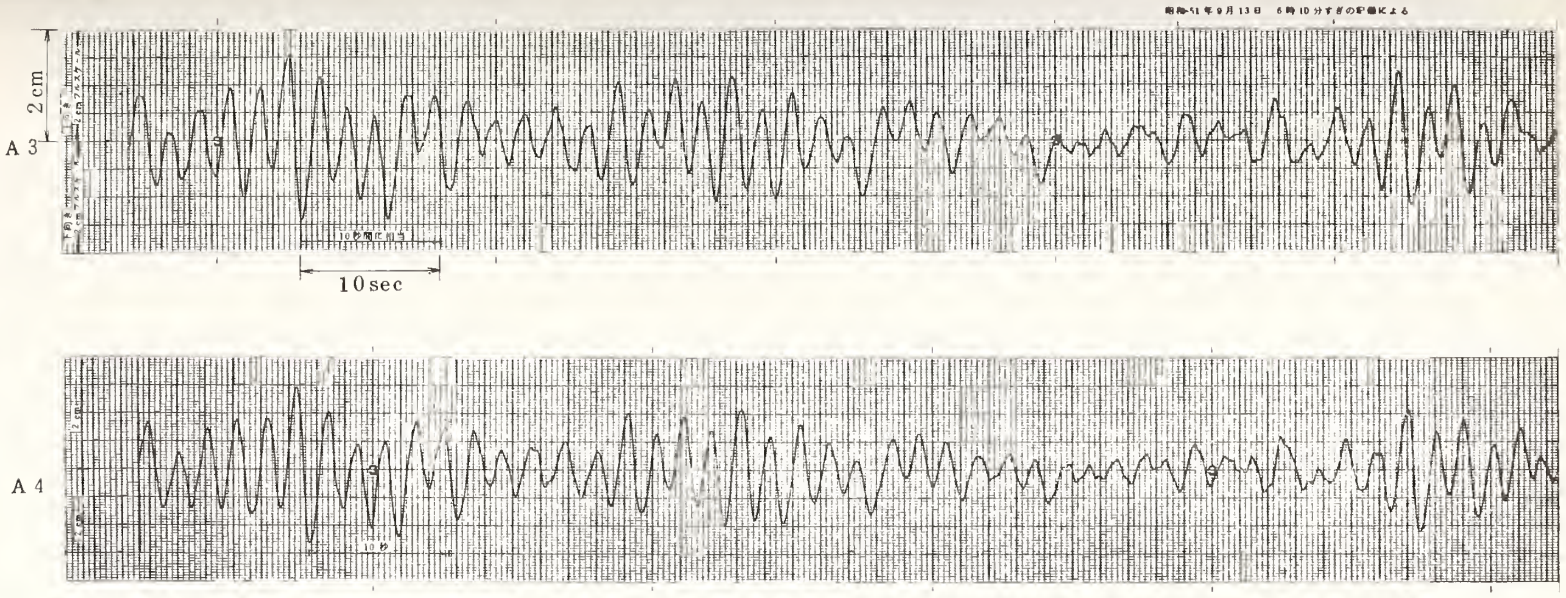

二重積分器によって変位変換された加速度記録

FIGURE 14. HEAVING VIBRATION OF DECK (DERIVED FROM ACCELERATION DATA)

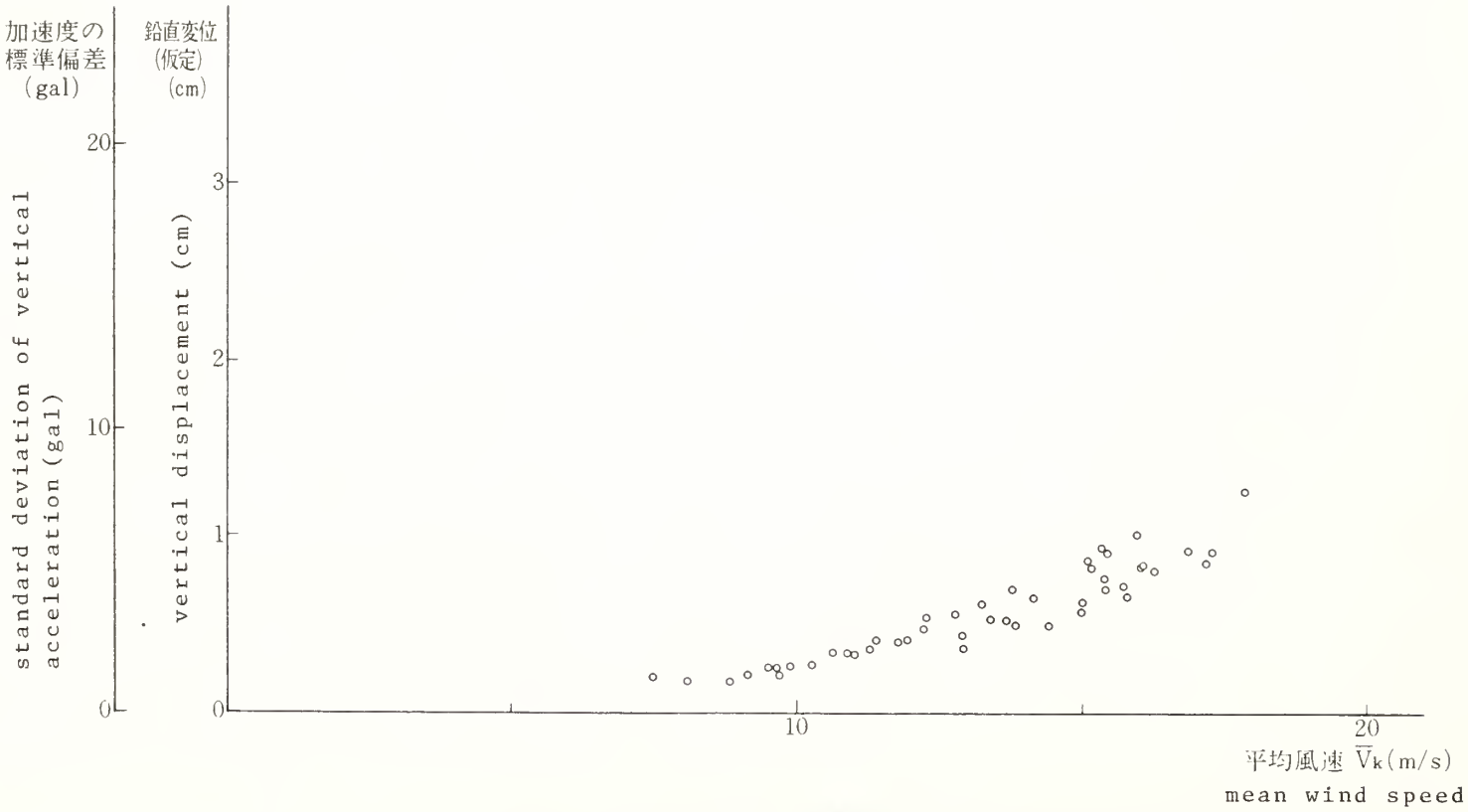

平均風速と加速度の標準偏差の関係

FIGURE 15. MEAN WIND SPEED AND STANDARD DEVIATION OF VERTICAL ACCELERATION OF BRIDGE DECK

16

AERODYNAMIC STABILITY OF PROPOSED OHIO RIVER CABLE-STAYED BRIDGE

Lloyd R. Cayes

Federal Highway Administration
Washington, D.C.

Aerodynamic Stability of Proposed Ohio River Cable-Stayed Bridge

This report presents the results of wind tunnel tests on a model of the proposed cable-stayed bridge across the Ohio River at Huntington, West Virginia, to determine the aerodynamic stability of the suspended span. There is also a discussion of the background of this type of section model testing and the procedure used by the Federal Highway Administration in carrying out such an investigation. The test was conducted for the West Virginia Department of Highways. The object of the investigation is the determination of the bridge dynamic deflection under vortex shedding and the critical wind velocity for flutter.

Background

There are several accounts of suspension bridges that were severely damaged or collapsed in wind storms during the nineteenth century. However, most of these failures were of bridges of relatively short span length. In 1889, the 1,280-foot (390 m) span Niagara Clifton Bridge failed from wind action, giving the engineering world its last severe warning about the problem of aerodynamic stability until the collapse of the Takoma Narrows Bridge in 1940. During this period, suspension bridge spans were built increasingly longer and with lighter stiffening strutures. Investigations into the causes of the Takoma Narrows disaster were immediately undertaken at the University of Washington [1], where wind tunnel tests on a scale model reproduced quite faithfully the observed behavior of the bridge during its brief life. The stability of the proposed design for the new bridge was then established by wind tunnel testing. Further research revealed that a section model representing a limited length of the bridge and mounted on springs to reproduce to scale the frequency of a significant mode of motion could be used to determine the response of the bridge in a normal wind at various vertical angles of attack.

During the past decade there has been considerable interest in using wind tunnel techniques for the determination of the aerodynamic stability derivatives of suspension bridge models. These derivatives represent purely aerodynamic data -- as against overall dynamic response observations -- which are the consequence of just bridge cross-section geometry.

In earlier wind tunnel tests, bridge-deck section models were elastically suspended, with properly scaled vertical and torsional natural frequencies, and observed primarily for their tendencies to flutter at some air speed. The present practice is to extract the purely aerodynamic characteristics of the model, then employ these in the dynamic response calculations relative to full size or prototype bridge stability. This method has the advantage of divorcing test results from all model structural properties except geometric form.

There are two types of wind effects on structures -- static and dynamic. The static effect is the pressure that the moving air mass exerts against the structure, and it varies in direct proportion to the square of the wind velocity. The dynamic effects of wind are the forces created by flow separation and turbulence of the moving air as it passes around the structure or by changes in the wind speed such as gusting. This report will deal only with the dynamic instability, of which there are two main types. The first is due to the regular formation of vortices in the wake of the bridge. The vortices form alternately on the upper and lower lee-side corners of a body with a pronounced degree of periodicity. This phenomenon

is known as vortex shedding. The vortices give rise to fluctuating forces, and the frequency is proportional to the wind speed. If the vortex shedding is equal to one of the natural frequencies of the structure, then a resonant condition can occur, if the structural damping is low, resulting in a buildup of vibration amplitude either in torsion or vertical bending. The amplitudes of vibration caused by vortex shedding are usually small, although they may cause human discomfort they are not normally catastrophic.

The second type of instability observed on bridges is much more serious and is referred to as flutter [2, 3] because of the aeroelastic studies on aircraft in the past. Unlike vortex shedding, once flutter is entered into, a higher wind velocity will not cause the structure to pass beyond the phenomenon and suppress it so that the structure again becomes stable. In flutter, the higher the velocity beyond onset of instability, the more violent the phenomenon becomes.

Basic Theory for Model Tests

The susceptibility of the prototype structure to aerodynamic instability is determined by wind tunnel tests. These tests are conducted on a section model of a bridge and subjected to laminar flow. Although the natural wind is turbulent there are some substantial reasons for testing under laminar conditions. The level of turbulence in the natural wind appears to decrease as wind velocity increases, and most serious wind problems of bridges occur at high wind velocities. Laminar testing appears to be more conservative for problems of instability such as flutter and vortex excitation. Laminar testing procedures and subsequent data reduction are considerably simpler than their counterparts in turbulent flow.

Section models, representing only a portion of a long-span bridge deck, are simple, cheap, and relatively easy to construct and modify. Their prime basic requirement is geometric similarity to the prototype.

The vortex shedding response was determined by References 3, 4, and 5 and is as follows:

Considering purely vertical motion of the section model, the homogeneous Equation (6) for the self-excited case of flutter is provided with a special forcing function applicable to the region of vortex shedding response:

$$m[\ddot{h} + 2\zeta_h \omega_h \dot{h} + 2\,\omega_h^2\, h] = \frac{1}{2}\rho v^2\,(2B\,[KH_o^* \frac{\dot{h}}{v} + C_{Lo} \sin \omega_s t]$$

where

H_o^* is an aerodynamic damping coefficient for decay to a "resonant" response amplitude

C_{Lo} is an "oscillating lift" coefficient

ω_s is the Strouhal circular frequency

H_o^*, C_{Lo}, and ω_s are experimentally determined where the vortex excitation frequency coincides with the natural frequency of the model to produce maximum response amplitude.

The equation for the prototype deck station is:

$$m(\chi)\ [\ddot{\eta} + 2\gamma_s\omega_s\dot{\eta} + \omega_s^2\eta]\ \psi(\chi) = P_s \sin \omega_s t$$

and the maximum half amplitude η is:

$$\eta_{max.} = \frac{P}{M\omega_s^2 \cdot 2\gamma_s}$$

where:

$$\gamma_s = \zeta - \frac{\rho B^2 H_o^*}{2m}$$

$P = \rho v^2\ B\ C_{Lo} \int_{span} \psi(x)\ dx$ = generalized force amplitude

$M = m \int_{span} \psi^2(x)\ dx$ = generalized mass span

ζ = structural damping ratio

ρ = mass density of air

B = deck width

m = section mass per foot of span

v = wind speed

$\psi(x)$ for the prototype was computed by the design engineers for the main span deflected shape with ℓ = 900 feet and obtained:

$$\int_o^\ell \psi(x)\ dx = 468.515$$

$$\int_o^\ell \psi^2(x)\ dx = 348.128$$

For a prototype frequency of oscillation N_p, the maximum acceleration of the deck section is:

$$g_{max} = (2\pi\ N_p)^2\ \frac{\eta_{max}}{32.2}$$

Scanlan with others (6) developed the following equations to predict flutter behavior of a rigid section model.

Assuming the typical bridge deck to be symmetrical about the vertical plane of the roadway centerline, equations of motion for the sectional structure may be written:

(1) $m\ [\ddot{h} + 2\zeta_h\omega_h\dot{h} + \omega_h^2 h] = L$

(2) $I\ [\ddot{\alpha} + 2\zeta_\alpha\omega_\alpha\dot{\alpha} + \omega_\alpha^2\ \alpha] = M$

16

where m and I are, respectively, mass and mass moment of inertia per unit span; h and α are vertical and torsional deflections of the given deck section (assumed uniform over the span); ζ_h and ζ_α are damping ratios-to-critical in the respective h- and α-degrees of freedom; ω_h and ω_α are the respective associated natural circular frequencies; and L and M are the respective dynamic lift and moment per unit span.

For the self-excited (flutter) problem that will be discussed here, the forms of L and M are intentionally taken as linearized, homogeneous functions of h, α, and their first derivatives only. Clearly, much more complex models can be assumed, but observations of model and full-scale structures in which aerodynamically induced responses at small structural amplitudes are dominated by structural-inertial vibrational characteristics suggest that linear models can quite adequately represent incipient aerodynamic instability.

Thus, L and M take on the simple forms:

$$(3)\quad L = m[H_1\dot{h} + H_2\dot{\alpha} + H_3\alpha]$$

$$(4)\quad M = I[A_1\dot{h} + A_2\dot{\alpha} + A_3\alpha]$$

where H_i and A_i (i = 1, 2, 3) are dimensional aerodynamic derivative coefficients to be determined by experiment, and the inertial factors m and I have been introduced for convenience.

To render such coefficients nondimensional, it is noted that they are essentially functions of the dimensionless parameter $K = B\omega/U$, where B is bridge deck width, ω is oscillation circular frequency, and U is horizontal wind velocity. They are then replaced by dimensionless coefficients H_i^* and A_i^* so that L and M can be shown to take the forms:

$$(5)\quad L = \frac{1}{2}\rho U^2\,(2B)\left[KH_1^*\frac{\dot{h}}{U} + KH_2^*\frac{B\dot{\alpha}}{U} + K^2H_3^*\right]$$

$$(6)\quad M = \frac{1}{2}\rho U^2\,(2B^2)\left[KA_1^*\frac{\dot{h}}{U} + KA_2^*\frac{B\dot{\alpha}}{U} + K^2A_3^*\alpha\right]$$

where ρ is air density.

Reference 6 describes test and data reduction methods for obtaining H_i^* and A_i^*. Essentially, test observations produce time histories of h and α; then with all quantities on the left-hand sides of equations (1) and (2) known, coefficients H_i^* and A_i^* are matched by system identification techniques to the test observations as functions of K.

The model damping was measured in terms of the logarithmic decrement $\delta = 1/n \ln \frac{x}{x_n}$, in which x and x_n are double amplitudes of oscillation separated by n cycles. For relatively low levels of damping such as exhibited by bridges, the damping ratios stated as a percent of critical can be determined by dividing the log decrement by 2π and multiplying by 100.

Damping can have a significant effect on the overall vibration of the structure. When the wind blows over a structure, it is inputting energy that is being dissipated by the movement of the structure. When the wind is removed, the vibration of the structure will decay or damp out as a result of the dissipation of energy. The rate of decay depends on the magnitude of the damping. The determination of the actual damping of any long-span capable-suspended structure can only be approximated because of the lack of data available. The design engineers have suggested a value of .08 log decrement for the proposed Ohio River Bridge prototype structure.

Design and Construction of Model

A selection model of a suspended bridge is a geometrically similar copy of a typical length of the suspended structure only. Any cables or hangers are not modeled because their aerodynamic effects are negligible. The section model is rigidly constructed so that all of the elastic behavior takes place in the springs from which it is suspended. The vertical and rotational movement of the section model supported by its springs simulates the vertical bending and torsional movement of the prototype structure.

The section model to be investigated for this study was designed to a scale of 1/45 to obtain a representative section of the bridge. The model is 60 inches (1.524 m) inside to inside of end plates, representing 225 feet (68.58 m) of the prototype. The width of the model is 9.6 inches (.244 m), resulting in an aspect ratio of 6.25. End plates are employed so that the air flow near the end of the model is two-dimensional. The model was scaled by the Froude number criteria for mass property and vertical natural frequency. Due to practical limitations of simulating the relatively high prototype torsional characteristics, values of polar mass moment of inertia and torsional natural frequency do not achieve Froude scaling. These scaling discrepancies in the torsional characteristics of the model were adjusted mathematically so that the prototype predicted results are proper.

The model was built from a variety of material to maintain the proper weight. The bottom and side panels are balsa wood, diaphragms and guard rails are aluminum, deck is plexiglass, and end plates are of balsa and aluminum sheets glued together. The model was fabricated by hand and assembled with double-sided tape and stainless steel machine screws. Aluminum extension brackets were used to provide crossbars 90 inches (2.286 m) apart for the attachment of the supporting spring connections, placing them completely out of the wind stream of the 6-foot by 6-foot (1.829 m) nozzle. The weight and center of gravity of the finished model were adjusted by adding brass weights to the end plates. The dynamic properties of the bridge section and deck configurations are shown in Figure 1. Photographs of the model are shown in Figures 8 through 11.

Tests

The tests were conducted in the George S. Vincent Memorial Wind Tunnel, which is a low-velocity wind tunnel designed particularly for testing bridge section models. A blower forces air through a diffusing section with a series of stainless steel wire screens into a cylindrical pressure chamber and through the nozzle from which the air is discharged onto the model. The velocity over the cross section of the wind stream is very uniform to a point 6 feet (1.829 m) beyond the end of the nozzle.

A constant wind velocity, with a range of 0 to 40 feet per second (17.88 m/sec), is maintained with a micro-control rheostat in the blower circuit. The wind velocity is computed from the dynamic pressure head of the wind stream obtained by direct measurement with a pitot-static tube and an inclined manometer.

The nozzle can be rotated about the horizontal axis of the pressure chamber, allowing tests at various wind angles of attack. The angle of attack is the vertical angle between the wind velocity vector and a horizontal plane; a positive angle of attack indicates an upward wind.

The section model was suspended in front of the wind tunnel nozzle by means of four supports with coil springs. The vertical length of the springs was adjusted to set the proper vertical frequency of oscilation. The torsional frequency was set by adjusting the spacing between the springs at each end of the model.

Horizontal restraining wires were attached to the end bracked crossbars at the center of gravity of the model to prohibit longitudinal or lateral movement during the tests. The restraining wires, which were tensioned with 2-pound (.903 kg) weights, were sufficient length that vertical force components would have no significant effect upon the vertical or torsional motion of the model.

Electrical resistance strain gages were attached to beryllium copper flexure plates above the coil springs. The strain gages at one end of the model were wired to indicate the vertical component of oscillation, and those at the other end were wired to indicate the torsional component. The two components were recorded side by side on an oscillograph.

The model is tested in smooth air flow at wind angles of attack varying from +6 degrees to -4 degrees. While maintaining a steady wind velocity at each of a series of increasing values, the model is displaced (if necessary) in the respective vertical and torsional degree of freedom, and the oscillatory dynamic response is recorded.

The damping values of the model setup were determined by displacing, then releasing the model in a no-wind condition and recording the rate of decay. The log decrement varied slightly from test to test but always around .01 for both vertical and torsional motion. Preliminary tests showed the model to be active due to vortex shedding with low levels of model damping. Therefore, it was deemed necessary to test the models at damping values that would more closely correspond to what may be expected for the prototype. Variable damping was achieved by attaching a small copper plate to each corner of the model and bringing a fixed permanent magnet in close proximity to the plate. Varying the small air gap between the magnets and plates gave the desired levels of model damping.

Discussion of Test Results

The different test configurations of the deck with their dynamic properties are shown in Figure 1.

Figure 2 is a summary of all the model tests that were conducted. A section model designation number was used throughout the investigation for easy identification and was determined as follows: take as an example model 3-2.4-.08; the first number, 3, refers to the prototype deck configuration; the second number, 2.4, refers to the model vertical frequency of oscillation; and the third number, .08, refers to the approximate log decrement of model damping at which the test was conducted. The x's in the columns for wind angles tested in Figure 2 signify tests that were conducted.

Figures 3, 4, and 5 summarize the results of all the tests conducted. The critical wind velocities for vortex shedding and flutter, and the amplitudes given in these figures are prototype values.

The critical flutter velocities shown in the summary Figures 3, 4, and 5 are for single-degree of freedom torsion and were determined from plots of the aerodynamic coefficients and computations

of the critical A_2^* coefficient. As can be seen, the flutter velocities are all well above the design wind velocity of 125 mph (201 kph) when any amount of damping is present. Flutter instability is not a threat to this bridge; therefore, no further discussion will be made.

Vortex shedding response in the torsional mode was only slightly evident in configurations 3 and 3H at the lowest level of damping, that is, without any added damping only model damping of approximately .01 log decrement, and occurred at prototype wind velocities around 75 mph (121 kph). But because the model torsional frequency was only about one-half of the proper scaled frequency, this motion, if possible at all with higher prototype damping, could only occur at much higher wind velocities. Therefore, torsional vortex shedding excitation is not a threat to this structure.

Vortex shedding response in the bending or vertical mode was evident in all tests of prototype configurations 3, 3H, 2, and 2H, and in many of the tests of configuration 1.

Configuration 1 represents a construction stage of the bridge deck system before the asphalt pavement wearing surface and curb barriers are installed. This model was tested at three different vertical frequencies of oscillation because of the uncertainty of the actual frequency as the bridge is being erected. The lowest equivalent prototype frequency tested was .247 cps. No vortex shedding response was present, apparently because the wind velocity required to excite vortex motion was so low that not enough energy was present to cause motion for the levels of damping tested. When the vertical frequency was increased to .29 cps, vortex response did occur between 8 (12.9) and 12 mph (19.3 kph) but very weak and slow to respond. When tested at frequency of .39 cps, approximately the same as used for 3, 3H, 2, and 2H, it showed no more response than the previous frequency tested.

Models 2 and 3 were of the same geometric shape, as well as 2H and 3H, the only difference being in the weight of the models due to the lack of a wearing surface on 2 and 2H. The weight of the wearing surface was added to 3 and 3H by attaching brass weights to the end plates inside the model. The "H" designation signifies vent holes in the curb barriers.

Configurations 2 and 2H were tested at one level of damping of approximately .08 log decrement. (See Figure 4.) There is insignificant difference in vortex response between these two tests indicating that the vented barriers have no effect. Models 2 and 2H are more active than 3 and 3H with the same level of damping. This indicates that the addition of weight to the bridge deck system, if the natural frequencies remain constant, tends to decrease vortex motion.

Model 3H was tested at model damping of .01 log decrement and with added damping to bring the total closer to the estimated prototype damping. (See Figure 5.) Model 3 was tested at model damping as well as three levels of added damping. Figure 6 is a curve showing the effect of damping on the maximum accelerations of the bridge deck for a wind angle of zero degrees. Positive wind angles of attack cause greater vortex response than negative angles for all tests and models. For the higher levels of damping, the vent holes in the curb barriers have little effect on vortex motion. It is also evident that this shape box section is slightly more stable without curb barriers than with curb barriers as a result of vortex shedding. The vent holes in the barrier rail evidently were not

large enough to be effective, but a more open type of barrier rail may prove to be beneficial.

Summary and Conclusions

The proposed steel box cross section of the Ohio River Bridge at Huntington, West Virginia, has critical wind velocities for flutter above 280 mph (450 kph) for wind angles of attack from -4 degrees to +6 degrees. This velocity is well above any expected winds at the bridge site.

Vertical motion caused by vortex shedding took place at all wind angles of attack with plus angles causing more deck motion than minus angles. With assumed prototype damping, maximum calculated vertical deck accelerations ranged between 4 percent g and 8 percent g. However, it is unlikely that the wind over the full span of the prototype would be steady and turbulent-free enough to cause motion of quite this magnitude.

The following conclusions are present:

(1) The prototype bridge will not experience any aerodynamic instability due to flutter.

(2) Vortex-induced oscillations are not a threat to bridge safety; however, pedestrains or passengers in stationary vehicles may feel some vertical motion if wind conditions are right.

(3) The vent holes in the curb barriers, as designed for this bridge, have no significant aerodynamic effect.

References

1. "Aerodynamic Stability of Suspension Bridges with Special Reference to the Takoma Narrows Bridge." University of Washington Engineering Experiment Station Bulletin No. 116.

2. "The Mathemetical Theory of Vibration in Suspension Bridges" by Freidrich Bleigh, C. B. McCullough, Richard Rosecrans, and G. S. Vincent, U. S. Bureau of Public Roads, Government Printing Office.

3. "Recent Methods in the Application of Test Results to the Wind Design of Long, Suspended-Span Bridges" by R. H. Scanlan, Report No. FHWA-RD-75-115, October 1975, Federal Highway Administration, Washington, D. C.

4. Scanlan, R. H., "Vortex-Shedding Response," Private Communication, R. Scanlan to R. Gade, 1974.

5. Scanlan, R. H., "Theory of the Wind Analysis of Long-Span Bridges Based on Data Obtainable from Section Model Tests." Proc. 4 International Conference on Wind Effects. London, England, September 1975.

6. Scanlan, R. H. and Tomko, J. J., "Airfoil and Bridge Deck Flutter Derivatives," Journal of the Structural Division, ASCE, Vol. 97, No. EM6, December 1971.

Acknowledgments

This investigation was carried out at the request of the West Virginia Department of Highways. The bridge was designed by E. Lionel Pavlo Engineering Company of New York, New York. Thanks are due them for computing the modes of motion and supplying information needed to design the scaled model.

The author wishes to thank Harold Bosch, Structural Research Engineer, for designing the model, Rick Ablaza, draftsman, who did the shop and detail drawings for the section model of the bridge, and Robert K. Taylor, machinist, who machined the many parts and fabricated the model. Special thanks are due Ronald Nelson, Technician, who assisted in conducting the tests and reducing the data.

DECK CROSS SECTION AND SECTION IDENTIFICATION	DESIGN	VERTICAL NATURAL FREQUENCY (CPS)	TORSIONAL NATURAL FREQUENCY (CPS)	VERTICAL LOCATION OF C. C. FROM BOX BOTTOM	WEIGHT PER FOOT MODEL (lb)	WEIGHT 5-FOOT MODEL (lb)	MASS/FT OF SPAN $\frac{lbs\text{-}sec^2}{ft^2}$	POLAR MASS MOMENT OF INERTIA/FT OF SPAN $\frac{lbs\text{-}sec^2}{ft}$
1 Box section without curbs and wearing surface. 36′ (Prototype) 0.8′ 1/45 Model 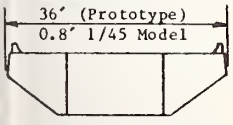	PROTO	.36	1.97	5.613 ft	3445		106.99	11017
	MODEL FROUDE SCALE	2.415	13.215	1.50 in	1.7013	8.506	.05284	.002687
	ACTUAL MODEL	2.63 1.96 1.62	6.20 4.29 3.42	1.50 in	1.463 1.485 1.506	7.315 7.427 7.531	.04640 .04981 .05042	.02418 .03041 .02866
2 Box section without 2H wearing surface. H is with vented curb barriers. 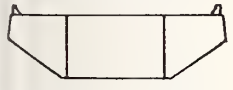	PROTO	.36	1.97	5.613 ft	3807		118.23	14218
	MODEL FROUDE SCALE	2.415	13.215	1.50 in	1.880	9.400	.05838	.003467
	ACTUAL MODEL	2.48	5.95	1.50 in	1.631	8.157	.05127	.02666
3 Box section with 3H wearing surface. H is with vented curb barriers. 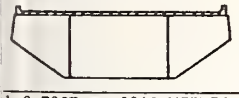	PROTO	.36	1.97	5.613 ft	4677		145.25	16107
	MODEL FROUDE SCALE	2.415	13.215	1.50 in	2.310	11.548	.07172	.003928
	ACTUAL MODEL	2.51 2.43 2.54	6.80 6.50 7.76	1.50 in	2.009 2.014 2.044	10.044 10.073 10.220	.06809 .07552 .06934	.02692 .03100 .02200

1.0 FOOT = .3048 METRES 1.0 POUND = .4536 KILOGRAMS

FIGURE 1. DECK CONFIGURATION AND DYNAMIC PROPERTIES.

16

PROTOTYPE DESIGNATION FOR DECK CROSS SECTION	PROTOTYPE VERTICAL NATURAL FREQUENCY (CPS)	SCALED MODEL VERTICAL FREQUENCY (CPS)	APPROXIMATE MODEL DAMPING LOG DEC	SECTION MODEL DESIGNATION	WIND ANGLES TESTED DEGREES					
					+6	+4	+2	0	-2	-4
1	.36	2.41	.08	1-2.4-.08	X	X	X	X	X	X
1	.30	2.00	.08	1-2.0-.08		X		X		X
1	.30	2.00	.05	1-2.0-.05		X		X		X
1	.30	2.00	.02	1-2.0-.02				X		
1	.24	1.61	.08	1-1.6-.08		X		X		X
1	.24	1.61	.05	1-1.6-.05		X		X		X
1	.24	1.61	.02	1-1.6-.02						
2	.36	2.41	.08	2-2.4-.08	X	X	X	X	X	X
2H	.36	2.41	.08	2H-2.4-.08	X	X	X	X	X	X
3	.36	2.41	.08	3-2.4-.08	X	X	X	X	X	X
3	.36	2.41	.05	3-2.4-.05		X		X		X
3	.36	2.41	.02	3-2.4-.02				X		
3	.36	2.41	.01	3-2.4-.01	X	X	X	X	X	X
3H	.36	2.41	.08	3H-2.4-.08	X	X	X	X	X	X
3H	.36	2.41	.01	3H-2.4-.01	X	X	X	X	X	X

FIGURE 2. SUMMARY OF WIND TUNNEL TESTS CONDUCTED.

MODEL TESTED AND WIND ANGLE OF ATTACK	NO WIND DAMPING LOG DECREMENT	NO WIND VERTICAL FREQUENCY OF PROTOTYPE CPS	VORTEX SHEDDING RESPONSE			FLUTTER RESPONSE	
			PROTOTYPE WIND VEL. MPH	VERTICAL MOVEMENT OF DECK D.A. FT.	MAXIMUM ACC. OF DECK q's	CRITICAL PROTOTYPE WIND VELOCITY MPH ZERO DAMPING	WITH DAMPIN
1-2.4-.08							
+6°	.094	.39	15.7	.645	.051	55	*
+4°	.102	.39	16.0	.352	.028	100	*
+2°	.099	.39	14.1	.195	.016	105	*
0°	.103	.39	15.6	.188	.015	270	*
-2°	.096	.39	-	0	0	400	*
-4°	.105	.39	-	0	0	425	*
1-2.0-.08							
+4°	.080	.29	11.9	.519	.029	270	440
0°	.081	.29	10.9	.210	.012	295	470
-4°	.076	.29	-	0	0	325	460
1-2.0-.05							
+4°	.053	.29	11.8	.747	.041	235	350
0°	.051	.29	9.2	.219	.012	255	400
-4°	.053	.29	8.3	.222	.012	290	430
1-2.0-.02							
0°	.025	.29	11.5	.698	.038	255	320
1-1.6-.08							
+4°	.082	.24	-	0	0	140	320
0°	.074	.24	-	0	0	150	380
-4°	.079	.24	-	0	0	285	450
1-1.6-.05							
+4°	.056	.24	-	0	0	155	280
0°	.057	.24	-	0	0	190	360
-4°	.055	.24	-	0	0	240	400
1-1.6-.02							
0°	.025	.24	-	0	0	200	280

* Wind velocity was well above the range of the test. 1.0 FOOT = .3048 METRES; 1.0 MPH = 1.6093 KPH

FIGURE 3. SUMMARY OF RESULTS.

MODEL TESTED AND WIND ANGLE OF ATTACK	NO WIND DAMPING LOG DECREMENT	NO WIND VERTICAL FREQUENCY OF PROTOTYPE CPS	VORTEX SHEDDINC RESPONSE			FLUTTER RESPONSE	
			PROTOTYPE WIND VEL. MPH	VERTICAL MOVEMENT OF DECK D.A. FT.	MAXIMUM ACC. OF DECK q's	CRITICAL PROTOTYPE WIND VELOCITY MPH ZERO DAMPINC	WITH DAMPINC
2-2.4-.09							
+6`	.083	.37	14.8	1.130	.090	110	390
+4`	.086	.37	14.9	.933	.074	120	350
+2`	.085	.37	15.0	1.020	.081	135	350
0`	.084	.37	13.6	.715	.057	120	350
-2`	.084	.37	13.1	.676	.054	190	335
-4`	.084	.37	13.1	.676	.054	150	300
2H-2.4-.08							
+6`	.082	.37	15.0	1.160	.092	110	*
+4`	.088	.37	15.4	1.060	.084	175	335
+2`	.084	.37	15.4	.968	.077	120	370
0`	.085	.37	13.4	.654	.052	200	390
-2`	.089	.37	13.0	.659	.052	210	390
-4`	.087	.37	13.0	.678	.054	210	*
3H-2.4-.08							
+6`	.099	.38	14.4	.684	.054	*	*
+4`	.099	.38	13.5	.586	.046	*	*
+2`	.106	.38	14.2	.618	.049	*	*
0`	.101	.38	13.4	.521	.042	*	*
-2`	.103	.38	13.9	.473	.038	*	*
-4`	.103	.38	14.4	.558	.044	*	*

* Wind velocity was well above the range of the test. 1.0 FOOT = .3048 METRES; 1.0 MPH = 1.6093 KPH

FIGURE 4. SUMMARY OF RESULTS.

MODEL TESTED AND WIND ANGLE OF ATTACK	NO WIND DAMPING LOG DECREMENT	NO WIND VERTICAL FREQUENCY OF PROTOTYPE CPS	VORTEX SHEDDING RESPONSE			FLUTTER RESPONSE	
			PROTOTYPE WIND VEL. MPH	VERTICAL MOVEMENT OF DECK D.A. FT.	MAXIMUM ACC. OF DECK q's	CRITICAL PROTOTYPE WIND VELOCITY MPH ZERO DAMPING	WITH DAMPING
3-2.4-.08							
+6`	.076	.38	12.8	.992	.079	*	*
+4`	.083	.37	13.9	.819	.065	*	*
+2`	.083	.37	14.1	.684	.054	*	*
0`	.082	.37	13.4	.567	.045	*	*
-2`	.096	.37	13.8	.564	.045	*	*
-4`	.093	.37	13.2	.494	.039	*	*
3-2.4-.05							
+4`	.065	.36	15.0	1.530	.122	120	425
0`	.057	.36	15.0	.958	.076	175	375
-4`	.056	.36	13.0	.867	.069	120	425
3-2.4-.02							
0`	.023	.36	17.2	2.48	.197	*	*
3-2.4-.01							
+6`	.010	.38	21.0	5.41	.430	135	*
+4`	.012	.38	20.6	3.30	.262	120	*
+2`	.007	.38	16.9	3.68	.293	120	*
0`	.009	.38	15.2	3.00	.239	120	*
-2`	.010	.38	16.1	2.63	.209	115	*
-4`	.009	.38	17.4	1.86	.148	115	*
3H-2.4-.01							
+6`	.008	.38	18.2	5.74	.456	125	*
+4`	.010	.38	19.7	5.63	.447	120	*
+2`	.006	.38	21.5	5.02	.399	125	*
0`	.010	.38	18.8	4.99	.396	125	*
-2`	.008	.38	17.2	2.80	.223	120	*
-4`	.009	.38	14.8	1.80	.143	110	*

* Wind velocity was well above the range of the test. 1.0 FOOT = .3048 METRES; 1.0 MPH = 1.6093 KPH

FIGURE 5. SUMMARY OF RESULTS.

16

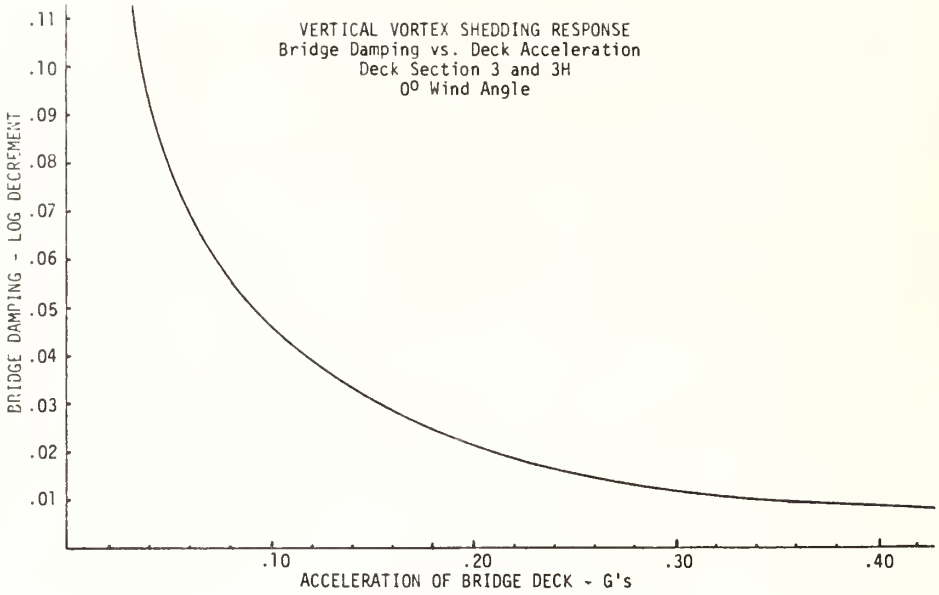

FIGURE 6. VERTICAL VORTEX RESPONSE VS. DAMPING.

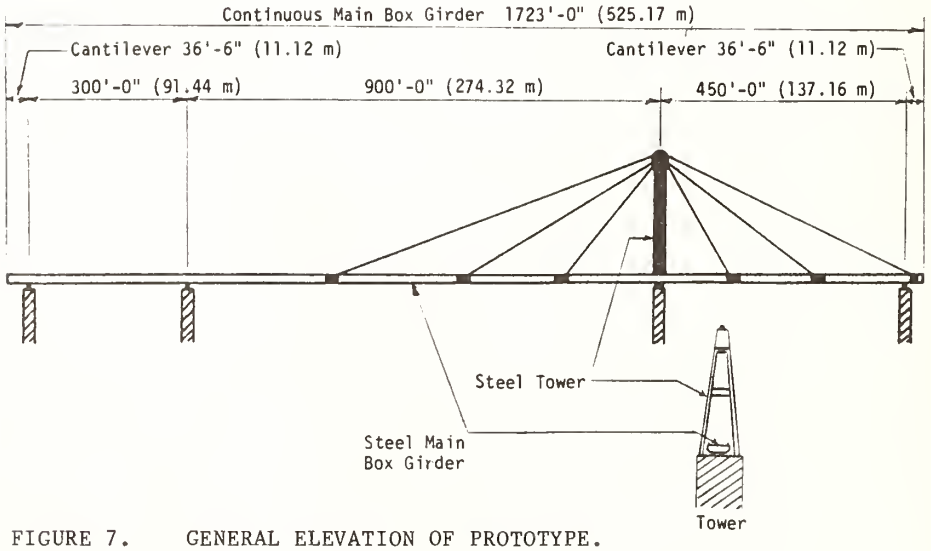

FIGURE 7. GENERAL ELEVATION OF PROTOTYPE.

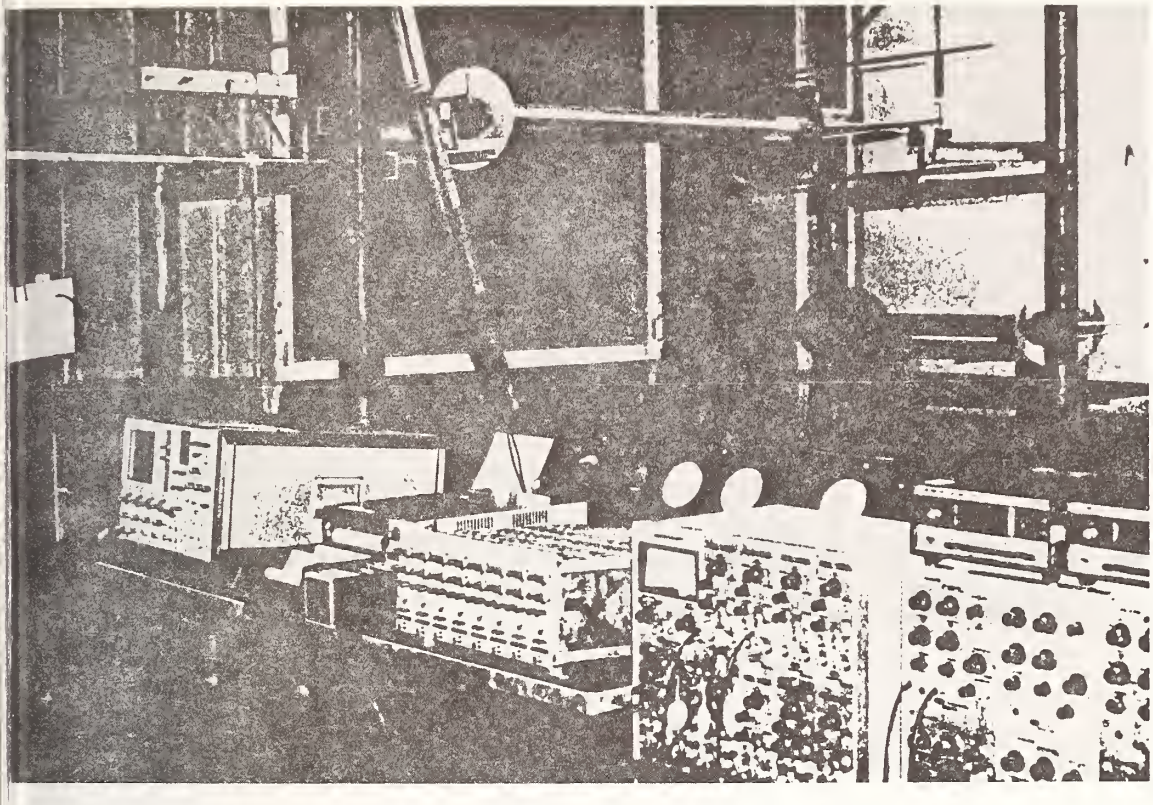

16

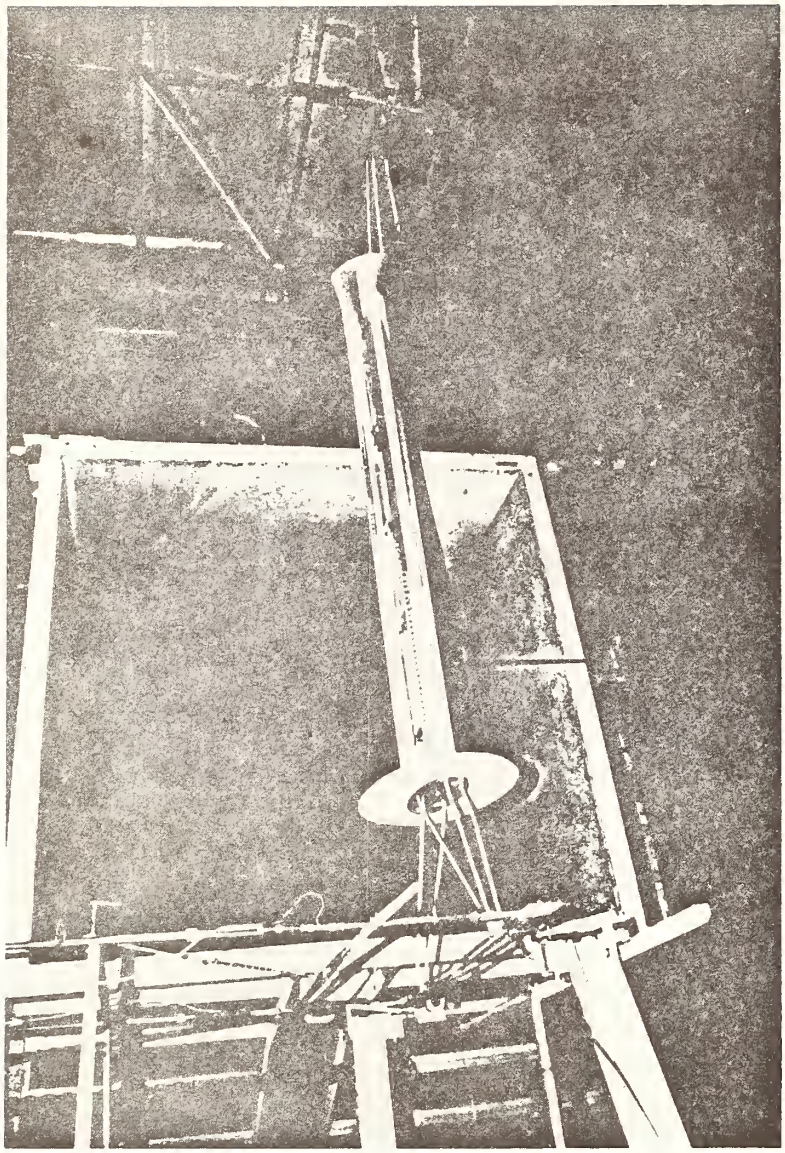

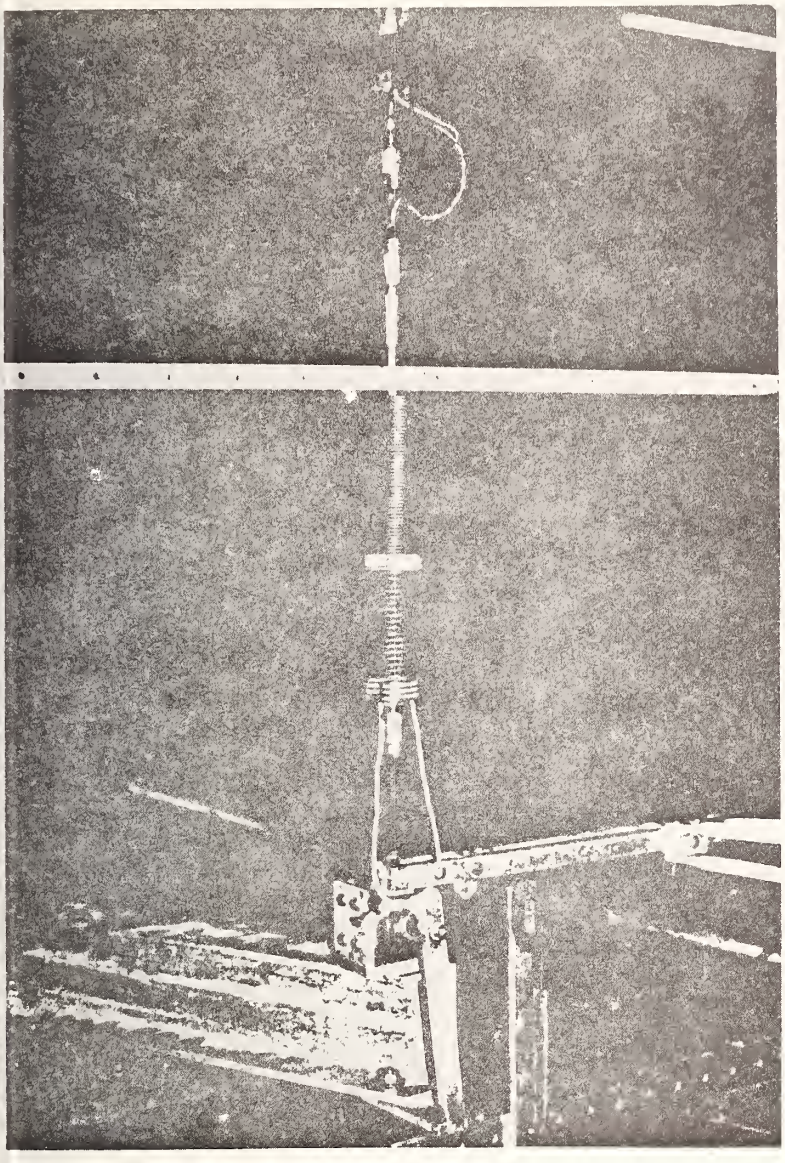

16

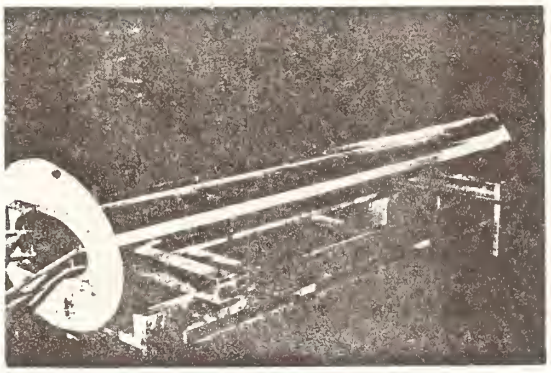

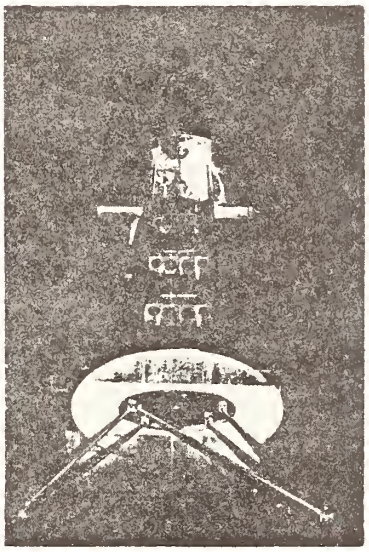

17

SOME AERODYNAMIC CONSIDERATIONS IN THE DESIGN OF THE RUCK-A-CHUCKY BRIDGE

Robert H. Scanlan

Department of Civil Engineering
Princeton University

Some Aerodynamic Considerations in the Design of the Ruck-A-Chucky Bridge

The design of the Ruck-a-Chucky bridge over the American River, upstream of the proposed Auburn dam near Sacramento, California is unique in several respects. The bridge, spanning 1200 feet, is cable-strayed, suspended by a spectacular "web" of cables from the rock of the adjoining hillsides, and curved in plan. It was designed by T. Y. Lin International of San Francisco. Ref. 9 presents a few of the interesting details of this bridge.

From an aerodynamics viewpoint the bridge was studied primarily with regard to the following questions:

(1) Maximum expected winds at the site and possible local terrain effects.

(2) Possible aerodynamic instabilities.

(3) Expected response to wind buffeting.

(4) Erection safety under wind.

(5) Possible wind-induced cable oscillations.

Steady Winds at the Bridge Site

Basic maximum winds for 50- and 100-year return periods in the region of the bridge were obtained from Thom's isotach maps [1], which show the maximum fastest-mile speeds in the region to be about 70 mph to 80 mph at 30 ft above ground in open terrain.

It was convenient in the subsequent calculations to work with wind speeds assumed to hold at bridge height, about 60 ft. above the expected water surface. The wind speed U at any elevation Z was calculated from the formula

$$U(Z) = 2.5u_* \ln \frac{Z}{Z_o} \qquad (1)$$

where

u_* = friction velocity, calculated from eq. 1 for given reference data, such as the Thom charts with $Z_o \cong 0.02$ meter. (Z_o = fetch roughness length)

$U(Z)$ = wind velocity at height Z

Table 1 below lists representative wind velocities U at bridge height and corresponding velocities U_{met} at the meteorological reference height of 10m.

Table 1

U(mph)	40	60	60	70	80	90	100	110
U_{met}(mph)	36	45	54	63	72	81	90	99

17

Study of Terrain Effects

To study the possible orographic and local topographic effects at the bridge site, a small-scale terrain model was built and tested in the boundary-layer wind tunnel at Colorado State University, Fort Collins, under the direction of Professors J. E. Cermak and J. Peterka. This model revealed no unusual channeling, wind intensification, or other local factors meriting special attention in the design of the bridge. Typical wind longitudinal gust spectra obtained at the bridge location with this wind tunnel model exhibited normal characteristics.

Study of Possible Aerodynamic Instabilities

The bridge deck is a box girder, curved in plan. The outline of the final external cross-sectional shape arrived at for this deck is shown in Figure 1. On the right side of the sketch is a grid-covered equestrian path, an unusual feature of the design. The basic section shape was arrived at by interaction among the T. Y. Lin design team, notably H. K. Lu, Alan Firmage, and the writer, with additional important contributions by J. E. Cermak of Colorado State. The shapes of the outermost edges were strongly influenced by other studies previously conducted by R. L. Wardlaw [2].

For suspended spans the shape of the deck cross-section lies at the heart of the wind stability problem. And the final cross-section in this study, indicated in Figure 1, had very stable tendencies against wind-induced flutter.

The method chosen for examination of the bridge aerodynamics was centered on the experimental study of a section model of the bridge deck. From this, basic aerodynamic force coefficients and self-excitation derivatives [3] were obtained in the wind tunnel at Colorado State University. This work was carried out by B. Bienkiewicz under the direction of Professor Peterka. Following the basic analog study in the wind tunnel, the aerodynamic data were employed in analytical studies by the writer to describe the expected responses of the full three-dimensional bridge.

The sectional test model proved to be economical and convenient and allowed rapid modifications of form leading to improved stability. A noteworthy item is that susceptibility to vortex-induced oscillation was found to be very low with the final cross-section.

Space does not permit a full discussion of the stability derivatives determined for this bridge deck, but it is of interest to comment on the key derivatives H_1^* and A_2^* [cf. Ref. 3], which govern aerodynamic damping in vertical motion and in torsion, respectively. These coefficients remained wholly negative--indicating increasingly safe conditions--for all reduced velocities U/NB where U = wind velocity across the deck, N = oscillation frequency, and B = 58 ft is the deck width.

The possibility of flutter was thus ruled out up to a wind velocity at bridge elevation of 150 mph or more.

Response to Wind Buffeting

The response to buffeting by gustiness was analyzed by an extension of methods described in Ref. 4 by Scanlan and Gade. Because of the curved plan form of the Ruck-a-Chucky bridge its vibration modes are more complex than with straight bridges, and

analytical extensions of the methods of Ref. 4 were needed, employing with the more complex modes the same basic aerodynamic derivatives and force coefficients obtained from the sectional model, plus additional information on natural wind spectra.

The following wind spectra were employed [5]

Longitudinal:

$$S_u(n) = \frac{200u_*^2 \frac{Z}{U}}{[1 + 50\frac{nz}{U}]^{5/3}}$$

Vertical:

$$S_w(n) = \frac{3.36u_*^2 \frac{Z}{U}}{1 + 10(\frac{nZ}{U})^{5/3}}$$

where u_* is the friction velocity, Z the altitude, U the wind velocity, and n frequency in H_z.

As an example of calculated buffeting results, the maximum expected vertical excursions of the bridge at center span are given in Table 2.

Table 2

U(mph)	40	50	60	70	80	90
Max. Vert. defl. (ft.)	0.48	0.71	0.99	1.41	1.73	2.07

Because of the stiffness and curved span form of the bridge buffeting deflections in torsion are negligible.

A full account of the generalized equations of linear buffeting theory, which grew out of the present study, is given in Ref. 6.

Erection Safety Under Wind

The inherent stability of the bridge cross-section is a strong indicator of primary safety from catastrophic oscillation during construction. However, some considerations were also given to the effects of temporary tie-downs and eventual dampers should the need arise. The detailed configuration of these will not be considered until the construction of the bridge is actively planned.

17

Measures Against Wind-Induced Cable Oscillations

Although a number of highly effective, external preventative measures against wind-induced cable oscillation, such as strakes, tuned-mass dampers, shock absorbers, etc., are well-known and documented in the literature [7] [8], full details of such devices have not been elaborated with respect to the present design, in view

of the following very important preventive measures already considered:

(1) Special study was undertaken by the T. Y. Lin design team, notably H. K. Lu, C. Redfield, and the writer, to provide extensively for relief from possible oscillatory stresses at the cable terminations. These latter were provided with long transitions of gradually increasing stiffness before conducting the individual cable wires into hard points.

(2) The cables are to be grouted within their outer sheaths along their full lengths, providing greatly increased damping.

(3) The widely varying cable geometric pattern throughout the overall design renders very unlikely the possibility of wake-induced oscillations of one cable by another.

Conclusion

This paper has sketched the preventive measures taken against wind-induced oscillations related to the Ruck-a-Chucky Bridge. The Primary concern--of removing the possibility of catastrophic flutter--was fully met by careful attention to the design of the bridge cross-section so that both vertical and torsional aerodynamic dampings became such as to increase the stability of the design.

The wind tunnel section model was used as the basic study tool. Results from this, in the form of non-dimensional coefficients, were then incorporated into both flutter and buffeting analyses using methods developed by the writer.

Attention was given to avoiding or alleviating the vortex-shedding problem, both as regards the deck cross-section itself, and the possible effects on the cables. Peripheral aerodynamic eventualities were also given consideration.

References

1. Thom, H. C. S.: "New Distributions of Extreme Wind Speeds in the United States" J. Struct. Div., ASCE, 94, No. ST7, Proc. Paper 6038 (July 1968) 1787-1801.

2. Wardlaw, R. L.: "A Preliminary Wind Tunnel Study of the Aerodynamic Stability of Four Bridge Sections for the Proposed New Burrard Inlet Crossing" Report No. LTR-LA-31, NAE, National Research Council, Ottawa, Canada, 1969.

3. Scanlan, R. H. and Tomko, J. J.: "Airfoil and Bridge Deck Flutter Derivatives" J. Eng. Mech. Div., ASCE, 97, No. EM6, Proc. Paper 8609, (Dec. 1971), 1717-1737.

4. Scanlan, R. H. and Gade, R. H.: "Motion of Suspended Bridge Spans Under Gusty Wind" J. Struct. Div., ASCE, 103, No. ST9, Proc. Paper 13222 (Sept. 1977), 1867-1883.

5. Simiu, E. and Scanlan, R. H.: Wind Effects on Structures J. Wiley & Sons, New York, 1978.

6. Scanlan, R. H.: "The Action of Flexible, Bridges Under Wind: I. Flutter Theory; II. Buffeting Theory Jnl. Sound and Vibration, Southampton, U. K. (in press, 1978).

7. Scanlan, R. H. and Wardlaw, R. L.: "Reduction of Flow-Induced Structural Vibrations" in Isolation of Mechanical Vibration, Impact, and Noise AMD Vol. 1, Sect. 2, ASME, New York, 1973, pp. 33-63.

8. Scanlan, R. H. and Wardlaw, R. L.: "Aerodynamic Stability of Bridge Decks and Structural Members" Proc. Engrg. Symposium on Cable-Stayed Bridges, Pasco Wash., FHWA and ASCE, Dec. 6-7, 1977 (in press).

9. _____. "Get Ready for Ruck-a-Chucky", Western Construction, Mar. 1977, pp. 34-35.

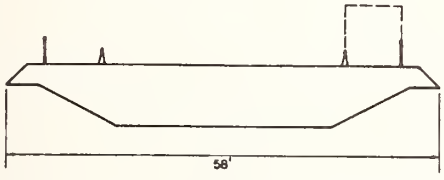

FIGURE 1: MODIFIED DECK SHAPE USED IN WIND STABILITY CALCULATIONS

18

A SUMMARY OF WIND-TUNNEL TEST RESULTS FOR THE LULING, LOUISIANA, CABLE-STAYED BRIDGE

Harold R. Bosch

Federal Highway Administration
Washington, D.C.

A Summary of Wind Tunnel Test Results for the Luling, Louisiana, Cable-Stayed Bridge

This paper summarizes the major results of a comprehensive aerodynamic investigation of the proposed cable-stayed bridge across the Mississippi River at Luling, Louisiana. The bridge, as illustrated in Figure 1, has a main span of 1,235 feet (376.4 m) comprised of double trapezoidal steel box-girders with an orthotropic deck. The supporting towers are 350 feet (106.7 m) in height with sloped, tapered steel box legs and upper and lower cross-struts which form an A-frame shape. It is important to note here that although cable-stayed bridge concepts have been used in Europe for many years, they are only recently receiving popularity by designers in the United States. The Sitka, Alaska Bridge was the first such bridge to carry vehicular traffic in this country.

This study was conducted in the George S. Vincent Wind Tunnel by the Federal Highway Administration (FHWA) for the Louisiana Department of Highways. The objectives of the study may be summarized as selection of an optimum superstructure cross-section, evaluation of the erection stability for the preferred section, evaluation of the erection stability for the main towers, and determination of flow field characteristics for purposes of preliminary design and development of field wind instrumentation. Structural response to vortex shedding and critical wind velocity for flutter together with aerodynamic data in the form of flutter coefficients are presented.

Historical Background

It has been well know for many years that serious vibration problems can arise with suspended bridge structures as a result of wind action. Perhaps one of the earliest well-documented examples is the failure of the Brighton Chain Pier Bridge in England in 1836 which was witnessed and reported on by Lt. Col. William Reid of the British Army. In fact, as noted by Farquharson [1], ten suspension bridges suffered major damage or collapsed during the period 1818 to 1889. Most of these failures were of bridges of relatively short spans.

The half-century following the 1889 failure of the 1,260-foot (384.1 m) Niagara-Clifton Bridge marked a period of rapid advance in design and construction techniques as well as materials and led to the appearance of lighter structures with significantly increased span lengths. The original Tacoma Narrows Bridge was the product of such progress and its dramatic failure in 1940 is, perhaps, the best-known example of an aeroelastic bridge deck instability. This event sparked vigorous examination of the aerodynamic stability of bridge superstructures. The University of Washington immediately conducted a series of analytical and experimental investigations [1] to determine the causes of the Tacoma Narrows disaster and establish design criteria for the new structure. Shortly thereafter, similar but more extensive studies [2] were conducted on the Golden Gate Bridge. Since these early endeavors, many wind tunnel research studies have been performed to evaluate proposed designs or determine appropriate modifications for existing "problem" structures and have made invaluable contributions to the understanding of the bridge stability problem.

During the past decade there has been considerable interest in employing wind tunnel techniques for the determination of the aerodynamic stability derivatives of suspended bridge models [3].

18

These derivatives represent purely aerodynamic data, as opposed to overall dynamic response observations, which are the consequence, uniquely, of bridge cross-section geometry.

In earlier wind tunnel tests, bridge deck section models were elastically suspended, with properly scaled vertical and torsional natural frequencies, and observed primarily for their tendencies to flutter at some air speed. The present practice is to extract the purely aerodynamic characteristics of the model first and then employ these in the dynamic response calculations for the full bridge. This practice has the inherent advantage of divorcing test results from all model structural properties, such as inertia, damping, and frequency, except for geometry.

Wind Environment

The rational treatment of interactions between wind in the atmospheric boundary layer and man and his works on the surface of the earth is currently termed "wind engineering." During the last decade, intense interest in the field of wind engineering has led to considerable advances in defining the wind environment likely to affect a given structure. The wind engineer's task is not only to minimize loss of life and damage to property that result from adverse wind, but also to maximize human comfort and economy by using beneficial wind effects.

Before conducting a bridge wind stability investigation, it is important to determine the overall characteristics of the wind environment at the proposed bridge site. Such site studies usually include the gathering of applicable strong-wind data for a number of years, with emphasis on wind velocity, direction, and frequency of occurrence. The U.S. Weather Bureau and similar records have historically been the primary source of this information. From these data, plots of high wind speeds versus probability of occurrence may be developed. For areas within the United States, Thom [4] has provided extremely valuable wind data in the form of maps of the distribution of extreme "steady" winds for different anticipated recurrence intervals ranging from 2 to 100 years. The data given are for mean high winds at a nominal height of 30 feet (9.1 m). Local plots, called "wind rows", may also be developed showing the probability of exceeding different velocity levels at each value of horizontal azimuth.

Among the important elements in wind environment studies is attention to the upstream conditions, or fetch, which strongly affect the vertical wind profile and degree of turbulence in the wind. For relatively small surface roughness, such as over a long fetch of open sea, the velocity profile flattens and turbulence level decreases, resulting in potentially higher ground level velocities and a possible enhancement of bridge vortex shedding response or flutter. High surface roughness, as encountered in urban areas, generates strong turbulence in the oncoming wind which is a principal factor in bridge buffeting.

When the bridge site is unique or subject to severe storms such as hurricanes or tornadoes, the aforementioned information should be supplemented by topographic wind tunnel studies or detailed field investigations. These provide a better understanding of the turbulence structure, maximum velocities, and angles of attack to be expected at the bridge site.

Wind Effects on Suspended Bridges

The designer has before him many possibilities when selecting the type of superstructure for a modern bridge. Whatever the choice, he must ensure that the aerodynamic stability of the section is satisfactory. To this end, it is necessary to understand the character of wind forces acting on the structure.

There are two basic types of wind effects on structures, static and dynamic. The static effect is the pressure that the moving air mass exerts against the structure, and it varies in direct proportion to the square of the mean velocity. The dynamic effects are the forces generated by flow separation and turbulence of the moving air as it passes around the structure or by changes in wind speed such as gusting.

In consideration of the static stability of bridge structures under steady wind, the critical wind direction is normally taken to be perpendicular to the longitudinal axis of the bridge. Lift, drag, and moment coefficients are assumed or measured in the wind tunnel for use in calculating the respective uplift, side thrust, or twist forces on the structure. When lift or drag forces become excessive, an unstable bridge may undergo lateral buckling or torsional divergence.

As a result of interaction with the earth's surface, the natural wind is not smooth but turbulent and gusty, with velocity fluctuations in both the vertical and horizontal directions. These fluctuations are random in nature, occurring over a wide range of frequencies. When the dominant frequencies of the wind spectrum are at or near the natural vibration frequencies of the structure and the winds are strong, buffeting can become a problem and lead to overstressing of structural elements. Fortunately for a majority of cases, the peak in the wind energy spectrum occurs at frequencies somewhat lower than those expected for large bridges.

Another form of wind-induced vibration of bridges is that of vortex shedding response. When wind blows across a slender bluff object, such as a bridge superstructure, the large wake that is formed consists of an array of vortices which are spaced in a characteristic pattern. The vortices form alternately on either side of the body in a periodic fashion, with the shedding frequency proportional to wind speed. The fluctuating nature of the wake causes an oscillatory force on the bridge and as shedding frequency approaches the natural frequency of the structure, it is possible for vibrations to result. This response occurs over a range of wind velocities in the vicinity of the resonant value, with maximum amplitude obtained when the "lock-in" condition is achieved. Both the velocity range and maximum amplitude are functions of structural damping and degree of streamlining. Since vortex shedding response is amplitude limited, structural problems arising from this mechanism are seldom catastrophic, although local fatigue damage and human discomfort are possible and warrant consideration.

The final class of instability, and perhaps the most important, is commonly referred to as flutter, following terminology developed in early work on aeroelastic instabilities of aircraft. In this case, wind forces interact with bridge deck motions to create a self-excited oscillation of growing amplitude, possibly leading to destruction. Unlike the vortex shedding problem, the flutter phenomenon is not limited to a velocity range beyond which structural stability returns. Increasing velocity beyond the threshold value

causes oscillations to buildup more rapidly and leads to more violent action.

Mathematical Modeling

To extract detailed aerodynamic derivative data from the wind tunnel section model studies, it is necessary to provide an analytical model of the physical situation. For this purpose, a symmetrical two-degree-of-freedom system is assumed. As discussed by Scanlan [5], the equations of motion for the section structure may be written in the form:

$$m[\ddot{h} + 2\zeta_h \omega_h \dot{h} + \omega_h^2 h] = L \tag{1}$$

$$I[\ddot{\alpha} + 2\zeta_\alpha \omega_\alpha \alpha + \omega_\alpha^2 \alpha] = M \tag{2}$$

where I and m are mass moment of inertia and mass per unit span of model; h and α are vertical and torsional deflections of the given deck section (assumed uniform; ζ_h and ζ_α are the damping ratios-to-critical in the h and α degree-of-freedom; ω_h and ω_α are the circular frequencies in the h and α degrees-of-freedom; L and M are the dynamic lift and moment per unit span. For the self-excited flutter problem, L and M are taken as linear and may be written in the form:

$$L = m[H_1 \dot{h} + H_2 \dot{\alpha} + H_3 \alpha] \tag{3}$$

$$M = I[A_1 \dot{h} + A_2 \dot{\alpha} + A_3 \alpha] \tag{4}$$

where H_i and A_i (i = 1, 2, 3) are dimensional aerodynamic derivatives determined by experiment, with inertial factors introduced for convenience. By noting the fact that L and M are essentially functions of the "reduced frequency" dimensionless parameter $K = B\omega/U$, nondimensional derivatives or coefficients may be obtained as:

$$L = 1/2\rho U^2(2B)\ [KH_1^* \frac{\dot{h}}{U} + KH_2^* \frac{B\dot{\alpha}}{U} + K^2 H_3^* \alpha] \tag{5}$$

$$M = 1/2\rho U^2\ (2B)\ [KA_1^* \frac{\dot{h}}{U} + KA_2^* \frac{B\dot{\alpha}}{U} + K^2 A_3^* \alpha] \tag{6}$$

where H_i^* and A_i^* (i = 1, 2, 3) are nondimensional aerodynamic coefficients and U is oncoming wind velocity; ρ is air density. These equations have been reduced to experimental form to enable direct use, and the details of this reduction are included in Reference 5. Essentially, test observations produce time histories of h and α; then with all quantities on the left-hand side of equations (1)

and (2) known, coefficients H_i^* and A_i^* are matched by system indentification techniques to the test observations as functions of K.

The coefficients are important in evaluating the stability characteristics of a section. The A_2^* coefficient measures aerodynamic damping in the torsion mode and thus is an indicator of single-degree flutter in that mode. The A_3^* coefficient is usually small and is sometimes assumed zero in analysis. In general, it is a measure of the aerodynamic stiffening effect upon frequency. The H_1^* coefficient measures the aerodynamic damping in the vertical mode.

When vortex shedding response is exhibited either indirectly in the aerodynamic coefficients, namely H_i^*, or directly in observations of the model test, the aforementioned mathematical model must be augmented to be applicable to the region of response [6]. This can be done for the case of purely vertical motion by providing equation 5 with a special forcing function:

$$L(t) = \frac{1}{2}\rho U^2 (2B) C_{Lo} \sin \omega_s t \tag{7}$$

The resulting combined equation takes on the form:

$$m[\ddot{h} + 2\zeta_h \omega_h \dot{h} + \omega_h^2 h] = \frac{1}{2}\rho U^2 (2B) \left[KH^* \frac{\dot{h}}{U_o} + C_{Lo} \sin \omega_s t\right] \tag{8}$$

where H_o^* is an aerodynamic damping coefficient for decay to a resonant response amplitude; C_{Lo} is an oscillating lift coefficient and ω_s is the Strouhal circular frequency. It should be noted here that a completely analogous model could be developed for the torsional case. The values of H_o^*, C_{Lo}, and ω_s are determined experimentally from records of oscillations at the vortex "lock-in" condition and enable the ultimate prediction of prototype response amplitude.

The "strip" equation for the prototype deck section is expressed as:

$$m(x)\,[\ddot{\eta} + 2\gamma_s \omega_s \dot{\eta} + \omega_s^2 \eta]\,\Psi(x) = P_s \sin \omega_s t \tag{9}$$

and the maximum mid-span amplitude is computed as:

$$\eta_{max} = \frac{P}{2M\,\omega_s^2\,\gamma_s} \tag{10}$$

where

$$\gamma_s = \zeta - \frac{\rho B^2 H_o^*}{2m},$$

$P = \rho U^2 B C_{Lo} \int_{span} \Psi(x)\,dx$ = generalized force amplitude,

$M = m \int_{span} \Psi^2(x)dx$ = generalized mass,

$\Psi(x)$ = normalized span deflection

18

$\Psi(x)$ is approximated by assuming that the main span deflected shape is represented by a half wave sine curve.

Design and Construction of Models

A section model of a suspended bridge superstructure is a geometrically similar copy of a typical length of the suspended structure only. Any cables or hangers are not modeled because their aerodynamic effects are considered negligible. The section model is rigidly constructed to ensure that all elastic behavior takes place in the springs from which it is suspended. The vertical and rotational movement of the section model supported by its spring suspension simulates the vertical bending and torsional twist of the prototype structure.

Four basic section models with 15 potential configurations were designed and constructed for this test program. Design was performed by Carroll Associates, Inc., of Maryland, while fabrication and assembly were performed by Frazier Precision Instrument Co., Inc., of Virginia, and the FHWA Mechanical Design and Experimental Fabrication Group, respectively. All models were designed to a geometric length scale of 1:60 to ensure adequate reproduction of significant structural details. Model length was set at 60-inches (1.524 m) inside to inside of end plates representing a 300-foot (91.46 m) section of prototype span. Model widths vary from 16.85-inches (.4281 m) to 19.95-inches (.5070 m), resulting in aspect ratios between 3.56 and 3.00. End plates were employed so that two-dimensional flow could be maintained near the model ends. The models were scaled according to Froude number criteria for mass properties and vertical natural frequency. Due to practical limitations of simulating the relatively high prototype torsional characteristics, values of polar mass moment of inertia and torsional natural frequency do not, however, achieve Froude scaling.

To maintain proper weight and weight distribution, develop sharp edges, and provide necessary model strength and rigidity, a variety of lightweight materials were incorporated into the model designs. Girder webs, floor beams, and asphalt decks are constructed of aircraft birch plywood. Girder and beam flanges, edge strips, and railing lips are aluminum. Balsa wood was used for diaphrams, ribs, traffic barriers, stiffeners, and concrete decks. The end plates are of "sandwich" construction, with balsa wood between aluminum sheets. Edges were tapered to reduce drag effects, and an elliptical shape was chosen to minimize weight and polar mass moment of inertia. Trusses with tubular aluminum members were extended from the end plates to provide crossbars 90-inches (2.286 m) apart for attachment of the supporting springs. Traffic barriers are attached with machine screws to facilitate removal for modification of the cross-section. Details of the seven Luling configurations tested are illustrated in Figure 2 and Table 1.

Test Procedure and Instrumentation

The tests were conducted in the FHWA open-circuit, low-velocity wind tunnel, which was designed particularly for testing bridge section models. A blower forces air through a diffusing section with a series of stainless steel wire screens into a cylindrical pressure chamber and through the nozzle from which the air is discharged onto the model. The velocity over the cross-section of the wind stream is very uniform to a point 6 feet (1.8 m) beyond the end of the nozzle.

A steady wind velocity, with a range of 0- to 30-feet per second (9.1 mps), is maintained with a micro-control rheostat in the blower circuit. The wind velocity is computed from the dynamic pressure head of the wind stream obtained by direct measurement with a pitot-static tube and an inclined manometer. Corrections are made for changes in air or fluid temperature and barometric pressure.

The nozzle can be rotated about the horizontal axis of the pressure chamber, allowing tests at various wind angles of attack. The angle of attack is the vertical angle between the wind velocity vector and a horizontal plane; a positive angle of attack indicates an upward wind.

The section models were suspended in front of the wind tunnel nozzle by means of four supports with upper and lower coil springs at each support, as illustrated in Figure 3. The vertical length of the springs was adjusted to set the proper vertical frequency of oscillation. The torsional frequency was set by adjusting the spacing between the springs at each end of the model. Although it was not possible to attain the relatively high torsional frequency desired, attempts were made to obtain as high a frequency as possible. The total mass of the section model, end plates, support trusses, end bracket crossbars, and "moving" springs was tuned to the desired scaled quantity by the addition of small weights to the end plates at the model center of gravity.

Horizontal restraining wires were attached to the end bracket crossbars at the center of gravity of the model to prohibit longitudinal or lateral movement during the tests. The restraining wires, which were tensioned with 2-pound (0.9 kg) weights, were of sufficient length that their vertical components would have no significant effect upon the vertical or torsional motion of the model.

Electrical resistance strain gages were attached to beryllium copper flexure plates above the coil springs. The strain gages at one end of the model were wired to indicate the vertical component of oscillation, and those at the other end were wired to indicate the torsional component. Strain gage outputs were amplified and the two components were recorded side-by-side on an oscillograph.

The models were tested only under laminar flow conditions. The tests were conducted at wind angles of attack varying from +6° to -4°. While maintaining a steady wind velocity at each of a series of increasing values, the models were displaced in the respective vertical and torsional degrees-of-freedom, released, and the oscillatory dynamic response recorded. For the vertical mode, the initial displacement was accomplished manually. For torsion, however, it was necessary to "hold" the model at a 4° displacement and release it using solenoids. The velocity and response data were processed on the FHWA computer system to obtain the aerodynamic derivatives and vortex response information discussed earlier.

18

Discussion of Results

Test results for each of the seven Luling configurations are summarized in Figures 4 through 9.

No vertical flutter (self-excited, divergent, vertical oscillations) was exhibited by any of the model configurations during laboratory testing. This observation is verified by the computer

plots of the aerodynamic derivatives. The H_1 derivative, the function for aerodynamic damping of vertical oscillations, shows positive damping over the full test range. A typical plot of this derivative is presented in Figure 4. Torsional critical flutter velocities at zero damping and 1 percent damping are illustrated for prototype wind speed and wind angle (angle of attack) in Figures 5 and 6. Torsional flutter (self-excited, divergent, torsional oscillations) was exhibited at horizontal wind speeds greater than equivalent prototype design requirements of 150-miles per hour (240 km/h). The greatest flutter stability was demonstrated by the most "streamlined" models, C-6-C-A, C-6-C-B, and C-2C-A, with critical velocities in excess of 250-miles per hour (400 km/h). As angle of attack increases in the positive direction, flutter stability generally decreases.

Since high wind velocities at high angles of attack are not considered likely in view of data obtained at the Severn and Newport Bridges, critical flutter velocities of less than design wind speed at high angles of attack are not considered a point of concern. Again, these observations are verified by computer plots of the A_2^* derivative, indicative of torsional aerodynamic damping. When A_2^* becomes positive, self-excitation tendencies are restrained only by the structural damping. A typical plot of this derivative is presented in Figure 7.

An excitation of the bridge deck in vertical and torsional modes by the resonant action of the periodic shedding of vortices in the wake of the structure was exhibited by all models. The amplitude-limited oscillation can be an unacceptable characteristic of the design when it occurs at moderate wind speeds, and resulting accelerations are disturbing to the user. Generally, vertical vortex shedding response was exhibited at various velocities or ranges of velocities between 15- and 30-miles per hour (24 and 48 km/h), while torsional vortex shedding response was exhibited between 60- and 100-miles per hour (96 and 160 km/h). Since torsional response occurs at relatively high velocities, its effect on the user may be disregarded. For the vertical response which occurs at moderate wind speeds, deck accelerations of 2 percent of "G" are considered acceptable [7]. Estimates of prototype accelerations are illustrated in Figure 8 for vertical response in a horizontal wind. Models C-2C-C and C-2C-A demonstrated the least overall vertical response, while Model C-2-C-2 exhibited the most. These estimates are considered conservative since it is probable the real wind over the bridge span will be gusty enough to cause poor spanwise correlation and decrease the likelihood of "lock-in" to occur.

Drag coefficients were obtained for the preferred Luling cross-section, C-2C-A, and its three erection stages as illustrated in Figure 9. For stage A1, the median barrier was removed; A2, median barrier and fairings removed; A3, median barrier, fairings and railings removed. Horizontal pressures were computed from the coefficients for a moderate wind angle of $\pm 2°$ and were found to be somewhat less than recommended AASHTO values for configuration C-2C-A and about equal to the AASHTO values for stage A2.

Summary and Conclusions

This paper summarizes the major results of a comprehensive wind tunnel study of a major suspended bridge structure. The bridge studied is an example of the cable-stayed, box-girder type which, until recently, has not often been constructed in the United States. In general, all the cross-sections tested in a horizontal wind have

critical velocities for flutter in excess of the appropriate design wind speeds. At other wind inclinations, the critical velocities remain high enough to exceed expected winds. Varying degrees of vertical motion are caused by vortex shedding at speeds between 15- and 30-miles per hour (24 and 48 km/h). Vertical vortex shedding response amplitudes and accelerations are minimal and considered neither damaging to the structure nor discomforting to the user. Drag forces measured in the wind tunnel appear reasonably relative to recommended design values. Further details regarding results presented as well as results for other parts of the test program may be found in the recent study report: "Aerodynamic Investigations of the Luling, Louisiana, Cable-Stayed Bridge," FHWA-RD-77-161. This report will be available through the National Technical Information Service, 5285 Port Royal Road, Springfield, Virginia 22161.

Acknowledgments

This project was carried out at the request of the Louisiana Department of Highways. The author gratefully acknowledges the technical support and guideance provided by Mr. Richard H. Gade, Project Manager for FCP Project 5A. Despite Mr. Gade's failing health in recent years, he never ceased to serve as a guiding force on this and other projects in the Wind Engineering field. Mr. Gade died on September 25, 1977, and he will be deeply missed by all those who knew him.

References

1. Farquharson, F. B., et al., "Aerodynamic Stability of Suspension Bridges with Special Reference to the Tacoma Narrows Bridge," University of Washington Engineering Experiment Station, Bulletin No. 116.

2. Vincent, G. S., "Golden Gate Bridge Vibration Studies," Journal of the Structural Division, ASCE, October 1958.

3. Gade, R. H. and Scanlan, R. H., "Experimental Measurement and Interpretation of Aerodynamic Stability Coefficients for the Decks of Two Cable-Stayed Bridges," Proceedings of ASCE and EMD Symposium on Dynamic Response of Structures, UCLA, March 1976.

4. Thom, H. C. S., "New Distributions of Extreme Winds in the United States," Journal of the Structural Division, ASCE, Volume 94, pp. 1787-1801, July 1968.

5. Scanlan, R. H., and Tomko, J. J., "Airfoil and Bridge Deck Flutter Derivatives," Journal of Engr. Mech., Volume 97, ASCE, December 1971.

6. Scanlan, R. H., Recent Methods in the Application of Test Results to the Wind Design of Long, Suspended-Span Bridges, Federal Highway Administration, Report No. FHWA-RD-75-115, October 1975.

7. Wardlaw, R. L., and Buckland, P. G., "Some Aerodynamic Considerations in Bridge Design," The Journal of the Engineering Institute of Canada, April 1972.

TABLE 1: CROSS-SECTIONAL DATA

Section model designation (1)	Prototype section depth, in feet (2)	Roadway surface (3)	Railing type (4)	Vertical natural frequency, in cycles per second (5)	Torsional natural frequency, in cycles per second (6)
C-2-C-1	14	Concrete	Basic	2.62	5.29
C-2-C-2	14	Concrete	Alternate	2.56	5.20
C-2C-C	14	Concrete	Alternate	2.56	5.35
C-2C-A	14	Asphalt	Alternate	2.80	5.25
C-2A-C-1	12	Concrete	Basic	2.53	5.24
C-6-C-B	14	Concrete	Basic	2.49	5.33
C-6-C-A	14	Concrete	Alternate	2.48	5.24

1 ft = 0.3048m

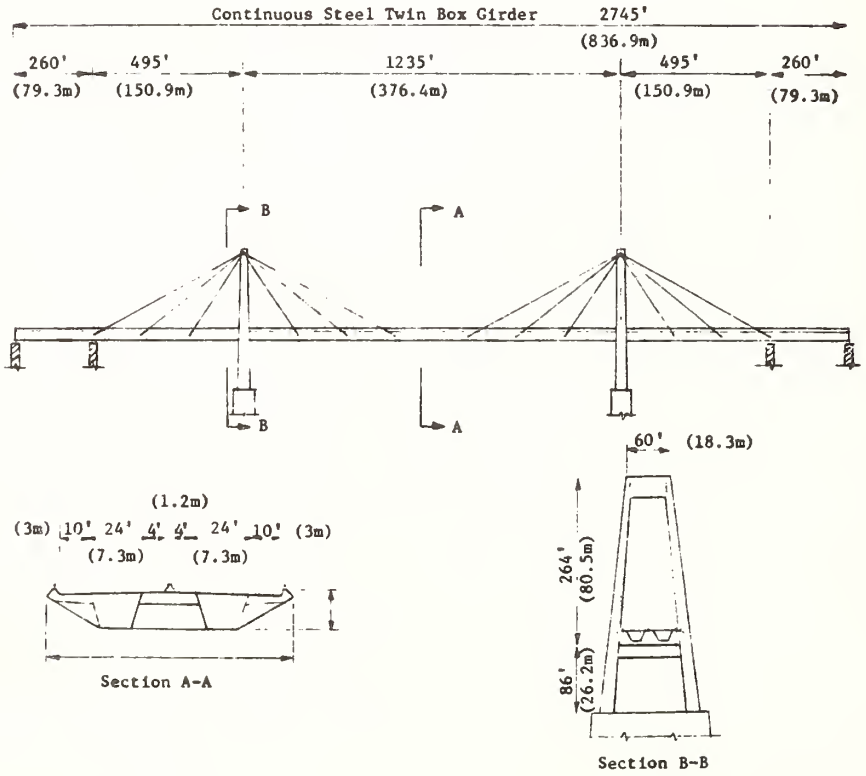

FIGURE 1: BRIDGE ELEVATION AND CROSS-SECTIONS

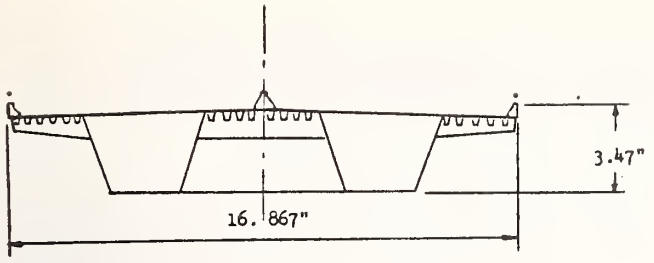

C-2-C-1

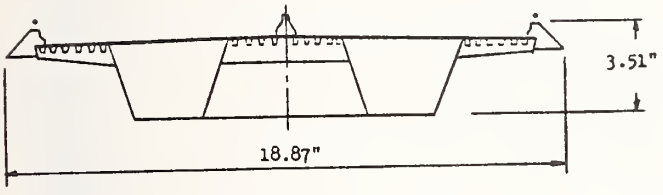

C-2-C-2

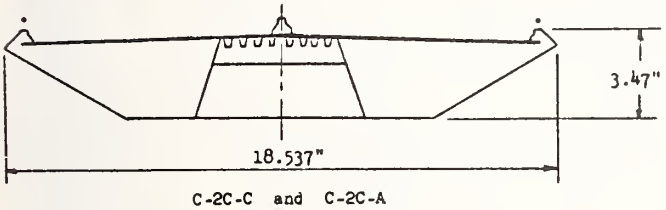

C-2C-C and C-2C-A

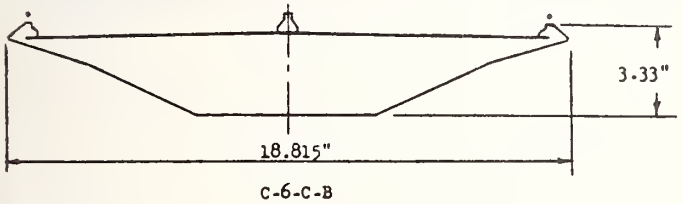

C-6-C-B

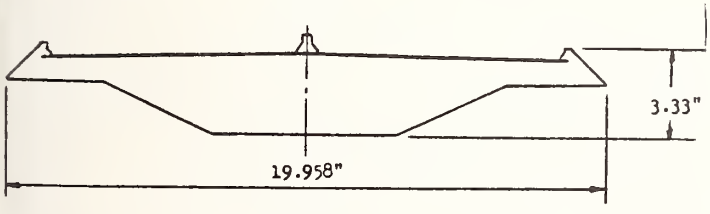

C-6-C-A

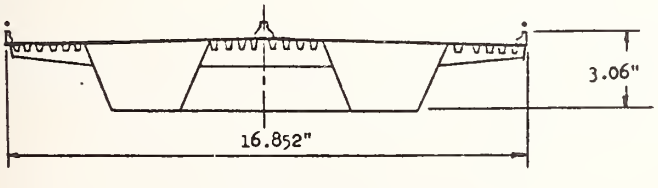

C-2A-C-1

FIGURE 2: MODEL CONFIGURATIONS

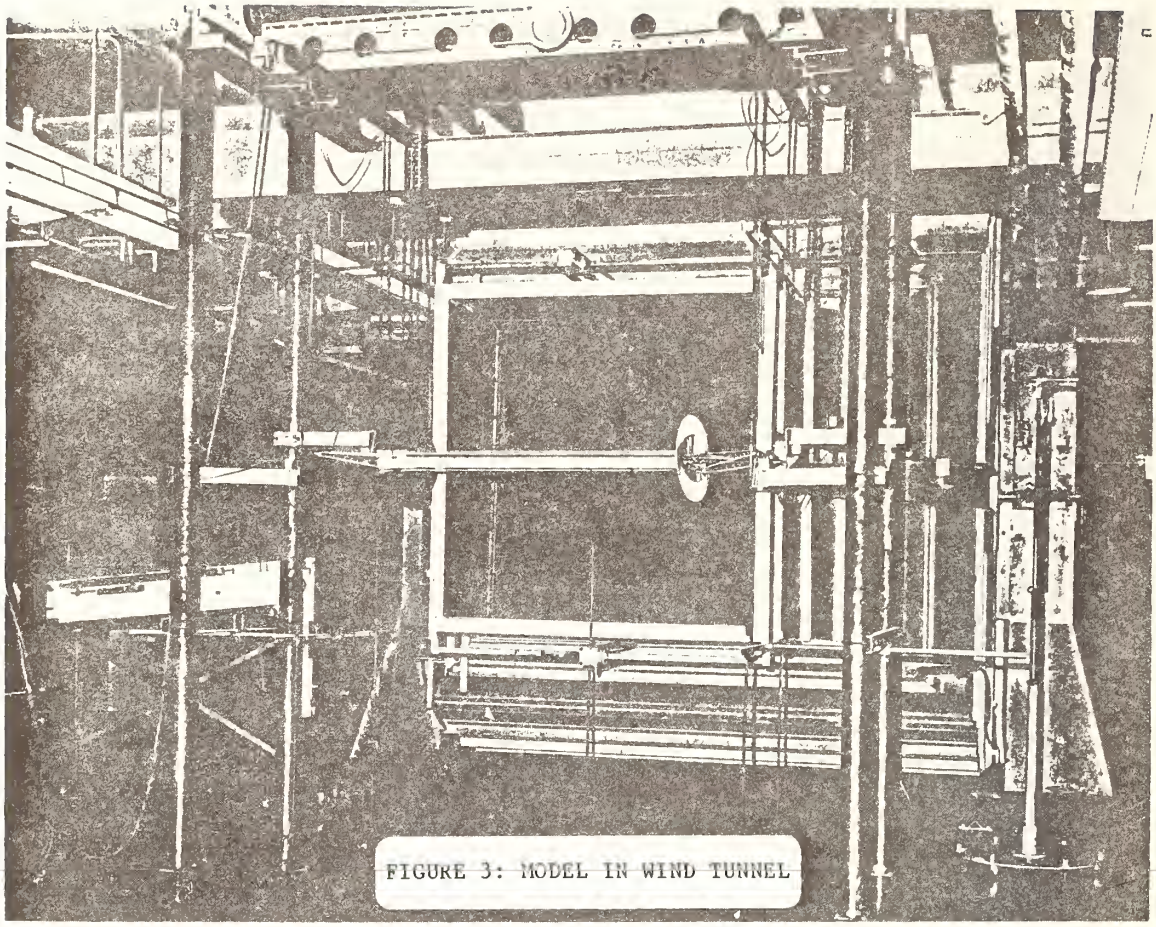

FIGURE 3: MODEL IN WIND TUNNEL

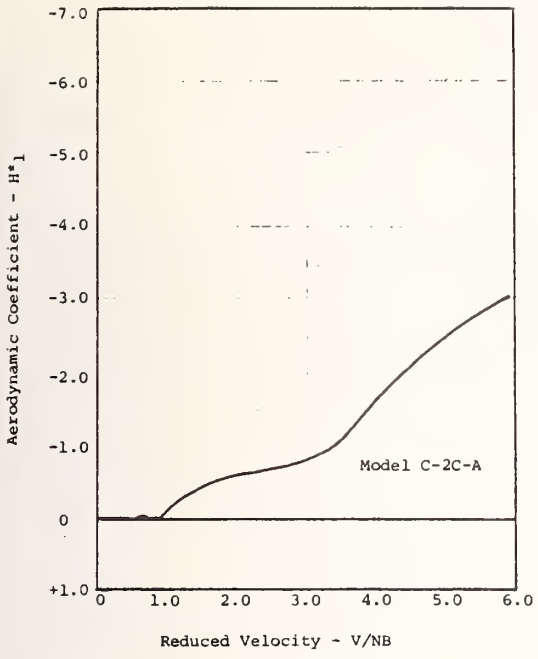

FIGURE 4: FLUTTER DERIVATIVE FOR VERTICAL - ANGLE OF ATTACK = 0°.

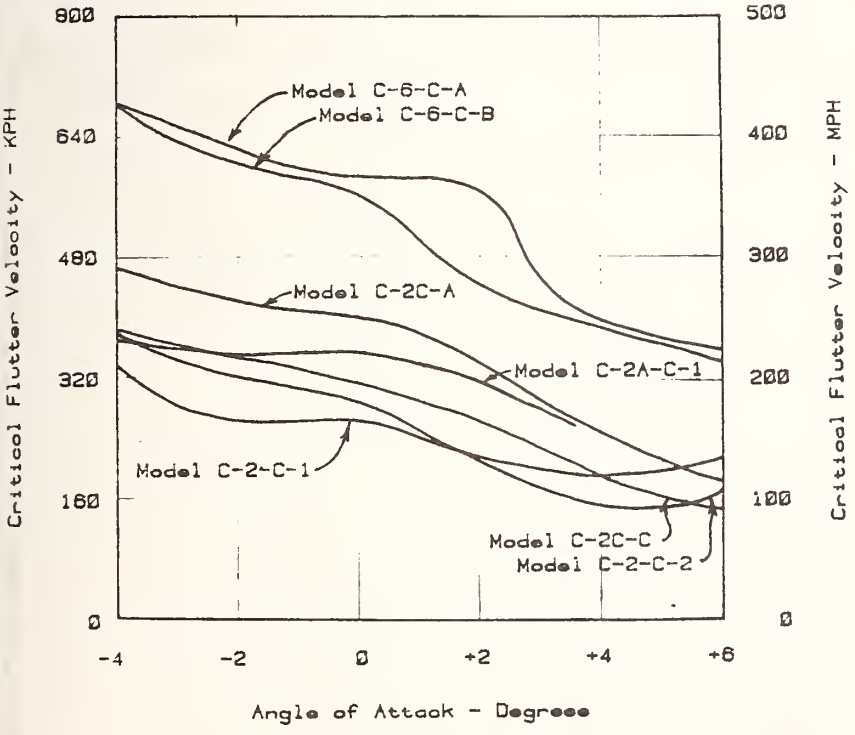

FIGURE 5: CRITICAL FLUTTER VELOCITY - NO DAMPING

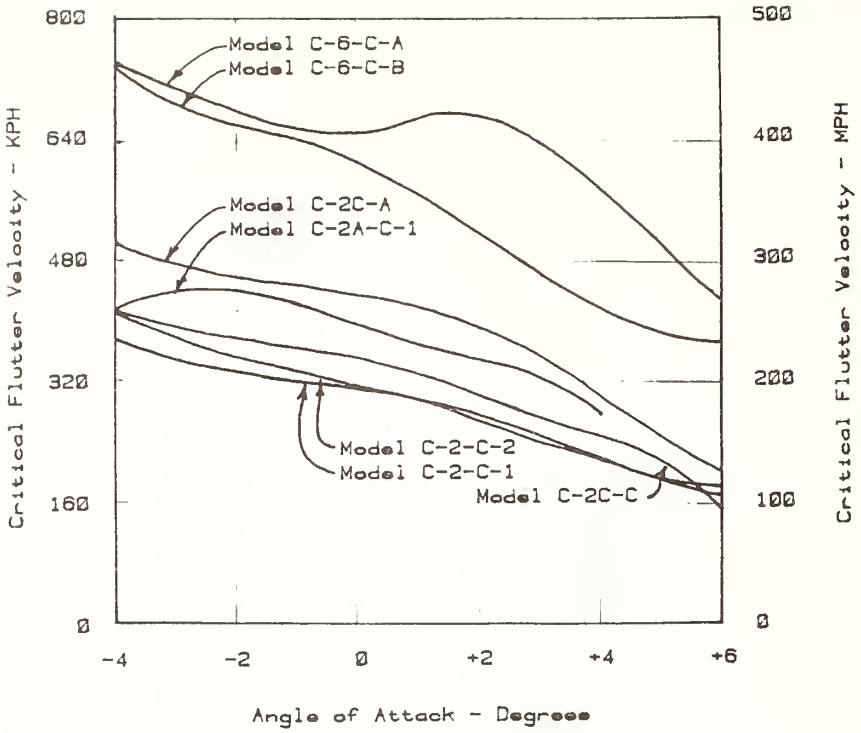

FIGURE 6: CRITICAL FLUTTER VELOCITY - 1% CRITICAL DAMPING

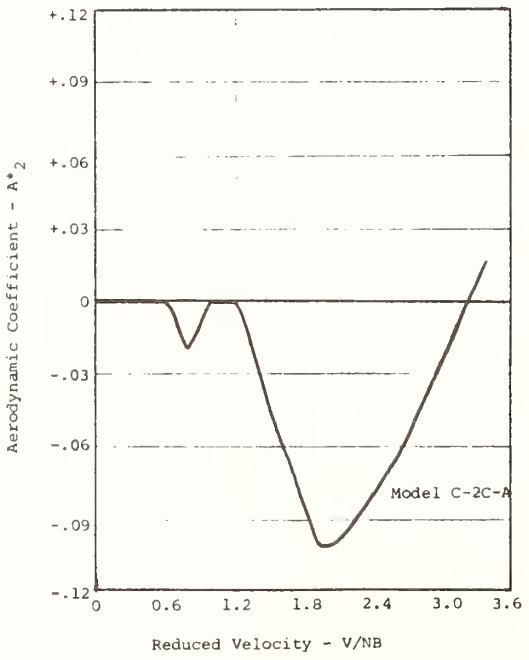

FIGURE 7: FLUTTER DERIVATIVE FOR TORSION - ANGLE OF ATTACK = 0°

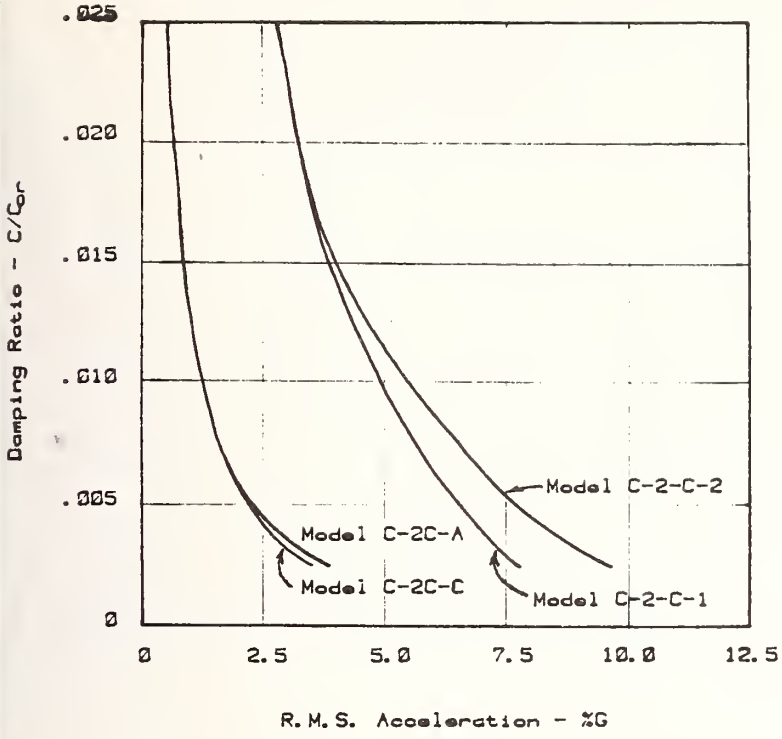

FIGURE 8: ESTIMATE OF PROTOTYPE ACCELERATIONS RESULTING FROM VERTICAL VORTEX EXCITATION - ANGLE OF ATTACK = 0

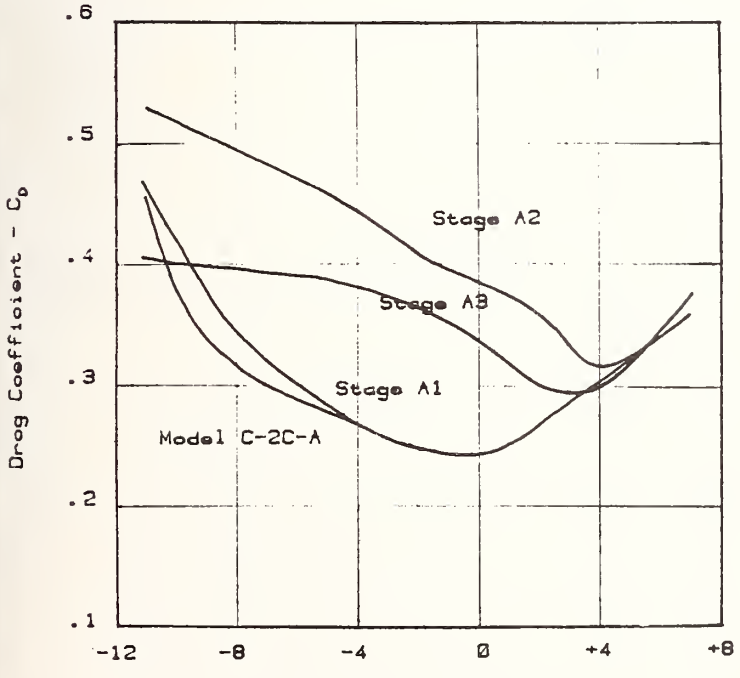

FIGURE 9: DRAG COEFFICIENTS

19

A TECHNIQUE FOR MEASURING FLUCTUATING WIND LOADS ON A TALL-BUILDING MODEL IRRESPECTIVE OF MODEL MOTION

Timothy A. Reinhold

National Bureau of Standards
Washington, D.C.

A Technique for Measuring Fluctuating Wind Loads on a Tall-Building Model Irrespective of Model Motion

Models used to determine resultant fluctuating loads on structures can be divided into two categories. The first category includes aeroelastic and elastic models for which loads are determined from the movement of the model. The second category involves direct measurement of wind pressures. Direct measurements of wind pressures have been made since the earliest wind tunnel model tests and involve a model with a number of pressure taps on its exterior surface. Pressure measurements made at each tap are usually analyzed to determine mean values, root mean-square (RMS) values, and possibly spectra. Cross-correlation betwen pressure measurements at two points may also be obtained to determine the correlation of the pressure fluctuations over the model surface. However, it has been extremely difficult to use pressure measurements to obtain information about resultant fluctuating loads in a form that is useful to a design engineer. Consequently, aeroelastic or elastic models, which require measurement of the motion of the model, are used in practically all tests where information on the fluctuating motion or the resultant loads is sought.

Aeroelastic and Elastic Models

Aeroelastic models constitute the most widely recognized type of model for use in determining the motion of a building and in determining resultant fluctuating loads acting on the building as a whole (base bending moments and base shear). The requirements for simulation of building response to wind loads using aeroelastic models have been well established and are discussed by Whitbread [1]. The nondimensional parameters which must be modeled have been listed often in the literature, for example, see references [1 and 2], and will not be reproduced here. The important observation relative to these parameters is that a number of structural properties of the prototype building must be modeled to simulate the dynamic response of the structure to wind loading. The problem associated with attempts to satisfy the similarity requirements are discussed by Whitbread [1] and Scruton [2], who have shown that construction of an aeroelastic model which satisfies rigorously all the similarity requirements is generally impossible. A common simplification involves use of a semi-rigid model, which incorporates a gimbal and a set of springs at its base, to simulate the motion of tall buildings where the predominant mode of vibration is linear [3 and 4].

Aeroelastic models can be used to measure both mean and dynamic components of the building deflection or base moment along two orthogonal axes (usually chosen perpendicular to the faces of a rectangular prismatic building). However, even with expensive and elaborate aeroelastic models, it is difficult to account for torsional movements which have been shown to be an important component of the dynamic response of a building, even for symmetrical buildings [5]. Tests must be conducted for a number of different wind speeds at various angles of attack, and structural parameters must be varied. The structural properties, including stiffness, damping, and mass distribution, must be varied in the test to bracket the possible values that may ultimately exist in the prototype. Measurements of the dynamic characteristics of existing buildings [6] have shown that estimates of stiffness and damping (based on design calculations and judgment) may be extremely inaccurate. Furthermore, application of the results is usually limited to the particular building being designed because of specific modeling of the range of frequency and damping parameters [7].

A second type of model that relies on measurements of motion to determine the loading is the elastic model. These models are rigid members mounted on elastic foundations and allow measurement of the so-called quasi-static force spectrum (i.e., the spectrum of actual wind loads), which is independent of the natural frequency and damping of the model [7]. The spectrum is quasi-static because it does not reflect the amplification of the loads due to resonance. For example, while aeroelastic models may have natural frequencies of a few Hertz, the model used by Whitbread [7] had a natural frequency of 450 Hz and the spectrum of loads was determined for the frequency of 0 - 250 Hz. Models such as this are too stiff in the torsional mode to allow measurements of twisting moments.

Determination of the spectra of wind loads has been attempted for aeroelastic models by measuring the displacement spectrum and determining the mechanical admittance function for the model. The mechanical admittance is a function of frequency and represents the ratio between the spectra of the amplitude of deflection and load. For a building, a modal approach is used and the response of the building in each mode is expressed as a single degree-of-freedom system [8]. Normally first-mode (linear) response is assumed and the corresponding first-mode mechanical admittance function is determined. Saunders and Melbourne [9] used this technique to determine normal force spectra for several models.

All of the techniques described can be used to obtain only the resultant fluctuating loads on the building as a whole and it is not possible to determine the manner in which the wind loads are distributed over the surface of the building. A more complex model, which yields information on the nature and distribution of the wind loads throughout the building height, has been investigated by Ellis [10]. The technique used a multi-force transducer composed of 6 elements to measure dynamic strains and acceleration at various levels throughout the building. Dynamic bending moments are found from the output of calibrated strain gages; and inertia forces are found from the measured accelerations and known mass distribution of the model. Random loads on each element are determined from these strains and accelerations. The model can not be used to measure fluctuating twisting moments.

Direct Pressure Measurements

Mean forces and moments on buildings have often been determined by integrating mean pressure measurements made at numerous points over the entire building [11]. However, this procedure has not been used previously to determine resultant fluctuating loads. Ellis [10] noted that fluctuating loads at various levels throughout a building could be determined by using numerous pressure transducers. However, he rejected the method because of the high cost of the large number of transducers needed and because subsequent data gathering and integration would be expensive and cumbersome.

The analog manipulation of the data performed in the present investigation streamlined the data gathering and integration procedures. Three analog signals were produced to represent the resultant fluctuating load components on a discrete segment of the building. Consequently, analysis of the load records to determine load spectra was no more difficult than analysis of turbulent velocity records. The transducers did represent a significant initial investment but the cost of all parts, including printed

circuit boards, used in the electronic network for signal conditioning and integration was less than the cost of three transducers. The transducers and electronics can be readily used in future model tests.

The technique can be used to determine fluctuating forces simultaneously at several levels throughout the building height. Twisting moments can be determined in addition to normal forces for each level. Consequently, it is possible to determine both the nature and distribution of fluctuating normal forces and twisting moments throughout the height of the model. Furthermore, since the loads are measured simultaneously, it is possible to sum the loads at various levels, weighted by a mode shape, to determine the modal forces on the building. These modal forces can then be used together with an appropriate admittance function to calculate the building response.

Test Program

Environment

A series of model tests, which employed numerous transducers to measure directly resultant fluctuating pressures, were carried out at Virginia Polytechnic Institute and State University. Square prisms with sharp edges were used in the wind tunnel model tests. The models fulfilled the requirements of having simple geometric shape and of having relative dimensions (height-to-width ratio) similar to realistic structures and to previously tested aeroelastic models. Experiments were conducted in a 1.8 m square by 8.0 m long test section of a low-speed wind tunnel. Models were placed in a turbulent shear layer which was designed to simulate the atmospheric boundary layer over an urban area. The turbulent shear layer was developed over the test section floor using a combination of spires at the entrance of the test section and 6.1 m fetch of 102 mm cubic roughness elements.

A detailed description of the mean flow and the three turbulence components for the wind tunnel shear flow, together with a comparison of the flow properties with those of the atmospheric boundary layer over urban terrain, are contained in references [12 and 13]. It is sufficient for the purposes of this discussion to note that the mean velocity profile followed the power law with a power index of 0.37 (corresponding to flow over urban terrain) and that the turbulence properties were found to compare reasonably well with full-scale estimates at a geometric scale ratio ranging from 1/400 to 1/600 [12 and 13].

Models

Two models of identical geometry (76.2 mm x 76.2 mm x 635.0 mm) were used. One model was fitted with 96 pressure taps, connected by flexible tubing to two Scanivalve systems. This arrangement was used to obtain mean pressure measurements because the flush mounting pressure transducers (Kulite model COH-125-5) often exhibited a slow voltage drift. The second model was fitted with the flush mounting pressure transducers, having an exposed diaphram of 2.16 mm diameter. The transducers were used to measure fluctuating pressures at the same locations as the pressure taps. The pressure taps and transducers were located in groups of 16 about the perimeter of the model, with 4 transducers on a side, at 6 elevations throughout the model height.

Selection of the locations for pressure taps and transducers was based on results of experiments conducted using a section-model of square cross-section placed in a two-dimensional uniform turbulent flow. Tests were conducted for four different orientations of transducers on a single model face. The configurations used are illustrated in Figure 1 and range from the use of seven transducers to the use of three. The signals from the transducers were summed to obtain the resultant normal force on the model face and the resultant twisting moment about the center of the model face. The objective was to determine the positioning across the face of no more than four transducers on a side, which would closely reproduce the loads measured using seven transducers on a side. A comparison was made of both RMS values and autocorrelation functions for the normal forces and twisting moments measured with the four configurations of transducers shown in Figure 1. Measurements were made at a number of orientations of the model face to the flow described by the angle of attack, α, in Figure 1.

The positions of the transducers adopted for the boundary layer model tests are shown in Figure 2. This configuration reflects the observation that the outer transducers had to be as close to the edge as possible. It was necessary to offset the outer transducers to accomplish this. The maximum estimated error obtained by using the four tranducers on a side as opposed to seven is less than 5 percent for the normal force and less than 15 percent for the twisting moment associated with any wind direction. More detailed information concerning the placement of transducers can be found in reference [2].

Determination of Resultant Fluctuating Loads

Accumulation of a large mass of data representing simultaneous instantaneous pressures on each transducer was avoided by performing an analog summation of the transducer output signals to obtain single signals representing the resultant fluctuating loads. The electronics necessary to perform this task consisted of two units. The transducer output signals had to be amplified to obtain uniform pressure sensitivity weighted by the area factor associated with the transducer location. Finally, these signals had to be added and subtracted in proper combinations. Moment arm factors had to be introduced in order to obtain a signal representing the resultant fluctuating moment. Figure 3 outlines the network of electronics used to obtain the resultant fluctuating loads.

Each transducer had its own pressure sensitivity and surface pressure fluctuations produced output voltage fluctuation of less than one millivolt peak to peak. Consequently, a differential amplifier capable of producing gains of between 500 and 2,500 was connected to the output of each transducer. A schematic diagram of the amplifiers is shown in Figure 4. Design helps for such items are available in books on operational amplifiers such as the one by Graeme, Tobey and Huelsman [14]. The amplifiers contained two stages because it is difficult to obtain both high common model rejection and high gain using a single operational amplifier. The first stage provided a gain of 10 and the common mode rejection necessary to remove noise, primarily 60 Hz generated by fluorescent lights and equipment which was picked up by the wires carrying the signal from the transducer to the amplifier. Two conductor shielded cables were used in transmitting signals to ensure that most noise picked up would be common to both leads. The second stage provided a variable gain of between 50 and 250. A variable DC voltage offset feature was available on the first stage of the amplifier.

The offset adjustment feature allowed any DC voltage produced by the transducer to be removed so that the average output voltage of the amplifier could be set to zero.

The amplifier gain was set so that the output signals of all transducers located at one level represented identical pressure sensitivities weighted by the proper area factor. For example, if identical differential pressures were applied to transducers 1 and 2 in Figure 2 then the ratio of the changes in output voltages for the transducers would equal the ratio of the area factors.

Signals were added and subtracted using inverting summing amplifiers. A schematic of the network used to sum the signals is shown in Figure 5. Precision resistors were used in these networks to ensure accuracy since the equation for determining gain of these amplifiers involves only the input resistance and the feedback resistance. Offset of the operational amplifier output voltage was reduced by matching the resistor between the non-inverting input and ground to the parallel equivalent resistance of the input resistors and the feedback resistor.

Four summing amplifier networks were used to produce the resultant fluctuating loads at each level. One network was used to produce each of the normal loads. Two networks were needed to obtain the moment. By referring to Figure 2, the details of the procedure can be easily explained. F'_x was produced by connecting tranducers 1, 2, 3, and 4 to inputs A, while transducers 9, 10, 11, and 12 were connected to inputs B. F'_y was produced in a similar manner using a second network and connecting transducers 13, 14, 15, and 16 to inputs A, and transducers 5, 6, 7, and 8 to inputs B. The moment was produced in two segments. The first segment, called M1, was obtained by connecting transducers 1, 5, 9, and 13 to inputs A, and transducers 4, 8, 12, and 16 to inputs B of the third network. The second segment, M2, was produced by connecting transducers 2, 6, 10, and 14 to inputs A, and transducers 3, 7, 11, and 15 to inputs B of the fourth network. The signal from segment M1 was multiplied by a factor of 1.0 and the signal from segment M2 was multiplied by a factor of 0.384 to express the relative lengths of the associated moment arms. These products were then added using an Electronics Associates, Inc., Mini AC analog computer to obtain the resultant moment. The output voltages were multiplied by appropriate factors to obtain the loads in engineering units. The actual length of the moment arm was incorporated in the factor for the moment.

Sample Results

Resultant normal forces and twisting moments were determined at each of the 6 levels at which instrumentation was placed. The levels were located at 0.16, 0.32, 0.48, 0.64, 0.80, and 0.96 of the model height, measured from the tunnel floor upward. Because of a limited number of transducers, it was only possible to instrument three levels simultaneously. Consequently, three tests were conducted. Test 1 had transducers at 0.64, 0.80, and 0.96 of the model height (levels 4, 5, and 6). Test 2 had transducers at 0.32, 0.64, and 0.96 of the height (levels 2, 4, and 6), and test 3 had transducers at 0.16, 0.48, and 0.64 of the height (levels 1, 3, and 4). This combination of tests allowed measurements of the fluctuating loads to be made a level 4 (0.64 of the height) in each test. Consequently it was possible to determine the correlations of resultant fluctuating loads between all levels and level 4. RMS values of the resultant fluctuating loads were measured as the tests were conducted and the signals representing the loads were

recorded on a 14 channel FM tape recorder. The records were subsequently analyzed to determine the power spectra of the loads and the cross-spectra between loads at different levels.

Examples of the detailed information concerning the nature and distribution of the loads which could be obtained from analysis of the wind load measurements are illustrated in Figures 6 through 9. The loading illustrated is the cross-wind component for a single tall building with one face normal to the mean flow. Normalized power spectra obtained at each of the six instrumented levels are shown in Figure 6. The shift in frequency of the vortex shedding with height is clearly shown. Figures 7 and 8 together illustrate the relationship between the loads at level 4 and each of the other levels. The coherence functions, Figure 7, indicate the degree of correlation between the loads while the phase shift, Figure 8, contains the information on the relationship of the timing of the loads. From observations of the cross-correlation functions computed between the load components, it was determined that the maximum cross-correlation generally occurred when the signal from the upper of the two levels was delayed in time with respect to the signal from the lower level. This shows up as a negative phase shift between level 4 and level 5 or level 6 and as a positive phase shift between level 4 and the lower levels, Figure 8. Consequently, the load fluctuations applied on the upper levels of the model propagated downward. The double lines in Figure 8 correspond to the range of frequencies where the coherence function was greater than 0.2.

Estimates of the modal forces were also obtained by using data from test 1. The signals representing the forces at levels 4, 5, and 6 were scaled to represent their relative magnitude, the areas over which they were assumed to act and a linear mode shape factor to represent the first mode of vibration of a tall building. The signals were summed by passing them through an analog computer circuit. The resultant signal represented the modal force and was analyzed to obtain the modal force spectrum and the RMS value of the modal force was also determined. These modal force estimates only incorporated forces which acted over roughly the top half of the model. It is estimated that the maximum error obtained from neglecting forces at the lower levels in determining the modal forces and torques is less than 30 percent. The nondimensional modal force spectrum for the cross-wind forces on the single model with one face normal to the mean wind direction is shown in Figure 9. The magnitude of the RMS value of the modal force can be determined from the following equation:

$$\overline{F}_y = 1/2 \; \rho \; \overline{U}_H^2 \; BH \; C'_{F_y} \qquad (1)$$

where C'_{F_y} is the RMS modal force coefficient and was found to be 0.118 for the cross-wind force.

Comparison of Results

The true test of the validity of model test results is a comparison with results of full-scale measurements. In the absence of full-scale measurements for a similar building, results are compared with those obtained from aeroelastic tests where models of similar geometric shape were used. Tests of an aeroelastic model with reasonably similar geometry were conducted by Rosati at the University of Western Ontario [15]. The only difference in the geometric shape of the models is that the Rosati model was

shorter (aspect ratio of 7.0 instead of 8.33). Measurements of the response of the aeroelastic model were made in a flow with similar properties to the one used in this study for a wide range of velocities.

It is possible to use the modal force spectrum shown in Figure 9 together with an appropriate mechanical admittance function to predict the RMS level of response of the Rosati model. The necessary equations are presented in reference 16. Assuming that the response is first mode with a linear mode shape, the equation for the response spectrum is given by:

$$G_y(n) = \frac{H^2(n)}{K^2} G_{F_y}(n) \tag{2}$$

where

$$H^2(n) = \frac{1}{(1 - \frac{n^2}{n_0^2})^2 + (\frac{2\gamma n}{n_0})^2} \tag{3}$$

and

$$K = (2\pi n_0)^2 \int_0^H m \, \mu_1^2 \, dz. \tag{4}$$

The RMS level of response, σ_y, is given by:

$$\sigma_y^2 = \int_0^\infty G_y(n) \, dn. \tag{5}$$

Predictions of the response of the Rosati model were made using these equations and are compared with the actual response measurements reported by Rosati [15]. The comparison is shown in Figure 10. The open symbols represent measured response and the solid symbols represent the predicted response. The agreement is within 25 percent for all cases up to reduced velocities of about 15. At high values of reduced velocity the predictions become considerably lower than the measured values for low values of structural damping. The differences may be attributable to differences in the properties of the shear layers used in the tests or to aeroelastic effects, i.e., aerodynamic damping. Negative aerodynamic damping would cause greater building response and would be especially noticeable when the structural damping is low. There are some indications that use of more levels of transducers in determining the modal force would lead to a reduction in the difference between the measured and predicted levels of building response, at least up to values of reduced velocity of about 15.

Conclusions

19

The multiple transducer technique described in this paper provides a method for directly determining the resultant dynamic wind loads on a building. The technique can be used to obtain detailed information concerning the distribution of the loads over the surface of the model as well as the characteristics of the loads at various levels. Twisting moments can be readily obtained.

Forces at various levels can be integrated to determine modal forces. Results of response predictions for first mode (linear)

agree reasonably well with response measurements of similar aeroelastic model test for values of the reduced velocity of practical interest in design. Other mode shapes could also be used since information concerning the distribution of the loads over the surface of the structure is available.

The experimental work reported here shows that it was possible to use analog computer circuits to reduce the data handling to a manageable scale with very little expense.

Since the transducers provide measurements of wind loads which are obtained independently from measurements of model motion, the transducers can also be used in conjunction with aeroelastic models. Use of transducers on an aeroelastic model could lead to a better understanding of body-motion related forces.

Acknowledgments

The experimental work and some of the data analysis reported in this paper were supported by the National Science Foundation, Grant No. ENG-75-05327 A01. Further data analysis was conducted by the author under the NRC/NBS Postdoctoral Research Associateship. The author also wishes to acknowledge the guidance of Professor F. J. Maher and H. W. Tieleman of Virginia Polytechnic Institute and State University during the course of experimental work.

References

1. Whitbread, R. E., "Model Simulation of Wind Effects on Structures," Proceedings of the Conference on "Wind Effects on Buildings and Structures," National Physical Laboratory, England, 1963, pp. 284-302.

2. Scruton, C., "Aerodynamics of Structures," Proceedings of International Research Seminar, "Wind Effects on Buildings and Structures," Ottawa, Canada, 1967, pp. 115-161.

3. Davenport, A. G. and Isyumov, N., "The Application of the Boundary Layer Wind Tunnel to the Prediction of Wind Loading," Proceedings of International Research Seminar, "Wind Effects on Buildings and Structures," Ottawa, Canada, 1967, pp. 201-230.

4. Robertson, L. E. and Chen, P. W., "Application of Design of Research and Wind Effects," Proceedings of International Research Seminar, "Wind Effects on Buildings and Structures," Ottawa, Canada, 1967, pp. 83-113.

5. Jeary, A. P. and Sparks, P. R., "Some Observations on the Dynamic Sway Characteristics of Concrete Structures," paper presented at ACI Symposium on Vibration of Concrete Structures, New Orleans, October 1977.

6. Jeary, A. P., Lee, B. E., Paquet, J., De Souza, V. C. M. and Sparks, P. R., "The Dynamic Behaviour of the Arts Tower, University of Sheffield," paper presented at the International Conference on Slender Structures, City University, London, September 1977.

7. Whitbread, R. E., "The Measurement of Non-Steady Wind Forces on Small-Scale Building Models," Proceedings of the Fourth International Conference on "Wind Effects on Building and Structures," Heathrow, England, 1975, pp. 567-574.

8. Wyatt, T. A., "The Calculation of Structural Response," Proceedings of the Seminar "The Modern Design of Wind-Sensitive Structures," Construction Industry Research and Information Association, London, 1971, pp. 83-93.

9. Saunders, J. W. and Melbourne, W. H., "Tall Rectangular Building Response to Cross-Wind Excitation," Proceedings of the Fourth International Conference on "Wind Effects on Buildings and Structures," Heathrow, England, 1975, pp. 369-379.

10. Ellis, N., "A New Technique for Evaluating the Fluctuating Lift and Drag Force Distributions on Building Structures," Proceedings of the Fourth International Conference on "Wind Effects on Buildings and Structures," Heathrow, England, 1975, pp. 527-536.

1. Cermak, J. E., "Wind Tunnel Testing of Structures," Proceedings ASCE/EMD Specialty Conference, "Dynamic Response of Structures: Instrumentation, Testing Methods and System Identification," March 30 and 31, 1976, University of California Los Angeles.

2. Reinhold, T. A., Measurement of Simultaneous Fluctuating Loads at Multiple Levels on a Model of a Tall Building in a Simulated Urban Boundary Layer, Thesis (Ph.D.) Virginia Polytechnic Institute and State University, November 1977.

3. Reinhold, T. A., Tieleman, H. W. and Maher F. J., Wind Tunnel Simulation of Urban Winds for the Study of Tall Buildings, Report No. VPI-E-77-12, College of Engineers, Virginia Polytechnic Institute and State University, April 1977.

4. Graeme, J. G., Tobey, G. E. and Huelsman, L. P., Operational Amplifier Design and Applications, McGraw Hill, New York, (1971).

5. Rosati, P. A., The Response of a Square Prism to Wind Load, Report No. BLWT-II-68, Faculty of Engineering Science, The University of Western Ontario, London, Canada, March 1968.

6. Engineering Sciences Data Unit, "The Response of Flexible Structures to Atmospheric Turbulence," ESD Item No. 76001, London, England, September 1976.

otation

B	Width or depth of square prismatic model - mm
C'_{F_y}	RMS modal force coefficient for the cross-wind force component
F'_y	Fluctuating cross-wind force component - N
$\overline{F}_y$	RMS modal force for cross-wind force component - N
$\overline{F'^2_y}$	Variance of fluctuating cross-wind force component - N^2
$_y(n)$	Cross-wind displacement spectrum - m^2s
$_y(n)$	Cross-wind modal force spectrum - N^2s

19

H	Height of model - mm
$H^2(n)$	Mechanical admittance function
K	Modal stiffness - N/m
m	Mass per unit length of model - Kg/mm
n	Frequency - Hz
n_0	Natural frequency for a particular mode of vibration - Hz
$\overline{U}_g$	Mean wind velocity at the gradient height - m/s
$\overline{U}_H$	Mean wind velocity at the top of the model - m/s
Z	Height above ground level - mm
α	Angle of attack - deg.
γ	Structural damping, expressed as fraction of critical damping
μ_1	Mode shape function for first mode = Z/H
ρ	Density of air - Kg/m^3
σ_y	RMS displacement of top of model - mm

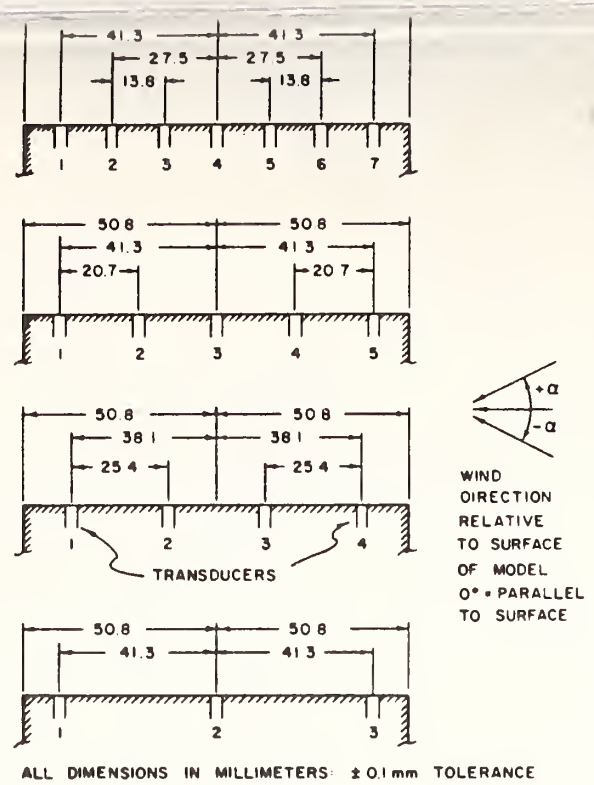

FIGURE 1: TWO-DIMENSIONAL, SECTION MODEL TESTS TO DETERMINE PLACEMENT OF TRANSDUCERS

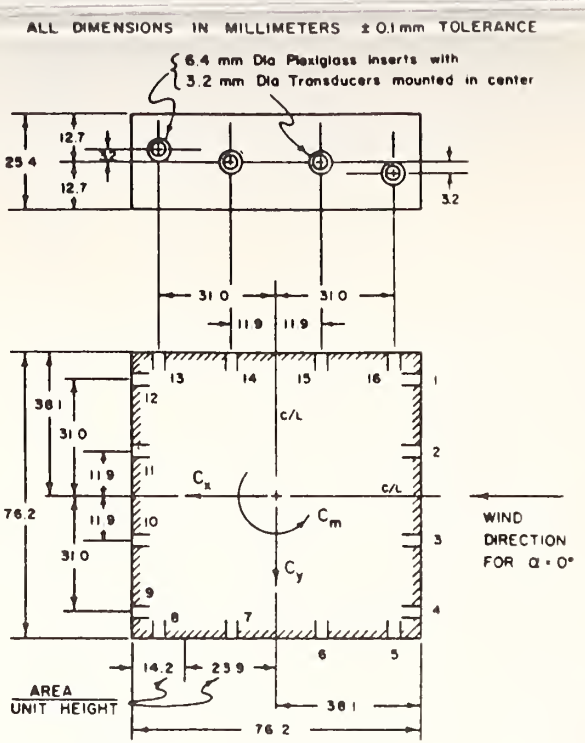

FIGURE 2: INSTRUMENTED SECTION OF MODEL - PLACEMENT OF TRANSDUCERS ADOPTED FOR 3-DIMENSIONAL MODEL STUDY

19

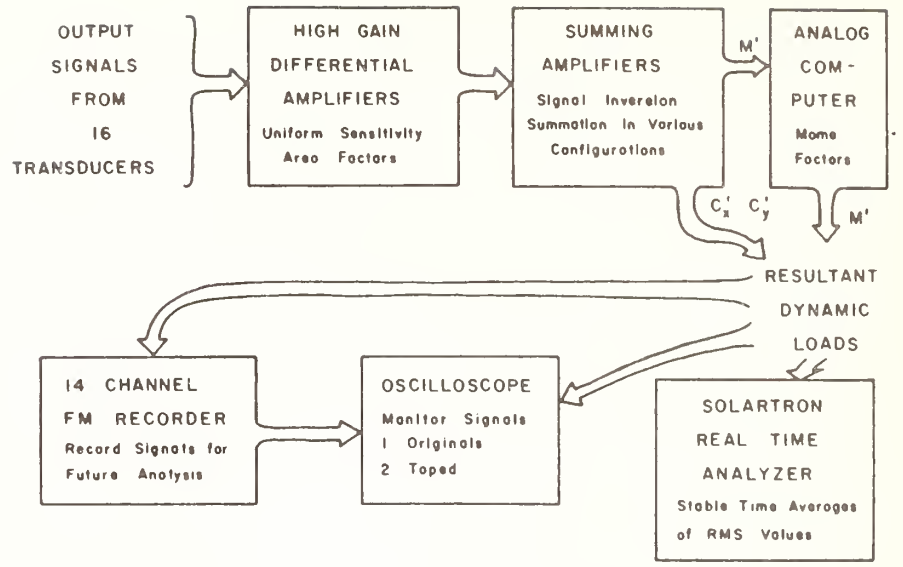

FIGURE 3: DETERMINATION OF RESULTANT DYNAMIC LOADS FOR ONE LEVEL

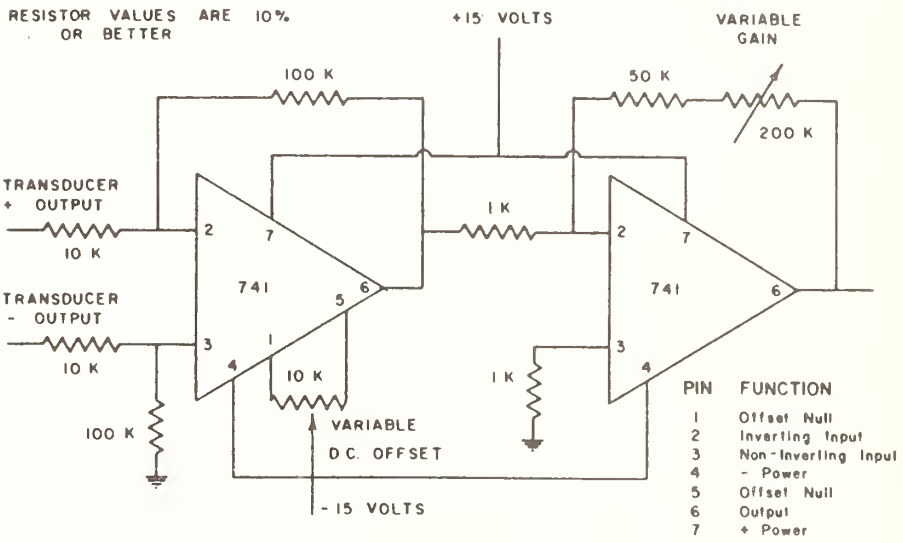

FIGURE 4: SCHEMATIC OF HIGH GAIN DIFFERENTIAL AMPLIFIER - GAIN 500 - 2500

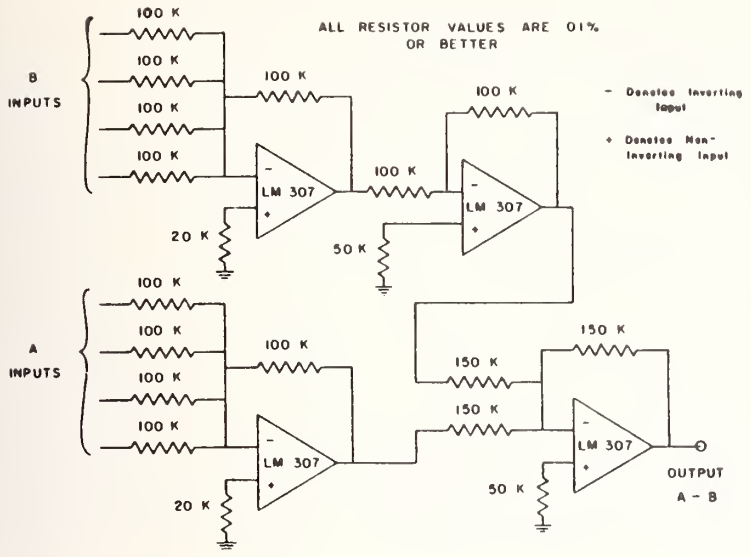

FIGURE 5: SCHEMATIC OF SUMMING AMPLIFIER NETWORK FOR ONE UNIT OF TWELVE

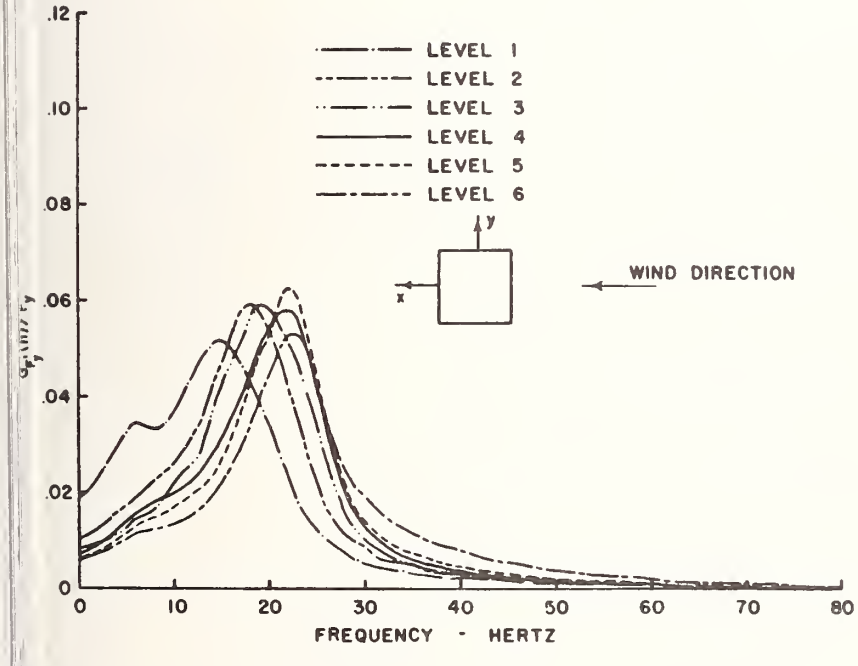

FIGURE 6: NORMALIZED POWER SPECTRA FOR F_y' AT 6 ELEVATIONS, CONFIGURATION 0

19

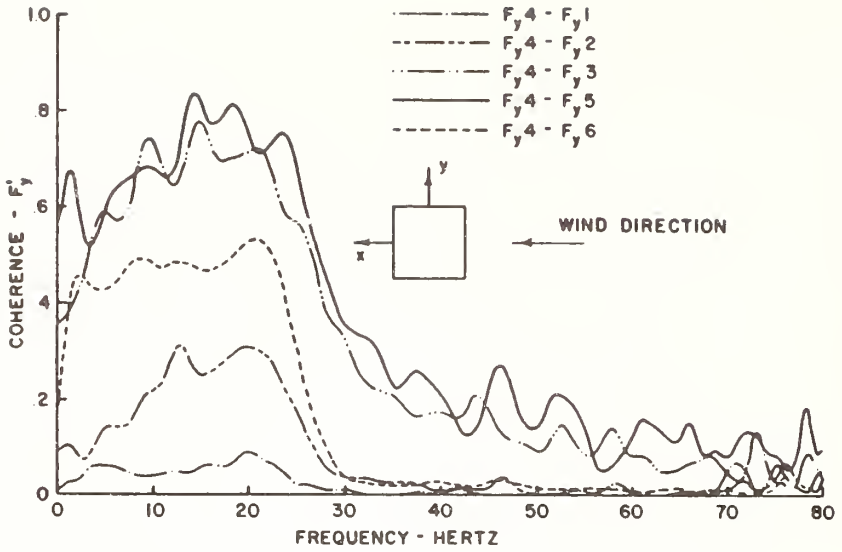

FIGURE 7: COHERENCE FUNCTIONS FOR F_y' BETWEEN LEVEL 4 AND OTHER LEVELS, CONFIGURATION 0

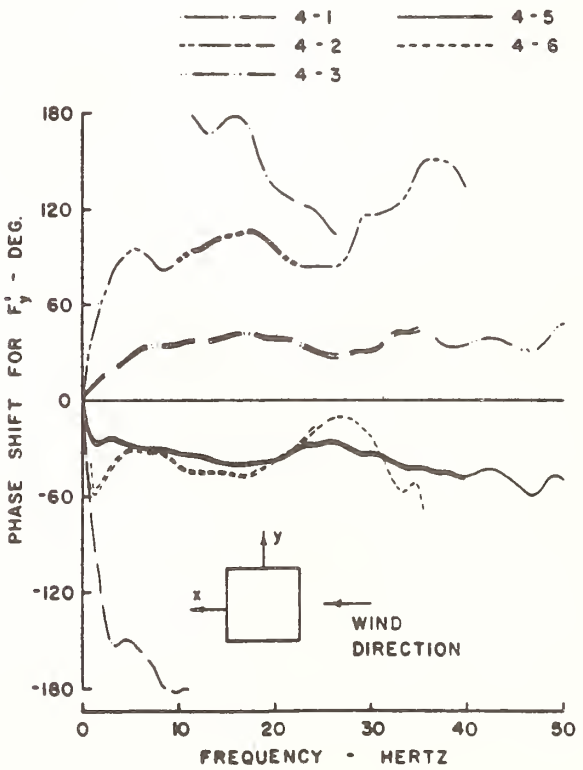

FIGURE 8: PHASES ASSOCIATED WITH COMPLEX CROSS-SPECTRA FUNCTIONS AND COHERENCE BETWEEN LEVELS FOR F_y', CONFIGURATION 0

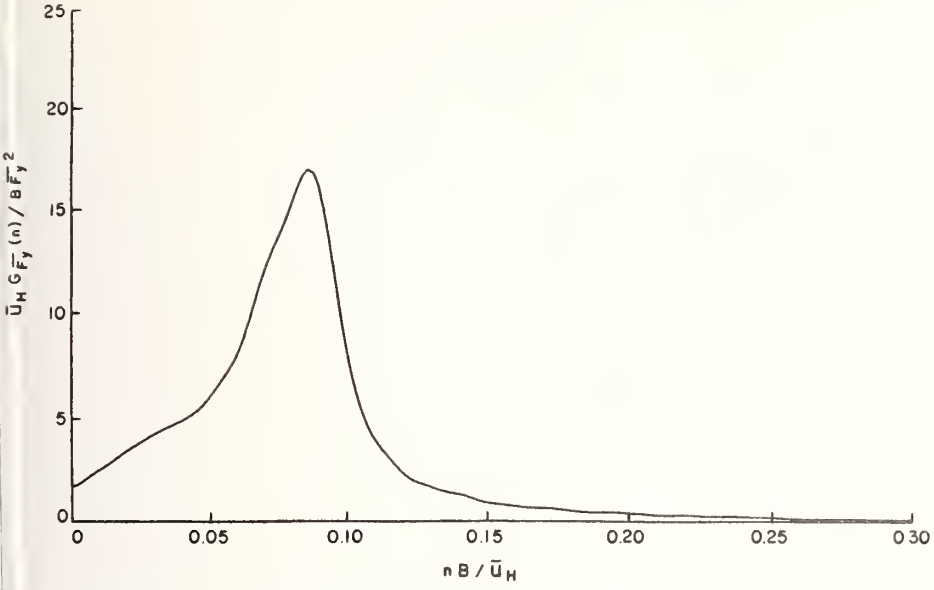

FIGURE 9: MODAL FORCE SPECTRUM FOR CROSS-WIND FORCE COMPONENT

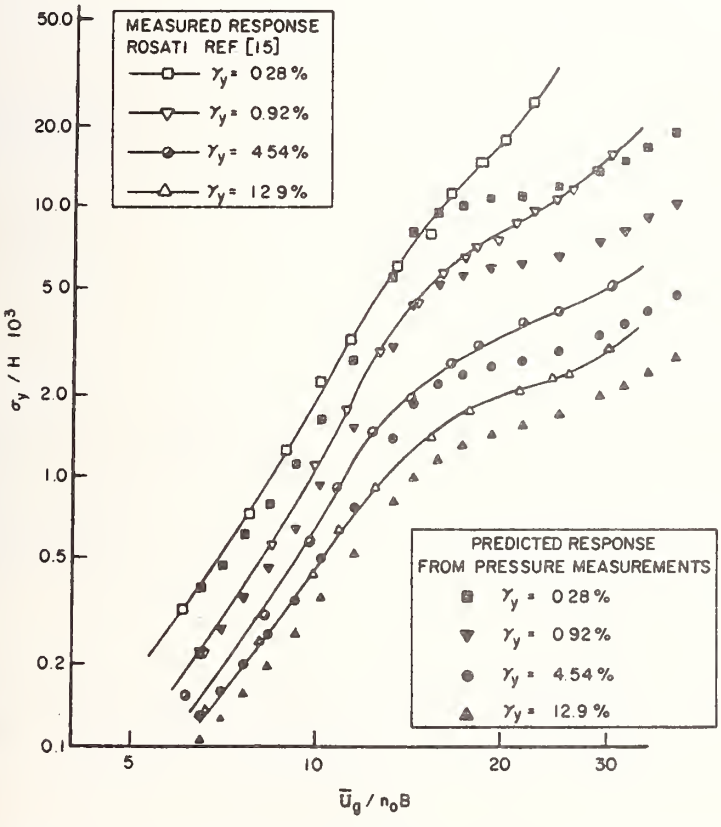

FIGURE 10: COMPARISON OF PREDICTED AND MEASURED RESPONSE OF AN AEROELASTIC MODEL

19

20

A STUDY OF BUILDING DAMAGE CAUSED BY WIND

James R. McDonald
Patrick A. Lea

Institute for Disaster Research
Texas Tech University
Lubbock, Texas

Prepared for
The Veterans Administration

NOTE: TABLES NOT AVAILABLE FOR THIS PAPER

A Study of Building Damage Caused by Wind

Each year more than $800 million in property damage is caused by wind forces from tornadoes, hurricanes, and extratropical storms in the United States. In addition, there are thousands of injuries and the loss of hundreds of lives. Much of the property loss and many of the deaths and injuries might be mitigated by changes in building design for resistance to wind-induced forces. Recognizing the potential of property damage and the need for protection against injury and loss of life, the Veterans Administration (VA) has implemented a program to evaluate its present design standards, and, where necessary, to develop new design criteria and construction standards for use by A/E's and VA personnel in the design of VA facilities. The need for new design criteria can best be established from a historical survey of wind damage and casualties to hospitals and major buildings in the United States. From the historical survey those construction subsystems which are most susceptible to wind damage can be identified. With the knowledge of how construction subsystems behave in windstorms, a methodology also can be developed for evaluating the wind resistance potential of existing VA hospital facilities.

The purpose of this report is to present the results of a historical survey on the kinds of significant damage caused by wind forces to hospitals and major buildings in the United States. The survey was conducted by members of the Texas Tech University Institute for Disaster Research Team, which, in the past seven years, has surveyed building damage in more than 30 windstorm events. The survey team is made up of structural engineers who are familiar with wind design criteria and standard construction practices.

From results of the historical survey, evaluations of structural, architectural, mechanical, and electrical subsystems are presented relative to their performance in wind storms and the consequences of their failure on hospital operations. Based on the data compiled during the historical survey, a questionnaire was developed for surveying existing VA hospital buildings to assist in establishing potential for wind damage. By making an inspection of a faculty and completing the questionnaire, a trained engineer can make a rational judgment as to how the facility will perform in a windstorm. An evaluation of a small private hospital in West Texas is presented as an example of the methodology and as an illustration of the use of the questionnaire.

Windspeed data for each of 185 VA hospital sites were assembled from storm records available from the National Oceanic and Atmospheric Administration. Tabulated in Table 5 for each VA site is the maximum annual extreme fastest-mile windspeed and the windspeeds associated with 50- and 100-year mean recurrence intervals.

The information from the historical survey, evaluations of the construction subsystems, and use of the questionnaire provides the information needed by VA personnel for developing new design criteria, if needed, and for assessing the condition of existing facilities with regard to their resistance to windstorms.

20

Historical Survey

The purpose of the historical survey is to make an assessment of the performance of hospital buildings in the United States that have been subjected to severe windstorms, including tornadoes,

hurricanes, and straight-line winds. Tabulated in the survey are five basic types of information:

(1) Type of damage to architectural, structural, electrical, and mechanical subsystems

(2) Outages caused by windstorms, including power, water, sanitary, and gas

(3) Associated damage by flooding, rain, hail, slides, and storm surge

(4) Fire, if related to the windstorm incident

(5) Number of casualties, including cause of injury and death

(6) Impact on building operation.

Because relatively few hospitals have suffered major damage in windstorms and in order to consider a variety of construction features, major buildings, other than hospitals, are included in the survey.

Four basic data sources were used:

(1) Windstorm damage documentation files at Texas Tech University and other institutes engaged in storm research

(2) Storm Data, a publication of the National Oceanic and Atmosphere Administration, Environmental Data Service, Asheville, NC

(3) Technical literature, including published papers and reports from both the meteorological and engineering professions

(4) Magazine and newspaper accounts of storm characteristics and damage.

The searches have been thorough within the limits of the proposed efforts. However, no guarantee can be made that every significant hospital or major building damage has been reported.

Windstorm damage documentation files were searched for hospitals and major buildings which either experienced windstorm damage or which survived an extreme windstorm without significant damage. Questionnaires were sent to individuals and organizations engaged in windstorm damage research, requesting information on hospital damage. Table 1 includes a list of those contacted. Written or oral responses were received from eight of the nine groups. Except for Bishop Bergen-Mercy Hospital in Omaha, NB, no other major hospital damage could be recalled by the groups.

The windstorm records in Storm Data were searched for references to hospital damage. This monthly publication lists each windstorm incident in the United States, along with a verbal description of damage. The search proved to be arduous and time consuming. A total of eleven hospitals and three nursing homes were identified from the Storm Data listings in the period 1973-1976. Individuals at the hospitals were contacted by phone and a questionnaire was sent requesting specific information regarding the storm characteristics, the building description, and the extent of damage. Unfortunately, the questionnaire did not prove to be

an effective means of getting information. Follow-up telephone calls were needed to get action and to get the specific information requested.

Specific geographic areas known to have been hit by tornadoes, hurricanes, or straight-line wind events were examined for possible damage to hospitals. Once the affected hospitals were identified, authorities at the hospitals were contacted by telephone to obtain detailed information. This approach was very effective in obtaining information on hurricanes.

Once all of the available information on hospitals was assembled, other major buildings were selected for study, because of the need to complete the windstorm damage data matrix with respect to type of windstorm and type of structural system. Information similar to that tabulated for hospitals was obtained for each building. Preference was given to convalenscence homes, special activities buildings, and nurses' quarters because of the association or similarity to hospital buildings.

The findings of the historical survey are summarized in Table 2. This table is referred to as the Windstorm Damage Data Matrix. The information furnished is divided into four categories:

(1) Building Identification and Description

(2) Windstorm Identification and Description

(3) Building Damage Information, which includes damage to architectural, structural, electrical, and mechanical subystems

(4) Ancillary Information, which includes outages, associated damage, fire, casualties and impact on operations.

Sixteen separate buildings or additions are included in the survey. Eight buildings were hit by tornadoes, five were affected by hurricanes, and three were victims of straight-line winds. Tornado intensities ranged from weak to one of the most intense on record. The two specific hurricanes (Camille and Celia) were chosen because the damage attributed to the buildings was primarily due to wind. The three buildings affected by straight-line winds are typical of the type of damage caused by straight-line winds. Substantial structures that have received adequate engineering attention do not generally suffer major damage from straight-line winds. The windstorms cited had windloads within plus or minus 20 percent of local building code windload criteria.

Among the damage to architectural subsystems, which includes windows, nonload bearing exterior walls, interior partitions, parapet walls, canopies, covered walkways, fascia and roofing material, window damage appears to be the most significant. Window damage is caused by a combination of wind pressure and debris impact. Thus, upwind conditions, such as gravel roofs, and window glass design considerations affect the performance of window glass in windstorms. Broken windows in windward walls allow the wind to get inside a building. This situation creates additional outward acting pressures and creates havoc with interior partitions and the contents of the building.

Little damage to electrical subsystems was observed except in the case of complete collapse of the building. Mechanical equipment located on the roof is particularly susceptible to wind

damage. Cooling towers, compressors, vents and intakes should be protected by some type of substantial wind screens or a penthouse.

The most common outage was electrical power. Power failure normally occurs outside of the hospital facility. Power failure to pumps can result in reduction or elimination of water pressure and the failure of sanitary systems. This study emphasized the importance of adequate auxiliary electrical generating equipment. The most common type of associated damage was rain. Carpets, draperies, furnishings, and medical equipment are damaged or ruined by water. The point should be emphasized that if the roof or exterior cladding is breached, significant damage can occur to the interior of a building.

Fire was not a factor in any of the buildings studied. And the number of casualties was small -- chiefly because most hospitals are tied into some type of windstorm warning system, emergency plans are formulated and practiced, and interior rooms, hallways, or basements provide occupant safety. The impact on building operations depends on utility outages and extent of damage.

The historical survey shows that adequate engineering attention to architectural, structural, electrical, and mechanical subsystems result in minimum damage and interference with building operations. If deficiencies in existing buildings can be identified prior to a windstorm, retrofit or redesign may be possible. The ultimate objective of this research project is to develop a questionnaire for surveying VA building sites in order to identify wind damage potential. The findings of the survey and its subsequent evaluation will be used by the VA as a basis for making necessary corrections to existing buildings and to design improvements into new buildings to reduce the probability of injury or property loss caused by windstorms.

Assessment of Performance

In this section the performance of the various construction subsystems identified in the historical survey are assessed. Included in the evaluations are discussions relating to strength, performance criteria, and consequences of failure.

For purposes of this report construction subsystems are divided into two classifications: structural and architectural. The structural subsystem includes all load carrying elements of the building. All nonmechanical and nonelectrical components that do not function as load carrying members are considered to be part of the architectural subsystem. The architectural subsystem classification, thus, goes beyond what is normally considered to be architectural elements to include windows, exterior nonload bearing walls, interior partitions, parapet walls, canopies, covered walkways, facia details, and roofing materials.

The strength of a structural subsystem is defined in terms of subsystem's ability to withstand windloads without compromising the integrity of the structure. The structural subsystems of the buildings included in the historical survey can be placed in five categories. Table 3 lists the categories and the names of the buildings or additions in each one. Each structural subsystem is discussed in the paragraphs below.

Cast-In-Place Reinforced Concrete Frame

The components of this structural system include the columns, the beams, and the floor and roof slabs. The primary advantage of this type of system is its inherent rigidity, which is produced by strong connections and diaphragm action of the floor or roof slabs. Lateral deformations due to windloads are extemely small. None of the buildings surveyed suffered any structural damage to the concrete frame itself. Where extensive damage to a building with a reinforced concrete frame did occur, it was because of failures of wall cladding and/or removal of roofing material.

Steel Frame with Nonload Bearing Walls

This type of structural subsystem has considerable reserve strength, although lateral deflections may be excessive. The Great Plains Life (GPL) Building survived the Lubbock, Texas tornado of 1970 even though the average wind pressures were more than double the 20 psf uniform wind pressure used in the original design. In this case the building used additional stiffness from the exterior masonry walls and the rather stiff interior partitions. Older buildings such as the GPL have greater inherent resistance from the nonstructural elements than a modern steel framed building with metal curtain walls and lightweight moveable interior partitions. Particular attention should be paid to lateral load resistance. If not provided for, excessive wind drift will cause damage to interior partitions and plaster ceilings.

If the reserve strength of a moment-resistant frame is to be realized, it must have adequate connections. Standard connections of riveted, bolted, or welded types have evolved over a long period of years that perform well under extreme loads. Such connections, however, must have proper engineering attention, correct fabrication (including quality control), and timely inspection. None of the connections or splices in the GPL Building failed.

The weak links in a building with a steel framed structural system are the attachments of the nonstructural elements, specifically the curtain walls and the roof rather than the steel frame itself. Three of the four buildings in this category suffered extensive damage because of wall or roof failure, even though the steel frames proved to be adequate.

Steel Frame with Load Bearing Walls

This type of construction is typical of 1-story wings and additions to hospitals, or to support facilities such as maintenance buildings, or storage facilities. Three examples were considered in the historical survey (see Table 2). A typical 1-story structure consists of metal deck on open web steel joists supported on steel beams or load bearing masonry walls. Interior supports are furnished by steel wide-flange sections or pipe columns. Roof overhangs of 2-4 ft. are not uncommon.

Two modes of failure were observed for this type of construction. In the case of the Ambulatory Care Unit, Bishop Bergen-Mercy Hospital, the windward wall collapsed because of inadequate vertical reinforcing steel in the wall. Uplift forces on the roof tend to negate the axial compressive stresses in the wall due to dead load, thus making the flexural tensile stresses in the wall due to wind more critical. The other mode of failure, observed in Ward Memorial Hospital, occurred because of insufficient anchorage of the

the roof to the top of the wall. Roof uplift forces arose from wind flowing over the top of the building, from stagnation pressures that develop underneath the overhang and from wind getting inside the building. Roof members were anchored securely to a continuous bond beam at the top of the wall. However, the bond beam itself was not anchored. The only uplift resistance was provided by the mortar joint underneath the bond beam. The joists remained anchored to the bond beam, but the bond beam itself was lifted from the top of the wall. In addition to the roof failure, pieces of the bond beam became windborne missiles.

Precast-Prestressed Concrete Structural Subsystem with Load Bearing Walls

The observations concerning load bearing walls stated above also applies to this structural subsystem. The primary cause of failure of the Xenia High School Addition "C" was collapse of the load bearing walls on the windward side of the building. Precast concrete members provide considerably more dead weight on the load bearing wall than a roof consisting of steel deck. The additional axial stresses are beneficial to the wall in resisting flexural tensile stresses due to wind. However, if the wall does collapse, the subsequent roof collapse is catastrophic.

Wood Frame Construction

This type of construction is more frequently used for apartment and motel applications rather than hospital facilities. Some retirement and convalescent facilities use this type of construction. The systems generally receive little or no engineering attention and as a result suffer considerable damage from straight-line winds, which are little, if any, above building code requirements.

Roof overhangs and inadequate roof-to-wall anchorages were the primary causes of failure in the two buildings studied. Tornado damage to this type of construction often involves removal of an entire second story of the building. The incidence of occupant injury or death is extremely high for this type of structure.

Strength of Architectural Subsystems

Strength as implied here can mean material strength or strength with regard to anchorage of the architectural subsystem to the structure.

Windows

As was pointed out in the conclusions of the historical survey, window breakage is the major cause of damage to buildings in windstorms. Associated damage from rain and the wind getting inside the building is the main factor in the large dollar value of damage.

Window glass has traditionally been designed only for wind pressures. Recent investigations have revealed that impacts from small pieces of debris such as roof gravel may be the major cause of window glass breakage. Two buildings in the survey emphasize the effects of debris on window glass and breakage. The Great Plains Life building, located in a downtown area adjacent to numerous gravel roofs, had extensive window glass breakage at the lower floors. The Mississippi Power Company building is located on an isolated beach front area. Very few windows were broken

in this building because of screens on the first floor windows and because of the absence of small debris around the building.

Exterior Nonload Bearing Walls

Metal curtain walls and nonload bearing masonry walls are included in this discussion. Metal curtain walls generally perform well under windloads because most curtain wall systems must pass certain wind and water leakage tests. Problems generally occur with curtain walls because of inadequate or improper anchorages to the main structural frame. Localized wind pressures at wall corners due to turbulence and oblique wind incidence angles place additional requirements on wall anchors and reinforcement. Navarro County Memorial Hospital was an example of this type of failure, although in that case the consequence of failure was negligible. Nonload bearing masonry walls must have adequate support on all four sides. Parkwood High School is an example where support details can be overlooked in the design and construction of such a wall. Control joints serve the purpose of retarding cracks in the wall, but they also can be the weak link in the support system.

Interior Partitions

Interior partitions, being nonload bearing, do not always receive the design attention required. Because wind can get inside a building, permanent partitions should have some type of positive anchorage on all four edges. Interior hallway partitions should receive special attention, because the hallways may be used for occupant protection. The consequence of interior partition failure, as was pointed out in the survey, is to make hospital room unuseable.

Parapet Walls

Parapet walls were damaged by wind forces and by impact from flying debris (GPL building and Ward Memorial Hospital, respectively). Sometimes the coping material, which can be either stone or metal, is ripped off the wall and becomes flying debris. The wall itself may collapse and cause damage to the roof.

Canopies and Covered Walkways

The consequences of these failures are minimal, although the repairs may be expensive. The major danger is that the canopy material may become airborne and strike other vulnerable areas.

Facia Details

Facia damage is usually of little consequence, with one possible exception. If facia damage allows wind to get underneath the roof deck, additional uplift pressures can cause the roof deck to pull up and subsequently an entire roof section can be ripped off. The same wind forces also will cause damage to suspended ceilings and fluorescent light fixtures.

Built-up Tar and Gravel Roofs

Aside from the roof gravel becoming flying debris, the primary problem with roofing material is inadequate anchorage to the roof deck. In all too many instances there is no bonding of the felt paper to the roof. The only thing that keeps the roof in place is diaphragm action of the layers of roofing material. Removal of roofing material occurred at almost all structures that were included in the historical survey. Next to glass breakage, this

may be the single most severe problem with hosptials and other buidings in windstorms.

Summary

Regarding structural subsystems, the following observations are made based on the results of the historical survey:

(1) Cast-in-place reinforced concrete is the most suitable structural subsystem for wind resistance, because of its inherent rigidity and strength.

(2) Steel frames perform satisfactorily, if wind drift is limited and if adequate engineering attention is paid to moment-resistant connections.

(3) Load bearing walls are dangerous, if vertical reinforcing steel is not provided to resist tensile stresses due to flexure.

(4) Precast-Prestressed concrete subsystems used with loadbearing walls have the same potential problems as those walls used with steel structural subsystems.

(5) Wood frame construction rarely receives the engineering attention required for it to adequately resist extreme windloads.

With respect to architectural subsystems, two major observations are summarized:

(1) Window glass breakage from wind pressure and flying debris is the most serious wind failure because of the associated damage to the interior of a building.

(2) Inadequate bonding of built-up tar and gravel roofs to the roof deck results in excessive damage to interior of buildings from rain.

One other observation that should be made is that from the appearance of damage to a specific building, one cannot distinguish the type of windstorm that caused the damage. Conversely, a well-designed structure will adequately resist wind forces whether they are created by tornadoes, hurricanes, or straight-line winds.

TABLE 1: ORGANIZATIONS AND INDIVIDUALS ENGAGED IN WINDSTORM DAMAGE RESEARCH

TABLE 2: WINDSTORM DAMAGE DATA MATRIX

TABLE 2: WINDSTORM DAMAGE DATA MATRIX (CONTINUED)

TABLE 2: WINDSTORM DAMAGE DATA MATRIX (CONTINUED)

TABLE 2: WINDSTORM DAMAGE DATA MATRIX (CONTINUED)

TABLE 2: WINDSTORM DAMAGE DATA MATRIX (CONTINUED)

TABLE 2: WINDSTORM DAMAGE DATA MATRIX (CONTINUED)

TABLE 2: WINDSTORM DAMAGE DATA MATRIX (CONTINUED)

TABLE 2: WINDSTORM DAMAGE DATA MATRIX (CONTINUED)

TABLE 2: WINDSTORM DAMAGE DATA MATRIX (CONTINUED)

TABLE 2: WINDSTORM DAMAGE DATA MATRIX (CONTINUED)

TABLE 3: CLASSIFICATION OF STRUCTURAL SUBSYSTEMS

21

RECENT EARTHQUAKE-RESISTANT DESIGN METHODS FOR DIFFERENT TYPES OF BRIDGE FOUNDATIONS IN JAPAN

Yukitake Shioi
Toshio Furuya
Michio Okahara
Yasuo Mitsuie

Public Works Research Institute
Ministry of Construction

Recent Earthquake-Resistant Design Methods for Different Types of Bridge Foundations in Japan

This paper presents a survey of 31 examples of bridges built in Japan. Their foundations are classified into four types: spread, pile, caisson, and a multi-column. For each type, the authors surveyed design methods and the methods used to set up models to study the interaction of soil and foundation.

Spread Foundations

Earthquake Calculation Method

Even in the case of a large-scale structure, model analysis by a simple system with two degrees of freedom is possible because the earthquake behavior of the entire foundation can be examined by assuming it as a rigid foundation. Calculations are made by response spectra, treating the maximum response alone.

Modeling

For the purpose of maintaining the continuity between superstructure and substructure, a part of the weight of superstructure is treated as a weight added to substructure and superstructure and substructure are separated. When substructure is under water, dynamic water pressure during earthquake is to be calculated in terms of virtual mass.

$$M_w = \frac{0.6\rho A h_w}{(a/h_w)^{2/3}}$$

where

ρ = bulk density of water

A = section area

a = width in the direction of vibration

h_w = depth of water ($0.8 \leqq a/h_w \leqq 4.0$)

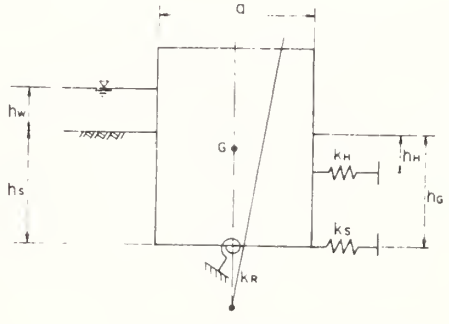

(In the direction of length b)

The soil surrounding substructure is to be calculated in terms of virtual mass, assuming it to vibrate together with the structure during earthquake.

$$M_s = 1/2(\gamma_s/g)a^2 d$$

where

γ_s = weight of soil

g = acceleration of gravity

d = thickness of soil layer

21

Earthquake force is to be calculated by the use of response accleration spectrum (statistical value obtained from observations made in the vicinity).

Related Constants

As for the dynamic spring constant of the subgrade, the lowest value of the modulus of deformation of the original position measured by the pressionmeter is to be used. The spring constants in the horizontal, vertical, rotational, and shearing directions are to be determined as instructed in the "Specification for Highway Bridge Substructure Design (Caisson)."

$K_H = k_H \cdot (b/D)^{-3/4}$, $k_H = \frac{1.2}{D} E_p$, b: width ($b = \sqrt{A_H}$)

$K_V = k_V \cdot (a/D)^{-3/4}$, $k_V = \frac{1.0}{D} E_p$, a: length ($a = \sqrt{A_V}$)

Flowchart of earthquake resistant design calculation:

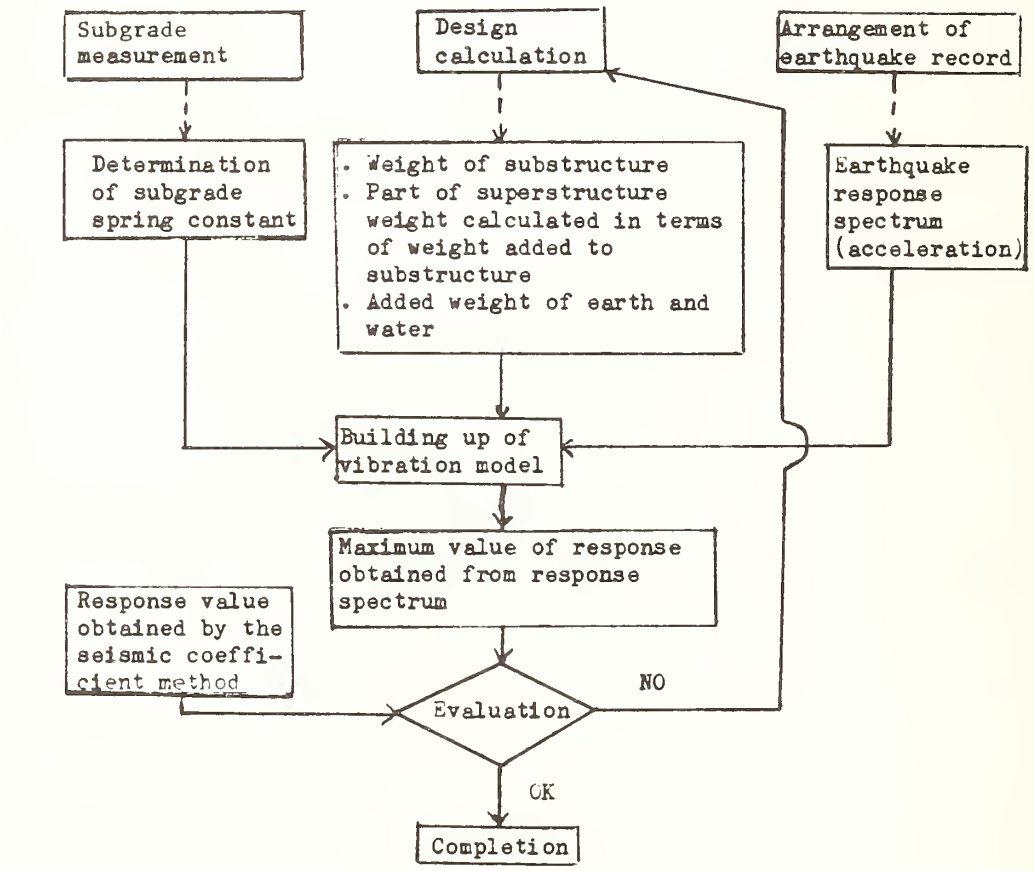

$K_R = Kv \cdot I$, I: moment of inertia of the bottom

$K_s = \lambda K_v$, $\lambda = 1/3$

Or Blot's equation $K_R = \frac{E_R}{(1-\nu^2)k} a^2 b, K_s \frac{E_R}{2(1+\nu)bk}$

E_R: Voigt's elastic module, ν: Poisson's ratio

Evaluation

The values to be obtained by calculations are natural period, center of rotation, displacement of gravity center and angle of rotation of the model. The above values are used to evaluate the subgrade reaction, distance of eccentricity, bearing power, sliding and tipping.

Pile Foundations

Earthquake Resistant Design Objectives

When the soft soil stratum extends deep beneath the surface, the ground movement is estimated to be large. Since the structural type and dimensions are fixed, it is necessary for the bearings to be flexible to reduce the section force.

Earthquake Calculation Method

When the piles are likely to vibrate, coupled with the surrounding soils, the ground is to be replaced by a multiple-layer shearing model. When there are no seismic wave records available for the same stratum of soil, the incident wave to the pile bearing stratum is to be estimated from the estimated acceleration of the seismic foundation, using the shearing wave theory. Since the coefficient of subgrade reaction cannot be obtained, the dynamic reaction coefficient is to be obtained by modeling the subgrade by the finite element method.

Modeling

The ground is replaced by shearing models, stratum by stratum. In the case of superstructure, only damping is to be considered, neglecting the reaction characteristic. In the footings, the righting moment of rotation and rotational inertia are to be considered.

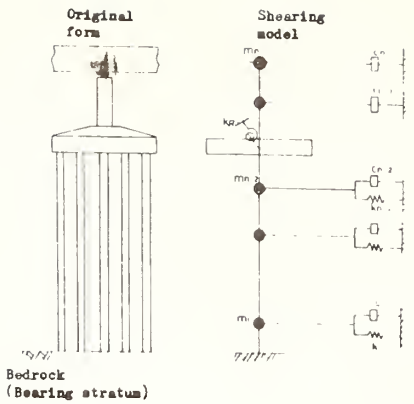

The incident wave to the bearing stratum is to be calculated by means of the following equation, using the laws of reflection and refraction.

$$u_k(t,z) = f_k\left(t - \frac{z}{V_k}\right) + g\left(t - \frac{H_k - z}{V_k}\right)$$

The stratum where the response $U_k(t,z)$ changes little is to be regarded as input bedrock (bearing stratum).

Related Constants

The spring constant of subgrade is to be estimated, using FEM in plane strain.

$$K = \frac{1}{x} = k - S^T K^{-1} S$$

As for the added mass, it is assumed that footing or piles have kinetic energy equal to that of the subgrade.

$$m_a = \frac{1}{2} X^T M X$$

Evaluation

In the case of soft ground, there is so great a difference in the acceleration of seismic waves between the bedrock and ground surface that it is necessary to make investigations on the ground responses. The bending moment in a pile is greater in its lower part because the seismic waves are rapidly amplified.

There may be a limit to the application of the theory of sheering wave (multiple-stratum ground, great earthquake). The effects of a group of piles on the shearing model, as well as the damping mechanism and nonlinearity, must also be considered. A flowchart of this calculation follows:

Flowchart of earthquake resistant design calculation:

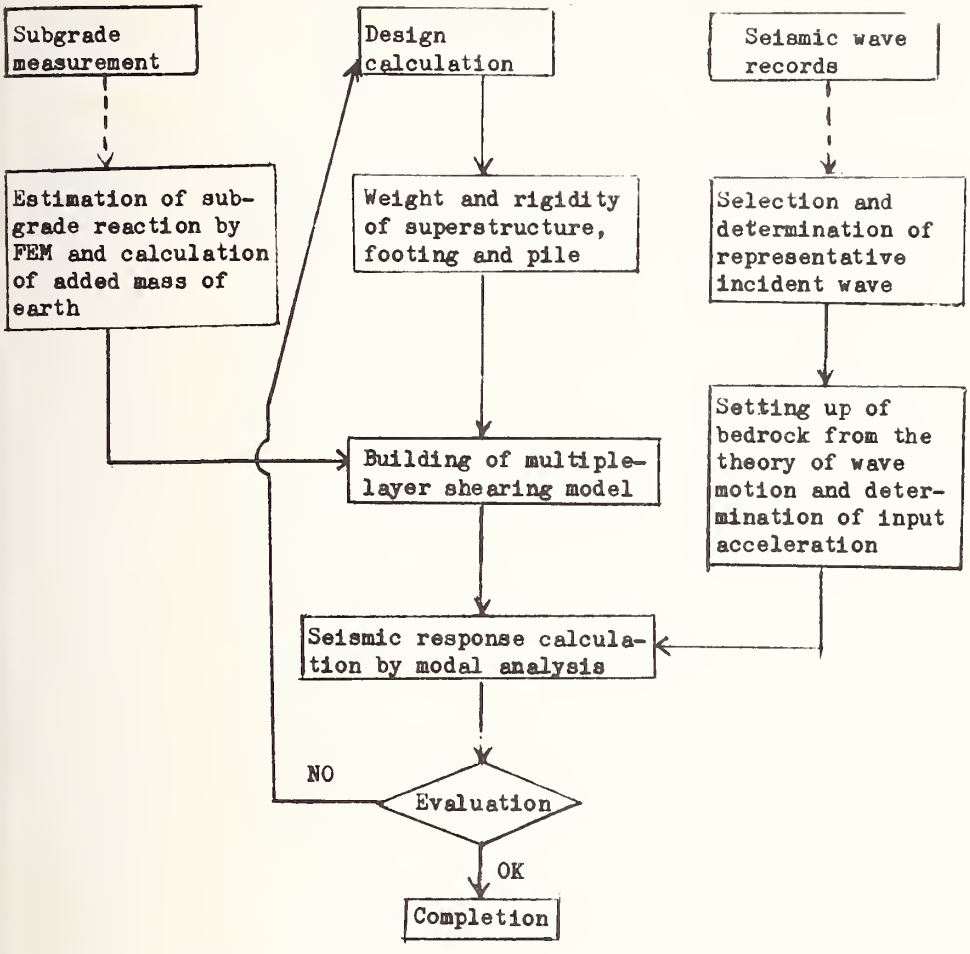

Caisson Foundation

Design Objectives

In the case of soft ground, there are problems with the caisson behavior during earthquake. The type of superstructure can also have special effects.

Earthquake Calculation Method

As for the ground modeling, the model of spring-dashpot system is to be used from a practical veiwpoint, although the wave motion theory and finite element method are also available. Response spectrum analysis is done on a model with two degrees-of-freedom, horizontal translation, and rocking motion.

21

Modeling

Effects of superstructure and water are to be treated as added mass.

$$M_w = \frac{0.6\gamma_w A_w h_w}{(b/h_w)^{2/3}}, \quad M_s = \frac{1}{2}\gamma_s g b^2 d$$

When the side ground is very soft, it is to be treated as a plastic state if the horizontal reaction exceeds the allowable bearing capacity. In the case of a large caisson, the response spectrum of earthquake records in the vicinity is to be used. The maximum design acceleration is 180 to 250 gal.

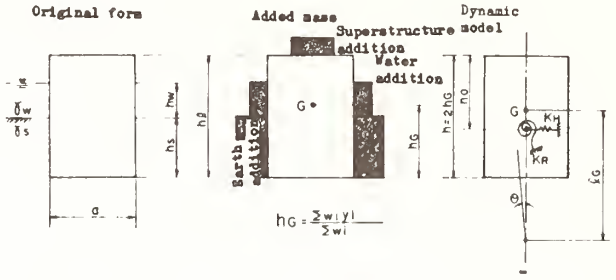

Related Constants

It is necessry to examine the subgrade spring constant by a variety of Boussinesq's equation, as given below, and other methods (Pauw, Tajimi, Richart):

$$K_V = \frac{E}{l_p\,(1-\nu^2)B_V^{3/4}}$$

where

E = Ground deformation modulus = $6E_o$ ∿ $5E_o$

E_o = Pressiometer deformation modulus

B_V = Foundation conversion width = $\sqrt{A_V}$

ν = Poisson's ratio

I_p: Shape factor

Evaluation

Although there are some problems about the conversion of superstructure by added mass, in general there is not much difference from the results of analysis by the whole system model. The response is governed by the evaluation of the subgrade spring constant. Particularly, the evaluation of the effects of caisson shape.

The values to be calculated are the natural period, the horizontal and rotational displacement of gravity center, and maximum acceleration response. Since the substructure response is influenced by the type of superstructure, it is necessary to make response analysis at the basic design stage. A flowchart follows:

Flowchart of earthquake resistant design calculation:

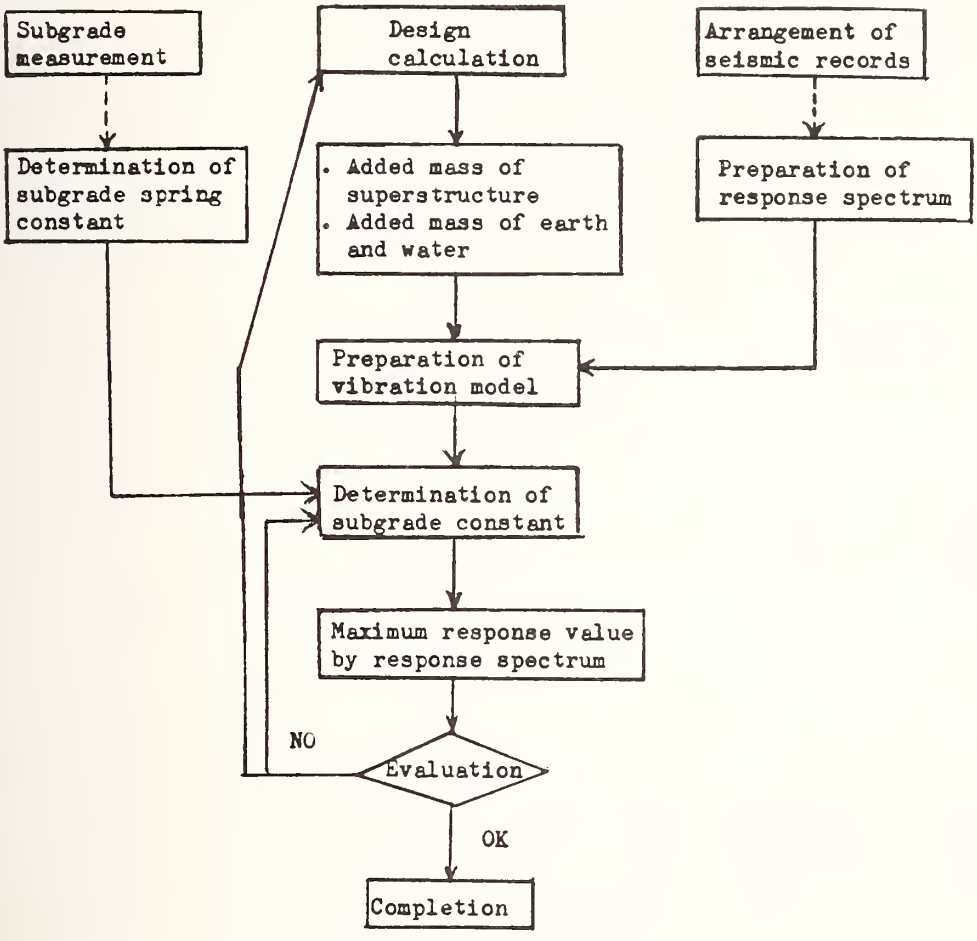

Multi-Column Foundation

Design Objectives

Since this is a flexible structure, the elastic behavior of the foundation and footings are to be investigated. The coupled vibration with the superstructure must also be considered.

Earthquake Calculation Method

It is necessary to investigate the three-dimensional behavior for reasons of topographic inclination, arbitrarity of earthquake input direction, eccentricity of superstructure reaction, and asymetry for the foundation structure. Since it is impossible to estimate the condition in which the foundation and ground are bound together (the spring constant is not uniform), added mass of ground and damping constant, there is the necessity for analysis of three-dimensional vibration. To make the calculation in terms of a multiple system of material points, modal analysis is to be used.

Modeling

Considering the three-dimensional vibration, the deformations are to be taken as unknown quantities.

Pier: Horizontal x and y displacements (2)

Footing: Horizontal x and y displacements, torsional angle and rotational angle (10)

Superstructure: Horizontal x and y displacements and torsional (4)

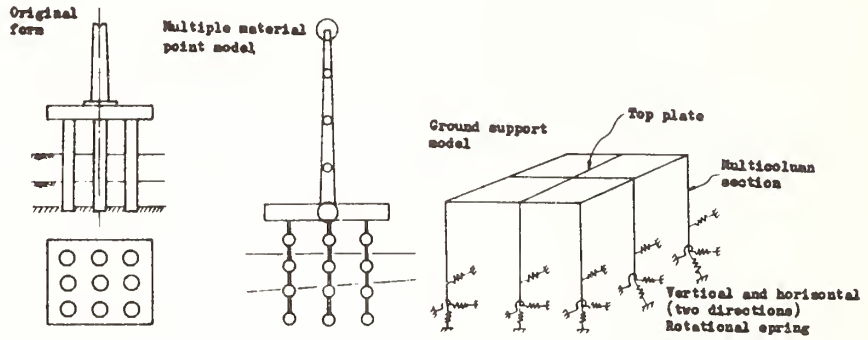

Evaluation

Static and dynamic calculation results must be compared. Likewise, calculated values must be compared with vibration experimental results. It is also necessary to check the responses by varying the subgrade reaction coefficient. Since the foundation has so great an influence on the superstructure, its coupling to the superstructure is also important. A flowchart of this analysis follows:

Flowchart of earthquake resistant design calculation.

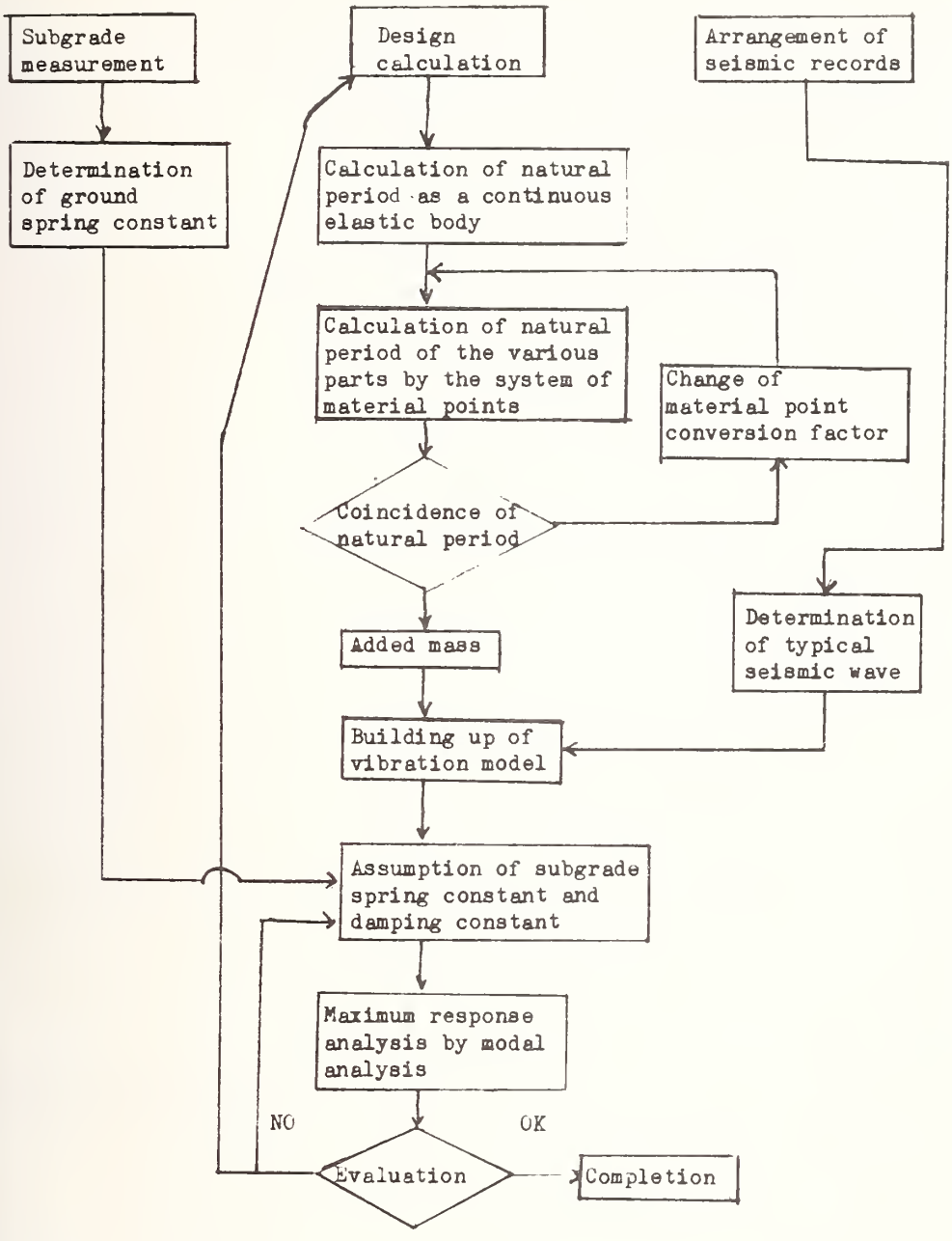

Conclusion

As seen from the examples, the objectives of earthquake resistant design mainly concern two cases: Either when the bridge is very long, or the ground is poor. The details of these two items are found by studying:

- The effects of the seismic responses of substructure on the superstructure due to the long span of the bridge.
- Dynamic characteristics of the substructure.

21

- The ground behavior during earthquake.

- The behavior of the foundation structure itself during earthquake. The current trend is obviously toward evaluating the behavior during earthquake due to seismic force characteristics, and the response characteristics (natural period) of ground and structures. However, the behavior during earthquake has not yet been fully clarified in the analysis of seismic response.

Many studies involving actual observations and analysis of experimental results have been made about the way the subgrade spring constant, damping constant, and added mass are to be treated. However, from the methodological standpoint, the earthquake resistant design calculation has now reached a state in which safe bridges are becoming the norm.

22

RECENT DEVELOPMENTS IN SEISMIC DESIGN CODES

Roland L. Sharpe

Applied Technology Council
Palo Alto, California

Recent Developments in Seismic Design Codes

The need for a coordinated effort to review existing requirements and state of knowledge and to develop comprehensive seismic design provisions applicable to all of the country was recognized several years ago. It was realized by design professionals and government representatives that the effort would take many years to complete if performed by volunteer committees as codes have been developed in the past. After numerous discussions and careful planning, ATC started work in November 1974 on a detailed study comprising:

- A comprehensive review of seismic provisions
- An evaluation of the latest state of knowledge and state of practice
- Development of a coordinated set of provisions which could be used as a resource document in developing seismic design provisions for all areas of the United States.

The 85 participants involved in the development of the provisions were organized into 5 working groups composed of 14 task committees, 2 advisory groups, 1 independent review group, and a project executive panel; the author was Project Director.

Two working drafts were submitted to several hundred outside reviewers. These reviewers represented practice, industry, professional organizations, government agencies, code promulgating groups, and universities. The numerous comments received for each draft were reviewed by the task committees, and changes and clarifications were made as deemed appropriate.

The basic concepts and approaches followed in the review and evaluation are described and a summary of some of the provisions developed by the 85-member group assembled and retained by the Applied Technology Council (ATC) are presented. The development of seismic risk maps, and analysis and design provisions for structural and nonstructural systems are discussed.

Basic Concepts

The primary basis for development of the seismic design provisions for buildings was to protect life safety and to ensure continued functioning of essential facilities needed during and after a catastrophe. Another major premise was that provisions should be developed so they could be applicable to all areas of the United States.

In the development of the U.S. codes currently in use, it was recognized that the specified seismic design forces might be considerably smaller than those encountered in moderate or major earthquakes. Primary consideration is given to seismic design for the main structural framing system. Consideration is given either explicitly or implicitly to the effects (both good and bad) of interior partitions, exterior covering, different types of materials, and damping. However, this approach has caused misunderstandings resulting in building designs with serious deficiencies such as inadequate tying together of building components and inadequate provisions for the occurrence of building deformations in excess of those calculated for the design forces.

22

The ATC-3 tentative provisions are intended to be logically based with explicit consideration given to factors that are generally implicit in present code design provisions. There are a number of new concepts that are significant departures from existing seismic building codes, such as:

1. More realistic ground motions.

2. Consideration of the effects of distant earthquakes on long period buildings.

3. Response modification coefficients (reduction factors) which are based on consideration of the inherent capacity for energy absorption and damping associated with inelastic response, and observed past performance of various types of framing systems.

4. Complexity of analysis and design dependent on seismic motion intensity, building importance or use, and assigned building seismic performance.

5. Simplified seismic response coefficient formulas related to fundamental period of building but with certain restrictions.

6. Detailed requirements for architectural, electrical, and mechanical sytems, and components.

7. Material design stresses approaching yield.

8. Guidelines for assessment and systematic abatement of seismic hazards in buildings.

9. Guidelines for assessment of earthquake damage, and strengthening or repair of damaged buildings and potential seismic hazards in existing buildings.

Items 1 through 6 are discussed in this paper. The remaining items are contained in the ATC-3 project report [2].

It should be noted that the provisions are intended to apply only to buildings and do not contain design requirements for special structures such as bridges, transmission towers, offshore structures, piers and wharves, industrial towers and equipment and nuclear reactors.

Ground Motions

In developing the seismic risk maps, four basic factors were considered: (1) a realistic appraisal should be made of the expected ground motion intensity, (2) the probability of the design ground shaking being exceeded should be approximately the same in all parts of the country, (3) the effects of distant earthquakes on long period buildings should be considered, and (4) areas should not be microzoned or actual faults shown on the maps and variations of ground shaking over short distances of about ten miles or less should not be delineated.

The recommended seismic design regionalization maps in Figures 1 and 2 are based on an evaluation of historical seismicity, frequency of occurrence of the earthquake motions and underlying geology where possible. They reflect the collective judgment of several committees based upon the best data available in 1976, adjusted and tempered by

experience and judgment. It is probable that the maps and coefficients will change with time as more knowledge is gained about earthquakes and their ground motions and as society better understands the establishments of acceptable risk.

Seismic Design Coefficients

The effective peak acceleration (A_a in Figure 1) and effective peak velocity-related acceleration (A_v in Figure 2) should be considered as normalizing factors for construction of smoothed elastic response spectra for ground motions of normal duration. Motions of high seismic areas near active faults could exceed these values, especially in locations inside the 0.4g contour.

The development of the A_a map was facilitated by the work of Algermission and Perkins of the United States Geological Survey (USGS) and is in may ways quite similar to their maps [3]. The A_v was constructed to consider the effects of distant earthquakes. The velocity attenuation study by McGuire and the attenuation of modified Mercalli intensity by Bollinger in conjunction with review of other data from large earthquakes were used to develop the A_v contours [4, 5]. It is felt that considerable further study should be given to this area. The maps were literally drawn by a committee after considering input from many sources, but they are judged to provide the best current estimate of the geographical variations of A_a and A_v for purposes of design of buildings.

After the contour maps in Figures 1 and 2 were prepared, the country was divided into seven map areas. Each map area, for purposes of design, is assigned a seismicity index as shown in Table 1. To facilitate administration by regulatory agencies, maps were then prepared showing the A_a and A_v values on a county-by-county basis. A_a and A_v values are given for each of the over 4,000 counties in the United States.

Applicability to All Areas of the United States

The seismic hazard varies from very low to high across the United States. In order to make the provisions adaptable to all parts of the United States, four seismic performance categories were established to which buildings would be assigned based on the seismicity index of site and the seismic hazard exposure (occupancy or use) of the buildings, see Table 2.

Buildings in Seismic Hazard Exposure (SHE) Group III include critcal or essential facilities that should function during and after an earthquake such as hospitals, communication and control centers, and buildings with a high density of occupants. SHE Group II includes buildings, housing a large number of occupants or buildings in which the occupants' movements are restricted or their mobility is impaired such as public assembly for 100 or more persons, schools, large retail stores, hospitals, and ambulatory health facilities. SHE Group I includes all other buildings not classified in Group III or II.

For Seismicity Index I (the lowest risk), SHE Group III buildings are required to have limited analysis and design for seismic forces. All other buildings do not have to be designed for seismic forces; however, a number of basic details are specified such as connections of walls to roofs and floors, and interconnections of other building elements. Experience has shown that the tying together of parts of buildings can be of material assistance in resisting earthquake forces.

All buildings in Seismicity Index 2 must have limited seismic analysis and design. For Seismicity Index 3, all SHE Group III and II buildings must be designed to requirements roughly comparable to the 1973 Edition of the Uniform Building Code for California conditions of seismicity. SHE Group I buildings need only limited seismic analysis and design.

Buildings in Seismicity Index 4 area, assigned to SHE Groups II and I, must meet the seismic analysis and design requirements for critical or essential facilities in Seismicity Index 3. SHE Group III buildings must also meet restricted height limitations if they are constructed with shear walls or braced frames and certain additional restrictions on use of materials are specified.

Design Steps: Structural

The seismic analysis and design procedures to be used in the design of a building and its components are dependent on the Seismic Performance Category (Table 2) to which the building is assigned. The seismic design forces are established considering the values of A_a and A_v, the effects of site conditions, the type of framing employed, and the fundamental period of the building based on the elastic properties of the seismic resisting system.

The internal forces in the members of the building shall be determined using a linearly elastic model. Individual members shall be sized for the shears, axial forces, and moments determined in accordance with the analysis and design provisions. The deformation of the building when subjected to the design seismic forces shall not exceed prescribed limits.

Analysis and design of the structural system would proceed as follows:

1. Locate site A_a and A_v maps; determine the map area number.

2. Using the map area number, select the coefficients A_a and A_v and the Seismicity Index from Table 1.

3. Considering the use or importance of the building, establish the Seismic Hazard Exposure Group and determine the Seismic Performance Category from Table 2.

4. The Seismic Performance Category to which a building is assigned determines the analysis and design requirements.

Category A

The structural frame components in Category A buildings are required to be tied together, but no overall seismic design is required. Category A buildings can be used in areas of low seismicity.

Category B

Must meet the Category A requirements and in addition have minimum seismic design such as collector elements, diaphragm design, design of bearing walls for for seismic forces normal to the flat surface of the wall, reinforcement of openings in shear walls, or diaphragms, and certain minimum pile foundation design requirements. Category B buildings are used

for essential facilities in areas of low seismicity and for all buildings in areas of moderate seismicity.

Category C

Must meet the requirements for Category B and also must conform to certain framing limitations for buildings over 160-feet (49 meters) in height. The seismic resisting system for buildings over 160-feet in height must be one of the following:

- A moment resisting frame system with Special Moment Frames (Special Moment Frames are ductile-moment resisting frames).
- A dual system; see Table 3.
- A braced frame (steel or concrete) or shear wall system with the braced frames or shear walls arranged so that the frames or walls in any plane do not resist more than 33 percent of the seismic design force including torsional effects; this system is limited to buildings less than 240-feet (74 meters) in height.

Moment resisting space frames which are enclosed by or adjoined by more rigid elements not considered to be part of the seismic resisting system shall be designed so that the action or failure of those elements will not impair the vertical load and seismic force resisting capability of the space frame. The design shall consider and provide for the effect of these rigid elements on the structural system at building deformations corresponding to a total story design drift Δ where:

$$\Delta_s = C_d \Delta_a (1 + a_d) \qquad (1)$$

C_d is the deflection amplification factor from Table 3, Δ_a is the story drift calculated using the seismic design forces and the elastic stiffness of the seismic resisting system, and a_d is the amplification coefficient related to P-Delta effets (P-Delta effects in a given story are the secondary effects due to eccentricity of the gravity load above that story). If the P-Delta effects are small, a_d can be taken as zero.

All structural elements not considered in the design to be part of the seismic resisting system in Category C buildings shall be investigated and shown to be adequate for the vertical load-carrying capacity and the induced moments resulting from the total story design drift Δ_s.

ategory D

ust conform to Category C requirements and are also subject o more restrictive height requirements; the 160-feet and 240-eet height limitations given above are reduced to 100-feet 31 meters) and 160-feet (49 meters), respectively.

It was also recognized that there can be potential adverse ffects when the ratio of the strength provided in any story to he strength required is significantly less than that ratio for he story immediately above. No specific provisions were devel-oed; however, a proviso is made that the story strengths shall

22

be adjusted to compensate for this effect. Possible methods for evaluating these ratios are presented in the Commentary included in the ATC-3-06 document.

Similarly, the requirement is stipulated that the design of a building shall consider the potentially adverse effect that the failure of a single member, connection, or component would have on the stability of the building and appropriate design modifications shall be made to mitigate this effect.

5. The building should be classified as regular or irregular considering both the plan and vertical configuration.

6. The analysis and design procedures are determined based on the Seismic Performance Category (SPC) and whether the building is regular or irregular. SPC B buildings, both regular and irregular, must be analyzed as a minimum using Equivalent Lateral Force (ELF) procedure. SPC C and D buildings that are regular shall, as a minimum, be analyzed using the ELF procedure. Irregular buildings shall be analyzed considering their dynamic characteristics. For vertical irregularities only, a modal analysis procedure is specified.

7. Assuming an SPC B, C, or D building, the following steps 8 through 16 apply.

8. Determine the site soil profile and select the soil factor S. The factor S varies from 1.0 for rock sites to 1.5 for soft to medium -stiff clays and sands.

9. Select the Response Modification Coefficient R and the deflection amplification factor C_d from Table 3. R is dependent on the type of structural system and the vertical seismic resisting system. The deflection amplification factor C_d, is used to determine the total story drift.

10. For the ELF procedure, the total seismic shear at the base $V = C_s W$. Where W equals total gravity load plus portions of other loads such as permanent equipment, effective snow loads, and 25% of the floor live load for warehouses.

$$C_s = \frac{1.2\ A_v\ S}{RT^{2/3}} \qquad (2)$$

The fundamental building period T_a equals

$$T_a = C_T h_n^{3/4}$$

where

C_T = 0.035 for steel frames

C_T = 0.025 for concrete frames

h_n = height in feet above the base.

For all other buildings $T_a = 0.5\ h_n/\sqrt{L}$, where L equals the overall length of the building in the direction being considered.

For lower buildings, the fundamental period need not be calculated. In such cases, the minimum value of C_s shall be 2.5 A_a/R, except for soft-soil sites when A_a is equal to or greater than 0.3 the minimum value of $C_s = 2A_a/R$.

The total lateral shear force at the base, V, may be reduced for soil-structure interaction effects. Soil-structure interaction should reduce the shear force but because of rotation about the base the total building deflection would be increased.

11. The total lateral shear force at the base, V, is distributed the height of the building as follows:

$$F_x = V \frac{w_x h_x^k}{\sum_{i=1}^{n} w_i h_i^k} \qquad (3)$$

where k is an exponent related to building period and has the following value:

- For buildings having a period of 0.5 seconds or less, k = 1
- For buildings having a period of 2.5 seconds or more, k = 2
- For buildings having periods between 0.5 and 2.5 seconds, k may be taken as 2 or may be determined by linear interpolation between 1 and 2.

F_x is the seismic force applied to level x, w_i or w_x is the portion of W located at or assigned to level i or x, and h_i or h_x is the height above the base to level i or x.

12. The seismic shear and torsion in any horizontal plane is distributed to the vertical resisting elements in accordance with the relative stiffness of the elements and the horizontal diaphragm. Torsional moments due to building irregularities plus a 5 percent "accidental" torsion are considered.

13. A reduction in overturning moment M_x is allowed for buildings ten stories or higher as follows:

$$M_x = B \sum_{i=x}^{n} F_i (h_i - h_x) \qquad (4)$$

where

B = 1.0 for the top ten stories

B = 0.8 for the twentieth story from the top and below

B = a value between 1.0 and 0.8 determined by a linear interpolation for stories between the twentieth and tenth story below the top.

22

The foundation of buildings, except inverted pendulum-type structures, may be designed for an overturning moment at the foundation-soil interface determined using B = 0.75 in the above formula for all building heights providing the resultant of the seismic forces and vertical loads at the foundation-soil interface does not fall outside the middle one-half of the base of the component(s) resisting the overturning.

14. For buildings requiring a modal analysis, a lumped mass model may be used. The design value for each of the story-shear moments and drifts and the floor deflection quantities shall be determined by combining their modal values by taking the square root of the sum of the squares of each of the modal values. The base shear thus determined shall not exceed a base shear calculation using Equation 2 with a value $T = 1.4\ T_a$. The design story shears, moments, and drifts and the floor deflections shall be adjusted accordingly.

15. The story drifts should be calculated to ensure they do not exceed the values in Table 4.

16. Using the analytical results and material design stresses approaching yield, the framing system is resized from the preliminary model.

17. The design should be reviewed to confirm that final member sizes are in conformance with those assumed in the analysis. Revisions and reanalysis should be made as appropriate.

18. The design details should conform to general requirements for tying together of parts of buildings, concrete or masonry wall anchorage, collector elements, diaphragms, bearing walls, inverted pendulum-type structures, vertical seismic motions, and deflection and drift limits.

Design Steps: Nonstructural

Architectural systems and components are required to be designed to resist seismic forces as follows:

$$F_p = A_v\ C_c\ P\ W_c$$

where

F_p = The seismic force applied to a component of a building or item of equipment at its center of gravity

C_c = The seismic coefficient for components of architectural systems as given in Table 6 (dimensionless)

W_c = The weight of a component of a building or item of equipment

P = Performance criteria factor as given in Table 5 (dimensionless).

Attachments of exterior wall panels to the building seismic resisting system are required to have sufficient ductility and rotational capacity to accomodate the total story drift.

Mechanical and electrical systems are required to be designed to resist seismic forces as follows:

$$F_p = A_v\ C_c\ P\ a_c\ a_x\ W_c$$

where

C_c = The seismic coefficient for components of mechanical and electrical systems in Table 7 (dimensionless)

a_c = The amplification factor related to the response of a system or component as affected by the type of attachment (varies from 1 to 2).

a_x = The amplification factor at level x related to the variation of the response with height of the building.

$$a_x = 1.0 + (h_x/h_n)$$

where

h_x = the height above the base to level x

h_n = the height above the base to level n.

Conclusions

The ATC-3 document is predicated on the assumption that the analysis and design provisions must be used in conjunction with the material provisions covering wood, steel, concrete, and masonry because the design details and requirements are based on strength design. The A_a and A_v values, the response modification coefficients (R), the defletion amplication factors (C_d), and the T_a formulas were determined by considering their interdependence with the materials requirements.

Because of the new concepts and approach, it is strongly recommended that the ATC-3 provisions be tested by making numerous building designs and comparing the results with the same buildings designed using current seismic codes. It is also recommended that further detailed study be given to the A_a and A_v maps and their values, the values of R and C_d, the method of the limitations on determination of building periods, design requirements for torsional response, the effects of and design for irregularities in framing and discontinuities in strength, the design of foundations for overturning forces, and design for the effects of orthogonal ground motions.

References

1. Sharpe, R. L., "Evolution of Codes and Standards for Earthquake-Resistant Reinforced Concrete Building Construction," Proceedings of Workshop on ERCBC, University of California, Berkeley, California, July 11-15, 1977.

2. Applied Technology Council, "Tentative Provisions for Development of Seismic Design Regulations for Buildings," (ATC-3-06), prepared for the National Bureau of Standards - National Science Foundation, Washington, D.C., 1978.

3. Algermissen, S. T., and Perkins, D. M., "A Probabilistic Estimate of Maximum Accleration in Rock in the Contiguous United States," United States Geological Survey Open-File Report 76-416, 1976.

4. McGuire, R. K., "Seismic Structural Response Risk Analysis, Incorporating Peak Response Progressions on Earthquake Magnitude and Distance," Department of Civil Engineering, Massachusetts Institute of Technology, Cambridge, Massachusetts, Report R-74-51, 1975.

5. Bollinger, G., "Reinterpretation of the Intensity Data for the 1886 Charleston, South Carolina Earthquake," Bulletin of Seismological Society of America (in publication).

FIGURE 1: MAP OF EFFECTIVE PEAK ACCELERATION, A_a

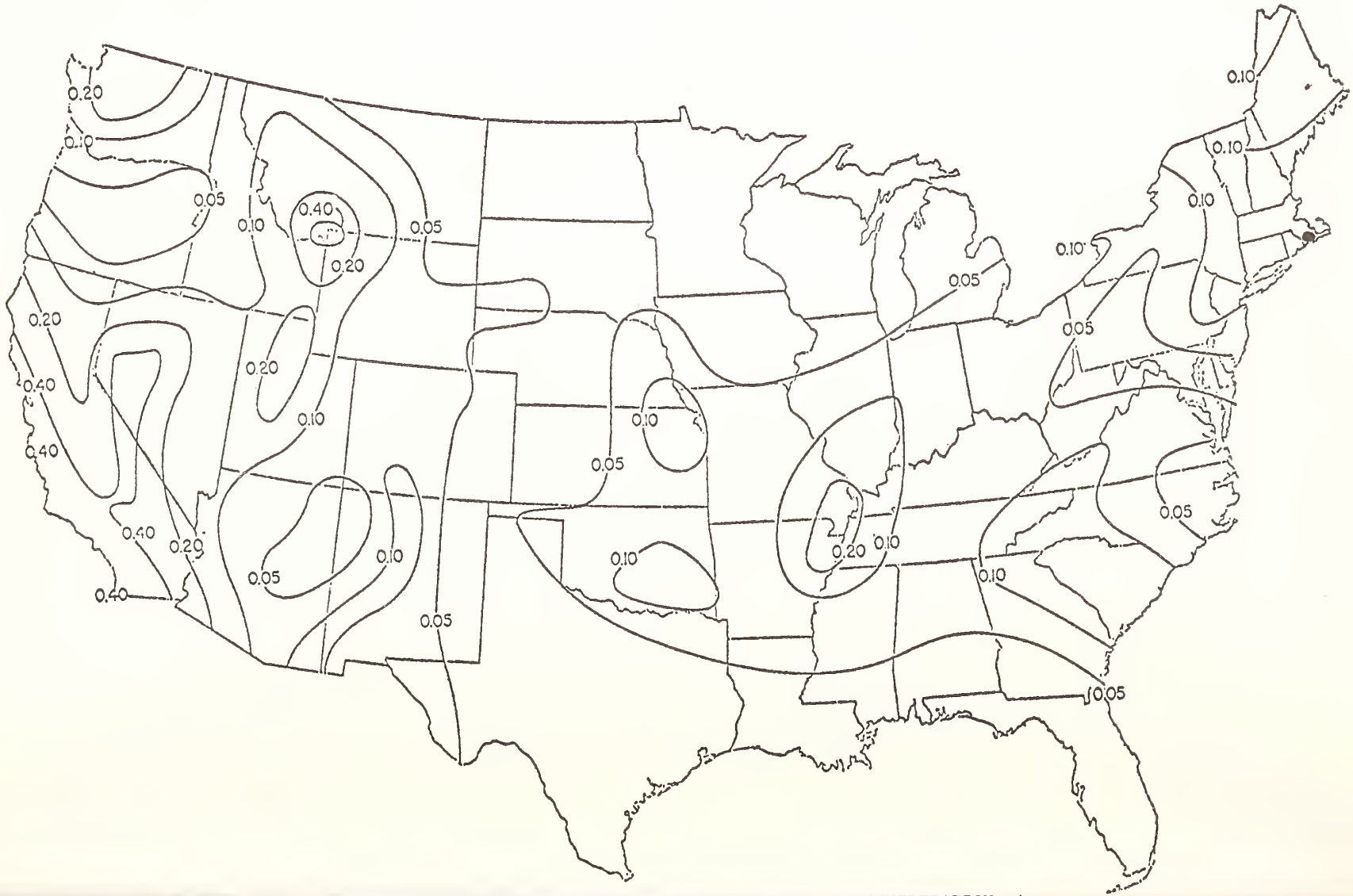

FIGURE 2: MAP OF EFFECTIVE PEAK VELOCITY-RELATED ACCELERATION, A_v

TABLE 1: COEFFICIENTS A_a, A_v, AND SEISMICITY INDEX

Coefficient A_a Figure 1	Map Area Number	Coefficient A_v Figure 2	Seismicity Index
0.40	7	0.40	4
0.30	6	0.30	4
0.20	5	0.20	4
0.15	4	0.15	3
0.10	3	0.10	2
0.05	2	0.05	2
0.05	1	0.05	1

TABLE 2: SEISMIC PERFORMANCE CATEGORY

Seismicity Index	Seismic Hazard Exposure Group III	II	I
4	D	C	C
3	C	C	B
2	B	B	B
1	B	A	A

22

TABLE 3: RESPONSE MODIFICATION COEFFICIENTS

Type of Structural System	Vertical Seismic Resisting System	Coefficients R	Coefficients C_d
BEARING WALL SYSTEM: A structural system with bearing walls providing support for all, or major portions of, the vertical loads. Seismic force resistance is provided by shear walls or braced frames.	Light framed walls with shear panels	6½	4
	Shear walls		
	Reinforced concrete	4½	4
	Reinforced masonry	3½	3
	Braced frames	4	3½
	Unreinforced masonry shear walls	1¼	1¼
BUILDING FRAME SYSTEM: A structural system with an essentially complete Space Frame providing support for vertical loads. Seismic force resistance is provided by shear walls or braced frames.	Light framed walls with Shear panels	7	4½
	Shear walls		
	Reinforced concrete	5½	5
	Reinforced masonry	4½	4
	Braced frames	5	4½
	Unreinforced masonry Shear walls	1½	1½
MOMENT RESISTING FRAME SYSTEM: A structural system with an essentially complete Space Frame providing support for vertical loads. Seismic force resistance is provided by Ordinary or Special Moment Frames capable of resisting the total prescribed forces.	Special moment frames		
	Steel	8	5½
	Reinforced concrete	7	6
	Ordinary moment frames		
	Steel	4½	4
	Reinforced concrete	2	2
DUAL SYSTEM: A structural system with an essentially complete Space Frame providing support for vertical loads. A Special Moment Frame shall be provided which shall be capable of resisting at least 25 percent of the prescribed seismic forces. The total seismic force resistance is provided by the combination of the Special Moment Frame and shear walls or braced frames in proportion to their relative rigidities	Shear walls		
	Reinforced concrete	8	6½
	Reinforced masonry	6½	5½
	Wood sheathed shear panels	8	5
	Braced frames	6	5
INVERTED PENDULUM STRUCTURES. Structures where the framing resisting the total prescribed seismic forces acts essentially as isolated cantilevers and provides support for vertical load.	Special Moment Frames		
	Structural steel	2½	2½
	Reinforced concrete	2½	2½
	Ordinary Moment Frames		
	Structural steel	1¼	1¼

TABLE 4: STORY DRIFT Δ_a

	Seismic Hazard Exposure Group		
	III	II	I
Δ_a	0.010 h_{sx}	0.015 h_{sx}	0.015h_{sx}

h_{sx} is the story height below level x.

1 Where there are no brittle-type finishes in buildings three stories or less in height, these limits may be increased one-third.

TABLE 5: PERFORMANCE CRITERIA

Designation	Performance Characteristic Level	P
S	Superior	1.5
G	Good	1.0
L	Low	0.5

22

TABLE 6: SEISMIC FORCE AND PERFORMANCE CHARACTERISTIC LEVELS REQUIRED FOR ARCHITECTURAL SYSTEMS OR COMPONENTS

Architectural Systems or Components	C_C Factor	Required Levels Seismic Hazard Exposure Group III	II	I
Appendages				
Exterior Nonbearing Walls	0.9	S	G	L
Wall Attachments	3.0	S	G	L
Veneers	3.0	G	G	L
Roofing Units	0.6	G	G	NR
Containers and Miscellaneous Elements (free standing)	1.5	G	G	NR
Paritions				
Stairs and Shafts	1.5	S	G	G
Elevators and Shafts	1.5	S	L	L
Vertical Shafts	0.9	S	L	L
Horizontal Exits Including Ceilings	1.5	S	S	G
Public Corridors	0.9	S	G	L
Private Corridors	0.6	S	L	NR
Full-Height Separation Partitions	0.9	S	G	G
Full-Height Other Partitions	0.6	G	L	L
Partial-Height Partitions	0.6	G	L	NR
Structural Fireproofing	0.9	S	G	L
Ceilings -- Fire-Rated Membrane	0.9	S	G	G
-- Nonfire-Rated Membrane	0.6	G	G	L
Architectural Equipment -- Ceilings, Wall, or Floor Mounted	0.9	S	G	L

NR - Not required

TABLE 7: SEISMIC FORCE AND PERFORMANCE CHARACTERISTIC LEVELS REQUIRED FOR MECHANICAL/ELECTRICAL COMPONENTS

Mechanical/Electrical Components	C_C Factor	Seismic Hazard Exposure Group III	II	I
Emergency Electrical Systems (code required)				
Fire and Smoke Detection System (code required)	2.00	S	S	S
Fire Suppression Systems (code required)				
Life Safety System Components				
Boilers, Furnaces, Incinerators, Water Heaters, and Other Equipment Using Combustible Energy Sources or High Temperature Energy Sources, Chimneys, Flues, Smokestacks, and Vents				
Communication Systems				
Electrical Bus Ducts and Primary Cable Systems				
Electrical Motor Control Centers, Motor Control Devices, Switchgear, Transformers, and Unit Substations	2.00	S	G	L
Reciprocating or Rotating Equipment				
Tanks, Heat Exchangers, and Pressure Vessels				
Utility and Service Interfaces				
Machinery (manufacturing and process)	0.67	S	G	L
Lighting Fixtures	0.67	S	G	L
Ducts and Piping Distribution Systems -- Resiliently Supported	2.00			
Ducts and Piping Distribution Systems -- Rigidly Supported	0.67	S	G	NR
Electrical Panelboards and Dimmers	0.67			
Conveyor Systems (non-personnel)	0.67	S	NR	NR

23

LOGICAL ANALYSIS OF SEISMIC DESIGN PROVISIONS

James Harris

National Bureau of Standards
Washington, D.C.

Logical Analysis of Seismic Design Provisions

In early 1976, the National Bureau of Standards (NBS) and Carnegie-Mellon University (CMU) undertook a collaborative project to apply logical and systematic techniques of analysis and information display to the earthquake resistant design criteria then being developed by the Applied Technology (ATC). The project is funded by the National Science Foundation (NSF) and has three objectives:

1. To aid the participants in ATC's project in their task of developing the new provisions by applying existing techniques of analysis to detect ambiguities, omissions and inconsistencies.

2. To document our analysis and ATC's provisions by preparing and publishing the provisions expressed tabular, logical format.

3. To prepare alternative arrangements of ATC's provisions that would meet the needs of some special audiences more directly than the orginal arrangement.

ATC has produced a large and impressive set of provisions. Because these provisions will now be considered by the building codes and standards community for adaption into many codes and standards, it is imperative that they be correctly understood. Yet, like nearly all technical provisions, they will be subject to misinterpretation. This need for precise communication is exactly what the techniques used in this study are design to bolster.

Overview of the Techniques

A set of provisions can be analyzed to determine that they are clear, complete, consistent and, to some extent, correct. The analysis is conducted in an objective fashion at several levels of detail. The primary benefit to the user of the analysis is that it raises questions about clarity, completeness, etc. The technique does not provide corrective answers, for that generally involves actual change in the wording of the provisions.

There are three principal tools used in the analysis:

1. The decision table is used to represent the meaning of individual provisions. It is simply an orderly presentation of the reasoning controlling a set of decisions. It is easily analyzed to assure that the reasoning process will lead to a unique result and that no possibility exists for encountering a situation not defined. Decision tables present an overall analysis of situations involving parallel thought processes, whereas written text and, to some extent, flow charts both describe more of a sequential thought pattern.

2. The information network is used to represent the precedence relations among the provisions. Each decision table occupies one node in the network. The nodes are connected to their ingredient nodes by branches that represent the flow of information through a set of provisions from the input data to the terminal criteria. The ingredients of any node are simply all those nodes that may be required for the direct evaluation of the node.

3. The outline/classified index is used to represent the arrangement and scope of the provisions. The subset of the overall

set of provisions which contains the likely points of entry by users of the provisions is selected as a set of basic provisions. Each of these basic provisions is then classified using key words that define the scope of the provision. The classifiers allow outlines and indexes to be constructed, and the basic provisions are entered at the appropriate points. Several different arrangements of the basic provisions can be generated, allowing one to select the best arrangement for any given use.

Examples of the use of each of these tools in the analysis of ATC's provisions are presented in the following sections. The complex documentation will be available in a few months. Further examples and explanations of the techniques are available in several publications [1, 2, 3].

Decision Table

A decision table is a tabular arrangement of conditions, actions, and rules. A condition is a logical statement that must have one of only two values: true or false. An action is any operation; generally, in the context of this study it is the assignment of a value to a variable. A rule is a statement that prescribes a set of condition values in order that a specified set of actions can be performed. Thus, the simple provision, "No single floor area shall exceed that permitted for a one-story building," is shown in decision table form as follows:

		Rule 1	Rule 2
Condition 1	Actual story area ≤ allowable one-story building area	T	F
Action 1	Single story area check = satisfied	X	
Action 2	Single story area check = violated		X

The table is read rule by rule, "If the actual story area is less than the allowable one-story building area, then the single-story area check is satisfied; if it is not, then the check is violated"

The following text is taken from an intermediate draft of ATC's provisions. The subsequent decision table represents those same provisions, except that the three rules at the right edge of the table represent situations for which the text gives no action.

Site Effects

Site effects on building response shall be established based on three soil profile factors defined as follows:

SOIL PROFILE TYPE A is a profile with:

1. Rock of any characteristic, either shale-like or crystalline in nature. Such material may be characterized by a shear wave velocity greater than 2,500-feet per second, or

2. Stiff soil conditions where the soil depth is less than 200-feet and the soil types overlying rock are stable deposits of sands, gravels, or stiff clay.

SOIL PROFILE B is a profile with deep cohesionless or stiff clay conditions, including sites where the soil depth exceeds 200-feet and the soil types overlying rock are stable deposits of sands, gravels, or stiff clay.

SOIL PROFILE C is a profile with soft- to medium-stiff clays and sands, characterized by 30-feet or more of soft- to medium-stiff clay with or without intervening layers of sand or other cohesionless soils.

In locations where the soil profile type is not known in sufficient detail to determine the soil profile type and where foundations are supported without the use of piles, Soil Profile B or C shall be used whichever produces the larger base shear.

		1	2	3	4	5	.	.	.
1	Soil type = rock	T	-	-	-	·	·	F	F
2	Soil type = stiff	-	T	T	-	·	·	F	F
3	Soil depth 200'	+	T	F	·	·	·	·	·
4	Soil type = soft clay	-	-	-	T	·	·	F	F
5	Depth of soft clay 30'	-	·	·	T	·	·	·	F
6	Soil type known	+	+	+	+	F	F	T	T
7	Piles support foundation	·	·	·	·	F	T	·	·

1	Soil Profile Type = A	x	x						
2	Soil Profile Type = B			x					
3	Soil Profile Type = C				x				
4	Soil Profile Type = B/C					x			

Note: + means true predetermined by another condition value
- means false predetermined by another condition value
· means either true or false is acceptable

23

The analysis of the provisions for completeness and conflicts begins with the construction of the decision table. For the preceding provisions, the result was the decision table shown without the three rules at the right edge. The upper right quadrant of the table is then analyzed to see that no two rules could be matched simultaneously and that all possible rules are included. The easiest and most reliable way to do this is by decomposing the table into a decision tree. This analysis is easily performed with a computer [4, 5]. The decision tree for the preceding table is shown in Figure 1. Note that there are three nodes labeled "Else" in that tree. They each represent possible rules that are not in the original table, and it was from them that the three rules at the right edge of the table were constructed. These rules do represent possible situations for which the provisions, as written, provide no answer. Thus, the analysis has raised a question.

Also note that none of the nodes in Figure 1 contain more than one of the rules in the original table. If that had been the case, a situation would have existed in which the provisions contained a contraction, at worst, or were redundant, at best.

The logical problem in the provision for soil profile type was solved by ATC by rewriting the last paragraph as follows:

> In locations where the soil properties are not known in sufficient detail to determine the soil profile type or where the profile does not fit any of the three types, Soil Profile B shall be used.

Information Network

The information network represents the flow of information through the decision points in a set of provisions. The entire network can be assembled once each of the nodes and their direct ingredients are known. The assembly is easily performed with a computer program [4, 5]. The complete information network can then be used for two general operations: to trace global ingredients of a particular node (that is, all the nodes that have any possible influence on the mode in question) and to trace the global dependence of a particular node (that is, all the nodes that might be influenced by the node in question). These two operations are useful to those actually complying with a set of provisions (particularly in the use of automatic data processing) because they provide all the necessary cross references. They are also useful in the development of a set of provisions; the global ingredients, in particular, can be used to guide the ordering and written expression of provisions. The network can also be used to detect loops in the precedence and detached (uncrossreferenced) sets of provisions.

In the analysis of one of ATC's intermediate drafts, it was found through examination of the information network that a provision for the effects of vertical motion was misplaced. It was originally located in the chapter that described the "Equivalent Lateral Force" procedure of analysis, although it was not functionally related to any other provisions in that chapter. The information network clearly showed that it was functionally related to the load combination provisions for component design (see Figure 2) and thus a recommendation was made to ATC that the provision be moved to a more appropriate location in the section on component design. This move provided for a more direct agreement between the written expression and actual use of the provisions.

Outline/Classified Index

The classification of provisions in a systematic fashion offers considerable insight into the overall organization of a set of provisions for better access and retrieval. Algorithms exist to automatically generate outlines of headings once a set of provisions has been classified [5, 7] and guidelines exist for the classification of provisions [8, 9]. Two brief examples of the use of classification in analyzing the organization of ATC's provisions are offered here.

In the first example, a chapter contained several sections, two of which were "Framing Systems," which dealt with parameters and restrictions for certain framing systems, and "Site Effects," which included the provisions for soil profile type analysed earlier and certain restrictions on the use of some sites. The section on framing systems was the first of the two. These two sections were not functionally related through the information network, so that had no influence on their order. On the basis of classifying provisions by their positions in the process of design and construction, it was recommended that their order be reversed, for the site selection process almost always occurs before the decision on a framing system.

In the second example, the intermediate draft of the provisions contained a chapter and an appendix dealing with wood construction. The original section headings are shown on the left in the following, while the recommended reorganization is shown on the right. The recommendation came about as a result of classifying each of the provisions on several different bases and noting that there was a significant division between the provisions for those buildings that were analyzed for seismic loads ("Engineered") and those for buildings that were not analyzed ("Non-engineered"). This allowed a clear decision as to the applicability of each provision and eliminated the need for the appendix.

Comparative Outlines, Chapter 10

ATC-3-05		Recommended	
10.	Wood	10.	Wood and Related Materials
10.1	Reference Documents	10.1	Reference Documents
10.2	Strength of Members and Connections	10.2	Non-engineered Construction
		10.2.1	Wall
		10.2.2	Wall Sheathing Requirements
		10.2.3	Acceptable Types of Wall Sheathing
10.3	Category A	10.3	Engineered Construction
10.4	Category B	10.3.1	Strength of Members and Connection
10.5	Category C		
10.6	Category D	10.3.2	Framing Requirements
10A	Wood Construction	10.3.3	Requirements for All Shear Panels
10A.1	General		
10A.1.1	Diagonally Sheathed	10.3.4	Diagonally Sheathed Diaphragms
10A.2	Wood Diaphragms		
10A.2.1	Diagonally Sheathed Diaphragms	10.3.4	Diagonally Sheathed Diaphragms
10A2.2	Plywood Diaphragms	10.3.5	Plywood Diaphragm
10A.3	Shear Panels Sheathed with Various Materials	10.3.6	Shear Panels Sheathed with Various Materials
		10.4	Category A
		10.5	Category B
		10.6	Category C
		10.7	Category D

Conclusion

The joint NBS-CMU project to aid in the development of new seismic design provisions for building codes by applying systematic, logical analyses to the provisions is nearly complete. During the first phase several recommendations were made to ATC as questions were raised by the decision table, information network, and classification/organization analyses of their interim drafts. The final phase of the project will conclude with a report documenting the analysis of the provisions and containing decision tables for the final version of ATC's provisions.

References

1. Fenves, S.J., "Tabular Decision Logic for Structural Design," Journal of the Structural Division, American Society of Civil Engineers, Vol 92, No. ST6, December 1966.

2. Fenves, S.J., and Wright, R. N., The Representation and Use of Design Specifications, Technical Note 940, National Bureau of Standards, Washington, D.C., June 1977.

3. Harris, J.R., Melin, J. W., Tavis, R. L., and Wright, R. N. "Technology for the Formulation and Expression of Specifications, Volume I: Final Report, "Civil Engineering Studies, SRS 423, University of Illinois, Urbana, Ill., December 1975.

4. Harris, J.R., Melin, J. W., and Albarran, C., "Technology for the Formulation and Expression of Specifications, Volume II: Program User's Manual" Civil Engineering Studies, SRS 424, University of Illinois, Urbana, Ill., December 1975.

5. Wright, R.N., Harris, J. R., Melin, J. W., and Albarran, C. "Technology for the Formulation and Expression of Specifications, Volume III: Technical Reference Manual," Civil Engineering Studies, SRS 425, University of Illinois, Urbana, Ill., December 1975.

6. Wright, R.N., Boyer, J. T., and Melin, J. W. "Constraint Processing in Design," Journal of the Structural Division, American Society of Civil Engineers, Vol. 98, No. ST1, January 1971.

7. Nyman, D.J. and Fenves, S. J., "An Organizational Model for Design Specifications," Report R73-4, Department of Civil Engineering, Carnegie-Mellon University, Pittsburg, PA, September 1973.

8. Fenves, S.J., Rankin, K. and Tejuja, H., The Structure of Building Specifications, Building Science Series 90, National Bureau of Standards, Washington, D.C., September 1976.

9. Harris, J.R., and Wright, R. N., "Organization of Design Standards" (to be published) National Bureau of Standards, Washington, D.C.

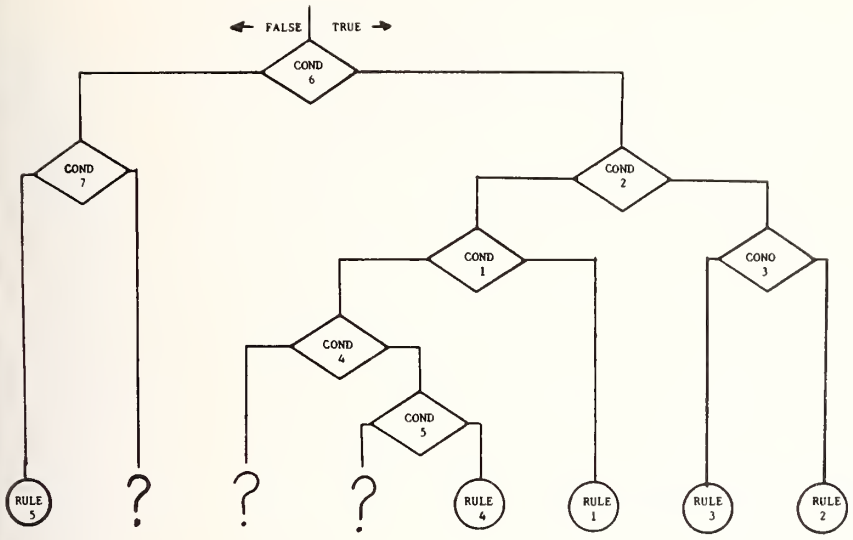

FIGURE 1: DECISION TREE GENERATED FROM DECISION TABLE BY TESTING THE CONDITIONS TO SUBDIVIDE THE TABLE

NOTE: the branches marked ? show possible rules that are missing from the original table, thus it is logically incomplete

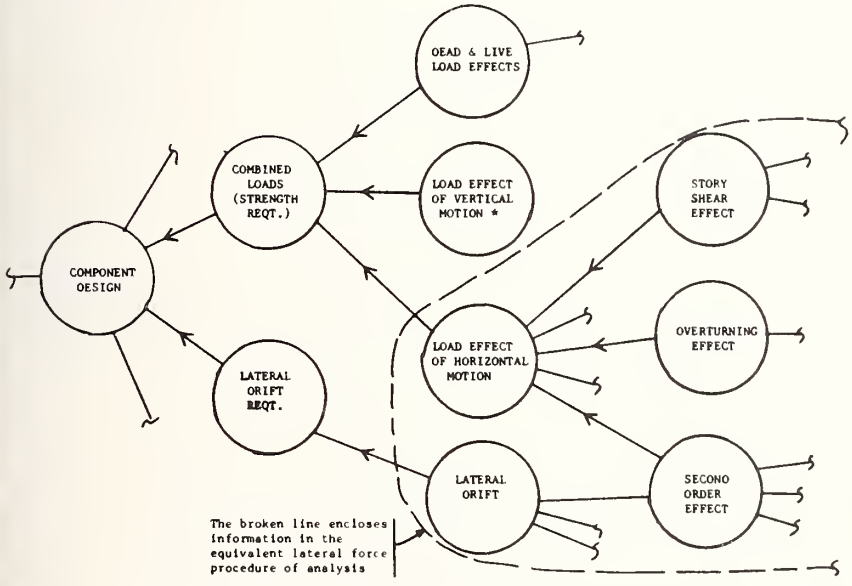

FIGURE 2: PORTION OF THE INFORMATION NETWORK FOR STRUCTURAL DESIGN

24

HIGHLIGHTS OF CALIFORNIA SCHOOL AND HOSPITAL BUILDING REGULATIONS

John F. Meehan

Office of the State Architect
California

Highlights of California School and Hospital Building Regulations

California public school buildings have performed very well in all earthquakes since the 1933 Long Beach earthquake. In that earthquake a great many public school buildings were badly damaged and innumerable deaths would have occurred if the earthquake would have occurred during school hours. Within one month following the earthquake, the California Legislature adopted the Field Act, which placed public school buildings under the jurisdiction of the State. Similarly, the 1971 San Fernando earthquake caused a great deal of damage to several hospital buildings, including one that was just completed a few months before the earthquake. Over 80 percent of the deaths in that earthquake occurred to hospital occupants. A year after that earthquake the Legislature enacted the Hospital Act, which also placed hospital buildings under State jurisdiction.

It is apparent that the schools performed well in past earthquakes because of the provisions of the Field Act. The act requires that the designers, from the private sector, must be registered architects or structural engineers; an independent review of the contract documents must be performed by the State; construction surveillance by all project designers and the State; and continuous inspection by an approved project inspector. Further, as the construction progresses and at the completion of the project, verified reports must be filed by the designers, inspector, and contractor indicating complete conformance with the approved construction documents. False reports carry a felony penalty. Regulations may be adopted and a fee may be collected to accomplish the intent of the Field Act. The complete Field Act is given in the Education Code, Section 39140-39156.

In 1967, the Legislature enacted statutes to require a geologic study of school sites.

Hospital statutes are somewhat similar except that the level of performance is higher; that is, they require that the hospital building "must be completely functional to perform all necessary services to the public after a disaster...." They require that a structural engineer perform the structural design; that a geologic investigation be made of the site; an independent plan review must be made by the State; construction surveillance must be provided by the State and all project designers; and the project must be continuously inspected by an approved inspector. Verified reports by all of those involved in the construction supervision, which are the designers, inspector and contractor, must be filed. The complete Hospital Act is given in the Health and Safety Code, Section 15000-15023.

Through delegation, the Field Act is enforced by the Structural Safety Section (SSS) of the Office of the State Architect in the Department of General Services. However, the Hospital Act is enforced by the Department of Health but the statutes require that the State structural plan review and construction supervision must be performed by the SSS under contract to the Department of Health.

24

Public School Regulations

All regulations applicable to public school buildings cannot be presented here. Only a few of those which may be considered somewhat unique to California schools will be discussed.

The basic building regulations adopted by California are those of the Uniform Building Code. Additions and deletions to it are adopted by various State agencies which relate to their specific interest or legislative assignment. Currently the 1973 edition of the Uniform Building Code (73 UBC) published by International Conference of Building Officials is the effective basic code. Procedures are underway at this moment to adopt the 1976 edition of the Uniform Building Code (76 UBC).

The Uniform Building Code is a widely distributed code and therefore those basic regulations will not be discussed here.

The regulations discussed in this paper will be only those proposed by the SSS as additions or deletions to the 76 UBC.

Snow Load

The 76 UBC Section 2305(d), permitting a reduction on snow load due to slope of roof was deleted because frequent measurements of actual snow loads on roofs of many buildings by this author did not justify any load reduction due to slope of the roof. Full load on half the span or the ridge of the roof and no load on the remaining portion of the span should also be used as a criteria in snow load design because of the likelihood of having that loading condition when snow is being removed from the roof.

Veneered Walls

An addition was made to 76 UBC Section 2307(c) to require that the perpendicular to the wall deflection of metal or wood stud walls providing lateral support to masonry veneer be limited to L/600 when resisting seismic loads. All masonry over 1/2" in thickness must be mechanically anchored to the structure with anchors capable of carrying, at working stress, in both tension and compression a load equal to twice the weight of the veneer. This is usually accomplished with a piece of 18ga galvanized strap cast in the horizontal mortar joint and fastened to the wall by means of dove-tail anchor slots which are nailed to the wood studs. Horizontal wire reinforcing must be placed continuously in mortar joints containing the anchors. Masonry veneer is not permitted over exitways or more than 25' above grade when the veneer is supported by wood framing.

Drift

An addition is made to 76 UBC Section 2307 to limit the story drift to 0.005 times the story height. The calculated story drift due to code level forces shall be multiplied by 1.00/K but this ratio need not exceed 1.0. Also the drift or the displacement in the plane of the wall from head to sill at a glazed opening shall not exceed 0.0025 times the height of the opening unless the glass therein is prevented from resisting shear or taking distortion, or tempered, safety or wire glass is used. Ordinary glass embedded in hard bedding material will fail at about 0.005 times the glass height. It is apparent that if a window is framed such that the head of the opening is anchored to the floor above and the sill is framed and anchored to the floor below, the permitted story drift is limited to 0.0025 times the opening height if ordinary glass is used. That is, if the window is 4 feet high and the glass is bedded into the frame the story drift limit would be 0.12 inches which is very stiff, indeed.

In this same section, 75 UBC Section 2307, an addition has been made to require a vertical resisting element in each resisting plane for every 100 feet of building length when the construction consists of a wood horizontal diaphragm or horizontal rod bracing and the walls are of wood. In buildings having horizontal wood diaphragms or rod bracing systems and with continuous structural steel reinforced concrete framing of continuous reinforced grouted masonry walls the element may then be at 125 feet of building length.

Unreinforced masonry is not permitted in school construction.

Requirements have also been added to limit the span-depth ratio of various diaphragm materials as related to the stiffness of the wall materials. For example, a flexible roof diaphragm material such as diagonal sheathing may have a 2:1 span-depth ratio if the walls are of wood or light steel but it cannot be used if the walls are of concrete masonry. If the roof diaphragm is plywood nailed at all edges of the panel, the span-depth ratio is 3:1 for any kind of wall materials.

Earthquake Regulations

The lateral force provision in the 76 UBC closely follows the current Structural Engineers Association of California Recommended Lateral Force Requirements and Commentary.

The seismic force due to soils acting against walls is a newly proposed regulation. Where buildings provide lateral support for walls retaining earth, and the exterior grades on opposite sides of the building differ by more than 6 feet, the load combination of the dynamic increment of active earth pressure due to earthquake acting on the higher side, as determined by a civil engineer qualified in soils engineering, plus the difference in active earth pressures, shall be added to the lateral forces provided in this Section. In lieu of a determination by a civil engineer qualified in soils engineering, the dynamic increment of active earth pressure for soils of low cohesion may be considered to be a constant uniformly distributed pressures, P_d, determined in accordance with the following formula:

$$P_d = Z(0.03\delta h)$$

where

P_d = Dynamic increment of active earth pressure due to earthquake in pounds per square foot

δ = Soil density in pounds per cubic foot

h = Height of retained earth above the bottom lateral support for the wall

In the base shear equation V = ZIKCSW the influence of snow load as related to elevation has been included in the factor W. Where the design snow load is 30 psf or less, no part need be included in the value of "W". Where the snow is greater than 30 psf, the snow load shall be included; however, the snow load may be reduced to 25 percent of the design snow load for sites below 5,000 feet in elevation and may be reduced to 33 percent of the design snow load for sites above 5,000 feet in elevation.

It is quite apparent that heavy snow load at the higher elevations will have a strong influence on the seismic design. The maximum measured snow load made by this author to date in California was 323 pounds per square foot, the snow depth was 141 inches, on a pitched roof of a structure located at 6900 foot elevation.

When considering the seismic design of single-mass structures laterally supported by cantilevered columns, the value of K has been increased to be not less than 2.0. The columns for such structures shall meet all the requirements for columns in ductible moment resisting space frames. Broadly speaking, single-mass structures are one-story structures whose columns have no moment resistance at the top and the moment resistance at the base is provided solely by the lateral soil pressure on the column foundation.

Overturning

When calculating the internal stresses in a structural system due to overturning effects produced by horizontal earthquake forces, the maximum tensile stresses may be reduced by not more than three-fourths of the vertical dead load stresses because of the effects of possible vertical earthquake acceleration. However, the total dead load resisting moment may be used in computing overturning forces at the foundation/soil interface.

Building Separations

The required separation distance between buildings has been increased. It must be determined by multiplying the calculated lateral force drift or deflection by a factor of 2.0/K but not less than 2.0. The total separation shall be not less than the sum of the displacements calculated for each building at that level. Any building elements, mechanical or electrical systems which cross or enclose the building separating space shall be designed and detailed to accomodate these calculated displacements.

Structural Systems. Ductility Requirements

The ductility requirements for school buildings have been raised to require that all moment-resisting space frames used to resist design seismic forces in any height school building shall meet ductile moment-resisting space frame requirements.

> Exception: Moment-resisting space frames not meeting ductile frame requirements may be used for one or two story structures provided their design is based on the basic lateral force formula using a K not less than 2.0. The columns for such structures shall meet all the requirements for columns in ductile moment-resisting space except that columns for single-story steel frames supporting tributary dead loads, including the weight of the frame, not exceeding five pounds per square foot need not comply with the requirements of the steel ductile moment-resisting space frames.

Braced Frames

The 76 UBC requires that all members in braced frames shall be designed for 1.25 times the force determined in accordance with the basic lateral force formula. Connections for all members in braced frames shall be designed to develop the full tensile or compression capacity of the member. However, an exception for school buildings

has been inserted to require that the connection need not develop the full capacity of the member if the connection is designed for 2.0 times the force determined in accordance with the basic lateral force formula. Also, all tension members shall be installed in a manner to remove any sag.

Flexible Horizontal Diaphragm Anchorage

Where diaphragms of wood or other materials of similar flexibility are used to laterally support concrete or masonry walls, the anchorage shall provide a positive direct connection capable of resisting the forces required by the lateral force formula or a minimum of 200 pounds per foot of wall length. Such connections shall be in addition to the diaphragm to wall connections provided for shear transfer.

Anchorage of framing members shall not be provided by use of toe nails or nails subjected to withdrawal; nor shall wood framing be used in cross-grain bending or cross-grain tension.

Lateral support of the wall may be provided by a 1/2" or thicker plywood diaphragm fastened with a double row of nails directly to a 3 x 6 minimum wood plate bolted on the top of the wall. The nails shall be 1" minimum from each edge of the plate and 1" minimum from the edge of the plywood.

Lateral Force on Non-Structural Components

Supporting structural elements and anchorage of architectural, mechanical and electrical components shall be designed for lateral forces in accordance with the following formula:

$$F_p = ZC_pW_p$$

The values of C_p for determining anchorage forces for architectural, mechanical and electrical components shall be as set forth in Table 1. Where the provisions of these tables do not specify C_p values for the anchorage of particular components which in the opinion of the Office of the State Architect should be designed and anchored to resist lateral forces for the safety of the occupants, the office may assign C_p coefficients with the advice of the architect or engineer based on coefficients specified for similar components listed in these provisions.

Seismic Hazard Zones

To establish clearly defined enforceable boundaries of the seismic hazard zones in California, the county lines, location of highways, latitudes and longitudes are employed. The zones shown in Figure 1 show these proposed boundaries. As a guide to determine these zones the suggestions given in the Commentary of the Recommended Lateral Force Requirements and Commentary were used to locate Zone 4 boundaries. It was recommended that Zone 4 should extend 25 miles from both sides and ends of a fault which could produce a Richter 7.0 or greater magnitude and 15 miles from a fault which can produce a 6.0 to 7.0 Richter magnitude earthquake.

Lay-in Panel T-Bar Ceilings

Portions of many lay-in panel T-bar ceilings have failed in earthquakes of magnitude of about 5.6 and greater. Following the 1971 San Fernando earthquake, the ceiling industry developed recommendation now found in the UBC Standards No. 47.18. Briefly, this

requires that the main and cross tees be anchored at the wall or a continuous member be provided which will prevent the bars from spreading and dropping the panels, a wire hanger shall be provided within 8" of the wall, and restraints consisting of four No. 12 gage wires secured to the main runner within 2" of the cross runner intersection and splayed 90° from the plane of the ceiling. These horizontal restraint points shall be within 4 feet of the wall and not over 12 feet on center each way. The splices of the main runners and the cross tees must be capable of resisting an ultimate test load of not less than 180 pounds in tension and compression provided that only the ceiling load is to be resisted. Where the ceiling system must resist additional loads from partitions, shelving, and light fixtures, the test load of at least twice the design load must be resisted. Also, it must be demonstrated that this load can be resisted in tension with a 5° misalignment of the members. In lieu of these arbitrary requirements, a ceiling may be designed to resist the lateral loads given in Table 1.

Hospital Regulations

Essentially all of the regulations adopted or proposed for school buildings also apply to hospital buildings. There are, however, a few differences due to the increased level of performance required by legislative intent -- "to be completely functional...." The basic code will be the 1976 UBC and will follow the "essential facilities" with the importance factor requirements; i.e., the value in the base shear equation will be 1.5.

The regulations do, however, stress the requirement that the static analysis as proposed by the 76 UBC is applicable only to regular buildings. Dynamic analysis will definitely be required for any structure which has highly irregular shape, larger differences in lateral resistance or stiffness between adjacent stories or other unusual structural features which would significantly affect the dynamic analysis shall be based upon the ground motion prescribed for the site in a geotechnic report. The report shall consider the seismic event which may be postulated with a reasonable confidence level within a 100-year period. The analysis may be based upon appropriate time-histories or response spectra with percentages of critical damping consistent with the strain levels in the structural materials. All natural modes of vibration with periods of vibration greater than 0.05 second shall be considered in the analysis. The base shear resulting from the dynamic analysis shall be not less than 80 percent of the base shear calculated from the basic lateral force equation. If the base shear, as determined by the dynamic analysis, must be increased to meet this requirement, the design response shall be normalized to a proportionately higher value.

Lateral Force on Non-Structural Components

The design and detailing of mechanical or electrical systems and non-structural components required to be completely functional to perform all necessary services after a disaster shall be based upon the formula

$$F_p = ZC_pW_p$$

when C_p is obtained from Table 2. The State review will be made for the anchorage of the item to the structure and not for the design or construction of the item.

References

1. Steinbrugge, K. V. and Moran, D. F., "An Engineering Study of the Southern California Earthquake of July 21, 1952, and of Its Aftershocks," Bulletin of the Seismological Society of America, April 1954, p. 244 and p. 255.

2. Steinbrugge, K. V., Cloud, W. K., and Scott, N. H., "The Santa Rosa California Earthquakes of October 1, 1969," Coast and Geodetic Survey, 1970, p. 38 and p. 10.

3. National Academy of Sciences, National Academy of Engineering, "The San Fernando Earthquake of February 9, 1971," p. 13.

4. Jennings, P. C., "Engineering Features of the San Fernando Earthquake," California Institute of Technology EERC 71-02, p. 276.

5. National Bureau of Standards, "Engineering Aspects of the 1971 San Fernando Earthquake," Building Science Series 40, 1971, p. 311.

6. Steinbrugge, K. V., Schader, E. E., "Earthquake Damage and Related Statistics, San Fernando Earthquake February 9, 1971," U. S. Department of Commerce, 1973, Vol. I, Part B, p. 713.

7. U. S. Department of Commerce, National Oceanic and Atmospheric Administration, "San Fernando, California, Earthquake of February 9, 1971," Vol. I, Parts A and B.

8. Steinbrugge, K. V., Schader, E. E., Bigglestone, H. C., and Weers, C. A., "San Fernando Earthquake of February 9, 1971," Pacific Fire Rating Bureau, p. 2.

TABLE 1: HORIZONTAL FORCE FACTOR "C_p" FOR ANCHORAGE OF SCHOOL NON-STRUCTURAL COMPONENTS*

CATEGORY	DIRECTION OF FORCE	VALUE OF C_p[1]
1. When connected to, part of, or housed within a building: a. All mechanical and electrical equipment or machinery[4] b. Tanks (plus contents) and support systems	Any direction	0.30[2,3]
2. Emergency power supply systems[5]	Any direction	0.75[2,3]
3. a. Storage racks with the upper storage level more than 5 feet in height (plus contents)[6,7] b. Floor supported cabinets and bookstacks more than 5 feet in height (plus contents)[6]	Any direction	0.30[3,7]
4. Wall hung cabinets and storage shelving (plus contents)	Any direction	0.30
5. Suspended ceiling framing systems (See Section T21-4701(e))	Any direction	0.30[8]
6. Suspended light fixtures[9]	Any direction	1.00
7. Power-cable driven elevators or hydraulic elevators with lifts over 5 feet: a. Car and counterweight guides, guide rails, and supporting brackets and framing[10] b. Driving machinery, operating devices and control equipment	See Part 7, Title 24	See Part 7, Title 24

Welded, bolted or other intermittent connections such as inserts shall not be allowed the one-third increase in allowable stress permitted.

[1] C_p may be two-thirds of value shown for components mounted on foundations at grade or on floor slabs on earth subgrade. C_p shall be not less than the ratio of Fx/Wx for floor or roof level under consideration. Where a dynamic analysis is used in the design of the building, the forces so determined may be used in the design of the elements or components with appropriate resistance criteria.

[2] For flexible and flexibly mounted equipment and machinery (fundamental period of vibration greater than 0.05 seconds), the appropriate values of C_p shall be determined with consideration given to both the dynamic properties of the equipment and machinery and to the building or structure in which it is placed but shall not be less than the listed values. For closely restrained flexible mountings with resilient snubbers, a factor of two times the values shown shall be used except where more appropriate values can be determined by a dynamic analysis.

[3] The component anchorage shall be designed for the horizontal force, F_p, acting simultaneously with a vertical seismic force equal to one-third of the horizontal force, F_p.

[4] Equipment or machinery shall include such items as tanks, boilers, chillers, pumps, motors, air handling units, cooling towers, transformers, switch gear, control panels, etc.

[5] Emergency equipment should be located where there is the least likelihood of damage due to earthquake. Such equipment should be located at ground level and where it can be easily maintained to assure its operation during an emergency.

[6] Floor supported storage racks, cabinets or bookstacks not more than 8 feet in height need not be anchored if the width of the supporting base or width between the exterior legs is equal to or greater than two-thirds the height.

[7] In lieu of the tabulated values, steel storage racks may be designed in accordance with UBC Standard No. 27-11.

[8] Ceiling weight shall include all light fixtures and other equipment or components which are laterally supported by the ceiling. For purposes of determining the lateral force, a ceiling weight of not less than four pounds per square foot shall be used.

[9] Suspension systems for light fixtures which have passed shaking table tests approved by the Office of the State Architect or which, as installed, are free to swing a minimum of 45° from the vertical in all directions shall be assumed to comply with the lateral force requirements of Section T21-2312(1).

Unless of the cable type, free swinging suspension systems shall have a safety wire or cable attached to the fixture and structure at each support capable of supporting four times the support load.

[10] W_p for elevator cars shall be the weight of the car plus 0.4 times its rated load. The lateral forces acting on guide rails shall be assumed to be distributed one-third to the top guide rollers and two-thirds to the bottom guide rollers of elevator cars and counter weights unless other substantiating data is provided.

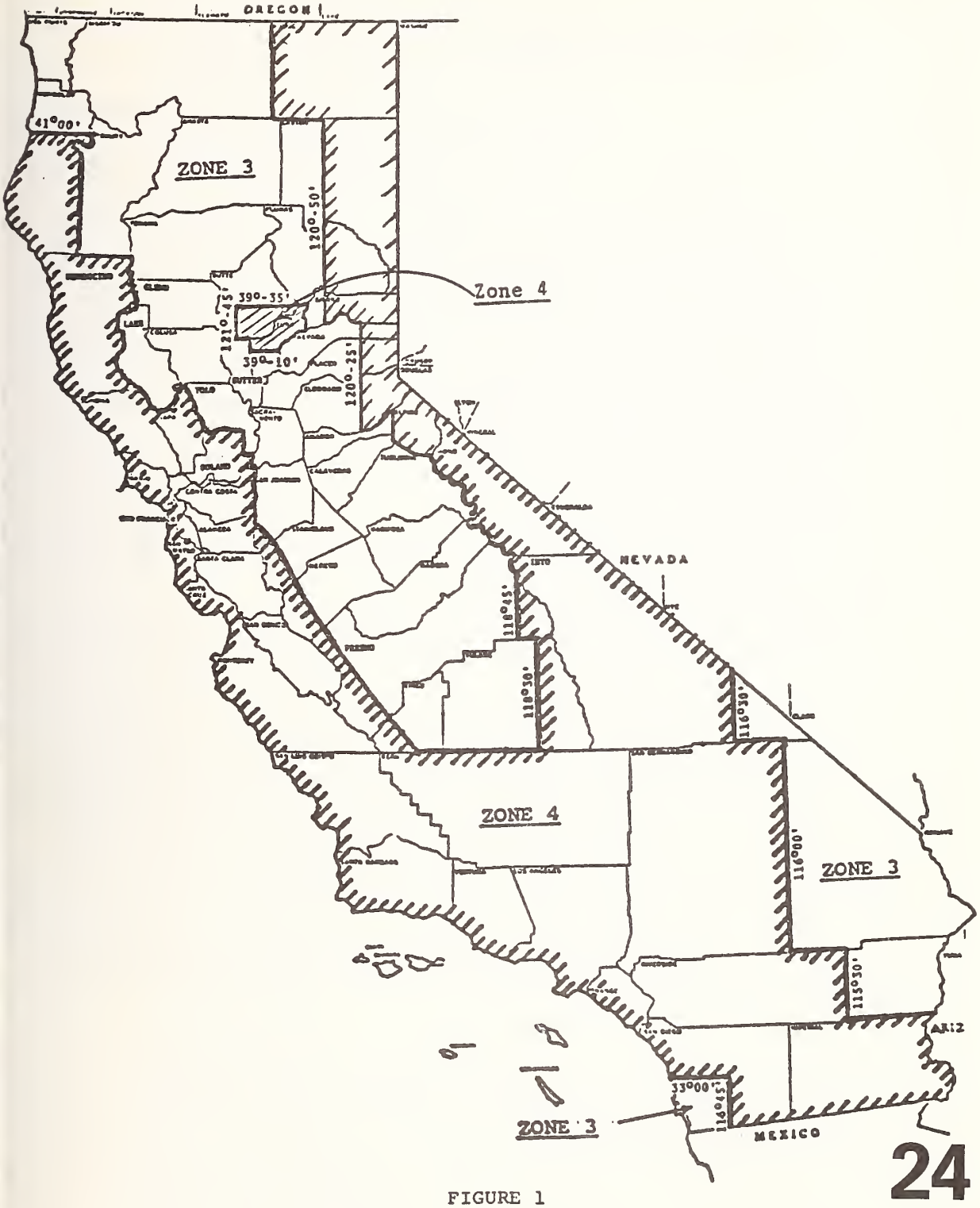
OREGON
41°00'
ZONE 3
120°-50'
Zone 4
121°-15'
39°-35'
39°-10'
120°-25'
NEVADA
118°-15'
118°-30'
114°-30'
ZONE 4
ZONE 3
114°00'
115°-30'
ARIZ
33°00'
114°-15'
ZONE 3
MEXICO

24

FIGURE 1

TABLE 2: HORIZONTAL FORCE FACTOR "C_p" FOR ANCHORAGE OF HOSPITAL NON-STRUCTURAL COMPONENTS*[p]

CATEGORY	DIRECTION OF FORCE	VALUE OF C_p[1,2]	
		I=1.0	I=1.5
1. Mechanical and electrical components			
a. Equipment or machinery[5] not required for life safety systems or for continued operations of essential facilities	Any direction	0.30[3,4]	0.50[3,4]
b. Equipment or machinery[5] required for life safety systems or for continued operation of essential facilities[6]		0.75[3,4]	0.75[3,4]
c. Essential communication equipment and emergency power equipment such as engine generators, battery racks and fuel tanks necessary for operation of such equipment[6]		0.75[3,4]	0.75[3,4]
d. Piping, electrical conduit, cable trays, and air handling ducts		0.50[7]	0.50[7]
2. Hospital equipment[6] when permanently attached to building utility services such as: surgical, morgue and recovery room fixtures, radiology equipment, food service fixtures, essential laboratory equipment, TV supports, etc.	Any direction	0.30[3,4]	0.50[3,4]
3. a. Storage racks with the upper storage level more than 5 feet in height (plus contents)[8]	Any direction	0.30[3,4]	0.50[3,4]
b. Floor supported cabinets and book-stacks more than 5 feet in height (plus contents)[8]		0.30[3,4]	0.50[3,4]
4. Wall hung cabinets and storage shelving (plus contents)	Any direction	0.30	0.50
5. Suspended ceiling framing systems (See Section T17-4701(e))	Any direction	0.30[9]	0.50[9]
6. Suspended or surface mounted light fixtures[10]	Any direction	1.00	1.00
7. Power-cable driven elevators or hydraulic elevators with lifts over 5 feet:			
a. Car and counterweight guides, guide rails, and supporting brackets and framing[11]	See Part 7, Title 24	See Part 7, Title 24	
b. Driving machinery, operating devices and control equipment			

Welded, bolted or other intermittent connections such as inserts shall not be allowed the 1/3 increase in allowable stress.

[1] C_p shall be not less than the ratio of Fx/Wx for floor or roof level under consideration. Where a dynamic analysis is used in the design of the building, the forces so determined may be used in the design of the elements or components with appropriate resistance criteria.

[2] For flexible and flexibly mounted equipment and machinery (Fundamental period of vibration greater than 0.05 seconds), the appropriate values of C_p shall be determined with consideration given to both the dynamic properties of the equipment and machinery and to the building or structure in which it is placed but shall not be less than the listed values. For closely restrained flexible mountings with resilient snubbers a factor of 2 times the values shown may be used except where more appropriate values can be determined. Where a dynamic analysis is not furnished the value C_p shall be doubled.

[3] For equipment and machinery mounted on foundations at grade or floor slabs on earth subgrade the value of C_p may be reduced 1/3.

[4] The component anchorage shall be designed for the horizontal force, F_p, acting simultaneously with a vertical seismic force equal to one-third of the horizontal force, F_p.

[5] Equipment or machinery shall include such items as tanks, boilers, chillers, pumps, motors, air handling units, cooling towers, transformers, switch gear, control panels, etc.

[6] Emergency equipment should be located where there is the least likelihood of damage due to earthquake. Such equipment should be located at ground level and where it can be easily maintained to assure its operation during an emergency.

[7] Seismic restraints may be omitted from the following installations:

(a) Gas piping less than 1 inch inside diameter.
(b) Piping in boiler and mechanical equipment rooms less than 1¼ inch inside diameter.
(c) All other piping less than 2½ inch inside diameter.
(d) All piping suspended by individual hangers 12 inches or less in length from the top of pipe to the bottom of the support for the hanger.
(e) All electrical conduit less than 2½ inch inside diameter.
(f) All rectangular air handling ducts less than 6 square feet in cross sectional area.
(g) All round air handling ducts less than 28 inches in diameter.
(h) All ducts suspended by hangers 12 inches or less in length from the top of the duct to the bottom of the support for the hanger.

[8] In lieu of the tabulated values steel storage racks may be designed in accordance with UBC Standard No. 27-11.

[9] Ceiling weight shall include all light fixtures and other equipment which are laterally supported by the ceiling. For purposes of determining the lateral force, a ceiling weight of not less than 4 pounds per square foot shall be used.

[10] Suspension systems for light fixtures which have passed shaking table tests approved by the Office of the State Architect or which, as installed, are free to swing a minimum of 45° from the vertical in all directions shall be assumed to comply with the lateral force requirements of Section T17-2312(1).

Unless of the cable type, free swinging suspension systems shall have a safety wire or cable attached to the fixture and structure at each support capable of supporting 4 times the support load.

[11] W_p for elevator cars shall be the weight of the car plus 0.4 times its rated load. The lateral forces acting on guide rails shall be assumed to be distributed 1/3 to the top guide rollers and 2/3 to the bottom guide rollers of elevator cars and counter weights.

25

SUMMARY OF RESEARCH PROJECTS IN THE LARGE-STRUCTURES TESTING LABORATORY FROM 1967-1977

Masaya Hirosawa
Yuji Ishiyama
Tetsuro Goto

Ministry of Construction

Summary of Research Projects in the Large-Structures Testing Laboratory from 1967-1977

Structural design should always be carried out on the basis of theory and test results. Test results obtained by using a small-scale model of a structure or a full-scale test of structural components give us invaluable information on the behavior of structures, but they do not always satisfy the practical engineer's requirements. The problem of dimensional similarity between the prototype and model structures frequently occurs.

To solve such problems, the Ministry of Construction suggested the construction of a Large-Structures Testing Laboratory and the budget was allocated to the Japan Housing Corporation in the fiscal year of 1966. The planning and basic design of the Laboratory were performed by the staffs of the Building Research Institute and the Japan Housing Corporation, and the Laboratory was built in 1967.

This Laboratory consists of a L-shaped testing bed and vertical reaction wall of prestressed concrete and the shed of reinforced concrete with several testing rooms. The height of the reaction wall is 16 meters and the size of the testing bed is 9.5 meters by 20 meters. Horizontal loads can be applied both in pushing and pulling directions against the wall and the vertical loads can be applied simultaneously keeping the vertical loads constant by the accumulation of oil. The capacity of the reaction wall is 1,000 tons in shear and 10,000 ton-meters in bending moment. Accordingly, five storied full-scale reinforced concrete buildings with two housing units on each floor can be tested in this Laboratory (see fig. 1).

Since the completion of the Laboratory, research projects testing full-scale or large-scale specimens of the buildings have been carried out. Summaries of the main projects are reported in the following chapters. 1977 will be its last year because the Laboratory will be demolished in 1978 or 1979 with the removal of Building Research Institute to Tsukuba Science City.

1967: Test on a Five-Story Apartment House of Precast Reinforced Concrete Panels

The test specimen was a full-scale five-story building with two living units on each floor designed by Japan Housing Corporation according to the general design method. The plan of the specimen was 14.3 meters long and 6.1 meters wide, the height was 12.8 meters, and the weight was 430 tons including the live load, which was not actually loaded in the test. The wall thickness was 15.cm and the wall ratio was 28.3 cm/m^2 at each floor. The vertical joints were the so-called wet joints that use cement mortar; the horizontal joints were dry joints that connect the embedded steel plates or bars with welding (see fig. 2).

The same amount of horizontal load was applied at each floor level in the longitudinal direction; these loads were alternated by pulling and pushing with three oil-jacks at each floor; 15 in total.

Bending cracks appeared in the beams at the design load, which can be calculated multiplying the sum of the dead load and the live load by the seismic design coefficient that is generally 0.2 according to the Japanese Building Standard. As the load increased bending cracks in beams and shear cracks in walls progressed. The maximum load carrying capacity was 651 tons, which was 7.6 times

the design load of 86 tons. The horizontal displacements at the maximum load were 4.7 cm at the top of the specimen and 1.9 cm at the second floor, which corresponded to 1/270 and 1/131 of the respective heights. As the deflection increased after this maximum point, the load-carrying capacity decreased gradually to 0.77 of the maximum load at a displacement of 16.7 cm at the top, which was 1/77 of the height. During this loading, shear cracks in walls progressed significantly and many new shear cracks appeared in the beams. The final failure mechanism was shear failure of the first and the second story walls. It is significant that the specimen could endure large deflection after this maximum load without appreciable strength deterioration (figs. 3 and 4).

Several conclusions were drawn from this work:

(1) This specimen would have enough reserve strength against severe earthquakes. Accordingly, it would be possible to reduce the wall ratio.

(2) It would be possible to reduce the number of reinforcing bars in the wall panels and vertical reinforcement in the vertical joints.

(3) The following assumptions could be used in design calculations: (a) the rigidity of the floor slabs could be assumed as infinite, and (b) the vertical joint could be considered as monolithic.

A recommendation for the structural design of such precast concrete buildings was completed in 1971 and thousands of apartment houses have been constructed by Japan Housing Corporation with this construction method.

1968: Test on a Five-Story Apartment House of Monolithic Reinforced Concrete

The plan of the specimen was 13 meters long and six meters wide. The height was 13 meters and the weight was 450 tons including the live load, which was not actually loaded in the test. The wall thickness was 15 cm and the wall ratio was 12 cm/m^2 at each floor. The specimen was designed to have a wall ratio and wall thickness that were smaller than the requirements of the Japan Housing Corporation (see fig. 5).

The horizontal loads were applied in the longitudinal direction same as in the 1967 project.

Bending cracks appeared in the beams at the design load and shear cracks in the walls gradually appeared as the load increased. The maximum load-carrying capacity was 390 tons, which was 4.1 times the design load of 90 tons. The displacements at the maximum were 4.9 cm at the top of the specimen and 1.8 cm at the second floor. These values were 1/266 and 1/140 of the respective heights. Thereafter the displacement at the top reached the maximum of 7.3 cm, was 1/180 of the height with a decreased strength to 0.74 of the maximum value. Shear failure in the first-story walls was critical to the load-carrying capacity (see figs. 6 and 7).

This work resulted in the following conclusions:

(1) This specimen was provided only with the minimum load capacity and ductility. According to the

dynamic analysis, this structure would be damaged heavily by a strong earthquake.

(2) Positions and sizes of openings in the walls should be changed for uniform distribution of wall rigidities.

(3) The wall in the first story should be reinforced with more steel bars to improve the ductility of the building.

From the results of this test, it became clear that the structural regulations that had been used for buildings up to four stories could also be used for the five-storied ones. The Japan Housing Corporation issued the structural design specifications of five-storied buildings of reinforced concrete wall construction. Wall ratios and wall thicknesses specified by the Japan Housing Corporation differ from the specimen of this test as follows:

	Specimen	Specification
Wall thicknesses	15 cm	18 cm (in the longitudinal direction) 15 cm (in the transverse direction)
Wall ratios	12 cm/m^2	15 cm/m^2

1969: Test on an Eight-Story Apartment House of Precast Prestressed Concrete

The project was to test a eight-story apartment house of precast prestressed concrete. This structural system had been developed in 1965 at the Building Research Institute. The main purpose was to obtain data to design and construct building that use this structural system.

The test specimen was the full-scale four-storied building corresponding to the lower four stories of an eight-story apartment house. Each floor had two of the half living units. This structure consisted of precast reinforced concrete structural elements, i.e., L, +, T, and I shaped wall columns, girders and slabs. The vertical connections between columns and girders are made by a post-tensioning method. The prestressing bars anchored in the foundation are extended through the column and girder coupling at each floor level. These bars are tensioned and grouted after completion of assembly. The joints between floor slabs and girders are made by welding the steel plates anchored in each element. The plan of the specimen was 11.7 meters long and 4.6 meters wide; the height was 10.8 meters and the weight was 600 tons including the upper four stories dead load and the total live load. The wall thickness was 18 cm and the wall ratio per unit floor area was 13.7 cm/m^2 (see fig. 8).

The horizontal loads were applied in the longitudinal direction by eight hydraulic jacks at the top of the specimen, four at the fourth floor level and two at the third and second floor levels. The vertical loads that corresponded to upper four-story dead load and the total live load of an eight-story actual building were also

applied by 12 hydraulic jacks connected to the accumulator to keep the vertical load constant during the application of the horizontal load.

Fairly linear relations between the loads and the displacements were observed up to 1.2 times the design load of 120 tons. No cracks in the columns but slight bending cracks in the beams were observed at this load. The bending cracks in the beams developed to shear cracks at 2.9 times the design load, while the initial shear cracks in the columns appeared at 3.2 times the design load. The maximum load-carrying capacity was 3.9 times the design load. The displacements at the maximum load were 10.5 cm at the top of the specimen and 3.3 cm at the second floor, which were 1/103 and 1/82 of the respective heights. The final failure mechanism was the shear failure of second and third floor beams; further repetition of the load did not cause any significant decreasing of the load-carrying capacity. At the final load the displacements reached to 1/62 at the top of the specimen and 1/47 at the second floor of the respective heights (see figs. 9 and 10).

The following conclusions were drawn:

(1) This specimen had a considerable ductility compared to the shear wall structures.

(2) In the actual eight-story buildings, the final failure would be caused by the failure of the first story columns and the shear reinforcement of the columns should be increased.

(3) Because of the early shear failure of the beams, shear reinforcement of the beams should be increased by twice of that of the specimen.

(4) The closely spaced reinforcement at the corner of the columns was very effective in preventing the development of shear cracks and the crushing of the enclosed concrete.

(5) From the dynamic analysis the specimen had a sufficient capacity to endure severe earthquakes with the maximum acceleration 300 gals.

In 1970, an eight-story apartment house with 104 units was built in Tokyo with this structural system. Since then, two thousand such housing units have been constructed.

1970: Test on a Five-Story Apartment House of Monolithic Reinforced Concrete with Staggered Plan and Elevation

The test specimen was the full-scale five-story building and had five living units on one side and four on the other. The floor levels of both sides were staggered by half of a story and the longitudinal walls of both sides were also staggered by the half a wall. The plan of the specimen was 13 meters long and 5.4 meters wide, the height was 14 meters and the weight was 450 tons including the live loads, which were not actually loaded in the test. The wall thicknesses were 18 cm from first to the fourth story and 15 cm at at the fifth story. The wall ratio was 15 cm/m^2 at each floor (see fig. 11). The horizontal loads were applied in the longitudinal direction same as the 1967 project.

At the design load there were only few hair cracks at the corner of openings. At three times the design load, diagonal shear cracks occurred. The maximum load was 452 tons, which was 5.0 times the design load. The displacements at the maximum load were 8.8 cm at the top of the specimen and 2.8 cm at the second floor, which were 1/150 and 1/100 of the respective height. At the maximum load, the first story walls failed in shear severely and bars in the walls were exposed.

The load-carrying capacity decreased after the maximum load with increased displacement and at the maximum displacement the load capacity was 0.65 of the maximum load. At this load the displacements were 1/100 at the top and 1/35 at the second floor of the respective heights and the shear failure progressed continuously. A great many broken pieces of concrete fell down (see Figs. 12 and 13).

The following conclusions were drawn:

(1) This specimen had enough strength to withstand severe earthquakes.

(2) The effect of staggered plan and elevation would not cause any structural defects.

(3) The first story, which had higher floor level than the other, would be damaged most heavily.

(4) The cracks around the small openings of the first story walls would be 20 mm wide at the maximum load, so more ductility around the openings would be advisable.

1971: Test on a Ten-Story Apartment House of Precase Prestressed Concrete

The test specimen was the full-scale four-storied frame model corresponding to the lower four stories of a ten-storied apartment house. The plan of the specimen was 7.2 meters long and two meters wide, the height was 10.8 meters and the weight was 518 tons including the upper six stories dead load and the total live load. The wall thickness was 18 cm and the wall ratio per unit floor area was 17.4 cm/m^2 (see fig. 14).

A horizontal load was applied in the transverse direction of the building, i.e. in the longitudinal direction of the specimen, by eight hydraulic jacks at the top of the specimen. The vertical load, which corresponded to the upper six stories dead load and the total live load of a ten-story actual building, was intermittently applied by 12 hydraulic jacks.

Fairly linear relations between the loads and the displacements were observed up to two times the design load of 104 tons. No cracks appeared at the design load. Bending cracks in the beams and vertical cracks along the vertical joints appeared at two times the design load. At three times the design load, the bending cracks in the beams and the columns developed into shear cracks. The maximum load carrying capacity was 400 tons, 3.85 times the design load. The displacements at the maximum load were 4.1 cm at the top of the specimen and 1.4 cm at the second floor, which were 1/261 and 1/188 of the respective heights. The final failure mechanism was the shear failure of the second floor beams. At the final load, 2.4 times the design load and 0.61 of the maximum load, the displacements

reached 18.3 cm at the top and 6.0 cm at the second floor, which were 1/59 and 1/45 of the respective heights (see Figures 15 and 16).

This test underscored the following:

(1) The final failure mechanism would be the shear failure of the beams both in the longitudinal direction and transverse direction.

(2) At three times the design load, cracks would be slight.

(3) The maximum load-carrying capacity would be four times the design load.

About two thousand housing units have been constructed with this structural system in Tokyo and Kanagawa Prefecture. The number of stories are five or eight. A ten-story apartment house like this has been constructed in Shizuoka Prefecture; it has 70 living units.

1972: Test on an Eight-Story Apartment House of Reinforced Concrete

The specimen was a full-scale four-story building corresponding to the lower four stories of an eight-story apartment house and each story had two living units. The plan of the specimen was 11.2 meters long and 7.0 meters wide, the height was 10.4 meters and the weight was 1,090 tons including the upper four stories dead load and the total live load. The wall column thickness was 30 cm and the wall ratio per unit floor area was 6.6 cm/m^2 in the longitudinal direction, while in the transverse direction the wall thickness was 18 cm and the wall ratio was 22.8 cm/m^2 (see fig. 17).

The horizontal load was applied in the longitudinal direction by eight hydraulic jacks at the top of the specimen, four or eight at the fourth floor level and two at the third and second floor levels. The vertical load, which corresponded to the upper four stories dead load and the total live load of a eight-storied actual building, was also applied by 12 hydraulic jacks keeping the vertical load constant.

Fairly linear relations between the loads and the displacements were observed up to two times the design load of 218 tons. Bending cracks appeared in the beams at half the design load. After that the bending cracks in the beams and the wall columns progressed gradually and at two times the design load shear cracks in the wall columns were observed from the first story to the fourth story. Cracks did not concentrate but spread over the beams and the wall columns. As the load increased, the bending cracks at the end of the beams became severe and at the final loading the first story wall columns were crushed. No deterioration of strength was seen at the final loading. The final load was 990 tons, 4.5 times the design load. The displacements were 15 cm at the top of the specimen and 7.0 cm at the second floor, which were 1/69 and 1/37 of the respective heights (see Figs. 18 and 19).

The maximum displacement at the top was limited by the strokes of the hydraulic jacks.

The following points were concluded:

(1) The final failure mechanism would be the bending failure of the beams.

(2) The maximum load carrying capacity was 4.5 times the design load. Accordingly, the strength could be minimized within limits not spoil the ductility of the structure.

(3) The minimum required ductility was satisfied, which was considered to be 1/50 of the height.

1973: Test on a Eleven-Story Apartment House of Precast Concrete

The test specimen in the longitudinal direction was the full-scale four-story frame with two spans, which corresponded to the lower four of an eleven-story 14-span apartment house. The basic precast concrete members were beams with halves of upper and lower columns on both ends. The specimen was 11.1 meters long, the height was 10.8 meters, and the weight was 650 tons including the dead load of the upper seven stories and the total live load. The columns were 87 cm wide and 55 cm thick. The beams were 40 cm thick and 55 cm high. The special coupler joints were used to connect the beams. Mortar-filled sleeve joints were adopted to connect the columns (see fig. 20).

The test specimen in the transverse direction was a half-scale eight-story shear wall with one span, which corresponded to the lower eight stories of an eleven-story with one span apartment house. The main precast concrete members were the columns with beams, which also composed the longitudinal rigid frame, and the shear walls with the beams on the tops. The specimen was 4.5 meters long, the height was 10.8 meters, and the weight was 125 tons including the dead load of upper three stories and the live load. The cross section size of the columns was 27.5 cm by 43.5 cm and the walls were 7.5 cm thick with 15 cm by 25 cm beams at the tops. To connect between the columns, mortar filled sleeve joints were used and the embedded bars were welded to connect the columns to the beam. To connect the walls to the columns and the beams, so-called wet joints were adopted using the spiral reinforcements (see fig. 21).

In the longitudinal direction, the horizontal load was applied at the top of the specimen by eight hydraulic jacks. The vertical load was also applied by 12 hydraulic jacks.

In the transverse direction, the horizontal load was applied at the top of the specimen by two oil jacks. The vertical load was also applied by four oil jacks.

In the longitudinal direction, bending cracks appeared in the third floor beams at the load of 40 tons, which was 0.31 of the design load of 130 tons. Fairly linear relations between the loads and the displacements were observed up to the design load. At the design load, cracks appeared at the connections between the beams along the main bars of the beams, diagonal cracks appeared at the panel zones of the columns and the beams, and the displacement at the top of the specimen was 3.7 cm which was 1/292 of the height. At 1.2 times the design load, the compression bars in the columns began to yield and at 1.4 times the design load the tension bars in the beams began to yield, causing a gradual decreasing of the stiffness. At 1.7 times the design load, the outside first story column began to crush and the displacement at the top was 11.4 cm, which was 1/94 of the height. After this load, the displacement increased without an obvious increase in load. At the maximum load, 1.8 times the design load, the displacement at the top became 21 cm, which was 1/51 of the height. At the final stage, the

displacement at the top became 43 cm, which was 1/25 of the height without any evident decreasing of the load. The final failure mechanism was the bending failure of the columns and the beams (see figs. 22 and 23).

In the transverse direction, fairly linear relations between the loads and the displacements were observed up to the design load of 25 tons. At the design load bending shear cracks appeared in the first story wall, bending cracks also appeared at the joint between the first story columns, and the displacement at the top of the specimen was 0.63 cm, which was 1/1690 of the height. At 1.3 times the design load, bending cracks in the foot of the first columns appeared and at 1.4 times the design load, shear cracks appeared in the walls from the fourth to the sixth story, causing a gradual decreasing of the stiffness. The maximum load was 1.9 times the design load. At this load the displacement at the top was 4.2 cm, which was 1/256 of the height. At the final stage, the load was 0.85 of the maximum load and the displacement at the top was 7.2 cm, which was 1/147 of the height. The final failure mechanism was the yielding of the main tension bars of the first-story columns, which caused a slippage between the foundation and the first-story shear wall (see figs. 24 and 25).

This test led to the following conclusions:

(1) Since the final failure mechanism of the rigid frame in the longitudinal direction was a bending failure of the columns and beams, it was felt that this frame had a considerable ductility to resist a strong earthquake.

(2) The final failure mechanism of the shear wall in the transverse direction was the yielding of the main tension bars of the first story columns; there was no obvious destruction in the other parts. The connections between the main bars of the columns should be improved.

1974: Test on a Eight-Story Apartment House of Precast Concrete

The test specimen was the full-scale five-story shear wall that corresponded to the lower five stories of an eight-story apartment house in the transverse direction. The wall was 18 cm thick precast concrete from the first to th fourth story; the fifth-story wall was cast-in-place reinforced concrete. The test specimen was 8.3 meters long, the height was 13 meters, and the weight was 283 tons, including the upper three stories dead load and the total live load (see Fig. 26).

In the longitudinal direction the test specimens were the full-scale precast members of the beams with columns; test results are not discussed here.

The horizontal load was applied at the top of the specimen by six hydraulic jacks. The vertical load was applied by eight oil jacks.

Fairly linear relations between the loads and the displacements were observed up to 1.5 times the design load of 57 tons. At the design load, bending cracks appeared in the wall beams that faced the openings. Shear cracks occurred at 2.5 times the design load. The maximum load was five times the design load. At this load, the displacement on top of the specimen was 7.0 cm, which was 1/200

of the height. At the final stage the displacement at the top reached 30 cm, which was 1/46 of the height and the load became 0.67 of the maximum load. The final failure mechanism was the shear failure of the wall beams (see figs. 27 and 28).

This test resulted in the following conclusions:

(1) The specimen had enough strengtH7fK7resist strong earthquakes.

(2) The allowable maximum displacement at the top of the specimen would be 7.0 cm, which was 1/200 of the height.

(3) Shear failure in the wall beams should be avoided.

1975: Test on an Eleven-Story Apartment House of Steel-Encased Reinforced Concrete

The test specimens were a half-scale five story shear wall corresponding to the lower five stories of an eight-story apartment house in the transverse direction. The first specimen (A) was a cast-in-place steel-encased reinforced concrete wall without openings; the second one (B) was a cast-in-place steel-encased reinforced concrete wall with openings; and the last one (C) was a precast steel-encased reinforced concrete wall. Each specimen was 4.3 meters long, the height was 6.8 meters, and the weight was 180 tons, including the upper six stories dead load and the total live load. The wall thicknesses were 7.5 cm for the one with no openings (A) and 9.0 cm for the ones with openings (B) and (C). The size of the columns was 42.5 cm by 30 cm and the beams were 20 cm by 37.5 cm (see fig. 29).

The horizontal load was applied at the top of the specimen by two oil jacks. The vertical load was also applied by eight oil jacks not only to compensate for the upper six stories dead load and the total live load of the eleven-story building but to give the same shear span ratio as to the actual shear wall applying more load at the compression side than the tension side.

Specimen (A) (no openings)

Fairly linear relations between the loads and the displacements were observed up to the design load of 26 tons. At this load, bending cracks appeared in the foot of the first-story column and the displacement at the top of the specimen was 0.4 cm, which was 1/1680 of the height. At 1.2 times the design load, shear cracks appeared in the walls. The maximum load was 3.5 times the design load and the displacement at the top was 1/100 of the height. At the final stage, the load decreased to 0.1 of the maximum load. After a triple repetition the displacement was 1/100 of the height. The final failure mechanism was the shear failure of the wall and the compression side column (see Figs. 30 and 31).

Specimen (B) (with openings)

Bending cracks appeared in the foot of the first-story column at 0.8 times the design load of 36 tons. Fairly linear relations between the loads and displacements were observed up to the design load. The displacement at the top of the specimen was 0.7 cm, which was 1/960 of the height. At 1.2 times the design load, shear cracks appeared in the walls. The maximum load was 3.2 times the design load; the displacement at the top was 1/100 of the height. At the final stage, the displacement at the top was 1/60 of the height and

the load became 0.6 of the maximum load. The final failure mechanism was almost the same as specimen (A). See Figures 32 and 33.

Specimen (C) (precast concrete with openings)

Bending cracks appeared in the foot of the lst-story column and in the 2nd and 3rd floor beams facing to the openings at 0.7 times the design load of 26 tons. At the design load, shear cracks appeared in the walls from first to fourth story and the displacement was 0.7 cm, which was 1/960 of the height. Fairly linear relations were observed up to the design load. As the load increased, shear cracks in the walls progressed to bending shear cracks and bending cracks in the beams progressed to shear cracks. The maximum load was 3.4 times the design load and the displacement at the top was 1/100 of the height. Diagonal bars in the compression side first-story shear wall buckled at the maximum load. At the final stage, the displacement at the top reached 1/50 of the height and the load decreased to 0.7 of the maximum load. The final failure mechanism was almost the same as specimens (A) and (B). See Figs. 34 and 35.

This test resulted in the following conclusions:

(1) Bending failure occured before the shear failure in all three specimens.

(2) After the maximum load, the stiffness decreased because of the shear failure in the first-story walls and columns.

(3) Allowable displacements would mainly depend on whether the shear walls had openings or not.

1976: Test on an Eleven-Story Apartment House of Steel-Encased Reinforced Concrete

The test specimen was a half-scale five-story building corresponding to the lower five stories of an eleven-story apartment house. The plan of the specimen was 4.3 meters long and 2.7 meters wide, the height was 6.3 meters, and the weight was 240 tons, including the upper six stories dead load and the total live load. The thickness of the shear walls was 9.0 cm and the thickness of the partition walls was 6.0 cm (see Fig. 36).

The horizontal load was applied at the top of the specimen by four hydraulic jacks. The vertical load was also applied by eight hydraulic jacks not only to compensate for the upper six stories dead load and the total live load but to give the same effect as that of an eleven-story building, changing the tension and the compression side vertical loads according to the overturning moment caused by the horizontal load.

Fairly linear relations between the loads and the displacements were observed up to the design load of 48 tons. At 1.3 times the design load, bending cracks appeared in the lst-story columns and partition walls. At two times the design load, shear cracks appeared in the shear walls and at three times the design load, shear cracks appeared in the partition walls. At 4.7 times the design load, the displacement at the top of the specimen reached 1/200 of the height, shear cracks spread over the shear walls and partition walls, and the reinforcements yielded in the tension side of the first story columns. The maximum load was 5.7 times the design load and the displacement at the top was 1/100 of the height.

At the final stage, the displacement at the top reached 1/50 of the height and the load decreased to 0.6 of the maximum load. The final failure mechanism was the shear failure of the first-story shear walls and columns (see Figs. 37 and 38).

This test resulted in the following conclusions:

(1) The partition walls bear 0.3 of the horizontal load at the early stage.

(2) At the final stage the partition walls could not resist the horizontal load because of the slippage between the foundation and the walls.

(3) The final failure was the shear failure of the first-story shear walls and compression side columns.

1977: Test on an Eleven-Story Apartment House of Steel-Encased Reinforced Concrete

The test specimens were a half-scale three-story frame corresponding to the lower three stories of eleven-story apartment house in the longitudinal direction. Specimen (D) was a cast-in-place steel-encased reinforced concrete frame without walls, specimen (E) had walls along the columns, and specimen (F) had walls with openings in the frame. Each specimen was 6.5 meters long, the height was 4.2 meters, and the weight was 250 tons including the upper eight stories dead load and the total live load. The columns were 30 cm thick and 42.5 cm wide. The beams were 22.5 cm thick and 37.5 cm deep. The wall thickness was 6.0 cm (see fig. 39).

The horizontal load was applied at the top of the specimen by four hydraulic jacks. The vertical load was also applied by six hydraulic jacks corresponding to the upper eight stories dead load and the total live load.

Although precise data are not yet available, the following conclusions could be drawn:

(1) The effect of the nonbearing walls would be 0.2 of the horizontal stiffness and strength at the early stage.

(2) At the final stage, nonbearing walls would bear no load.

(3) The nonbearing wall would cause no significant structural defects.

References

1. Koizumi, Y. and Others, "Lateral Load Test on Multi-storied Full-size Building of Reinforced Concrete Wall Construction for Earthquake Resistant Design", BRI Research Paper No. 49, May 1971, Building Research Institute, Ministry of Construction.

2. Annual Reports of BRI, from 1967 to 1976, Building Research Institute, Ministry of Construction.

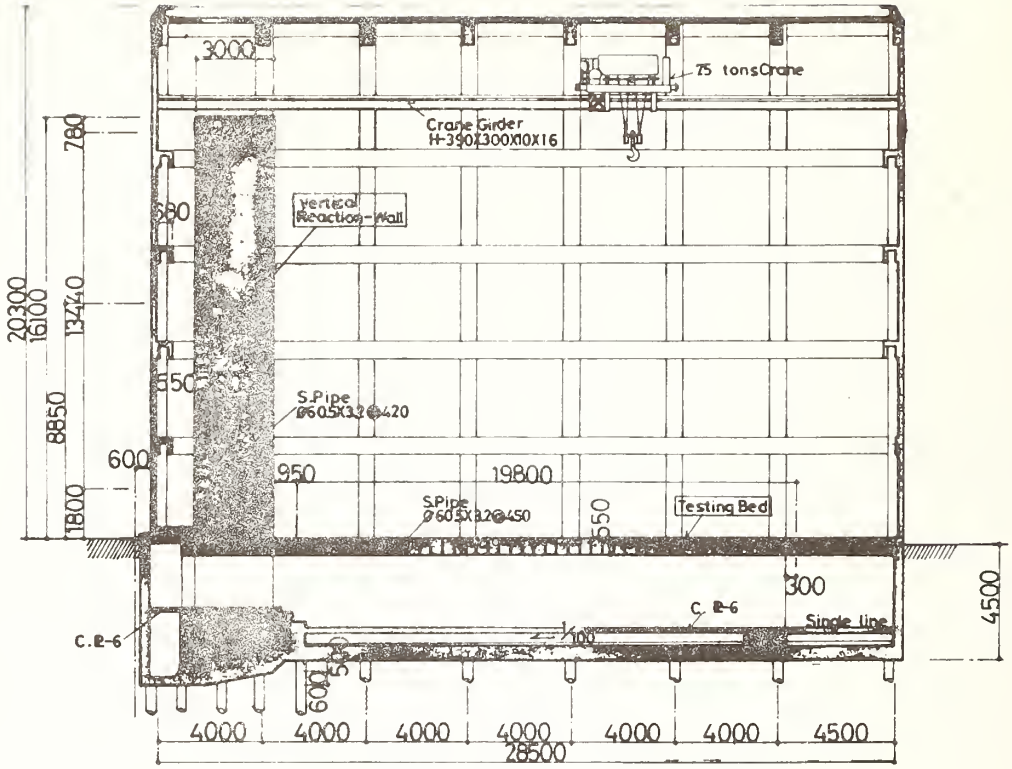

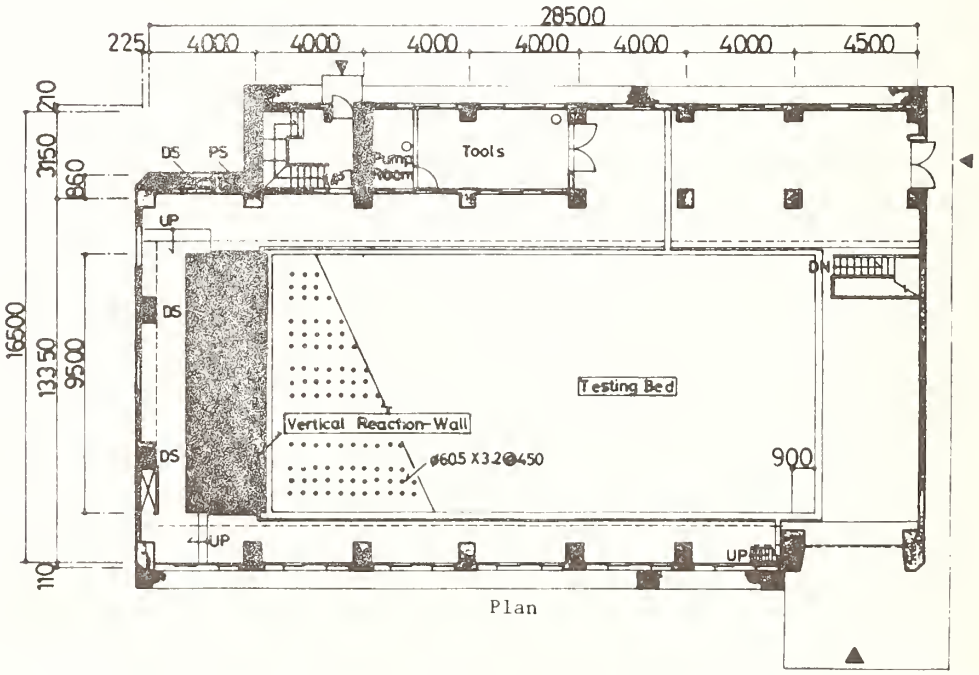

FIGURE 1. LARGE SIZE STRUCTURES TESTING LABORATORY (Unit:mm)

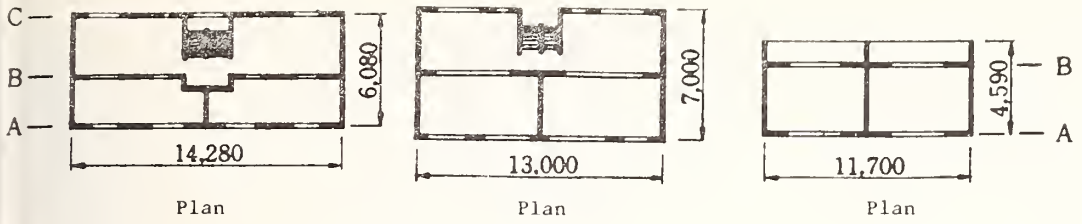

Plan Plan Plan

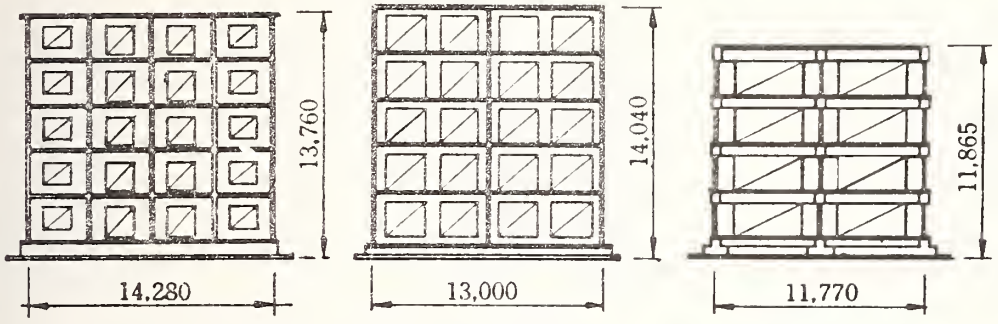

Skeleton(A) Skeleton(A) Skeleton(A)

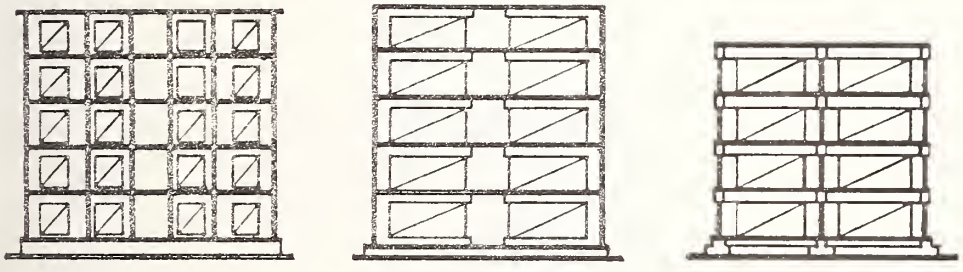

Skeleton(B) Skeleton(B) Skeleton(B)

FIGURE 8 (1969)

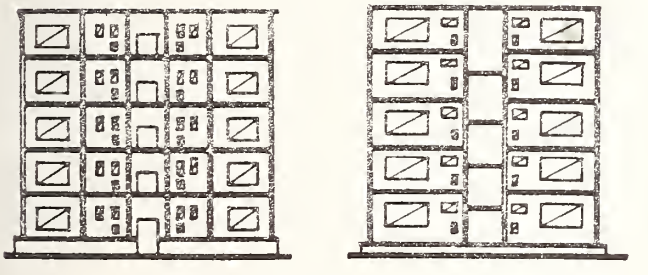

Skeleton(C) Skeleton(C)

FIGURE 2 (1967) FIGURE 5 (1968)

Plans and Elevations of Test Specimens (from 1967 to 1969) (Unit:mm)

25

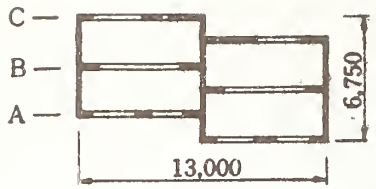

Plan

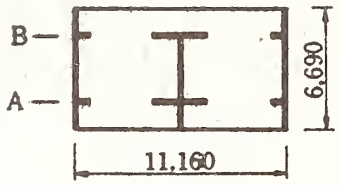

Plan

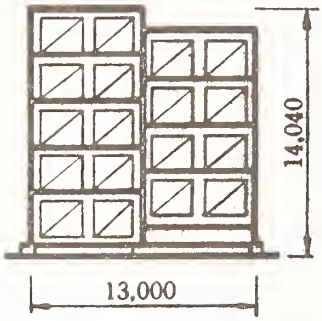

Skeleton(A)

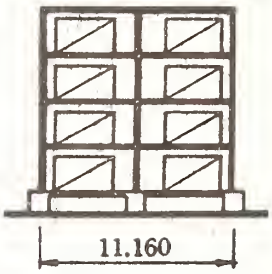

Skeleton(A)

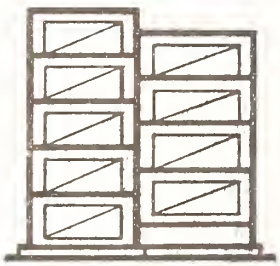

Skeleton(B)

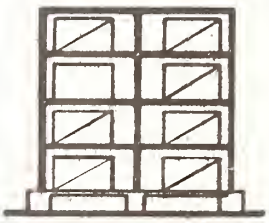

Skeleton(B)

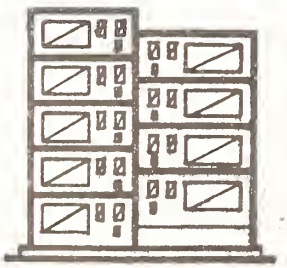

Skeleton(C)

FIGURE 11 (1970)

FIGURE 17 (1972)

Plans and Elevations of Test Specimens (1970 and 1972) (Unit:mm)

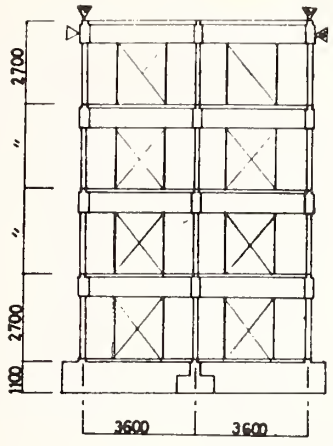

FIGURE 14: TEST SPECIMEN (1971)

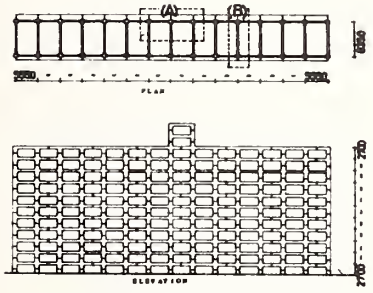

Prototype Building (1973)

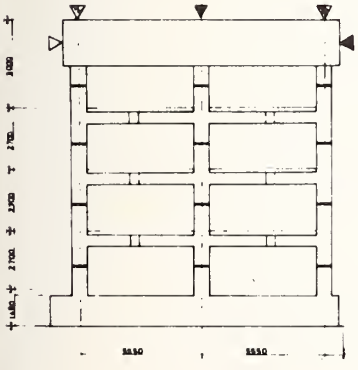

FIGURE 20: TEST SPECIMEN (1973)

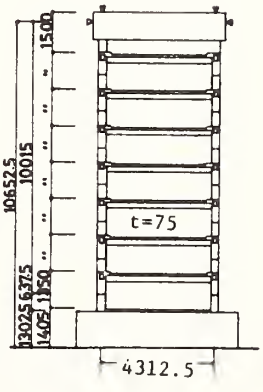

(Unit:mm)

FIGURE 21: TEST SPECIMEN (1973)

25

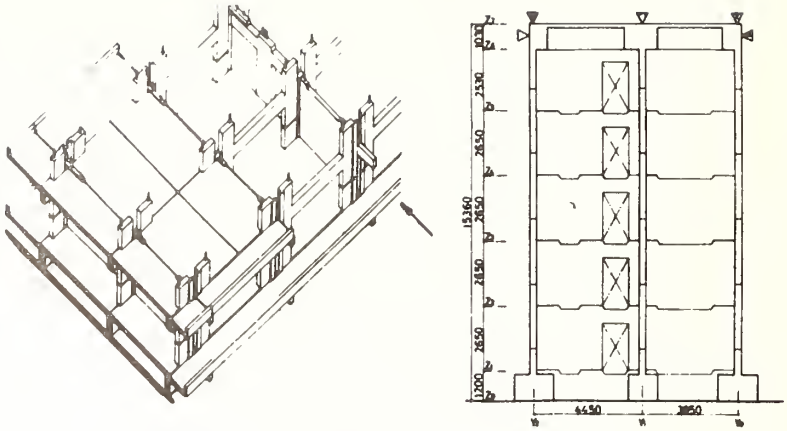

FIGURE 26 TEST SPECIMEN (1974)

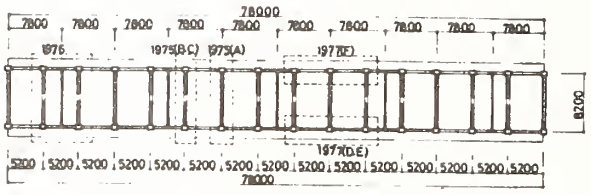

Plan of the Prototype Building (1975,'76 and '77)

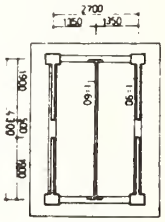

FIGURE 36 TEST SPECIMEN (1976)

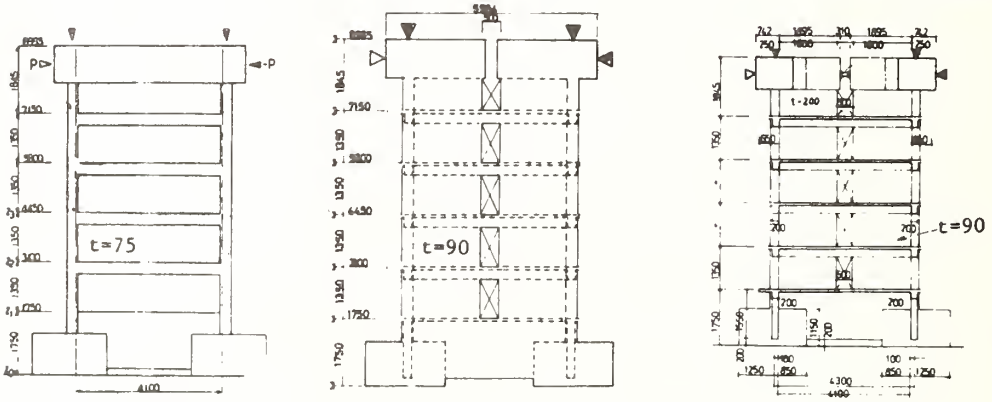

Specimen(A) Specimen(B) Specimen(C)

FIGURE 29 TEST SPECIMEN (1975)

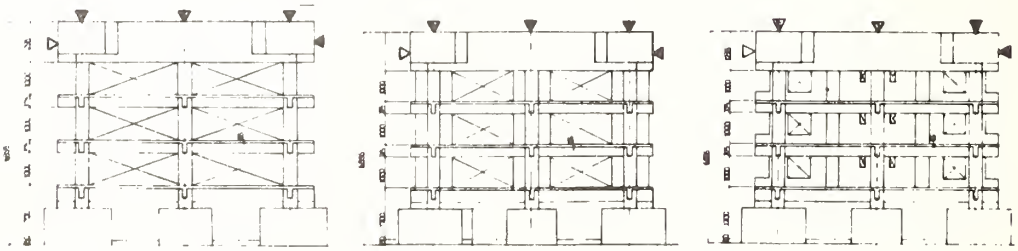

Specimen(D) Specimen(E) Specimen(F)

FIGURE 39 TEST SPECIMEN (1977)

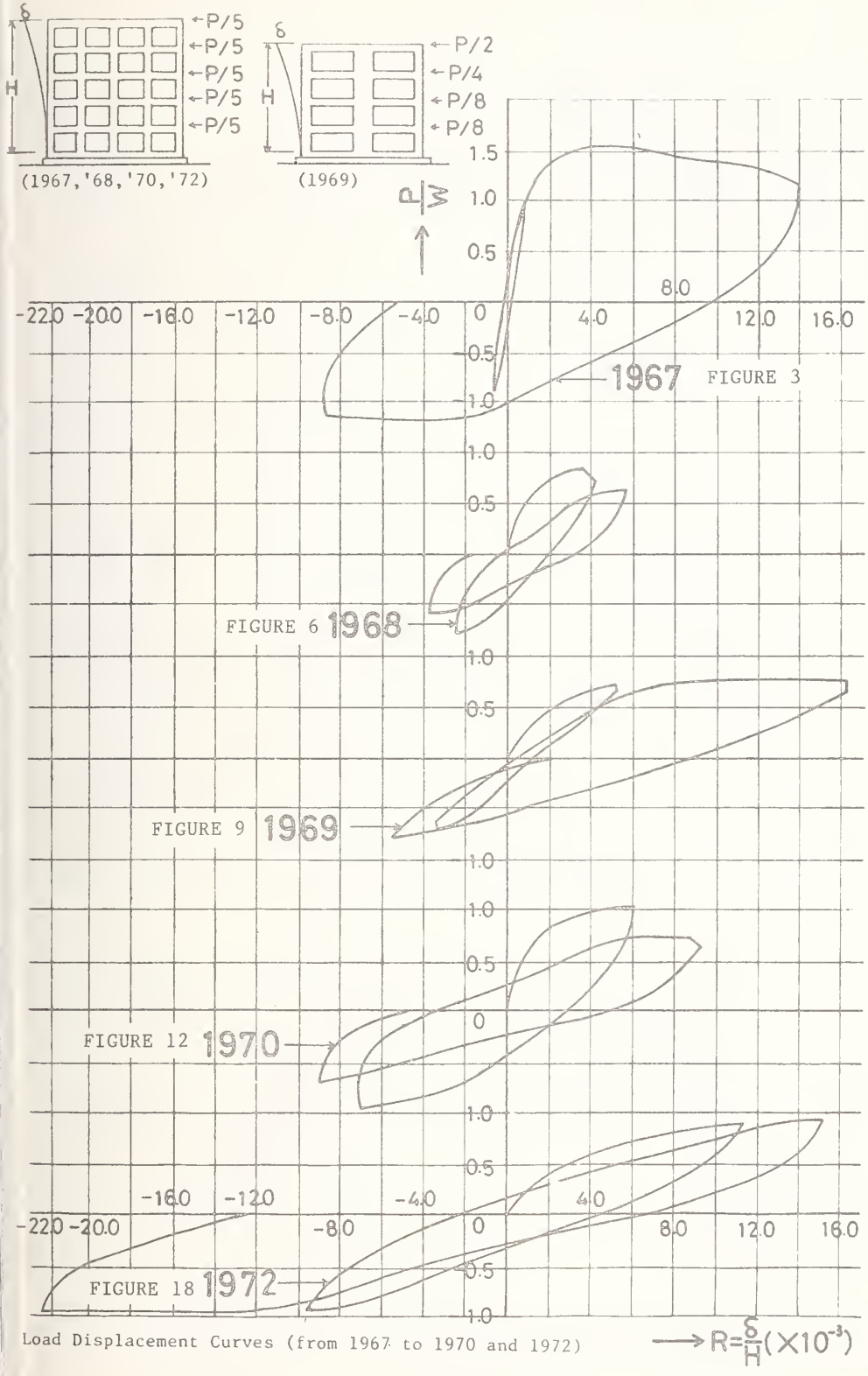

Load Displacement Curves (from 1967 to 1970 and 1972)

25

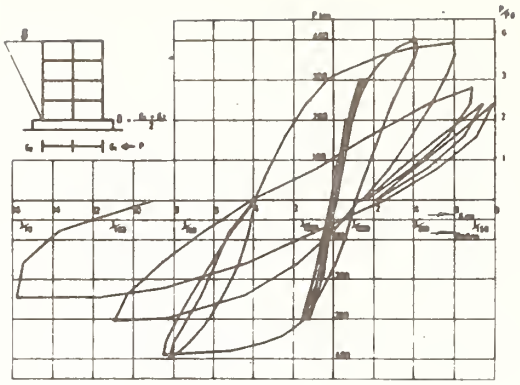

FIGURE 15 LOAD DISPLACEMENT CURVE (1971)

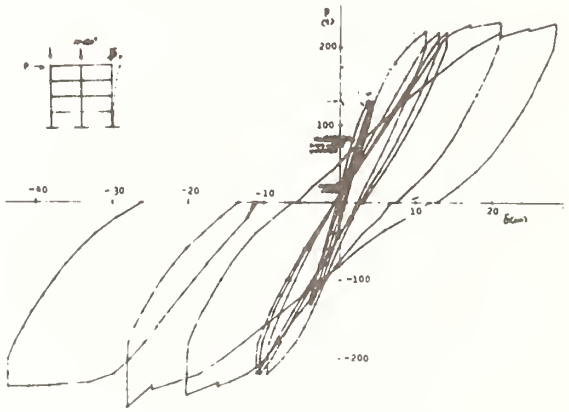

FIGURE 22 LOAD DISPLACEMENT CURVE OF SPECIMEN(A) (1973)

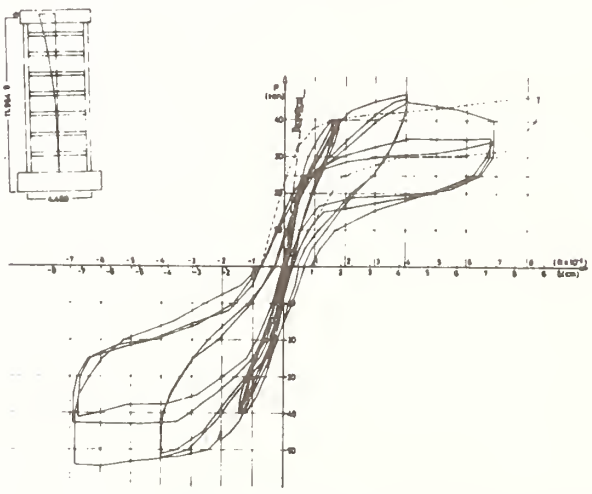

FIGURE 24 LOAD DISPLACEMENT CURVE OF SPECIMEN(B) (1973)

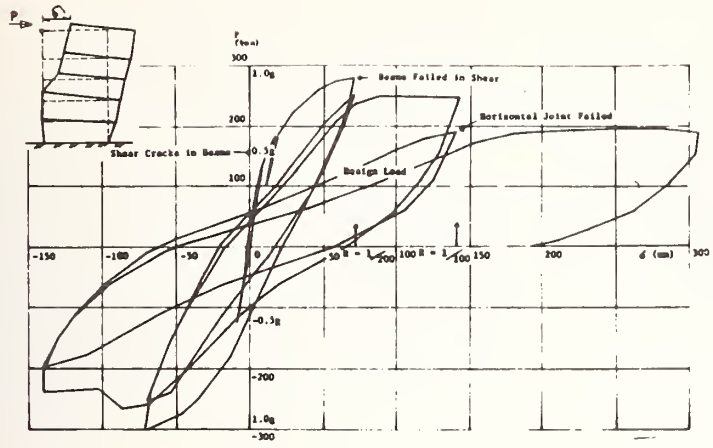

FIGURE 27 LOAD DISPLACEMENT CURVE (1974)

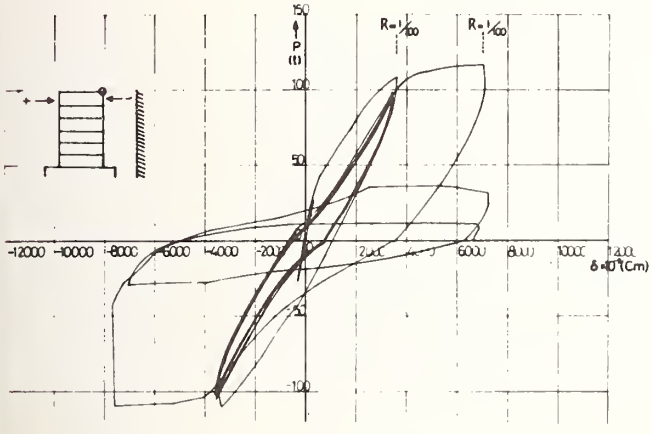

FIGURE 30 LOAD DISPLACEMENT CURVE OF SPECIMEN(A) (1975)

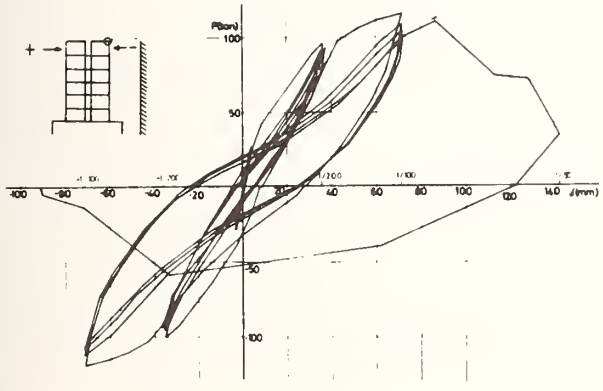

FIGURE 32 LOAD DISPLACEMENT CURVE OF SPECIMEN(B) (1975)

25

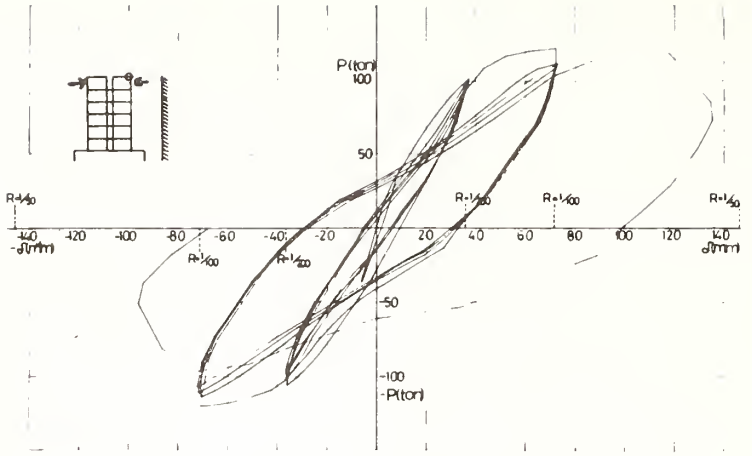

FIGURE 34 LOAD DISPLACEMENT CURVE OF SPECIMEN(C) (1975)

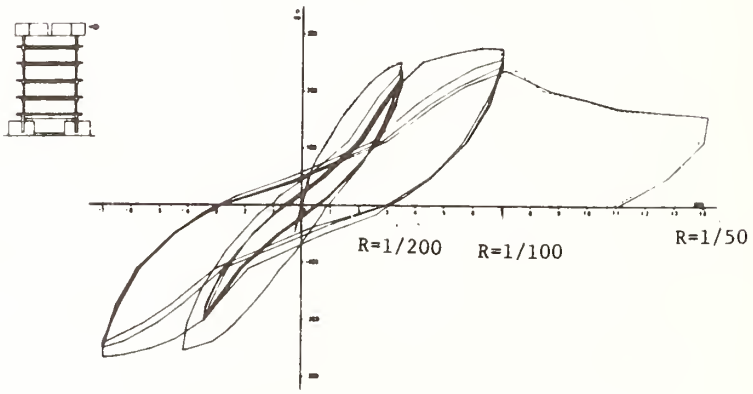

FIGURE 37 LOAD DISPLACEMENT CURVE (1976)

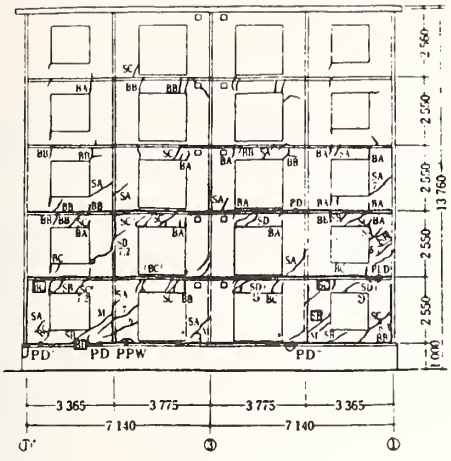

Skeleton(A)

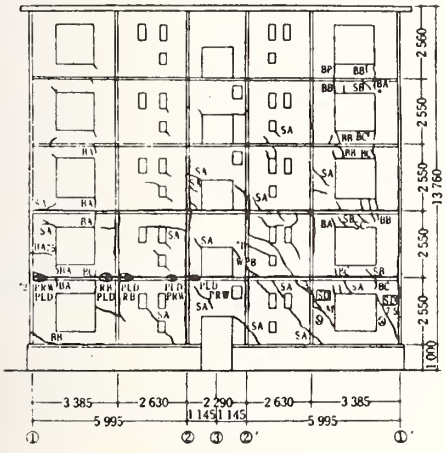

Skeleton(C)

REMARKS

P.P.W.	Rupture of welding between setting plates.
P.R.W.	Rupture of welding between setting plate and anchored bar.
P.D.	Deformation of setting plate.
P.L.D.	Severe deformation of setting plate.
R.B.	Rupture of anchored bar.
W.R.B.	Rupture of reinforcement in panel.
S.A.	Shear crack (less than 1mm)
S.B.	Shear crack (1 to 5 mm)
S.C.	Shear crack (5 to 10mm)
S.D.	Shear crack (larger than 10 mm)
B.A.	Bending crack (0.5 to 1 mm)
B.B.	Bending crack (1 to 3 mm)
B.C.	Bending crack (larger than 3mm)
	Crack accompanied by crush of concrete
	Crack accompanied by spalling-off of concrete

25

FIGURE 4 FINAL CRACK PATTERNS (1967)

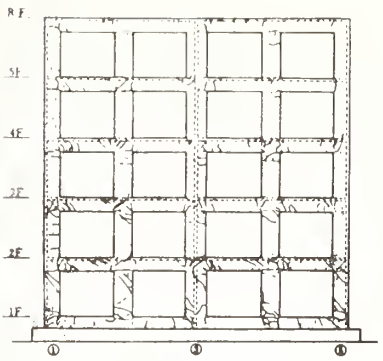

Skelton (A)

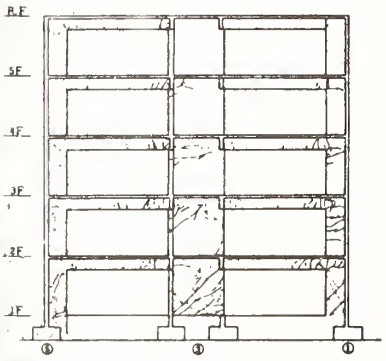

Skelton (B)

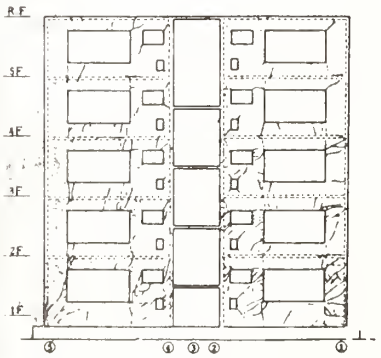

Skelton (C)

FIGURE 7. FINAL CRACK PATTERNS .(1968)

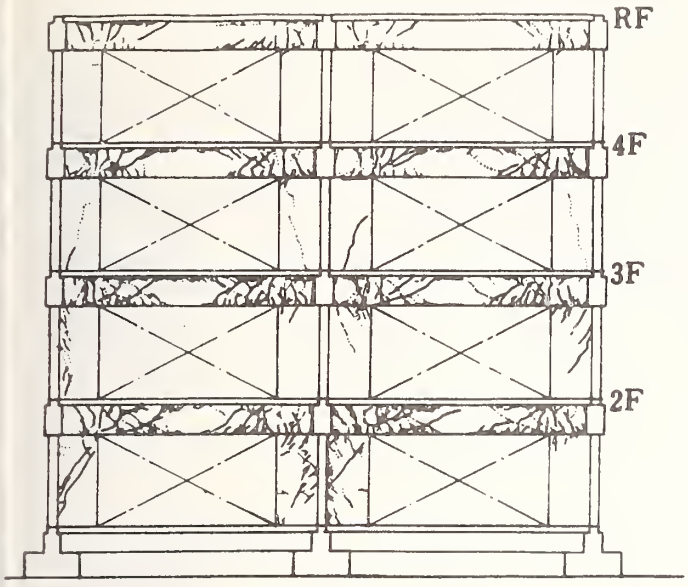

FIGURE 10 FINAL CRACK PATTERNS (1969)

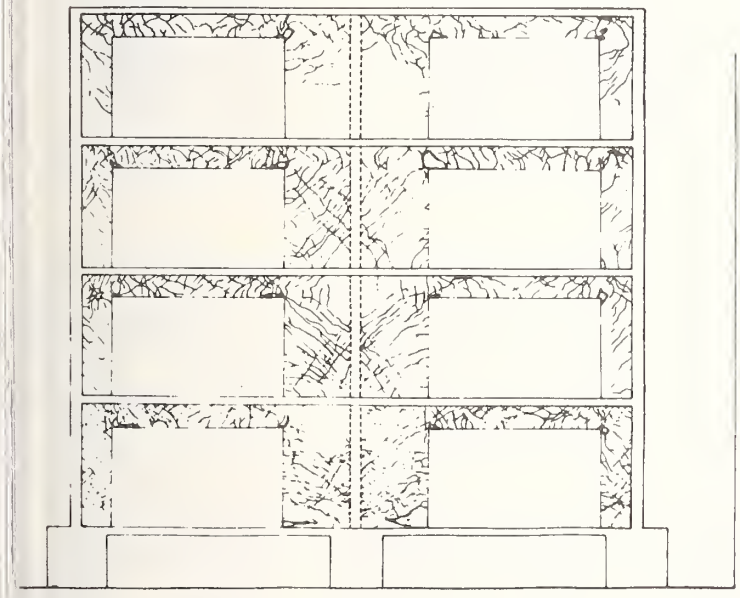

FIGURE 19 FINAL CRACK PATTERNS (1972)

25

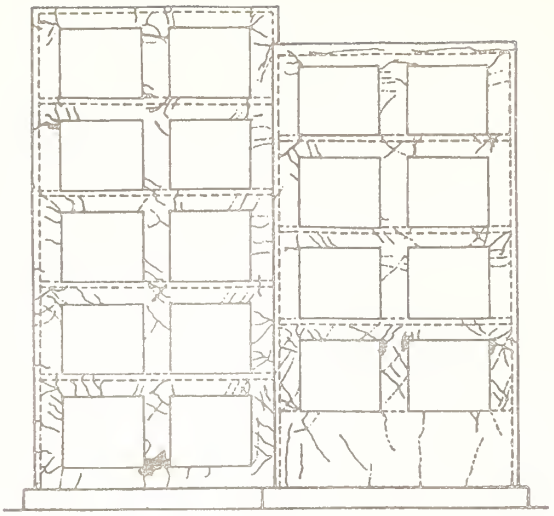

Skeleton(A)

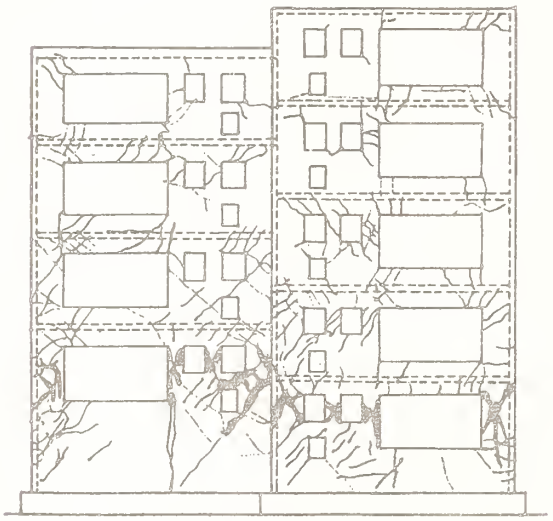

Skeleton(B)

FIGURE 13 FINAL CRACK PATTERNS (1970)

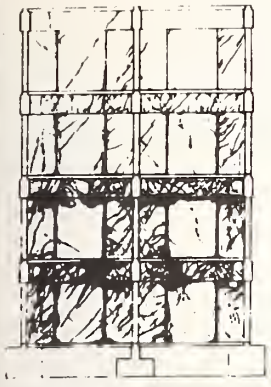

FIGURE 16 (1971)

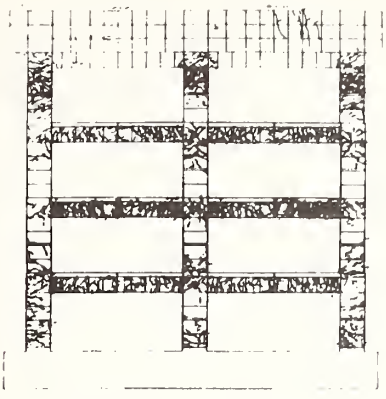

FIGURE 23 (1973)

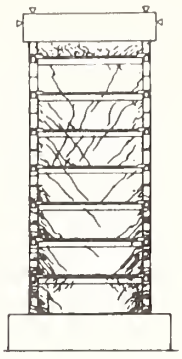

FIGURE 25 (1973)

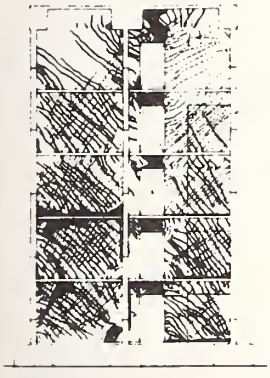

FIGURE 28 (1974)

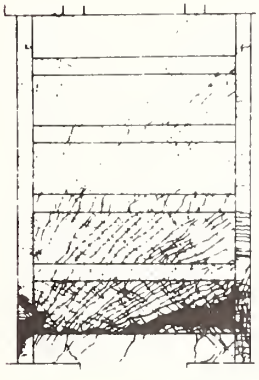

FIGURE 31 (1975)

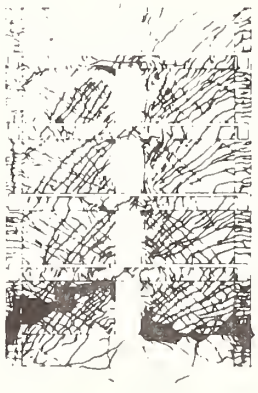

FIGURE 33 (1975)

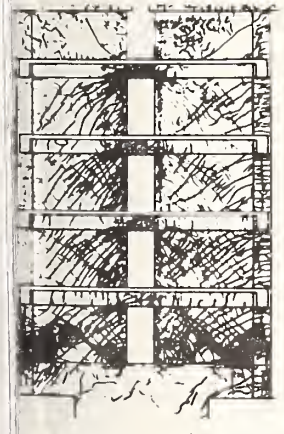

FIGURE 35 (1975)

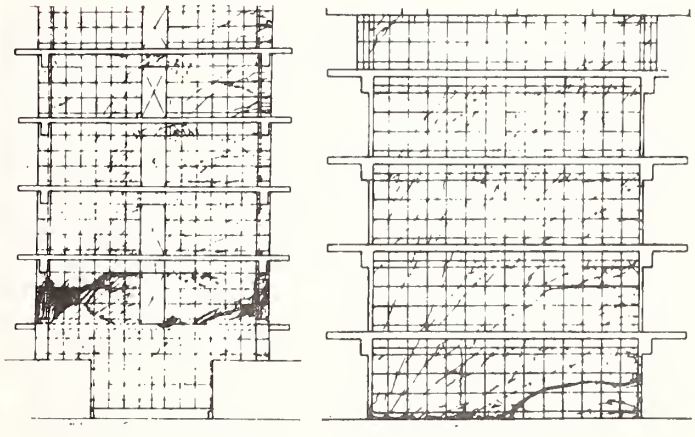

FIGURE 38 (1976)

FINAL CRACK PATTERNS (1971, and from 1973 to 1976)

26

DYNAMIC BEHAVIOR OF RECTANGULAR WATER TANKS ASSEMBLED WITH PANELS

Keiichi Ohtani
Chikahiro Minowa

National Research Center for Disaster Prevention
Science and Technology Agency

Dynamic Behavior of Rectangular Water Tanks Assembled with Panels

The dynamic behavior of rectangular tanks were studied by W. G. Housner and Fumiki Kito. In the formula developed by Housner, the elasticity of the side walls was not considered. Dr. Kito analyzed the natural frequencies of elastic side walls, by the energy method, assuming simply supported edges, clamped edges, and so on.

This paper describes theoretical and experimental studies concerning rectangular water storage tanks. In the theoretical study, the Kito's method is employed. The bending displacements of the walls perpendicular to an excitational direction (which are called the pressure walls), and the shear displacements of the walls parallel to this direction (which are called the side walls) are assumed. The water in the tank is regarded to have the velocity potential that satisfies the conditions of free surfaces, the continual conditions of velocities on the pressure walls, and the three-dimensional Laplace's equation. From these assumptions, the potential energies and the kinematic energies would be obtained. The vibrational equations of this system would be expressed by substituting these energies into the Eular's equation. This analysis is concluded by solving multi-degrees vibrational equations.

The dynamic tests concerned two tanks with dimensions of 1m x 1m, one was made from fiber-reinforced plastic, and the other was made from steel. The F.R.P. tank with a capacity of 52.5 tons (5m x 3m x 3.5m) was strengthened by bracings. The steel tank with a capacity of 38 tons (4m x 3m x 3.5m) was investigated in two cases. In the first case, the steel tank was not strengthened (the standard test). In the second case, the steel tank was braced. The large-scale shaking table of National Research Center for Disaster prevention in Tsukuba was used in these experiments. Frequency properties of displacements and hydro-dynamic pressures were measured in these tests.

The mathematical simulations were carried out in the frequency domains, in which the sloshing would be negligible. Natural frequencies, the sinusoidal responses of displacements, and hydrodynamic pressures were calculated. The same elastic analysis for cylindrical liquid tanks has already reported[4]

Analysis

In this section, the vibrational equation for the rectangular water storage tanks supported by base frames is obtained by Rayleigh-Ritz's methods. The coordinates and dimensions of rectangular water storage tanks are shown in Figure 1. The vibrational direction is only x-axis. The bending deformations of pressure walls and the shear deformations of side walls are considered, and other deformations are neglected in this analysis. So, the absolute displacements of the pressure wall u(y,z) are assumed as follow.

$$u(y,z) = \sum_{m=1,3} \sum_{n=1,2} \xi_{mn}(t) \sin\left(\frac{m\pi x}{b}\right) \sin\left(\frac{n\pi z}{d}\right) + \sum_{k=1,3} \zeta_k(t) \sin\left(\frac{k\pi z}{2d}\right) + \eta(t)\frac{z}{d} + u_o(t) + u_g(t)$$

The first term means the bending deflection of the pressure wall with the simply supported edges. The second and third terms represent the shear deflections of the side wall. Because of the

roof mass, a third term is added to this virtual displacement. $u_o(t)$ is the relative displacement of the base frame, and $u_g(t)$ is the ground displacement.

The water would be regarded to be incompressible, non-viscous fluid. The velocity potential[2,3] of the water in a rectangular tank is assumed as follows:

$$\phi = -\left(u_o(t) + u_g(t)\right)\left(x - \frac{a}{2}\right) + \sum_{s=1,3} \psi_s(t) \cos\left(\frac{s\pi x}{a}\right) \cosh\left(\frac{s\pi z}{a}\right)$$

$$+ \sum_{i=0,2} \sum_{j=1,3} \delta_{ij}(t) \sinh\left(\pi\sqrt{\left(\frac{i}{b}\right)^2 + \left(\frac{j}{2h}\right)^2}\left(x - \frac{a}{2}\right)\right) \cos\left(\frac{i\pi y}{b}\right) \cos\left(\frac{j\pi z}{2h}\right)$$

This potential ϕ satisfies the three-dimensional Laplace's equation, and the continuous conditions of velocity on the pressure wall are expressed as follows:

$$\left.\frac{\partial \phi}{\partial x}\right|_{x=0,a} = -\dot{u}(y,z)$$

To calculate any particular coefficient $\delta_{ij}(t)$ of the velocity potential, both sides of this equation are multiplied by $\cos\left(\frac{i\pi}{b}y\right)$ $\cos\left(\frac{j\pi}{2h}z\right)$ and integrated from 0 to b with respect to y and from 0 to h with respect to z. The orthogonality $\delta_{ij}(t)$ may be given by the following expression:

if, i=0

$$\delta_j(t) = \frac{-h}{\cosh\left(\frac{j\pi a}{4h}\right)}\left(\sum_{m=1,3} \sum_{n=1,2} \dot{\xi}_{mn}(t) H_\xi(j,m,n) + \sum_{k=1,3} \dot{\zeta}_k(t) H_\zeta(j,k) + \dot{\eta} H_\eta(j)\right)$$

if, i≠0

$$\delta_{ij}(t) = \frac{-h}{\cosh\left(\frac{\pi a}{4h}\sqrt{\left(\frac{2hi}{b}\right)^2 + j^2}\right)} \sum_{m=1,3} \sum_{n=1,2} \dot{\xi}_{mn}(t)\, H_{\xi\xi}(i,j,m,n)$$

where

$$H_\xi(j,m,n) = \frac{8}{j\pi^3}\left(\frac{n\frac{h}{d} - \frac{j}{2}\sin\left(\frac{n\pi h}{d}\right)\sin\left(\frac{j\pi}{2}\right)}{m\left(\left(n\frac{h}{d}\right)^2 - \left(\frac{j}{2}\right)^2\right)}\right)$$

$$H_\zeta(j,k) = \frac{4}{j\pi^2}\left(\frac{k\frac{h}{2d} - \frac{j}{2}\sin\left(\frac{k\pi h}{2d}\right)\sin\left(\frac{j\pi}{2}\right)}{\left(k\frac{h}{2d}\right)^2 - \left(\frac{j}{2}\right)^2}\right)$$

$$H_\eta(j) = \frac{8h}{j^2\pi^2 d}\left(\sin\left(\frac{j\pi}{2}\right) - \frac{2}{j\pi}\right)$$

$$H_{\xi\xi}(i,j,m,n) = \frac{16}{\pi^3\sqrt{\left(\frac{2hi}{b}\right)^2 + j^2}}\left(\frac{m\left(n\frac{h}{d} - \frac{j}{2}\sin\left(\frac{n\pi h}{d}\right)\sin\left(\frac{j\pi}{2}\right)\right)}{(m^2 - i^2)\left(n^2\left(\frac{h}{d}\right)^2 - \left(\frac{j}{2}\right)^2\right)}\right)$$

The next procedure is to derive the potential and kinematic energies of this system. The potential (strain) energy of one pressure wall u_b is given by the following expression:

$$U_b = \frac{D}{2} \int_0^b \int_0^d \left(\left(\frac{\partial^2 u}{\partial y^2} + \frac{\partial^2 u}{\partial z^2} \right)^2 - 2(1-\nu) \left(\frac{\partial^2 u}{\partial y^2} \frac{\partial^2 u}{\partial z^2} - \left(\frac{\partial^2 u}{\partial y \, \partial z} \right)^2 \right) \right) dy \, dz$$

The potential energy of one side wall U_s and the potential energy of a base frame U_f are given by the following expressions:

$$U_s = \frac{G}{2} \int_0^d \left(\frac{\partial u}{\partial z} \Big|_{y=0} \right)^2 dz \quad , \qquad U_f = \frac{k_f}{2} u_o^2$$

The potential energy of the water surface (U_w) is given by the following:

$$U_w = \frac{\rho_w g}{2} \int_0^b \int_0^a w^2 \Big|_{z=h} dx \, dy$$

In these energy expressions, D is the flexual rigidity of the pressure walls, G is the shear rigidity of the side walls, k_f is the stiffness of the base frame, g is the gravity acceleration, and w is the up-down displacement of water.

The kinematic energies of one pressure wall (T_b), one side wall (T_s), a roof (T_r), and a bottom plate (T_f) are given by the following expressions:

$$T_b = \frac{\rho_b}{2} \int_0^b \int_0^d \dot{u}(y,z)^2 dy \, dz \quad , \qquad T_s = \frac{\rho_s}{2} \int_0^d \dot{u}(0,z)^2 dz$$

$$T_r = \frac{m_r}{2} \dot{u}(0,h)^2 \quad , \qquad T_f = \frac{m_f}{2} \dot{u}(0,0)^2$$

Where ρ_b is the unit area mass of the pressure wall, ρ_s is the unit height mass of the side wall, m_r is the roof mass, and m_f is the bottom plate mass. The kinematic energy of the tank water T_w is given by the following expression:

$$T_w = \frac{\rho_w}{2} \int_0^a \int_0^b \int_0^h \left(\left(\frac{\partial \phi}{\partial x} \right)^2 + \left(\frac{\partial \phi}{\partial y} \right)^2 + \left(\frac{\partial \phi}{\partial z} \right)^2 \right) dx \, dy \, dz$$

Because the tank displacements except x-direction are neglected, the above expression may yield the following:

$$T_w = \frac{\rho_w}{2} \int_0^a \int_0^b \phi \frac{\partial \phi}{\partial z} \Big|_{z=h} dx \, dy + \rho_w \int_0^a \int_0^h \phi \Big|_{x=a} \dot{u}(y,z) dx \, dy$$

The Lagragian L, that is, the difference between total potential energies and total kinematic energies, is defined by

$$L = U_f + 2U_b + 2U_s + U_w - (T_r + T_f + 2T_b + 2T_s)$$

Substituting the Lagragian L into Eular's equation, will give the vibrational performance of this rectangular water storage tank. Eular's equation is defined by

$$\frac{\partial L}{\partial v_r} - \frac{d}{dt} \left(\frac{\partial L}{\partial \dot{v}_r} \right) = 0$$

Where v_r is the generized coordinate corresponding to ξ_{mn}, ζ_k, η, u_o, ψ_s. ψ_s would be obtained by integrating ψ_s with respect to time t.

After all, the vibrational equations of this system can be written in the matrix form as follows:

$$[M]\{\ddot{v}\} + [K]\{v\} = -\{m_o\}\ddot{u}_g$$

where

$$\{v\}^T = (\xi_{11}, \xi_{12}, \xi_{13}, \cdots \xi_{mn}, \zeta_1, \zeta_3, \cdots\cdots \zeta_k, \eta, \Psi_1, \Psi_3, \cdots\cdot)$$

$$[M] = \begin{vmatrix} m_{11} & m_{12} & \cdots\cdots \\ & m_{22} & \cdots\cdots \\ & & \cdots\cdot \\ \text{SYM} & & \\ & & m_{rr} \end{vmatrix} \qquad [K] = \begin{vmatrix} k_{11} & k_{12} & \cdots\cdots \\ & k_{22} & \cdots\cdots \\ & & \cdots\cdot \\ \text{SYM} & & \\ & & k_{rr} \end{vmatrix}$$

$\{m_o\}$ is the column vector of matrix [M], corresponding to u_o. The result of this procedure, the dynamic behavior of rectangular storage tanks, would be represented by the similar vibrational equations for the general structures. But, the mass matrix has no components of zero, because of the influence of the water. Vector $\{v\}$ should be obtained by direct computation for any input $\ddot{u}_g$. Regarding the right side of the matrix equation as zero, the natural frequencies and the eigenvectors can be derived by using the modal-analysis method. Accordingly, the vector $\{v\}$ may be shown as follows:

$$\{v\} = \mu_1\{v_1\}q_1(t) + \mu_2\{v_2\}q_2(t) + \cdots\cdots + \mu_p\{v_p\}q_p(t)$$

The following equation will be attained by using the orthogonalities of eigenvectors $\{v_p\}$:

$$\ddot{q}_p(t) + \omega_p^2 q_p(t) = -\ddot{u}_g(t)$$

Adding the damping factor to this equation, one has

$$\ddot{q}_p(t) + 2h_p\omega_p\dot{q}_p(t) + \omega_p^2\,\ddot{q}_p(t) = -\ddot{u}_g(t)$$

μ_p is the participation factor which is given by the following expression:

$$\mu_p = \frac{\{v_p\}^T\{m_o\}}{\{v_p\}^T[M]\{v_p\}}$$

Using this method, the deformation and hydrodynamic pressure of the pressure wall would be obtained like follows.

$$u(y,z) = \sum_{p=1,2} \mu_p\, q_p(t) \Big\{ \sum_{m=1,3} \sum_{n=1,2} {}_p\xi_{mn} \sin\left(\frac{m\pi y}{b}\right) \sin\left(\frac{n\pi z}{d}\right)$$

$$+ \sum_{k=1,3} {}_p\zeta_k \sin\left(\frac{k\pi z}{2d}\right) + {}_p\eta\,\frac{z}{d} + {}_pu_o \Big) + u_g$$

$$P(y,z)=\rho_w \frac{\partial \phi}{\partial t}\Big|_{x=0} = \rho_w \Big(\sum_{p=1,2} \mu_p \ddot{q}_p(t) \Big(\sum_{s=1,3} {}_p\Psi_s \cosh\Big(\frac{s\pi z}{a}\Big) + {}_pu_o \frac{a}{2}$$

$$+ h\Big(\sum_{m=1,3} \sum_{n=1,2} {}_p\xi_{mn} \sum_{i=2,4} \sum_{j=1,3} H_{\xi\xi}(m,n,i,j) \tanh\Big(\sqrt{\Big(\frac{2hi}{b}\Big)^2 + j^2}\,\frac{a}{4h}\Big)$$

$$\cos\Big(\frac{i\pi y}{b}\Big)\cos\Big(\frac{j\pi z}{2h}\Big) + \sum_{j=1,3} H_\xi(m,n,j)\tanh\Big(\frac{j\pi a}{4h}\Big)\cos\Big(\frac{j\pi z}{2h}\Big)\Big) + \sum_{k=1,3} {}_p\zeta_k$$

$$\sum_{j=1,3} H_\zeta(j,k)\tanh\Big(\frac{j\pi a}{4h}\Big)\cos\Big(\frac{j\pi z}{2h}\Big) + {}_p\eta \sum_{j=1,3} H_\eta(j)\tanh\Big(\frac{j\pi a}{4h}\Big)\cos\Big(\frac{j\pi z}{2h}\Big)\Big)\Big)$$

$$+ \ddot{u}_g(t)\frac{a}{2}$$

where

$$\{v_p\}^T = \{{}_p\xi_{11}, {}_p\xi_{13} \cdots {}_p\xi_{mn}, {}_p\zeta_1 \cdots {}_p\zeta_k, {}_p\eta, {}_p\Psi_1, {}_p\Psi_3 \cdots {}_p\Psi_s\}$$

In the computational analysis, the sloshing effects of free surface are assumed to be negligible. Thus, vibrational equations are obtained by neglecting the first terms of U_w and T_w.

The sloshing equation in this case becomes, as generally known,

$$\ddot{\Psi}_s + \frac{s\pi}{a} g \tanh\Big(\frac{s\pi h}{a}\Big)\Psi_s = -\frac{4a}{s^2\pi^2 \cosh\Big(\frac{s\pi h}{a}\Big)} (\ddot{u}_o + \ddot{u}_g)$$

The circular frequency ω_s is

$$\omega_s{}^2 = \frac{s\pi}{a} g \tanh\Big(\frac{s\pi h}{a}\Big)$$

In the high frequency range, where the circular frequency ω is greater than ω_s, the second term in the left hand side in the sloshing equations may be negligible. So the sloshing equation would be rewritten in the following form:

$$\ddot{\Psi}_s = -\frac{4a}{s^2\pi^2 \cosh\Big(\frac{s\pi h}{a}\Big)} (\ddot{u}_o + \ddot{u}_g)$$

Substituting this $\ddot{\psi}$ into the matrix equation, the approximate equation for the dynamic behavior of rectangular water storage tanks was obtained.

Shaking Table Experiments and Numerical Computations

In the first shaking-table experiment, the rectangular water storage tank 1m x 1m and 1m x 0.5m F.R.P. panels with bolts and sealing materails was investigated. This test tank was fixed to the steel base frame, and set on the shaking table. To gain the bending rigidities, the F.R.P. panels have the convex patterns and the ribs along the edges as shown in Picture 1. Because of hydrostatic pressures, the panels' thickness increases with depth. Furthermore, this tank was strengthened by the inside braces as shown in Picture 2. In practical use the tanks should have roofs. In this experiment, the roof was taken off, and the upper panels were replaced with transparent acrylic plates so the behavior of the free surface could be seen. The dimensions of this tank were 5m in parallel with the excitational direction, 3m perpendicular to this direction, and 3.5m in height. The water levels employed in this experiment were 0m, 1.25m and 2.5m. The relative displacements to the shaking table foundation, the accelerations, and the hydrodynamic pressures acting on the walls were measured. The natural frequency for the empty

tank was recognized at about 2.65 Hz, the natural frequency for the water level of 1.25m was about 12.5 Hz, and the natural frequency for 2.5m was about 7.0 Hz. The case with a water level of 2.5m will be discussed in detail. The deformation shapes at natural frequency 7.0 Hz, as shown in Figures 2, 3, 4, 5, look like the shear deformation mode for the side wall, and also look like the superpositional mode of the side wall shear deformation and the plate bending deformation for the pressure wall. The peak of hydrodynamic pressure was recognized at 7 Hz as well as the deformations. Peak value of hydrodynamic pressure was about $1.5 g/cm^2$ for 1 gal input amplitude, and the profiles of the hydrodynamic pressure distributions are shown in Figures 6 and 7.

In the numerical analysis for this tank, one bending mode $(\sin\frac{\pi y}{b}\ \sin\frac{\pi z}{d})$ of the pressure wall, two shear modes $(z/d,\ \sin\frac{\pi z}{2d})$ of the side wall, and the deformation on the base frame, the 4 virtual displacements are employed. The constants of tank are taken as Table 1. Assuming the damping ratios as 5 percent and 4 percent the theoretical results would fairly agree to the experimental data.

In the second shaking-table experiment, the rectangular water storage tank assembled with 1m x 1m steel panels with bolts and sealing materials was investigated. This tank was only placed on the steel base frame, and held with frail devices. The dimensions of this tank were 4m in parallel with the excitational direction, 3m in perpendicular with the excitational direction, and 4m in height. For this test tank, a roof was installed. To examine the effects of the inside braces, both braced and unbraced tanks were observed.

In the standard test, the natural frequencies of the tank were recognized at about 9.5 Hz for the empty stage, 3.5 Hz for the water level of 2m, and 2.0 Hz for the water level of 3.7m. In the test of water level 3.7m, 5.5 Hz and 10 Hz were observed. Deformations were found in the pressure wall, but scarcely in the side wall. The deformations of the pressure wall were similar to the bending modes of the plate. The amplification ratios decrease with the increase of water level as shown in Figure 10. The amplificational ratios for higher natural modes wouldn't be always larger than for the first mode, as shown in Figure 11. Using the natural frequency 9.5 Hz for the empty tank and the average unit area weight 44kg of a panel, the flexual rigidity for the pressure wall would be evaluated about 5500~6000kg•m.

In the numerical analysis for this standard case, 6 bending modes of the pressure wall, 3 shear modes of the side wall, and the deformation of the base frame were used. The constants are shown in Table 1. In the numerical computations, the dampings are considered by 2 percent for the first mode, 10 percent for the second mode, and 10 percent or 5 percent for the third mode. The numerical and experimental results are shown in Figures 10, 11, 12, 13, and 14.

In the strengthened case, the natural frequency was recognized at about 6.5 Hz for the water level 3.7m. The base frame gave the large deformations in comparison with other experiments. The bending deformations of the pressure wall were measured smaller than the case of the F.R.P. tank. The hydrodynamic pressures at the natural frequency were about $2 g/cm^2$ for 1 gal input amplitude, as illustrated in Figure 16. Increasing the input amplitudes at the natural frequency, a slip occurred between the tank and the base

frame. The same numerical analysis for the F.R.P. tank was conducted. The numerical and experimental results are shown in Figures 15, 16, 17, and 18. The constants are given in Table 1.

It is reasonable that the flexual rigidity of the pressure wall strengthened by bracings is larger than the standard case. The reason that the shear rigidity of the side walls is estimated to be smaller than the standard case, are considered to be given by the bending deformations of the side wall which are not assumed in the theoretical analyzed.

Earthquake Damage to Water Storage Tanks

In the Near Izu-Oshima earthquake on January 14, 1978, and in the Off Miyagi Prefecture earthquake on February 20, 1977, many water storage tanks were damaged. Distortions of base frames, tank slips, and breaks at pipe connections occurred at many buildings. The wall of one F.R.P. tank had broken out because of the increase of hydrodynamic pressure. A water tank that was set on the penthouse of a seven-story hotel survived because it was held by eight bolts rather then the two that are ordinarily seen; one bolt was completely cut away by the earthquake force. In Izu Inatori, we estimate that half the water tanks set on the roofs would probably suffer some damage in some future earthquake.

Conclusion

In this study, a method for calculating the natural frequencies of rectangular water tanks was developed and compared with the experimental data. The pressures and deformations of rectangular water storage tanks, obtained by the shaking table experiments and the numerical analysis, indicated that conventional estimates for these tanks would be small.

Acknowledgments

The authors are grateful to Mr. Harada and Mr. Wakana, who are the members of Bridge-Stone Tire Co., Ltd., and Mr. Hirata and Mr. Takeuchi, who are the members of Mitsubishi Plastics Industries Ltd., for their cooperation in the experiments. Special thanks are due to the staff of the maintenance section of National Research Center for Disaster Prevention.

References

1. Housner, W. G., (1961) Shock and Vibration Handbook, Vol. 3, 50 26-50, 29, Mac Graw-Hill.

2. Kito, F., (1959-1964) On Vibration of a Rectangular Tank Filled With Water, I-VIII, Journal of the Society of Naval Architects of Japan, (in Japanese).

3. Simizu, N., Yamamoto, S., (1974) The Influences That the Long Period Components of Earthquake Waves Give On the Long Period Structures, Kenchiku-Gijutsu, No. 274, 381-388, (in Japanese).

4. Hori, N., Tani, S., Tanaka, Y., (1977) Dynamic Analysis of Cylindrical Shells Containing Liquid, 6th. WCEE.

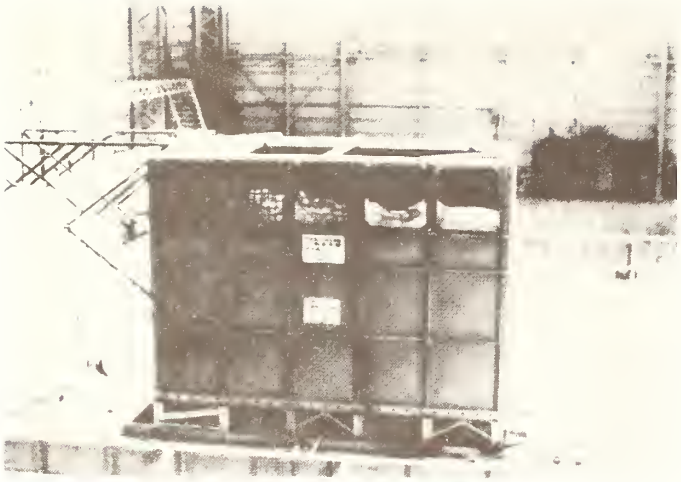

PICTURE 1: RECTANGULAR WATER STORAGE TANK ASSEMBLED WITH 1m x 1m F.R.P. PANELS

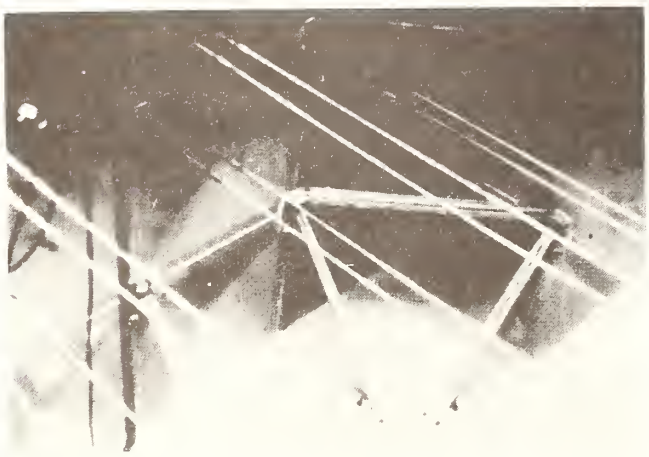

PICTURE 2: REINFORCING BRACES

INPUT DATA FOR COMPUTATIONS

ITEMS	SYMBOL	F.R.P TANK WITH BRACES	STEEL TANK	STEEL TANK WITH BRACES
DIMENSIONS BREADTH	b	3m	3m	3m
LENGTH	a	5m	4m	4m
HEIGHT	d	3.5m	4m	4m
AVERAGE UNIT AREA WEIGTH	ρ	16kg/m^2	44kg/m^2	44kg/m^2
FLEXURAL RIGIDITY OF THE PRESSURE WALL	D	65000kg.m	6000kg.m	150000kg.m
SHEAR RIGIDITY OF THE SIDE WALL	G	3×10^6 kg	9.72×10^7 kg	6.48×10^6 kg
STIFFNESS OF THE BASE FRAME	k_f	10^{10} kg/m	10^8 kg/m	10^8 kg/m

TABLE 1: INPUT DATA FOR COMPUTATIONS

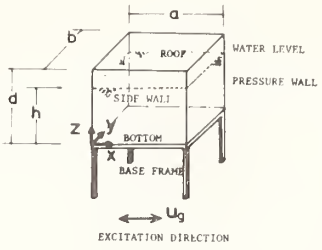

FIGURE 1: ANALTYICAL MODEL FOR A RECTANGULAR WATER TANK

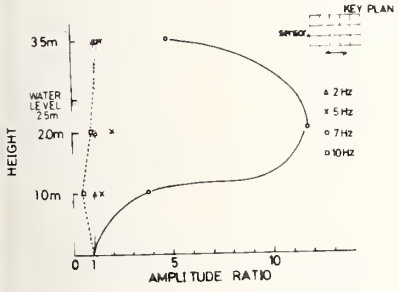

FIGURE 2: MEASURED DEFORMATION PROFILES OF PRESSURE WALL (F.R.P. TANK REINFORCED BY BRACES)

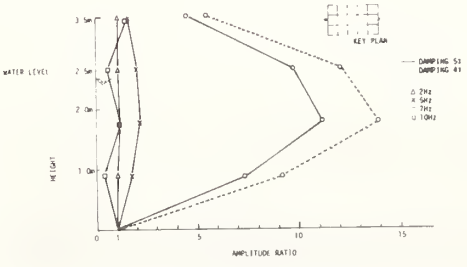

FIGURE 3: THEORETICAL DEFORMATION PROFILES OF THE PRESSURE WALL (F.R.P. TANK REINFORCED BY BRACES)

26

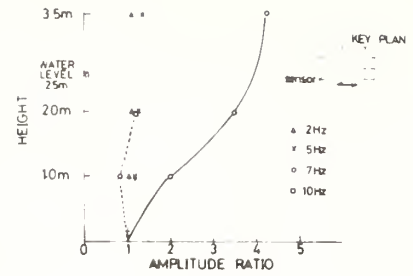

FIGURE 4: MEASURED DEFORMATION PROFILES OF SIDE WALL (F.R.P. TANK REINFORCED BY BRACES)

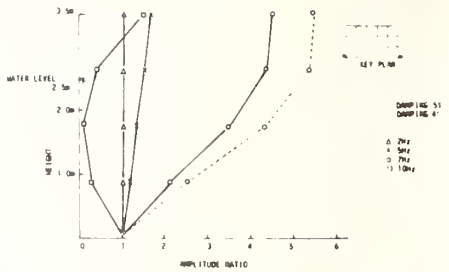

FIGURE 5: THEORETICAL DEFORMATION PROFILES OF THE SIDE WALL (F.R.P. TANK REINFORCED BY BRACES)

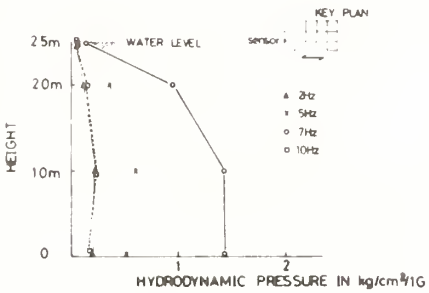

FIGURE 6: MEASURED HYDRODYNAMIC PRESSURE PROFILES CAUSED BY SINU SOIDAL EXCITATION (F.R.P. TANK REINFORCED BY BRACES)

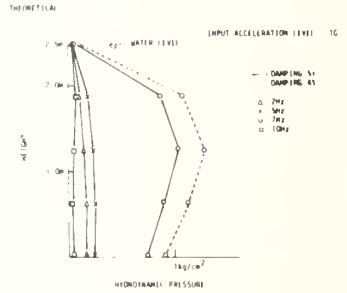

FIGURE 7: HYRODYNAMIC PRESSURE PROFILES (F.R.P. TANK REINFORCED BY BRACES)

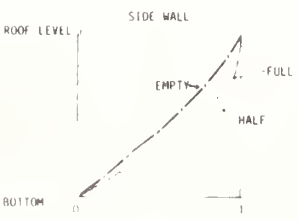

FIGURE 8 1:

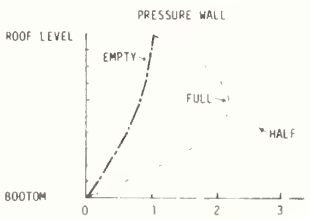

FIGURE 8-2:

THEORETICAL FIRST MODES WITH WATER LEVEL CHANGES (F.R.P. TANK REINFORCED BY BRACES)

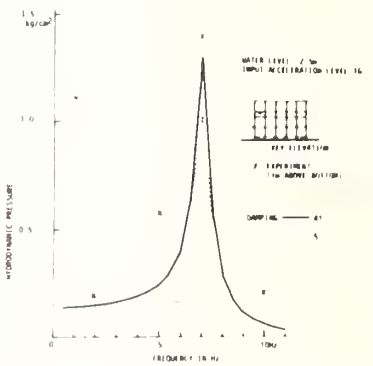

FIGURE 9: THEORETICAL HYDRODYNAMIC PRESSURE AT THE MIDHEIGHT OF WATER LEVEL (F.R.P. TANK)

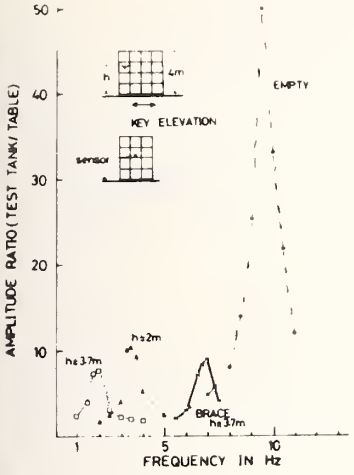

FIGURE 10: MEASURED RESONANCE CURVES FOR THE FIRST NATURAL MODE (STEEL TANK)

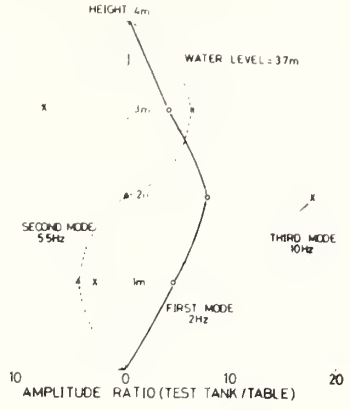

FIGURE 11: MEASURED MODES OF PRESSURE WALL (STEEL TANK)

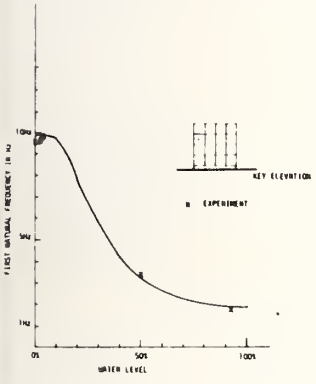

FIGURE 12: THEORETICAL FIRST NATURAL FREQUENCY (STEEL TANK)

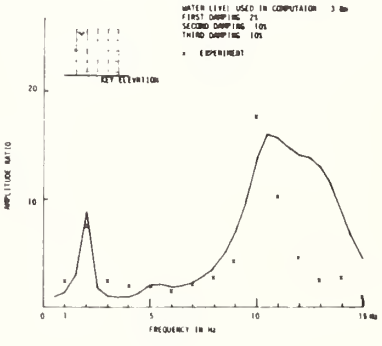

FIGURE 13: THEORETICAL RESONANCE CURVE OF PRESSURE WALL DEFORMATION AT THE MIDHEIGHT (STEEL TANK)

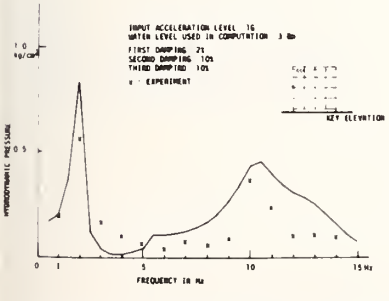

FIGURE 14: THEORETICAL RESONANCE CURVE OF HYDRODYNAMIC PRESSURE AT THE MIDHEIGHT OF WATER LEVEL (STEEL TANK)

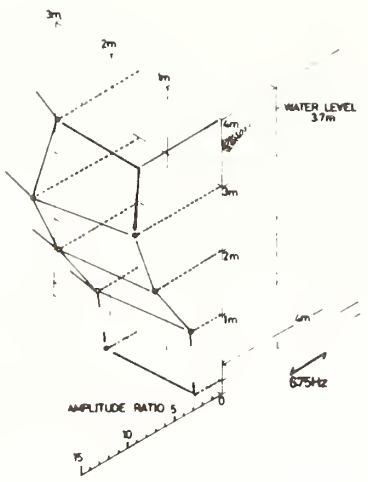

FIGURE 15: MEASURED DEFORMATION PROFILE (STEEL TANK REINFORCED BY BRACES)

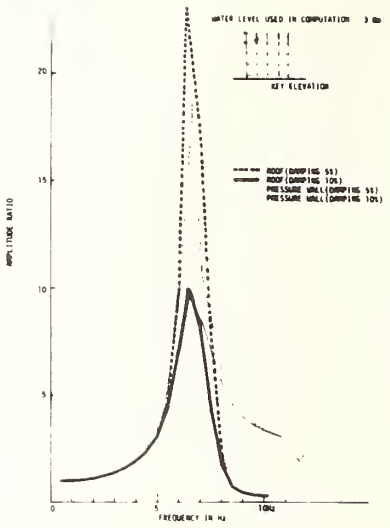

FIGURE 16: THEORETICAL RESONANCE CURVES OF THE WALL (STEEL TANK REINFORCED BY BRACES)

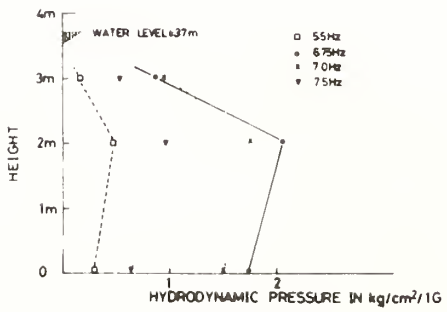

FIGURE 17: MEASURED HYDRODYNAMIC PRESSURE PROFILES CAUSED BY SINUISOIDAL EXCITATION (STEEL TANK REINFORCED BY BRACES)

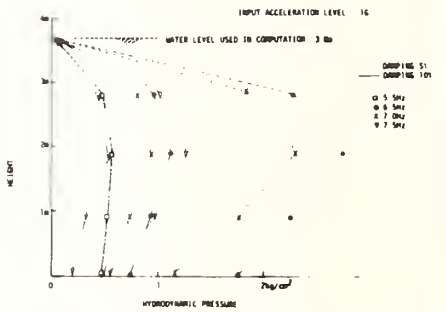

FIGURE 18: THEORETICAL HYDRODYNAMIC PRESSURE PROFILES (STEEL REINFORCED BY BRACES)

27

INELASTIC BEHAVIOR OF NON-BEARING WALLS IN AN 11-STORY STEEL-REINFORCED CONCRETE FRAME

AND

PART ONE

ASEISMATIC SAFETY OF EXTERNAL SURFACE FINISHES AND COATINGS

Makoto Watabe
Toshiyuki Kutoba
Akio Baba
Toshibumi Fukuta
Hiroshi Ito

Building Research Institute
Ministry of Construction

Inelastic Behavior of Non-Bearing Walls in an 11-Story Steel-Reinforced Concrete Frame

Shear walls and shear walls with openings have been designed for many high-rise steel-reinforced concrete buildings. Many studies have been carried out on the inelastic behavior of such bearing walls and their success has been accepted as a part of the seismic design procedure. In recent years, there have been many requests to enlarge the floor area per unit of public high-rise apartment buildings. To answer these requests, the structure shown in Figure 1 was proposed. To estimate the seismic safety of this structure, which consists of shear walls, shear walls with openings, and non-bearing walls, lateral loading tests were performed in 1975[1]. To clarify the effect of the non-bearing wall on the structural behavior as a whole, a lateral loading test on the half-scale test specimen simulating an eleven-story apartment building was carried out in 1976. In this paper, the inelastic behavior of a test specimen is summarized.

Lateral Loading Test

A high-rise steel-reinforced concrete apartment building has been designed according to the design provisions in the Architectural Institute of Japan Standards. The distribution of the seismic coefficient along the height is inverse triangular and the seismic coefficient at the eleventh floor is 0.401. The non-bearing wall is designed under the Provision of the minimum reinforcement ratio of shear walls. The test specimen shown in Figure 1 is the half-scale space frame consisting of one non-bearing wall and two shear walls with an opening surrounded by steel-reinforced concrete frames and is four stories high. To apply lateral and axial forces, walls and beams are assembled on the top of the test frame. The lateral force is transferred to the non-bearing wall through the floor slabs and the beams in the ridge direction. Axial forces shown in Figure 2 are applied to the four columns around the shear walls, so that the stress distribution of the test frame may be simulated to those of the actual eleven-story apartment building in the elastic range. Figure 2 also shows the relation of axial force N_1, N_2, and lateral force Q. Figure 3 shows the loading program. Materials used are normal concrete, SS41 steel plate, SD30 and SR24 reinforcements, and mesh. Properties of these materials are described in Tables 1 and 2. The test frame details are described in Figures 4 through 7.

Test Results

Figure 8 shows the lateral force-displacement relation, measured at the top of the test frame, 7.055 m high from the first-floor face. Table 3 is the list of the forces when flexural cracks, flexural shear cracks, and shear cracks are observed at each elements and the list of the forces at reinforcements or steel frame yielding. Figures 9 through 14 describe the crack distribution at three stages, R = 1/200, 1/100, and 1/50 where R is the rotation angle measured over total height.

The lateral load-displacement curve is nearly straight prior to the load, which is a little higher than the design load (48 tons). The test-frame load at the maximum displacement of the sixth loading cycle is about 85 percent of that of the second loading cycle. After this, the test frame load increases only 9.2 percent of the load at the maximum displacement of the second loading cycle prior to failure. This shows that the test frame yielding occurs at the load of 224 tons. At 265 tons in the seventh loading

cycle, crushing occurs in compression near the foot of the first floor of the non-bearing wall. At the load 274 tons in the same cycle, rupture of some vertical reinforcements occurs at the first floor of the non-bearing wall. Before this loading, the breadth of the flexure shear crack spreads to about 14 mm at the rupture point. Rupture of some vertical reinforcements occurs in the tensile regions of the first floor of shear walls with openings at the stage of the maximum displacement in the seventh cycle. The maximum test frame load is 274 tons, 5.7 times higher than the design load (48 tons). The rotation angle measured over total height is 1/114. The test frame load at the maximum displacement of the ninth loading cycle is about 85 percent of that of the seventh cycle. Restoring force of the test frame subjected to lateral load reversals is stable. After this loading stage, the test frame load decreases gradually and failure of the test frame occurs at the stage when the rotation angle measured over total height is 1/51. Damage to the test frame is concentrated on the first-floor elements; the rotation angle measured at the first floor is 1/16. The failed test frame showed crushed columns and shear failure of the shear walls with opening. Reinforced by full-web steel plates and mesh, spandrels of the shear wall with opening were damaged only a little.

Analysis

The following are the methods of the analyses for the elastic stiffness and the cracked loads of the test frame. The shear with opening is idealized to the model with rigid zones shown in Figure 14 and is analyzed by the slope-deflection method. The deflections caused by bending moment and shear force are considered in this method. The non-bearing wall is idealized to a cantilever whose fixed end is the first-floor face of the wall and is analyzed by the method considered alone with deflections by bending moment and shear force. The stiffness effects of floor slabs and beams in the ridge direction and the cracked loads are neglected here.

The elastic stiffness of the test frame is given as the sum of the elastic stiffnesses of each wall.

In case of the flexure cracked load, the following equation is applied to the section of the each wall's foot at the first floor and the flexure cracked moments of the section given are substituted in the lateral load-bending moment relation:

$$cMb = 1.8\sqrt{Fc}\ Ze + \frac{Ze}{Ae} N \qquad \text{(ref. 2)}$$

Fc = compressive strength of concrete
Ze = section modulus (includes reinforcement)
Ae = sectional area (includes reinforcement)
N = Axial load

In case of the shear cracked load, the following equation is applied to the section of the each wall at the first floor:

$$cQ = r \cdot t \cdot L \cdot (7.5 + 0.015\sqrt{Fc}) \qquad \text{(ref. 3)}$$

r = 1 - (equivalent opening peripheral ratio)
t = thickness of wall
L = distance bewteen columns

The flexure strength is calculated by applying the following equation to the walls:

$$uMb = A_t \cdot \sigma_y \cdot L + 0.5\Sigma(A_w \cdot \sigma_{wy}) \cdot L + 0.5N \cdot L \quad \text{(ref. 4)}$$

At = total section areas of axial reinforcement of tention side column
σ_y = yield strength of above reinforcement
A_w = total sectional areas of reinforcement of wall
σ_{wy} = yield strength of above reinforcement

The shear wall with opening is assumed to be a cantilever as a whole. The following equation is the relation between the lateral load and the ultimate flexure moment of the wall:

$$Q = (uMb - N \cdot L/2)/H$$

The non-bearing wall is assumed to be a cantilever whose fixed end is the first floor face of this wall. The flexure strength of the test frame is given as the sum of the flexure strength of each wall.

The shear strength of each wall is calculated by the following equations and the shear strength of the test frame is given in the same way as the flexure strength of the test frame:

$$Q = \min.(uQs_1, uQs_2) \quad \text{(ref. 4)}$$

$$uQs_1 = (0.068Pt_e(Fc + 180)/\sqrt{M/Q \cdot D + 0.12} + 2.7\sqrt{P_{we}\,\sigma_{wy}})\, be \cdot j + sQ$$

$$uQs_2 = \max.\ (r \cdot t \cdot L \cdot (7.5 + 0.015\sqrt{FC}) \ ,\ \ r(Qw + \Sigma Qc))$$

b_e = equivalent depth of wall
= (total section areas of wall and column)/L
L = end-to-end distance between columns
P_{te} = 100 x $A_t/b_e \cdot L$
A_t = total sectional areas of axial reinforcemnt of tension side column
P_{we} = equivalent lateral reinforcement ratio of wall
σ_{wy} = yield strength of above reinforcement
sQ = shear strength of steel frame within wall

Results given from the foregoing analytical methods are listed in Table 4; loading test results are shown too. These analytical methods make a good estimate of cracked loads and ultimate strengths of the test specimen.

Inelastic Behavior of Non-Bearing Wall

Load-Displacement Curve

The load-displacement curve of the non-bearing wall is calculated from the test results of the Reference 1. The properties of the materials used for this test are almost the same as those of the materials used for the Reference 1. But the compressive strength of concrete used for this test is about 18 percent higher than that of concrete used in Reference 1. After flexure yielding, both test specimens collapsed at shear failure. These points lead to the assumption that the behavior of the shear wall with opening in Reference 1 is the same as the shear walls with opening here. If the effect of floor slabs and beams in the ridge direction on the restoring force are neglected, then the restoring force on the non-bearing wall is given as the difference between the restoring force of this space frame and two times of the restoring force of the shear wall in the Reference 1.

Response Analysis

This eleven-story apartment building has been modeled as a one-mass system with a single degree of freedom. Responses to several earthquakes are calculated to clarify the effect of the non-bearing wall on the structural behavior as a whole.

The restoring force of this one-mass system is obtained through the following process. The height of the loading point of both tests in the reference 1 and this report is almost identical to the height of the center of gravity of the half scale eleven-story apartment building considered. Therefore load-displacement relations of walls shown in Figure 16 are adopted as restoring forces of walls constituting this one-mass system. The restoring force of this system is assumed to be the sum of those of walls in this system. The restoring force of the non-bearing wall is taken into account in case A and put out of account in case B. Shown in Figure 17, the whole restoring force of the system is approximated to several segments. Dimensions of the system adopted to response analysis are listed in Table 5. The elastic stiffness and the maximum strength of the system in case A are 1.18 times and 1.11 times larger than those of the system in case B, respectively. The displacement at the ultimate stage of the system in case A is nearly equal to that in case B. The undamped natural frequency of the system in case A is a little shorter than that in case B.

Earthquakes for response analysis are listed in Table 6. Responses described there are part of the results of the analysis. The maximum displacements subjected to earthquake loadings in case A are about 60 percent or 90 percent of those in case B. The maximum velocities subject to earthquake loadings in both cases are nearly equal. The maximum acceleration subjected to earthquake loadings in case A are 30 percent of those in case B.

In this analysis, the effects of damping and basement rocking are not considered.

Conclusion

Loading test results clearly show the effect of the non-bearing wall on the flexure-cracked load, the shear-cracked load, and the maximum strength of the test specimen. These loads and maximum strength increase, compared with those of only shear walls with openings.

The rotation angle measured over total height of the non-bearing wall is considerably small ($R = 1/284$) at the stage of its maximum strength, but at the ultimate stage the rotation angle measured over total height is nearly equal to that of the shear wall in-filled in Reference 1. It appears that non-bearing walls may indeed absorb the input energy under earthquake loadings. Despite the above results however, it is recommended that non-bearing walls be neglected in the seismic design of the structures.

References

1. Endo, T. and Goto, T. "Experimental Study of Steel-Reinforced Concrete Shear Wall with Opening," (November 1976).

2. Hirosawa, M. "Past Tests Results of Reinforced Concrete Shear Wall and Analyses," (March 1975).

3. The Architectural Institute of Japan, "The Design Provisions on the Reinforced Concrete Structure and Their Explanations."

4. The Architectural Institute of Japan, "Earthquake Load and Seismic Safety of the Structure - 1976," (January 1977).

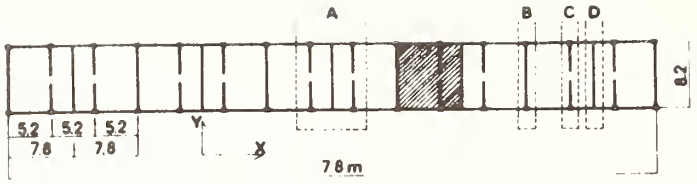

FIGURE 1: PLAN OF HIGH RISE FLATS

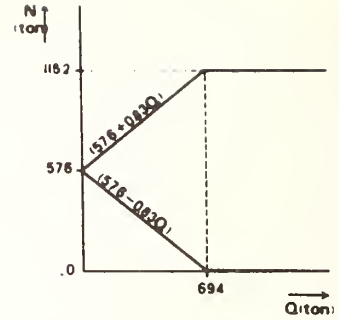

FIGURE 2: AXIAL LOADING - LATERAL LOADING RELATION

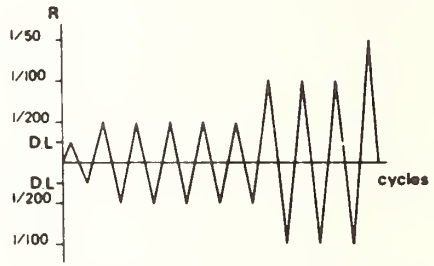

FIGURE 3: LOADING PROGRAM

			σ_y (kg/cm²)	ε_y (μ)	E (×10⁵ kg/cm²)	σ_{max} (kg/cm²)
column	flange		3070	1490	205	4407
	web		3407	1620	212	4549
	main reinforcement	D10(SD30)	3503	2116	1.90	5103
		D13(SD30)	3963	2146	190	5680
	hoop (SR24)		4073	2221	188	5810
beam	L shape		3283	1580	210	4356
	web		3330	1570	209	4630
	lattice (SR24)		3858	2089	180	4718
wall	mesh		4925	2661	203	5173

TABLE 1: PROPERTIES OF MATERIALS: STEEL

	σ_{max} (kg/cm²)	ε (μ)	E (×10⁵ kg/cm²)	poisson's ratio
base	266	2190	2.15	
1fl-4fl	263	2440	1.98	0.21

TABLE 2: PROPERTIES OF MATERIALS: CONCRETE

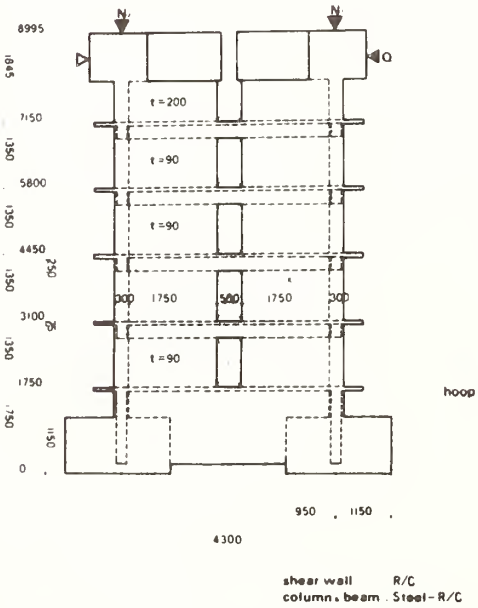

FIGURE 4: SHEAR WALL WITH OPENING

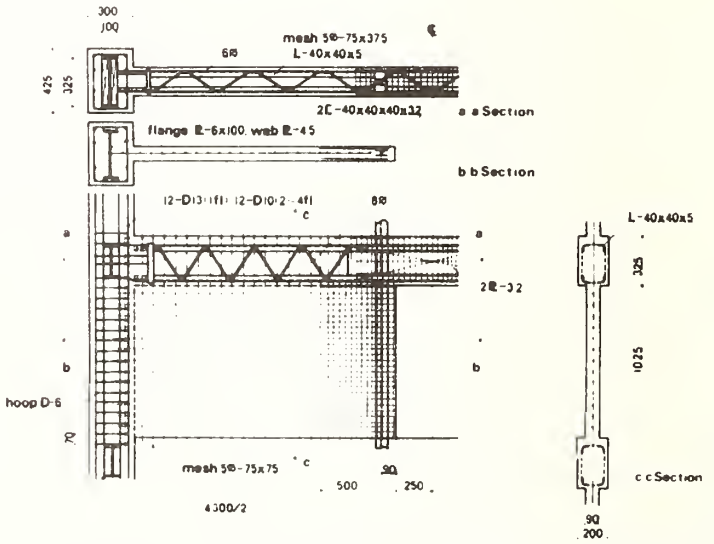

FIGURE 5: REINFORCEMENT: SHEARWALL WITH OPENING

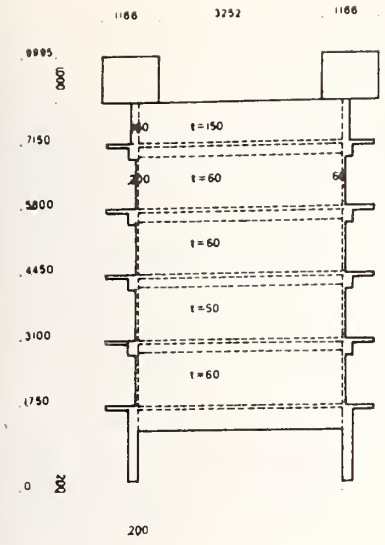

FIGURE 6: NONBEARING WALL

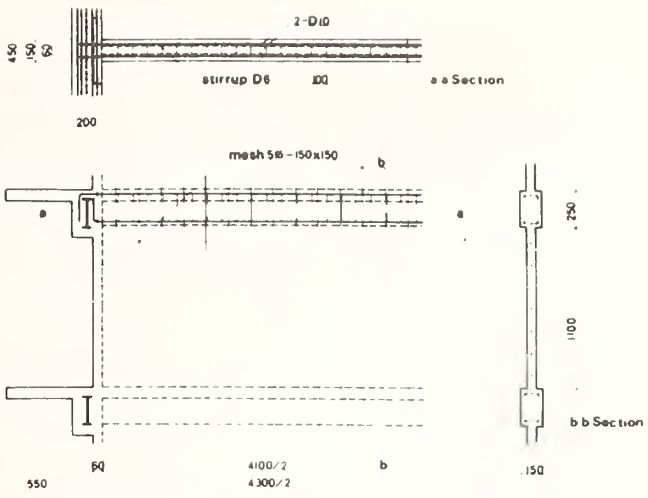

FIGURE 7: REINFORCEMENT: NONBEARING WALL

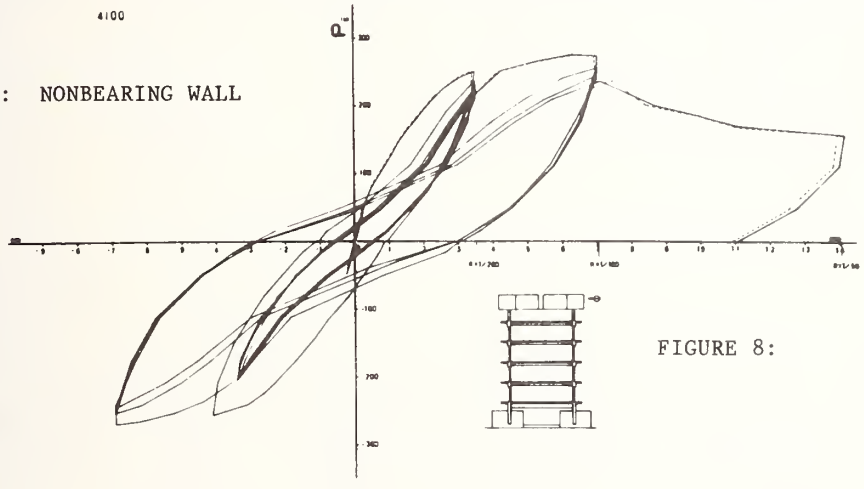

FIGURE 8:

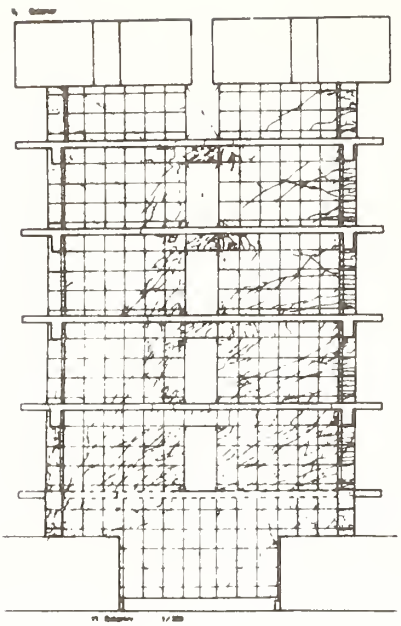

FIGURE 9: R = 1/200

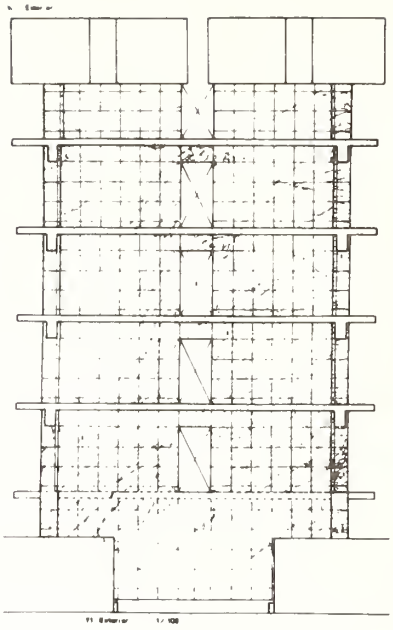

FIGURE 10: R = 1/100

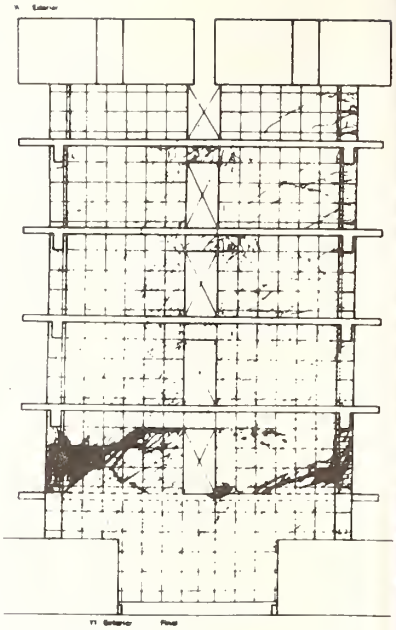

FIGURE 11: R = 1/50

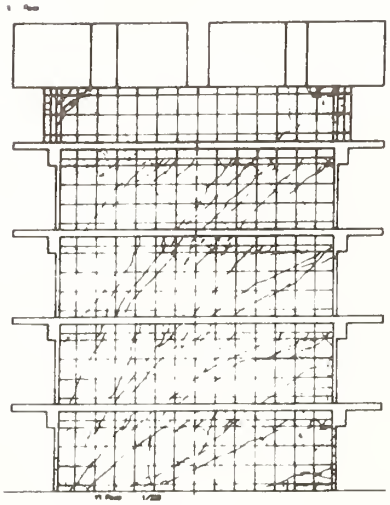

FIGURE 12: R = 1/200

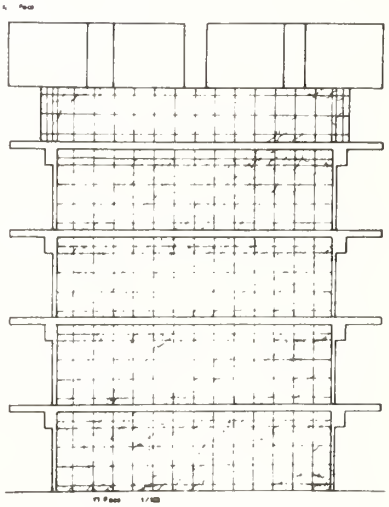

FIGURE 13: R = 1/100

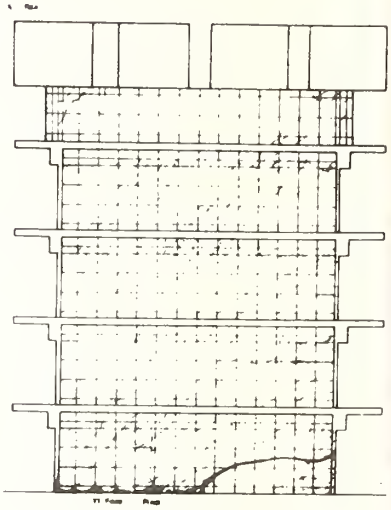

FIGURE 14: R = 1/50

	shear wall with opening										nonbearing wall			
	column				beam				wall					
	+		−		+		−		+		−		+		−	
	cycle	ton														
flexure crack	2	64	2	48	2	64	2	48	2	80	2	80	2	64	2	80
flexure shear crack					2	96	2	112	2	96	2	80	2	176	2	144
shear crack					2	80	2	112	2	96	2	80	2	96	2	80
yield point 1	2	208	2	208					2	144	2	176	2	208	2	112
yield point 2	2	176	2	176	2	240	7	235								

yield point 1 reinforcing bars yield
yield point 2 H or L shaped steel members yield

TABLE 3: TEST RESULTS

	stiffness in elastic range	flexural cracked load	shear cracked load	ultimate flexural strength		ultimate shear strengnth	
experiment	224.4 (t/cm)	64.0 t	96.0 t	274.0 t		274.0 t	
				case 1	case 2	case 1	case 2
theoretical	391.3 (t/cm)	58.2 t	77.5 t	248.1 t	228.1 t	184.8 t	164.4 t

case 1 this includes nonbearing wall strength
case 2 this doesn't incrude nonbearing wall strengh

TABLE 4: MAXIMUM STRENGTH OF TEST FLAME

	m	K_0 (t/cm)	K_1 (t/cm)	K_2 (t/cm)	K_3 (t/cm)	K_4 (t/cm)	K_5 (t/cm)
case A	2.055	1579.0	613.7	39.2	−2303.3	−77.6	1579.0
case B	2.055	1333.0	353.8	68.4	−5095.0	−77.6	1333.0

	K_6	K_7 (t/cm)	X_1 (cm)	X_2 (cm)	X_3 (cm)	X_4 (cm)	X_5 (cm)	h
case A	473.7		0.41	2.44	6.90	7.30	12.8	0.0
case B	399.9		0.42	3.36	7.16	7.30	12.8	0.0

case A 6 shear walls in-filled + 10 shear walls with opening + 5 NONBEARING WALL
case B 6 shear walls in-filled + 10 shear walls with opening

TABLE 5: DIMENSIONS OF MODEL FOR RESPONSE ANALYSIS

27

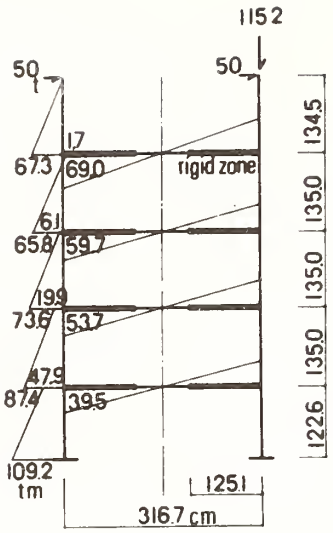

		Ae (cm²)	Ie (cm⁴)
column	1 FL	3388	1390
	2~4FL	3324	1369
beam		1596	1497

FIGURE 15:
MOMENT DISTRIBUTION OF
SHEAR WALL WITH OPENING

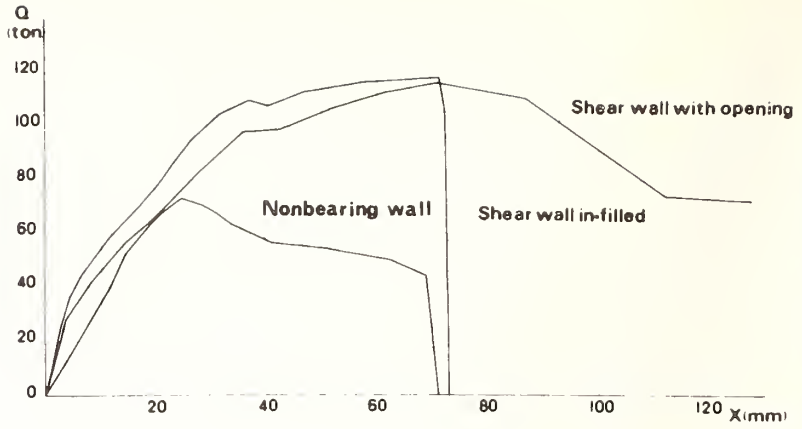

FIGURE 16: EXPERIMENTAL ENVELOPE CURVES OF WALLS

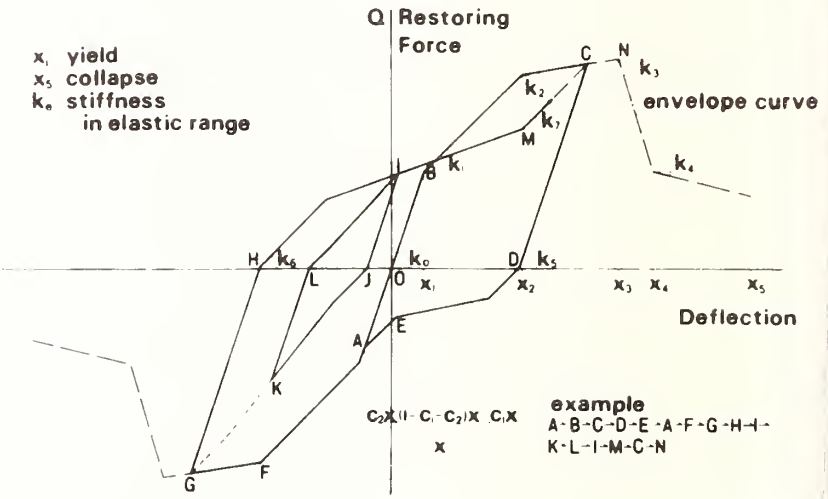

FIGURE 17: MODEL OF RESTORING FORCE CHARACTERISTICS

		El Centro		Taft		Vernon		Hiroo		Hachinohe	
		A	B	A	B	A	B	A	B	A	B
y_o max = 332.850 (gal)	x (cm)	1.20	1.33	1.30	1.92	1.18	1.72	1.86	1.56	1.37	2.33
	x (kin)	2.38	2.10	2.36	2.45	2.14	2.50	3.23	2.98	1.96	2.54
	x+y (gal)	551.2	428.2	580.9	532.8	545.3	495.9	747.4	469.0	602.8	600.2
y_o max = 500.0 (gal)	x (cm)	1.76	3.05	2.10	3.32	1.68	2.90	2.52	2.21	2.49	4.40
	x (kin)	3.20	4.20	3.52	3.45	2.67	3.88	4.63	4.23	3.22	4.27
	x+y (gal)	719.9	725.9	820.8	771.2	694.5	699.9	922.9	581.1	922.2	831.3

TABLE 6: MAXIMUM RESPONSE TO SEVERAL EARTHQUAKES

27

INELASTIC BEHAVIOR OF NON-BEARING WALLS IN AN 11-STORY STEEL-REINFORCED CONCRETE FRAME

PART TWO

AND

ASEISMATIC SAFETY OF EXTERNAL SURFACE FINISHES AND COATINGS

Makoto Watabe
Toshiyuki Kutoba
Akio Baba
Toshibumi Fukuta
Hiroshi Ito

Building Research Institute
Ministry of Construction

Aseismatic Safety of External Surface Finishes and Coatings

Though few structural members are destroyed, many non-structural elements and components are often destroyed in earthquakes. Worse, these sometimes threaten human life. In view of the fact that relatively little previous work has been conducted on the safety aspects of non-structural elements and components, this study evaluates the seismic safety of non-structural elements such as wall tiling, terrazzo block, brick masonry, and cement mortar rendering, etc.

Experiment

Specimens were the external surface finishing (Table 1, Figure 1) applied on the face of 20 load bearing walls with openings. The clearance of the boundary of each non-structural elements was 10 mm. The loading method and program were explained in the previous paper. The measuring method for each non-structural element was as follows:

cracking: visual observation
delamination: visual observation by tapping the surface of specimens with a steel bar
shear movement of joints: contact gage
adhesive strength: adhesion testing apparatus

Evaluation Method

First, each surface is divided into a cross-sectional square grid. Then the rate of cracking and rate of delamination can be defined as follows:

$$\text{Rate of cracking (ROC)} = \frac{\text{number of grids having any crack}}{\text{total number of grids}} \quad (1)$$

$$\text{Rate of delamination (ROD)} = \frac{\text{number of grids having any delamination}}{\text{total number of grids}} \quad (2)$$

Evaluation of Density of Cracks by Rate of Cracking (ROC)

When the size of grids is a cm x a cm, density of cracks D cm/cm^2 can be expressed by rate of cracking as follows:

$$D = \frac{P}{\sqrt{2}\, a \sin(\theta + \pi/4)} \qquad (0 \leq \theta \leq \pi/2)$$

θ = angle between horizontal line and cracking line.

This equation is based on the following assumptions:

A cracking line is straight with a certain gradient.
The distance of adjacent cracking lines is greater than the size of grid.
Cracking is expected to be caused at any part of wall.

As for the relation between density of cracks and ROC, the comparison between the theoretical value and the experimental value is shown in Figure 2. As shown there, ROC is proportional to density of cracks or the length of cracking. Therefore the concept of ROC is used instead of density of cracks or the length of cracking.

Evaluation of Delaminated Area by Rate of Delamination (ROD)

Since it is hard to identify the boundary of delamination, the following method (Grid Method) is proposed here. In the case of tiling wall the grid is the same as the dimension of the tile; with cement mortar and sprayed finishing, it is 10 cm x 10 cm. In this method, ROD is varied by the size of grid. Therefore in order to exclude the size effect, initial ROD is converted to normalized ROD as follows. Supposing initial ROD is P, ROD on the enlarged size of grid by n-times is P_n. If the delamination area is small and distributed randomly, $P_n = 1 - (1 - P)^{n^2}$ (n: natural number). If each delamination area is larger than the enlarged grid, $P_n = P$. As the actual delamination consists of those two phases, the relationship between P and P_n can be provided as follows:

$$P_n = \{1 - (1 - P)^{n^2}\} \alpha + P(1 - \alpha)$$

α = weight coefficient
which can be derived from the experimental data
(Figure 3)

In case of n = rational number, P_n can also be provided by this equation. Normalized ROD can be based to compare certain delamination areas with other different-size grid areas.

Results

Some results of the cracking and the delamination in non-structural elements are shown in Figures 4, 5, and 6. In these figures, a filled-in square shows an element having any cracking or any delamination up to the horizontal displacement of structure reached at R = 1/200.

The cracking and the delamination of non-structural elements occur along with the cracking in the load-bearing walls, while the delamination in the stoneware tile on the first story appears to be caused by relatively large compressive stress.

Generally more cracking in load bearing walls and more cracking and delamination in non-structural elements can be recognized on lower stories than on uppers.

At first cycle (design load), the cracking and the delamination in non-structural elements was scarcely recorded. At second cycle (horizontal displacement R = 1/200), a great amount of cracking and delamination occurred, while no falling out was observed. At seventh cycle (R = 1/100), a few fell out of the first story.

Characteristics of Cracking and Delamination in Various Surface Finishings

The relationship among ROC in load bearing walls and ROC or ROD in non-structural elements is shown in Figures 7 and 8. Because the behavior and the degree of destruction is different in each load-bearing wall, the characteristics of various non-structural elements are expressed by applying ROC in load bearing wall as the parameter. There is a limit to the length of crack propagation in the plane of load bearing wall even with a stepwise increase in loading. Within this limit, ROC in non-structural elements is relatively proportional to ROC in the load-bearing wall, and its proportional coefficient depends upon the individual non-structural element. Elements

having large proportional coefficient, such as cement mortar and and epoxy-based sprayed finishing, are liable to be cracked. The cracking on porcelain mosaic tile wall was only within the joints in a stepwise pattern.

The relationshup between ROC in load bearing walls and ROD in nonstructural elements is shown in Figures 8 and 9. This result represents the following:

Specimen -4, -5 (porcelain mosaic tile)

ROD in non-structural elements was relatively proportional to ROC in a load-bearing wall.

Specimen -1, -2 (stoneware tile), Specimen -6 (cement mortar rendering)

When the length of cracking in load bearing wall reached its limit, phenomenon of delamination in non-structural elements was started.

Specimen -3 (stoneware tile), Specimen -7, -8 (sprayed finishing)

No delamination occurred.

The pattern of the delamination on Specimen -1 (1F) appears to be a combination of the first two shown above. In brick masonry, there appears only a slight cracking, while in terrazzo block slight cracking and the falling out of several blocks were observed.

Results of Adhesion Test and Measuring of Joint Movement

Figure 10 shows result of adhesion test. At R - 1/200, the shearing movement of joints in Specimen -9 (brick masonry) was very little, and in Specimen -1 (stoneware tile fixed by ordinary cement mortar method) and Specimen -10 (terrazzo block) it was about 0.25 and 0.75 mm, respectively.

Conclusion

On the basis of this experiment, the following can be pointed out:

Our "Grid Method" for evaluating the cracking and delamination of external surface finishing, is simple and rational.

More work needs to be done to clarify the fundamental mechanism of the delamination--rigidity, strength, thickness, strain, adhesive strength.

"Specimen -3" (stoneware tile embedded at concrete) and "Specimen -7, -8" (sprayed finishing) were concluded to have sufficient aseismatic performance; the rest were relatively safe provided that no structural members were destroyed.

External forces, such as the relative displacement between the stories and the strain at the time of the collapse of non-structural elements, also need more study.

27

material	specimen number	applied story
stoneware tile 60x108x20mm	1	1 3
	2	1 3
	3	2 5
porcelain mosaic tile 47x47x4mm	4	2 4
	5	4 5
cement mortar	6	3 5
epoxy based sprayed finishing	7	2 3
urethan based sprayed finishing	8	2 5
brick masonry 50x50x210mm	9	1 4
terrazzo block 500x580x28mm	10	1 4

TABLE 1: SPECIMENS

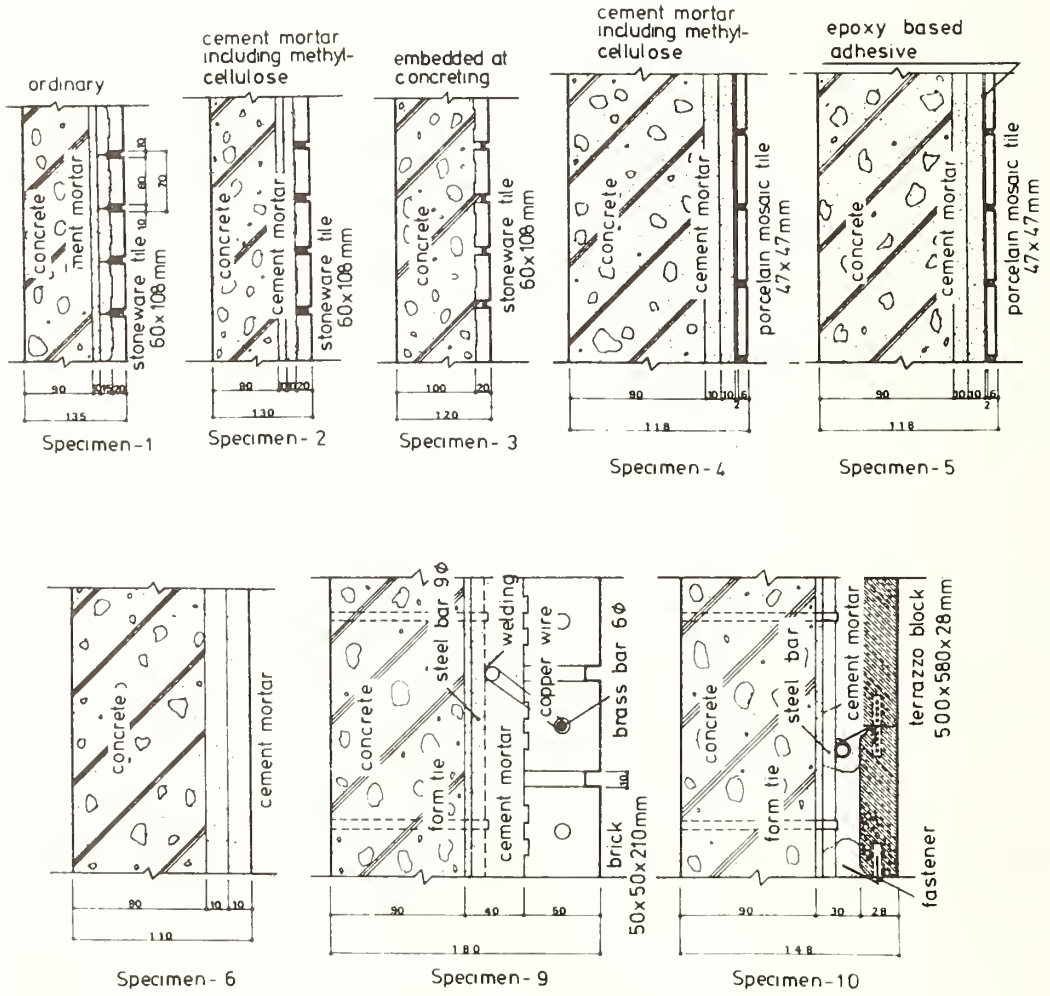

FIGURE 1: SPECIMENS

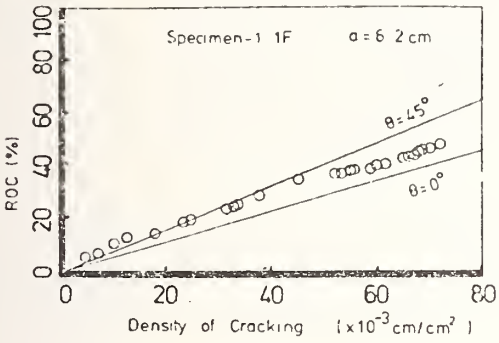

FIGURE 2: RELATION BETWEEN DENSITY OF CRACKING AND ROC

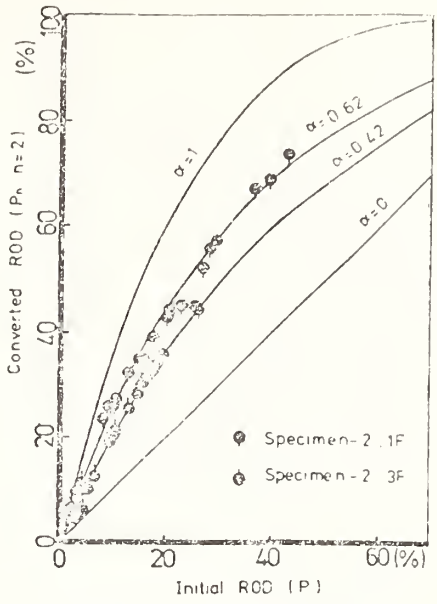

FIGURE 3: P-Pn RELATION

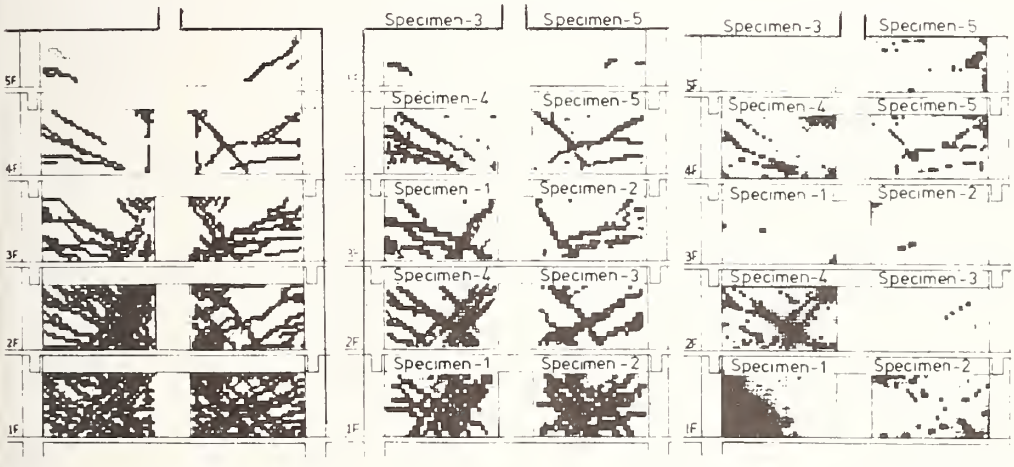

FIGURE 4: DISTRIBUTION OF CRACKING IN STRUCTURES

FIGURE 6: DISTRIBUTION OF DELAMINATIONS IN OBJECTED FINISHINGS

FIGURE 5: DISTRIBUTION OF CRACKING IN OBJECTED FINISHINGS

27

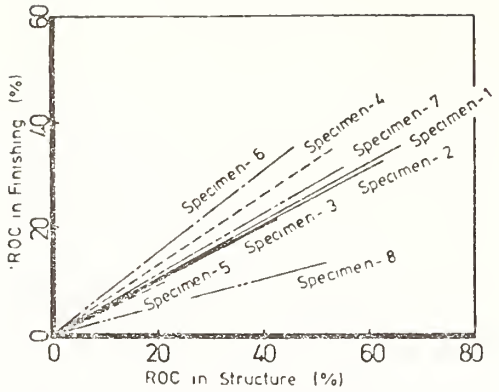

FIGURE 7: RELATION BETWEEN ROC IN STRUCTURE AND ROC IN FINISHING

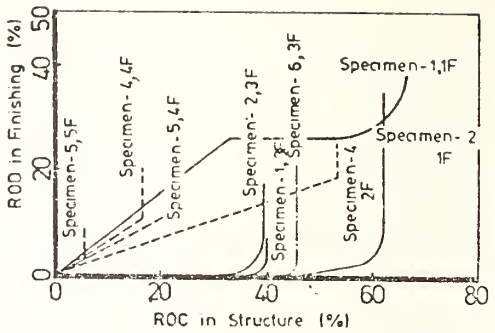

FIGURE 8: RELATION BETWEEN ROC IN STRUCTURE AND ROD IN FINISHING

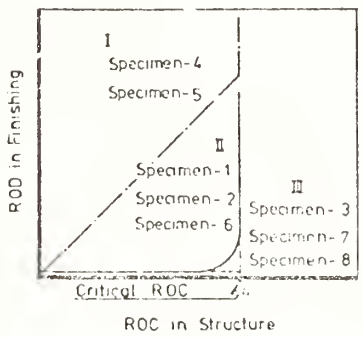

FIGURE 9: DELAMINATION PATTERN

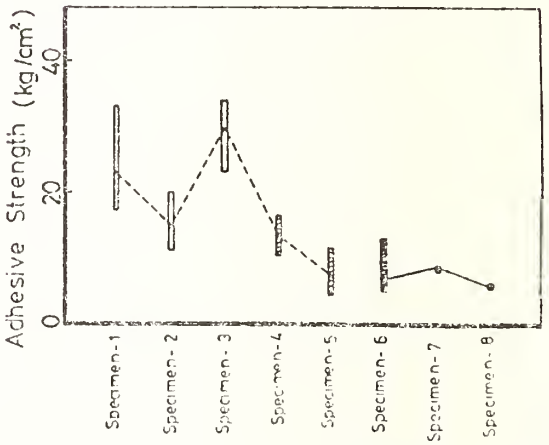

FIGURE 10: RESULTS OF ADHESION TEST

28

SEISMIC EVALUATION OF EXISTING MULTISTORY RESIDENTIAL BUILDINGS

G. Robert Fuller

Department of Housing and Urban Development
Washington, D.C.

Seismic Evaluation of Existing Multistory Residential Buildings

There has been a recent demand, caused by increased construction costs, for rehabilitation and restoration of existing multistory buildings, originally constructed for other occupancies such as commercial offices or hotels. A complex problem then arose for HUD's technical personnel and consultants to evaluate the structural resistance of existing buildings to earthquake loads.

The response of an existing building to earthquakes reflects the performance level inherent in codes, standards, and construction practices existent at the time of design and construction of the building. Building practices generally improve during the life of a building, reflecting an improved state of knowledge. Thus, implied margins of safety also change, depending on whether a comparison is made with the code in force at the time of design or with the current code. In addition, deterioration and alterations during the service life of a building affect the actual margin of safety provided by the structure. The need exists, therefore, to evaluate the potential seismic hazard of buildings. Following this evaluation, the cost of appropriate strengthening or retrofit may be determined so that the feasibility of various schemes to mitigate unacceptable hazards may be established.

The evaluation procedure discussed here is based on a feasibility and cost study of alternative strengthening techniques. It is intended to provide a method for upgrading existing buildings by identifying elements needing strengthening or repair and by verifying the adequacy of rehabilitation. The methodology can be applied nationally.

Methodology

The Methodology is based on the "Approximate Analytical Evaluation Method" developed by S. B. Barnes and Associates for the National Bureau of Standards. This analysis technique is contained in Building Science Series 61 (BSS 61), titled "Natural Hazards Evaluation of Existing Buildings" (National Bureau of Standards, 1975). The standard for determining structural integrity is based on compliance with the 1973 Edition of the Uniform Building Code (International Conference of Building Officials, 1973).

Data collection forms are included to provide a guide for compiling the type of information necessary to evaluate the building. Guidance is also given on methods available to verify properties of existing structural elements. If structural drawings of the original building are available they are very helpful, but it may still be necessary to verify how well the drawings define the actual building. Structural calculations for the original structure can also be of help, particularly in understanding the basis of the original design.

At the completion of the data collection, a first decision point is reached. Information in the data collection must be sufficiently complete and detailed to decide whether or not further analysis is desirable. The data collection information may result in termination of retrofit studies if the magnitude of renovation is obviously excessive.

To analyze a building as a whole it is necessary to assume an analytical model of the framing system. This is true whether a static or dynamic analysis is used and whether analysis is

accomplished by hand or computer methods. The model is determined by the building layout, physical properties of materials in structural frame or walls, and by their size, shape and location.

Once the model is established, the elastic fundamental period of the building can estimated. This may be done by hand calculation using the simplified formulas contained in the 1973 Uniform Building Code (UBC) based on building layout only, or by computer analysis to any degree of analytical complexity desired. Once this period is determined, the minimum design base shear can be obtained from formulas in UBC. The distribution of forces on the building may be accomplished either by simplified methods in the Code or by modal analysis of the lateral force resisting system.

The distribution of base shear as given by the Code should be modified if the building is highly irregular. This modification may be accomplished by approximation or by use of modal analysis, which is solely dependent upon the user's preference.

As part of the development of the structural model, it is necessary to determine paths through which loads are transmitted. This identifies the methods provided by the building frame for resisting lateral forces. In most buildings within the scope of this methodology, the resisting system will be structural bearing or filler walls. Some buildings may have lateral force resisting systems composed of moment frames or braced frames.

Once the forces on the building have been determined, an analysis of the structural model is performed in which the imposed loads are translated into moments, shears, and axial loads on the individual members composing the structural model. This analysis may be performed by using hand methods or the computer program included as part of the Manual.

From the basic data used to construct the structural model, the strengths of the individual members are determined by using UBC '73 criteria. These are the same methods provided by material specifications generally available for various systems such as structural steel; reinforced concrete; reinforced, unreinforced, or partially reinforced masonry and wood.

Also discussed are methods for determining appropriate basic strength of materials in existing construction, as distinct from methods in the Code required for new construction. This particular facet of evaluation is usually one of the most difficult to establish with any consistency or realism.

The basic design equation states that a member's strength shall not be less than load effects on that member, with an appropriate specified or implied factor of safety. The ratio of stress from load effects to nominal code stress limit is called the Stress Ratio. However, it is only necessary to determine the stress ratios from those members of the structural frame that can be seen to be most critical to the stability of the building.

The steps in the analysis discussed to this point are capable of being completed by either hand calculations or by using a computer program called the "ACE Program." It is emphasized that this computer program was included in our original research only on the surmise that it would be of help. Hand calculation methods are usually adequate for the types of buildings generally proposed for residential use.

Once critical stress ratios are determined, another decision point in the evaluation is reached. That is, to determine whether the building is adequate without retrofit or whether some form of structural strengthening is required.

In our study, various methods used to strengthen existing structures are discussed in a general manner. Specific methods of strenghening for individual conditions are left open to the designer. Methods not included may also be used when appropriate for the particular building being strengthened.

Some of the more general considerations on strengthening methods. are as follows:

(1) Increased shear resistance can be provided by adding new shear walls, adding encased reinforcement or by increasing thickness of shear walls upon replacement. However, added weight should be considered in its effect upon foundations, foundation pressures, and the building's inertial response to earthquake motions.

(2) Increased capacity of structural steel frames can be provided by adding material, reinforcing joints, or by additional bracing of members.

(3) Concrete frames can be strengthened by adding reinforced shotcrete.

(4) Infill walls can be isolated to be compatible with building motions or they can be strengthened by adding reinforced shotcrete.

(5) Removal of the upper stories of a building may reduce the overall hazard to an acceptable level.

During strengthening of the building, the status of existing stresses should not be ignored. Shoring may be required. In addition, the resulting effect on the stiffness of the building should be considered when selecting the method of strengthening. The joinery of strengthening elements to the rest of structure should also be considered in the design.

After the methods of strengthening are determined, a detailed cost of the strengthening should be made so that the cost of retrofit can be made a part of the decisionmaking process.

Finally, a decision at this stage of the evaluation should conclude that either retrofit strengthening is cost-effective, further iteration of strengthening is required, or retrofit is uneconomical. If further iteration is required. The process is repeated until the desired level of strengthening is reached.

28

Computer Analysis

Basic steps of the computer program are as follows:

Step 1:	Definition of properties of building.
Steps 2-4:	Calculation of 1973 UBC loads.
Step 5:	Definition of critical elements.
Step 6:	Calculation of moments, shears, and axial forces in critical element.
Steps 7-10:	Calculation of critical stress ratios.

The computer program is constructed in modular form so that the user can modify any one of the modules with a minimum of inconvenience. It is very important to note that the computer program can serve multiple uses. The program can be used to calculate UBC loads on the building, or additionally, it can be used to calculate moment and shear forces or element critical stress ratios for the UBC loading. The computer program is capable of modeling buildings with flexible or rigid diaphragms or buildings for which torsional response is significant.

To demonstrate the versatility of the program let us consider the UBC loading module of the ACE program. In the calculation of lateral forces due to earthquakes, the UBC requires the specification of building period. The user may directly input the desired building period, or he may input building properties and calculate a building period and then multiply that calculated building period by a scale factor based on experience, or he may calculate the period from formulas given in the 1973 UBC.

Once lateral forces are calculated they must be distributed over the building height. The program enables the user to either use the UBC formula for distributing forces, or alternately to distribute forces using the dynamic properties of the building and the calculated fundamental mode shape of vibration, and should be used when the building's lateral stiffness is not uniform over the building height.

The module of the computer program which performs the structural analysis is referred to as ETABS. This is a structural analysis program especially created for multistory buildings by Professor E. Wilson and his associates at University of California at Berkeley. This building analysis program was selected over the other potential building analysis programs for the following reasons (Wilson, et al., 1975):

(1) It is a computer program which has been used by the professional structural engineering community to calculate building response for comparison with San Fernando earthquake building response records.

(2) The computer program enables us to do a complete three-dimensional model of the building when existenance of either mass or stiffness eccentricity indicates that torsional response may be significant.

(3) There are many lateral force resistance systems available within the program for use in modeling. For example, shear walls, brace frames, and infill walls can all be modeled.

(4) It has the flexibility of adding equivalent springs to the stiffness of each story. These equivalent springs have been found to be useful in representing the stiffness characteristics of structural members which are exceedingly difficult to model in an exact fashion.

(5) The program has considerable flexibility in the treatment of loads. The user may calculate the stress ratios for only lateral loads or alternately the stress ratios can be calculated for any combination of dead, live or lateral loads.

As previously noted, the computer program is designed to be modular in form. In the masonry component, for example, the critical stress ratios can be calculated for axial and bending or just for shear stress.

The concrete critical element portion of the program branches off into separate modules for shear walls, beams or columns.

The steel critical element portion of the program has options for beams, columns or members that only carry axial loads.

To help the user in learning the program, our original research contained a hypothetical example with several different types of lateral forces resistance systems. The example is a two-bay by three-bay frame, two stories high. Floor diaphragms are rigid. Properties of one-bay are varied in the example in order to demonstrate how to input data for different lateral force resistance systems.

Example One

The first building is a six-story apartment building with basement. The building is 39' x 112' in plan and 63' high. It has unreinforced brick masonry exterior walls with wood interior framing.

A 'K' factor of 1.33 is used for determining the base shear. The diaphragms are flexible. After an examination of the masonry, an allowable shear stress of 7.5 psi was chosen as being appopriate. The building is rectangular in plan, providing diaphragms having a span-depth ratio of almost three.

Elevations of exterior walls were drawn indicating that first story strength and stiffness would be a problem. Critical elements were chosen for specific analysis. A wall analysis similar to those used for new buildings was made. The members of the building frame were modeled and the elastic distribution of the shear on the wall was determined. Shears and moments resulting from this analysis were calculated.

Critical stress ratios and results for 100 percent compliance with UBC 73, as well as for 75 percent, 50 percent, and 25 percent are tabulated.

Various potential strengthening methods are discussed, and the following were chosen for a detailed cost analysis:

(1) Diaphragm span reduction by providing interior transverse resisting elements.

(2) Reinforcement of exterior walls with shotcrete.

(3) Transverse interior shotcrete shear walls.

(4) Transverse interior steel moment frame.

28

Steel frames are placed on one side of the building corridor, and are used to provide flexibility for later room modifications. Consideration is also given to frame deformation and problems of erection.

Shear walls are located in positions to minimize room layout problems. First story flexibility and weakness is corrected by filling in walls with windows consistent with room layout.

A summary of the cost of structural modiifcation is provided to assist in decisionmaking. Very little difference in cost was found in providing for 25 percent or 100 percent of UBC 73 forces. This indicates that in some cases design forces have little effect on the cost of providing earthquake resistance.

Example Two

This example is a six-story building with basement, having a concrete frame and brick masonry filler walls. The base of the building is 110' x 200' in plan and 81' high. A 'K' factor of 1.00 was used to determine the base shear. Rigid diaphragms were assumed. The masonry was considered somewhat better than that in Example 1 so an allowable shear of 10 psf was used.

A complexity offered to hand calculations is the fact that the west edge of the building is skewed with respect to the other side. Upper floors in the "L" shaped tower provided an eccentricity of mass to the base structure. Elevations again indicate that the first story flexibility would require analysis. The wall adjacent to the building next door is concrete and solid except for a vent shaft.

A force diagram on the building layout indicates the severity of first floor eccentricity. Distribution of the base shear and story shears were calculated and tabulated. A compatible design level for diaphragms was also determined.

This building, having rigid diaphragms and having a large torsional moment required a torsional analysis to be made so that the appopriate design shears on each wall could be determined. Once the forces on each wall were determined, a wall analysis was performed similar to that in Example 1. Critical stress ratios were tabulated to assist in determining the method of strengthening.

Again, tables were assembled for 100 percent compliance with UBC 73, Zone 3, and for 75 percent, 50 percent, and 25 percent to assist in the evaluation.

Interior shear walls were added. Exterior masonry walls were strengthened using 6" reinforced shotcrete in place of one wythe of brick. After providing what was deemed to be the appropriate strengthening, analysis was again performed. The final critical element stress ratio table indicated that further strengthening was not required.

As part of the required strengthening, such detail items as struts to shear walls were included. First-story archways were partially filled, with consideration given to continued functioning of first-story shops.

Cost analysis was tabulated to provide the data necessary for final decision making.

Conclusions

This methodology was developed for use by HUD technical personnel to determine the feasibility of rehabilitating existing property for residential use under HUD programs. It should also be a valuable tool for consulting engineers, under contract with HUD, to evaluate proposed rehabilitation projects.

The computer program is available through the National Information Service, Eathquake Engineering, Computer Applications at the University of California at Berkeley. Copies of our three-volume manual may be purchased from the Superintendent of Documents, U.S. Government Printing Office, Washington, D.C. 20402.

Acknowledgments

The information in this paper was primarily obtained from a taped slide presentation prepared by Clarkson W. Pinkham of S. B. Barnes and Associates and Gary C. Hart of J. H. Wiggins Co. for HUD technical personnel. Special thanks goes to Andrei Gerich, HUD Structural Engineer, for reviewing the paper and Sheila Lockwood for typing.

References

1. International Conference of Building Officials, 1973, Uniform Building Code, 1973 Edition, Chapters 23-28.

2. National Bureau of Standards, January 1975, Natural Hazards Evaluation of Existing Buildings, Building Science Series 61 (BSS 61), "Approximate Analytical Evaluation Method."

3. Wilson, E. L., Hollings, J. P. and Dovey, H. H., Three-Dimensional Analysis of Building Systems (Extended Version), April 1975, Earthquake Engineering Research Center Report No. 75-13.

29

DAMAGE TO ENGINEERING STRUCTURES DURING THE NEAR IZU-OHSHÍMA EARTHQUAKE OF JANUARY 1978

Kazuto Nakazawa
Toshio Iwasaki
Kazuhiko Kawashima
Makoto Watabe
Hiroyuki Yamanouchi
Yutaka Yamazaki

Ministry of Construction

Damage to Engineering Structures During the Near Izu-Ohshima Earthquake of January 1978

The details of this January 14, 1978, earthquake have been presented in Paper 12 of this volume. Seismic intensity on the JMA Scale at various sites is shown in Figure 1

Many fore-shocks were observed near Izu-Oshima Island; after-shocks, including a shock registering a magnitude of 5.8, occurred in the middle part of Izu Peninsula (see Figure 2). The fault line of the main shock was directed from the near Izu-Ohshima to the middle part of Izu Peninsula, in an east-west direction. Other parameters about the fault are as follows:

Length of the fault line -- 20 km

Dip angle -- 90°

Dislocation -- 1 m

Topography and Geology of the Izu Peninsula

The central part of Izu Peninsula is a mountainous area with steep hills. Volcanic topography is seen in this area, with famous volcanic Mt. Amagi near the center of the peninsula. Mountain ridges have a nearly constant height.

As shown in Figure 3, a map of the peninsula from the Shizuoka Prefecture, the geology of this area is represented by the Yugashima Group and the Shirahama Group consisting of Neocene volcanic ejecta, volcanic lavas, and volcanic mud flows and pyroclastics. The Yugashima Group and the Shirahama Group are surface-soil strata made from tuffaceous sandstones, siltstones, breccia, and volcanic conglomerates.

In the areas of Inatori, Higashi Izu Town and Mitaka, Kawazu Town, terraces with moderate slopes are made of volcanic mud flows including site gravels. In the areas of Naramoto, Higashi Izu Town, and Mitaka Iriya Nanamagari, Kawazu Town, pyroclastics cover the surface. These are loose layers made of scoria, loam, and light yellow volcanic ash, with moderate slopes of about 25°.

As in the Off-Izu Peninsula earthquake of May 9, 1974, active faults were disclosed after the recent earthquake. Surface dislocations were found along a line connecting Inatori and Neginota.

Right lateral dislocations of 18 cm were seen on the pavement of National Highway Route 135 (see Figure 4) located in front of Inatori and Neginota. Considerable damage was concentrated close to the active faults.

Earthquake Ground Motions

The maximum values of the observed earthquake accelerations at the sites are shown in Figure 5. The accelerograms closest to the fault were on a basement floor of Itoh Denden Office, the epicentral distance to which is nearly 30 km. Time histories and response spectra of the accelerograms are shown in Figures 6 and 7. The maximum vlaues of acclerations, velocities, and displacements of the earthquake motions were:

Accelerations -- 101.1 gal (EW), 71.9 gal (NS), 31.9 gal (UD)

Velocities -- 16.2 kine (EW), 10.0 kine (NS), 5.1 kine (UD)

Displacements -- 10.5 cm (EW), 2.8 cm (NS), 2.4 cm (UD)

The maximum values of the EW component are considerably larger than those of the NS component. On the other hand there are some differences in frequency characteristics between the spectra, shown in Figure 7 in EW and NS components. The differences on the maximum values of the motions and the spectra between both of the components are explained by the fact that the earthquake records were obtained near the fault and that the direction of the fault line was EW.

The following are pointed out in Figures 6 and 7:

- The duration of the main earthquake motion is 15 to 20 seconds.
- The predominant periods in EW component are 0.4 and 0.7 seconds. The maximum amplification factor 3.07 for 5 percent of critical damping at the former peak period.
- The predominant period in NS component is 0.5 seconds, with the maximum amplification factor 3.9 for 5 percent critical damping.
- The ratio A_v/A_h of the maximum acceleration of UD component to that of horizontal components is 0.32 and 0.44 for EW and NS components, respectively. According to the maximum values observed at the various sites as shown in Figure 5, the ratio, A_v/A_h is 0.45 on an average.

Figure 8 shows the distribution of overturned tombstones in graveyards in Izu Peninsula (171 graveyards were investigated). In the 3 areas,Higashi-Izu Town to Kawazu Town, Amagi-Yugashima Town, and Nishi-Izu Town, ratios of overturned tombstones to total number of ones in each yard exceeds 50 percent. However, it may be that the overturned tombstones in the latter two areas were due to after-shocks rather than the main shock. Epicenters of major after-shocks are plotted in Figure 8.

Statistics of Damage

Regions hit by the earthquake cover the administrative districts of Shizuko Prefecture and the Tolyo Metropolis (Izu-Ohshima Island). Twenty-five persons were killed in all by slope failures and landslides. Earthquake damage in Shizuoka Prefecture is summarized in Table 1. The total amount of the damage is estimated at 31 billion yen (104 million U.S. dollars) -- far greater than the damage from the Off-Izu Peninsula Earthquake of 1974 by a factor of 12. Approximately 40 percent of this amount was damage to roads. Damage to public works is summarized in Table 2.

Damage to Civil Engineering Structures

The major damage mode to roads in the 1978 earthquake was landslides occurring on natural slopes, while major damage in the Off-Izu Peninsula Earthquake of 1974 resulted from settlements in road embankments and cracks in pavements. Nevertheless, several failures took place in embankments, retaining walls, and tunnels but highway bridges and pedestrian overcrossings suffered little damage.

Road damage seemed isolated to Route 135 (national road), the Higashi-Izu Toll Road, and Shuzenji-Shimoda Route (principal prefectural road) as shown in Figure 10. The areas heavily damaged are considered to be in good agreement with the areas where after-shocks took place (shown in Figure 2).

Landslides

The field observations revealed that the slope failures could be classified into three categories: failures of soil slopes, failures of rocky slopes, and rockfalls.

Typical soil failure could be observed in Naramoto Area (Higashi-Izu Town), Mitaka-Iraya-Nanamagari Area (Kawazu Town), and Nashimoto Area (Kawazu Town). In the former two areas, surface soils with a depth of 1 to 2 meters were underlaid by scoria with a depth of 2 to 3 meters and loam. The sliding of soils generaly took place in the scoria stratum or between scoria and loam strata. The amount of soil that fell was estimated to be from several thousand to two hundred thousand cubic meters in this type of failure. In the case of rocky and weathered surface soils, the amount of falling soils was estimated to be from several thousand to ten thousand cubic meters. Figure 11 shows a representative failure of this type at Nashimoto Area (Kawazu Town). It was noted the failure of this sort most likely happened at convex parts of slopes as shown in Figure 12.

The falling stones consisted chiefly of rocks with few joints and volcanic and site gravels, such as Yugashima Group, in both Kawazu and Amagi-Yugashima Towns. The amount of falling stones was on the order of several hundreds of cubic meters.

In addition to the slope failures described above, failures of cutting slopes were also observed. However, later investigation showed that the cutting slopes themselves did not generally fail. The natural slopes above them sometimes fell on the cutting slopes. It was also observed that slopes retained by concrete walls, concrete frames, or concrete or mortar covering could survive the earthquake.

Embankment and Retaining Walls

In the case of embankments constructed by both cutting and filling, filled parts generally settled, resulting in cracked pavements. In the Yugano Area along the Shuzenji-Shimoda Route, several embankments failed. Figure 13 shows a reprsentative failure 3.5 m in width, 60 m in length, and maximum settlement of about 60 cm.

In the area hit by the earthquake there were a number of retaining walls for cutting and embanking slopes. The most common retaining walls were concrete or masonry. Although some of them were damaged as shown in Figure 14, they could survive safely with minor non-structural damages such as cracks, gaps, or small settlements. There were several high embankments with a height of more than 10 to 20 meters in the east Izu area as shown in Figures 15 and 16. It should be noted that these high embankments could perform quite well against the earthquake when adequately retained.

29

Tunnels and Bridges

In the 425 m-long Tomoro Tunnel (Higashi-Izu Toll Road), a piece of lining concrete near the arch crown and side wall fell down as shown in Figure 17. Large amounts of soil also fell near the tunnel entrances, blocking transportaion in the Shirata, Kitoh, and Kurone

Tunnels on Route 135. In the Inatori Tunnel (Izu-Kyuko Railway) lining concrete was crushed by fault movements, and uplifts shifted the railbeds.

On the Shin-Shimoda Bridge (Shimoda City), Figure 18 shows that the free end of a prestressed concrete girder moved horizontally about 7 cm. This lateral movement crushed concrete handrails at both sides since they were rigidly connected to the abutments to set the mermaid statues. It was also observed that several pieces of concrete at parapets and piers fell down in Shimoda Bridge on Route 135 and that a pier of the Minato Bridge in Shimoda City settled approximately 0.5 meter.

Two pedestrian overcrosses survived with a few minor cracks, although they were located only 20 meters away from faults near Inatori Junior High School (Figure 19). Ground motion at the site was estimated to be very severe since several wooden residential houses and most gravestones around the site were overturned.

Other Damage

Two tailing dams for storing mining wastes collapsed as shown in Figures 20 and 21. The slimes that overflowed polluted the Mochikoshi River, Kano River, and Suruga Bay.

Damage to Building Structures

Damages to buildings were classified into 4 groups:

- Damage due to vibrational response of structures
- Damage due to cracks caused by faults
- Damage due to landslides
- Damage due to instability in road-shoulders

Wooden Structures

Roof tiles fell off around roof ridges in many places (Figure 22). Mortar finishing exterior walls were cracked and some fell off because of underlying dry rot (Figure 23). Moreover, some wooden structures collapsed due to heavy roof weights or weak ground (Figures 24, 25, and 26).

Continuous footings of wood structures lying on faults were deformed and cracked, and by these deformations the structures were distorted. Mortar concrete covering dirt floors had many and large cracks (Figures 27, 28, and 29).

Landslides took the greatest toll of property and lives (Figure 30). Many houses were swept away and crushed by earth and sand (Figure 31).

Structures standing close to roads began to lean over because of the instability of road-shoulders or failure of the retaining walls on the opposite sides of the roads (Figures 32 and 33).

All damage in East-Izu seemed to be caused by the main shock, while those in West-Izu were caused by the after-shock.

Reinforced Concrete Structures

In general, no reinforced concrete structure had severe structural damage. The 3-story school building (Inatori lower secondary school), which was about 100 meters from the fault line, had many great cracks in the joint between the stair hall and the school-rooms.

Most buildings built near slopes settled unevenly. Figures 34 through 37 show this typical damage and Table 3 classifies reinforced concrete buildings according to the types of damage they suffered.

Damage to Steel Structures

It is said that steel buildings were more severely damaged than reinforced concrete and wooden ones. In fact, the damage that actually occurred to steel buildings was limited to non-structural members. This fact gave the impression that the steel buildings were especially hard hit.

No buildings with severe damage to main structural members could be observed outside of an apartment house and hotel. Damages to non-structural members are typified by the damage to the exterior walls of a hotel in the Inatori region (Figure 38). In the Izu district, mortar finish on metal lathing, similar to this hotel, is widely used for exterior walls of steel buildings. In many cases, connectors -- usually steel wires used to tie the exterior walls to furring strips -- were rusted by sea breezes.

As for structural problems, some buckling of diagonal braces and fracture of their connections were observed, especially in the gymnasiums of schools. However, the fabrication and execution of these works were poor, particularly in welded or bolted connections to fasten braces to gusset plates and to fasten gusset plates to beams or columns. Since this kind of damage to connections around braces has also been seen in past earthquakes, such as the Tokachi-Oki earthquake, this shows that recent seismic prevention recommendation have not been put to practical use.

The restaurant that collapsed (Figure 39) was result of poor building practices in column supports, end connections, and gusset plate connections of diagonal braces and beam-to-column connections. By contrast, the apartment house (Figure 40) and the hotel (Figure 41) failed because of poor structural planning. For the apartment house, the first-story columns were too slender. As for the hotel, the plan of the building was so complicated and each H-shaped column was arranged so irregularly with respect to the sectional axis that the details of beam-to-column connections were neglected.

In the Izu district, most steel buildings are a kind of mixed construction -- the first story is often reinforced concrete and the stories over it are made of structural steel. In general, steel in this type of building tended to whip from the earthquake excitations, because of the large difference among ratios of story rigidity to story weight. Because of this, a great deal of damage occurred to exterior walls and interior partitions that were not deformable enough to follow the large deflection of the steel frames.

Acknowledgments

The Public Works Research Institute and Building Research Institute received a great deal of assistance from the Headquarters of the Ministry of Construction, the Chubu Regional Construction Bureau, and Shizuoka Prefectural Government. Seismic data and strong-motion records were collected from the Earthquake Research Institute of the University of Tokyo, the Seismology Division of the Japan Meteorological Agency, the National Research Center for Disaster Prevention of the Science and Technology Agency, the Port and Harbour Research Institute of the Ministry of Transport, the Kanto Regional Construction Bureau, Japanese National Railways, Nippon Telegraph and Telephone Public Corporation, and Japan Highway Public Corporation. The authors express their sincere thanks to the staff members of these above organizations.

References

1. Public Works Research Insitute, "Progress Report on Earthquake Damages Due to the Near-Ohshima Earthquake in 1978," Journal of Public Works Technics 20-4, April 1978.

2. Public Works Research Institute, "Earthquake Damages Due to the Near-Ohshima Earthquake in 1978, Technical Note No. 1346, Ministry of Construction, March 1978.

3. Shizuko Prefecture, Geological Map of Shizuoka Prefecture, Naigai Map Ltd., March 1973.

4. Public Works Research Institute, "Progress Report on Earthquake Damage Due to the Off-Izu Peninsula Earthquakes," Journal of Public Works Technics 16-7, July 1974.

5. Assoication for Promoting Strong-Motion Acceleration Measurements, Progress Report No. 13 -- Near Izu-Ohshima Earthquake in 1978, National Research Center for Disaster Prevention, Science and Technology Agency, March 1978.

6. Public Works Research Institute, Final Report for Research and Development on Earthquake Engineering Technics, Technical Note No. 1250, Ministry of Construction, March 1977.

7. Building Research Institute, Progress Report on Earthquake Damage Due to the Near-Ohshima Earthquake 1978, Ministry of Construction, January 1978.

8. Makoto Watabe, "Research on Design Earthquake," B R I Research Paper No. 67, September 1976.

TABLE 1: EARTHQUAKE DAMAGE IN SHIZUOKA PREFECTURE

Damages		Unit	Total	Higashi-Izu T.	Amagi Yugashima T.	Kawazu T.	Shimoda T.	Nishi-Izu T.	Matsuzaki T.	Toi T.	Ito C.	Minami-Izu T.	Kamo V.	Atami C.	Naka-Izu T.
Damage to Human Beings	Dead	Person(s)	25	9	5	11					1				
	Heavily Injured	"	34	23	3	2	4	1							
	Slightly Injured	"	171	86	5	26	47	1	2		3	1			
	Total	"	205	109	8	28	51	2	2		4	1			
Damage to Residential Houses	Completely Collapsed	House(s)	96	56		16	12	7	4		1				
		Family(ies)	100	56		16	16	7	4		1				
		Person(s)	410	251		77	44	23	14		1				
	Heavily Collapsed	House(s)	616	460		56	24	34	11		4		27		
		Family(ies)	633	478		56	25	34	11		2		27		
		Person(s)	2,587	1,998		236	87	105	41		12		108		
	Partially Collapsed	House(s)	4,170	2,097	124	879	77	229	195	100	304	29	114	1	21
		Family(ies)	4,256	2,125	124	879	81	283	194	100	306	29	114	1	20
		Person(s)	16,335	8,053	521	3,581	291	1,023	701	400	1,166	119	392	4	84
Damage to Non-Residential Houses	Public	House(s)	24	6	2		12	2	1				1		
	Non-Public	House(s)	538	145		78	57	124	9	60	45		20		
Other Damages	Overburden Rice Field	ha	5.662	0.500	0.742		1.180	1.09	0.4			0.300			1.45
	Overburden Field	ha	13.112	10.500	2.012		0.02	0.15		0.100		0.300			
	Educational Facilities	Point(s) Damaged	84	14	5	6	33	7	4		10	3	1	1	
	Hospitals	"	44	25		14			3				2		
	Roads	"	1,126	375	13	494	30	92	4	22	12	3	65	3	13
	Bridges	"	3			2	1								
	Rivers	"	65	18	10	27	2	3							5
	Fishery Ports	"	12	4		1		4			2		1		
	Sabo	"	2									1			1
	Waterwork Facilities	"	532	78	116	85	31	106	4	12	7	3	90		
	Cleaningwork Facilities	"	5	1		2		1			1				
	Slope Failure	"	191	57	22	38	12	5	21	9	25	2			
	Rail Roads Damaged	"	26	12		12					2				
	Communication Service Facilities	No.	579	330		140		109							
Number of Family Damaged		House(s)	733	534		72	41	41	15		3		27		
Number of People Damaged		Person(s)	2,997	2,249		313	131	128	55		13		108		

TABLE 2: AMOUNT OF EARTHQUAKE DAMAGE TO PUBLIC WORKS

Administrative District	Classification	No. of Damaged Points	Amount of Damages (million yen)	Notes
Tokyo Metropolis	Roads	3	38	Town Road No. 38 in Izu-Ohshima Town
Shizuoka Prefecture	River	51	245	Kawazu River, etc.
	Sabo	5	108	Shirata-River, Nigori-River, etc.
	Roads (except Bridges)	737	12,175	Routes 135 and 136(National Road), Shuzenji-Shimoda Route and Ito-Nishiizu Route(Prefectural Road)
	Bridges	7	39	Shin-Shimoda Bridge and Minato Bridge(Shimoda City), Shiratagawa Bridge(Kawazu Town)
	Toll Roads	44	1,800	Higashi-Izu Toll Road, Amagi Tunnel Toll Road
	Sub total	844	14,367	
Total		847	14,405	

TABLE 3: DAMAGED REINFORCED CONCRETE BUILDINGS CLASSIFIED ACCORDING TO CAUSES

Region		Due to Response	Due to Ground	Due to Faults	Other Causes	Slight Damages
East-Izu	Inatori	Preschool(1F)	Apartment House(4F) Hotel(4F+2B)	Lower Secondary School(3F)		High School(4F) Primary School(4F)
	Nashimoto	Hotel(3F)				Hotel(3F) Dormitory(3F)
	Mine					Hotel(4F)
	Kawazu					Public Office(2F)
	Imaihama	Hotel(4F) Hotel(6F)				
	Shirahama				Dormitory(3F)	
	Atagawa	Lower Secondary School(3F) Primary School (3F)	Hotel(3F)			
	Katase-shirata	Hotel(4F+1B)				Apartment House(4F) Hostel(3F)
West-Izu	Matsuzaki					Lower Secondary School(3F)
	Arazato		Office(1F)			

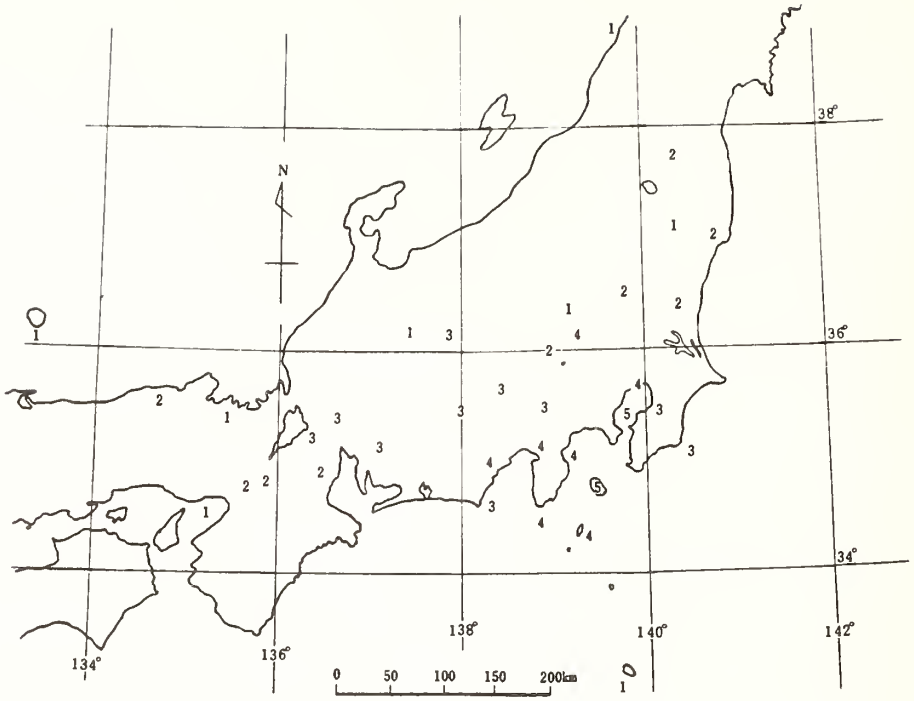

FIGURE 1: SEISMIC INTENSITY, THE NEAR IZU-OHSHIMA EARTHQUAKE OF JANUARY 14, 1978

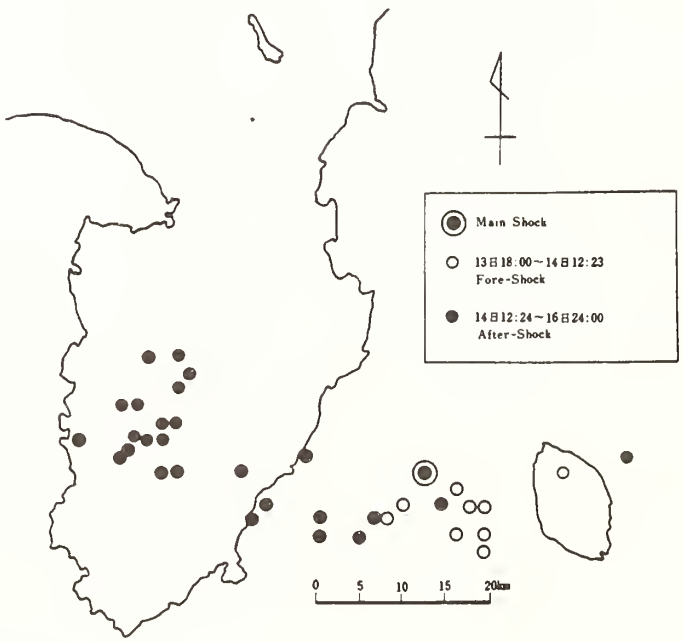

FIGURE 2: DISTRIBUTION OF EPICENTERS OF SHOCKS

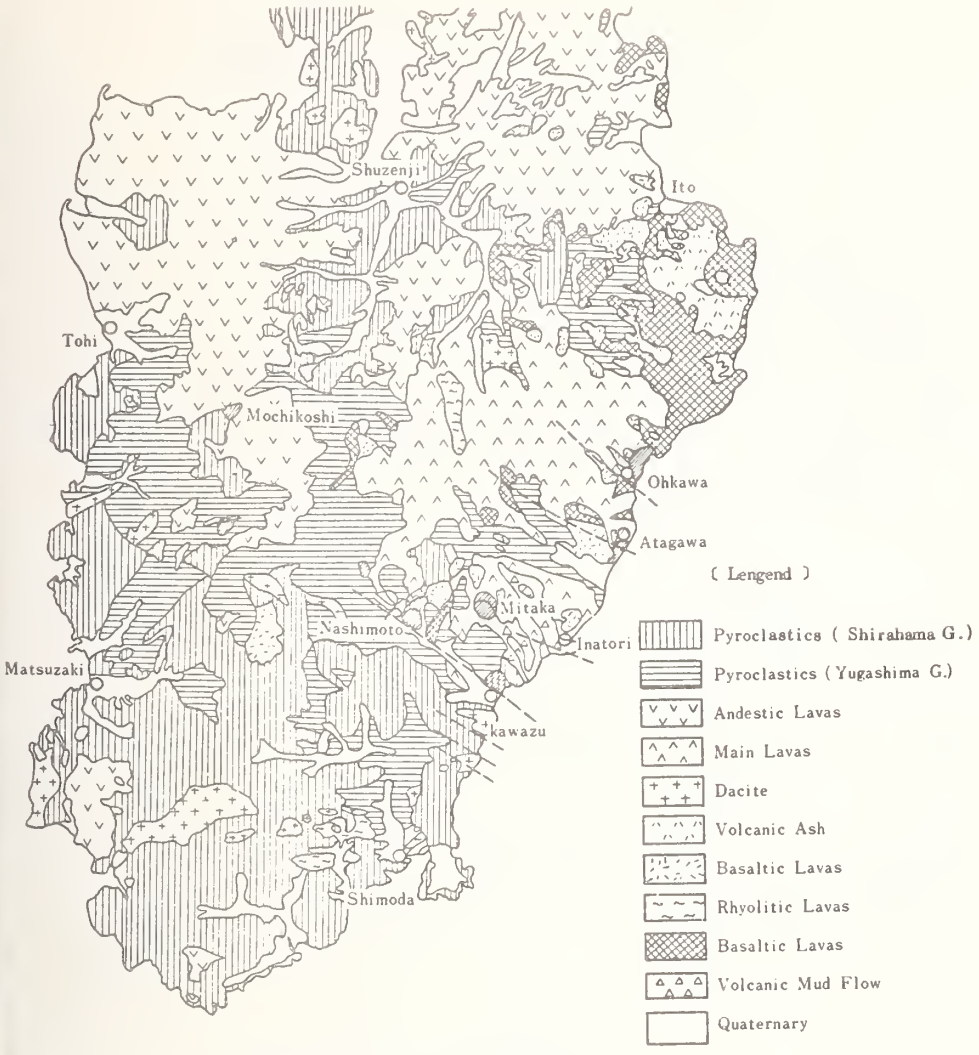

FIGURE 3: GEOLOGICAL MAP OF IZU PENINSULA

IGURE 4: TRACES OF EARTHQUAKE FAULT ON ROUTE 135 IN FRONT OF INATORI JUNIOR HIGH SCHOOL (LIGHT LATERAL DISPLACEMENT WITH A MAGNITUDE OF 18 cm)

29

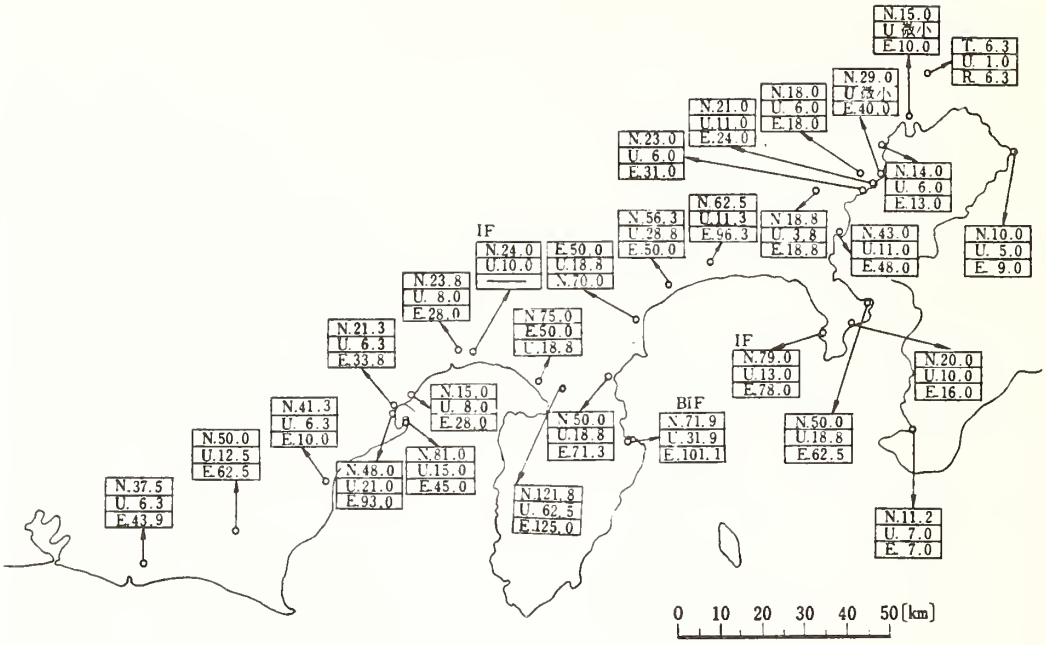

FIGURE 5: THE MAXIMUM GROUND ACCELERATIONS

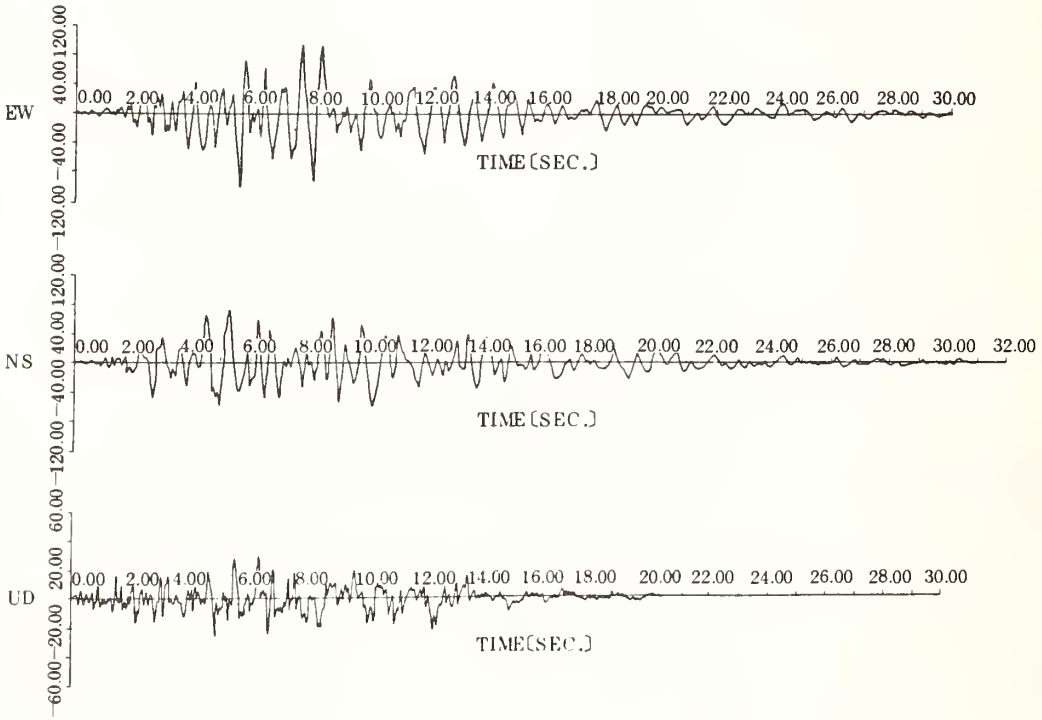

FIGURE 6: TIME HISTORIES: ITOH DENDEN OFFICE

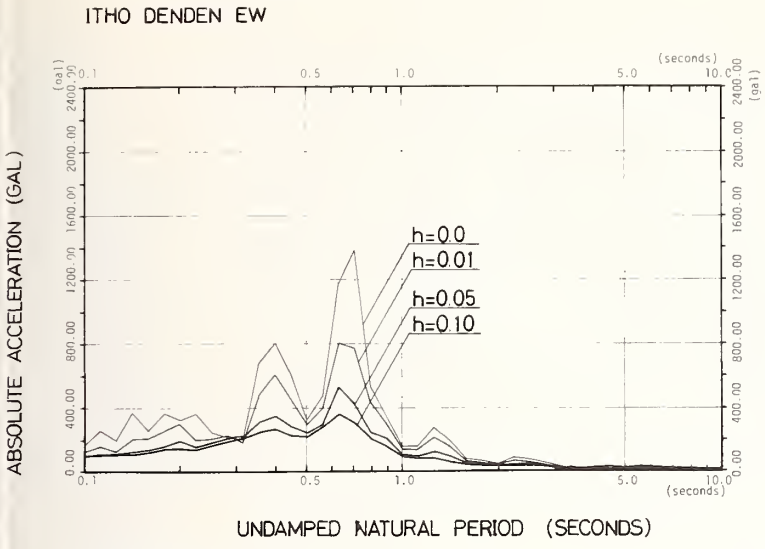

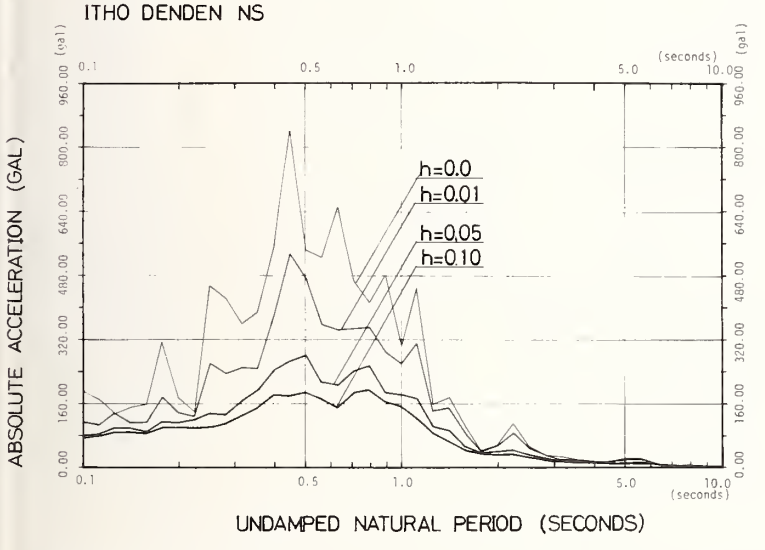

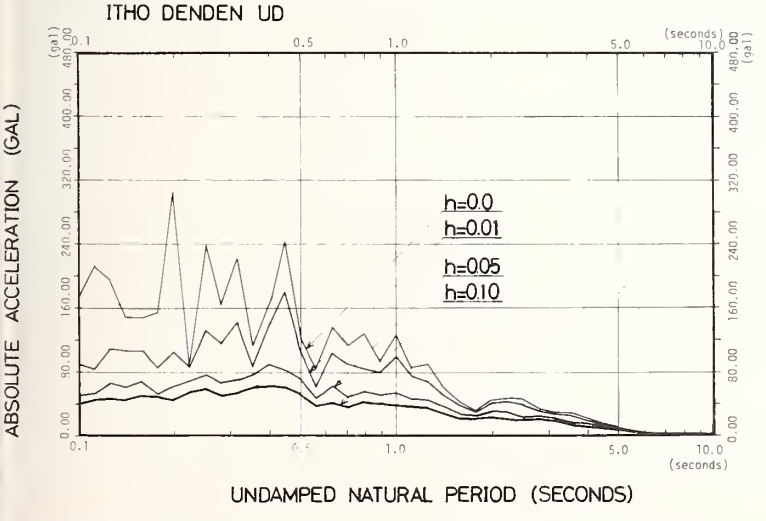

FIGURE 7: RESPONSE SPECTRA: ITOH DENDEN OFFICE

29

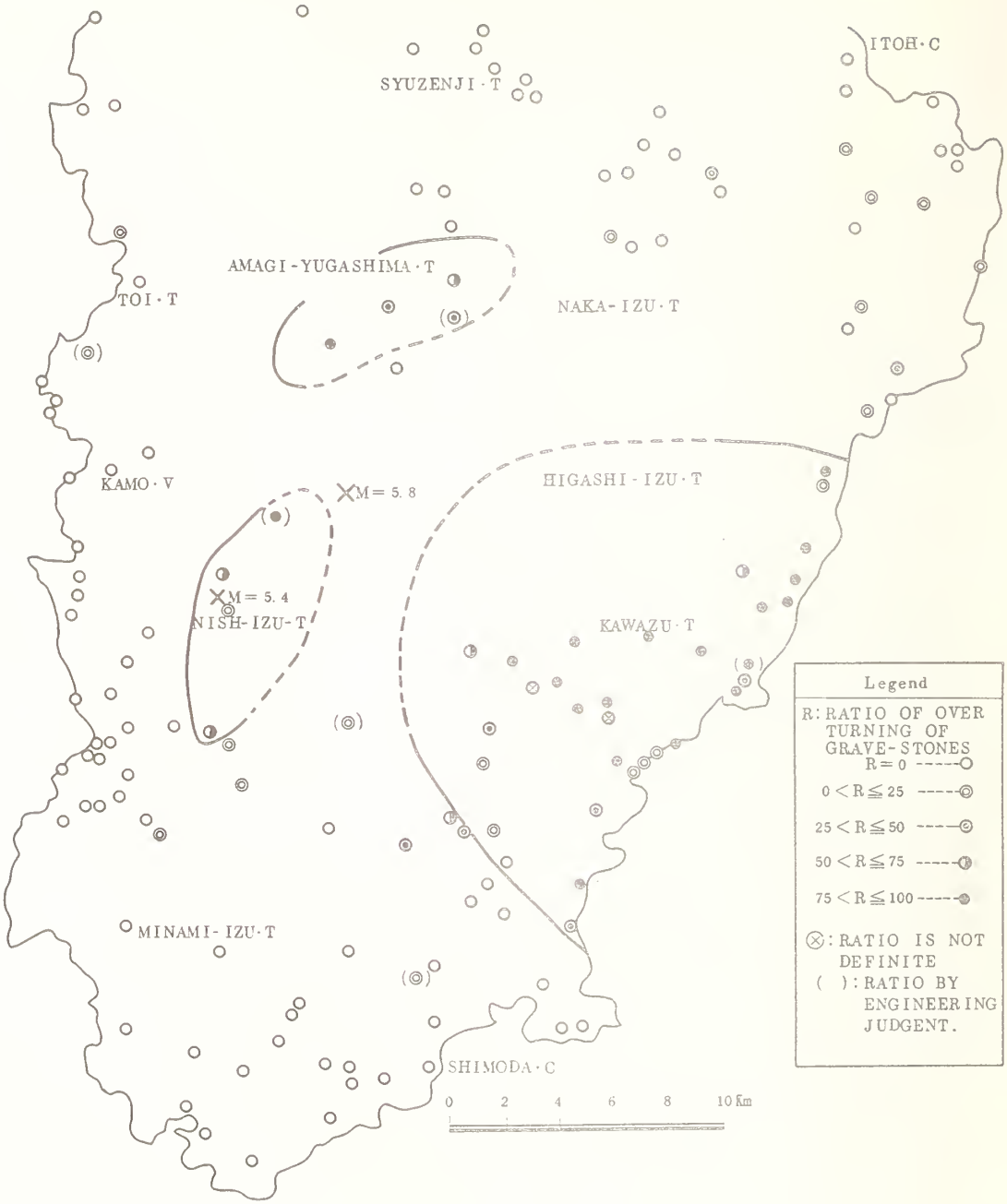

FIGURE 8: DISTRIBUTION OF OVERTURNED GRAVESTONES

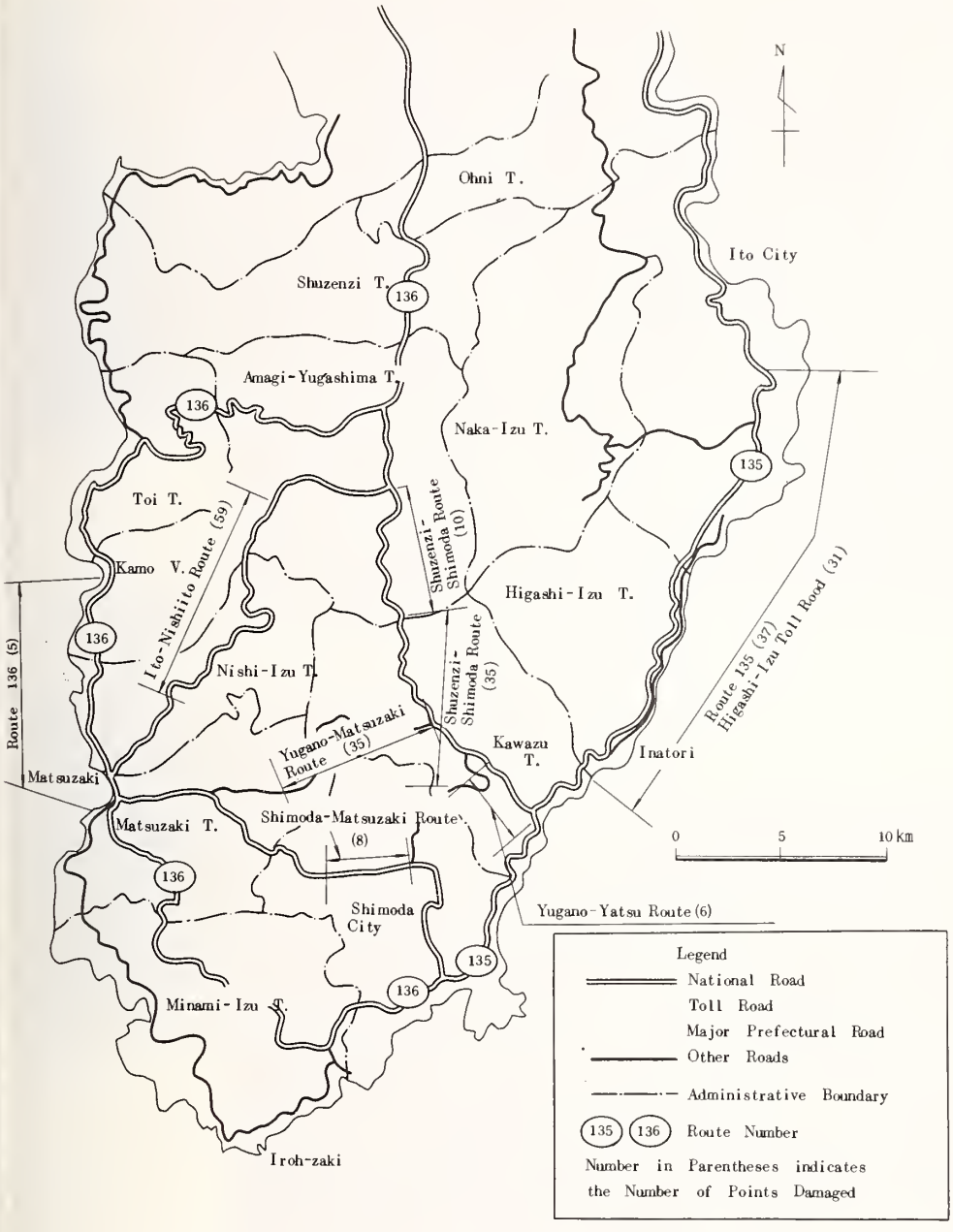

FIGURE 10: DISTRIBUTION OF ROADS DAMAGED

29

FIGURE 11: SLOPE FAILURE AT NASHIMOTO AREA IN KAWAZU TOWN (SHUZENJI-SHIMODA ROUTE, PHOTOGRAPH FROM SHIZUOKA PREFECTURE)

FIGURE 12: SLOPE FAILURE AT OHKAWA AREA IN HIGHSHI-IZU TOWN (ROUTE 135, PHOTOGRAPH FROM SHIZUOKA PREFECTURE)

FIGURE 13: SETTLEMENT OF EMBANKMENT IN YUGANO AREA (SHUZENJI-SHIMADA ROUTE)

FIGURE 14: FAILURE OF MASONRY WALL AT INATORI AREA IN HIGASHI-IZU TOWN (ROUTE 135)

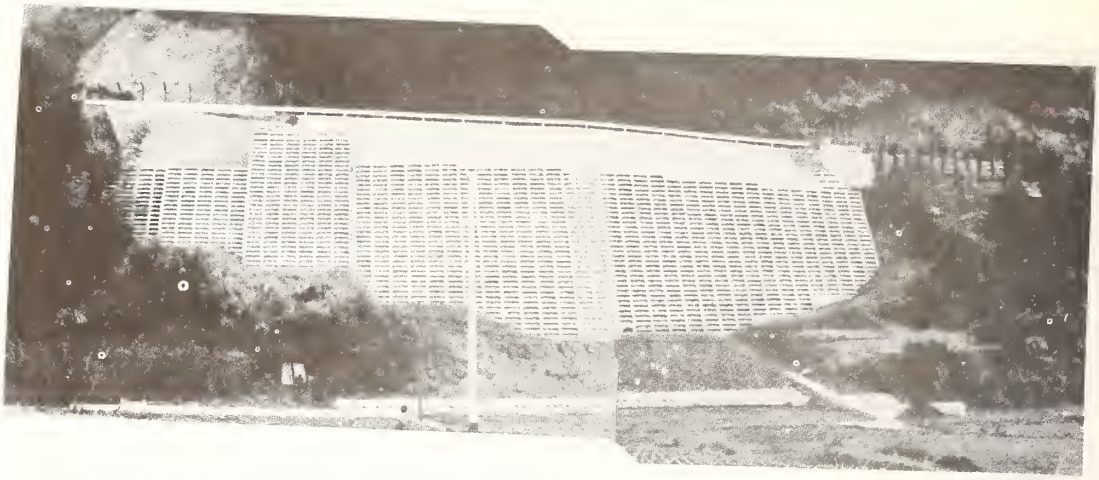

FIGURE 15: PLANE VIEW OF HIGH EMBANKMENT, RETAINED BY CONCRETE FRAME, WHICH SURVIVED THE EARTHQUAKE, AT NASHIMOTO AREA IN KAWAZU TOWN (SHUZENJI-SHIMODA ROUTE)

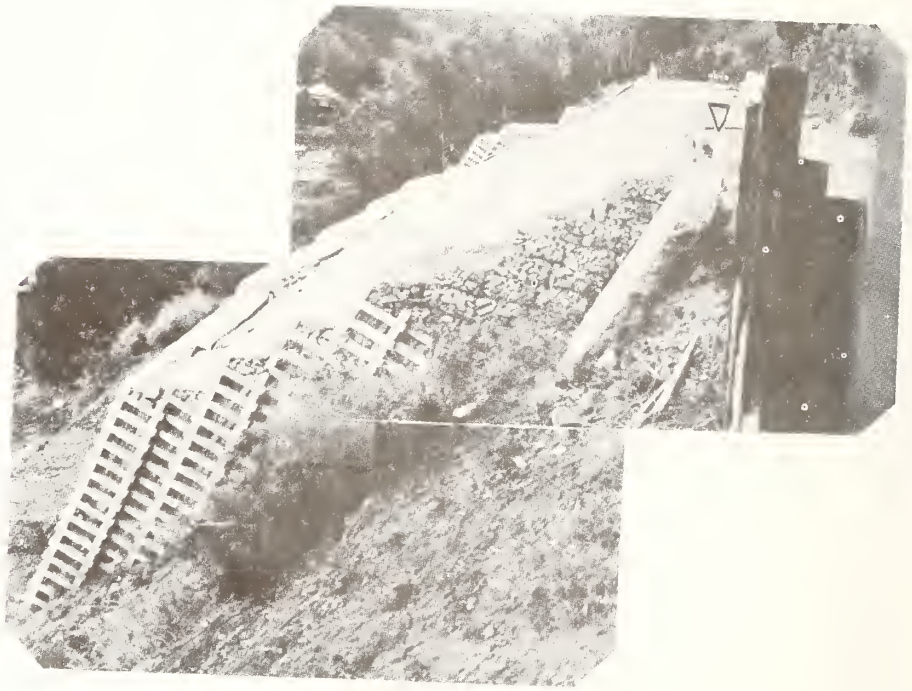

FIGURE 16: SIDE VIEW OF THE HIGH EMBANKMENT (SHUZENJI-SHIMODA ROUTE)

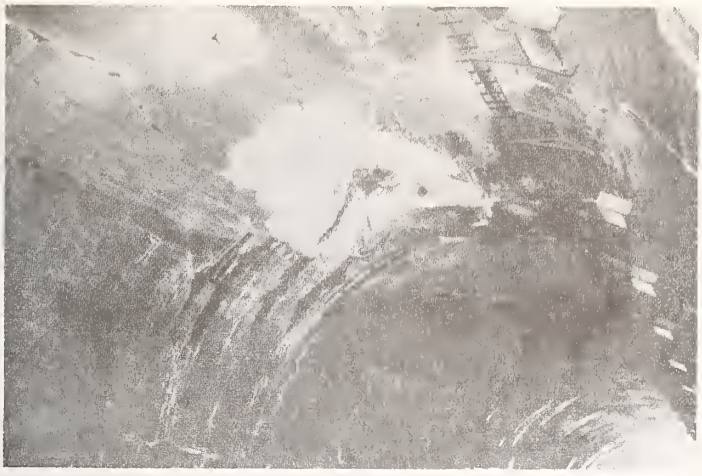

FIGURE 17: FAILURE OF LINING CONCRETE NEAR ARCH CROWN AT TOMORO TUNNEL (HIGASHI-IZU TOLL ROAD)

FIGURE 18: FAILURE OF CONCRETE HANDRAIL AND LATERAL MOVEMENT OF CONCRETE GIRDER (SHIN-SHIMODA BRIDGE, SHIMODA CITY)

FIGURE 19: OVERCROSSING FOR PEDESTRIAN LOCATED ONLY 20 m FROM FAULTS NEAR INATORI JUNIOR HIGH SCHOOL AT INATORI AREA IN HIGASH-IZU TOWN, WHICH SURVIVED WITH MINOR CRACKS AT PARAPETS

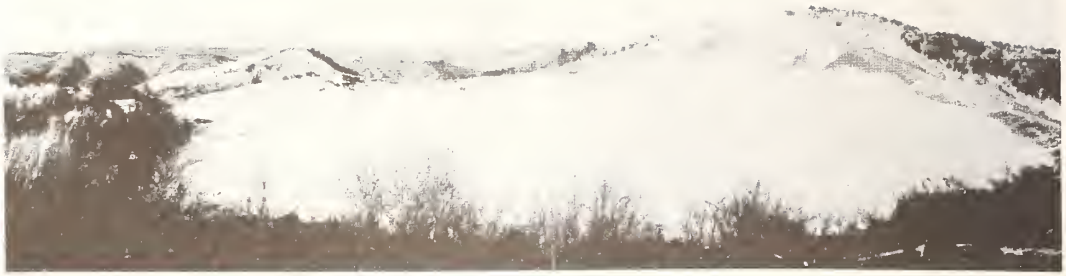

FIGURE 20: OVERALL VIEW OF COLLAPSED HOHZUKI-ZAWA TAILINGS DAMS FOR STORING MINING WASTE - FOREGROUND SHOWS THE FIRST DAM COLLAPSED JUST AFTER THE MAIN SHOCKS (JANUARY 14, 1978); RIGHT SHOWS SECOND DAM COLLAPSED FROM AFTER-SHOCK AT ABOUT NOON IN JANUARY 15; LEFT SHOWS THE THIRD DAM WITH NO DAMAGES.

FIGURE 21: COLLAPSED DAM AND TEMPORARY DAM

FIGURE 22: ROOF TILES FELL OFF AROUND RIDGES -- SIMILAR DAMAGE COULD BE SEEN EVERYWHERE (KATASE-REGION)

FIGURE 23: ROTTEN EXTERIOR WALLS WERE PEELED OFF (KATASE-REGIONAL)

FIGURE 24: LEANING HOUSE, DAMAGE CAUSED BY HEAVY ROOFS AND STRUCTURAL ROTTENNESS (KATASE-REGION)

FIGURE 25: FALLEN SHINTO SHRINE (TANAKA-REGION)

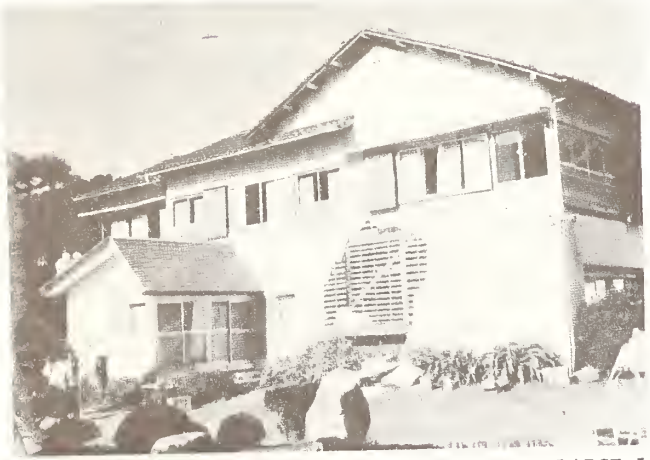

FIGURE 26: THE HOTEL ON WEAK GROUND HAD LARGE LOSS OF INTERIOR NON-STRUCTURAL MEMBERS (KATASE-REGION)

FIGURE 27: FAULT PASSED GROUND UNDER THIS HOUSE (INATORI-REGION)

FIGURE 28: HOUSE LYING ACROSS A FAULT LINE (INATORI-REGION)

FIGURE 29: NEW HOUSE (THE LEFT-HAND ONE WAS LEANING, AND ITS STRIP FOOTINGS WERE CRACKED) (NEMOTONOTA-REGION)

FIGURE 30: LANDSLIDE, CAUSING THE DEATH OF SEVEN PERSONS BENEATH THE FALLEN HOUSES (MITAKAIRIYA-REGION)

FIGURE 32: CRACKS DUE TO LOOSENESS OF THE STONE WALL (NASHIMOTO-REGION)

FIGURE 31: HOUSES SWEPT AWAY AND CRUSHED BY THE FLOW OF EARTH AND SAND (NASHIMOTO-REGION)

FIGURE 33: CRACKS IN THE CONCRETE MORTAR COVERING DIRT FLOORS (KADONO-REGION)

FIGURE 34: CONCRETE MORTAR CRACKED AND DROPPED OFF NEAR THE BASE (HOTEL, 4-STORIES HIGH, IMAIHAMA-REGION)

FIGURE 35: BENDING CRACKS IN EXTERIOR WALLS (PRESCHOOL HOUSE, ONE-STORY, INATORI-REGION)

FIGURE 36: THE DAMAGED RETAINING WALL AND 4-STORY APARTMENT HOUSE, INCLINED AT AN ANGLE OF 0.5° - 1.5° (INATORI-REGION)

FIGURE 37: SHEARING CRACKS IN A GIRDER OF THE UNDERGROUND ROOM (HOTEL, 4-STORIES HIGH AND 2-STORIED BASEMENT, INATORI-REGION)

FIGURE 38: DAMAGE OF MORTAR FINISH ON METAL LATHING (HOTEL, INATORI-REGION)

FIGURE 40: DEFORMED COLUMN (ALREADY REPAIRED) (KAWAZU-REGION)

FIGURE 39: COMPLETE COLLAPSE OF STEEL FRAMES (RESTAURANT, INATORI-REGION)

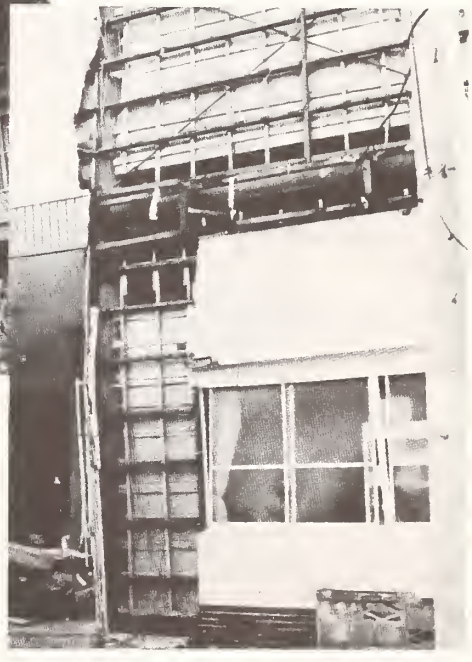

FIGURE 41: DEFORMED COLUMN AND DAMAGED WALLS (INATORI-REGION)

29

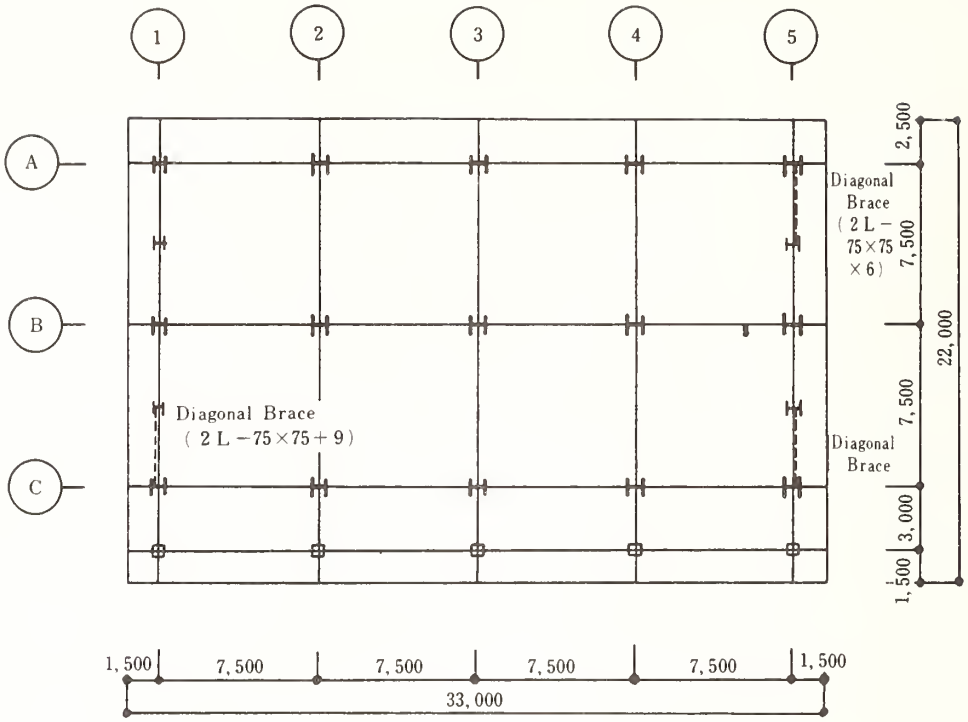

Dimension of Used Members

Column	H −340×250× 9 ×14	Brace	2 L −75×75× 6 and 9
Girder	H −396×199× 7 ×11	Beam	H −346×174× 6 × 9

(i) Plan (The part of structural steel)

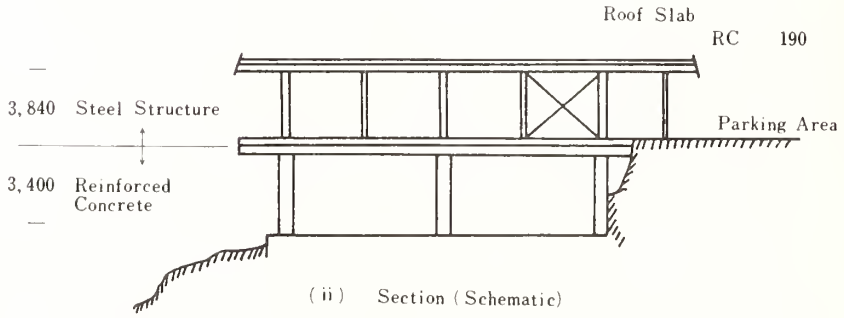

(ii) Section (Schematic)

FIGURE 39 b: RESTAURANT STRUCTURE

APPENDIX - COMPARISON OF SEVERAL SEISMIC INTENSITY SCALES

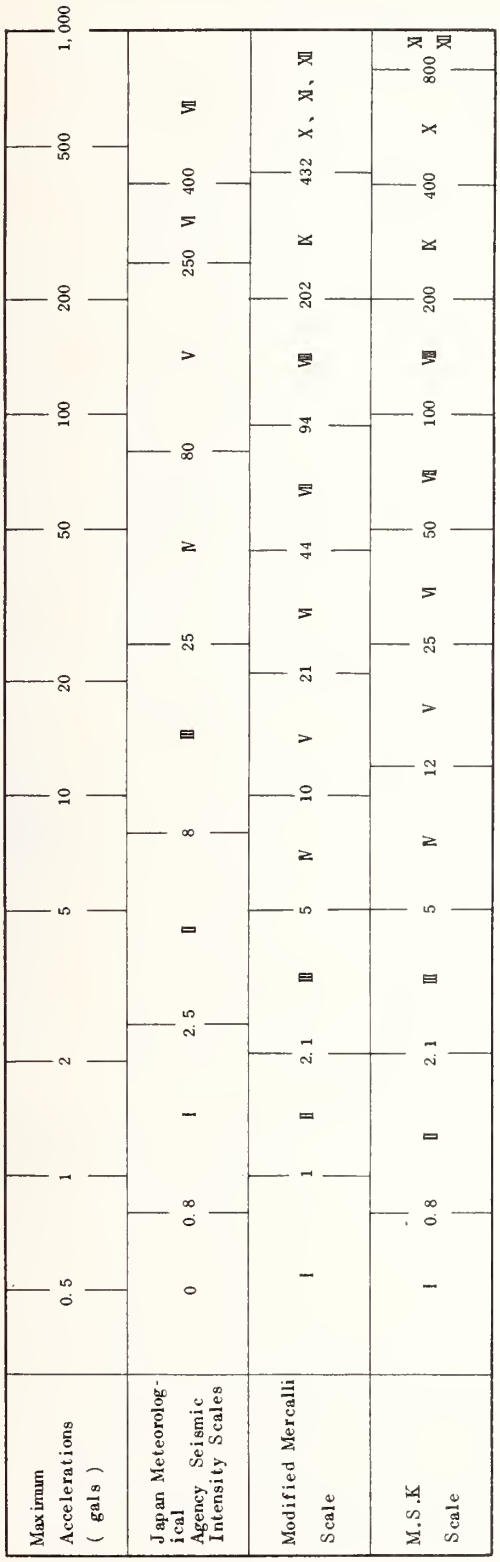

Notes) Roman numerals (0, I, II, etc) indicate seismic intensity values, and Arabic numerals (1, 2, 5 etc) denote maximum ground accelerations in gals.

29

30

REPAIR AND RETROFIT OF BUILDINGS

J. K. Wight
R. D. Hanson

Civil Engineering Deparment
University of Michigan

Repair and Retrofit of Buildings

Damage surveys after recent earthquakes in Alaska, Venezuela, California, Nicaragua, and Guatemala clearly demonstrate the need for two different, but closely associated technologies. First, because it is economically unfeasible to replace all "older" buildings, an ability to retrofit (increase earthquake resistance) buildings is required. Also, because no building new or old can ever be "earthquake proof," an ability to repair (restore original strength and stiffness) is required. In many instances, repair and retrofit would be carried out simultaneously in buildings damaged during a recent earthquake. However, extra care must be exercised for both repair and retrofit situations. If poorly planned or poorly executed, the earthquake resistance of a building may actually be diminished rather than improved by a repair and/or retrofit procedure. Interest in repair and retrofit of buildings has increased dramatically in the U.S. since the San Fernando earthquake (1970) and a summary of research needs was formulated during a workshop [1] sponsored by the National Science Foundation.

Repair of Reinforced Concrete Buildings

In general, many reinforced concrete structures will survive a medium or large earthquake with only minor or moderate damage. For such structures, a combination of the following two repair techniques has been used in the past. If the damage is minor, consisting of narrow cracks with no significant spalling or loss of concrete, an epoxy injection technique is used. More extensive damage will require a removal of all unsound concrete and filling of the resulting void with a concrete-type material that has strength and stiffness properties approximately equal to those of the existing concrete. In either case, it is desireable to use a high-early-strength material so the building can be repaired and reoccupied in the shortest possible time.

Experimental investigations into the behavior of reinforced concrete members and subassemblages repaired by one of the two techniques described above have been carried out at the University of California [2, 3], the University of Michigan [4], and the Portland Cement Association [5]. A summary of the results from the University of Michigan tests are given below.

Epoxy Injection

Epoxy injection has been widely used as a post-earthquake repair procedure, but the success of the repair is strongly influenced by a skill of the operator and the quality of the epoxy resin. In a laboratory situation where a high-quality material and a highly skilled operator is used, the epoxy injection technique has been shown to be quite successful.

In the University of Michigan tests, beam to column subassemblages (Figure 1) were subjected to cyclic load reversals of varying intensity to produce different levels of damage. Specimens with only a small amount of damage, consisting primarily of narrow flexural and shear cracks in the region of the beam adjacent to the column, were repaired by the epoxy-injection technique. The repaired specimens were then subjected to the same loading routine and the results were compared with the original test results. The beam load vs. deflection relationships for a typical original and repaired specimen are given in Figures 2(a) and 2(b), respectively. The behavior of the repaired specimens generally compared favorably with that of the original specimens. Strength and energy dissipation

capacities were restored with only a minor loss in initial stiffness. The inability of the epoxy injection technique to fully restore bond between reinforcement and concrete is assumed to be primarily responsible for the loss of stiffness.

Removal and Replacement

The only effective method of repairing severely damaged structural elements is to remove all unsound concrete and replace it with a new material. Before the new material is placed, some modification of the reinforcement will probably be needed. Longitudinal bars that are buckled or displaced will need to be straightened or replaced. Also, additional transverse reinforcement should be added to satisfy the latest code requirement [6, 7]. Finally, all of the reinforcement should be sand-blasted to remove any loose material that may adversely effect the bond between the reinforcement and the repair material.

In the test series conducted at the University of Michigan, various high-early-strength repair materials were used. In general, the best results were obtained when a standard concrete mix with high-early-strength was used. Specimens repaired with this material generally had the same strength and energy dissipation capabilities as the original specimens. When other high-strength repair materials were used, two general problems caused the behavior of the repair specimens to be considerably poorer than that of the original specimen. First, some of the stronger material tended to be brittle and had little or no energy dissipation potential. Second, the use of a higher strength material tended to alter the location and/or type of inelastic behavior for the repaired specimen. In all of the original specimens the majority of inelastic activity could be classified as flexural behavior and occurred in the region of the beam adjacent to the column. In some of the specimens repaired with higher strength material, the inelastic activity shifted into the joint and led to less ductile shear and anchorage failures.

Conclusions on Repair

(1) If well executed, epoxy injection is a useful method for restoring strength and energy dissipation capacity to a lightly damaged reinforced concrete member. (2) In more heavily damaged members, a removal and replacement technique using a concrete with properties equivalent to the existing concrete in the area of the repair region should be sufficient. Reinforcement in the damaged region may also need to be modified. (3) Brittle materials should be avoided in all repair situations. (4) To be successful a repair procedure must be well planned and should include a study of how the repair will effect members and connections adjacent to the repaired region and how the repair will effect the overall structural strength, stiffness, and probable response to a future earthquake.

Strengthening and Stiffening Existing Buildings

As mentioned in the introduction, there are numerous buildings in seismic zones that do not have adequate lateral resistance and are a potential life hazard in the event of an earthquake. However, instead of replacing these buildings it is economically more feasible to strengthen and stiffen the basic structural system. Unfortunately, a well-defined procedure for strengthening and stiffening cannot be developed because each building is unique and therefore requires a unique solution. Also the degree of strengthening and stiffening

required will vary from building to building depending on the existing lateral resistance of the building, the importance of the building, and the design earthquake intensity. It is generally accepted that emergency facilities must be kept operational after an earthquake. However, the degree of strengthening required for other buildings will probably be a social-political-economical decision made through a government agency acting on information supplied by professionals from all concerned fields.

Some strengthening and stiffening techniques that may be used alone or in various combinations are enlargement of existing frame members, addition of shear walls or other structural members, uncoupling of non-structural elements that may hamper the structure's response to lateral loads, and the strengthening of unreinforced masonry walls by the application of shotcrete. Examples of each of these techniques were reported at the previously mentioned workshop [1].

A recent investigation at the University of Michigan on the use of walls to strengthen and stiffen a single-story, single-bay reinforced concrete frame was reported by Kahn and Hanson [8]. The basic frame used in this investigation is shown in Figure 3. Various infilling techniques were used (Figure 3) and were compared with the behavior of a frame with a monolithically cast wall. All of the units were subjected to lateral load reversals applied at the top floor slab.

The results of this investigation indicated the general adequacy of each of the infilling techniques for strengthening and stiffening existing frames. The cast-in-place infill developed the same ultimate strength as the monolithic wall, but it was not as ductile because of problems with the horizontal dry-pack joint at the top of the infill. The single precast infill panel did not obtain the same ultimate strength as the monolithic wall, but it did exhibit a more ductile type of behavior. The multipanel infill with vertical openings between the panels obtained about one-half of the ultimate strength of the monolithic wall; but it was the most ductile of the specimens tested. This study clearly indicated that different strengthening techniques can result in significantly different stiffnesses, lateral load capacities, energy dissipation capacities and ductilities. Results such as this should be used in analytical studies of building behavior before deciding which infilling technique would be most appropriate in a given situation.

References

1. Hanson, R. D., "Repair, Strengthening and Rehabilitation of Buildings - Recommendations for Needed Research," Report to Workshop sponsored by the National Science Foundation, Department of Civil Engineering Report No. 77R4, The University of Michigan, October 1977.

2. Mahin, S., Bertero, V., Atalay, M., and Rea, D., "Rate of Loading Effects on Uncracked and Repaired Reinforced Concrete Members," Earthquake Engineering Research Center, University of California, Berkeley, California, Report No. EERC 72-9, December 1972.

3. Celebi, M. and Penzien, J., "Hysteretic Behavior of Epoxy-Repaired Reinforced Concrete Beams," Earthquake Engineer Research Center, University of California, Berkeley, Calfiornia, Report No. EERC 73-5, February 1973.

4. Lee, D. L. N., Wright, J. K., and Hanson, R. D., "Original and Repaired Reinforced Concrete Beam-Column Subassemblages Subjected to Earthquake Type Loading," Department of Civil Engineering Report No. UMEE 76S4, The University of Michigan, April 1976.

5. Oesterle, R. G., Fiorato, A. E., Johal, L. S., Carpenter, J. E., Russell, H. G., and Corley, W. G., "Earthquake Resistant Structural Walls - Tests of Isolated Walls," Report to the National Science Foundation, Portland Cement Association, November 1977.

6. American Concrete Insitute, Committee 318, "Building Code Requirements for Reinforced Concrete (318-77)," Detroit, Michigan, 1977.

7. International Conference of Building Officials, "Uniform Building Code," 1976 Edition, Whittier, California, 1976.

8. Kahn, L. F., and Hanson, R. D., "Reinforced Concrete Infilled Shear Walls for a Seismic Strengthening," Department of Civil Engineering Report No. 76S2, The University of Michigan, January 1976.

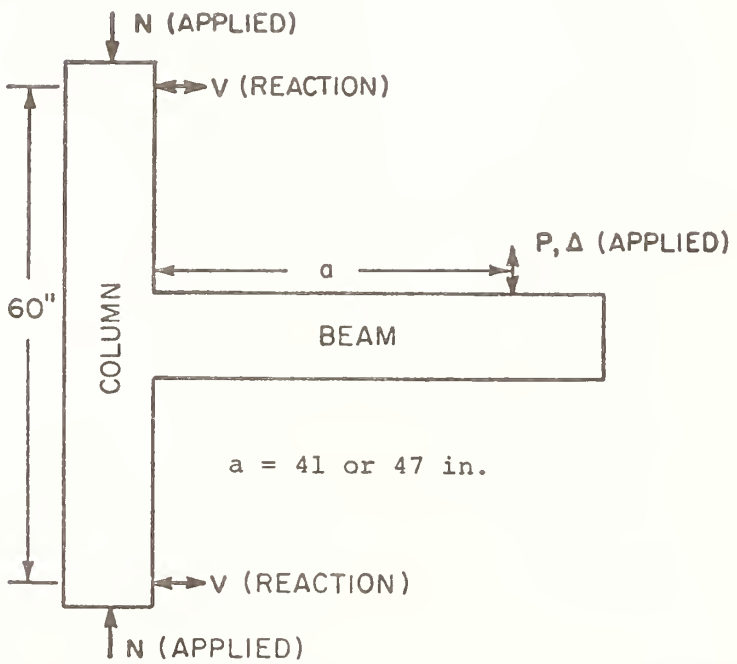

FIGURE 1: BEAM TO COLUMN SPECIMEN USED IN REPAIR INVESTIGATION (1 in. = 25.4 mm)

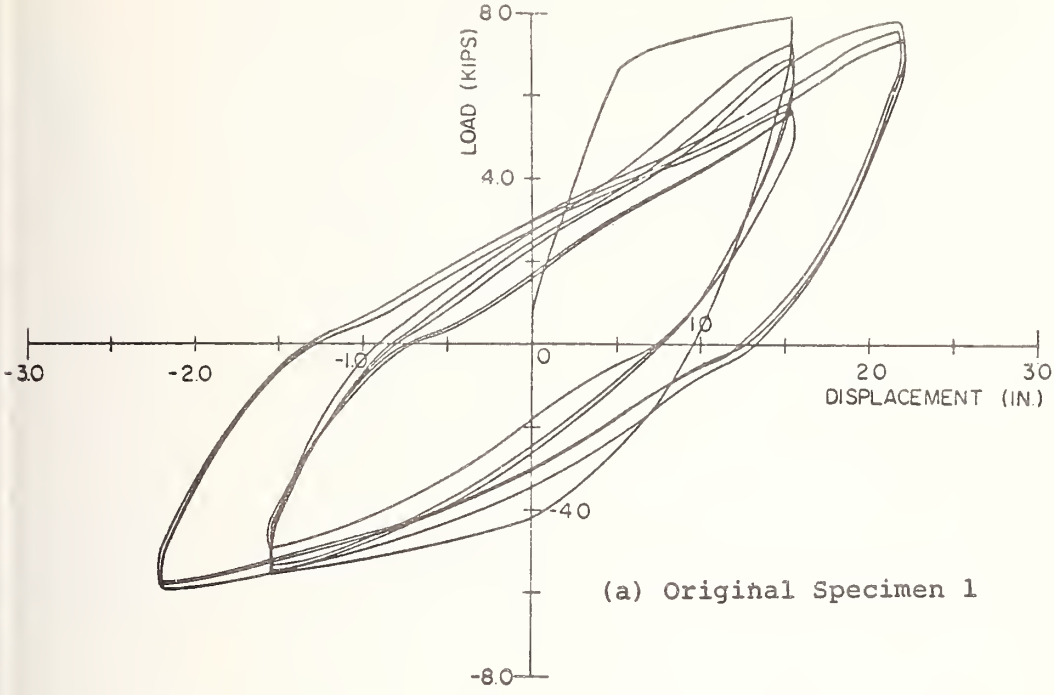

(a) Original Specimen 1

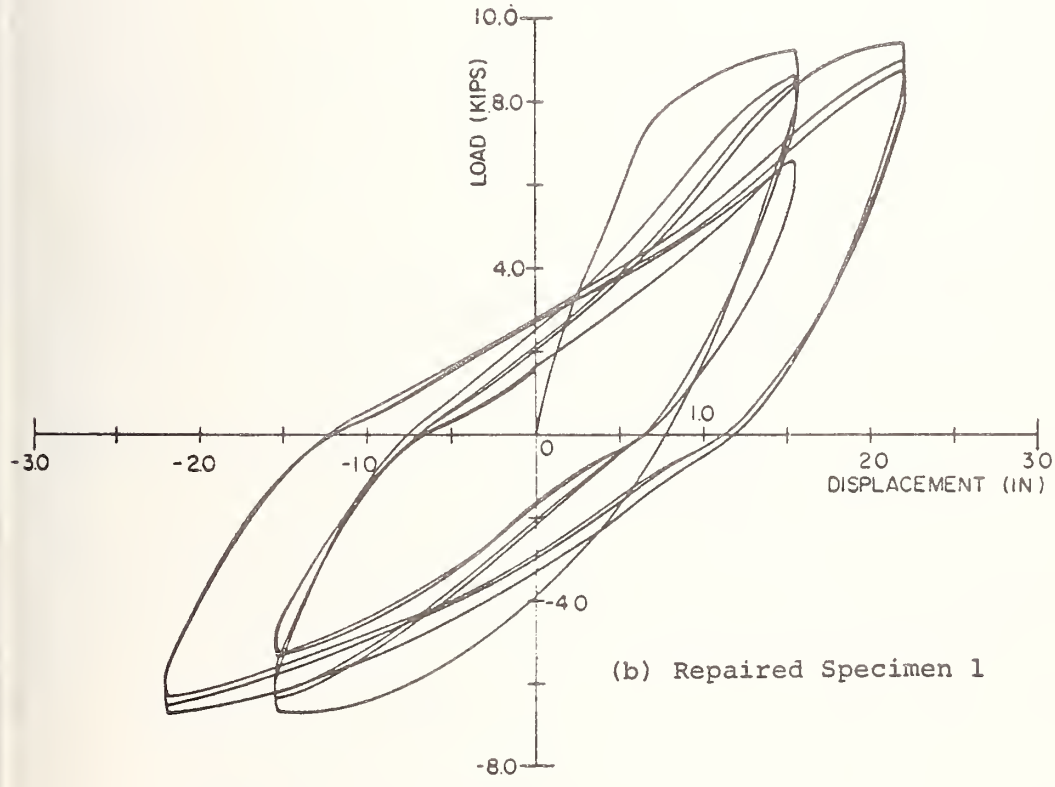

(b) Repaired Specimen 1

30

FIGURE 2: BEAM SHEAR FORCE VS. DEFLECTION RELATIONSHIPS

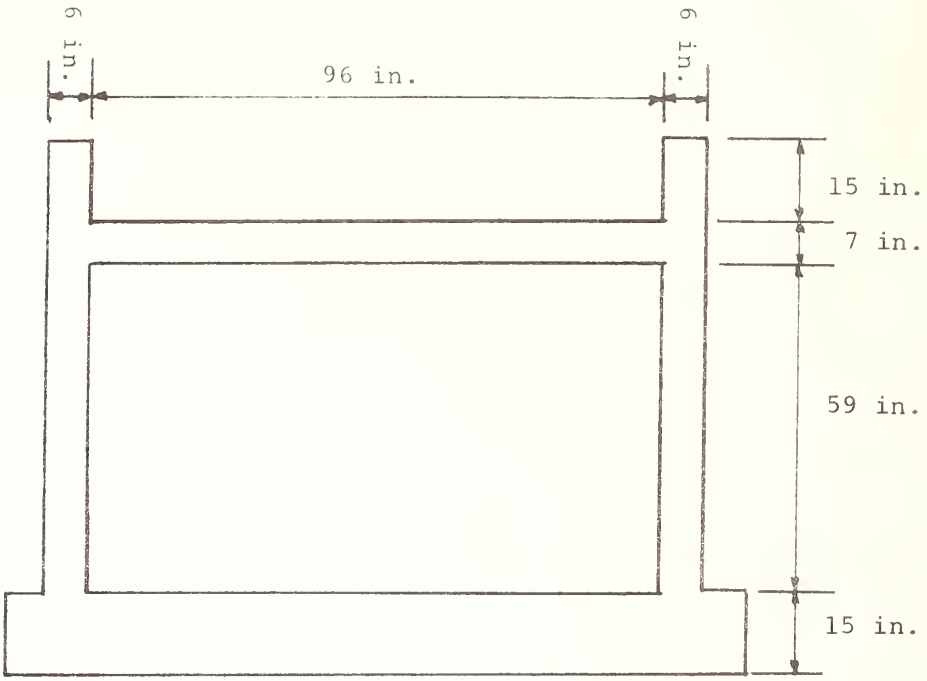

Basic Frame Dimensions

Infilling Techniques: 1. Cast-in-Place (not shown)

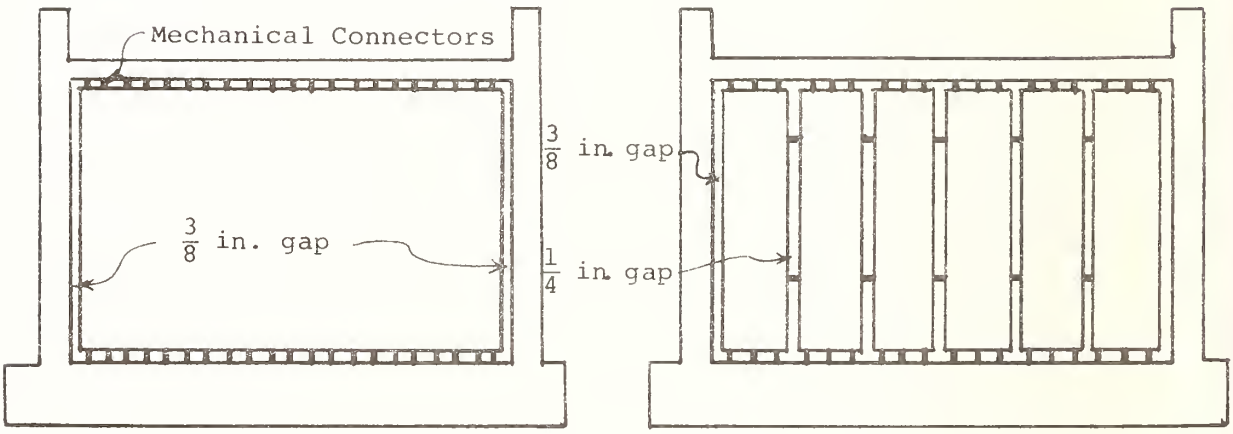

2. Single Precast Panel

3. Multiple Precast Panel

FIGURE 3: BASIC FRAME AND INFILLING TECHNIQUES (1 in. = 25.4 mm)

31

THE DISTRIBUTION OF PROPERTY LOSSES CAUSED BY HISTORICAL EARTHQUAKES

Eiichi Kuribayashi
Tadayuki Tazaki

Public Works Research Institute
Ministry of Construction

The Distribution of Property Losses Caused by Historical Earthquakes

A number of quantitative estimations of earthquake disasters have been carried out in the past. References [1-4] deal with the damage to existing wooden houses. References [5] and [6] investigate the damage to bridges and underground pipes, respectively. To express the amount of losses, various kinds of indexes are used such as the ratio of razed houses to standing ones or damaged spots per service line for underground pipes. However, a common index is necessary to evaluate the total loss from disasters and to compare them. The property loss valued in money meets with this requirement. With this in mind, the authors have investigated the evaluation method of property loss distribution by analyzing eighteen historical earthquakes in Japan.

Methodology

The authors assumed a ratio of property losses caused by earthquakes as an index of earthquake disasters. The property loss ratio can be defined as a ratio between property losses [l] and existing assets (w) valued in money and expressed as a function of earthquake magnitudes, epicentral distances, and subground conditions as follows:

$$D_I = G_I \, 10^{\alpha M + \beta \Delta} \tag{1}$$

$$D_{II} = G_{II} \, 10^{\alpha M + \beta \Delta} \tag{2}$$

where the suffixes I and II mean older subgrounds than diluvial deposits and younger than alluviam, respectively, and

G_I, G_{II} = constant for the subground types, I and II,
M = earthquake magnitudes in Richter scale,
Δ = epicentral distances in km
α, β = constants.

The ratio is to be evaluated in accordance with the subground condition as shown in Figure 1(A). The existing assets distribute independently from it like in Figure 1(B). The property loss caused by an earthquake can be evaluated by multiplying the existing assets and the ratio as shown in Figure 1(C).

The constants were determined by correlating actual property losses and the estimation of the losses of eighteen earthquakes in Japan since 1923.

A total property loss (L) in each earthquake can be estimated by summing up the losses of each mesh (l_i) which is appropriately divided into

$$L = \sum_i l_i = \sum_i \{\delta_i (D_I)_i + (1 - \delta_i)(D_{II})_i\} w_i \tag{3}$$

where

w_i = existing assets.
$(D_I)_i$ = property loss ratio in subground type I,
$(D_{II})_i$ = property loss ratio in subground type II,
l_i = loss in mesh i,
δ_i = identification index $\begin{cases} 0 & \text{for subground type I in mesh i} \\ 1 & \text{for subground type II in mesh i.} \end{cases}$

The assets at each mesh were estimated from the relationships between the assets and local populations. Table 1 shows the relationships between them in nine districts of Japan, from the National Wealth Survey and National Census as of 1970. It can be said that the assets correlate with the population in each district,

$$A_T = 2.77 \cdot P - 0.891 \tag{4}$$

A_T = Gross tangible fixed assets in trillion yen,
P = Population in million.

In Equation (4), the regression constant of 0.891 is negligible compared to the assets. Then Equation (3) becomes:

$$L = \sum_i \{\delta_i (D_I)_i + (1 - \delta_i)(D_{II})_i\} \; W \frac{p_i}{P} \tag{5}$$

where

W = National wealth in yen,
P = Population of Japan,
p_i = Population of mesh i.

The population of mesh $i(p_i)$ was estimated from the average population density of quake-damaged area, which was obtained from the sum of the population and area of the municipalities suffering an earthquake.

$$L = \frac{W}{P} \frac{P_D}{A_D} \sum_i \{\delta_i (D_I)_i + (1 - \delta_i)(D_{II})_i\} a_i$$

$$= \frac{W}{P} \frac{P_D}{A_D} \sum_i \{\delta_i G_I + (1 - \delta_i) G_{II}\} 10^{\alpha M + \beta \Delta_i} a_i \tag{6}$$

where

P_D = Population of the quake-damaged area,
A_D = Area of the quake-damaged area in km^2.
a_i = Area of mesh i in km^2,
Δ_i = Epicentral distance of the center of the mesh (km).

Figure 3 shows the procedure to estimate the losses caused by an earthquake as stated above. The mesh used in this analysis was made to coincide with that of a hundred times of the National Land Information Mesh Data of National Land Agency[8]. The size of mesh of National Land Agency varies in accordance with the latitude. Therefore the mesh in this analysis was determined to be the same size as shown in Table 2.

The loss was summed within the area where damage possibly occurred as shown in Equation (7).

$$\log R = 0.5M - 1.5 \tag{7}$$

where

R = Radius of the area where damage possibly occurred in km (See Figure 4),
M = Magnitude in Richter scale.

The unknown constant G_I, G_{Ii}, α and β were determined by minimizing the difference of the sum of square of $\log\left(\frac{LPA_D}{WP_D{}^a}\right)$ and its estimate $\log\left(\widehat{\frac{LPA_D}{WP_D{}^a}}\right)$.

$$\sum_j \left\{\log\left(\frac{LPA_D}{WP_D{}^a}\right)_j - \log\left(\widehat{\frac{LPA_D}{WP_D{}^a}}\right)_j\right\}^2 \rightarrow \text{Min} \qquad (8)$$

j = Suffix to denote earthquake j

Data Used in this Analysis

National Wealth Survey has been conducted twelve times until 1970 in Japan as shown in Table 3[10]. Usually it has been conducted every five years. However there is a twenty-year blank before and after World War II. To interpolate the national wealth during the blank years, it was estimated from the gross national product (GNP). Figure 5 shows the relationship between the gross national product and national wealth in nine districts of Japan. In the relationship, the definitions of the national wealth before and after World War II were quite different. For example, before the war it involved land and natural resources. After the war, it only consists of reproducible tangible assets. Moreoever, the definition of each survey year was slightly different. Figure 5 was drawn by roughly modifying the data to be uniform as for the definition of the national wealth.

$$\log_{10} W = 1.03 + 0.937 \log_{10} N \quad \text{(unit: million yen)} \qquad (9)$$

N = Gross National Product.

Population and Area of the Damaged Area

The population and area of the damaged area to be used in Equation (6) were the sum of those of municipalities which were involved within the radius (R') given by Equation (10). The radius R' corresponds to the area within which the seismic intensity of Japan Meterorological Agency is expected to be greater than V[12].

$$\log_{10} R' = 0.5M - 1.85 \qquad (10)$$

M = Magnitude in Richter scale.

The data of population and area were as of 1970[13]. Although the local population must have changed, the ratio of the population of Japan and that of the damaged area, which was used in Equation (6), is considered to have changed little. Figure 6a-r show the seismic intensity map and the area denoted by Equation (10). Table 5 shows the population and area of the damaged area used in the analysis.

Subground Condition

Each mesh was classified into subground type I or II according to Reference[14]. Figure 7 shows an example of the classification of subground in the northern part of Japan.

Earthquakes Used in the Analysis

Eighteen earthquakes, whose recorded property loss are listed in Table 6,[15-32] were used in this analysis. The influence of

inflation was not taken into consideration because both the loss and existing assets were values in current price.

Results of the Analysis

The regression formulas for Equations (1) and (2) were introduced as follows:

$$D_I = 7.9 \times 10^{-7} \times 10^{0.62M-0.0028} \quad (11)$$

$$D_{II} = 1.9 \times 10^{-6} \times 10^{0.62M-0.0029} \quad (12)$$

$$6.1 \leqq M \leqq 8.1$$

The multiple correlation coefficient by Equation (13) was 0.82,

$$R = \sqrt{1 - \frac{\sum_j \{(\frac{LPA_D}{WP_D{}^a})_j - \widehat{(\frac{LPA_D}{WP_D{}^a})_j}\}^2}{\sum_j \{(\frac{LPA_D}{WP_D{}^a})_j - \overline{(\frac{LPA_D}{WP_D{}^a})}\}^2}} \quad (13)$$

where

$\overline{(\frac{LPA_D}{WP_D{}^a})}$ = Average of $\frac{LPA_D}{WP_D{}^a}$ for all earthquakes,

$\widehat{(\frac{LPA_D}{WP_D{}^a})_j}$ = Regression estimate calculated by Equation (11) and (12) for earthquake j.

Figures 8 and 9 show the value of D_I and D_{II}. The relationship between the actual value $(\frac{LPA_D}{WP_D{}^a})$ and its estimate $\widehat{(\frac{LPA_D}{WP_D{}^a})}$ is shown in in Figure 10. As far as the multiple correlation coefficient and Figure 10 are concerned, the regressional formulas can be considered to estimate the property losses caused by an earthquake. An arrow at Kanto Earthquake shows the band of losses of various estimators. One reason that the loss value and its estimate of Fukui earthquake differ might be that the earthquake occurred just after the World War II and damage was not surveyed in detail.

Figure 11 illustrates the equivalent ratio of razed houses given in Reference*[3]. Comparing Figure 11 to Figures 8 and 9, the following can be said:

(1) Both property loss ratio and equivalent ratio of razed houses increase with the magnitude of earthquake, and decrease with the epicentral distance.

(2) In general, equivalent ratio of razed houses is greater than property loss ratio.

(3) Decreasing rate with the epicentral distance for equivalent ratio of razed houses is greater than that for property loss ratio. Decreasing rate with the magnitude is almost the same for both.

---

* Equivalent ratio of razed houses

$$= \frac{\text{Number of razed houses} + 0.5 \times \text{Number of half-razed houses}}{\text{Total number of razed houses}}$$

Comparison of Property Loss

Figure 12 shows the breakdown of the social capital according to the National Wealth Survey of 1970. If the composition of social capital can be assumed to be constant for a decade before 1970, the ratio calculated by Equation (14) of various kinds of lifeline facilities for eight earthquakes from 1961 till 1970 represents the individual loss ratio of facilities.

$$\text{Individual loss ratio} = \frac{L_k P}{W_k P_D} \qquad (14)$$

L_k = Loss valued in money of facility k
W_k = Existing assets of facility k
= National Wealth as of the year of the earthquake
x $\frac{\text{Assets of facility K as of 1970}}{\text{National wealth as of 1970}}$

Table 7 shows the result of calculation. Figures 13 to 20 show the relationships between the individual loss ratio of various kinds of facilities and the total property loss.

The procedure to evaluate the loss value is not always the same in each facility. Therefore it might not be accurate to compare the ratio of Equation (14) for different facilities. However, it tends to be that the loss ratios of buildings and highways are almost the same as that of the total property loss. The loss ratios of agriculture, river, and harbor facilities are higher than that of the total. The loss ratios of electric power, telecommunication, and water supply facilities are lower than that of the total, but they gradually reach the same level as the ratio itself comes to a greater value (see Figure 21).

Conclusions

Property loss can be used as the index to the scale of the earthquake disaster.

Property loss can be estimated from the magnitude of the earthquake, epicentral distance, and subground condition.

The property loss ratio is in general smaller than the equivalent ratio of razed houses.

Buildings and highway facilities are likely to suffer the average property loss. Agricultural, river, and harbor facilities are likely to suffer greater loss than the average. Electric power, telecommunication, and water supply facilities are likely to suffer less property loss.

References

All references listed below are written in Japanese.

1. Kawazumi, H., Damage Distribution and Earthquake in Tokyo, Architecture Magazine, 773, 1951.

2. Omote, S. and Miyamura, S., Relationship between Damage Distribution in Earthquake in Yokohama and Nagoya City, and Subground Conditions, Architecture Magazine, 773, 1951.

3. Kuribayashi, E., et al., Investigation on the Damage of Fukui, Yebino and Izuhanto-oki Earthquakes, Technical Memorandum of PWRI No. 1106, March 1976.

4. Kuribayashi, E., et al., Investigation on the Estimation Method or Razed Houses and Fire Distribution Caused by Earthquakes, Technical Memorandum of PWRI No. 1256, May 1977.

5. Katayama, T., A Methodology to Estimate the Bridge Capability Against Earthquakes, Journal "Column".

6. Kubo, K., et al., Quantitative Analysis of Seismic Damage to Buried Pipelines, Proceedings of the 4th Japan Earthquake Engineering Symposium, 1975.

7. Economic Planning Agency: 1970 National Wealth Survey of Japan.

8. National Land Agency, Regulation Bureau, General Affairs Section: Outline of National Land Data Collection Project.

9. Katsumata, M., Earthquake Magnitude and the Area Possibly to Suffer Damage. Proceedings of the Spring Session of Seismological Society of Japan, 1977.

10. Economic Planning Agency, Economic Institute: National Wealth Survey in Japan, March 1976.

11. Economic Yearbook, 1975, Toyo-Keizai-Shimpo-Sha.

12. Usami, T., List of the Earthquakes that Caused Damage in Japan, Tokyo University Press.

13. New Japanese Atlas of Each Prefecture, 1972, Kokusai-Chigaku-Kyokai.

14. Economic Planning Agency and National Land Agency: Classified Maps of Subground.

15. Reports of the Imperial Earthquake Investigation Committee, No. 100 C, p. 57.

16. Reports of the Imperial Earthquake Investigation Committee, No. 101.

17. Kyoto Prefecture, Report of Oku-tango Earthquake, March 1927.

18. Central Meteorological Observatory, Report of Kita-izu Earthquake of November 26, 1930; December 1930.

19. Nishi, et al., Report of Shizuoka Earthquake, Journal of Japan Society of Civil Engineers, Vol. 21, 1935.

20. Akita Prefecture, Report of Oga Earthquake, April 1942.

21. Tottori Prefecture, Report of Tottori Earthquake, p. 9, 1944.

22. Construction Authority, Report of Technology Institute No. 16, Report of Nankai Earthquake, June 1948.

23. Kochi Prefecture, Report of Nankai Earthquake.

24. Report of PWRI, No. 78, Report of Fukui Earthquake, March 1949.

25. Okamoto, S., and Kubo, K., Damage of Civilengineering Facilities Caused by Imaichi Earthquake of December 26, 1949, Proceedings of Japan Society of Civil Engineers, No. 10, December 1951.

26. Report of PWRI No. 113, Report of the Damage of Hyuganda Earthquake, October 1961.

27. Tada, H., et al., Investigation of the Damage of Miyagiken-hokubu Earthquake (I), Journal of PWRI, Vol. 4, No. 10, 1962.

28. Niigata Prefecture, Documents of Niigata Earthquake, June 1965.

29. Miyazaki Prefecture, Documents of Yebino Earthquake, April 1969.

30. Research Committee of Tokachi-oki Earthquake of 1968: Report of Tokachi-oki Earthquake of 1968, January 1969.

31. Report of Nemuro-hanto-oki Earthquake of June 17, 1973, Research Project of Natural Disaster, Ministry of Education.

32. Oyo Corporation, Damage of Ohitaken-chubu Earthquake, June 1970.

33. Kawaguchi, M., Introduction of Multivariate Statistical Analysis, Morikita Shuppan.

Appendix: Evaluation Method

The property loss valued in money used in this analysis is mostly issued by the disaster organizations of each administration. Its evaluation method is divided in two. The first is expressed as follows:

Property Loss = Current price x Loss ratio

Current price is evaluated by reducing the depreciation from the purchase price. Privately owned properties, which are not to be qualified for the national subsidy for reconstruction, belong to this category. Buildings (excluding public ones such as school buildings), agricultural products, and hatching products are the examples.

Second category is that the loss is evaluated as the price necessary to reconstruct the damaged facilities. It involves public facilities, which get the national subsidy. The assessed amount of subsidy by the upper administration becomes the loss. Water supply, education, agricultural, civil engineering, forestry, fishery, electric power, telecommunication, and railroad facilities belong to this category.

In each category, the method of evaluating the loss is not equal. For example, in the first category, the current price, which is very important in the loss evaluation, depends on the judgment of the personnel. In second category, the property loss is likely greater because the former does not take the depreciation into account.

Table 1 Relationship between Gross Tangible Fixed Assets and Population

District	Population (thousand)*	Tangible Fixed Assets (Bil.)
Hokkaido	5,392	14,569
Tohoku	11,774	26,559
Kanto	28,174	79,782
Hokuriku	2,785	9,444
Tokai	13,408	38,808
Kinki	16,498	46,469
Chugoku	7,129	20,621
Shikoku	4,059	12,032
Kyushu	12,770	25,875
Total	101,989	274,159

* As of Oct. 1, 1970.

Table 2 Sizes of a Mesh of Each Earthquake Used in the Analysis

Earthquake	Date	Magnitude	Maximum Seismic Intensity*	Epicenter		Size of a Mesh in Latitudinal Direction	Size of a Mesh in Longitudinal Direction
				λ	φ		
						Unit: Km	Unit: Km
Kanto	1923. 9. 1	7.9	6	131.1°E	30.6°N	9.243	11.41
Kita-Tajima	1925. 5.23	6.5	6	134.8°E	35.7°N	9.246	11.27
Kita-Tango	1927. 3. 7	7.5	6	135°06'E	35°36'N	9.245	11.27
Kita-Izu	1930. 6.26	7.0	6	139°00'E	35°06'N	9.245	11.42
Shizuoka	1935. 7.11	6.3	5	138.4°E	35.0°N	9.243	11.41
Oga	1939. 5. 1	7.0	6	139.8°E	40.0°N	9.250	10.67
Tottori	1943. 9.10	7.4	6	134.2°E	35.5°N	9.243	11.41
Nankai (Kochi Pref.)	1946. 7.21	8.1	6	135.6°E	33.0°N	9.243	11.68
Fukui	1948. 6.28	7.3	6	136.2°E	36.1°N	9.246	11.27
Imaichi	1949.12.26	6.7	6	139.7°E	36.7°N	9.249	11.13
Tokachi-oki	1952. 3. 4	8.1	6	143.85°E	42.15°N	9.255	10.36
Hyuganada	1961. 2.27	7.0	5	131°51'E	31°36'N	9.240	11.81
Miyagiken-hokubu	1962. 4.30	6.5	5	141°08'E	38°44'N	9.255	10.83
Niigata (Niigata Pref.)	1964. 6.16	7.5	6	139°11'E	38°21'N	9.255	10.83
Yebino	1968. 2.21	6.1	6	130°43'E	32°01'N	9.240	11.81
Tokachi-oki	1968. 5.16	7.9	5	143°35'E	40°44'N	9.255	10.52
Tokachi-oki (Hokkaido Pref.)	"	"	5	"	"	"	"
Tokachi-oki (Aomori Pref.)	"	"	5	"	"	"	"
Nemuro-hanto-oki	1973. 6.17	7.4	5	145°57'E	42°58'N	9.258	10.19
Ohitaken-chubu	1975. 4.21	6.4	5	131.4°E	33.2°N	9.243	11.68

* in JMA scale

Table 3 National Wealth Survey in Japan

Surveyed Year	Published Year and Month	Organization	Note
1905	Unidentified	Bank of Japan	
1910	1912	"	
1913	Oct. 1921	Census Authority	
1917	Unidentified	Bank of Japan	
1919	Oct. 1921	Census Authority	
1924	Feb. 1928	Statistics Bureau of the Cabinet	
1930	Nov. 1933	" "	Surveyed actually in Dec. 1932
1935	Oct. 1948	" "	Surveyed actually in Dec. 1935
1955	March 1958	Economic Planning Agency	Surveyed reproducible tangible assets only.
1960	Dec. 1964	" "	
1965	Aug. 1967	" "	
1970	Feb. 1975	" "	

Table 4 Relationship between GNP and National Wealth

Year	GNP : N Unit: million yen	National Wealth (gross) : W Unit: million yen
1905	2,000	9,030
1910	2,757	12,904
1913	3,030	15,020
1917	3,527	28,605
1919	6,384	42,044
1924	12,904	63,824
1930	10,636	105,211
1935	14,532	132,073
1955	8,633,600	37,987,000
1960	15,499,200	57,602,000
1965	31,956,400	68,420,000
1970	70,730,900	302,219,600

Table 5 Population and Area of the Damaged Area.

Earthquake	Year	Population of the Damaged Area* Unit: thousand	Area of the Damaged Area Unit: Km^2
Kanto	1923	28,545	28,397
Kita-Tajima	1925	141	943
Kita-Tango	1927	1,247	10,130
Kita-Izu	1930	1,744	4,005
Shizuoka	1935	661	1,426
Oga	1939	225	1,392
Tottori	1943	1,035	9,264
Nankai (Kochi Pref.)	1946	787	7,105
Fukui	1948	1,310	6,115
Imaichi	1949	590	2,139
Tokachi-oki	1952	713	25,528
Hyuganada	1961	27	295
Miyagiken-hokubu	1962	535	1,955
Niigata (Niigata Pref.)	1964	1,203	4,886
Yebino	1968	102	970
Tokachi-oki	1968	2,040	23,410
Tokachi-oki (Hokkaido Pref.)	1968	277	6,880
Tokachi-oki (Aomori Pref.)	1968	953	6,504
Nemuro-hanto-oki	1973	66	846
Ohitaken-chubu	1975	144	1,149

* As of Oct. 1, 1970.

Table 6 Property Loss Cuased by Earthquakes

Earthquake	Year	Magnitude	Property Loss (Unit: million yen)	Estimated National Wealth (Unit: million yen)
Kanto	1923	7.9	5,500	77,000
Kita-Tajima	1925	6.5	89	78,000
Kita-Tango	1927	7.5	82.18	68,000
Kita-Izu	1930	7.0	25.46	63,000
Shizuoka	1935	6.3	10.32	96,000
Oga	1939	7.0	7.73	182,000
Tottori	1943	7.4	160	337,000
Nankai (Kochi Pref.)	1946	8.1	2,792	2,206,000
Fukui	1948	7.3	305,000	11,120,000
Imaichi	1949	6.7	3,500	13,860,000
Tokachi-oki	1952	8.1	15,183	24,200,000
Hyuganada	1961	7.0	163	70,380,000
Miyagiken-hokubu	1962	6.5	4,049	77,500,000
Niigata (Niigata Pref.)	1964	7.5	130,000	103,700,000
Yebino	1968	6.1	8,876	178,200,000
Tokachi-oki	1968	7.9	58,395	178,200,000
Tokachi-oki (Hokkaido Pref.)	1968	7.9	11,356	178,200,000
Tokachi-oki (Aomori Pref.)	1968	7.9	47,039	178,200,000
Nemuro-hanto-oki	1973	7.4	3,925	365,400,000
Ohitaken-chubu	1975	6.4	4,493	482,700,000

Table 7 Individual Loss Ratios of Various Kinds of Facilities

Property Loss, National Wealth: unit mil. yen

Earthquake	Property Loss: L	National Wealth: W	$\frac{LP}{WP_D}$	Building Loss: L_B	Building Assets: W_B	$\frac{L_B P}{W_B P_D}$	Highway Facility Loss: L_H	Highway Facility Assets: W_H	$\frac{L_H P}{W_H P_D}$
Hyuganada	163	70,384,000	0.009097						
Miyagiken-hokubu	4,049	77,507,000	0.01021	1,304	10,922,000	0.02333	145	2,083,000	0.01360
Niigata (Niigata Pref.)	130,000	103,708,000	0.1091	20,373	14,615,000	0.12132	3,808	2,787,000	0.1189
Yebino	8,876	178,266,000	0.05086						
(Miyagi Pref.)				2,616	"	0.37624	150	"	0.1129
Tokachi-oki	58,395	178,266,000	0.01021	7,805	25,121,000	0.01594	2,355	4,790,000	0.02523
(Hokkaido)	11,356	"	0.02405	226	"	0.003397	548	"	0.04320
(Aomori Pref.)	47,039	"	0.02899	7,579	"	0.03314	1,807	"	0.04143
Nemuro-hanto-oki	3,925	365,407,000	0.01715	411	51,493,000	0.01275	124	9,819,000	0.01731
Ohitaken-chubu	4,493	482,787,000	0.006753	1,327	68,934,000	0.01415	322	12,973,000	0.01800

Earthquake	Agricultural Facility Loss: L_A	Agricultural Facility Assets: W_A	$\frac{L_A P}{W_A P_D}$	River Facility Loss: L_R	River Facility Assets: W_R	$\frac{L_R P}{W_R P_D}$	Telecommunication Facility Loss: L_T	Telecommunication Facility Assets: W_T	$\frac{L_T P}{W_T P_D}$
Hyuganada	22	1,297,000	0.06580				1	1,131,000	0.003458
Miyagiken-hokubu	534	1,428,000	0.07311	671	1,073,000	0.1223			
Niigata (Niigata Pref.)	12,570	1,910,000	0.5726	4,804	1,435,000	0.2914	7,000	1,667,000	0.3655
Yebino	2,397	3,284,000	0.7456				13	2,865,000	0.004577
(Miyagi Pref.)				425	2,467,000	0.6228			
Tokachi-oki	14,032	3,284,000	0.2193	2,461	2,467,000	0.05120	1,087	2,865,000	0.01948
(Hokkaido)	1,678	"	0.1929	768	"	0.1175	330	"	0.04349
(Aomori Pref.)	12,354	"	0.4133	1,693	"	0.07541	757	"	0.02904
Nemuro-hanto-oki	353	6,731,000	0.08301	44	5,056,000	0.01380	10	5,872,000	0.002729
Ohitaken-chubu	1,316	8,893,000	0.1074	50	6,680,000	0.05453	5	7,759,000	0.0004962

(Table 7 continued)

Earthquake	Electric Power Facility Loss: L_E	Electric Power Facility Assets: W_E	$\frac{L_E P}{W_E P_D}$	Water Supply Facility Loss: L_W	Water Supply Facility Assets: W_W	$\frac{L_W P}{W_W P_D}$	Harbor Facility Loss: L_P	Harbor Facility Assets: W_P	$\frac{L_P P}{W_P P_D}$
Hyuganada	5	1,894,000	0.01234						
Miyagiken-hokubu				12	1,155,000	0.002097			
Niigata (Niigata Pref.)	2,011	2,791,000	0.06269	2,231	1,545,000	0.1257	12,177	712,562	1.487
Yebino	38	4,798,000	0.008124	67	2,656,000	0.02646			
(Miyagi Pref.)									
Tokachi-oki	414	4,798,000	0.004432	747	2,656,000	0.01443	2,247	1,224,839	0.09415
(Hokkaido)	52	"	0.004058	72	"	0.01025	465.2	1,224,839	0.1434
(Aomori Pref.)	363	"	0.008308	674	"	0.02790	1,781.8	1,224,839	0.1598
Nemuro-hanto-oki	2	9,835,000	0.0003781	533	5,443,000	0.01562	699	2,510,651	0.4444
Ohitaken-chubu	4	12,994,000	0.0002263	25	7,192,000	0.002472			

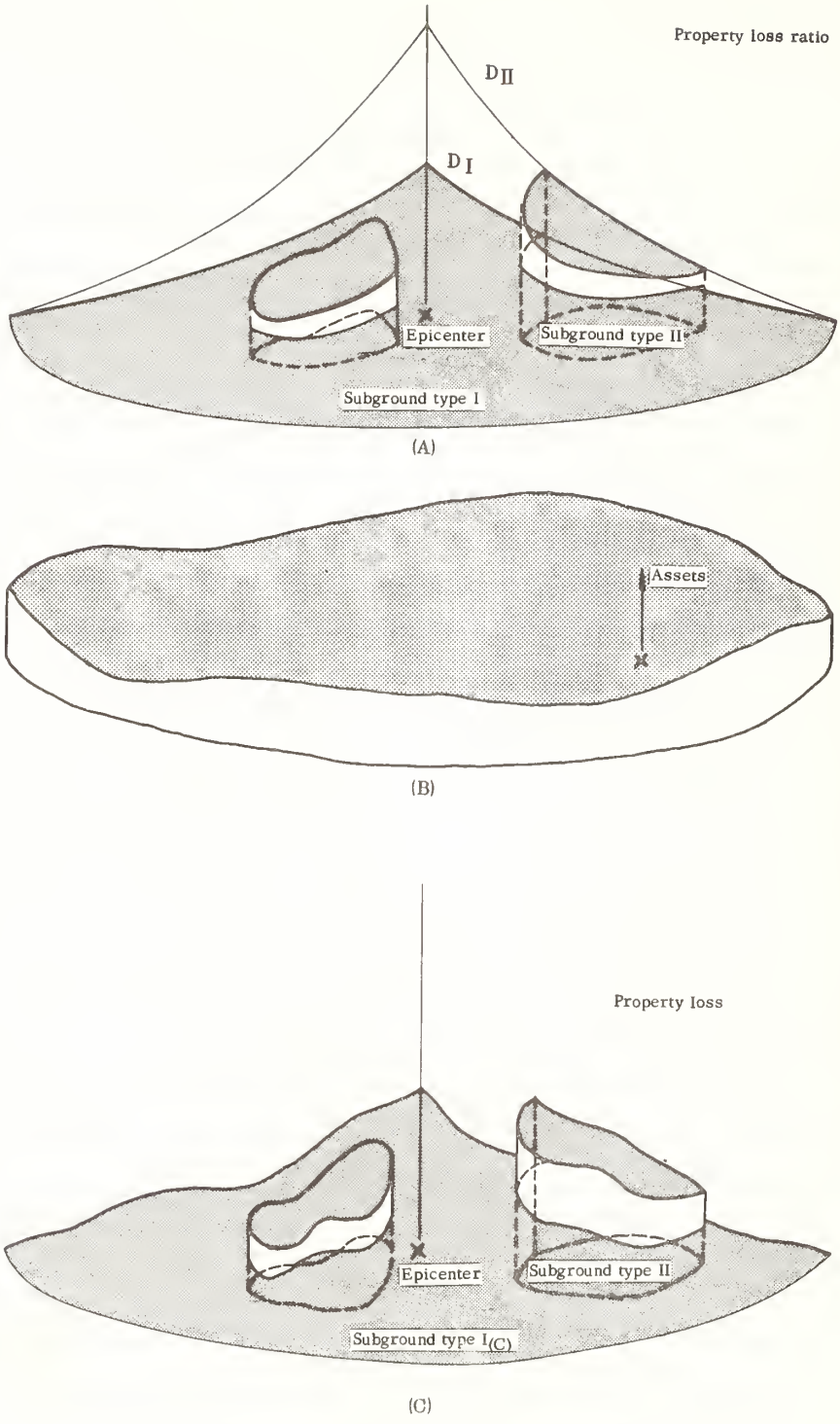

Fig. 1 Abstract of Property Loss Evaluation Caused by Earthquakes

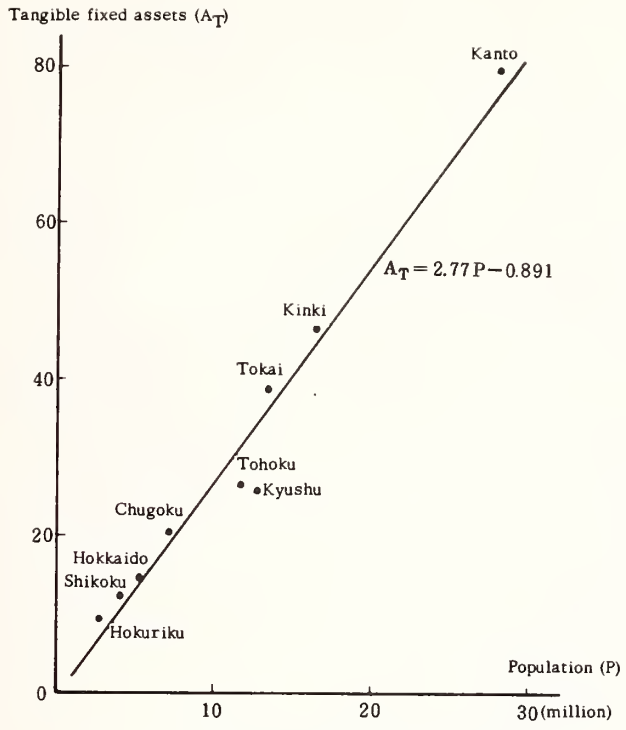

Fig. 2 Relationship between Gross Tangible Fixed Assets and Population

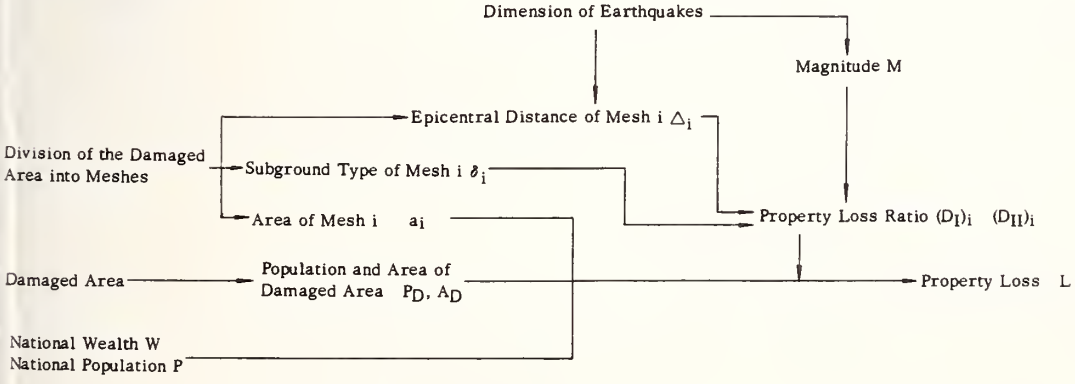

Fig. 3 Flow Chart to Evaluate Property Loss

31

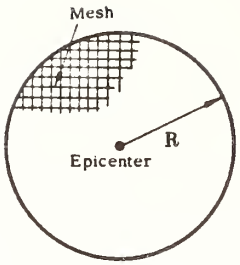

Fig. 4 Area of Loss Evaluation

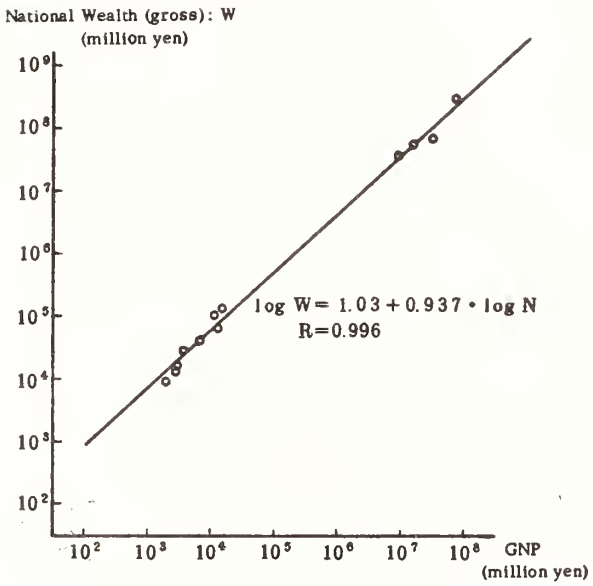

Fig. 5 Relationship between GNP and National Wealth

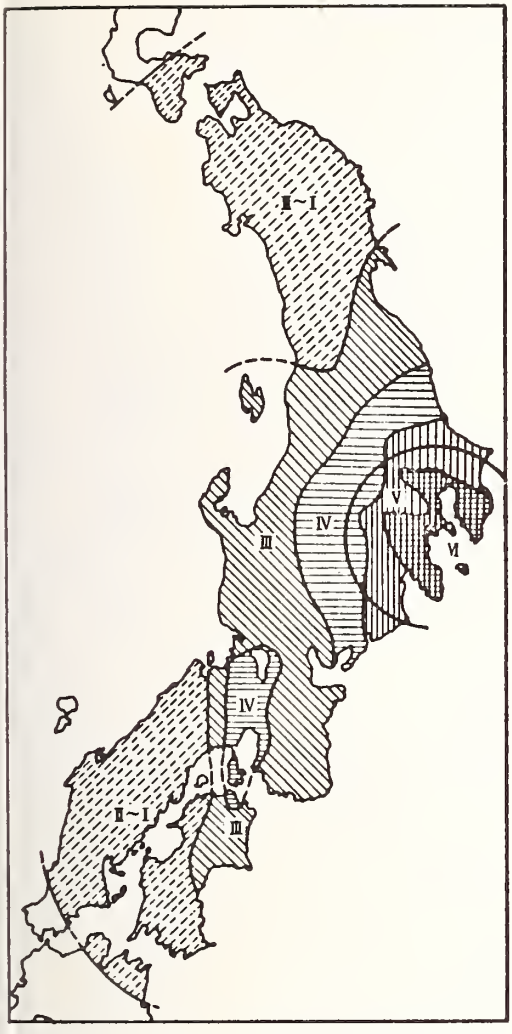

Fig. 6a Seismic Intensity Distribution of Kanto Eq. (1923)

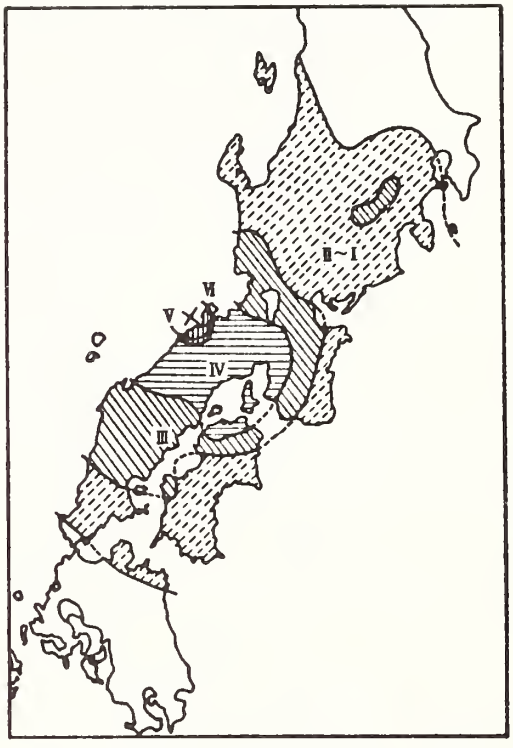

Fig. 6b Seismic Intensity Distribution of Kita-tajima Eq. (1925)

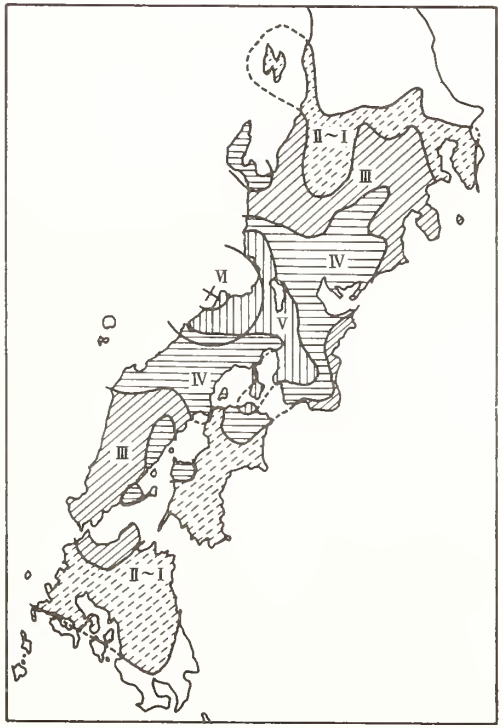

Fig. 6c Seismic Intensity Distribution of Kita-tango Eq. (1927)

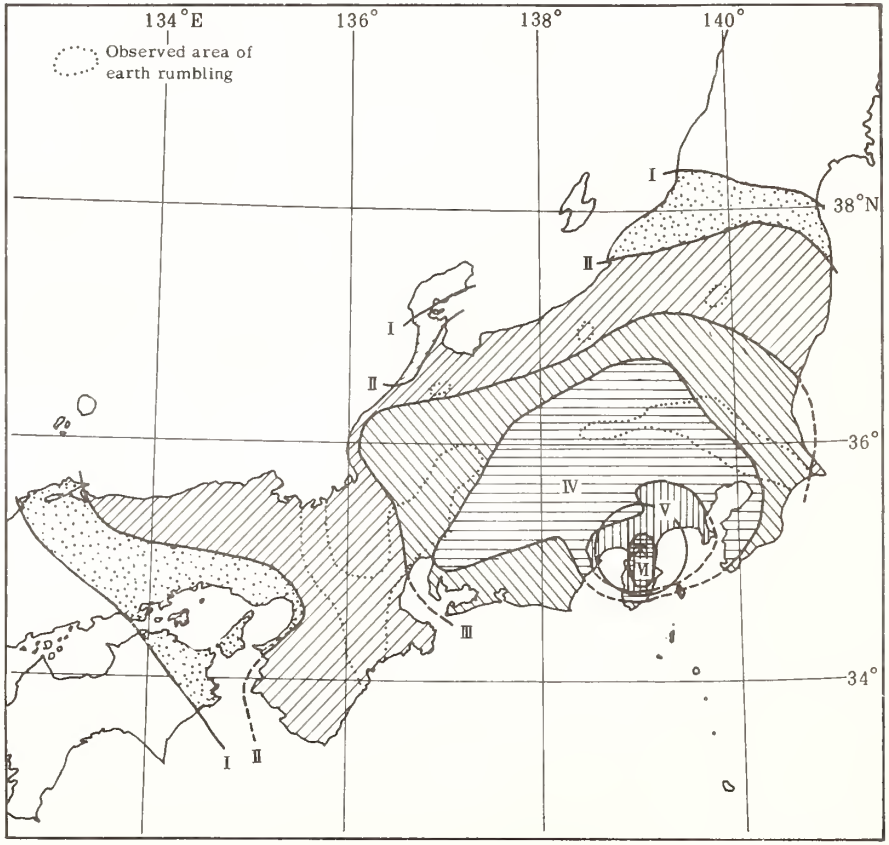

Fig. 6d Seismic Intensity Distribution of Kita-izu Eq. (1930)

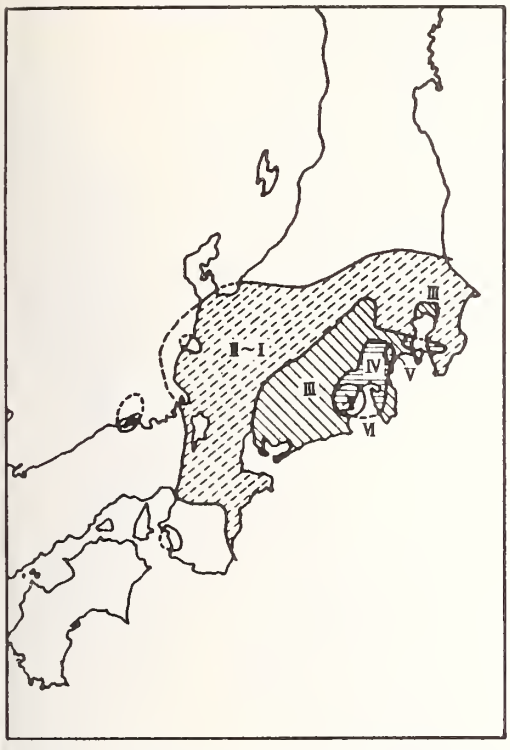

Fig. 6e Seismic Intensity Distribution of Shizuoka Eq. (1935)

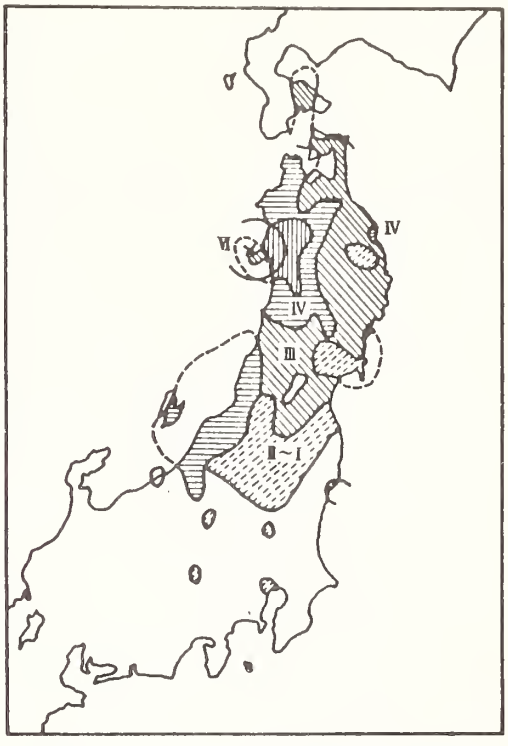

Fig. 6f Seismic Intensity Distribution of Oga Eq. (1939)

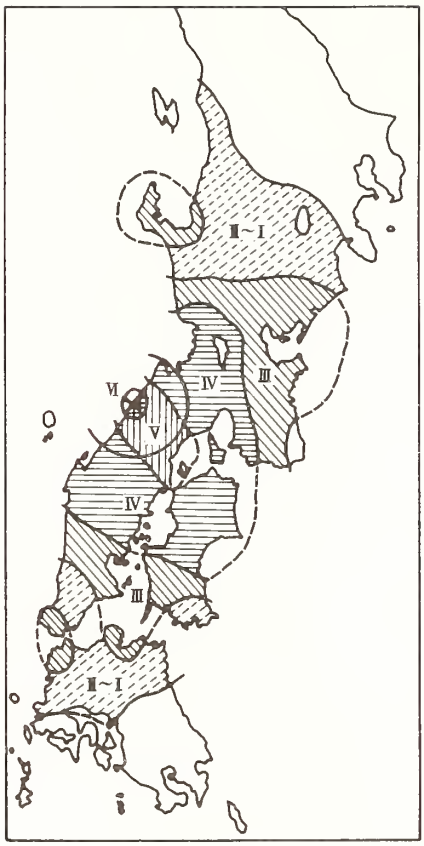

Fig. 6g Seismic Intensity Distribution of Tottori (1943)

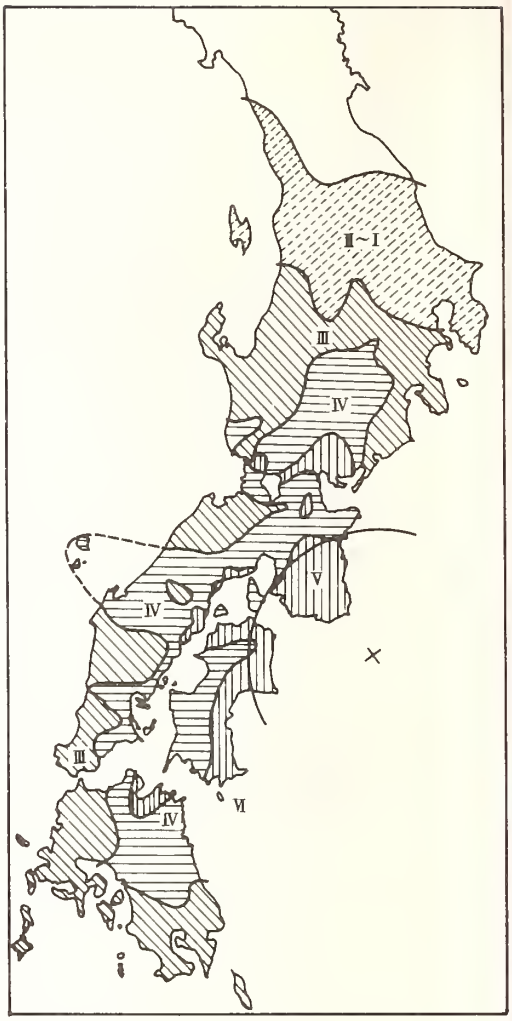

Fig. 6h Seismic Intensity Distribution of Nankai Eq. (1946)

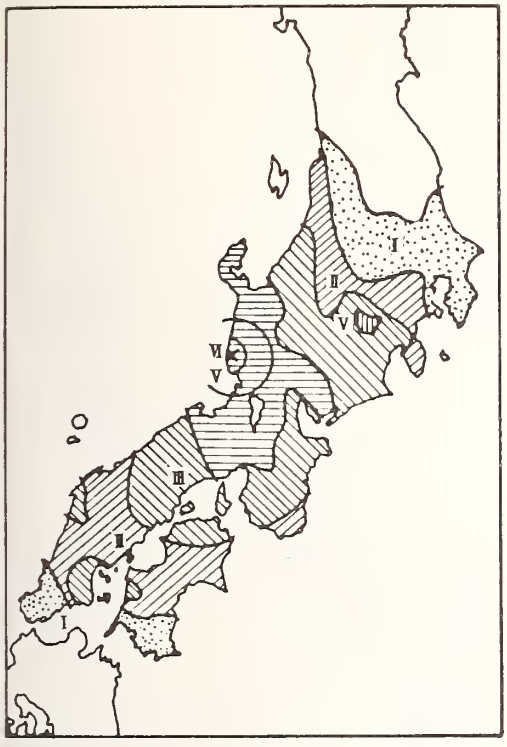

Fig. 6i Seismic Intensity Distribution of Fukui Eq. (1948)

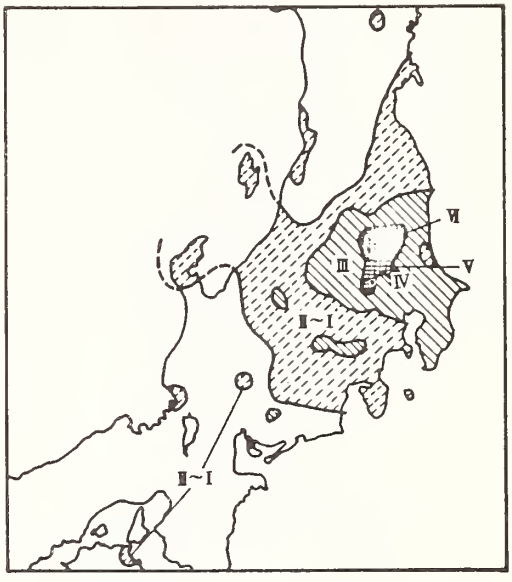

Fig. 6j Seismic Intensity Distribution of Imaichi Eq. (1949)

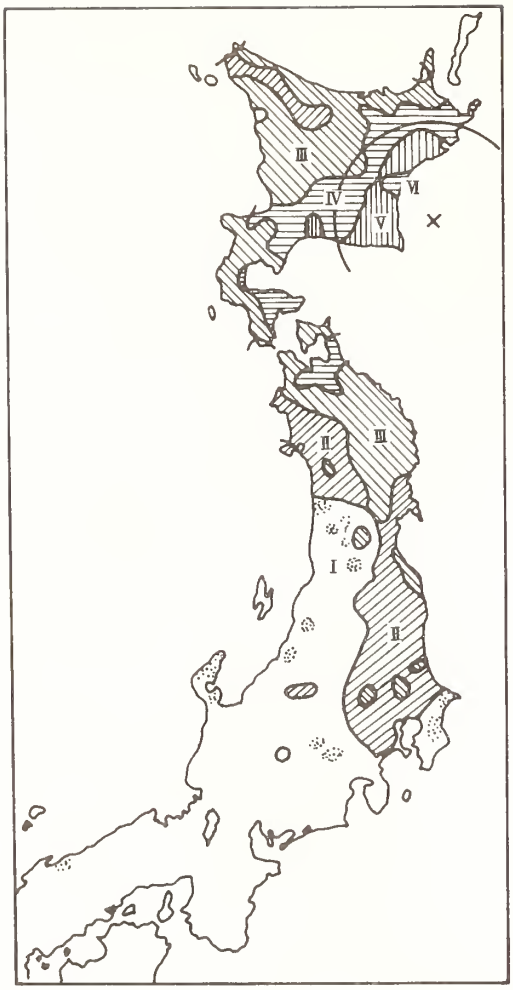

Fig. 6k Seismic Intensity Distribution of Tokachi-oki Eq. (1952)

Fig. 61 Seismic Intensity Distribution of Hyuganada Eq. (1961)

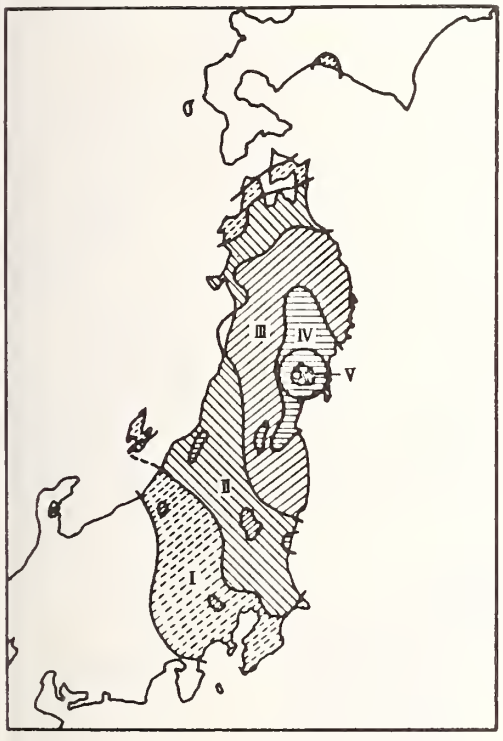

Fig. 6m Seismic Intensity Distribution of Miyagiken-hokubu Eq. (1962)

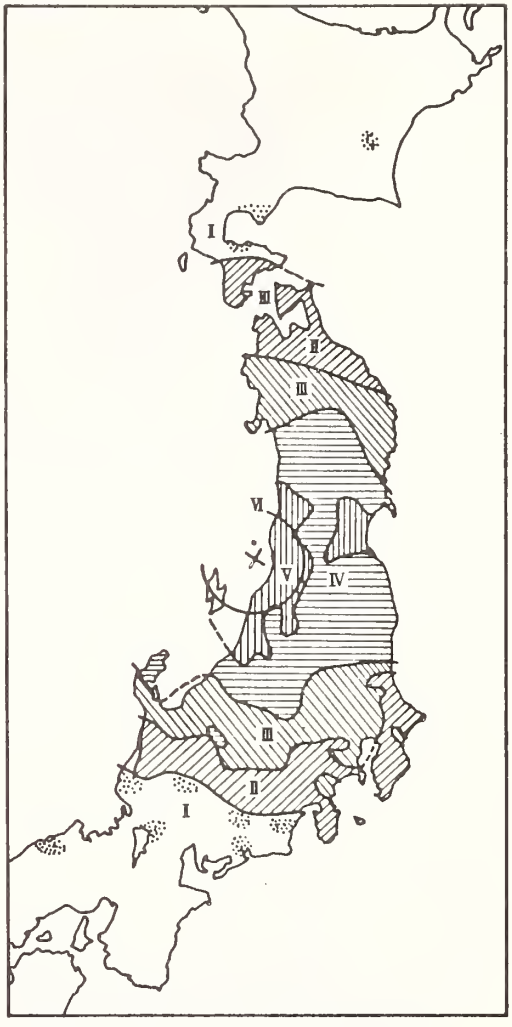

Fig. 6n Seismic Intensity Distribution of Niigata Eq. (1964)

31

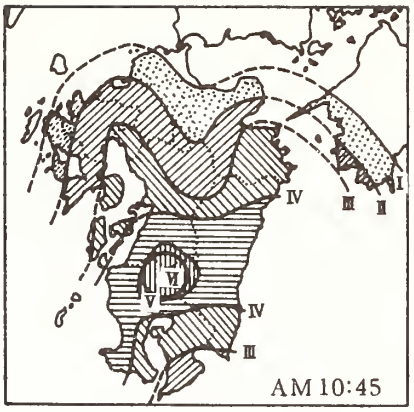

Fig. 6o Seismic Intensity Distribution of Yebino Eq. (1968)

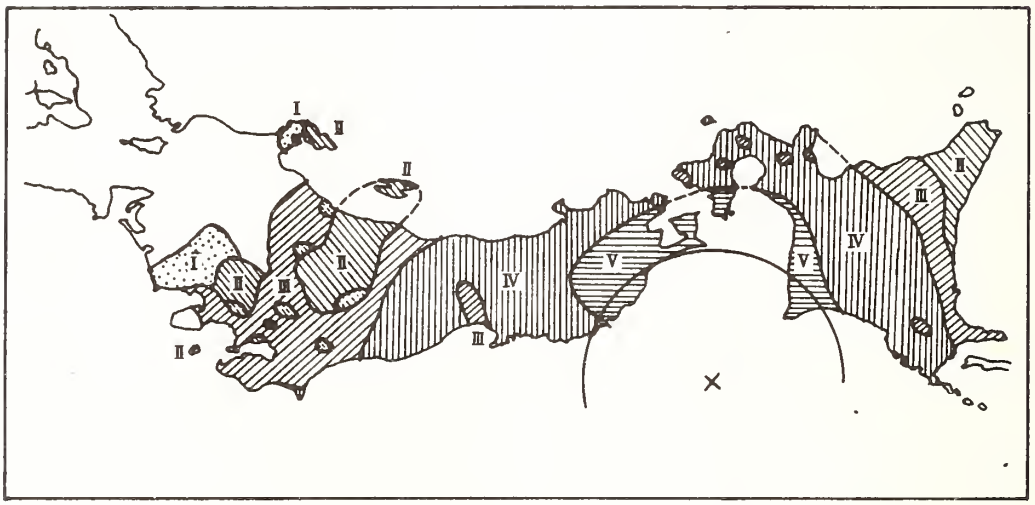

Fig. 6p Seismic Intensity Distribution of Tokachi-oki Eq. (1968)

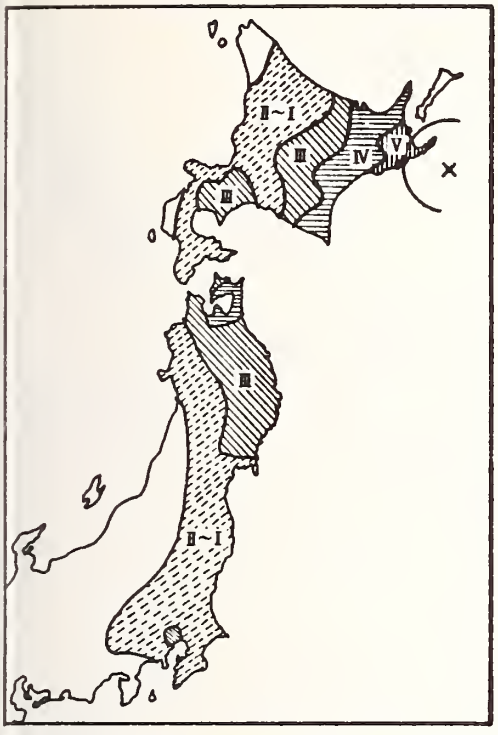

Fig. 6q Seismic Intensity Distribution of Nemuro-hanto-oki Eq. (1973)

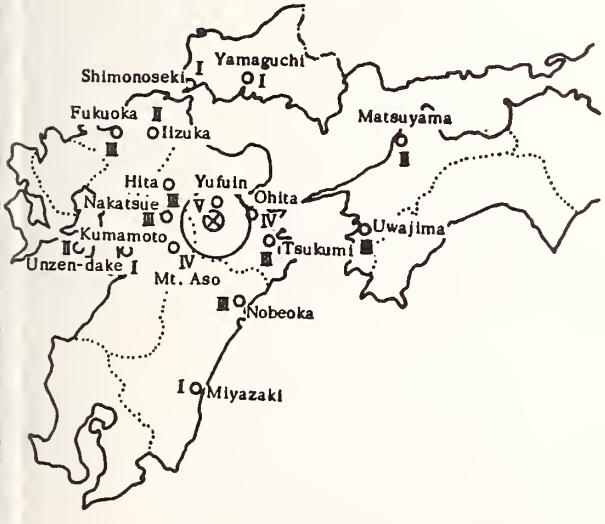

Fig. 6r Seismic Intensity Distribution of Ohitaken-chubu Eq. (1975)

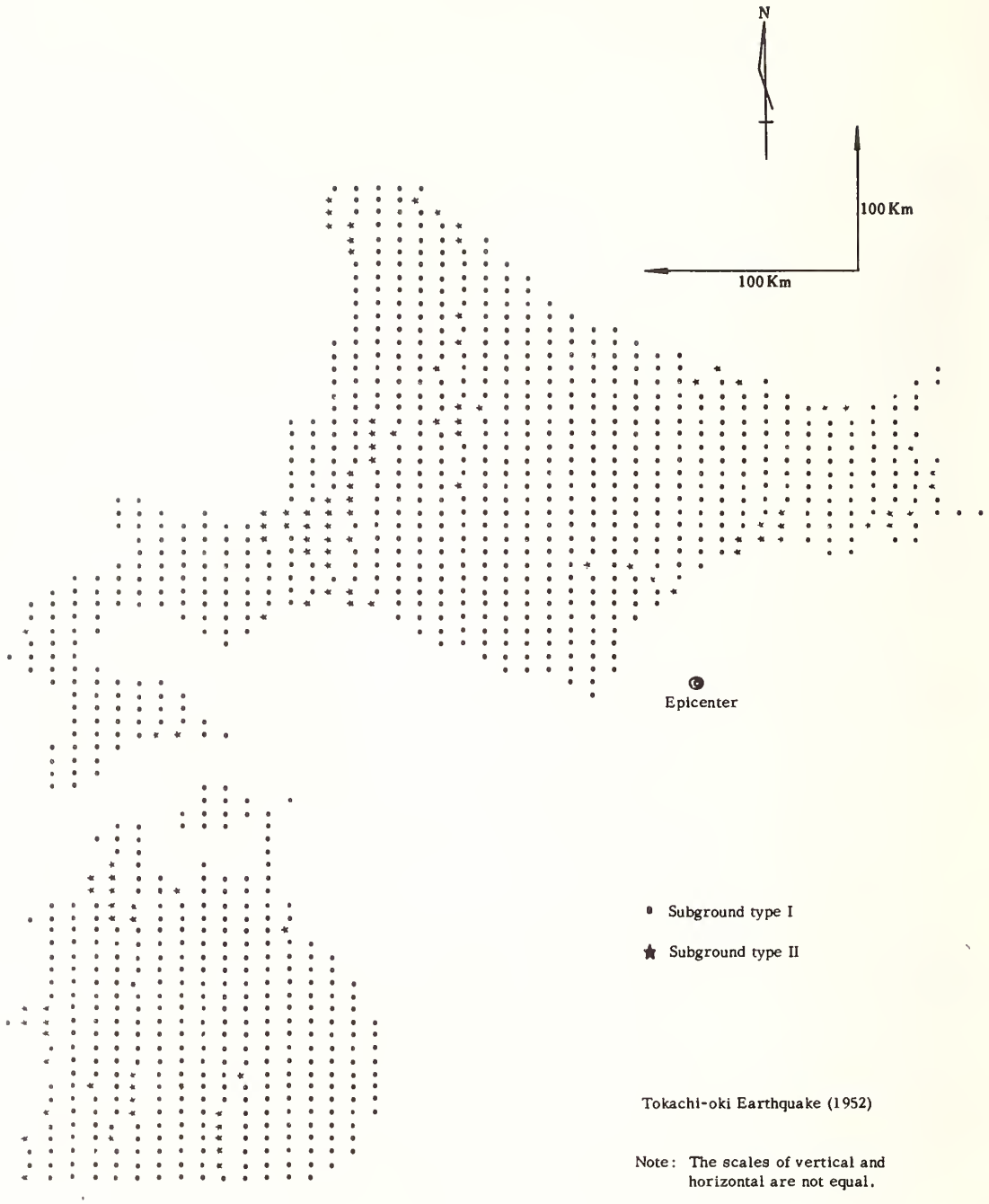

Fig. 7 An Example of Subground Types

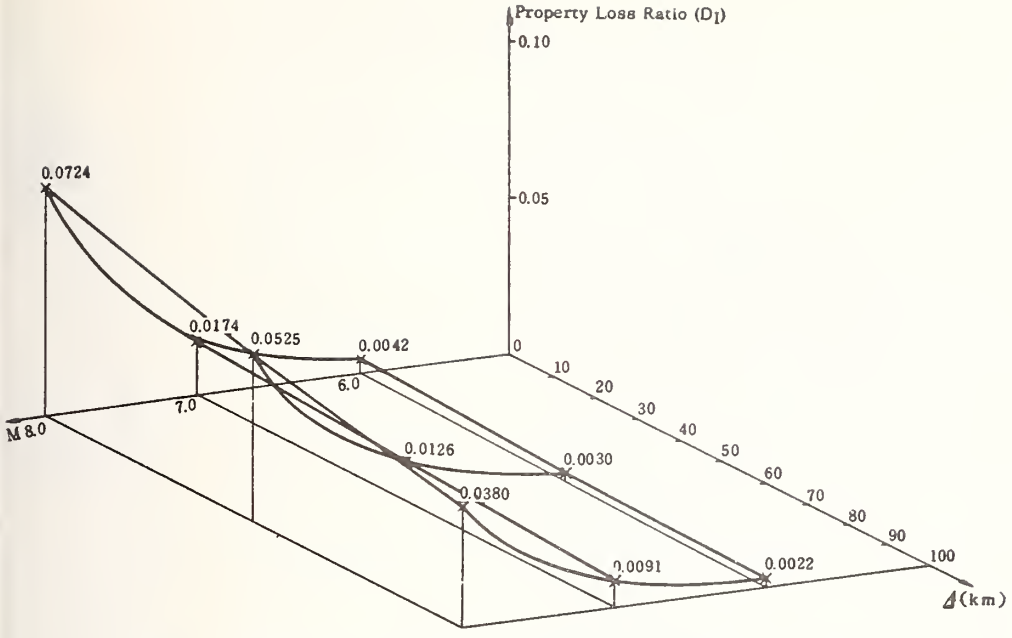

Fig. 8 Relationship between Magnitude, Epicentral Distance and Property Loss Ratio (Subground Type I)

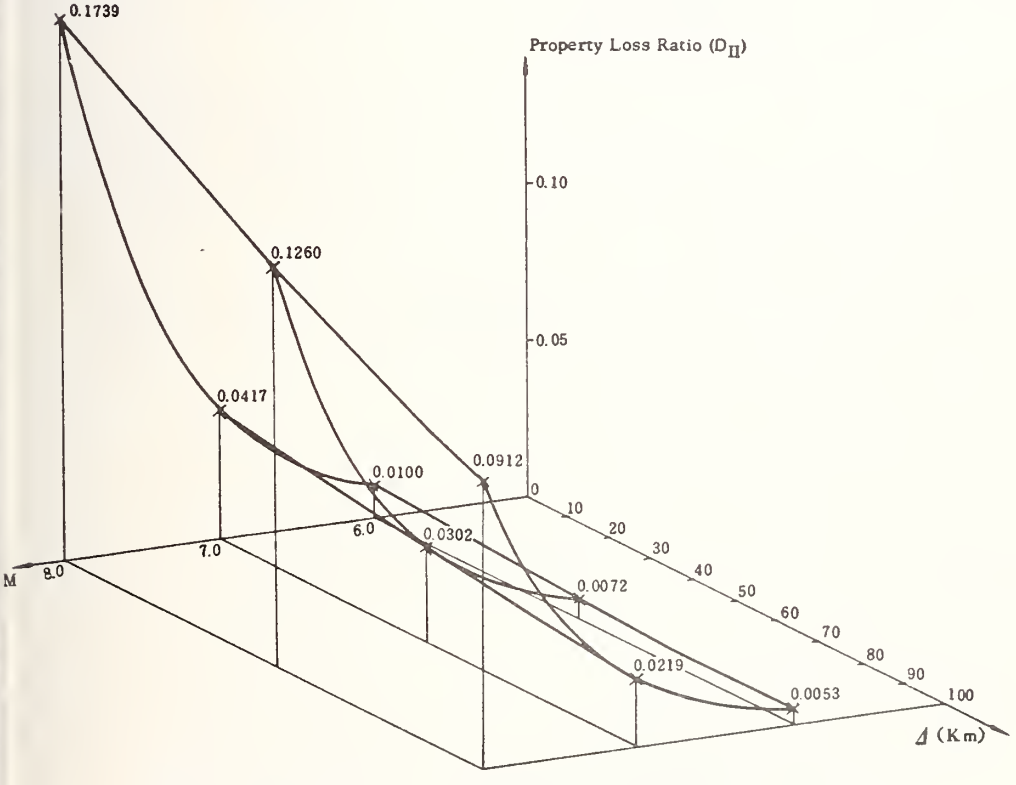

Fig. 9 Relationship between Magnitude, Epicentral Distance and Property Loss Ratio (Subground Type II)

31

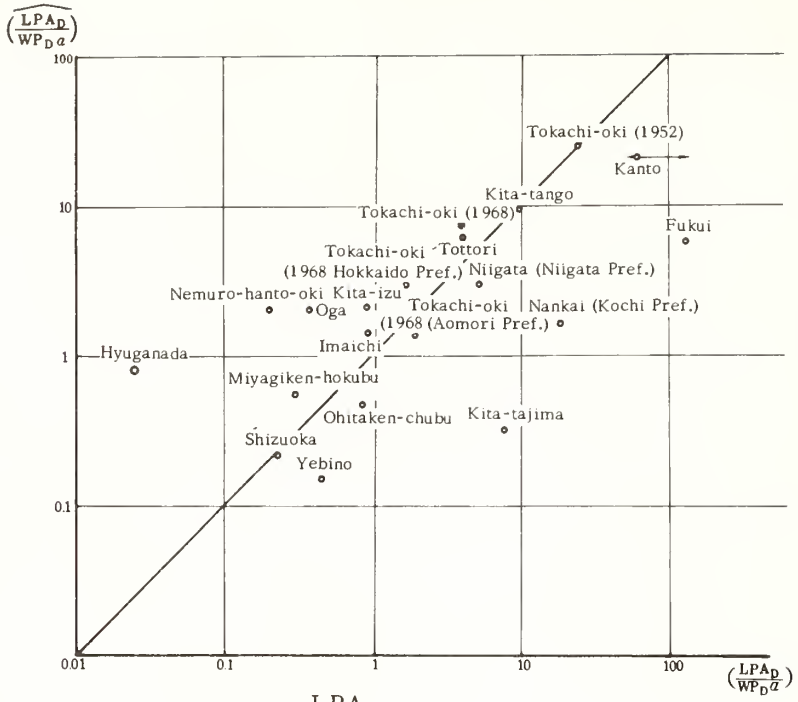

Fig. 10 $\left(\frac{LPA_D}{WP_D a}\right)$ and its Estimation

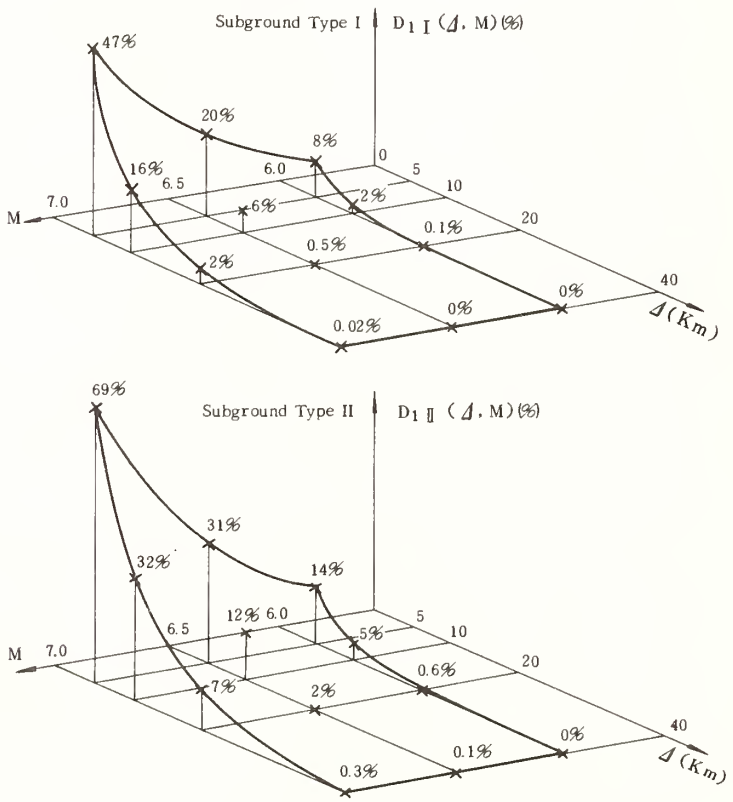

Fig. 11 Relationship between Magnitude, Epicentral Distance and Equivalent Ratio of Razed House

Social Capital (82,715 billion yen)

32,876.2 bil.yen	Assets of Public Corporations (39.7)	Transportation (44.2)
		Electric Power (24.7)
		Telecommunication (14.8)
		Water Supply (13.7)
		Gas Supply (2.6)
21,827 bil.yen	Public Service Assets (25.5)	Education (49.4)
		Public Organizations (16.6)
		Religion (12.4)
		Medical Service (11.0)
		Cooperation (8.1)
		Public Insurance (2.5)
20,986.3 bil.yen	Public Assets (25.4)	Highway (38.7)
		Agriculture, Fishery, Forestry (26.5)
		River (19.9)
		Harbor (9.9)
		Others (5.0)
7,769.8 bil.yen	Governmental Assets (9.4)	Central (29.8)
		Local (70.2)

( ): percentage.

Fig. 12 Breakdown of Social Capital in 1970 National Wealth Survey

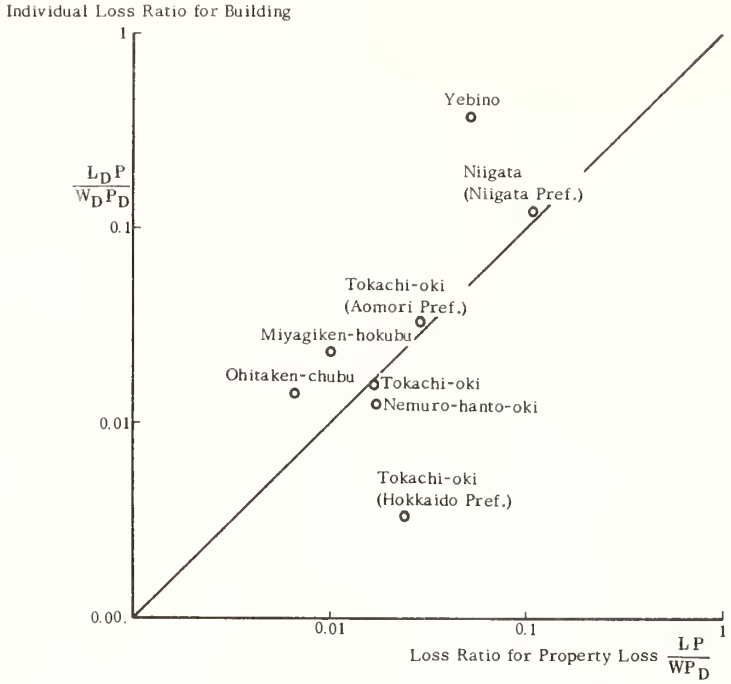

Fig. 13 Relationship between Loss Ratios of Property Loss and of Building

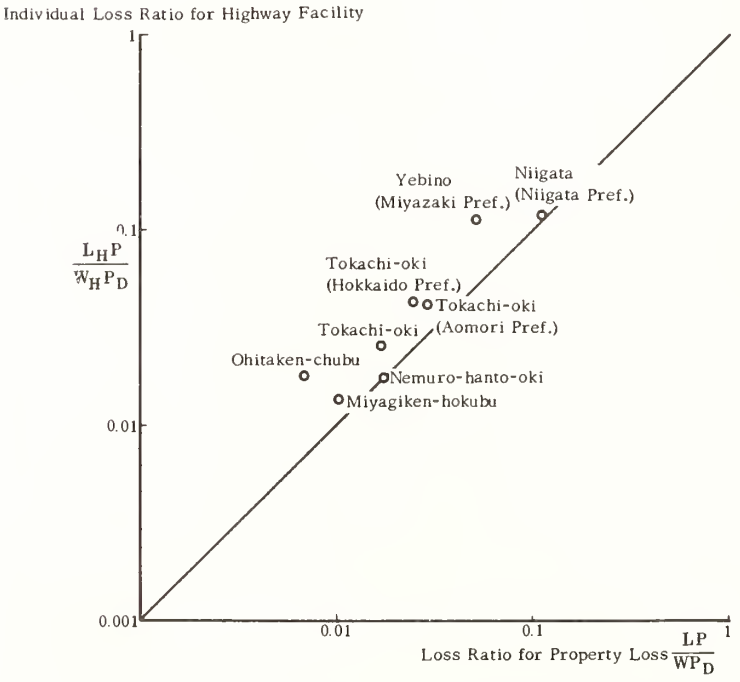

Fig. 14 Relationship between Loss Ratios of Property Loss and of Highway Facility

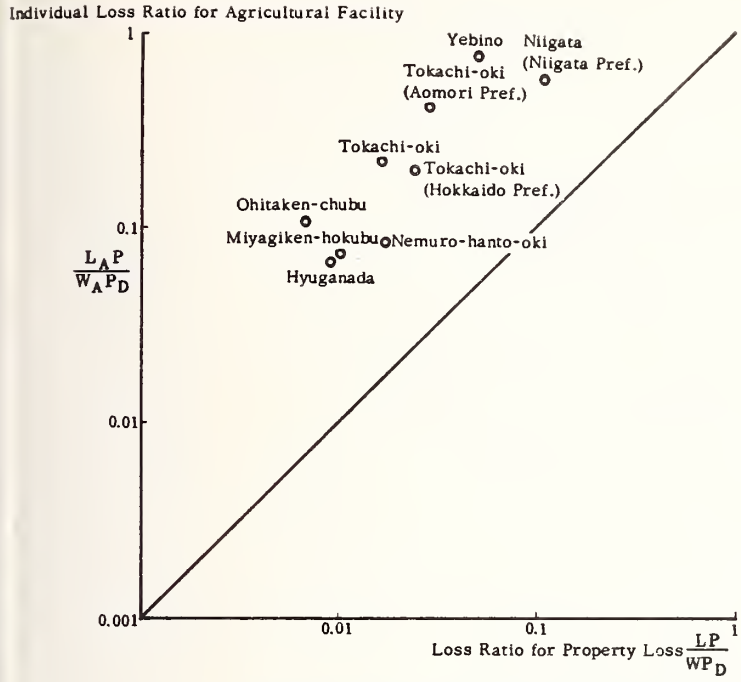

Fig. 15 Relationship between Loss Ratios of Property Loss and of Agricultural Facility

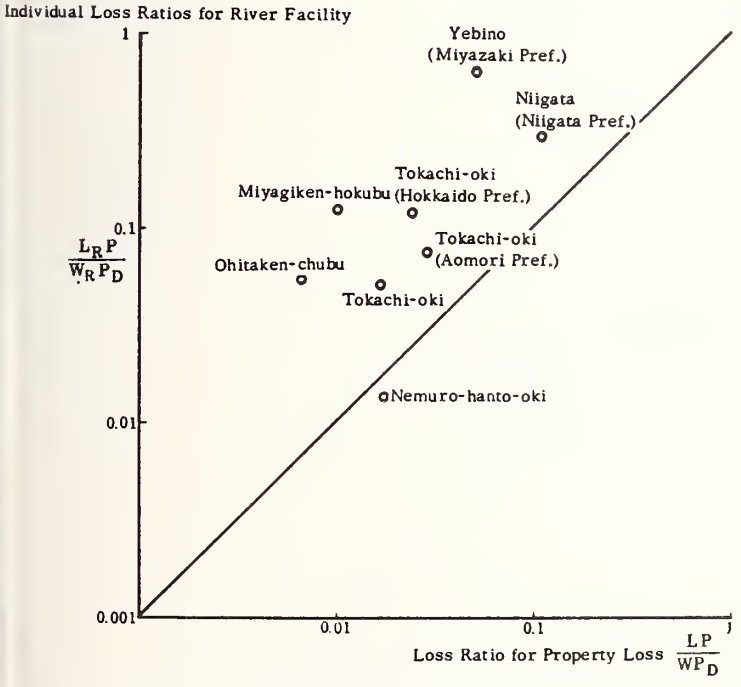

Fig. 16 Relationship between Loss Ratios of Property Loss and of River Facility

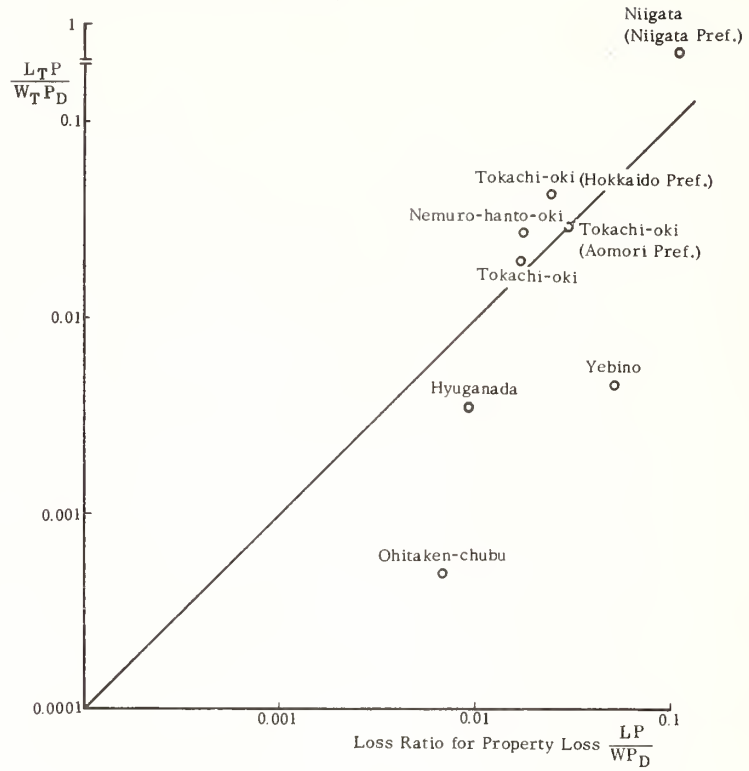

Fig. 17 Relationship between Loss Ratios of Property Loss and of Telecommunication Facility

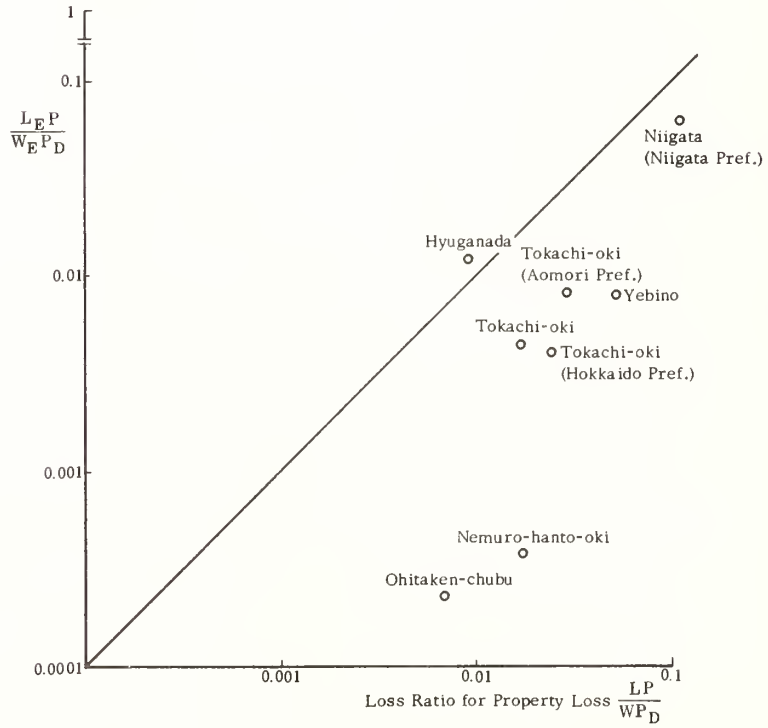

Fig. 18 Relationship between Loss Ratios of Property Loss and of Electric Power Facility

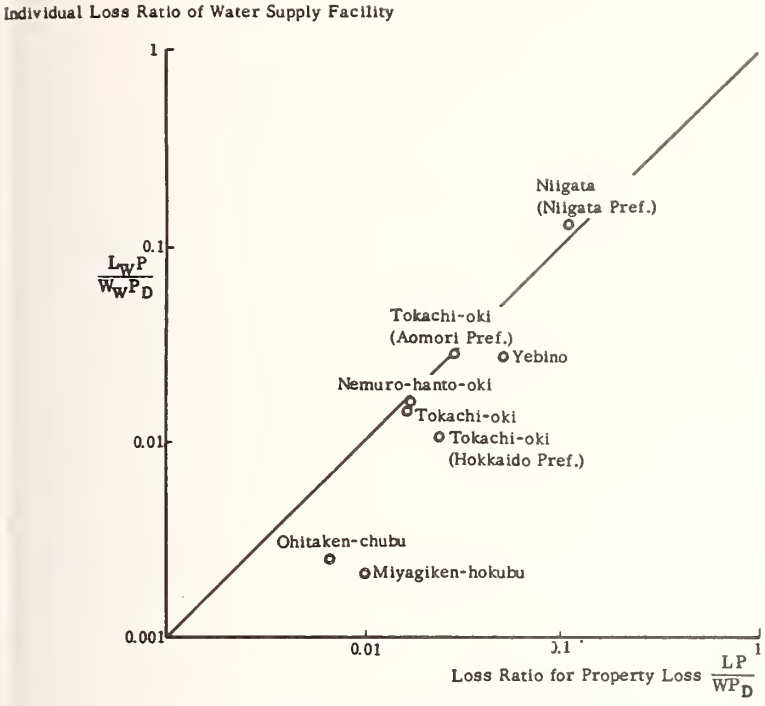

Fig. 19 Relationship between Loss Ratios of Property Loss and of Water Supply Facility

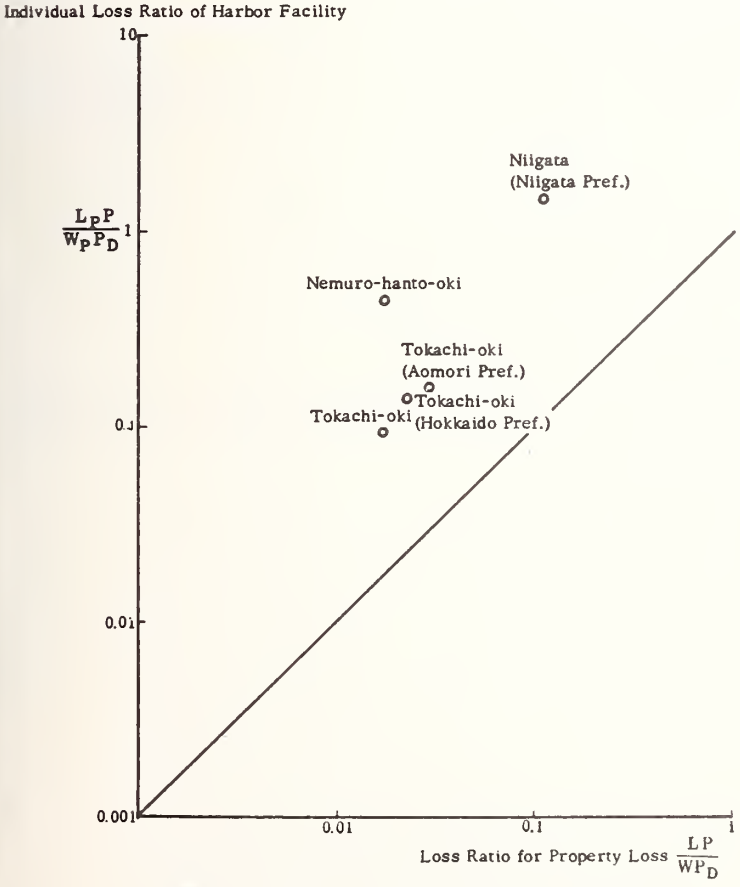

Fig. 20 Relationship between Loss Ratios of Property Loss and of Harbor Facility

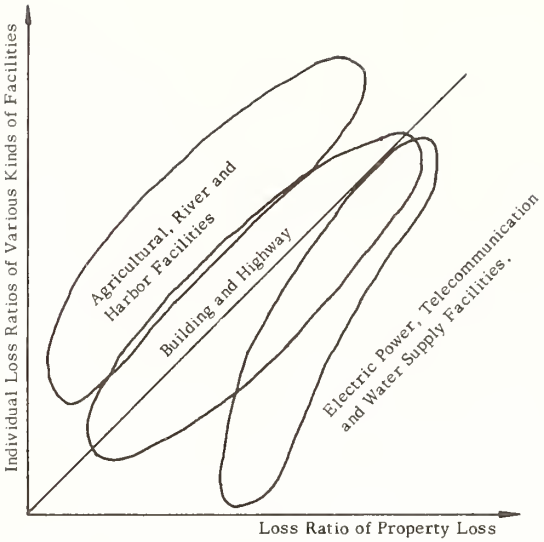

Fig. 21 Characteristics of Individual Loss Ratios of Various Kinds of Facilities

32

THE DISASTER-RESISTANCE OF CITIES AND THEIR LIFELINES

Kazuto Nakazawa
Eiichi Kuribayashi

Public Works Research Institute
Ministry of Construction

The Disaster-Resistance of Cities and Their Lifelines

Until recently, the phrase "earthquakes countermeasures" largely meant the design and construction of structures to withstand earthquakes. Today, however, it means much more than that, and typically includes studies of when earthquakes are likely to occur and assessment of the preparedness of cities, neighborhoods, and escalities to motion, fire, or tsunamis brought about by earthquakes. Such research is certainly justified by the awesome power of earthquakes. Among all natural disasters, earthquakes have taken the greatest toll of human life and property (see Table 1). If the highly populated central Pacific coast of Japan were to be hit today with a quake like the infamous Kanto quake of 1923, losses are estimated to be in the neighborhood of several tens of trillion yen ($200 billion).

Earthquake Prediction

The subject of earthquake prediction has always been shrouded in controversy. Early in the twentieth century, a debate began to grow up around two early practitioners of seismology -- Professor Omori and Professor Imamura. Imamura had predicted a large quake in the Tokyo area and insisted on countermeasures to protect the city. Professor Omori on the other hand belittled this prediction as being totally without scientific evidence. It is also said that Omori was anxious about needlessly panicking the public.

Unfortunately, the Kanto earthquake occurred in 1923 with 120,000 deaths and 5 billion yen in property losses. Based on this prediction, Imamura became the father of Japanese earthquake prediction. He followed this success with accurate predictions of the Tonankaido earthquake of 1944 and the Nankaido quake of 1946.

But Professor Imamura's predictions began to fail after World War II and the prediction of earthquakes as a scientific discipline began to fall into disuse. Not until 1962 was earthquake prediction study seriously undertaken again. In that year, three scientists, Tsuboi, Wadachi, and Hagiwara, outlined a new program, called the "blueprint", that would set earthquake research back on its feet and would require an investment of several billion yen over ten years. The program's budget rapidly increased -- in 1965 to 175 million yen; and in 1976 to 2,213 million yen. The organizational structure of this program is shown in Figure 1.

Today, earthquake prediction depends on many types of observations -- horizontal ground strain, vertical upheavals and subsidences, velocity changes in seismic waves, changes in the electromagnetic properties of rocks, and changes in ground water. Only synthesis of all this information can result in a useable prediction. Nevertheless, as Professor Imamura believed, "without prediction, there can be little prevention."

32

Disaster Resistance of Urban Districts

The Kanto earthquake of 1923 resulted in the following losses; where five can be seen as the predominant threat:

Burnt	447,128 houses
Razed	128,266 houses
Half Razed	126,231 houses
Lost by Floods	868 houses

By contrast, in the Tottori earthquake of 1943 and the Fuki earthquake of 1948, shaking was the culprit:

	Tottori Earthquake	Fukui Earthquake
Burnt	254 houses	3,960 houses
Razed	7,485 houses	35,420 houses
Half Razed	6,158 houses	11,449 houses
Lost by Floods	none	none

These facts suggest that while ground motion is the major threat in small towns, fire is what consumes the cities.

But fire and shaking are not the only enemies. Just as important are the economic and social disruptions that occur after the quakes. Indeed, Professor Toshihiko Kato of the Social Science Institute, University of Tokyo, suggests that the Kanto earthquake of 1923 led to a severe economic depression, which in turn led to militarism and expansion in Manchuria and China, and eventually to the disaster of World War II.

As a first step in ranking a city's resistance, a number of factors dealing with the city's layout, housing stock, and population must be investigated. They are:

- Geographical and Natural Elements

  Density of population and its concentration
  Kinds of industry and their distribution
  Vacant areas, aquatic areas
  Topography
  Meteorological and Hydrological phenomena

- Physical Properties

  Earthquake Frequencies and Intensities
  Geology and Soil Conditions
  Aseismic and Fire Resistance of Buildings
  Water and Energy Supply

- Dynamic Elements

  Population, Day and Night
  Dangerous Facilities
  Disaster-Prevention Facilities
  Traffic Volume
  Regional Redevelopment

- Social and Cultural Elements

  Communication Networks
  Governmental Control Organizations

Using this kind of information, the disaster-risk potential of each ward in a city can be profiled, as the Tokyo Metropolitan Government did in 1974. Their first step was to find, for each of the items shown below, the disaster risk for all 23 wards:

- Accumulated risk potential for wooden buildings
- Risk potentials due to local population, open spaces, and traffic volume
- Accumulated fire risk
- Risk potential of spreading fires
- Risk potentials for refugees

Based on this assessment, the five wards of the city at greatest risk are as follows:

	With Fire Fighting	Without Fire Fighting
1st	Sumida	Sumida
2nd	Arakawa	Arakawa
3rd	Taitō	Taitō
4th	Toshima	Toshima
5th	Kōtō	Shinagawa

The five safest wards were the following:

1st	Minato	Minato
2nd	Bunkyō	Nerima
3rd	Nerima	Setagaya
4th	Chūō	Chiyoda
5th	Setagaya	Chūō

Distribution of Earthquake Damage to Wooden Houses

Shaking Damage

How is earthquake damage distributed? The distribution of damage in the Fukui Earthquake of 1948 is shown in Figure 2. The circles in the figure indicate places where ground conditions are relatively sound, and the black spots indicate places where the ground is not sound. They suffered from the earthquake damage in ratios larger than 1%.

Fukui Earthquake of 1948 (M = 7.3, H = 20 km)
Izu Peninsula Earthquake of 1974 (M = 6.8, H = 20 km)
Ebino Earthquake of 1968 (M = 6.1, H = 0 km)

In the above medium-scale earthquakes, with magnitude of 6.1 through 7.3 and depths of hypocenters of 20 km or less, the distribution of ratios of earthquake damage to wooden houses were statistically as follows:

$$D_{1I} = \frac{1}{164} \times 10^{(0.625M + 0.025M \cdot \Delta - 0.272)}, \quad \text{----} \quad (1)$$

$$D_{1III} = \frac{1}{73} \times 10^{(0.576M + 0.026M \cdot \Delta - 0.248)}, \quad \text{----} \quad (2)$$

where

D_{1I} : ratios of earthquake damage to wooden houses (in %) in relatively sound ground conditions (I region),

D_{1III} : ratios of earthquake damage to wooden houses (in %) in bad ground condition (II region)

32

The earthquake damage ratios = $\frac{\text{Number of razed houses} + 0.5}{\text{Total number of}}$

$\frac{\text{x Number of half razed houses}}{\text{existing houses}}$ x 100, in %

M : Magnitude of earthquakes
Δ : epicentral distances (in km)

Research on the distribution of earthquake damage ratios has been done by Professors Omote, Minakami, Uchibori, and all of these researches find the ratio as being proportional to the exponent of epicentral distance. In Equations (1 and 2) the magnitude and ground conditions were taken into account. Ground condition I means layers of diluvium and tertiary; ground condition II, alluvium.

From the equations, it can be seen that in region I the earthquake damage ratio is smaller than in region II. Larger magnitude brings larger earthquake damage ratios and larger epicentral distances bring smaller earthquake damage ratios. These relationships are illustrated in Figure 3.

When these relationships are applied to actual earthquakes, comprehensive evaluations are possible. For example, the Ansei-Edo Earthquake of 1855 had its epicenter at the northern part of Tokyo at a location of N 35.8° and E 139.8°.

In each ward of Tokyo, the earthquake damage ratios corresponding to earthquakes of 6.0, 6.5, and 7.0 magnitudes were obtained as shown in Figure 4. In this figure great earthquake damage ratios are shown in the four wards of Adachi, Katsushika, Kita, and Arakawa near the epicenter and also the wards of Sumida, Taitō and Kōtō located in the delta.

In Figure 5, the distribution of the earthquake damage ratios for the Ansei Edo Earthquake is shown. Although the structural characteristics of houses 100 years ago are different, we can assume the thickness of the alluvium layers as being the same as today. The earthquake damage ratios of every ward in the area of the central part of Tokyo are compared with the actual ratios that occurred in Table 2. The three most dangerous wards are the same in both cases.

Fire Damage

At first glance, it seems that there is a correlation between earthquake damage ratio and the fire damage of earthquakes. However, in case of the Fukui Earthquake of 1948 there was no such similarity. (see Figure 6).

Damage by fires is affected by the possibility of outbreaks of fires, the possibility of expanding fires, the meteorological conditions, and fire-fighting ability. In macroscopic points of view, however, an equation of this evaluation was developed by Prof. Kawazumi as follows:

$$B = 10^{-5} \times N^2, \qquad (3)$$

where B = number of burnt houses,
N = number of razed houses,
$N = 0.2 \times 10^{2(M-5)}$,
and M = earthquake magnitude.

In Equation (3), it is known that about one house is burnt down at M = 6.5. However, at M = 8.0 a million houses are burnt down. The fact that 450 thousand houses were burnt down in the Kanto Earthquake with M = 7.9 supports Prof. Kawazumi's equation.

Lifeline Systems

Relations between various facilities and governmental agencies in charge in Japan are shown in Table 3. From this table, the facilities related to lifelines are as follows:

Facilities	Elements
Transportation - - -	Road, street, railway, airport and harbour
Communication- - - -	Telegram, telephone, mail, broadcasting and newspaper
Sanitary - - - - - -	Watersupply, sewerage and solid waste disposal
Energy - - - - - - -	Electricity, gas and liquid fuel
Vacant area- - - - -	River, lake park, greenzone and open space

All of them are indeed the indispensable facilities in and after earthquakes. Gases and liquid fuels are needed as heat sources, but on the other hand, they can help expand fires.

Here, a consideration will be presented about the improvement of the disaster-resistivity of lifelines by making use of a concept known as their residual lives. The residual life is the length of time obtained by subtracting the already-used time from the durable lifetime of a structure. The following is an example relating to the earthquake resistance of bridges in the Kanto district.

Assumptions:

i. Probability of earthquake damage (U*). Namely, the probability of earthquake damage (complete losses of the functions) of bridges that have existed since the Kanto Earthquake of 1923 is assumed to be 2.1×10^{-3}. (The probability of a human death during a earthquake is supposed to be 10^{-3} to 10^{-4} for reference.)

ii. The earthquake-resistance of bridges (R) is an exponential function of time.

iii. Durable life-time of a bridge is assumed to be 50 years.

Examples of the analyses are shown in Figures 7 and 8. Meanings of symbols in the figures are as follows,

Ro : Required capacities of bridge earthquake resistance.
ΔR : Ratios between capacities retrofitted and required.
Curve A : Changes of the existing capacity without any retrofitting.
Curve B : Changes of the retrofitted capacity to maintain the level of required capacities corresponding to the durable life of 50 years at any moment.
Curve C : Changes of the retrofitted capacity to maintain the level of the required capacities corresponding to the residual life at any moment, but with reductions of risks being proportional to ratios of the residual life-time and durable life-time.

32

In Figure 7 retrofitting ratios (ΔR: B-A and $\Delta R'$: C-A) are shown in the case of satisfying initially 96 percent of required capacity. In Figure 8 retrofitting ratios (ΔR and $\Delta R'$) are shown in the case of satisfying the full required capacity, but with reductions of probabilities of risks (1.05×10^{-3}) to half of the assumed probability before.

Although some technical specialists and planners may reject such a statistical approach and rely instead on their intuition, it is clear that the approach outlined there -- or one similar to it -- must underlie any future analysis that aims at thoroughness and dependability.

References

1. Okamoto, Shynzo: "Introduction to Earthquake Engineering," University of Tokyo Press, 1973

2. Ishibashi, Katsuhiko: "Re-examination of a Large Earthquake Expected in Tokai District," Autumn 1976 Meeting of Seismological Society, Draft Manuscripts of Presentations, No. 2, October, 1976 (in Japanese)

3. Sato, Yutaka: "Problems of Earthquake Prediction Research," Kensetsu Geppo (Public Relations Magazine of Ministry of Construction), Vol. 30, No. 2, Feb., 1977 (in Japanese)

4. "Planning of Earthquake Disaster Mitigation of U.S.A. Geologic Survey," Earthquake Prediction Data 2, Science and Technology Agency, Research and Coordination Bureau, Living Science and Technology Section, March 1976 (in Japanese)

5. Kuribayashi, Eiichi: "Introduction to Earthquake Engineering" (1) through (15) The Bridge and Foundation Engineering," Vol 4, No. 2 to Vol. 5, No. 5 Feb., 1969 through May, 1970 (in Japanese)

6. Yoneda, Shoji: "Catastrophic Circumstances Produced by Great Earthquake," Economist Magazine, Extraordinary Number, July 7, 1975, Mainichi Newspaper Co., Ltd (in Japanese)

7. "Earthquakes" University of tokyo, University Extension, No. 24, University of Tokyo Press, Nov. 15, 1976 (in Japanese)

8. "Rikanenpyo (Science Yearbook)," Published in 1960, edited by Tokyo Astronomical Observatory (in Japanese)

9. Kato, Toshihiko: "Chapter VI, Earthquakes and Economy," refer to reference book 7 above (in Japanese)

10. "Promotion of Urban Seismic Disaster Countermeasures," Ministry of Construction, City Bureau, Kensetsu Geppo, Vol. 28, No. 11, Nov. 1975 (in Japanese)

11. "A Guide-line for Drafting Projects on Mitigation of Earthquake Disaster in Three Major Metropolitan Areas, Tokyo, Nagoya and Ōsaka (draft)," Ministry of Construction, Aug., 1975 (in Japanese)

12. Kuribayashi, Eiichi, et al.: "Distribution Characteristics of Seismic Damage," Technical Journal of Civil Engineering, Vol. 18, No. 9, Sept., 1976 (in Japanese)

13. Umemura, Hajime, et al.: "Survey in Regard to Evaluations of Earthquake Damage in Building" Report of Disaster Prevention Committee of Tokyo Metropolitan Government, 1970 (in Japanese)

14. Kawazumi, Hiroshi: "On the Seismic Damage Distribution and Earthquakes in Tokyo," Journal of Architecture and Building Science, No. 775, 1951 (in Japanese)

15. "Review on Disasters of the Ansei-Edo Earthquake," Tokyo Metropolitan Government 1973 (in Japanese)

16. Kawazumi, Hiroshi: "Intensity and Magnitude of Shallow Earthquakes" Bureau Central Seism. Intern. Ser. A, Tran. Sci. 19, 99-114

17. Kuribayashi, Eiichi, et al.: "Stochastic Analysis on Professional Judgements on the Importance Factors in Aseismic Design," Technical Memorandom of Public Works Research Institute, Sept., 1976 (in Japanese)

18. Kuribayashi, Eiichi, et al.: "Retrofitting Vulnerable Structures to Earthquakes," Technical Journal Civil Engineering, Vol. 19, No. 9, Spet. 1976 (in Japanese)

TABLE 1: HISTORICAL RECORD OF THE DEATH BY NATURAL DISASTERS IN THE WORLD

Disasters	Year of Christian Era	Country	Number of Death
Earthquake	1556	China	830,000
Flood and Tidal wave	1642	China (Break on coastal embankment)	300,000
Storm	1876	India	200,000
Volcanic eruption	1693	Italy	60,000
Fire	1871	U.S.A. (Wood fire)	1,152

TABLE 2: THE RATIOS OF HOUSES DAMAGED BY THE ANSEI-EDO EARTHQUAKE OF 1855

ratio of houses damaged by earthquake place name	Evaluated ratios*	Observed ratio
(1) Sumida-ward	100 % or more	80 %
(2) Kōtō	84 %	76 %
(3) Taitō	54 %	51 %
(4) Bunkyō	46 %	68 %
(5) Chiyoda	35 %	46 %
(6) Minato	34 %	80 %
(7) Chūō	26 %	8 %

(note) * As to the structural characteristics of houses and the thickness of Alluvium layers in subgrounds, those of the present days are used.

TABLE 3: FACILITIES CORRESPONDING TO MINISTRIES OR AGENCIES IN CHARGE

Facilities \ Ministries or Agencies in charge		prime Minister's Office	M. of Justice	M. of Finance	M. of Education	M. of Health and Welfare	M. of Agriculture and Forestry	M. of International trade and Industry	M. of Transport	M. of Posts and Telecommunications	M. of Construction
Cultural and educational	School				0						
	Physical training				0						
	Social and educational				0						
	Cultural assets				0						
Health and Welfare	Water supply					0					
	Medical service					0					
	Social welfare					0					
	Environmental and sanitary					0					
Agriculture and Forestry	Farmland						0				
	Agricultural						0				
	Woodland path						0				
	Fishery						0				
	Cultivation						0				
Commercial and Industrial	Service and distribution							0			
	Light industries							0			
	Heavy industries							0			
	Mining and raw material manufactures							0			
	Energy							0			
Transport	Railroad								0		
	Land transport								0		
	Marine transport								0		
	Airport								0		
Communication	Telegraph and telephone									0	
	Mail									0	
	Broadcasting									0	
Urban	Sewerage										0
	Street and park										0
Public engineering works	Road										0
	Road-re-lated										0
	River										0
	River-re-lated										0
	Coastal										0
	Sabo										0
House	Individuals' housing										0
	Public housing										0
	Others	Self-Defence Forces of Japan	Criminal affairs	Government employees' housing etc.							

FIGURE 1: ORGANIZATION OF EARTHQUAKE PREDICTIONS
(PREPARED MAINLY BY YUTAKA SATO)

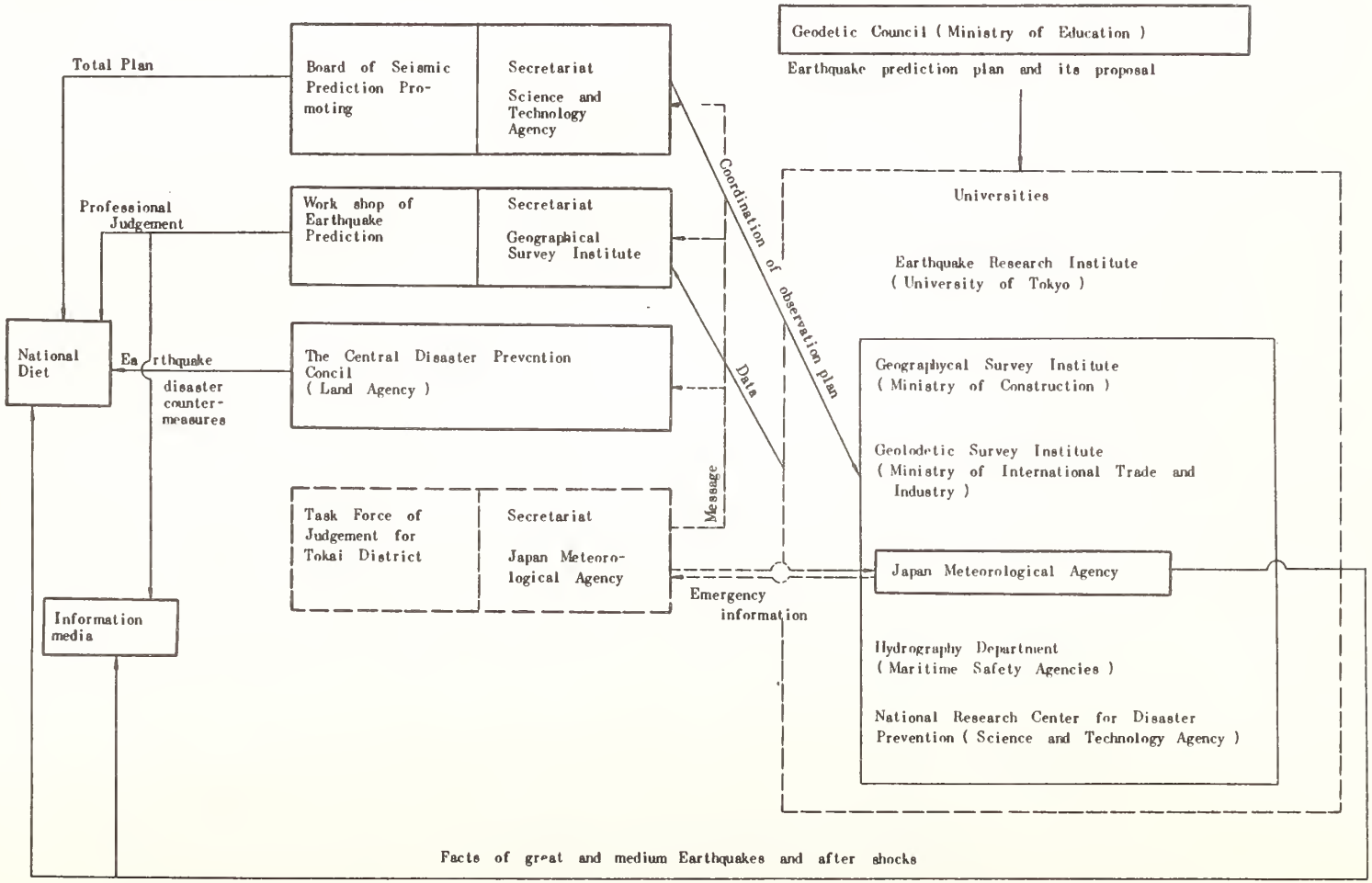

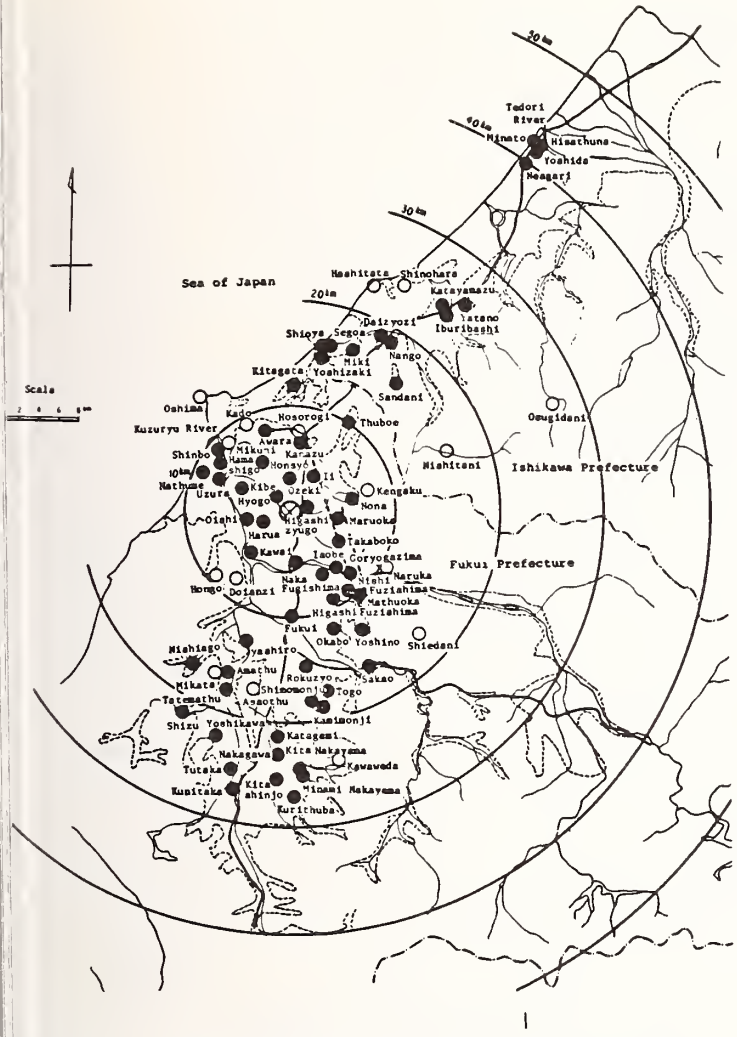

FIGURE 2: DISTRIBUTION MAPS OF TOWNS AND VILLAGES DAMAGED BY THE FUKUI EARTHQUAKE (WITH THE RATIO OF DAMAGED HOUSES OF 1% AND OVER), CLASSIFIED BY THE NATURE OF THE GROUND

(note) As to the faults, their curves are drawn according to the report of Mr. Yoshikatsu Ogasawara (1949): "On the Damage by the Fukui Earthquake and the changes in the ground, especially on the earthquake and the fault movement", Geodetic Survey Institute Review, Special Issue 2.

32

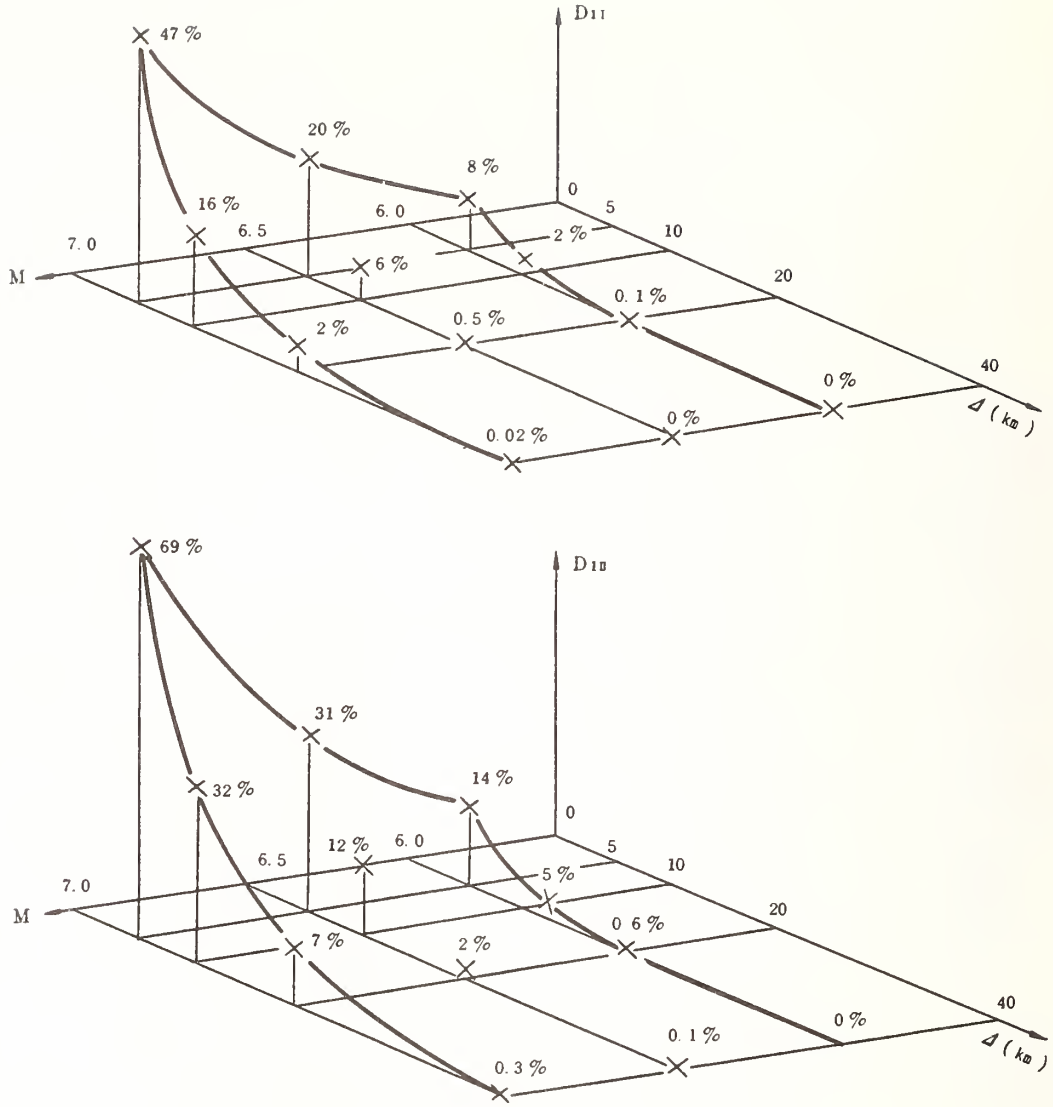

FIGURE 3: DISTRIBUTIONS OF THE RATIOS OF HOUSES DAMAGED BY EARTHQUAKES

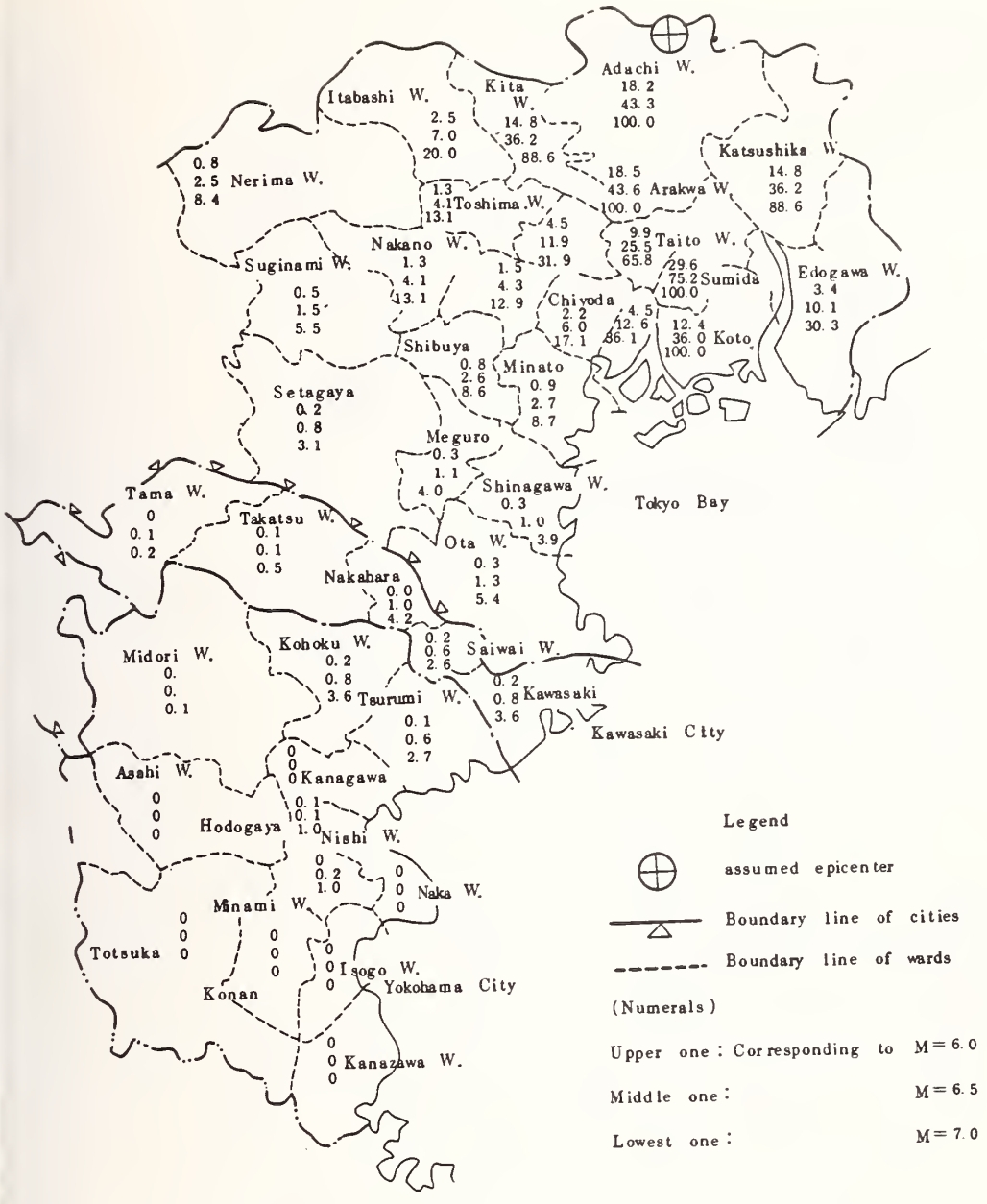

FIGURE 4: DISTRIBUTIONS OF THE RATIOS OF HOUSES DAMAGED BY HYPOTHETICAL EARTHQUAKES M=6, 6.5 AND 7, CLASSIFIED BY URBAN WARDS OF TOKYO, KAWASAKI AND YOKOHAMA

32

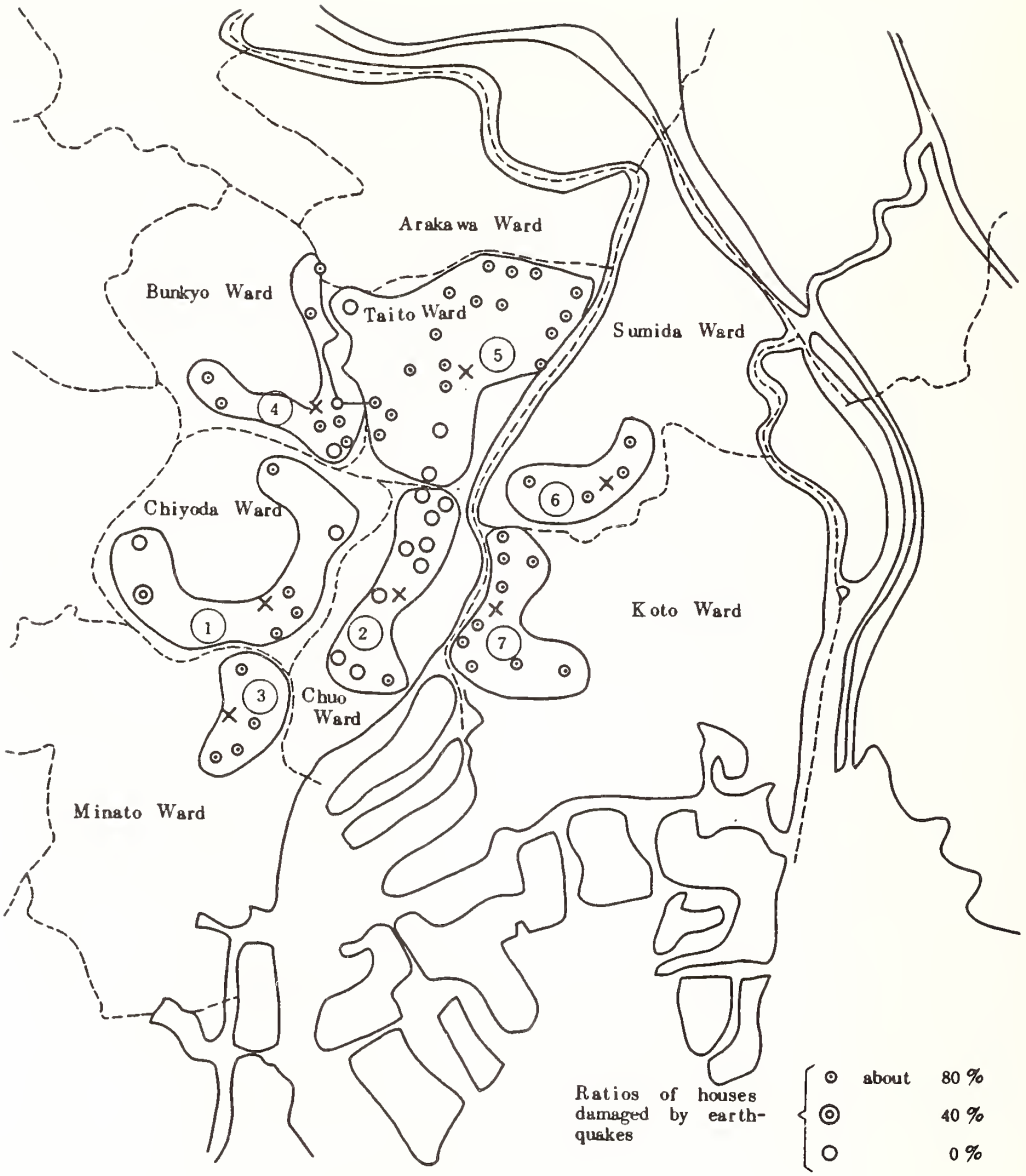

FIGURE 5: DISTRIBUTIONS OF THE RATIOS OBSERVED OF HOUSES DAMAGED BY THE ANSEI-EDO EARTHQUAKE OF 1855

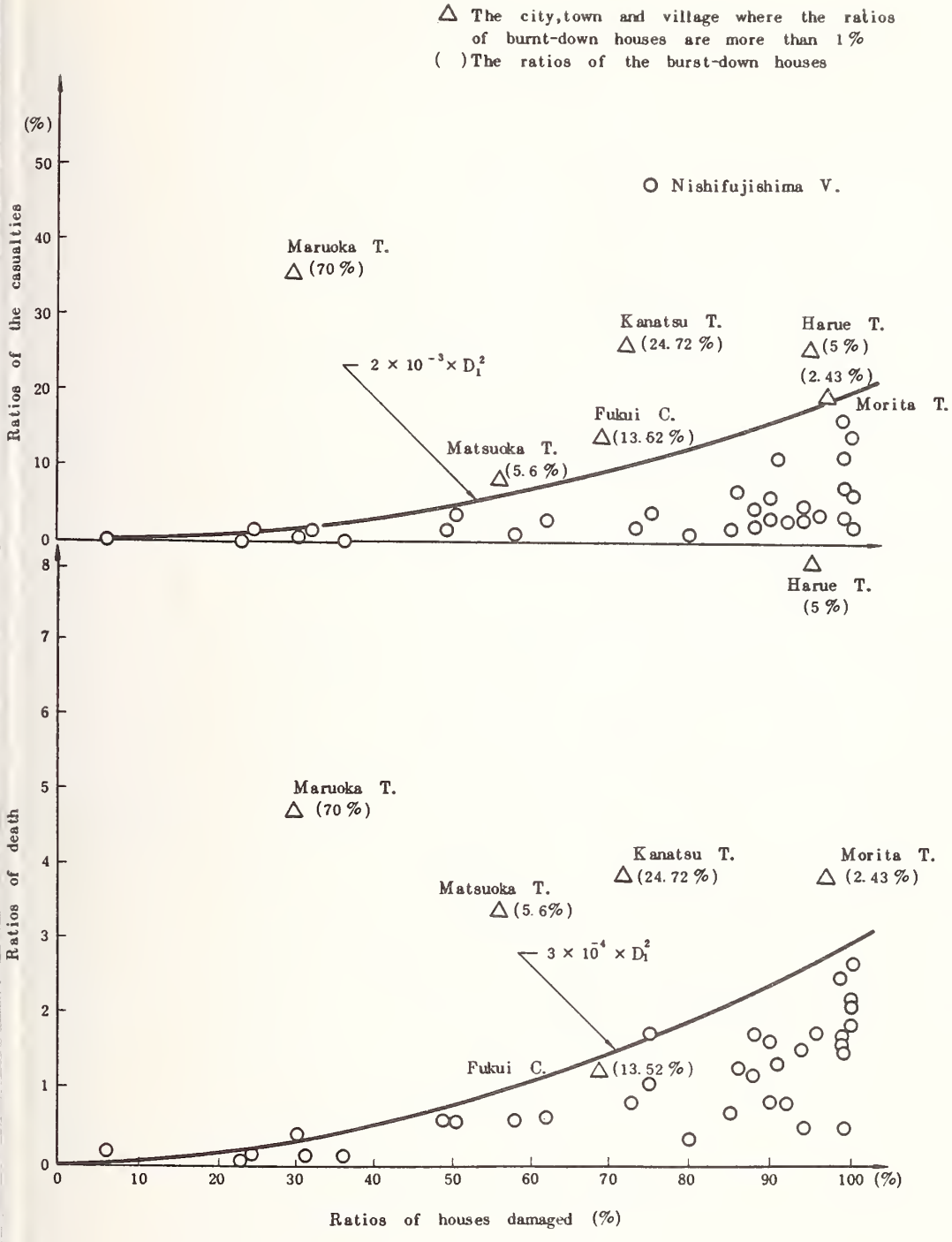

FIGURE 6: RELATIONS AMONG DEATH, CASUALTY, FIRE AND SHAKING DAMAGE IN THE FUKUI EARTHQUAKE OF 1948

32

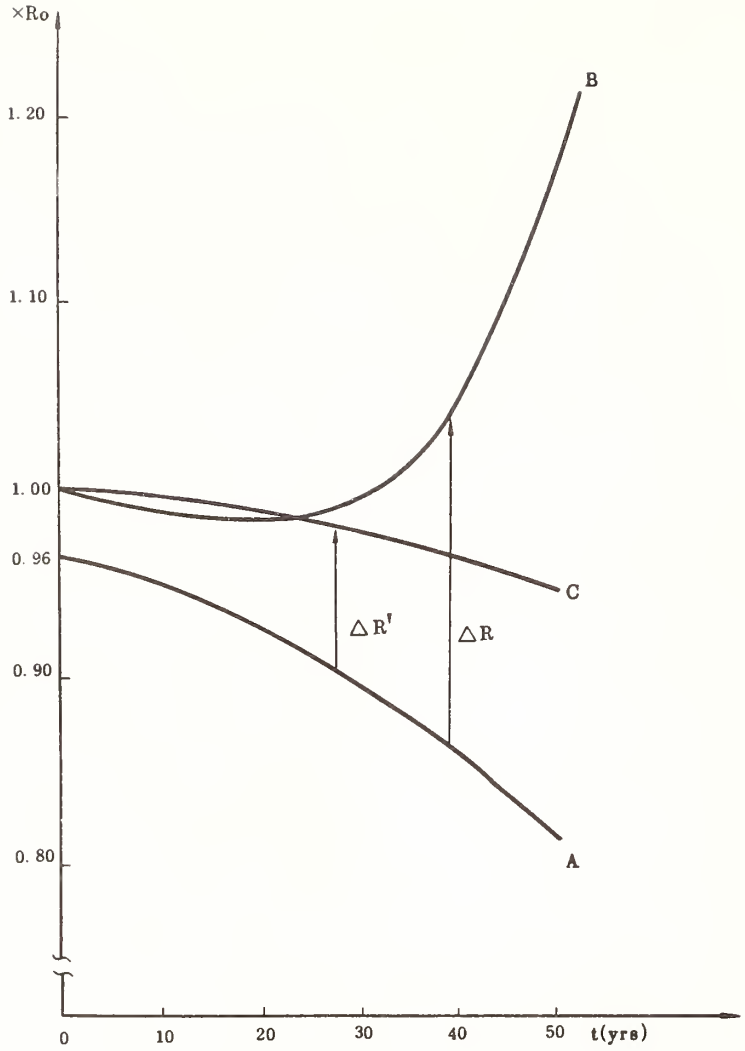

FIGURE 7: RETROFITTING REQUIRED, CASE 1

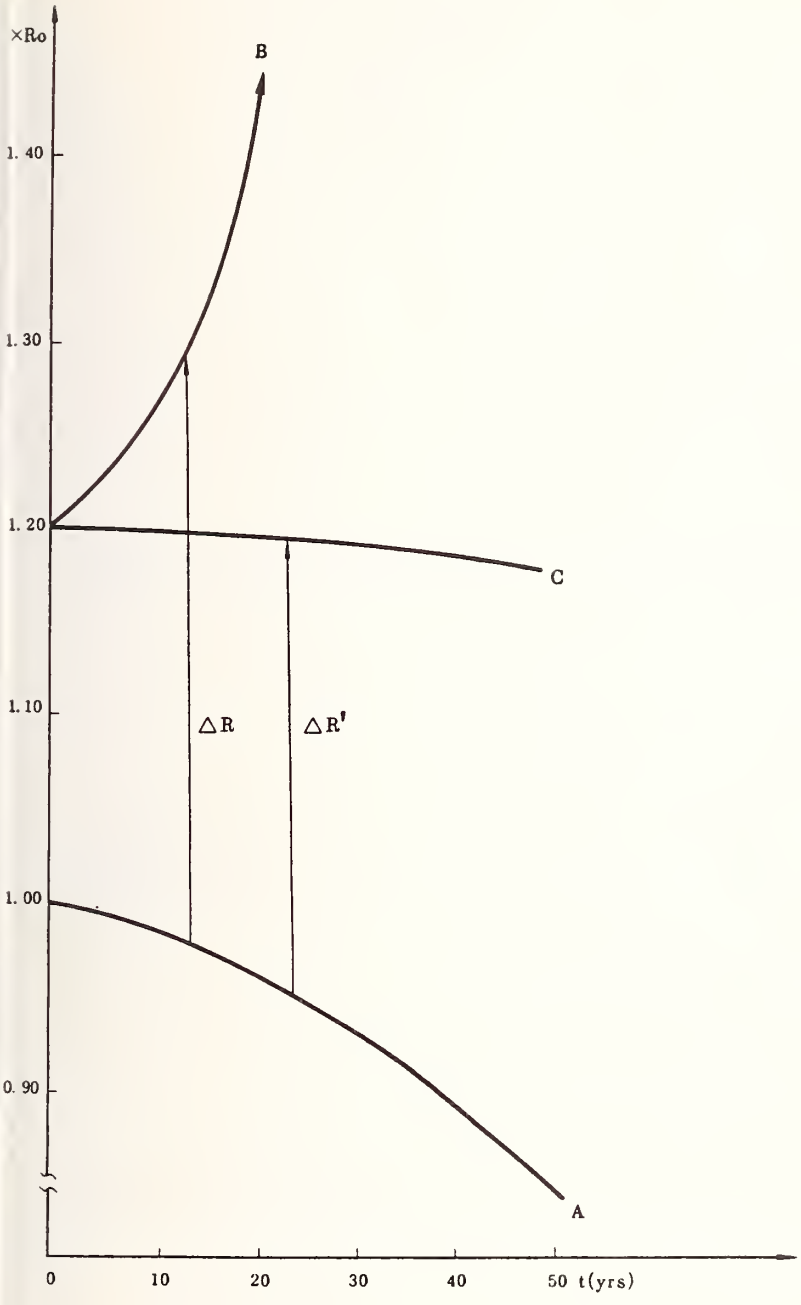

FIGURE 8: RETROFITTING REQUIRED, CASE 2

32

33

RESCUE AND REHABILITATION AFTER THE IZU-OHSHIMA KINKAI EARTHQUAKE OF 1978

Eiichi Kuribayashi
Tadayuki Tazaki
Takayuki Hadate

Public Works Research Institute
Ministry of Construction

Rescue and Rehabilitation After the Izu-Ohshima Kinkai Earthquake of 1978

General Information on the Earthquake

Date and time of the occurrence of the main shock: 1978, January 14th (Saturday), 12h 24m
Epicenter: 139°18'E, 34°48'N, depth 0 km
Location of the epicenter: Northern part of Ohshima Town, Ohshima island, Tokyo 26 km in east from Higashi-Izu Town, located along the east coast of the central part of the Izu Peninsula
Magnitude in Richter Scale: M=7.0 nominally, containing ±1/4 of error
Intensity distribution in JMA intensity scale: Shown in Figure 1-1, but 6 is considered the upper bound.
Intensity of JMA 5 and 6 corresponds to an 8 or 9 on the Modified Mercalli Intensity scale.
Focal Mechanism: A right lateral fault developed from the epicenter to almost western direction; lift zone was observed in the northern side.
Severest after-shock: 1978, Jan. 15th, 7h 32m a.m., M=5.7, the epicenter is estimated as 138°54'E, 34°53'N and 10 km in depth after Earthquake Research Institute, Tokyo University (see Figure 1-2)
Fore and after shock area: Fore and after shocks are distributed in a belt from Ohshima Island to the western coast of the Izu Peninsula across the middle of the peninsula as shown in Figure 1-3.

Fore-Shocks

From 36 to 55 minutes past 9 o'clock on January 14, four relatively big shocks (4th degree of JMA's intensity scale) were observed at Ohshima Meteorological Station.

In response to this information, the Shizuoka Prefectural Government sent the following wireless message to municipal governments in Shizuoka Prefecture at 11 o'clock: "The Japan Meteorological Agency informs us that occurrences of earthquakes and some damage are suspected in the very near future."

Weather in the Damaged Area

Before and after the earthquake, temperature changes and rainfall at Shimoda City, adjacent to the severest damaged area of Kawazu Town and Higashi-Izu Town, are shown in Table 1-1. In this table, the mean temperature is 8.0 degrees centigrade and the total rainfall is 50.5 mm during the whole of January, whose average is 7.5 and 66.1, respectively.

An Outline of the Disaster

In Kawazu Town and Higashi-Izu Town lifeline systems consisting of roads, railways, buried pipe lines, communication lines and power lines suffered damage from landslides and surface ruptures. Little damage occurred in buildings and houses. Incredibly, most of the damage occurred in two soilfill dykes for slime from a gold mine located at a point about 40 km from the epicenter of the main shock, along the upper stream of the Kano River.

In the limited district of Shizuoka Prefecture, the amount of the direct losses is estimated as 39.3 billion yen or more;

the indirect is still being estimated (refer to Table 1-2). Districts other than Shizuoka Prefecture suffered little damage.

Occurrences of Historical Earthquakes in the Izu Peninsula, their Geography and Geology

Since the seventh century A.D., 14 earthquakes on the Izu Peninsula and its adjacent area were recorded -- 6 times in the twentieth century, and 3 times stronger than 5th degree in this decade. On August 18, 1976, Kawazu Town was hit by an earthquake of Richter Magnitude 5.4 and Maximum Intensity 5.

The Izu Peninsula is covered with igneous rocks, and steep slopes with airslaked soils are seen along coasts and rivers. The whole of the peninsula is very sensitive to atmospheric, hydraulic, and geomechanical effects, especially heavy rain falls, which have frequently brought disasters (see Figure 1-4 and 1-5).

Damage and Losses

Most of the damage to buildings and houses resulted from landslides and surface ruptures; some damage occurred due to ground motions. As for the value of articles inside houses, they have been estimated as one third of the value of a house or three million yen for a house. Damage and losses are shown in Table 2-1.

Damage and losses to agricultural products, farm yards, forests, fishing ports, water sources for agriculture, water ways, roads for agriculture, canning plants for fruits and vegetables are shown in Table 2-2. Damage and losses to schools and play grounds are shown in Table 2-3. Damage and losses to hospitals, medical stations, relief facilities, and water supply systems are shown in Table 2-4.

Principal industries in the severest damaged area are tourism and agriculture. Damage to industries is shown in Table 2-5. Damage to roads is shown in Figures 2-1 to 2-4 and Table 2-6.

The failure of two dykes of Mochikoshi Gold Mine resulted in polluted river water from sodium cyanide contained in the slime. The effect to water quality is shown in Table 2-7.

Great damage occurred in railway facilities between Higashi-Izu and Kawazu railroad stations on the line operated by Izu Kyuko Railroad Co. Ltd. The damage is shown in Table 2-8.

There was no substantial damage to telephone systems except for cutting of an aerial wire caused by falling rocks in Kawazu Town. However, during about a half day after the main shock in all districts of the Izu Peninsula telphone service was not available. This problem was the result of countless receivers which had been shaken off their cradles due to the earthquake motion.

As for electrical power systems, minor damage occurred in two power plants, two transformer stations, two channels, and 24 towers for transmission lines, as shown in Table 2-9. In the severest damaged area there are liquid petrolium gas cylinders for domestic use, areal gas supply service, and kerosene storages for vehicles, ships, and machinery. Their damage was very slight.

Slight damage occurred in facilities for police and fire stations, but their activities were not disturbed.

The indirect losses are listed in Table 2-10. Losses due to this earthquake are compared with those of the Niigata Earthquake of 1964 in Table 2-11.

Countermeasures for the Emergency in and after the Earthquake

Shizuoka Prefectural Government Office and municipalities set up the Rescue and Rehabilitation Center as shown in Table 3-1, following the Regional Disaster Prevention Plan of each body. Figure 3-2 and 3 are the structures of the Center of Shizuoka Prefectural Government Office and Shimoda City Office.

At the same time, the prefectural center, headed by the Director of the Shimoda Tax Office, was established in Shimoda (see Figure 3-2). A forward base of the Branch was organized on Jan. 17 at Kawazu municipal office. Twenty people led by an accounting superintendent (a position second only to a vice governor) were dispatched to Kawazu. They assisted with information collection, rescue, and rehabilitation in cooperation with the Kawazu officials.

Collecting information about the damaged facilities overwhelmed the capacity of municipal offices and lower prefectural organizations. Several prefectural officials were also dispatched to Izu district. Three search groups were sent to the Prefectural Construction Office in Shimoda.

The Governor of Shizuoka Prefecture asked for the help of the Self Defense Forces (SDF). Several corps, including 400 men of the 34th regiment, moved to Izu on January 14. Some of them arrived at the damaged sites that night. They rescued unidentified and injured persons, and removed the fallen soil and rocks from slopes beside roads and behind houses. Table 3-2 shows the work of SDF.

Fire self-defense squads and community systems (private organizations) also contributed greatly to the rescue and rehabilitation. Table 3-3 shows the performance of these squads. Table 3-4 shows the list of other organizations related to rescue and rehabilitation.

Although the main shock took place at 12:24, 24 minutes after business hours, people who were on their way home quickly came back to the office and set up the emergency system.

When the Prefectural Government Office had transmitted the information about the foreshocks, which JMA had issued, to branch offices of prefectural government and municipal offices, Shimoda City Office announced it to its personnel in the building. But Kawazu Town regarded the message as having very little urgency, based on its previous experience with such warnings.

Refuge and Rescue

The damage brought by the earthquake was mainly caused by landslides. Moreover, there existed a possibility of relatively big aftershocks in an area that was dotted with the dangerous cliffs and slopes. Issued recommendations are listed in Table 3-5.

Some people in the districts other than those in Table 3-5 made their own decision to evacuate. They had detected the danger

of landslides. Table 3-6 shows numbers of evacuees and refuge places. Private residences were also used as refuges.

Restoration

Water supply facilities consist of municipal and areal water supplies. The scale of the latter is smaller. Although the water pipes sustained severe damage, the filtration plant did not. As shown in Table 3-7, municipal and areal water supplies were restored by Jan. 26 in Higashi-izu Town and Kawazu Town.

Drinking water shortage was not a severe problem during the suspended period. One reason is that each municipality usually prepares water wagons and can supply drinking water if only the water source survives the earthquake. The other is that the water wagon of the Ground Self Defense Force and the water boat of Maritime Self Defense Force took drinking water to the disaster area.

When the dykes of the sludge reservoir at Mochikoshi gold mine gave way, the sludge with sodium cyanide held there (about 58,500 m^3) flowed into the Mochikoshi river and its main river, the Kano river. Izu-nagaoka Town Office was forced to stop taking water from the Kano river. For several weeks they were using existing wells and narrow streams as their water source.

Telecommunication facilities of Japan Telegraph and Telephone Public Corporation (JTTPC) were restored by Jan. 17, except for 49 circuits in Kami-kawazu, Kawazu Town. The entire circuit was back in operation by Jan. 25 (see Table 3-8).

The electric power was cut off to 15,000 residents after the earthquake. Tokyo Electric Power Co. Ltd dispatched 888 people from the 14th through 16th of Jan. to repair the problem. It was finished by 19:15, Jan. 15 (see Table 3-8).

Shimoda City was the only one having areal gas supply service in Izu territory. The gas supply company in Shimoda City examined all gas pipes before resuming the service. Most houses in the area other than Shimoda City were installed with a liquid petroleum gas (LPG) cylinder. The gas company specialists inspected whole cylinders preceding the reopening on Jan. 17.

Resumption of Traffic and Traffic Control

The skelton of the highway in the Izu Peninsula consists of National Highway routes 135 and 136 and a Principal Prefectural Road, Shuzenji-Shimoda Line, part of which are toll roads. The railroad network is comprised of the Ito Line (JNR, Atami-Ito), Izu-Kyuko Line (Izu-Kyuko Railroad Co. Ltd, Ito-Shimoda) and Izu-Hakone Railroad Line (Mishima-Shuzenji) (see Figure 3-4).

Most of the damage to highways was generated by landslides. The damaged sites were too concentrated in the mountainous area to perform the rehabilitation all at once. The works were started from both sides of the damaged route and went forward to the middle.

Table 3-9 shows the traffic control. The numbers in the table correspond to those in Figure 3-4. The site indicated by X was still out of service as of Feb. 12. Out of the major highways, Route 136 first reopened at 12:00, Jan. 16. As for the route on the east coast, both the Higashi-izu Toll Road and ex-national highway route 135 administrated by Japan Highway Public Corporation

(JHPC) and Prefectural Construction Office run in parallel (Figure 3-5).

Priority was given to the Toll Road even though the restoration of the ex-national highway was obliged to be delayed. The ex-national highway was still suspended a month later because of the heavy damage, as shown in Photo 1. The Higashi-izu Toll Road was out of service from 14th through 16th of January. It opened from 17th through 29th exclusively to emergency vehicles only in the daytime. It was shut again from Jan. 30 through Feb. 9 for rehabilitation. Since Feb. 10 it has resumed with some one-lane sections. The Principal Prefectural Road, Shuzenji-Shimoda Line sustained extensive damage, where a tourist bus was buried in a landslide and three passengers were killed. The Prefectural Construction Office and SDF made a great effort to restore the road, but it was still out of service a month later.

Most damage to railroad facilities was to the Izu-kyuko Railroad Co. Ltd. The line was stopped after the earthquake and reopened as:

Ito-Izu-kogen	12:30, Jan 15
Izu-ogen-Katase-shirate	12:20, Jan 17
Katase-shirata-Inatori	6:55, Jan 30
Kawazu-Shimoda	6:30, Jan 31

The section between Inatori and Kawazu is still blocked by the tunnel whose lining was crushed due to the active fault. Inatori and Kawazu are connected by bus service.

The facilities of Japanese National Railroad (JNR) suffered no damage. However, according to its own regulations, JNR was forced to stop services and examine its facilites. The resumed time of each line was as below:

New Tokaido Line (superexpress)	16:55, Jan 14
Tokaido Line	15:15, Jan 14
Ito Line	15:00, Jan 14
Minobu Line	12:40, Jan 14
Futamata Line	14:50, Jan 14

Collection and Transmission of Information

Collecting information on the damage itself and the demand of goods and machinery for rehabilitation is a substantial problem in the beginning of an emergency. Most of the information on the damage to dwellings, water supply, electric power, and telecommunications facilities was gathered by midnight of Jan 14 by the administration and public organizations. Kawazu Town Office, the most heavily damaged area, could not finish, however, until the next day.

For example, Shimoda City Office dispatched 38 people immediately after the earthquake to investigate damage. They collected the number and scale of damage in a few hours and transmitted them to the headquarters of the Prefectural Government. Detailed investigation continued from the 15th through the 18th of January.

Community systems were well organized and each citizen knew his duty. This contributed effectively to the collection of information.

Collecting the information on the damage to roads was difficult, because the traffic route itself was blocked everywhere. For the Principal Prefectural Road, entering by automobile was impossible. The search party of the Prefectural Construction Office investigated the damaged sites on foot. It took 3 days to outline the damage and 3 more days for detailed investigation.

Three people of the Prefectural Government Office flew by SDF helicopter over the damaged territory on the afternoon of Jan 14. However, they could not see details because the pilot was not accustomed to the highway routes and his altitude was relatively high.

Some information on the damage of highways was brought in by the road monitors. When the tourist bus was buried in the landslide at Nashimoto, Kawazu Town was informed by one of the monitors living beside the Principal Prefectural Road, Shuzenji-Shimoda Line.

Telephone network of JTTPC was the principal means of communication in the emergency. However, for a few hours after the earthquake the demand for telephone calls exceeded the system's capacity. During this period, emergency wireless -- eleven circuits in Shizuoka Prefecture -- was used to communicate between Prefectural Government Office and municipal offices. Prefectural Government has planned to increase the circuits to 35 by October 1978.

An exclusive circuit was installed temporarily between the Prefectural Construction Office and Shimoda Branch in Shimoda Tax Office after the earthquake.

Other Measures

The collapsed dykes on the Mochikoshi and Kano Rivers were repaired temporarily with double-steel sheet piles. The toxic sludge was removed from the riverbed and deposited in abandoned mines. It was scheduled to be finished by Feb 20 (see Photo 2).

Reconstruction

Law Systems for Relief

The law systems applied by the relevant administrations are listed below:

(1) Disaster Relief Law
Disaster Relief Law was applied in;

Higashi-izu Town	19:30, January 15
Kawazu Town	19:30, January 15

(2) Designation of Violent Disaster
Designation of Violent Disaster is under consideration for the time being by the Cabinet. The damage to agriculture and minor enterprises in Higashi-izu and Kawazu Towns will possibly be designated. Only in Kawazu Town will it possibly be designated for public works.

(3) Loans
People whose dwellings were totally or half destroyed by the earthquake were qualified to have a disaster relief loan from the Housing Loan Corporation. Explanation meetings were held in Kawazu and Higashi-izu Towns on Jan 28 and 29. Tourism

enterprises received loans from the People's Finance Corporation and Minor Enterprises Finance Corporation.

(4) Exemption of Tax

The fixed property tax of the razed houses was exempted. Enterprises that suffered some damage were exempted from the enterprise tax, real estate acquisition tax, auto tax, and automobile acquisition tax. The restaurant tax was also deferred. Compulsive car inspection was deferred for a month in the damaged district.

(5) Aid

Shizuoka Prefectural Government decided to aid those people whose residential land was considered suceptible to further landslides when its preventive cost would exceed 500 thousand yen. The Government assumed half this expense, which totalled 53,900 thousand yen.

Reconstruction Work on Public Utilities

Reconstruction work on civil engineering, argicultural, and educational facilities have been performed or are being prepared. Table 4-1 shows the public structures qualified for the national subsidy. Ministry of Construction urgently qualified the first 39 reconstruction sites for the subsidy from 15th through 17th of February. Other qualifications by the ministry will follow.

Other Articles Concerning Reconstruction Measures

Izu-kyuko Railroad Co. Ltd has considered reconstruction of the Inatori tunnel to resume service as early as possible. The tunnel had been constructed in a circular section as illustrated in Figure 4-1. An interior lining inside the existing one is the most likely method of reconstruction.

As for the Mochikoshi mine, a Mochikoshi Mine Reconstruction Countermeasures Committee headed by Prof. H. Yamaguchi of Tokyo Institute of Technology had been established since Jan 28.

Specific Matters Referring Experiences of Past Disasters

The Izu Peninsula has suffered frequent natural disasters. The Kano-gawa typhoon of 1958 killed 1,269 people. As for the past five years, it has sustained:

Izu-hanto-oki earthquake	May 1974
Flood	July 1974
Heavy rain	July 1975
Heavy rain	July 1976
Kawazu earthquake	Aug 1976
Heavy rain	Oct 1976

People and administrative personnel in the district were thus well prepared for this disaster. Installing water wagons in each municipality was a typical example of preparation.

The Fuji-Hakone National Park on the Izu Peninsula is occupied by many tourists all year around. In the flood of July 1974, several traffic routes were blocked and tourists could not leave Shimoda City. They rushed into Shimoda Port causing some panic. Remembering this experience, tourists were ordered after the earthquake to remain in their hotels until transportation was assured. The municipal offices asked for or hired boats from SDF, Maritime

Safety Division, and private shipping companies to transport them to Atami and Ito Cities. Table 5-1 shows the number of tourists brought out by ships.

Because Route 135 on the east coast was damaged, the Prefectural Construction Office put a priority of reconstruction on its by-pass, a section between Shimoda City and Kawazu Town of the Principal Prefectural Road, Shuzenji-Shimoda Line.

Shimoda City has experienced many tsunamis (tidal waves) as shown in Table 5-2. The City Office has designated refugee places high up on the hills. They have also marked the anticipated water level of tsunamis on electric power poles to draw the attention of citizens.

Japan Meteorological Agency (JMA) issued the tsunami warning 12:31, Jan 14. However, Shimoda City is located only about 30 km from the epicenter and the first wave of the tsunami was estimated to reach about 10 minutes after the earthquake. There would be no time to evacuate. As a matter of fact many citizens decided on their own to evacuate to the designated refuge places. The observed tsunami was about 10 cm and the warning was canceled at 14:15.

Operation of Organizations

The Kawazu office of the Prefectural Government was exceptionally organized for this disaster. The Kawazu office, headed by an accounting superintendent of the prefectural government, controlled rescue, rehabilitation, and reconstruction throughout the damaged area. A meeting was held every morning at Kawazu office attended by staff from relevant municipalities, branch offices of the prefectural government, Higashi-izu Toll Road Office (JHPC), Izu-kyuko Railroad Co. Ltd, SDF, and police.

Lessons from this Disaster

In this disaster, the quick collection of information allowed the government to grasp its extent and severity. As for the highways, it took three days to grasp the damage.

It is recommended in Japan, where mountains are steep and many trunk lines of transportation are concentrated on a narrow flat strip of land, to develop an effective and quick way to survey the damage.

Telecommunication networks functioned satisfactorily except during one confused period for a few hours. Expanding and strengthening emergency networks should be encouraged.

Shizuoka Public Safety Commission (SPSC) was ordered to stop traffic where the road was blocked by landslides. But passes were granted. The owner of a vehicle who wanted to get such a pass applied to SPSC. When it was given, a seal had to appear on the front windshield. But the number of vehicles qualified reached 7,395, which disturbed the rehabilitation and reconstruction of road to some extent.

Lessons for Organizational Systems

The accounting superientendent sent to the disaster-hit area had supervised various organizations in emergency relief. He had visited Izu territory five times for previous disaster relief.

He knew the area in detail. This contributed a lot to the rehabilitation and reconstruction after this disaster.

Other Lessons from the Earthquake

The organziational systems to cope with natural disasters have been satisfactorily developed in Japan. Shizuoka Prefectural Government had improved its organization system and information network, and had stored daily goods for the emergency, especially because a seimologist had warned of the possibility of a "Great Tokai Earthquake" to occur within Suruga Bay [10]. The Government had newly established its Earthquake Countermeasures Section in 1977. These measures created an awareness of what to do in earthquakes. For example, no fire broke out after this earthquake. This is because most people turned off their gas, even though some of them got burned doing it.

Most roads in the Izu Peninsula are constructed by cutting and banking on a steep slope. The possibility of landslides along the roads is considered to be higher than that of any other territory in Japan. To improve the situation the road administrator is planning to construct a new disaster-proof highway consisting mostly of long-span bridges and tunnels. This plan is quite reasonable if all the disaster countermeasures are used.

References

1. Rika-Nenpyo (Science Yearbook): Tokyo Astronomical Observatory, Maruzen Co., Ltd, 1978.

2. Preliminary Report of the Izu-Ohshima Kinkai Earthquake of 1978: Ohshima Meteorological Station, Tokyo Meteorological Observatory, Jan 21, 1978.

3. Executive Office of the President, Office of Emergency Preparedness: Report of the Congress, Disaster Preparedness, Jan 1972.

4. J. Haas and R. Ayre: the Western Sicily Earthquake of 1968, National Academy of Sciences, 1969.

5. R. Dynes, J. Haas and E. Quarantelli: Some Preliminary Observations on Organizational Responses in the Emergency Period after the Niigata, Japan, Earthquake of June 16, 1964, Disaster Reserch Center, The Ohio State University, 1964.

6 and 7 A case Study on the Rescue and Reconstruction after An Unexpected Disaster - The Eruption of Mt. Usu, 1977 - : Technical Memorandum of Public Works Research Institute, No. 1292 (in Japanese) and No. 1293 (in English), 1978

8. Classified Maps of Subground in Shizuoka Prefecture: Development Bureau, Economy and Planning Agency, Prime Minister's Office, 1971.

9. R. Wallace: Goal, Strategy and Tasks of the Earthquake Hazard Reduction Program, Geological Survey Circular 701, 1974

10. Katsuhiko Ishibashi: Re-Examinations of Estimated Great Earthquake in Tokai Region - About the Great Earthquake in Suruga Bay -, Preprint of Autumnal Meeting, the Seismological Society of Japan, 1976.

11. The Outline of Road Works, Shizuoka Highway Works Office, Ministry of Construction, 1977.

12. Protective Treatments to the Izu-Ohshima Kinkai Earthquake, Numazu Construction Office, Ministry of construction, 1978.

13. Lists of Density of Cyanide from Jan 14 to Feb 5 in 1978.

14. Geometrical Plane of Stock Pile for Slime of Mochikoshi Mine in Houzuki Azawa Swamp.

15. Geometrical Plane of Sabo Works along Kano River.

16. Outline of Road and River Works, Numazu Construction Office, 1977 [12-16: provided by Numazu Construction Office, Chubu Regional Construction Bureau, Ministry of Construction].

17. The Izu-Oshima Kinkai Earthquake of 1978, and Damage, Feb 14, 1978.

18. Occurrence of Sensible Earthquakes in the Izu-Ohshima Kinkai Earthquake of 1978.

19. The Outline of Damage and Losses to the Izu-Ohshima Kinkai Earthquake of 1978, Feb 13, 1978.

20. Lists of Damage of Public Facilities Caused by the Izu-Ohshima Kinkai Earthquake of 1978, Feb 13, 1978.

21. Damage of Railroad of Izu-Kyuko Co. Ltd. Caused by the Izu-Ohshima Kinkai Earthquake of 1978.

22. Rehabilitation of Roads, Jan 15, 1978.

23. Traffic Control after the Izu-Ohshima Kinkai Earthquake of 1978, from Jan 14 to Jan 16.

24. Record of Reports of Air Reconnaissance.

25. Report on Enforcement of the Traffic Control Based on the Disaster Countermeasures Basic Law.

26. Dangerous Zones for Landslide and Slope Failure.

27. Manuals for the Headquarters of Countermeasures Against Disasters of Shizuroka Prefecture.

28. Map of Jurisdiction of Shizuoka Prefectural Government.

29. A Guide to Earthquakes
[17-29: provided by Main Office of Shizuoka Prefectural Government].

30. Record of the Izu-Ohshima Kinkai Earthquake of 1978.

31. Information Transfer Systems for Earthquake Prediction Information in the Shimoda Branch 1977.

32. Manuals of the Shimoda Branch for Countermeasures against Disasters.

33. Manuals in Details for Generalizing Corps in Shimoda Branch.

34. Refuge and Inducement of Tourists from Jan 14 to Jan 15.

35. The Activity of the Fire-brigade
[30-35: provided by Shimoda Tax Office, Shizuoka Prefecture].

36. Lists of Damage Caused by Disasters in Fiscal Year of 1974.

37. Information File of Roads.

38. Disposition Systems for Disasters in Emergency.

39. Designated Dangerous Zone for Landslide and Slope Failure.

40. Tidal Wave Investigation on the Ansei Earthquake of Nov 4, 1860.

41. Map of Jurisdiction of Shimoda Construction, Shizuoka Prefecture.

42. The Izu-Ohshima Kinkai Earthquake of Jan 14, 1978 and Distribution Maps of Public Works Damaged, Prefectural Works and Municipal Works
[35-41: provided by Shimoda Construction Office, Shizuoka Prefecture].

43. Report of Earthquake Damage and Losses (Jan 31, 1978).

44. Distribution of Damage in Shimoda Town.

45. Lists of Rehabilitation of Public Facilities.

46. Emergency Disposition System.

47. Great Tidal Wave of the Ansei Earthquake of 1860.

48. Earthquake Disaster Mitigation Program of Shimoda City 1977: Ordinance of Regional Disaster Prevention Conference and its References.

49. Public Information on Tidal Waves, Oct 20, 1977.

50. Explanatory Data on Budget of Municipal Gov. of Shimoda City Jan 20, 1978
[43-50: provided by City Office of Shrimoda].

51. Outline of Water Services Managed by Amagi-Yugashima Town.

52. Map of Jurisdiction of the Amagi-Yugashima Town
[51-52: provided by Amagi-Yugashima Municipal Office].

53. Outline of Damage and Losses caused by the Izu-Ohshima Kinkai Earthquake of 1978, Feb 4, 1978.

54. Manuals of Headquarters for Countermeasures against Disasters of Kawazu Town.

55. Outline of Kawazu Town, 1976
[53-55: provided by Municipal Office of Kawazu Town].

56. Earthquake Frequency of Fore-shocks and After-shocks, Jan 30, 1978.

57. Estimated Losses on the Izu-Ohshima Kinkai Earthquake of 1978, Jan 15, 1978.

58. Manuals of Headquarters for Countermeasures against Disasters of Higashi-Izu Town.

59. Outline of Higashi-Izu Town, 1977
[56-59: provided by Municipal Office of Higashi-Izu Town].

60. Distribution of Damage along Higashi-Izu Toll Road, Administration Office of Higashi-Izu Toll Road, Japan Highway Public Corporation.

61. Damage and Rehabilitation Caused by the Izu-Ohshima Kinkai Earthquake of 1978, Feb 2, 1978.

62. Outline of Izu-Kyuko Co. Ltd.
[61-62: provided by Izu-Kyuko Co. Ltd].

63. Damage of Electric Power Facilities caused by the Izu-Ohshima Kinkai Earthquake of 1978
[63: provided by Tokyo Electric Power Co. Ltd.].

Questionnaire Used in Interviews with the Personnel of Administrative Organizations

1. Outline of the Damage
2. Organization Response of the Administration
3. Damage of Urban and Housing Facilities
4. Damage of Hydraulic Facilities
5. Damage and Rehabilitation of Lifeline System

    a. Highway
    b. Railroad
    c. Electric Power
    d. Telecommunication
    e. Water Quality
    f. Water Supply
    g. Fuel

6. Financial Aids, Loans and Tax Exemptions
7. Losses Valued in Money
8. Other Related Comments

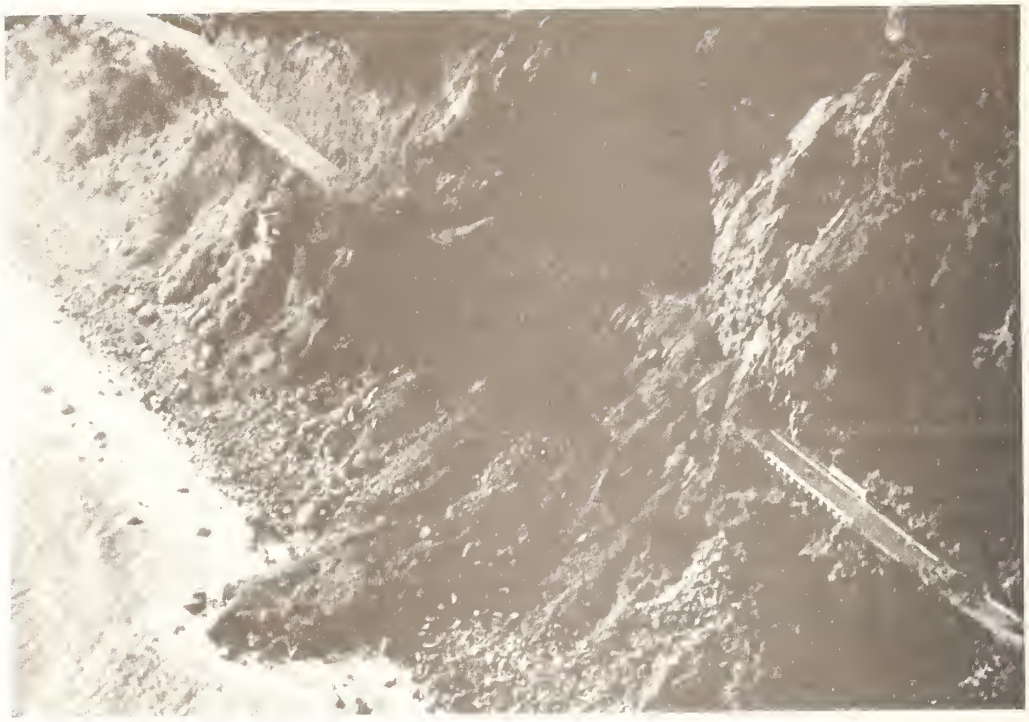

Photo 1. Failure of Ex-national Highway Route 135 Caused by a Landslide in Higashi-izu Town

Photo 2. Sludge Removal from the Mochikoshi River

Photo 3. Flowing Out of Sludge Caused by the Failure of Dykes of its Reservoir

Photo 4. Temporary Countermeasures to Prevent Rock Fall in Shimoda City

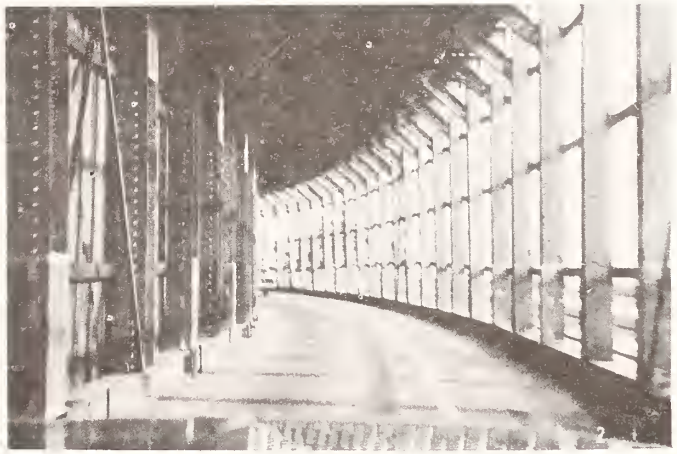

Photo 5. Temporary Structure to Prevent Rock Fall on the Higashi-izu Toll Road

Photo 6. Residensial Damage in Shimoda City

Table 1-1. Weather Condition before and after the Main Shock

(after Shimoda Municipal Government)

Date	Weather	Temperature in atmosphere (Centidegree)			Rain fall mm/day
		Max.	Min.	Mean	
Jan. 1	◎	20.5	14.0	15.1	1.0
2	◎ ①	14.5	11.0	9.8	4.0
3	● ①	12.0	7.0	7.3	8.5
4	①	12.5	5.5	7.5	0
5	①	11.0	5.5	7.3	0
6	①	13.5	6.5	9.8	0
7	①	15.5	5.5	9.5	0
8	● ①	13.5	7.0	9.2	1.0
9	①	14.5	6.0	10.3	0
10	①	10.5	2.0	5.9	0
11	①	13.5	2.0	6.5	0
12	①	15.5	7.0	10.3	0
13	①	13.5	7.0	9.2	6.0
14	●	14.5	9.0	9.3	7.5
15	①	17.5	7.0	12.3	1.0
16	◎	14.5	6.0	8.8	0
17	①	9.5	6.0	6.9	0
18	●	13.0	6.0	6.8	1.0
19	①	12.0	8.0	7.8	0
20	①	13.0	3.0	7.1	0
21	①	13.0	5.5	7.1	4.0
22	①	9.5	2.0	4.5	0
23	①	12.0	0	5.1	0
24	◎	12.5	1.8	6.8	7.0
25	①	11.0	2.0	5.9	0
26	◎ ●	12.5	4.0	6.8	5.5
27	①	15.0	6.0	9.8	0.5
28	◎	12.5	6.0	9.3	1.0
29	◎	8.0	4.0	4.9	0
30	● ①	11.5	2.0	5.8	2.5
31	①	10.0	3.0	5.4	0
–	–	–	–	Average 8.0°C	Total 50.5 mm

Note: Weather: ① fine. ◎ cloud, ● rainy

Table 1–2. Damage and Losses
(as of Feb. 15, 1978, Shizuoka Prefecture)

Classification	Evaluated Loss (in 1,000 yen)	Note
Direct Damage	38,709,501	
Buildings and Houses	5,838,400	
Agriculture and Fishery	6,892,490	
Facility for Education	494,838	
Facility for Welfare and Sanitary	972,783	
Industrial Facility	8,407,582	
Public Works	14,375,408	
Facility for Electricity	228,000	Not Official
Railroad	1,500,000	Not Official
Indirect Damage	Unidentified	Delay of Resumption, etc.
Total	38,709,501	

33

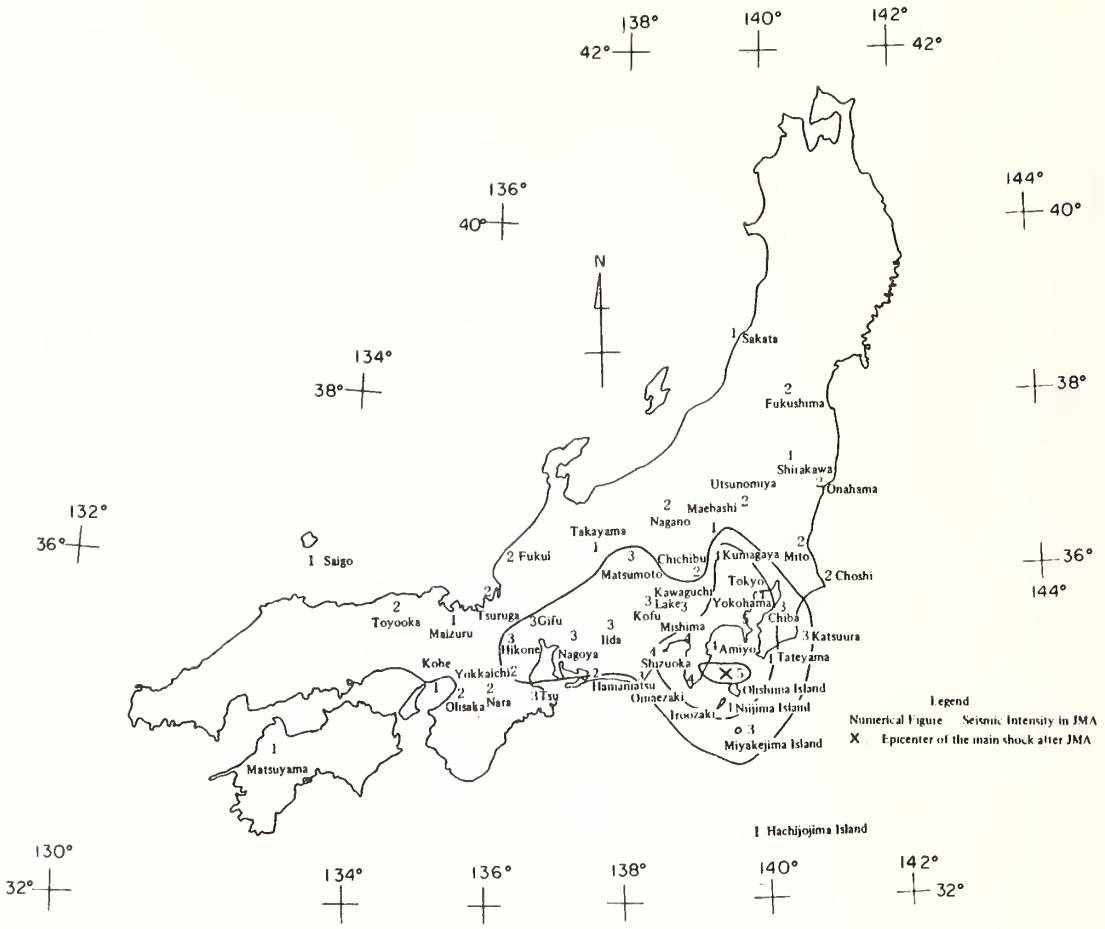

Fig. 1–1 Intensity Distribution Map of the Izu-Ohshima Kinkai Earthquake of 1978

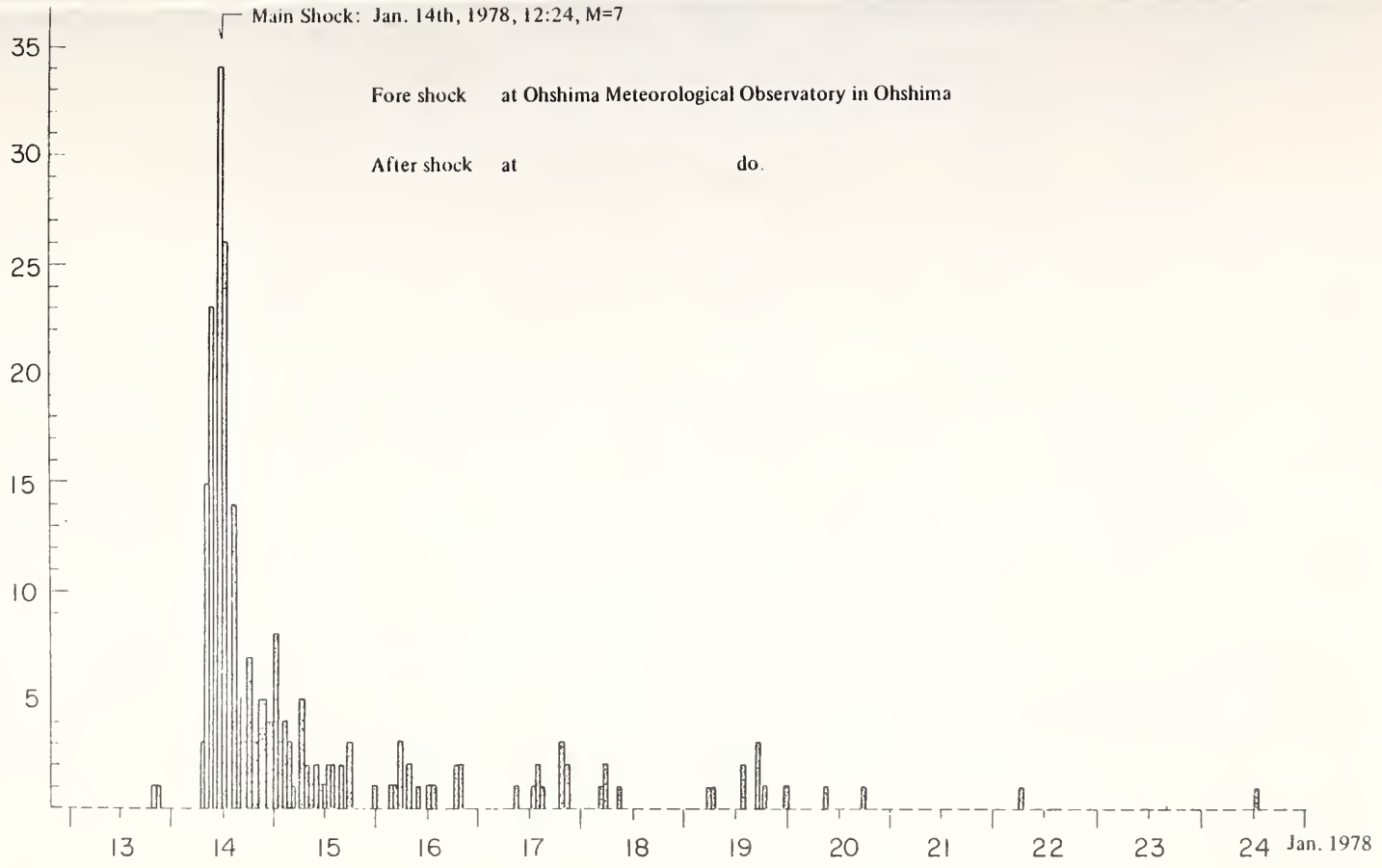

Fig. 1-2 Fore and After Shocks

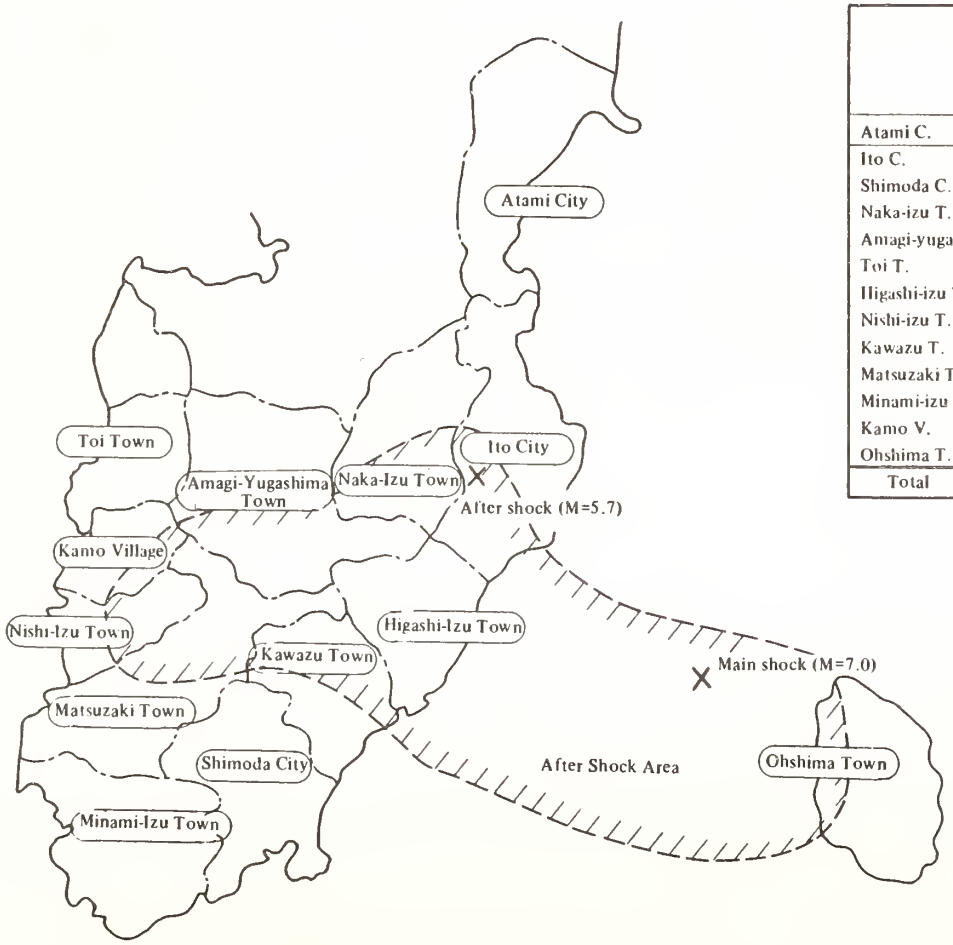

	Loss of Lives		Damage of Dewelling Houses		Affected Households and Sufferers	
	Dead	Injured	Totally Razed	Half Razed	Affected House-holds	Sufferers
Atami C.	0	0	0	0	0	0
Ito C.	0	4	1	4	3	13
Shimoda C.	0	51	12	24	41	131
Naka-izu T.	0	0	0	0	0	0
Amagi-yugashima T.	5	8	0	0	0	0
Toi T.	0	0	0	0	0	0
Higashi-izu T.	9	109	49	381	440	1,807
Nishi-izu T.	0	2	7	34	41	128
Kawazu T.	11	28	16	56	72	313
Matsuzaki T.	0	2	4	11	15	55
Minami-izu T.	0	1	0	0	0	0
Kamo V.	0	0	0	27	27	108
Ohshima T.	0	0	0	0	214	677
Total	25	205	89	537	853	3,232

Fig. 1–3 Distribution Map of the Earthquake Damage

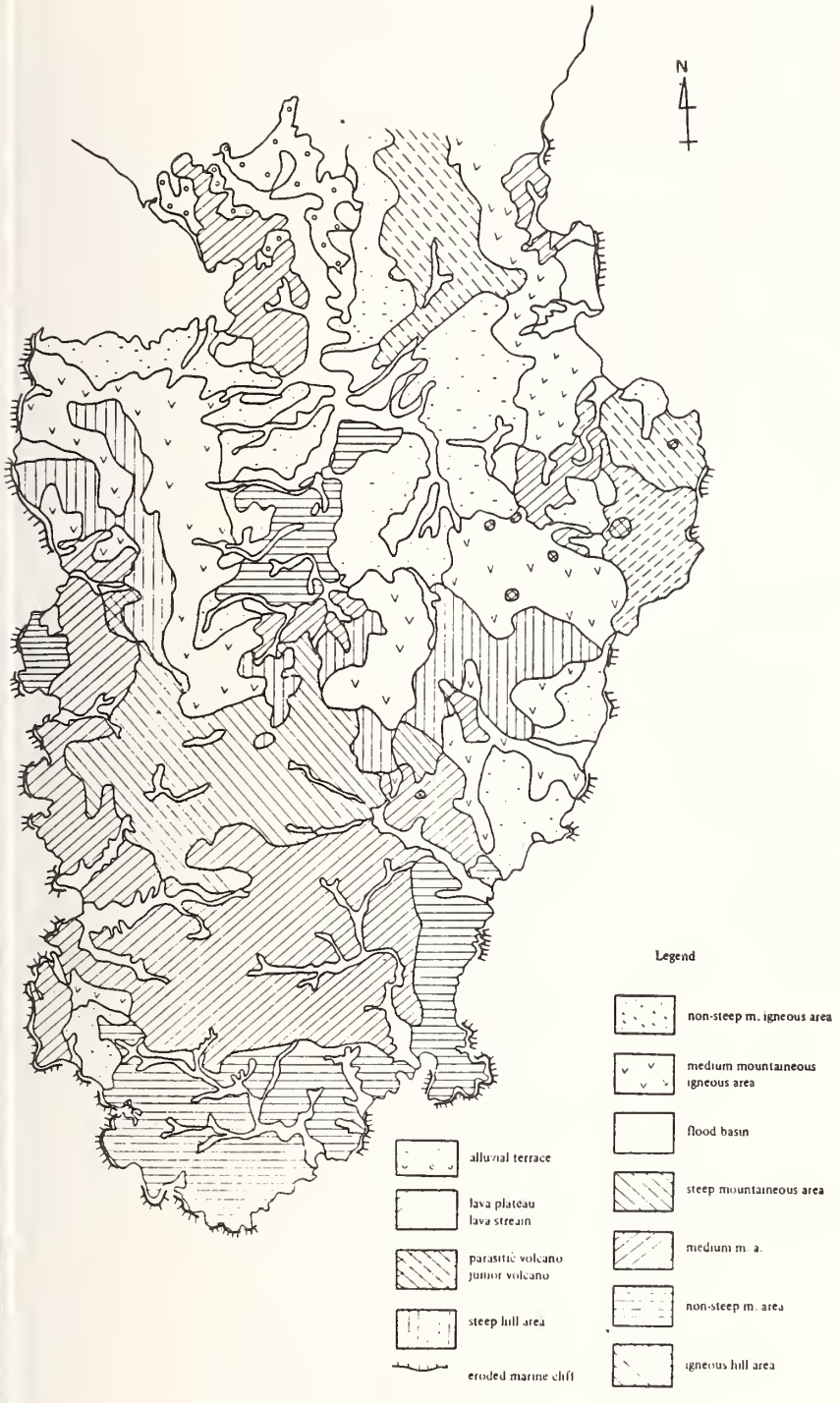

Fig. 1–4 Geographical Feature of Izu Peninsula

33

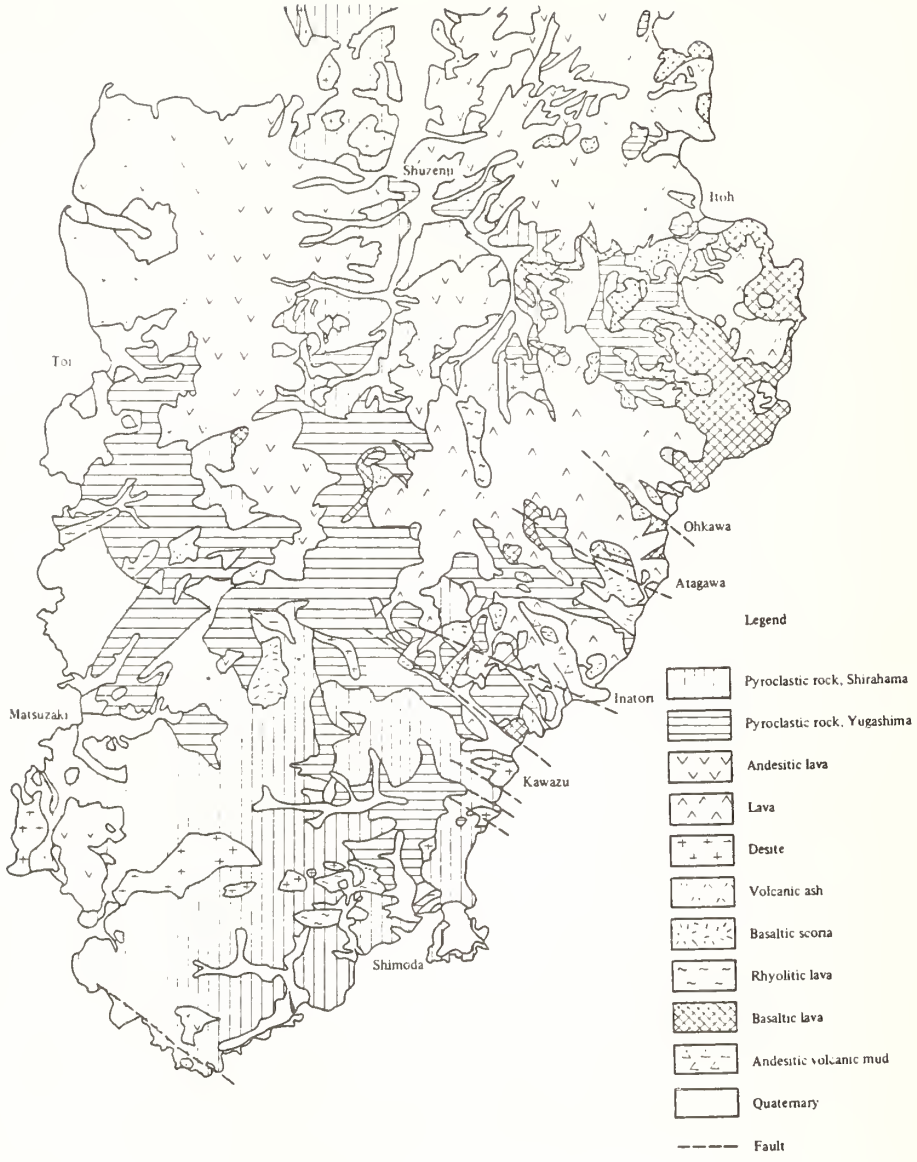

Fig. 1–5 Subsurface Geology of Izu Peninsula

(Damaged buildings and houses in Shizuoka Pref.)

Classification		Location	Higashiizu T.	Amagiyugashima T.	Kawazu T.	Shimoda C.	Nishiizu T.	Matsuzaki T.	Toi T.	Ito C.	Minamiizu T.	Kamo V.	Atami C.	Nakaizu T.	Total
Dwelling	Totally Razed House	House	49		16	12	7	4		1					89
		Family	49		16	16	7	4		1					93
		Sufferer	180		77	44	23	14		1					339
	Half Razed House	House	381		56	24	34	11		4		27			537
		Family	391		56	25	34	11		2		27			546
		Sufferer	1,627		236	87	105	41		12		108			2,216
	Partially Destroyed House	House	1,739	124	879	77	208	195	100	304	29	114	1	21	3,791
		Family	1,760	124	879	81	252	194	100	306	29	114	1	20	3,860
		Sufferer	7,001	500	3,581	291	959	701	400	1,166	119	392	4	84	15,198
Non-dwelling	Public Building	House	6	2		12	2	1				1			24
	Others	House	145		78	57	120	9	60	45		20			534

(Losses of Three Municipalities, Severely Damaged)

Classification \ Location	Higashi-izu T.	Kawazu T.	Shimoda C.	Total
Dwelling	3,720,600	1,087,300	155,100	4,963,000
Non-dwelling	357,800	475,000	22,600	855,400
Total	4,078,400	1,562,300	177,700	5,818,400

Table 2–2. Damage and Losses in Agriculture and Fishery

Classification	Number of Damage	Loss in thousand yen	Note
Agriculture	20.8 ha, 1,706	4,969,518	Crops, Agricultural land, Facility for agriculture
Forestry	19.9 ha, 101	1,623,972	Forest, Facility for forestry
Fishery	49	299,000	Facility for fishing port
Total	40.7 ha, 1,856	6,892,490	

Table 2–3. Damage and Losses in Facilities for Educations

Classification	Number of Damage	Loss in thousand yen
Kinder Garten	12	24,972
Primary School	22	136,603
Junior High School	13	107,355
Senior High School	11	201,250
Hutte	1	1,030
Public Hall	5	1,918
Gymnastic Facility	1	10,000
Cultural Estate	5	11,610
Library	1	100
Total	71	494,838

Table 2–4. Damage and Losses in Facilities for Welfare and Sanitary

Classification	Number of Damage	Loss in thousand yen
Hospital	61	523,288
Water Supply Services		327,747
Solid Waste Disposal Plant	2	20,885
Hospital for Epidemic	1	200
Others	54	100,663
Total	–	972,783

Table 2–5. Damage and Losses in Industries

Classification	Number of Damage	Loss in thousand yen
Commercial	1,699	2,566,697
Mining and Industry	474	558,773
Tourism and Service	1,053	5,282,112
Total	3,226	8,407,582

Table 2–6. Damage and Losses in Roads

Classification	Number of Damage	Loss in thousand yen
Shizuoka Prefectural Government	283	10,632,771
Shimoda City	31	42,037
Kawazu Town	269	1,165,990
Higashi-izu Town	123	234,000
Prefectural Highway Public Corporation	16	102,000
J.H.P.C.	31	1,700,000
Total	753	13,876,798

Table 2–7 Water Pollution Due to Sodium Cyanide in Kano River

(in PPM)

	Mizunuki Bashi		Endo Bashi		Chitose Bashi		Kurose Bashi	
	Time	Density	Time	Density	Time	Density	Time	Density
Jan. 14					18:50	ND	18:15	ND
Jan. 15					9:45	1.34	9:50	ND
					10:30	ND	10:30	ND
					13:25	1.25	14:20	0.016
Jan. 16					9:40	0.19	10:25	0.13
					13:20	0.14	13:55	0.14
Jan. 17					9:35	ND	10:20	ND
					14:20	ND	15:10	ND
Jan. 18					10:25	153 ND	11:45	61 ND
					14:15	143 ND	15:10	78 ND
Jan. 19					10:30	97 ND	12:00	50 ND
					14:25	76 ND	15:00	56 ND
Jan. 20	8:00	2,230	8:00	153	9:45	100 ND	10:35	43 ND
					14:10	62 ND	14:50	41 ND
Jan. 25	8:00	615	8:00	89.3	9:30	30 ND	10:15	14 ND
					14:05	30 ND	14:40	14 ND
Jan. 30	8:00	666	8:00	46.7	10:00	20 ND	10:35	10 ND
					14:10	15 ND	14:45	13 ND
Feb. 4	9:00	325	9:00	21.0	9:20	22 ND	10:00	7 ND
					13:50	12 ND	14:30	10 ND

Note: upper, suspended solid (SS) lower, density of sodium cyanide (CN^{-1})
ND: not detected

Table 2–8 Damage and Losses in Izu-Kyuko Railroad Co. Ltd.

Number	Damage
1	Subsidence of rail, Inclination of poles
2	Rock fall (50 cm ~ 10 m)
3	Subsidence of rail
4	Subsidence of rail, Inclination of signal and poles
5	Peel off of tunnel lining
6	Subsidence of rail
7 a	Subsidence of rail and platform
7 b	〃
7 c	Inclination of signals
7 d	Subsidence of rail and platform, Inclination of poles
7 e	Subsidence of rail and platform
7 f	〃
7 g	〃
8	Deformation of tunnel lining
9	Subsidence of rail
10	Rock fall, Landslide, Subsidence of rail
11	Deformation of tunnel lining
12	Collapse of rock shed by landslide (10,000 m^3)
13	Collapse of retaining wall
14	Crack in wall
15	〃
16	Deformation of tunnel lining, Dislodgement of wall
17	Rock fall (16 m x 6 m x 5 m)
18	Rock fall, Disconnection of cables, Damage of poles
19	Landslide (70 m^3, 500 m^3)
20	〃 (50 m^3)
21	Dislodgement of abutment (80 mm)
22	〃 (60 mm)
23	Landslide (100 m^3)

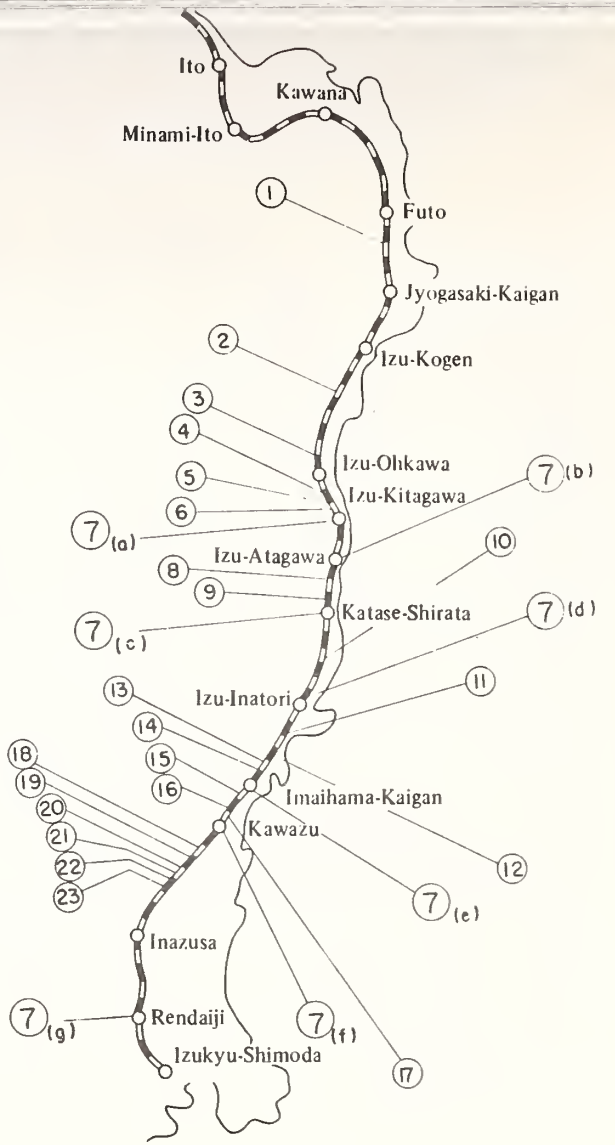

Table 2–9 Damage and Losses in Facilities for Electric Power

Classification	Number of Damage	Loss in thousand yen
Power Plant	2	
Transformer Station	2	
Water Channel	2	
Tower for Transmission Line	Several	
Total		228,000

Table 2-10 Indirect Losses

Classification	Indirect loss	Note
Agriculture		Decrease of agricultural product by damage of agricultural land and agricultural facilities
Industry		
Trade		Decrease of income by interruption of business
Industry		Decrease of product by interruption of work
Tourism		Decrease of income by interuption of work and decrease of tourist
Electric Power		Decrease of income by interruption of power supply
Railroad		Decrease of income by interruption of service

Table 2–11 Damage and Losses in Comparison between the Izu-Ohshima Kinkai Earthquake of 1978 and the Niigata Earthquake of 1964

Classification / Eq.	Direct Loss (bil. yen)	Indirect Loss (bil. yen)	Indirect/Direct
Izu Ohshima Kinkai	39		
Niigata	130	122	0.94

Fig. 2–1 Distribution Map of Damage to National Highways and Prefectural Roads

33

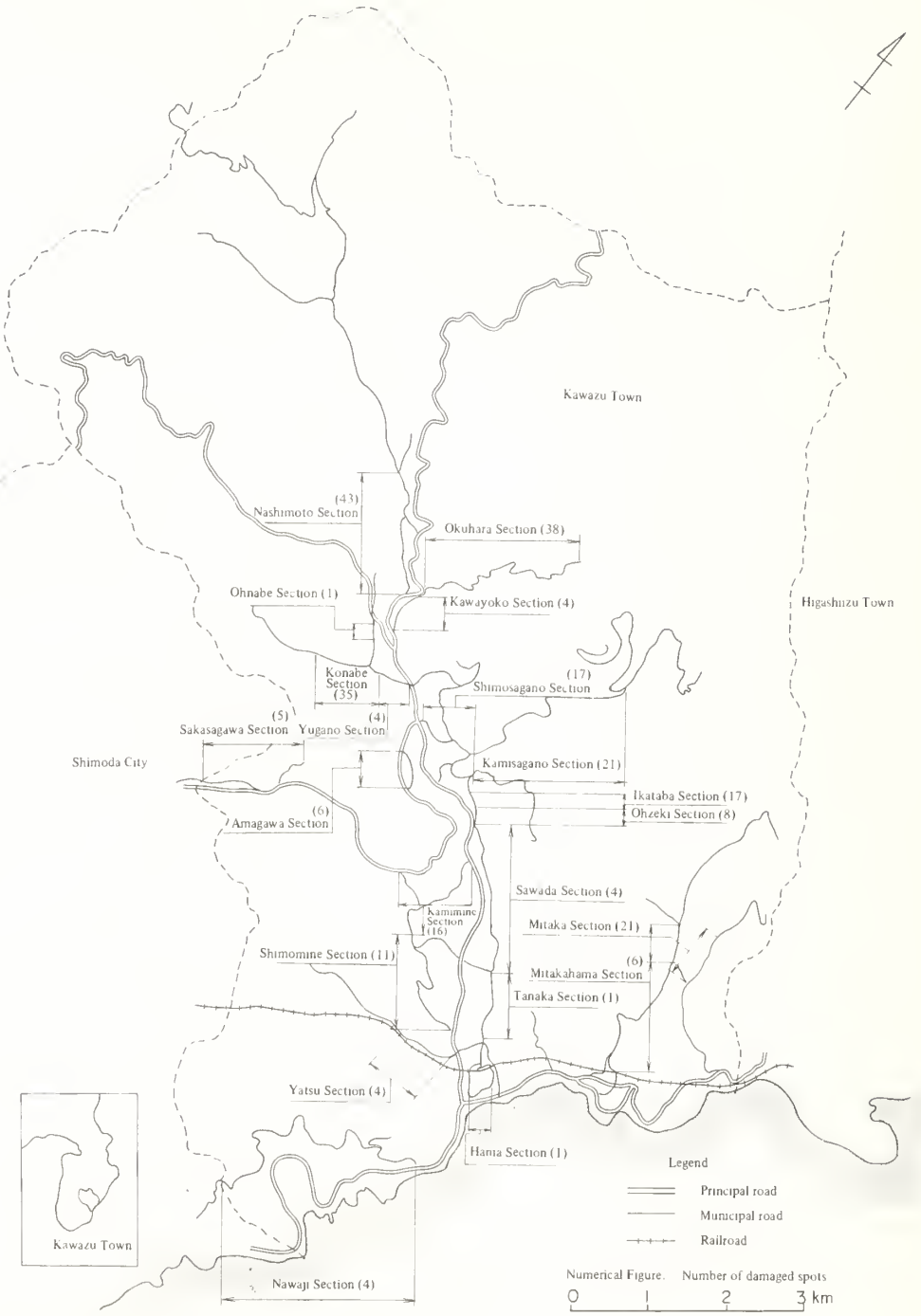

Fig. 2–2 Damage Distribution of Municipal Roads in Kawazu Town

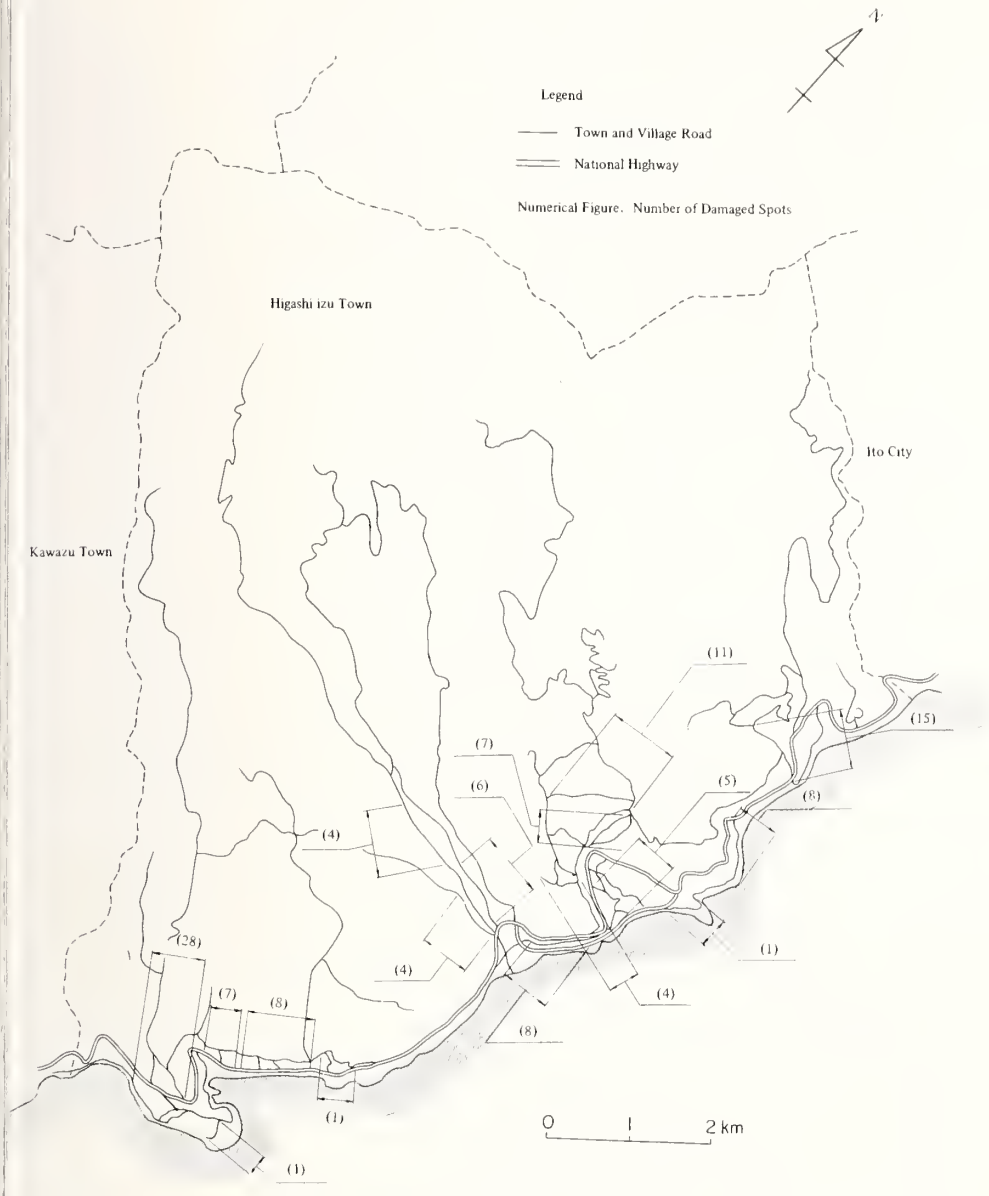

Fig. 2–3 Damage Distribution of Municipal Roads in Higashi-izu Town

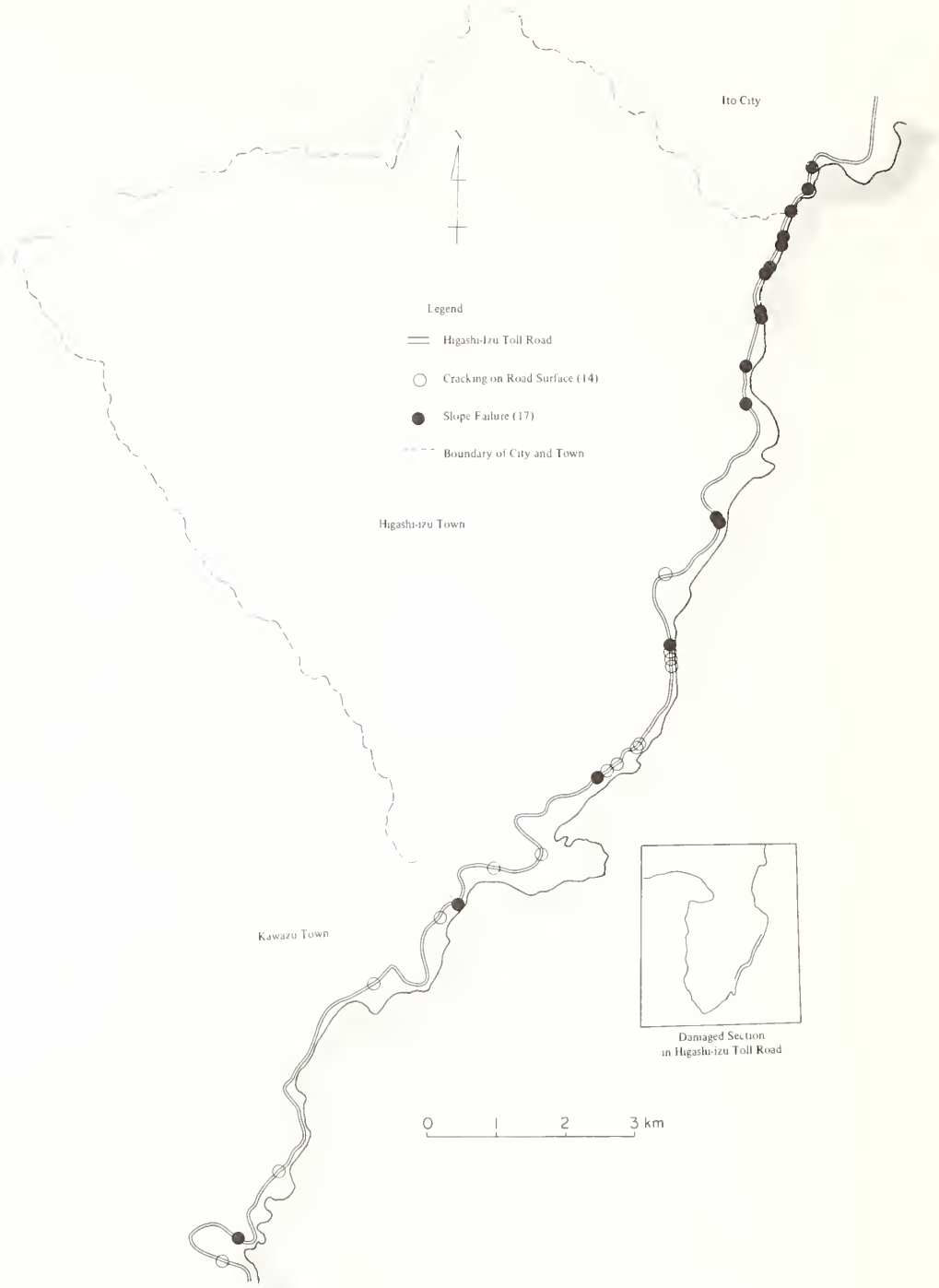

Fig. 2–4 Damage Distribution of the Higashi-izu Toll Road

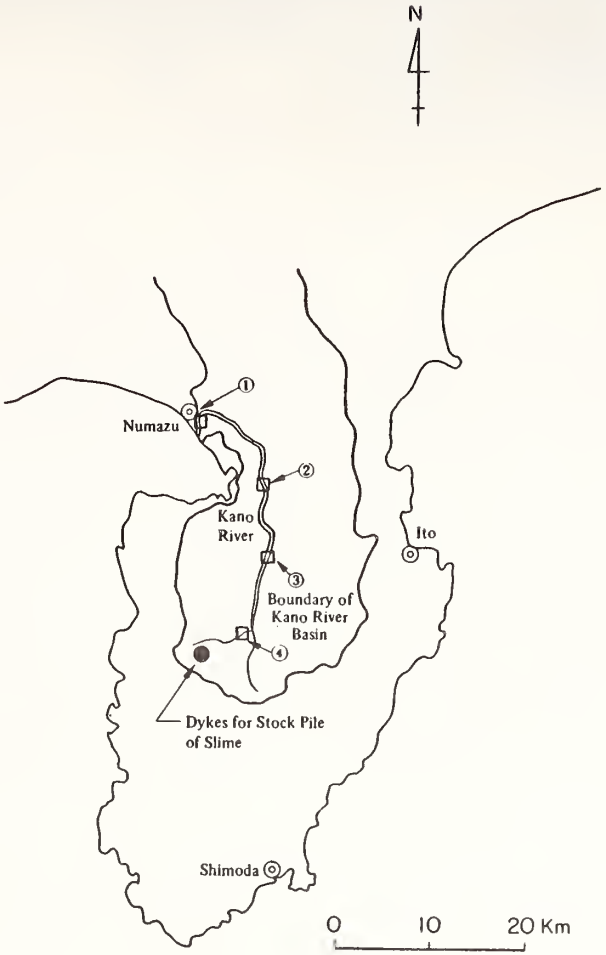

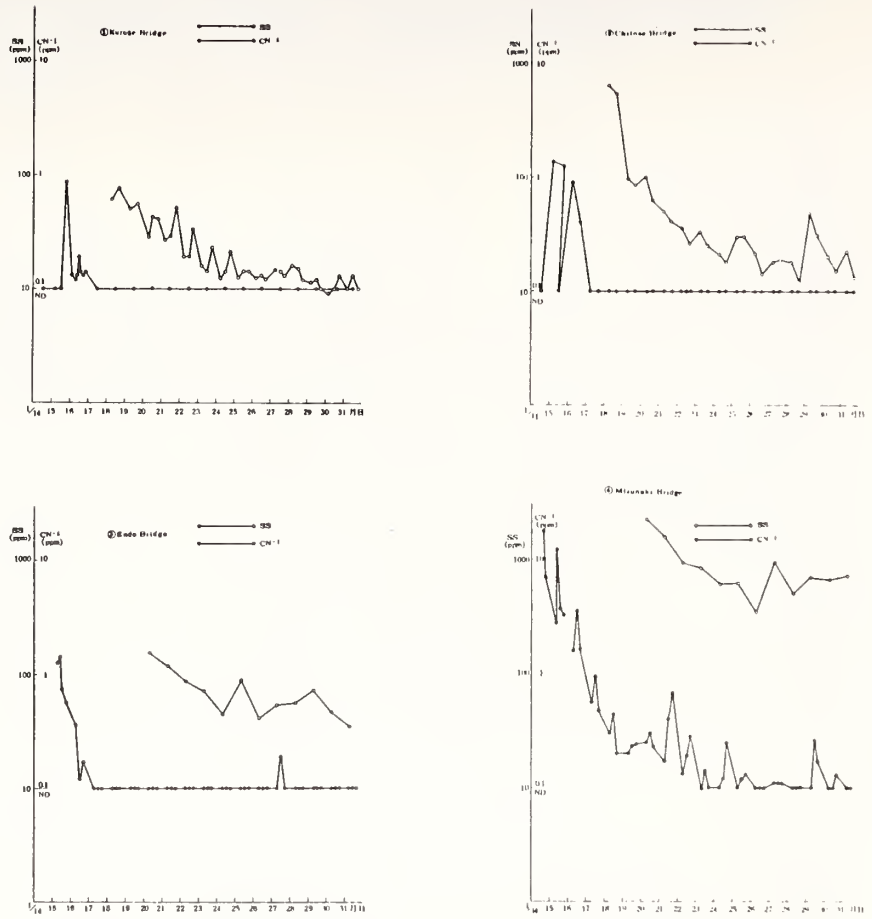

Fig. 2–5 Water Pollution due to Sodium Cyanide in Kano River

Table 3–1 Established Date of Rescue and Rehabilitation Center in each Administration

Administration	Established Date of Rescue and Rehabilitation Center
Shizuoka Prefectural Government Office	January 14, 14 : 10
Shimoda Office, do	January 14, 14 : 10
Kawazu Office, do	January 17,
Higashi-izu Town Office	January 14, 13 : 10
Matsuzaki Town Office	January 14, 12 : 45
Kawazu Town Office	January 14, 14 : 10
Shimoda City Office	January 14, 14 : 50

Table 3–2 Dispatched Self Defense Forces to Damaged Area

Destination	Ground, Maritime, Air	Period	Man-days	Vehicle-days
National Highway Route 136 (Restoration of the Highway)	Ground	Jan.14	680	Tractor Shovel (2) Bulldozer (7) Dump Truck (3) Power Shovel (7)
Amagi-yugashima Town (Restoration of the Highway)	Ground	Jan.18~22	743	(49)
Mitakairiya, Kawazu Town (Searching the Missings)	Ground	Jan.15~29	11,364	Tractor Shovel (10) Trailer (18) Bulldozer (77) Bulldozer for Soft Ground (48) Dump Truck (23) Power Shovel (93) Wrecker (40) Drugshovel (131) Others (535) Oil Pressure Shovel (2) Drain Pump Fire Engine
Nashimoto, Kawazu Town Onabe, Kawazu Town (Rescue for the Bus Accident)	Ground	Jan.15~17	2,344	Wrecker (6) Water Trailer (39) Food Supply Car (21) Ambulance Others (416)
Yugano, Kawazu Town	Ground	Jan.18	50	Dump Truck (3) Power Shovel (2) Others (1)
Numanokawa, Kawazu Town (Watching the Waterlevel of a Stream)	Ground	Jan.20~21	40	Chain Saw Others (4)
Kawazu Town (Water Supply)	Ground	Jan.18~22	139	Water Wagon (22) Filtration Equipment
Kawazu Town (Information Exchange)	Ground	Jan.26~29	490	Aircraft (5)
Mochikoshi, Amagi-yugashima Town (Rehabilitation of the Dyke)	Ground	Jan.15~18	305	Helicopter (60) Bulldozer (8) Trailer (6) Power Shovel (4) Dump Truck (8) Others (14)
Naramoto, Higashi-izu Town (Restoration of the Highway Rescue at a Destroyed Hotel)	Ground	Jan.15~19	1,078	Power Shovel (13) Bulldozer (40) Wrecker (9) Tracter Shovel (4) Dump Truck (64) Air Compressor (9)
Inatori-ko, Higashi-izu Town (Water Supply)	Maritime	Jan.14~24	2,349	Guardboat (4) Troopship (13) Special Ship (2)
Izu Territory (Transportation, Survey)	Air	Jan.14~15	8	Aircraft (2)

Table 3–3 Fire Self Defense Squad Performance

	Jan. 14		Jan. 15		Jan. 16		Jan. 17	
	Persons	Performance	Persons	Performance	Persons	Performance	Persons	Performance
Shimoda C.	530	Dissemination of Tsunami Alarm Survey of Damaged Area	184	Rehabilitation	20	Rehabilitation		
Higashi-izu T.	480	Rescue at Takami Hotel Dormitory Rescue at Landslide Site of Higashi-izu Toll Road Rehabilitation Rescue at the Collapsed Building	480	Rehabilitation Water Supply	320	Rehabilitation Water supply	296	Rehabilitation Soil Removal from Road Repair Water Pipe Investigation of Drinking Water
Kawazu T.	330	Rescue at Landslide Site	392	Rescue at Landslide Site	330	Rescue at Landslide Site Rehabilitation	184	Rescue at Landslide Site
Minami-izu T.	200	Dissemination of Tsunami Alarm Watching Tidal Level	45	Reinforcement to Kawazu T.	45	Reinforcement to Kawazu T.	15	Reinforcement to Kawazu T.
Matsuzaki T.	360	Survey of Damaged Area Rehabilitation	360	Survey of Damaged Area Rehabilitation	10	Survey of Damaged Area Rehabilitation		
Nishi izu T.			81	Clearing Up the Damaged Area				
Kamo V.			60	Survey of Damaged Area Investigation of Dangerous Site				
Total	1,900		1,602		725		495	

(Table 3–3 continued)

Jan. 18		Jan. 19		Jan. 20		Jan. 21	
Persons	Performance	Persons	Performance	Persons	Performance	Persons	Performance
5	Dissemination of Recommendation of Refuge						
270	Traffic Control Soil Removal from Road Assistance for the Removal of Evacuees Investigation of Drinking Water	38	Water Supply	38	Water Supply	57	Water Supply Rehabilitation Patrol
68	Rescue at Landslide Site	83	Rescue at Landslide Site	90	Rescue at Landslide Site	109	Rescue Draining
16	Patrol						
359				128		166	

Table 3 4 Man-days Persued for Rescue and Rehabilitation of Organizations

Organization \ Item		Period	Man-days	Vehicle-days
Police		Jan. 14	11,551	2,341
Fire Defense	Fire Fighting Squal	Jan. 14 ~ Jan. 30	8,069	—
	Local Public Official	Jan. 14 ~ Jan. 20	471	—
Self Defense Forces	Ground	Jan. 14 ~ Jan. 30	23,065	4,268
	Maritime	Jan. 14 ~ Jan. 24	2,315	23
	Air	Jan. 14 ~ Jan. 15	8	2
Maritime Safety Division		Jan. 15	—	2
JTTPC		Jan. 14 ~ Jan. 18	1,180	303
Tokyo Electric Power Co.		Jan. 14 ~ Jan. 23	2,164	644
LPG Association		Jan. 14 ~ Jan. 23	381	106
Shizuoka Gas Co.		Jan. 14 ~ Jan. 24	388	127
Total			49,592	Vehicles 7,789 Ships 25 Aircrafts 2

Table 3–5 Recommendations of Refuge

Municipality	District	Issued Date of Recommendation	Reason
Matsuzaki Town	Uchino	19:30, Jan. 17	Possibility of landslide
Matsuzaki Town	Ikeshiro	19:30, Jan. 17	Possibility of landslide
Shimoda City	Takeyama in Kakizaki	15:00, Jan. 18	Possibility of rock fall

33

Table 3 - 6 Number of Evacuees

Municipality	District	Refuge Place	Number of Evacuees	Refuged Date	Returning Home Date	Cause of Evacuation
Kawazu Town	Mitakairiya	Acquaintance House Apartment House	48	Jan.16, 10:00	Each evacuee returned home by his judgement	Possibility of Landslide
	Mitakahama	Same as above	94	Jan.16, 17:00		Possibility of Rock Fall
	Nashimoto	Same as above	80	Jan.18, 16:00		Possibility of Landslide
	Nawaji	Same as above	1			Possibility of Landslide
	Total		223			
Higashi-izu Town	Kitagawa	Public Hall	8	Jan.14, 12:50		Possibility of Landslide
	Tamachi-ohata	Acquaintance House	53	Jan.21, PM		Possibility of Overturning of a Hotel Building
	Inatori	Hotel	48	Jan.21, PM		
	Total		109			
Amagi-yugashima Town	Kayano	Acquaintance House	7	Jan.14, 16:00		Possibility of Landslide
	Total		7			
Grand Total			339			

Table 3--7 Rehabilitation of Water Supply Facilities

Area	Supplying Population	Capacity	Restored Date	Emergency Measures
Shimoda City Water Supply	29,982	Ochiai 25,000 m^3/day Kawauchi 2,000 m^3/day	Jan. 17, 17:00	Water Wagon of 1.5 t (1)
Higashi-izu Town Water Supply	14,498	Shirata River 20,000 m^3/day	Jan. 24, 17:00	Water Boat (2), SDF Water Wagon (22)
Kawazu Town Water Supply	6,302	Ozeki Mine Sasahara 11,500 m^3/day Mitakairiya 500 m^3/day	Jan. 20, 14:00	Water Wagon (7)
Minami-izu Town Water Supply	5,662	Ishii 5,159 m^3/day	Jan. 14, 20:00	
Higashi-izu Town Okawa Areal Water Supply	1,095	225 m^3/day	Jan. 15, 15:00	
Kawazu Town Kami Areal Water Supply	1,768	360 m^3/day	Jan. 21, 15:00	Water Wagon (1)
Kawazu Town Onabe Areal Water Supply	245	60 m^3/day	Jan. 21, 12:00	Water Wagon (1)
Kawazu Town Kamisagano Areal Water Supply	279	70 m^3/day	Jan. 19, 15:00	Water Pool (1)
Kawazu Town Nashimoto Areal Water Supply	320	100 m^3/day	Jan. 26	Water Pool, 500 l (2)
Matsuzaki Town Water Supply	519	6,200 m^3/day	Jan. 17, 18:00	
Nishi-izu Town Water Supply	8,500	7,500 m^3/day	Jan. 18, 18:00	
Nishi-izu Town Shirakawa Areal Water Supply	160	60 m^3/day	Jan. 16, 18:00	
Nishi-izu Town Miyagahara Areal Water Supply	178	45 m^3/day	Jan. 17, 17:00	
Nishi-izu Town Yoshinohata Areal Water Supply	160	85 m^3/day	Jan. 16, 18:00	
Kamo Village Ukusu Areal Water Supply	1,760	635 m^3/day	Jan. 16, 15:00	
Kamo Village Arori Areal Water Supply	2,311	465 m^3/day	Jan. 17, 18:00	

Table 3–8 Restoration of Electric Power, Gas and Telephone Facilities

	Municipality	Number of Residents out of Services	Restoration
Electric Power	Shimoda City Kawazu Town Higashi-izu Town	15,000	Restored temporarily by Jan. 15, 19:15
LPG	Kawazu Town Higashi-izu Town	2,800 5,200	Inspected the overturned gas cylinder by Jan. 17
Gas Supply	Shimoda City	2,000	Inspected the gas pipes by Jan. 14
Telephone	Higashi-izu Town Kawazu Town Shimoda City Ito City Nishi-izu Town	160 140 30 30 70	Restored temporarily by Jan. 16 except Nashimoto, Kawazu Town by Jan. 25

Table 3–9 List of Traffic Control

Number	Route	Site	Traffic Control			
			Cause	Started Date	Rescinded Date for Emergency Vehicles	Retrieval
1	Route 135 (Ex-national Highway)	Akazawa, Ito City	Landslide Rock Fall	Jan. 14, 13:00		X
2	〃	Okawa, Higashi-izu Town	Landslide	Jan. 14, 13:00		X
3	〃	Atagawa, Higashi-izu Town	Landslide	Jan. 14, 13:00	Jan. 14, 19:00	
4	〃	Kurone, Higashi-izu Town	Landslide	Jan. 14, 13:00		X
5	〃	Kurone, Higashi-izu Town	Landslide	Jan. 14, 13:00		X
6	Route 136	Kami-funahara Amagi-yugashima Town	Landslide	Jan. 15, 8:00	Jan. 15, 9:40	Jan. 15, 17:00
7	〃	Yagisawa, Doi Town	Landslide	Jan. 15, 8:00	Jan. 15, 9:40	Jan. 16, 12:00
8	〃	Komine, Doi Town	Landslide	Jan. 15, 8:00	Jan. 15, 9:40	Jan. 16, 12:00
9	〃	Fukada, Kamo Village	Landslide Rock Fall	Jan. 15, 8:00		Jan. 16, 12:00

(Table 3–9 continued)

Number	Route	Site	Traffic Control			
			Cause	Started Date	Rescinded Data for Emergency Vehicles	Retrieval
10	P.P.R. Shuzenji-Shimoda	Yoichizaka, Amagi-yugashima Town	Rock Fall	Jan. 14, 13:00	Jan. 14, 15:00	X
11	〃	200 m far from Toll Gate	Landslide	Jan. 14, 13:00	Jan. 14, 15:00	
12	〃	more 200 m far from Toll Gate	Landslide	Jan. 14, 13:00		X
13	〃	Kawaaino, Kawazu Town	Landslide	Jan. 14, 13:00		X
14	P.P.R. Shimoda-Matsuzaki	Akebuse, Matsuzaki Town	Rock Fall	Jan. 14, 13:00	Jan. 14, 13:00	
15	〃	Yokokawa, Shimoda City	Rehabilitation Works	Jan. 16, 11:00		
16	P.P.R. Ito-Nishiizu	Miyagahara, Nishi-izu Town	Landslide	Jan. 14, 14:00		X
17	〃	Yaemeno, Nishi-izu Town	Landslide	Jan. 15, 8:00		X
18	〃	Mochikoshi, Nishi-izu Town	Landslide	Jan. 14, 13:00	Jan. 14, 13:00	X
19	〃	Kokushi-toge, Naka-izu Town	Landslide Rock Fall	Jan. 15, 9:30		Jan. 15, 14:25
20	P.R. Ito – Kawana–Yawatano	Futo, Ito City	Landslide Rock Fall	Jan. 14, 13:00		Jan. 14, 19:00 (One Lane)
21	P.R. Atagawa–Katase	Atagawa, Higashi-izu Town	Landslide	Jan. 14, 13:00		X
22	P.R. Yugashima –Matsuzaki	Onabe, Kawazu Town	Landslide	Jan. 15, 8:00		X
23	〃	Ikeshiro, Matsuzaki Town	Landslide	Jan. 15, 8:00		X
24	P.R. Shimodako	Benten-bridge, Shimoda City	Subsidence of Bridge	Jan. 14, 13:00		
25	P.P.R. Shuzenji-Shimoda	Sakagawa, Kawazu	Rehabilitation Works	Jan. 17, 9:00		X
26	Route 135 (Higashi-izu Toll Road)	Okawa, Higashi-izu Town	Slope Failure	Jan. 14, 13:00		
27	〃	Naramoto, Higashi-izu Town	Slope Failure	Jan. 14, 13:00		

P.P.R. : Principal Prefectural Road
P.R. : Prefectural Road

33

Fig. 3–1 Sequential Document before and after the Earthquake

Date	Earthquake phenomena	Countermeasures			
		Establishment of Disaster Rehabilitation Center	Relief and Rehabilitation	Reconstruction	Information
Jan. 13	20:38 III in JMA intensity				
Jan. 14	8:12, 9:06 } III in JMA intensity 9:30 ~ 12:06 40 earthquakes greater than I in JMA intensity in which III and VI took place six and four times respectively.	9:49 Ohshima T., Tokyo Metropolis			9:00 Ohshima Observatory issued the temporary announcement on the volcano 10:50 JMA issued the announcement on the earthquake
	12:24 mainshock 12:28 ~ 23:50 II, 38 times III, 11 times in Shimoda	12:45 Matsuzaki T. 13:10 Higashi-izu T. 14:10 Prefectural Government, Shimoda Office. Kawazu T.	14:02 Kawazu T. asked to the Prefectural Government for dispatching SDF Traffic was forbidden at route 135		12:31 Warning of tsunami by JMA 12:49 Announcement on the earthquake by JMA 13:35 Announcement on the tsunami by JMA 14:05 Announcement on the earthquake by JMA 14:15 JMA canceled the tsunami warning 14:20 Announcement on the tsunami by JMA 14:20 Numazu Construction Office received the information of the sludge outflow at Mochikoshi 14:35 Announcement on the earthquake by JMA

Date	Earthquake phenomena	Countermeasures			
		Establishment of Disaster Rehabilitation Center	Relief and Rehabilitation	Reconstruction	Information
		14:50 Shimoda C.	Five hundred tourists evacuated from Higashi-izu T. by ship		15:50 Temporary Announcement on the volcano by Ohshima Observatory
			16:00 Accounting Superintendent of Prefectural Government left to Kawazu		
			20:45 SDF arrived at Kawazu		22:20 Temporary Announcement on the volcano by Ohshima Observatory
Jan. 15	0:12 ~ 18:53 II, 15 times III, 10 times in Shimoda in which 5.7 of magnitude was the maximum	8:00 Nishi-izu T. Kamo V.	9:30 Investigation group of National and Prefectural government set off to the damaged area		
			19:15 Electric power supply in Higashi-izu and Kawazu T. was resumed	19:30 Disaster Relief Law was adopted to Higashi-izu and Kawazu T.	
Jan. 16	II, 5 times III, 3 times in Shimoda				

(Fig. 3-1 continued)

Date	Earthquake phenomena	Countermeasures			
		Establishment of Disaster Rehabilitation Center	Relief and Rehabilitation	Reconstruction	Information
Jan. 17	9:44 ~ 21:06 II, 4 times in Shimoda	8:00 Kawazu Office of Prefectural Government	Route 135 was resumed exclusively for the emergency vehicles		Exclusive circuit between Shimoda Construction Office and Shimoda Branch Office
			19:30 Residents evacuated in Matsuzaki T. because of the possibility of landslide		
Jan. 18	5:22 ~ 9:38 II, 2 times in Shimoda		11:40 Governmental investigation group came to the damaged area		13:30 Announcement on the aftershocks to Shimoda Branch Office
			15:00 Residents evacuated in Shimoda C. because of the possibility of rock fall		Slight panic was generated.
Jan. 19	17:45 III in Izu-Ohshima				
Jan. 20			Temporary dwellings were constructed in Kawazu T.		
Jan. 21			Works to prevent rock fall in Shimoda C. was completed		
Jan. 22			15:00 Evacuees in Shimoda C. returned home		

(Fig. 3-1 continued)

Date	Earthquake phenomena	Countermeasures			
		Establishment of Disaster Rehabilitation Center	Relief and Rehabilitation	Reconstruction	Information
Jan. 24			17:00 Water supply in Inatori, Kawazu T. was recovered		
Jan. 25			Facilities of JTTPC were recovered		
Jan. 26					Shimoda Branch Office reported the outline of the loss
Jan. 27					
Jan. 28				Explanation meeting on disaster relief loan of the Housing Loan Corporation in Kawazu T.	
Jan. 29			SDF withdrawed from Mitaka-iriya, Kawazu T.	Explanation meeting on disaster relief loan of the Housing Loan Corporation in Higashi-izu T.	
Jan. 30					
Jan. 31		Closed in Shimoda C., Amagi-yugashima T.	Resumption of the sections of Ito ~ Inatori and Kawazu ~ Shimoda of Izu-kyuko Railroad Co. Ltd.		

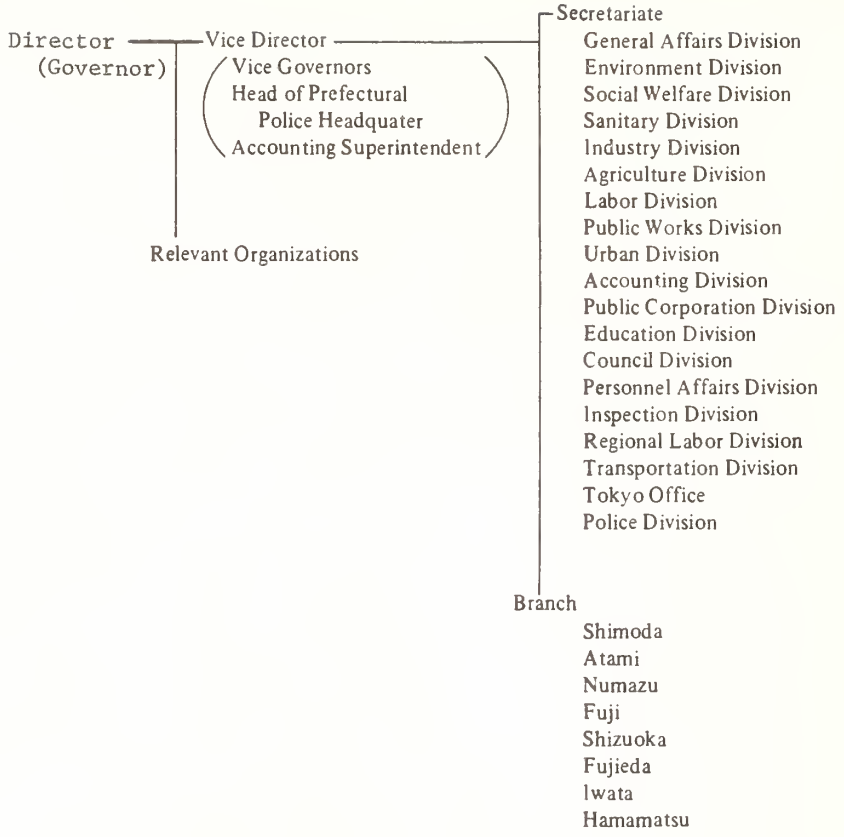

Fig. 3–2 Structure of Rescue and Rehabilitation Center of Shizuoka Prefectural Office

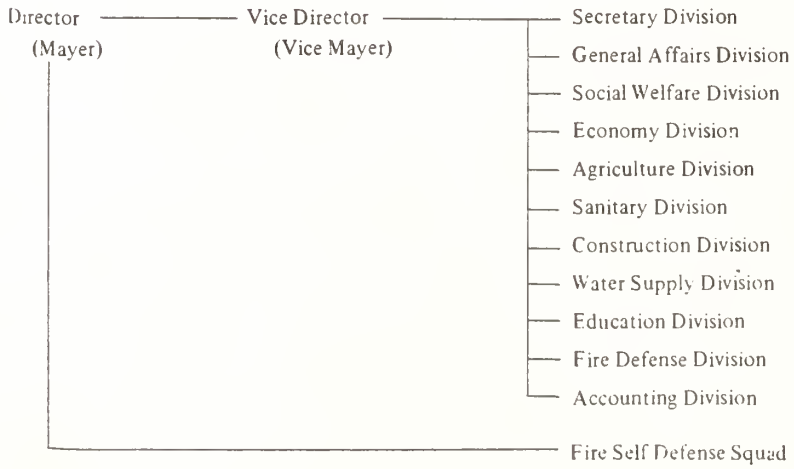

Fig. 3 3 Structure of Rescue and Rehabilitation of Shimoda City Office

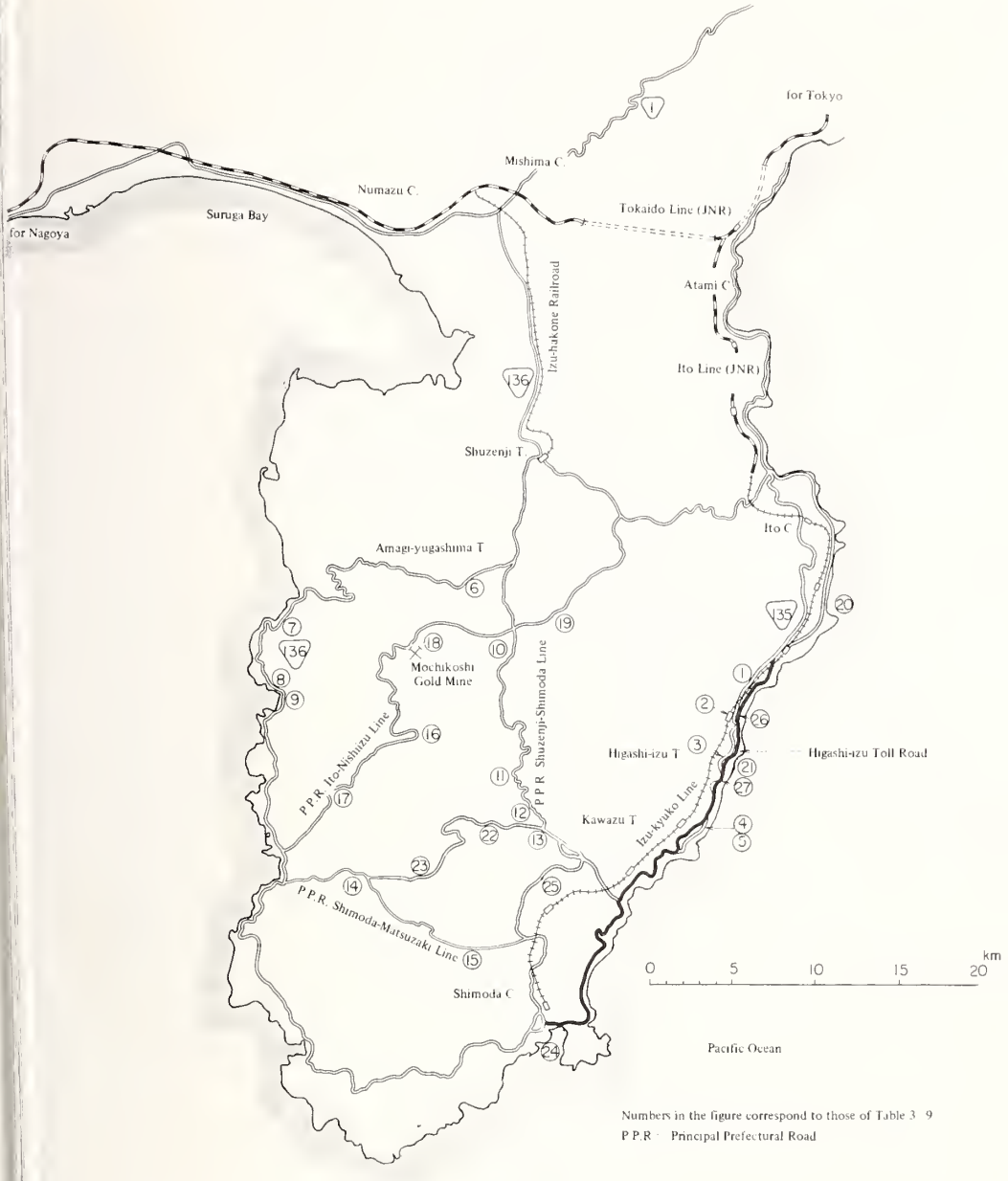

Fig. 3–4 Transportation Network in Izu Territory

Fig. 3–5 Route of 135th National Highway

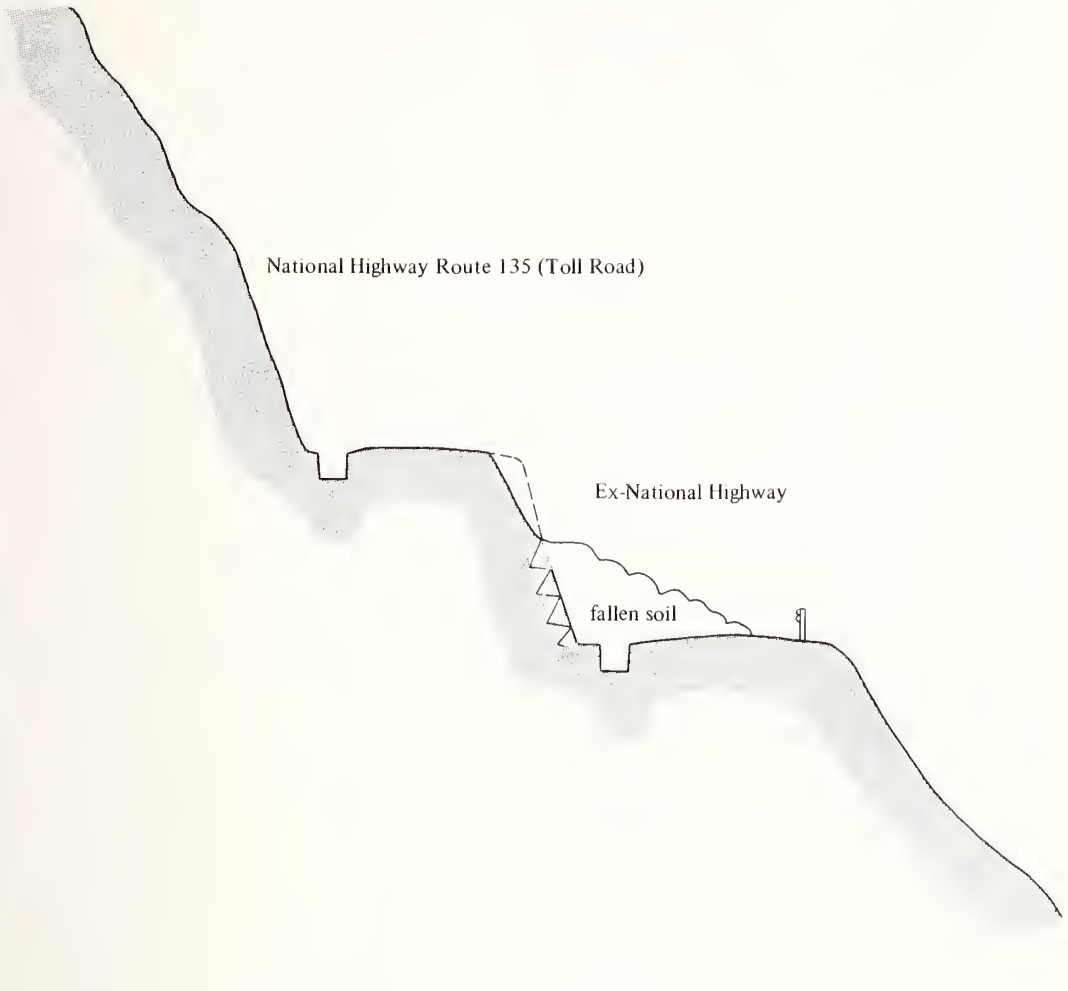

Fig. 3–6 Abstract of the Landslide at Route 135

Table 4－1 Budget of Rehabilitation Works of Public Civilengineering Facilities

(Budget : 1000 yen)

Construction Office of Prefectural Government	Administrator	River Works		Coastal Works		Sabo Works		Road Works		Bridge		Total	
		Sites	Budget	Sites	Budget	Sites	Budget	Sites	Budget	Sites	Budget	Sites	Budget
Shimoda	Prefecture	16	58,056			5	108,200	253	10,181,371	3	4,298	277	10,351,925
	Municipalities	35	186,905					442	1,480,998	4	35,080	481	1,702,983
Atami	Prefecture							5	36,750			5	36,750
	Municipalities							1	7,500			1	7,500
Numazu	Prefecture							25	414,650			25	414,650
	Municipalities							11	53,600			11	53,600
Total	Prefecture	16	58,056			5	108,200	283	10,632,771	3	4,298	307	10,803,325
	Municipalities	35	186,905					454	1,542,098	4	35,080	493	1,764,083
	Grand Total	51	244,961			5	108,200	737	12,174,869	7	39,378	800	12,567,408

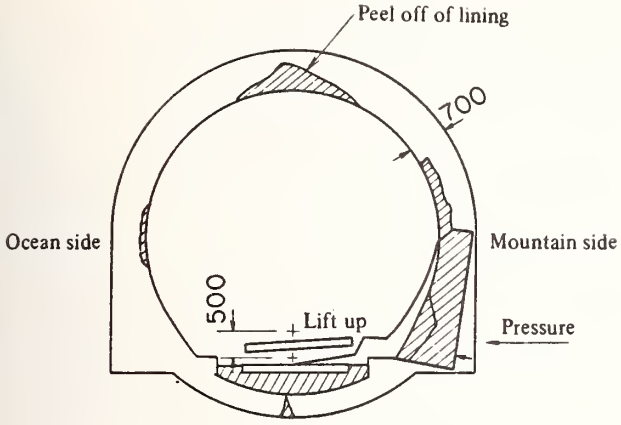

Fig. 4–1 Cross Section of Inatori Tunnel, Izu-kyuko Line

33

Table 5–1 Emergency Conveyance of Tourists by Ships (as of Jan. 14 and 15)

Departure Place	Ship Owner	Destination	Member of crew
Shimoda City	Self Defense Forces	Ito	227
	Tokai Shipping Co.	Atami	743
	Tokai Shipping Co.	Inatori	143
	Izukyu Shipping Co.	Inatori	121
	Total		1234
Higashi-izu Town	Izukyu Shipping Co.	Ito	300
	Self Defense Forces	Ito	70
	Tokai Shipping Co.	Atami	450
	Fishing Boat	Kitagawa ~ Yawatano	50
	Total		870
Matsuzaki Town	Izu-hakone Railroad Co.	Numazu	402
Nishi-izu Town	Izu-hakone Railroad Co.	Numazu	640
Grand Total			3146

Table 5–2 Tsunamis Having Affected Shimoda City

Date	Epicenter	Magnitude	Maximum Water Level Observed (m)		Dead	Houses Carried Away by Tsunami	Half-destroyed Houses	Flooded Houses	Sunk Ships
Feb. 3, 1605	Off Nankaido Off Boso Peninsula	7.9							
Dec. 31, 1703	Sagami Bay	8.2			27	332	160		81
Oct. 28, 1707	Tokaido, Nankaido	8.4	Shimoda	5.6	11	857	55		93
			Okakata	4.4					
			Kakizaki	6.7					
Dec. 23, 1854	Off Tokaido	8.4	Shimoda	5.7	122	841	30		about 30
Dec. 24, 1854	Off Nankaido	8.4	Okakata	4.8					
			Kakizaki	6.7					
Sept. 1, 1923	Sagami Bay	7.9	Kakizaki	4.6		2	9	334	
			Sotoura	4.1					
Dec. 7, 1944	Kumano-nada	8.3	Suzaki-Town	2.1				186	86
			Daiku Town	1.9					
			Kakizaki	2.5					
Dec. 21, 1946	Off Nankaido	8.1						245	26
Nov. 5, 1952	Off Kamchatka Peninsula	8.3	Shimoda	1.5				120	
May 24, 1960	Off Chile	8.3~8.5	Shimoda	1.14				38	

I. Historical Earthquake Records in Shizuoka Prefecture after Documents No. 19

Date and year	Epicenter	Magnitude
Nov. 29, 684 A.D.	Off Tokaido	Very large
July 4, 715	Totomi Area	6.4
818	Sagami Bay	7.9
July 30, 841	Izu Area	7.0
Aug. 22, 887	Nankaido Area	8.6
Oct. 29, 937	Izu Area	–
Dec. 11, 1096	Off Tokaido	8.4
1406	Suruga Area	–
Sep. 11, 1498	Off Tokaido	8.6
Sep. 10, 1510	Off Tokaido	–
March 21, 1589	Off Ohigawa Riv.	6.7
Feb. 4, 1605	Off Tokaido	7.9
Oct. 1626	Off Tokaido	–
March 1, 1633	Sagami Bay	7.1
Sep. 10, 1699		–
Dec. 31, 1703	Sagami Bay or off Boshyu	–
Jan. 2, 1704		8.2
Oct. 28, 1707	Tokaido or Nankaido Area	8.4
Sep. 18, 1711		–
Dec. 23, 1854 (Ansei-Tokai)	Off Tokaido	8.4
Dec. 24, 1891	Middle of Ohigawa Riv.	–
Sep. 1, 1923 (Kanto)	Off Odawara	7.9
Feb. 21 ~ May 17, 1930 (Swarm of Ito Ear.)	Off Ito	
Nov. 26, 1930 (Kitaizu)	North of Izu Peninsula	7.3
July 11, 1935 (Shizuoka)	Shizuoka City	6.7
Dec. 17, 1944 (Tonankai)	Gulf of Kumano	8.3
Apr. 20, 1965	Estuary of Ohigawa Riv.	6.1
May 9, 1974 (Izuhanto oki)	Off Izu Peninsula	6.9
Aug. 18, 1976 (Kawazu)	East of Izu Peninsula	5.4

33

II. Questionnaire Used in the Interviews to the Personnel of Administrative Organizations

1. Outline of the Damage
2. Organizational Response of the Administration
3. Damage of Urban and Housing Facilities
4. Damage of Hydraulic Facilities
5. Damage and Rehabilitation of Lifeline System
    a. Highway
    b. Railroad
    c. Electric Power
    d. Telecommunication
    e. Water Quality
    f. Water Supply
    g. Fuel
6. Financial Aids, Loans and Tax Exemptions
7. Losses Valued in Money
8. Other Related Comments

34

NATIONAL SCIENCE FOUNDATION ACTIVITY IN EARTHQUAKE HAZARD MITIGATION

Charles C. Thiel
J. Scalzi

National Science Foundation
Washington, D.C.

National Science Foundation Activity in
Earthquake Hazard Mitigation

This paper presents a brief review of grant ac tivity undertaken by the Earthquake Hazards Mitigation program from January 1977 through March 1978. Information given on each activity includes the title, principal investigator, institution, and a brief description of the research to be undertaken. The objective for each element of the program is briefly stated.

The NSF's Earthquake Hazards Mitigation program has expanded substantially in the past year from an $8.8 million expenditure in FY 77, ending September 30, 1977, to an $18 million research program in FY 78 beginning October 1, 1977. This paper presents a brief review of the objectives of the current program and of each individual award made between January 1, 1977 and March 30, 1978. Table below shows the allocation of program funds among the three components of the program for the past two years and the projection for FY 79.

Program Subelement	Actual FY 1977	Budget Request FY 1978	Current Plan FY 1978	Estimate FY 1979	Difference FY 1979/78
Siting - - - -	$3,020,412	$6,000,000	$6,856,600	$9,800,000	$2,943,400
Design - - - -	4,517,390	9,000,000	8,750,000	11,800,000	3,050,000
Policy - - - -	1,732,492	6,500,000	2,500,000	4,800,000	2,300,000
TOTAL	$9,270,294	$21,500,000	$18,106,600	$26,400,000	$8,293,400

The objectives of the Earthquake Hazards Mitigation program are to develop methods and techniques that can provide effective protection for man, his works and institutions from life loss, personal injury, property damage, social dislocations, and economic and ecological disruption associated with potential or realized earthquake hazards.

The Siting category of the Earthquake Hazards Mitigation program provides research support for the elucidation of the physical basis of earthquake energy generation and the transmission and propagation of the generated shock waves through various geologic and soil conditions; with the impact of earthquake ground motion on structures; and with development of criteria and guidelines for the mitigation of potential impacts on the built environment. The specific objectives of the Siting program are to:

- Develop a comprehensive data base on the nature of earthquake motion at typical construction sites and for representative structures;
- Establish the physical basis for characterizing the nature of earthquake motions and the dynamic forces generated by such motions and other natural hazards;
- Develop capabilities for prediction of the magnitude and frequencies of ground motion;
- Develop a methodology for qualitative and quantitative estimates of local or regional risk associated with earthquakes and other types of hazards and combined hazards;

34

- Develop a comprehensive and unified program to improve geotechnical engineering practices applicable to soil dynamics, foundation design, failure and instability, and other aspects of earthquake ground motion; and
- Identify procedures for integrating informatin on natural hazards into land use planning, urban and coastal zone planning, offshore engineering and siting procedures.

The specific objectives of the Design program are to:

- Improve the characterization of earthquake and natural hazard loadings necessary for the economical design of structures subject to dynamic loading;
- Develop new methods of analysis and design of buildings and structures of all types which will take into account nonlinear and inelastic behavior of materials;
- Develop methods to assess the hazard potential and risk assessments applicable to existing structures and facilities, and devise innovative methods for improving performance within economically acceptable bounds;
- Obtain information for engineering analysis and design by observing the damage of facilities following actual earthquakes, and incorporate this information into standard design practice;
- Develop improved computational capability for dynamic analysis of structures and facilities and improve user access to any computer software which is developed;
- Develop model standards and design criteria for design of structures and facilities subjected to earthquake and natural hazard loadings; and
- Conduct detailed studies of the behavior of smaller nonengineered structures and secondary components of buildings to improve recommended minimum analysis and design guidelines.

The specific objectives of the Policy program are to:

- Expand the base of knowledge on alternative social adjustments to earthquakes;
- Identify the social, economic, political, legal, and related factors which facilitate or hinder the adoption of both social and technological solutions to earthquake hazards;
- Facilitate the beneficial use of earthquake hazards mitigation measures by devising effective techniques for disseminating information to the public and to decision-makers at the local, State, and national levels; and
- Investigate measures which will reduce possible negative social, economic, and political consequences of earthquake predictions and warnings.

If you wish to be apprised of the grant activity in this program on a quarterly basis please notify one of the authors to be placed on our mailing list.

The following text presents the summary of awards in each of the individual program element areas: siting, design, and policy.

Siting

Underground Lifelines in a Seismic Environment; Melvin L. Barron; Weidlinger Associates, 110 East 59th Street, New York, New York 10022; Grant #76-80982; Supplemental Award.

Study the behavior of underground lifeline structures such as pipelines, conduits, and channels in seismic environments. Apply the technical knowledge gained with cost-benefit and optimization studies in order to plan, design, and construct such structures.

Earthquake Ground Motion Modeling for the Central United States; Robert H. Hermann; Dept of Earth and Atmospheric Sciences; St. Louis University, St. Louis, Missouri 63103; Grant #76-20875; New Award.

Conduct theoretical and observational studies to re-examine the available data base and improve the empirical model for predicting ground motion. Predict strong motion parameters and time histories in the distance range of up to 500 kilometers for earthquakes with a magnitude equal to or stronger than five, based on the study.

Operation of the National Program in Strong Motion Instrumentation; Robert B. Matthiesen; U.S. Geological Survey, 345 Middlefield Road, Menlo Park, California 94025; Grant #76-82207; Renewal Award.

Develop and operate a national program in strong-motion instrumentation and data management with respect to network design, network operations, and data management. The data development forms the basis for analysis, design, and construction of structures of all types to be earthquake resistant in order to mitigate the losses of life and property.

Induced Seismicity at the Nurek Reservoir, Tajikistan, USSR; David W. Simpson; Lamont-Doherty Geological Observatory, Columbia University, Palisades, New York 10027; Grant #01092; New Award.

Study the induced seismicity near a reservoir. Investigate spatial and temporal variations in the seismicity and their relationship to water level. Perform studies on the frequency characteristics of earthquakes and various geological and geophysical effects to the induced seismic nation.

Seismic Vulnerability, Behavior and Design of Underground Piping Systems; Leon R. L. Wang; Department of Civil Engineering, Rensselaer Polytechnical Institute, Troy, New York 12181; Grant 77-10390; New Award

Develop a systematic way of assessing the adequacy of existing water/sewer distribution systems. Determine the earthquake vulnerability of the systems and study the cost-effectiveness of new designs to various magnitudes of earthquakes.

Partial Support of the Committee on Seismology; Joseph W. Berg; National Academy of Sciences, 2102 Constitution Avenue, N.W., Washington D.C. 20418; Grant #76-24167; Renewal Award.

Provide Earth Sciences reserch data needs imput into RANN program planning for its program in strong-motion instrumentation.

Processing and Analysis of Oroville Earthquake Aftershock Ground Motion Records; Thomas C. Hanks; U.S. Geological Survey, 12201 Sunrise Valley Drive, Reston, Vriginia 22092; Grant #76-81816; New Award

Process the large set of earthquake records obtained after the Oroville earthquake of 1975 with the data arranged into a four volume set. Carry out an analysis of this data to develop methods for predicting potential ground motions of specific sites taking into account frequency band and variables which are of engineering interest. The survey is processing 100 aftershock accelerograms, analyzing data in terms of ground motion parameters, body wave spectra, seismic source parameters, and performing studies on synthesis of ground motion time histories. This project is being pursued in conjunction with the California Institution of Technology.

Processing and Analysis of Oroville Earthquake Aftershock Ground Motion Records; Donald V. Helmberger; Department of Geology and Planetary Sciences, California Institute of Technology, Pasadena, California 91104; Grant #76-21652; New Award

Process the large set of aftershock records obtained after the Oroville earthquake of 1975 with the data arranged into a four volume set. Carry out an analysis of this data to develop methods for predicting potential ground motions of specific sites taking into account frequency bands and variables which are of engineering interest. More specifically, it is processing long period data in terms of velocity and displacement time histories of 40 seismograms, analyzing data for the elasto-dynamic response of half space to faulting motions and generating synthetic motion histories. This project is in conjunction with the U.S. Geological Survey (above).

United States-Republic of China Cooperative Research in Earthquake Engineering-Part II; Le-Wu; Department of Civil Engineering, Lehigh University, Bethlehem, Pennsylvania 18015; Grant #77-07470; New Award

Conduct joint research on ground motion studies and seismic response of embedded structures (siting problems) and on strengthening concrete buildings with differential foundation settlements (design problems) which will be beneficial to both countries. This portion of the research will deal with earthquake resistance and strengthening of concrete buildings with foundation settlement and partial structural damage.

United States-Republic of China Cooperative Research in Earthquake Engineering-Part I; Joseph Penzien, Department of Civil Engineering, University of California, Berkeley, California 94720; Grant #76-06006; New Award.

Conduct cooperative research on ground motion studies and seismic response of embedded structures (siting problems) and on strengthening concrete buildings with differential foundation settlements (design problems) which will be

beneficial to both countries. This portion of the research will study attenuation laws, maximum acceleration and other ground motion characteristics in order to find common features, correlations, and discrepancies.

esearch Initiation-Behavior of Buried Conduit Structures Subjected o Seismic Loading; Jack Rosenfarb; Department of Civil Engineering, exel University, Philadelphia, Pennsylvania 19140; Grant #77-06421; ew Award.

Investigate the behavior of buried conduit-type structures such as pipelines and tunnels. Assess the effects of structure flexibilities as influenced by conduit geometry, material, and connection restraint conditions.

orkshop on Research Priorities for Geotechnical Earthquake Engineer-ng Applications; Kenneth H. Stokoe, III; Department of Civil ngineering, University of Texas, Austin, Texas 78122; Grant #77-9861; New Award: and Felix Y. Yokel; Center for Building Technology, ational Bureau of Standards, Washington D.C. 20234; Grant #77-4157; New Award.

This joint project is to organize, administer, and conduct a workshop on Geotechnical Earthquake Engineering Applications. It is also to review needs and priorities for future research and establish liaison among the various research groups.

arthquake and Strong-Motion Instrument Development and Array esign; Francis T. Wu; Department of Geophysical Sciences, tate University of New York, Binghamton, N.Y. 13901; Grant #76-3897; New Award.

Provide strong-motion instrument coverage in Eastern United States. Collect data for resolving the nature of strong-motion waves and for future predictive use in engineering design. Study the dynamic seismic source mechanisms by using near field data.

orkshop on Research Priorities for Geotechnical Earthquake ngineering Applications; Felix Y. Yokel; Center for Building echnology, National Bureau of Standards, Washington D.C. 0234; Grant #77-14157; New Award.

Analyze midwest convective cloud data, synthesize the results, and assess the potential for effective modification to augment precipitation.

Strong-Motion Seismography Array in Northern Baja California--ortheastern Sonora, Mexico; James N. Brune; University of alifornia, San Diego, LaJolla, California 92037; Grant #75-2939 A01.

Install and maintain a timed strong-motion seismograph system array in Northwest Mexico near the Cerro Prieto, Imperial, Agua Blanca and San Miguel Faults.

arthquake Response of Dams Including Hydrodynamic and Foundation nteraction; Anil K. Chopra; University of California, Berkeley, alifornia 94720; Grant #76-80073 A01.

Develop reliable techniques, including computer programs, for earthquake analysis of concrete gravity, concrete arch, and earth dams.

Seismic Response of Three-Dimensional Dam Reservoir Systems; Allen T. Chwang; California Institute of Technology, Pasadena, California 91125; Grant #77-16085.

Determine the seismic response of a dynamically coupled, three-dimensional dam reservoir system including the hydrodynamic interaction effect, the flexibility effect, the effect of phase variation and spatial attenuation of seismic waves, and the effect of the side confinement of the dam.

A Portable Vibrating Structure for Soils Investigations; Paul Ibanex; Applied Nucleonics Company, Inc., Los Angeles, California 90024; Grant #77-19653.

Develop a method for high strain in situ measurement of soil properties.

International Workshop on Strong-Motion Earthquake Instrument Arrays; Wilfred D. Iwan; California Institute of Technology, Pasadena, California 91101; Grant #77-24726.

Organize and convene an International Workshop on Strong Motion Earthquake Instrumentation Arrays (three dimensional) in the spring of 1978. The workshop will provide a basis for development of a plan for the future deployment of dense, three-dimensional strong-motion earthquake resistant arrays.

Distant and Local Tsunamis in Coastal Regions; Jiin Jen Lee; University of Southern California, Los Angeles, California 90007; Grant #77-01599.

To conduct research into the behavior of tsunamis in coastal regions with complicated topography for use by coastal zone engineers and planners for efficient design of coastal structures and communities.

Soil-Structure Interaction with Arbitrary Seismic Environment; John Lysmer; University of California, Berkeley, California 94720; Grant #76-23277 A01.

Develop a theory and associated finite element code CREAM (Complex Response Earthquake Analysis Method) and make this available thorough the NTIS and other appropriate channels.

Earthquake Response and Aseismic Design of Underground Piping Systems; Teoman Ariman; University of Notre Dame, Notre Dame, Indiana 46556; Grant #77-23236.

Investigate the earthquake response and earthquake-resistant design of underground piping systems utilized in energy transport, particularly buried gas pipelines; study the failure of pipes by fracture and other failure mechanisms, and develop design guides for piping systems subject to seismic hazard.

Underground Lifelines in a Seismic Environment; M.L. Baron; Weidlinger Associates, 110 E. 59th Street, New York, New York 10022; Grant #76-09838.

Study the behavior of underground lifeline structures such as pipelines, conduits, channels, etc., in seismic environments, and apply the technical knowledge gained in conjunction with cost-benefit and optimization studies to the planning, design and construction of such structures.

Seismological Analysis of Strong Motion Records; Bruce Bolt; University of California, Berkeley, California 94720; Grant #78-02650.

Examine the consequences of using effective peak acceleration as a scaling parameter for response spectra rather than the dislocation pulse; conduct wave analysis of strong-motion records; and search for common physical features in terms of source mechanisms, fault rupture, and so forth.

Numerical and Experimental Study of Earthquake Strong-Motion; James N. Brune; University of California, San Diego, La Jolla, California 92037; Grant #77-23829.

Investigate earthquake ground motion characterization in terms of fault proximity, fault type, models and laboratory experiments; calibrate the computer methods for modeling earthquakes, simulate ground motion under a variety of conditions, and produce rules for characterizing ground motion which are suited to the needs of design engineers.

Seismic Response of Three-Dimensional Dam-Reservoir Systems; Allen T. Chwang; California Institute of Technology; Pasadena, California 91125; Grant #77-16085

Evaluate the seismic response of a dynamically coupled, three-dimensional dam reservoir system including hydrodynamic interaction effect, flexibility effect, effect of phase variation and spatial attenuation of seismic waves, and the effect of the side confinement of the dam.

Statistical Investigation of Engineering Seismology; Leon Knopoff; University of California, Institute of Geophysical and Planetary Physics, Los Angeles, California 90024; Grant #77-24742.

Introduce physics into the stochastic models of earthquake occurrence, source, and faults, and develop basic scientific procedures for the seismic risk estimation of a given region.

Dynamic Soil Structure Interaction; Jose M. Roesset; Massachusetts Institute of Technology, Cambridge, Massachusetts 02139; Grant #77-14174

Earthquake Engineering of Large Underground Structures; Roger Scholl; John A. Blume and Associates, 130 Jessie Street, San Francisco, CA 94105; Grant #77-06505.

Evaluate the current state-of-the-art in underground earthquake engineering practice, determine areas in which additional research is needed, and produce a report summarizing world-wide experience concerning underground earthquake engineering design and construction practices.

Induced Seismicity at Nurek Reservoir, Tadjikistan, USSR; David W. Simpson; Columbia University, Palisades, N.Y. 10027; Grant #77-01092 A01.

Study the induced seismicity near the Nurek reservoir; investigate spatial and temporal variations in seismicity and their relationships to water level; perform studies on the frequency characteristics of earthquakes and various geological and geophysical effects of the induced seismic motion; study the earthquake spectra using digital recorders.

Strong-Motion Accelerograph Network in the Los Angeles Basin; Ta-Liang Teng; University of Southern California, Los Angeles, California 90007; Grant #77-16983.

Install 100 accelerographs in a well-planned grid-shaped array in the Los Angeles Basin to record future earthquake data; use the data to study the distribution of strong shaking, the attenuation patterns, the shear velocity structure, and the effect of geological structure and local conditions.

A Methodology for Optimal Strong-Motion Instrument Locations in Building Structures; F.E. Udwadia; University of Southern California, Los Angeles, California 90007; Grant #77-07903.

Develop a scientific methodology for the location of strong-motion instruments in buildings for maximum possible information about the structure's dynamic characteristics; study both the number and position of instruments in relation to the amount of information obtained.

Prediction of Earthquake Resistance of Structures; P.C. Wang; Polytechnic Institute of New York, 333 Jay Street, Brooklyn, New York 11202; Grant #78-09990.

Continue development of a minimum method to generate design earthquakes, including development of critical response spectra; establish procedures for choice of design variables, and design computer programs in forms that can be directly used by practicing engineers.

Earthquake Design Criteria for Water Supply and Wastewater Systems; Leon Weinberger; Environmental Quality Systems, Inc., 1160 Rockville Pike, Rockville, MD 20852; Grant #77-22617.

Develop criteria for the design of water supply and wastewater pollution control systems to reduce damage during earthquake events and promote rapid post-quake recovery.

Analysis of Cape Ann Earthquake from Building Damage; Robert V. Whitman; Massachusetts Institute of Technology, Cambridge, MA 02138; Grant #77-15331.

Determine the strength of ground shaking caused by the earthquake of 1755 at Cape Ann, Massachusetts.

Design

Stability of Structures Under Static and Dynamic Loading -- International Colloquium, May 17-19, 1977; Lynn S. Beedle; Fritz Engineering Laboratory, Lehigh University, Bethlehem, Pennsylvania 18105; Grant #76-20825.

Bring together the generators of research information on the static and dynamic stability of structures and elements and the users of this information to evaluate the latest research results, identify further needed research and documentation of static and dynamic stability information in a form suitable to be incorporated into design guides.

Safety Evaluation of Buildings Exposed to Earthquakes and Other Catastrophic Environmental Hazards; Boris Bresler; Department of Civil Engineering; University of California, Berkeley, California 94720; Grant #76-82384.

Develop methods and criteria for assesing the damage potential of existing structures. Develop guidelines based on damage potential indices which would be suitable for use by practicting engineers and building regulation departments.

Seismic Resistance of Fossil-Fuel Power Plants; John L. Bogdanoff; School of Aeronautics and Astronautics; Purdue University, Lafayette, Indiana 47907; Grant #77-01392.

Examine the structural dynamic behavior and response of major components of large fossil-fuel steam power plants subjected to seismic forces. Develop computer codes for the analysis of the major components; develop analysis and design guidelines and criteria; and develop design recommendations for code groups to consider for adaptation.

Structural Loads Analysis and Specification; C. Allin Cornell; Department of Civil Engineering, Massachusetts Institute of Technology, Cambridge, Massachusetts 02139; Grant #77-01389.

Develop a practical, unified approach to the analysis and specification of structural loadings, including extremum value loads and continuous loads by developing a relatively simple, unified set of representatives from the random characteristics of loads and by developing alternative codifiable treatments of loading and load combination specification.

Formulation and Expression of Seismic Design Provisions; Steven J. Fenves; Carnegie-Mellon University, Pittsburgh, Pennsylvania 15213; Richard N. Wright; National Bureau of Standards, Gaithersburg, Maryland 20234; Grant #77-01497.

Facilitate the development, usefulness, and implementation of the seismic design provisions that are currently being developed by the National Bureau of Standards and the Applied Technology Council.

Conference on the Repair and Rehabilitation of Buildings; Robert D. Hanson; Department of Civil Engineering, University of Michigan, Ann Arbor, Michigan 48109; Grant #76-83884.

Conduct a conference and workshop consisting of professionals, faculty and researchers to assess the current practices and needs of the professionals concerned with the repair and rehabilitation of structures, including other hazardous buildings. Undertake a projection of future research.

Earthquake Induced Bond Deterioration of Reinforced Concrete, Neil M. Hawkins; Department of Civil Engineering, University of Washington, Seattle, Washington 98105; Grant #76-15366.

Study the bond deterioration between reinforcing bars and the surrounding concrete when reinforced concrete elements are subjected to reverse earthquake loadings. Recommend design regulations for seismically loaded reinforced concrete structures.

Effects of Damage from Strong Earthquakes; George W. Housner; Department of Civil Engineering and Applied Mechanics, California Institute of Technology, Pasadena, California 91125; Grant #76-17137.

Develop practical techniques for the analysis of non-linear structural response to seismic forces and apply the methods to control the damage of structures beyond the elastic range.

Seismic Safety Design for Policy and Fire Stations; Earle W. Kennett; American Institute of Architects, Research Corporation, 1735 New York Avenue, NW., Washington, D.C. 20006; Grant #76-80695.

Explore, define and record seismic design considerations to be used by the architectural and public safety professions in the design, construction, and operation of policy and fire stations, including recommendations for specific, prototypical architectural design alternatives.

Effects of Earthquake Motions on Reinforced Concrete Buildings, Mete A. Sozen; Department of Civil Engineering, University of Illinois, Urbana, Illinois 61805; Grant #77-01391.

Identify and understand the mechanisms of energy dissipation in slender reinforced concrete structures subjected to strong ground motion in an effort to develop simple but realistic design methods for earthquake resistance.

Earthquake and Wind Response of Segmentally Constructed Hyperbolic Natural Draft Cooling Towers; Chi C. Tung; Department of Civil Engineering; North Carolina State University, Raleigh, North Carolina 27607; Grant #76-19663.

Study the dynamic response of segmentally constructed pre-stressed hyperbolic cooling towers using model studies and develop linear and non-linear analytical models for predicting the dynamic response of such structures.

Seismic Behavior of Complete Structural Systems; Ray W. Clough; Department of Civil Engineering, University of California, Berkeley, California 94720; Grant #77-00280.

Develop computer procedures for predicting structural response to earthquakes. Formulate mathematical models to reproduce the observed behavior analytically. Develop and test special structural components for improving the seismic resistance and conducting reconnaissance surveys of earthquake damaged structures.

Summer Institute on Architectural Design for Earthquake Disaster Mitigation; John P. Eberhard; AIA Research Corporation, 1735 New York Avenue, NW., Washington, D.C. 20006; Grant #76-80799.

Conduct a one-week short course for faculty of architectural schools with respect to an understanding of the earthquake phenomenon and the methods to mitigate the damages as a result of a seismic event.

Earthquake Induced Bond Deterioration of Reinforced Concrete; Neil M. Hawkins; Department of Civil Engineering, University of Washington, Seattle, Washington 98105; Grant #76-15366.

Study the bond deterioration between reinforcing bars and the surrounding concrete when reinforced concrete elements are subjected to reversed earthquake loadings. Recommend design regulations for seismically loaded reinforced concrete structures.

Research Initiation-Strengthening of Reinforced Concrete Columns for Earthquake Resistance; Lawrence F. Kahn; Department of Civil Engineering, Georgia Institute of Technology, Atlanta, Georgia 30332; Grant #77-06478.

Determine the adequacy of various methods of strengthening and repairing concrete columns for improved earthquake resistance.

Third U.S. National Conference on Wind Engineering Research, February 26-March 1, 1978; Bernard M. Leadon; Department of Engineering Sciences, University of Florida, Gainesville, Florida 32601; Grant #77-10170.

Bring together researchers and practitioners interested in dynamic wind effects to exchange information, to improve communication between researchers and users, to identify areas of research which require further effort and to produce a proceedings of the conference.

Structural Response Under Random Wind Loading; Yu K. Lin; Department of Aeronautical Engineering, University of Illinois, Urbana, Illinois 51801; Grant #76-84171.

Develop stochastic models for wind forces in the along-wind and across wind directions and to establish the stability criteria for structural response in the non-linear range.

Reliability of Existing Buildings in Earthquake Zones-Part II; Hugh D. McNiven; Earthquake Engineering Research Center, University of California, Berkeley, California 94720; Grant #77-06489.

Investigate the earthquake reliability of existing buildings by establishing a non-linear mathematical model representing the building and subjecting the model to a large family of earthquake excitations. This institution will develop the model.

Seismic Behavior of Multistory Masonry Structures; Hugh D. McNiven; Earthquake Engineering Research Center, University of California, Berkeley, California 94720; Grant #77-00281.

Conduct experimental and analytical studies of the behavior of masonry wall panels subjected to earthquake excitation. Perform correlation studies with forced vibration test results and determine equivalent elastic constants of masonry structures.

Seismic Behavior of Structures; Analysis and Design; Joseph Penzien; Department of Civil Engineering, University of California, Berkeley, California 94720; Grant #77-00186.

Apply improved seismic analysis capabilities to complete structural systems and develop methods of design with increased reliability of controlling seismic damage with a proper balance between cost and safety.

Seismic Behavior of Structural Components; Egor P. Popov; Department of Civil Engineering, University of California, Berkeley, California 94720; Grant #77-00275.

Conduct experimental and analytical studies of the behavior of structural components subjected to earthquake excitation. Perform the experimental work on large-scale components which extrapolate the experimental results to practical situations.

Research Initiation-Nonproportional Damping of Interaction Systems Subjected to Earthquake Motions; David T. Tank; Department of Civil Engineering, State University of New York, Buffalo, New York 14214; Grant #77-06425.

Explore the concept of employing measured damping data in the computation of seismic response of interaction systems.

Shear Transfer in Thick-Walled Reinforced Concrete Structures Subjected to Seismic Loading; Richard N. White; Department of Structural Engineering, Cornell University, Ithaca, New York, 14850; Grant #76-23896.

Develop engineering and analytical models of the shear transfer mechanism in cracked concrete reinforced with large reinforcing bars. Test these models against structures damaged in actual earthquakes.

Summer Institute of Multiprotection Design; Bernard Wobbeking; American Society for Engineering Education, 1 Dupont Circle, Washington, D.C. 20036; Grant #77-01090.

Educate and train the participants in the methods of structural design to mitigate the losses as a result of natural hazards, such as earthquakes, tsunamis, fire, landslides, extreme winds, and others.

Reliability of Existing Buildings in Earthquake Zones Part I; James T. Yao; Department of Civil Engineering, Purdue University, Lafayette, Indiana 47907; Grant #77-05290.

Investigate the earthquake reliability of existing buildings by establishing a non-linear mathematical model representing the building and subjecting the model to a large family of earthquake excitations. This institution will formulate reliability criteria and analyze the test results in terms of damage probability and other probablistic response measures.

Building Configuration and Seismic Design; Christopher Arnold; Building Systems Development, Inc., 120 Broadway, San Francisco, California 94111; Grant #76-81821.

Provide a systematic body of knowledge and a useful methodology that will enable a better understanding between architects and engineers with respect to the influence of building plan configuration on the seismic resistance of the building.

Implementation Planning for Seismic Design Provisions for Buildings; Charles Culver; National Bureau of Standards, Gaithersburg, MD 20234; Grant #77-15084.

Enlist the support and endorsement of the various organizations involved in construction to facilitate the adoption of comprehensive design provisions for buildings.

The United States-Japan Cooperative Research Program on Large-Scale Structural Tests: A Planning Study; Joseph Penzien; Department of Engineering, University of California, Berkeley, California 94720; Grant #76-80835.

Establish a task committee under the United States-Japan "Panel on Wind and Seismic Effects" program to make detailed plans and recommendations for developing effective cooperative research programs on large-scale tests of structural systems.

Probability Distribution of Extreme Wind; Emil Simiu; National Bureau of Standards, Center for Building Technology, Washington, D.C. 20234; Grant #77-16113.

Establish a task committee under the United States-Japan a probabilistic approach taking into account sampling errors, data errors, use of short-term data and applicability of procedures to different types of wind climates.

Safety Evaluation of Structures to Earthquake and Other Natural Hazards; A.H-S Ang; University of Illinois at Urbana-Champaign, Urbana, Illinois 61801; Grant #77-09090.

Coordinate analytical program to develop the basis for structural safety evaluation and reliability design of structures to resist natural hazards.

Seismic Hardening of Unreinforced Masonry Walls Through a Surface Treatment; James R. Cagley; Martin & Cagley; 6000 Executive Blvd, Rockville, MD 20852; Grant #77-19888.

Develop a simple and economical method of reinforcing masonry to resist seismic forces through the use of a coating.

Seismic Behavior of Complete Structural Systems; Ray W. Clough; University of California, Berkeley, California 94720; Grant 76-04262 A02.

Develop computer procedures for predicting earthquake responses through the use of mathematical models and actual buildings.

Masonry Buildings--Response of Existing Systems to Earthquake Motions; Robert D. Ewing; Agbabian Associates, 250 N. Nash St., El Segundo, California 90245; Grant #77-19829.

Identify improved methods for analyzing the earthquake response of existing unreinforced masonry structures and develop methods for strength retrofitting.

The Use of Structural Foams to Improve Earthquake Resistance of Buildings; B. C. Gabrielsen; Scientific Service, Inc., Redwood City, California 94063; Grant #77-21426.

Investigate the feasibility of using polyurethane foams to increase the shear capacity of timber stud walls and timber joist floors and ceilings.

Earthquake Resistant Design of Braced Steel Frame Structures; Subhash C. Goel; University of Michigan, Ann Arbor, Michigan 48109; Grant #76-82209.

Study configurations of braced multistory steel frame systems subjected to seismic forces to determine their advantages and disadvantages.

Engineering Design for Natural Hazards; W.J. Hall; University of Illinois, Urbana, Illinois 01801; Grant #77-07190.

Develop simplified and improved methods of structure design to provide protection against natural hazards.

A Rational Approach to Damage Mitigation in Existing Structures Exposed to Earthquakes; Ben Kacyra; Earthquake Engineering Systems, Inc., 141 Battery Street, Suite 400, San Francisco, California 94111; Grant #77-19463.

Undertake a feasibility study of developing a rational decision analysis methodology for evaluating possible modifications for existing buildings exposed to a predicted earthquake.

Mitigation of Seismic Hazards in Existing Unreinforced Mansonry Wall Buildings; John Kariotis, Kariotis, Kesler and Allys; 1414 Fair Oaks Avenue, South Pasadena, California 91030; Grant #77-19651.

Analyze performance of buildings with unreinforced masonry walls built prior to adoption of seismic building codes; evaluate methods of revising performance of unreinforced elements; investigate changes in response caused by modifications.

Reliability of Existing Buildings in Earthquake Zones--Part II; Hugh D. McNiven; University of California, Berkeley, California 94720; Grant #77-06489 A01.

Develop a realistic method of evaluating seismic reliability of existing structures through development of mathematical models, development of "failure criteria," and tests of model structures.

Seismic Behavior of Multistory Masonry Structures; Hugh D. McNiven; University of California, Berkeley, California 94720; Grant #76-04265 A02.

Test the seismic shear resistance of single and double window piers in multistory masonry buildings; correlate results with various matematical models.

Structure-Fluid Interaction Due to Earthquakes; C.C. Mei; Massachusetts Institute of Technology, Cambridge, Massachusetts 02139; Grant #77-10236.

Conduct theoretical and numerical investigations of the phenomenon of structure-fluid interaction in dam-reservoir systems, offshore structures, and other structures of this type.

The Dynamic of Structure with Localized Nonlinearity; Richard K. Miller; University of California, Santa Barbara, California 93106; Grant #77-01096.

Develop a better understanding of earthquake behavior of localized nonlinear systems and develop more efficient analysis techniques for the transient and earthquake responses of such systems.

Seismic Behavior of Structures; Analysis and Design; Joseph Penzien; University of California, Berkeley, California 94720; Grant #76-06264.

Develop improved seismic analysis capabilities and apply them in structural designs for increased reliability of controlling seismic damage and costs.

The United States-Japan Cooperative Research Program on Large-Scale Structural Systems; Joseph Penzien; University of California, Berkeley, California 94720; Grant #76-80835 A01.

Undertake a planning study for development of an effective research program of maximum benefit to both the US and Japan on large-scale tests of structural systems.

Methodology for Mitigation of Seismic Hazards in Existing Unreinforced Masonry Buildings; C. W. Pinkham; S.B. Barnes & Associates; 2236 Beverly Boulevard, Los Angeles, California 90027; Grant #77-19523.

Review past work on methods of retrofitting unreinforced masonry buildings, determine the need for hazard mitigation, and determine methods to retrofit economically.

Seismic Behavior of Structural Components; Egor P. Popov; University of California, Berkeley, California 94720; Grant #76-04263 A03.

Conduct advanced experiments and studies of braced steel frames, reinforced concrete walls and filled frames, reinforced concrete ductile frames, and reinforced beam-column components; use results to construct mathematical models for analyzing inelastic behavior.

Seismic Behavior and Design of Buildings; Jose M. Roesset; Massachusetts Institute of Technology, Cambridge, Massachusetts 02139; Grant #77-14174.

Improve present knowledge on the non-linear dynamic behavior of buildings subject to earthquake excitation and on the effectiveness of various design procedures.

Reliability of Existing Buildings in Earthquake Zones--Part I; James T.P. Yau; Purdue University, Lafayette, Indiana 47907; Grant #77-05290.

Develop a realistic method of evaluating seismic reliability of existing structures through development of mathematical models, development of "failure criteria," and tests of model structures.

Conference on Stability Problems of Mixed Steel-Concrete Structures, Boston, Massachusetts, May 1978; Lynn S. Beedle; Lehigh University, Bethlehem, PA 18015; Grant #78-08818.

Bring together information on the static and dynamic stability problems and performance characteristics of mixed steel-concrete composite construction and publish this information for distribution.

Seismic Investigation and Design Criteria for Industrial Storage Racks; John A. Blume; URS/John A. Blume & Associates, 130 Jesie Street, San Francisco, California 94105; Grant #77-06505.

Analyze and test stacker-type industrial storage racks including standard pallet racks and their subassemblies, drive-in and cantilever racks to determine their behavior under seismic forces.

Earthquake Engineering Research Facility Support; Ray W. Clough; University of California, Berkeley, California 94720; Grant #77-21787.

Provide continuing support for the essential maintenance and operation of inelastic seismic performance experimental facilities required at the University of California, Berkeley, including the Earthquake Simulator Laboratory, dynamic controlled test systems, high speed digital data aquisition systems, and field vibration test systems.

Formulation and Expression of Seismic Design Provisions; Steven J. Fenves; Carnegie Mellon University, Pittsburgh, Pennsylvania 15231; Grant #78-11300.

Facilitate the development, use and implementation of the seismic design provisions that are currently being developed by the National Bureau of Standards and the Applied Technology Council.

Progressive Collapse of Transmission Line Structures Due to Dynamic Loads; John F. Fleming; University of Pittsburgh, Pittsburgh, Pennsylvania 15231; Grant #77-23519.

Investigate the effect of partial failures induced by earthquake or other dynamic loads in transmission line structures, with particular emphasis on predicting progressive collapse conditions, and develop design criteria which would prevent progressive collapse.

Scale Modeling and Testing of Structures for Reproducing Response to Earthquake Excitation; James M. Gere; Stanford, California 94305; Grant #77-14444.

Investigate the direct replica modeling of elastic behavior of civil engineering structures to achieve a routine capability for reproducing, on existing small-scale test facilities, the dynamic response of large structures subjected to prescribed earthquake motions.

Behavior of Buildings to Wind and Seismic Forces; Gary C. Hart; University of California, Los Angeles, California 90024; Grant #77-24062.

Study the behavior and response of full scale buildings in Century City/Los Angeles when subjected to strong winds and seismic forces; compare such responses with the soil structure interaction due to these forces.

Seismic Response of Structures and Strong-Motion Instrumentation; George W. Housner; California Institute of Technology; Pasadena, California 97125; Grant #77-23687.

This project includes the analysis of earthquake records, operation and upgrading of instruments and protable instrument networks analysis of buildings in the nonlinear range, and behavior of materials and structures.

Behavior of Reinforced Concrete Frame Elements Under Biaxial Lateral Loadings; James O. Jirsa; University of Texas, Austin, Texas 78712; Grant #77-20816.

Evaluate the importance of the path of lateral deformation on sequence of application of bidirectional lateral loads on the shear strength and response of columns and beam-column joints; evaluate the influence of axial load variations on the behavior of columns and beam-column joints; develop design recommendations for such members; and develop behavioral models to be used in analysis of structures to predict behavior for members subjected to large shear forces.

Seismic Safety Design for Policy and Fire Stations; Earle W. Kennett; American Institute of Architects Research Corporation (AIA/RC) 1735 New York Avenue, NW, Washington, D.C. 20006; Grant #77-28413.

Explore, define, and record seismic design considerations to be used by the architectural and public safety profession in the design, construction, and operation of police and fire stations, including recommendations for specific prototypical architectural design alternatives.

Unified Approach to the Design of Window Glass Subjected to Dynamic Loads; Joseph E. Minor; Texas Tech University, Lubbock, Texas 79409; Grant #77-24063.

Review the processes in which glass panels are selected for use in engineered structures to provide the practitioner with safe, economical designs for glass windows which utilize current knowledge of wind engineering, glass material properties, and structural response of thin rectangular panels.

An Evaluation of the Earthquake Rehabilitation Building Ordinance in the City of Long Beach, California; William J. Petak; J. H. Wiggins Company; 1650 South Pacific Coast Highway, Redondo Beach, California 90277; Grant #77-22621.

Review, assess and evaluate the Earthquake Hazard Regulations for Rehabilitation of existing structures adopted by the City of Long Beach in 1971; determine the effectiveness of the ordinance, the effectiveness of the City Government in implementing the Ordinance, the costs and consequences of implementation, and the transferability of this approach to other natural hazard areas.

Fire Resistance of Epoxy Repaired Concrete Structures; Joseph M. Plecnik; California State University, Long Beach, California 90840; Grant #77-22946.

Investigate the behavior of epoxy repaired concrete structural walls during fire exposure; determine the nature and extent of residual strength of epoxy repaired structural components after fire exposure; and prepare a Computerized Catalog of repaired structures to study their behavior during future fires and/or earthquakes.

Feasibility of Force-Pulse Generators for Earthquake Simulators; F.B. Safford; Agbabian Associates, 250 N. Nash Street, El Segundo, California 90245; Grant #77-15010.

Design, construct and evaluate prototype pulse systems to simulate earthquake wave forms in full scale structures.

Improving Earthquake Resistance of Elevators; Anshel J. Schiff; Purdue University, Lafayette, Indiana 47907; Grant #77-21268.

Investigate three specific problem areas for improvement of the earthquake provisions of the national elevator code: counterweight and guide rail design, the determination of seismic loads on elevator systems, and the analysis of cable dynamics.

Summer Institute on Design for Protection Against Natural and Manmade Hazards; Bernard Wobbeking; American Society for Engineering Education; 1 Dupont Circle, Washington, D.C. 20036; Grant #77-01090 A02

Conduct a Summer Institute to train selected participants in methods of structural design to mitigate losses as a result of natural hazards such as earthquakes, tsunamis, fire, landslides, extreme winds, and others. Participants will be requested to teach similar courses in their universities and local areas. The courses for engineers and architects are on a local basis to reach the practicing professionals who can apply the results of the course immediately.

Policy

National Information Service for Earthquakes-University of California Berkeley; Ray W. Clough; Earthquake Engineering Research Center, University of California, Richmond, California 94804; Grant #77-01934.

Develop an effective information service for earthquake engineering by developing a library of technical information; by preparing and publishing programs and an abstract journal; by disseminating information; and by providing educational opportunities for professional practitioners.

Inflationary Changes in Construction Costs Created by Earthquake Damage: Implications for Government Policy; Harold C. Cochrane; Department of Economics, Colorado State University; Ft. Collins, Colorado 80523; Grant #76-24169.

Assess the extent of disaster-related inflation following the occurrences of hazardous events. Prepare recommendations for legislative and administrative actions to counteract it.

National Information Service for Earthquake Engineering--California Institute of Technology; George W. Housner; Department of Civil Engineering and Applied Mechanics, California Institute of Technology, Pasadena, California 91125; Grant #77-07472.

Serve as a source of earthquake engineering information with particular emphasis on strong earthquake recording data such as digitized acceleration, velocity and displacement. Provide a unique earthquake engineering reference source collection and make available to researchers and practitioners copies of reports, recorded accelerograms, digitized card decks and tapes.

State Government Policy Options for the Utilization of Earthquake Prediction Technology; Hirst Sutton; Council of State Governments; 1225 Connecticut Ave., NW., Washington, D.C. 20036; Grant # 77-81112.

Examine public policy, legal, legislative, program, and administrative issues related to the evolving technology of earthquake prediction, with the objective of developing options in state policies and programs.

Tall Buildings and Urban Habitat: Impact on the Urban Environment and Planning for Natural Disasters; Lyn S. Beedle; Fritz Engineering Laboratory, Lehigh University, Bethlehem, Pennsylvania 18015; Grant #77-01598; New Award.

Develop utilization/implementation techniques to transfer the large quantity of research information and data collected by the Council on Tall Buildings and Urban Habitat on tall buildings and their interaction with the urban environment to decisionmakers, and others concerned with the conception, planning, design, and operation of tall buildings with particular emphasis on planning for natural hazards.

ymposium on Structural Engineering and Mechanics; Karl S. Pister; epartment of Civil Engineering, University of California, Berkeley, alifornia 94720; Grant #77-06518; New Award.

Conduct a symposium to bring researchers, faculty and professionals together to present and discuss current knowledge needed in several areas of dynamic behavior, and developments in education, with respect to structural engineering and mechanics.

Disaster Knowledge and Beliefs and Emergency Planning; Dennis E. Wenger; Department of Sociology, University of Delaware, Newark, Delaware 19711; Grant #77-10202; New Award.

Analyze public and official knowledge regarding the consequences of natural disasters. Assess community disaster preparedness.

Building Futures Forum--The Importance of the Built Environment to the Quality of American Life; Robert M. Dillon; National Academy of Sciences, Washington, D.C. 20418; Grant #77-13297; New Award.

Assemble a group of persons to examine some aspects of the interaction between the man-built enviromment and individual and societal health. Identify forces that are causing and are likely to precipitate changes.

A Longitudinal and Cross Cultural Study of the Post Impact Phases of a Major National Disaster; Frederick L. Bates; Department of Sociology, University of Georgia, Athens, Georgia 30602; Grant #77-12721; New Award.

Identify, describe and measure the impact of a major earthquake on a nation's socio-economic units and develop programs analyze external (U.S.) disaster relief and rehabilitation delivery systems and their long and short-term effects; and develop alternative approaches for programs.

Search and Rescue Missions in Natural Disasters and Remote Settings; Thomas E. Drabek; Department of Sociology, University of Denver, Denver, Colorado 80208; Grant #77-14162; New Award.

Determine the problems rated to search and rescue in large natural disasters in remote areas and develop policy and procedural alternatives for dealing with them.

Community Response to Natural Hazard Warnings; Robert K. Leik; Department of Sociology, University of Minnesota, Minneapolis, Minnesota 55455; Grant #77-01452; New Award.

Identify and analyze by field and laboratory procedures the variables that influence the manner, speed, and appropriateness of the response by families, organizations, and communities, to four major hazard warning systems. Develop alternative approaches as needed.

Post-Earthquake Land Use Planning; George G. Mader; William Spangle and Associates; 3240 Alpine Road, Portola Valley, California; Award #76-82756.

An Interdisciplinary team will investigate post-earthquake land use planning and reconstruction in San Fernando, Santa Rosa, and Alaska and will develop recommendations for post-earthquake planning procedures, programs and regulations.

Seismic Safety Preparedness by Local Governments in California; Dean E. Mann; University of California, Santa Barbara, Santa Barbara, California 93106; Award #77-03688.

Four communities in California will be examined to ascertain sources of resistance to adequate seismic safety planning. The study will provide officials at all levels of government

and in the private sector with improved strategies for overcoming resistance to effective seismic safety planning.

National Information Service for Earthquake Engineering (NISEE); Ray W. Clough; University of California, Berkeley, California 94720; Award #76-20744 A02.

Provide for the transfer of earthquake and other hazards information generated through research to the public users.

Community Response to Natural Hazard Warnings; Robert K. Leik; University of Minnesota, Minneapolis, Minnesota 55455; Award #78-10634.

Provide policy level officials with information on communities response to floods, hurricanes, tornadoes and earthquakes; clarify how warning responses are related to content and timing of messages; interorganizational relation, predisaster planning and individual decisions.

Extension and Utilization of Community Flood Model; Louis W. Miller; University of Pennsylvania; Philadelphia, Pennsylvania 19104; Award #77-26363.

Determine how the physical and economic characteristics of communities influence the decision-making process for hazard mitigation and recovery; determine the financial impact of natural disasters on individual households; access the role of financial institutions in disaster mitigation; and study the impact of a natural disaster on regional economies.

Social and Psychological Factors in Evacuation in Natural Hazards; Ronald W. Perry; Batelle Human Affairs Research Center, 4000 N.E. 41st Street, P.O. Box 5395, Seattle, Washington 98105; Award #77-23697.

Produce a theoretically and empirically grounded model of the factors affecting evacuation which will help isolate key issues in the design and implementation of evacuation plans.

Natural Hazards Research and Applications Information Center; Gilbert F. White; University of Colorado; Boulder, Colorado 80309; Award #77-05164.

Accelerate natural hazards research and the application of findings through an information center service which disseminates information on research findings, programs, and conferences; and conduct annual and special natural hazards workshops.

35

RAPID SEISMIC ANALYSIS PROCEDURES FOR BUILDINGS

T. K. Lew
S. K. Takahashi
C. V. Chelapati

Civil Engineering Laboratory
Port Hueneme, California

Rapid Seismic Analysis Procedures for Buildings

Naval installations are not exempt from earthquake hazards. In addition to the potential monetary loss, the damage to Naval installations from earthquakes can contribute to the loss of operative capacity and life-hazard. Thus, it would be desirable to obtain an overall estimate of damages to an installation when the site is subjected to a potential earthquake. A typical installation may contain 100 to 500 buildings constructed from different materials and built in different years. Understandably, it would not be economically feasible to analyze such a large number of buildings in detail. A rapid, systematic, and economical procedure is needed.

The rapid seismic analysis procedure discussed here has been developed for determining damage estimates from potential earthquake motions to buildings. The procedure does not consider other potential earthquake damage to the buildings from tsunamis (seismic sea waves) and soil failures such as liquefaction and differential settlement.

Based on the resulting damage estimates from the analysis, the potential damage to the installation is quantified and the relative seismic resistance of the buildings determined. The more vulnerable buildings are identified and recommended for further detailed study. Based on results from the detailed study, recommendations are made to (1) modify and strengthen the inadequate existing buildings against the potential earthquake, or (2) plan a systematic phasing-out of the unsafe buildings with new, adequately designed buildings.

The procedure presented here was originally developed by John Blume and Associates for their seismic study on Puget Sound Naval Shipyard, Bremerton, Washington to estimate the potential damage on the shipyard buildings from strong earthquake motions [1]. Results of the original procedure were presented at a Naval Facilities Engineering Command (NAVFAC) workshop given in San Francisco during December 1973 [2].

The procedure has been modified and adapted by the Civil Engineering Laboratory (CEL) for seismic studies on Naval Air Station, North Island (NASNI), San Diego [3], Naval Construction Battalion Center (NCBC), Port Hueneme, and Long Beach Naval Shipyard (LBNSY), Long Beach, California.

The major modifications that CEL has made are systematization of the analysis of the facility inventory assets at a Naval installation and the development of the response spectra for the design earthquakes. In addition, CEL has automated the computation of shear stiffness for concrete or masonry buildings, the first mode shape and natural period of multi-story buildings, and estimation of damage for peak ground accelerations from 0.05g to 0.50g.

Generally, the rapid seismic analysis procedure consists of the following steps:

1. Selection of buildings.
2. Determination of response spectra for design earthquakes.
3. Estimation of yield and ultimate capacities.
4. Estimation of natural periods
5. Estimation of damage from the response spectra.

In the following sections, each of the steps is discussed. Then, a brief discussion of accuracy of the results is given.

Because of the breadth and the complexity of earthquake engineering, it is not possible to discuss all the aspects of earthquake engineering here in detail. However, the pertinent aspects of earthquake engineering relating to the rapid seismic analysis procedure will be presented. Information on technical subjects may be found in references [4 to 7]. Reference [4] is highly recommended, for it covers the total field of earthquake engineering and contains many useful references for the practicing structural engineer.

Selection of Buildings

Because of the generally large number of buildings at the Naval Installation, it is not economically feasible to analyze all the buildings. Generally, about 40 mission-important and permanent buildings at the installation are screened visually. However, only the more critical buildings from this group are selected for analysis. The building selections are determined by the engineers performing the seismic study, NAVFAC personnel, the Public Works Officer (PWO), and Planning Department representative of the Naval installation.

The following procedure was used for the selection of the buildings:

(1) Make a site survey to visually screen the mission-important and major permanent buildings at the installation. The purpose of the survey is to determine the physical conditions of these buildings and take photographs for future reference.

(2) Meet with the PWO and planning department representative of the installation to select the mission-important and representative major permanent buildings for structural analysis.

(3) Gather structural drawings and calculations, if available, from the Public Works Office or NAVFAC field division. Sometimes, drawings for the older buildings are not available or details on the drawings are very sketchy. In the later case, some detective work was required to determine the size of the lateral-force resisting members from the available drawings. With the exception of some of the newer buildings, calculation sheets are generally not available.

(4) Copy information required for the rapid analysis onto standard forms.

(5) Make a final visit to the installation to verify that the buildings are built as shown on the drawings, especially the lateral-force resisting elements.

To facilitate the selection of the buildings for the visual screening, Facilities Systems Office (FACSO) has developed for CEL a computer program that takes the data tape files of NAVFAC P-164, Detailed Inventory of Naval Facilities, and reorders them according to:

(1) Replacement cost (largest to smallest)
(2) Year built (oldest to newest)
(3) Building size (largest to smallest square footage)

The program lists the buildings with the established category code numbers (CCN's) for Navy facility assets as follows:

CCN	Class	Category
100	2	Operational and Training Facilities
200	2	Maintenance and Production Facilities
300	2	Research, Development & Production Facilities
400	2	Supply Facilities
500	2	Hospital and Medical Facilities
600	2	Administrative Facilities
700	2	Housing and Community Facilities
800	2	Utilities and Ground Improvement
900	1	Real Estate

The output from the computer program is used as an aid to select buildings for visual screening.

A sample output from the FACSO computer program is given in Table A1 of the Appendix.

The Program is general and can be used to analyze the facility inventory assets of any Naval installation. The computer program is available at FACSO, NCBC, Port Hueneme.

Determination of Response Spectra for Design Earthquakes

In this section, determination of the regional and local geology for the site of the installation is discussed first. Special emphasis is placed on the regional geologic evidence of seismic activity because it can be used to estimate the probable magnitudes, locations, and frequencies of seismic events. Determination of the historic seismicity for the site is discussed. Determination of earthquake magnitudes on the selected faults is discussed. Then, estimation of the maximum accelerations for the site using the empirical formula for attenuation of earthquake acceleration versus distance and the Monte Carlo technique with random numbers is discussed. Finally, determination of the response spectra using the scaled actual earthquake response spectra compiled by the California Institute of Technology, Pasadena, California, is discussed.

The strength of the earthquake is measured by an intensity scale of the Richter Magnitude scale. The intensity scale is a subjective measure of the effects of an earthquake. It refers to the degree of shaking at a specified place. Intensity determinations can be heavily influenced by the site conditions and type of construction. Over the years, many scales were developed by different individuals, notably by Mercalli and by Rossi-Forel. The most widely adapted one is the Modified Mercalli (MM) scale. It has twelve grades denoted by Roman numberal I-XII.

On the other hand, the Richter Magnitude (M) scale is defined by the equation

$$M = \log (A/A_o) \leq 8.9 \qquad (1)$$

where M = Richter Magnitude

A_o = Recording on a standard Wood-Anderson Seismograph with 1/1000 mm amplitude.

A = Peak amplitude from the recording on a standard Wood-Anderson Seismograph at 100 km from the earthquake center.

The Richter Magnitude scale measures the energy released from the earthquake. Because it is a log scale, a magnitude 8 earthquake releases about 32 times more energy than a 7 earthquake.

Regional Geology

Geologic evidence of seismic activity of a region is valuable in the evaluation of the seismic risk for a given site. This information can be used to estimate the probable magnitudes, locations, and frequencies of future seismic activities in the area. Moreover, by knowing the type of movement along a given fault, some characteristics of the ground motions may be predicted.

Regional earthquake geology involves the study of Tectonic deformations, deformation of the rock structure from the deep-seated crustal and sub-crustal forces in the earth. The purpose of such study is to determine the nature, position, age, and movement history. The main geological features studied are warping, tilting, faulting, and tectonic structure. Faulting generally receive most of the attention. Because of its relevancy to earthquake engineering, only faulting will be discussed.

The main features of faulting pertinent to earthquake engineering are location, activity, and type.

Maps showing the location of faults can generally be obtained from the State's Division of Mines and Geology, oil or water company doing exploratory work, or U. S. Geodetic Survey. However, such maps are generally incomplete. The source of energy release from an earthquake may be under a thick layer of soft soils. Consequently, no evidence of surface faulting can be seen from such an earthquake. Therefore, inference, interpolation, or extrapolation from a fault map may be necessary to determine the locations of the faults in the vicinity of the site.

A fault is considered active if it is known to be associated with an earthquake during historic times. A potentially active fault is one that has had no historic seismic activity, but has shown evidence of activity during the last 35,000 years. When in doubt about the activity of a fault, assume it to be potentially active for conservatism.

The four types of faults that should be considered in a regional geology study are:

(1) Low-angle compressive, underthrust faults.
(2) Compressive, overthrusting faults.
(3) Extension faults.
(4) Strike-slip faults.

Apparently, the characteristics of strong ground motion in the vicinity of the causative fault can be influenced by the type of faulting. Large horizontal motions are associated with strike-slip faults. By contrast, large vertical motions are associated with the compressive, overthrusting faults.

A map showing portions of major faults near San Diego, California is shown in Figure 1. Many of the larger earthquakes are not associated with surface fault breaks. In the selection of faults in the vicinity of the site, be sure to include all those that are adjacent

to the site. Their exclusion would result in an underestimation of the maximum ground acceleration for the site and, hence, the damage.

Local Geology

As mentioned earlier, the primary effect of the local geology is its influence on the dynamic amplification or attenuation of the earthquake ground accelerations and its frequency content.

The depth of the soil overlaying bedrock affects the dynamic response and natural period of the ground. At distances less than or equal to 25 km from the earthquake source, the peak ground accelerations for alluvium sites and intermediate sites are 0.60 and 0.75, respectively, times that for rock sites [8]. By contrast, at distances between 26 km and 50 km, the peak ground accelerations for alluvium sites and intermediate sites are 1.09 and 1.16, respectively, times that for rock sites [8]. Furthermore, the natural period of the site increases with soil depth. The natural period determines frequency of the waves filtered out by the soil and relates to the amount of soil-structure interaction.

The effects of soil-structure interaction is illustrated by the response spectra in Figure 2 for alluvium, intermediate, and stiff (rock) sites. The peak ground acceleration is one. From the curves in this figure, it can be seen that the dynamic response of structures located in rock sites peaks at a period of about 0.15 second and decreases with increasing periods thereafter. The location of the maximum structural response is caused by the resonance effect of the structure with the site. The apparent site period is about 0.15 sec.

On the other hand, the location of the maximum response for structures located in alluvium and intermediate sites is at about 0.3 sec., the approximate natural period of these sites. At periods greater than 0.3 sec., the structural response for the alluvium and intermediate sites tends to greatly amplify the earthquake motions in the longer period range. Because it is softer, the response of structures in alluvium sites are larger than those for the rock site. This is because of the softer alluvium and intermediate sites in this range.

The topography of the bedrock and soil deposites has various effects on the seismic ground waves such as reflection, refraction, focusing, and scattering. It is possible that local geological features such as hidden irregularities in the bedrock topography may have caused the unexplained difference in response observed at two nearby sites in 1971 San Fernando earthquake. Accelerations of 0.21g and 0.11g were recorded at two locations at the California Institute of Technology campus. The local soil profiles at both locations were considered identical.

A ridge is another topographical feature that may affect the structural response. Magnification of basic bedrock motions may occur at these locations.

Soil failures which may result in liquefaction of the soil and/or differential settlement of the building are beyond the scope of the rapid seismic analysis procedure and are not considered.

Historical Seismicity

Background data on the historic seismicity of the site may be obtained from local officials, engineers, seismologists, local building regulations, published papers, and reference books. All earthquakes with magnitudes greater than or equal to 4 should be included in the data compilation. The reliability of the earthquake frequency predictions increases with the amount of data available.

A recurrence curve showing the number of earthquakes per year for a given area versus magnitude is prepared from the historical data. The resulting equation is expressed in log linear form,

$$\log n = a - bM \qquad (2)$$

where

n = recurrence interval in no. of events of magnitude M per year

a, b = empirical constants

For instance, the information required for Southern California area is available in reference 9. The curve for San Diego is shown in the middle of the top of Figure 3 and has a "b" constant of 0.92. Incidentally, the b constant in Figure 3 is the inverse function of the seismic activity of a region. The corresponding b constant for the western and eastern United States are 1.14 and 1.38, respectively. It is of interest to note on this curve that an earthquake of about 4 magnitude can be expected once a year in the San Diego area. However, it is very difficult to accurately predict the seismicity for a particular site, especially when historic seismic data are lacking.

Determination of Magnitude on Faults

Based on the data available, the maximum credible earthquake on the selected faults is determined from the relationship between earthquake and the length of slipped faults, Figure 4 [10,11]. The bilinear curve in the figure can be expressed as

For $L < 6.6725$ miles,

$$M = \ln L + 4.006 \qquad (3)$$

and for $L = \geq 6.6725$ miles,

$$M = 0.5 (\ln L + 10.7019) \qquad (4)$$

where M = earthquake magnitude

L = length of slipped fault in miles

The maximum earthquake magnitudes for the faults can be obtained by substituting the fault lengths into Equations (3) and (4).

Next, Equation (2) is rearranged into the following forms,

$$a = \log n + bM \qquad (5)$$

$$M_n = \frac{a - \log n}{b} \qquad (6)$$

$$M_{25} = \frac{a + 1.40}{b} \qquad (7)$$

where n = earthquake frequency (events/year)
M_{25} = magnitude of the 25 year earthquake

Equations 5 to 7 are used to determine the constant a and the 25 year earthquake magnitude, M_{25}.

An earthquake frequency n (either obtained from studies by seismologists or assumed) is assigned to each of the selected faults. The assigned frequency is substituted into Equation 5 to determine the constant a. The validity of a is then checked by substituting it into Equation 6 and computing the known earthquake magnitudes associated with the fault in the past. If the computed earthquake magnitudes are too large or small, the assumed frequency is adjusted and the whole process is repeated. When a satisfactory value is obtained, it is used in Equation 7 to compute the 25-year earthquake magnitude. For faults where seismic event data are lacking, judgment must be used to determine a reasonable value.

Examples:

1. San Andreas fault, one 8.0 in 100 years.

$$a = \log 0.1 + 0.93\,(8.0)$$

$$= -2.00 + 7.44$$

$$= 5.44$$

$$M_{25} = \frac{5.44 + 1.40}{0.93} = 7.35$$

2. Newport-Inglewood fault, one 6.2 in 100 years

$$a = \log 0.01 + 0.93\,(6.2)$$

$$= -2.00 + 5.77$$

$$= 3.77$$

$$M_{25} = \frac{3.77 + 1.40}{0.93} = 5.56$$

Next, the 90% probability acceleration level according to the NAVFAC criteria is computed.

Maximum Acceleration

The maximum ground acceleration from an earthquake along one of the nearby faults is an important parameter used in the estimation of structural response and damage at the site. In addition to this parameter, the duration of the earthquake motion and its frequency content are the other determining parameters in estimating the structural response and associated damage that may occur at the site.

The duration of the earthquake motion is a function of its magnitude while the earthquake magnitude depends on the energy release at the earthquake source. Relationships proposed by Housner [10, 11] between magnitude and duration, magnitude and maximum acceleration, and magnitude, distance to fault, and maximum acceleration are shown

in Figure 5. The upper curve in Figure 5 is used to determine the duration of earthquake acceleration. Understandably, for a given maximum acceleration, the potential damage to structures at a site increases with the duration.

As the maximum earthquake acceleration propagates from its source, its amplitude attenuates with increasing distance from the source. The amount of attenuation depends on a great many factors including the physical properties of the propagation medium and the actual path traveled. There are many empirical formulas for estimating the attenuation of the earthquake acceleration with distance from the source. An illustration of the variation in results that can be obtained from such a formula is given in Figure 6.

For the rapid seismic analysis procedure, the maximum ground acceleration according to the NAVFAC criteria is determined by using the Trifunac-Brady empirical relationship for the intermediate soil condition and the Monte Carlo method.

The Trifunac-Brady empirical relationship [reference 12] is based on the analysis of the voluminous earthquake ground motion data available to the California Institute of Technology (Cal Tech). This formula gives very large accelerations for earthquakes close to the site. These large values are caused by the lack of data for distances closer than 20 km and the large scatter of the data points for the range. Moreover, only a few data points are available for distances closer than 20 km from the source. To obtain more reasonable accelerations for earthquakes close to the site, CEL has modified the formula to use the focal distance instead of the epicentral (horizontal) distance from the earthquake source. This modification reduces the maximum accelerations from earthquake on nearby faults somewhat but have negligible effect on the maximum accelerations from earthquake far away.

To compute maximum accelerations at the site according to the NAVFAC criteria, CEL has developed a computer program CEL3, that incorporates the Trifunac-Brady empirical relationship and the Monte Carlo method for determining the maximum acceleration with 90% probability of not being exceeded in a 25-year period.

Briefly, the range of the 25-year earthquake magnitudes (M_{25}), the range of horizontal fault distances to the site (shortest to longest), the range of focal depth, the soil type, and the number of samples are input into the program. Generally, 1000 samples are specified to assure a good statistical distribution. The computer program varies the range of input parameters at random for each sample with the aid of a random number generator and computes at the maximum acceleration and keeps track of the number of occurrences at each acceleration level.

Example output from the computer program CEL3 for the San Andreas fault near San Diego is given in Table 3.

The 90% probability acceleration levels for a site is determined from the output. From similar tables, the controlling near field earthquake and the far field earthquake are determined.

The reason for selecting a far and near field earthquake for the development of the site response spectra is that the former is generally more damaging to structures with longer natural periods and the latter is more damaging to shorter period structures.

Furthermore, the computed 90% probability acceleration level for near and far field earthquakes may have to be adjusted before they can be used in the development of the site response spectra. The maximum acceleration for the near field earthquake, for instance, was reduced by one-third because typical earthquake acceleration records generally contain very few peaks greater than two-thirds times the maximum acceleration as illustrated in the acceleration records shown in Figure 7. There are 5 and 7 peaks above 2/3 times the maximum value, respectively for the upper and lower curves. Moreover, the duration of the near field earthquake may be relatively short in some instances and its damage potential is smaller than that from the longer duration far field earthquake. Because of the relatively long duration of the far field earthquake, a much smaller reduction was used.

A plot of the probability versus maximum acceleration for the 25-year earthquake at a Navy site in San Diego is shown in Figure 8. In this figure, the probability of being exceeded is plotted on the vertical axis and the maximum acceleration is plotted on the horizontal axis. The data for this curve were obtained by normalizing the results from the Monte Carlo program for the San Andreas fault for 10% probability of occurrance to 0.066g's. From the curve in the figure, it can be seen that there is 100% probability that the maximum acceleration at the site will be greater than 0.022g. The return period acceleration at the site will be greater than 0.066g. The return period for this 0.066g accelertion is 250 years (25 years/0.10). Furthermore, the shape of the curve is essentially identical for other faults.

Response Spectra

The response spectra determined for the site is a composite of the spectra from the near and far field earthquakes. The response spectra for each of the earthquakes were obtained by scaling selected spectra from the Cal Tech earthquake data records [13] which are available in both printed form and in magnetic tapes. The reference contains the following information:

Vol II - 987 corrected accelerogram records

Vol III - Response spectra for 987 corrected records of Vol. II.

The printed information in Volume III was recorded on Cal Tech's master tapes NIS159 and NIS160. The information in these tapes was processed by a CEL computer program, CEL4, to:

(1) Compute epicentral distance from coordinates of the recording stations and epicenters.

(2) Order all events according to the duration of the earthquake.

(3) Order all events according to the epicentral distance.

Unfortunately, the durations recorded on the tapes were the total recorded durations of the earthquakes and not the durations of the strong-motion phase. Hence, the events order according to duration were useless.

The response spectra from the Cal Tech tape used in the development of the site spectra were selected according to similarity in soils at the recording site, magnitude, and epicentral distances.

This selection criteria automatically includes the effects of strong-motion duration. With very few exceptions, a set of response spectra that requires a scaling factor larger than 2.5 to 3.0 is rejected. This is done to ensure the satisfaction of the similarity criteria.

The selected response spectra were scaled and plotted by program CEL5. To minimize confusion between data for different curves, no more than six spectra curves are plotted on each plot. A sample plot of the far field response spectra data is shown in Figure 9. A curve covering most of the data is drawn for each spectra plot for a given damping. Then, the corresponding spectra from different plots for the same damping ratio are combined to form the final plot. Finally, the corresponding near field and far field spectra are combined to form the composite spectra for the site.

The resulting composite response spectra for the San Diego Navy site is given in Figure 10. Curves are given for 0, 2, 5, 10, and 20% of critical damping.

Estimation of Yield and Ultimate Capacities

Upon completion of building selection, notes and construction drawings obtained were used for the analysis of the selected buildings. These materials were reviewed. Rough sketches were made of typical plans and elevations to determine the primary lateral force-resisting system or systems of each building.

The weight of the building is approximated by assuming unit loads for roof framing, floor framing, walls, actual live loads (if any), and other miscellaneous items. The base shear capacities are then estimated for each direction of motion, viz., transverse and longitudinal. The procedures used for computing the base shear capacities varied for the different types of buildings.

To facilitate the computation of the yield and ultimate capacities from the primary lateral force-resisting elements of a building the following descriptions of the failure sequence of these elements in different buildings are given below.

The yield capacity of a building is defined as the lateral force required to cause the yielding of the most rigid lateral force-resisting element in the building. By contrast, the ultimate capacity of a building is defined as the lateral force required to cause yielding initiation of the most flexible lateral force-resisting element of the building.

For example, a steel building with a lateral force-resisting system consisting of infill brick walls and X-brace may behave as follows. The brick walls and the X-braces may work together to resist the seismic forces until cracking of the brick walls is initiated. Then the X-braces and columns (only after the yielding of the X-braces) will take more and more of the seismic loading until they fail. For concrete frame buildings with shear walls, the shear walls will resist most of the seismic loading until they start to yield (crack). Thereafter, the frame will start to resist a small portion of the loading. Wooden frame buildings will behave like to concrete frame and shear wall buildings.

General descriptions of the procedures of estimating the yield and ultimate capacities of steel, concrete, wooden, and masonry buildings are given in reference 14.

After computing the weight and shear capacities for the buildings, the base shear coefficients are then computed by dividing the base shear capacity by the weight of the building. The base shear capacity coefficient is then converted to a spectral acceleration capacity by multiplying by a constant. This constant is 1.0.

Estimation of Natural Periods

The natural period for the buildings was determined by using the theoretical formula for a single degree-of-freedom system, using the Uniform Building Code formula modified by a constant, assuming a spectral displacement, or using a computer program developed by CEL for multi-story buildings (CEL8).

The natural period for a single degree-of-freedom system at yield can be computed from the formula

$$T_y = 2\pi \sqrt{\frac{m}{k}} \quad \text{(sec.)} \qquad (8)$$

where m = seismic mass, the mass of the building above the midheight of the first story

k = stiffness of the building in the direction considered by summing the contribution from the lateral force-resisting elements

For design purposes, the natural period of the building is often from

$$T' = \frac{0.05\ h_n}{\sqrt{D}} \quad \text{(sec.)} \qquad (9)$$

where h_n = height of the building (ft.)

D = base dimension of the building in the direction considered (ft.)

Note that this equation contains no stiffness or mass terms. It was derived empirically from the small vibration data for concrete frame and steel buildings and for use with the UBC criteria. It generally gives natural periods that are lower than the actual to provide conservative design base shear coefficients according to the UBC seismic criteria. For the rapid seismic analysis, this formula is modified by a constant depending on the building construction to account for variation in stiffness and weight per unit volume of the particular type of building.

The spectral displacement S_d' is related to natural period T and spectral acceleration capacity S_a for a single-degree-of-freedom system according to the following formula:

$$S_d' = 9.79\ T^2\ S_a' \quad \text{(in.)} \qquad (10)$$

where S_d' = spectral displacement (in.)

T = natural period (sec.)

S_a' = spectral acceleration (g's)

Equation (10) is useful for checking the assumed natural period for a building. If S_a' is known, the natural period can be determined by assuming a spectral displacement from

$$T = \sqrt{\frac{1}{9.79}\frac{S_d'}{S_a'}} = 0.32\sqrt{\frac{S_d'}{S_a'}} \qquad (11)$$

For multi-story buildings, CEL has developed a computer program, CEL8, for computing fundamental period and mode shape iteratively. The ductility factor, and masses and stiffness at the various floor levels are input into the program and the program does the rest. A sample output from the program is given as Table 5.

$$\frac{T_u}{T_y} = \sqrt{\mu \frac{S_{ay}'}{S_{au}'}}$$

where μ = ductibility factor, the ratio of the ultimate to yield deflections

S_{ay}' = spectral acceleration capacity at yield

S_{au}' = spectral acceleration capacity at ultimate

By selecting an appropriate μ and knowing S_{ay}' and S_{au}', the T_u/T_y ratio can be determined. However, the earthquake damage would be underestimated if the assumed ductibility is larger than that can be developed by the structural system.

Procedures for using the formulas and computer program presented above for steel, concrete, wood and masonry buildings are described in reference 14.

For a more precise computation of the natural period of the building, CEL has developed a computer program CEL7 for computing the equivalent stiffness of shear wall with cut-outs.

Briefly, the Young's modulus, thickness, configuration, and dimensions of the piers are input the program. The program then computes the equivalent stiffness for the combinations specified. An example output from the program is given in Table 4.

The individual stiffness of the shear walls in each direction can then be added and used in program CEL8 to determine the natural period of the building. An example output from the program for a 6-story building is given in Table 5.

Overestimating the natural period may have a completely different effect on the damage estimate, depending on the natural period of the building and the shape of the response spectra. If the estimated natural period is less than 0.3 sec. (0.15 sec. for rock sites), the predicted acceleration demand and hence damage on the building would be greater than the actual. If the estimated period is greater than 0.3 sec., the predicted damage would be less than actual. The converse of the above holds for underestimating the natural period.

Estimation of Damage From Response Spectra

To estimate the amount of damage a building experiences from an earthquake, damage must first be defined. Until the yield capacity of the building is reached, damage is assumed to be zero and the ductility factor equal to one. When the ultimate capacity is reached, damage is assumed to be 100%. For intermediate values of capacity the assessment of damage is assumed that the damage varies linearly

between the yield limit, S_{ay}', and ultimate limit, S_{au}' as shown in Figure 11.

Another assumption that must be made to estimate damage is the amount of damping applied to the response of the structure. Damping is related to a form of internal energy absorption of the building during its response to the earthquake ground motions. Damping is assumed to be a constant up to the yield capacity of the building. Above the yield capacity, the energy absorption capacity of the building increases because of inelastic response. The assumed damping is increased to reflect the increase in energy absorption. The assumed damping values for the different types of buildings are given in Table 1. Moreover, damping was assumed to vary linearly between the yield and ultimate limits of the building.

The NAVFAC criteria earthquake response spectra for 0, 2, 5, 10, and 20% of critical damping for San Diego, California Naval Station used for determining the damage estimates were presented in Figure 10.

The procedure for estimating damage is based on the reconciliation of the building in relation to the period and damping. The procedure is illustrated graphically in Figure 11. The capacities of the building are identified by the open circles. The corresponding demands for the site are identified by the black dots. The intersection of the lines drawn through the two sets of points determines the estimated damage, 50.5%.

For each building, the damage is computed for each of the principal directions of motion, longitudinal and transverse. To determine the combined damage for the two directions, it is assumed that one-third of the building depends on each direction of lateral resistance and the remaining one-third depends on both directions for lateral resistance. That is, if a structural element requires both directions for lateral resistance is damaged by one direction of motion, it is also damaged in the other direction. The procedure takes two-thirds of the damage of the more critical direction than one-third of the damages are 60% and 30% in the two principal directions, the combined damage is 50%.

To reduce the amount of time required to determine damage estimates, CEL has developed a computer program CEL9 for determining the damage estimates. The response spectra is digitized and input into the program together with the building identifications, costs, damping values, natural periods, and capacities. The program then computes the damage estimate for the NAVFAC criteria. In addition, the program computes the damage estimates for maximum ground accelerations between 0.05 and 0.50g increments.

The replacement cost of the selected buildings was obtained from the inventory listed for the installation generated by the computer program at FACSO.

The damage cost is computed by multiplying the replacement cost of the building by the precent damage. An example computer printout of the damage estimate of a seven-story building is shown in Table 6.

Accuracy

As mentioned earlier in the introduction, the purpose of the rapid analysis procedure is to determine earthquake damage estimates. Approximations were made at each step of the analysis. These approximations have been added and multiplied into the results. Theoretically, large discrepancy between the predicted and actual values may occur. However, checks were made at each step of the procedure to minimize potential inconsistencies. These checks were based mainly on engineering judgment and included in comparisons between different buildings and comparisons with data from other studies. A discussion of the accuracy of the various segments of the procedure follows.

Response Spectra

In our opinion, the response spectra developed for San Diego Navy site are reasonable estimates of the ground-motion effects from the 25-year earthquakes.

Variation in Site Characteristics

The use of about twenty earthquake response spectra records from different sites to develop the response spectra should cover the possible effects that the variation in the local soil characteristics would be no greater than the uncertainties associated with the earthquake criteria and analysis criteria.

Structural Analysis

Approximate methods were used to determine the capacity limits of the buildings. Only the primary lateral force-resisting elements were analyzed, assuming that the supporting elements and secondary elements were adequate. Stress and deformation capacities had to be assumed, but the actual values can have a wide range of variation. Steel has the smallest range of variation, but it can be about 20%. By contrast, wood, concrete and masonry have a large range of variation due mainly to difference in age, workmanship and original quality. Furthermore, capacities of connections can have a wide range of variation. In some cases, the exact details of the connections were not available. In addition, non-structural elements contribute to the lateral force-resisting capability of the building. Although estimates can be made for the capacities of non-structure members, their range of variation is very wide.

Individually, the capacities of the elements that make up the lateral force-resisting system of the building can have a large range of variation. However, when combined, the conservatism or redundancy in some of the elements will balance some of the weakness and inadequacies in others. As a result, the overall building may be represented adequately by the aproximate model. Even a rigorous analysis is subjected to many uncertainties.

The computed natural period may vary greatly, depending on the assumptions made in the structural analysis.

The damping values used in the analysis are fairly representative of the state-of-the-art. In the inelastic range, effective damping may be higher than the values used. However, insufficient data is available to justify using higher values.

Damage Criteria

Actual damage costs for buildings from earthquakes are difficult to define. In addition to analytical evaluations, social and administrative decisions must also be considered. For example, suppose an old brick building develops some cracks during a moderate earthquake. A subsequent investigation indicated some uncertainty about the safe future use of the building. Three possible administrative decisions for the building are:

(1) Ignore the potential hazard and continue using the building for a number of years (i.e., the cracks are not serious enough to justify repairs).

(2) Rehabilitate the building to eliminate the potential safety hazards (repair the cracks and add some additional bracing and reinforcements).

(3) Demolish the building and build a new one to replace it.

In case (1), the damage cost is zero. In case (2), it may be 30% of the replacement cost. In case (3), it is 100% plus the demolition cost. The results of the rapid seismic analysis procedure do not consider such administrative decision, but would give a damage estimate of about 50%.

Other Computer Programs

The other Computer Programs developed by CEL for the rapid seismic analysis procedure include CEL2, CEL6, and CEL10.

Program CEL2 can be used to determine the maximum ground accelerations from the various empirical acceleration attenuation versus earthquake magnitude, site condition, and distance to fault formulas built into the program. It can be used to get an idea of the range of predicted accelerations for the site from earthquake on the surrounding faults.

Program CEL6 may be used to compute the stiffness and strengths for concrete masonry shear panels (piers) with cantilever and fixed conditions for a range of panel sizes with constant thickness.

Program CEL10 can be used to check the correctness of hand digitized response spectra data before it is input into computer program CEL9. It plots the digitized data using the CALCOMP plotter so that any errors made during the digitization can be spotted visually and appropiate corrections made.

References

1. John A. Blume and Associates, "Seismic Study of Puget Sound Naval Shipyard, Bremerton, Washington," Phases I through VI, A-E Contract N62474-71-C-4324, for Western Division, Naval Facilities Engineering Command, San Bruno, California, June 1974.

2. Naval Facilities Engineering Command, "Structural Engineering Workshop at San Francisco, CA," prepared by John A. Blume and Associates, Engineers, September 1973.

3. Civil Engineering Laboratory, Technical Memorandum M51-78-08: Earthquake hazard reduction program, North Island, Naval Air Station, San Diego, CA, by C. V. Chelapati, S. K. Takahashi, and T. K. Lew, Port Hueneme, California, April, 1978.

4. Dorwick, D. J., Earthquake Resistant Design, John Wiley & Sons, New York (1977).

5. Weigel, R. C. (Ed.), Earthquake Engineering, Prentice-Hall, Inc., Englewood Cliffs, New Jersey 1970.

6. Newmark, N. M., and Rosenblueth, E., Fundamentals of Earthquake Engineering, Prentice-Hall, Inc., Englewood Cliffs, New Jersey, 1971.

7. Blume, J. A., Newmark, N. M., And Corning, L. H., "Design of Multi-story Reinforced Concrete Building for Earthquake Building for Earthquake Motions," Published by Portland Cement Association, Chicago, Illinois, 1961.

8. Kiremidjian, A., "Probabilistic Hazard Mapping: Development of Site Dependent Seismic Load Parameters," Ph.D Dissertation, Stanford University (1977). Report 77-12, 655, University Microfilms International, Ann Arbor, Michigan.

9. Hileman, J. A., G. R. Allen, and Nordquest, J. M., "Seismicity of Southern California Institute of Technology, Pasadena, California, 1974.

10. "Report on NSF-UCEER Conference on Earthquake Engineering Research, March," University Council for Earthquake Research, Pasadena, California, May 1969.

11. Housner, G. W., "Strength Ground Motion" (Chapter 4), "Design Spectrum" (Chapter 5), Earthquake Engineering, Weigel, R. L., Ed., Prentice-Hall, Inc., Englewood Cliffs, New Jersey, 1970.

12. Trifunac, M. D., and Brady, A. G., "On the Correlation of Peak Acceleration of Strong Motion with Earthquake Magnitude and Epicentral Distance," Procedures of U. S. Natural Conference on Earthquake Engineering - 1975. Earthquake Engineering Research Institute, June 1975, Ann Arbor, Michigan, pp. 42-52 .

13. California Institute of Technology, "Strong Motion Earthquake Accelergrams," Vol. II and III. Earthquake Engineering Research Laboratory, Pasadena, California (EERL71-50), September 1971.

14. Civil Engineering Laboratory, Technical Memorandum M51-78-02, "Rapid Seismic Analysis Procedure," by Lew, T. K., and Takahashi, S. K., Port Hueneme, California, April 1978.

TABLE 1. ASSUMED DAMPING VALUES

Building Type	Percent of Critical Damping	
	At Yield Limit	At Ultimate Limit
Steel	2	5
Concrete	5	10
Wood	10	20
Masonry	5	10

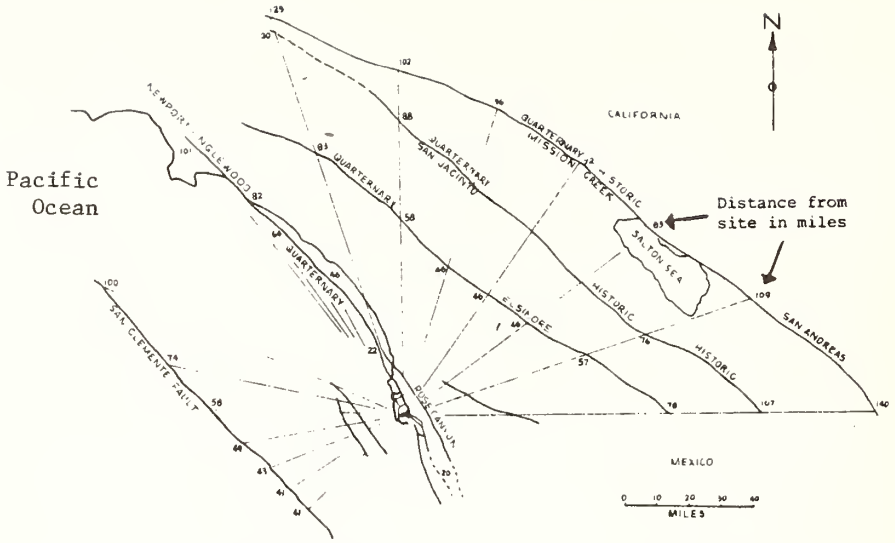

FIGURE 1. FAULTS USED FOR ESTIMATING GROUND ACCELERATIONS AT SITE OF NORTH ISLAND NAVAL AIR STATION.

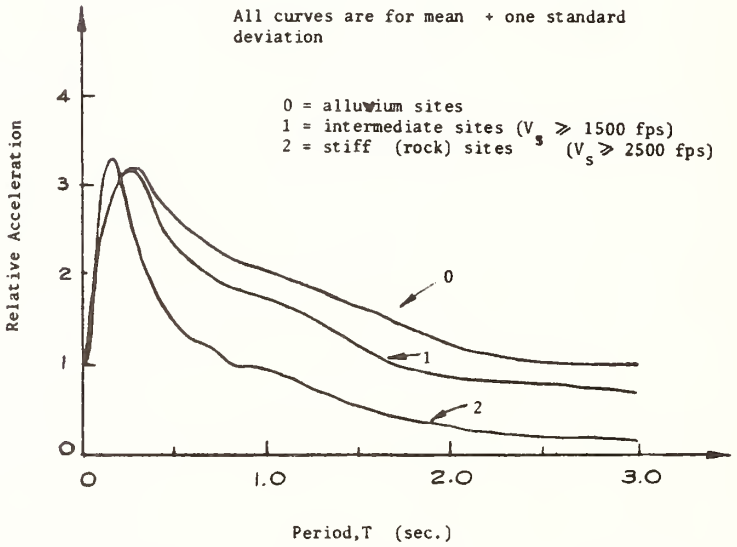

FIGURE 2. DYNAMIC AMPLIFICATION FACTORS (84 PERCENTILE, λ = 5%) FOR DIFFERENT SOIL CONDITIONS (AFTER REF. 8).

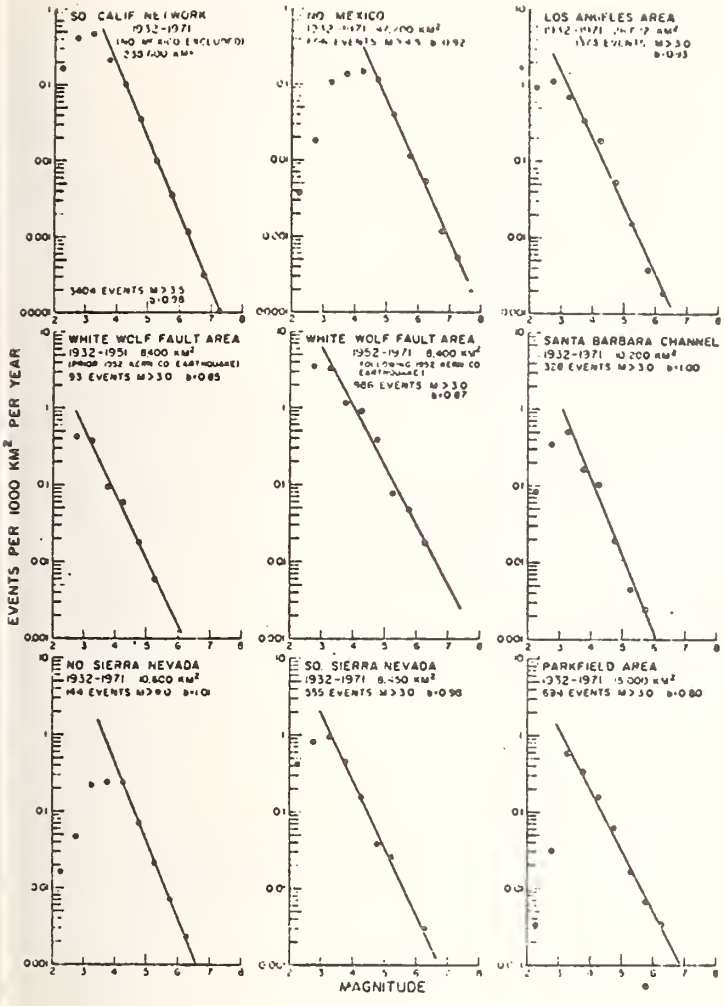

FIGURE 3. INTERVAL RECURRENCE CURVES FOR EACH OF THE AREAS SHOWN IN FIGURE 3.10. NOTE THAT THE ORDINATE SCALES ARE IDENTICAL FOR ALL CURVES EXCEPT FOR THE CURVES FOR THE SOUTHERN CALIFORNIA NETWORK AND NORTH MEXICO (FROM REF. 9).

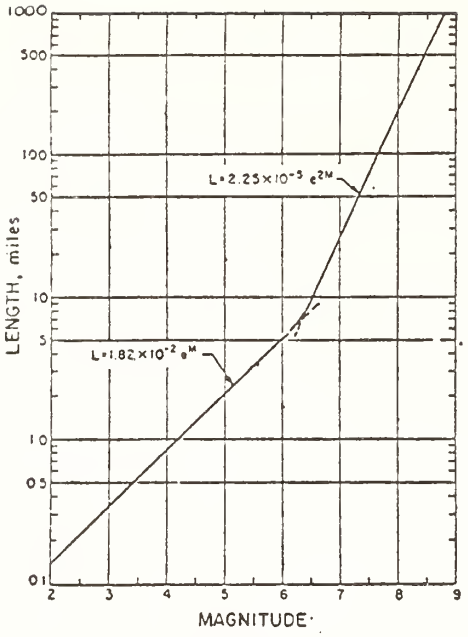

Idealized relation between length of slipped fault vs. Magnitude of earthquake.

IDEALIZED RELATION BETWEEN MAGNITUDE AND LENGTH OF SLIPPED FAULT

Magnitude	Length (miles)
8.8	1000
8.5	530
8.0	190
7.5	70
7.0	25
6.5	9
6.0	5
5.5	3.4
5.0	2.1
4.5	1.3
4.0	0.83
3.0	0.33
2.0	0.14(735')
1.0	0.05(270')
0	0.018(100')

INFERRED LENGTHS OF SLIPPED FAULT OF ACTUAL EARTHQUAKES

Earthquake	Magnitude	Length (miles)
Chile, 1960	8.5-8.6	600±
Alaska, 1964	8.4	450±
San Francisco, 1906	8.2	250±
El Centro, 1940	7.1	40±
Baja California, 1956	6.8	15±

FIGURE 4. RELATIONSHIPS BETWEEN EARTHQUAKE MAGNITUDES AND LENGTH OF SLIPPED FAULTS (FROM REF. 10 AND 11).

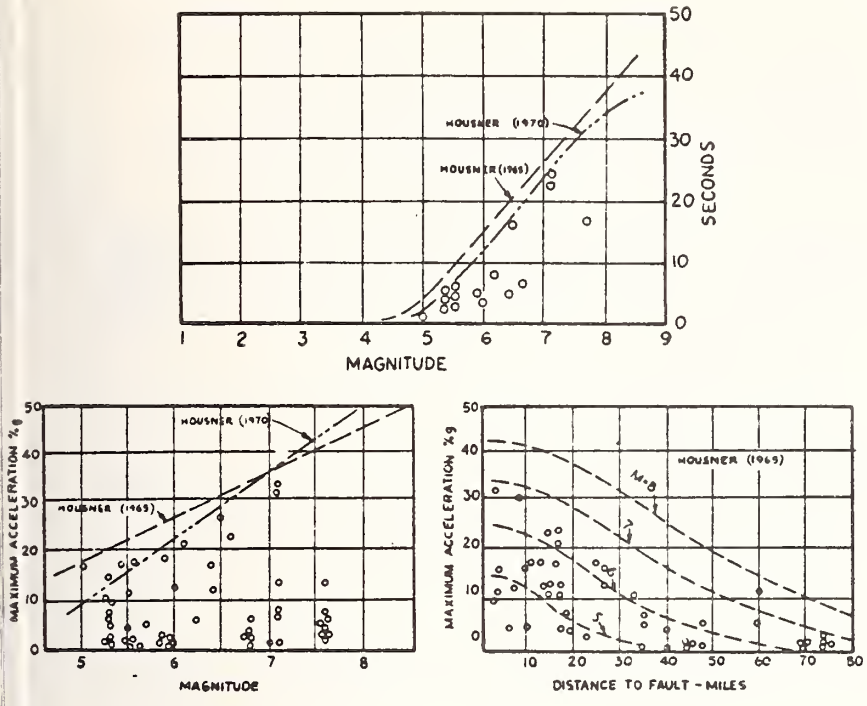

FIGURE 5. IDEALIZED RELATIONSHIPS BETWEEN MAGNITUDE, DURATION, ACCELERATION AND DISTANCE FROM FAULT FOR STRONG MOTION EARTHQUAKES (FROM REF. 10 and 11).

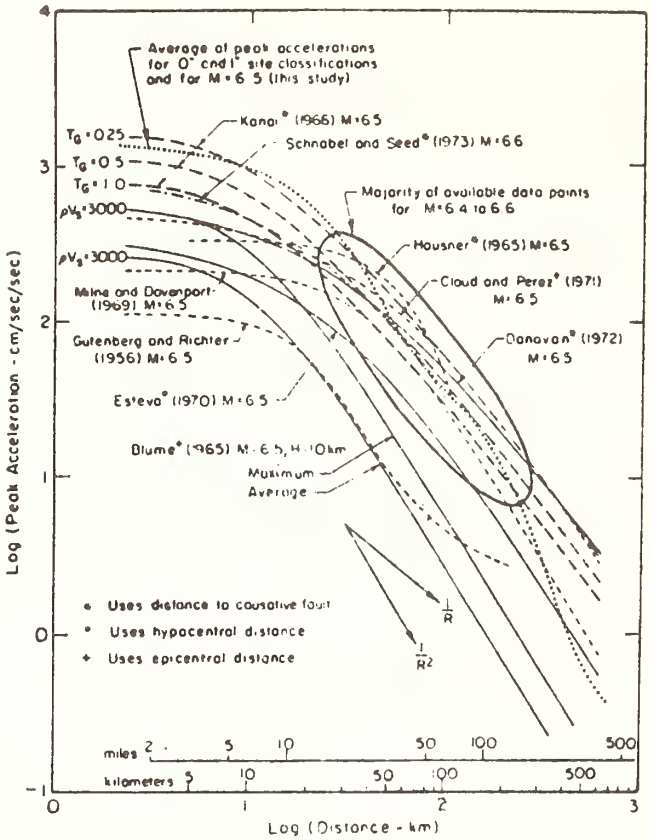

FIGURE 6. RELATIONSHIPS BETWEEN PEAK ACCELERATION AND DISTANCE FROM SOURCE FOR MAGNITUDE 6.5 EARTHQUAKES (AFTER REF. 12).

M = 6.5
Distance = 6.2 miles

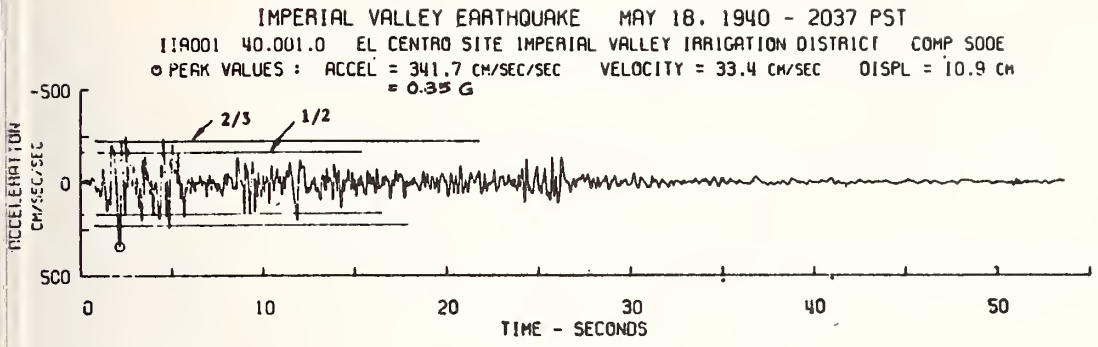

M = 7.7
Distance = 25.8 miles

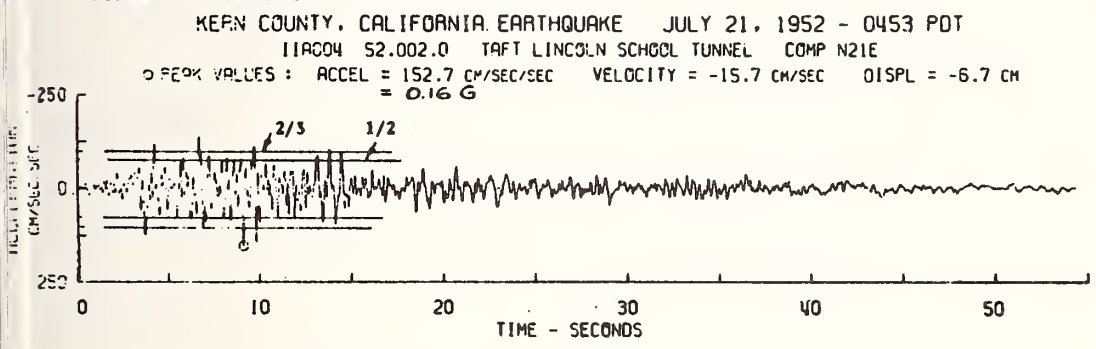

FIGURE 7. STRONG MOTION ACCELERATION RECORDS IN ALLUVIAL SITES FROM LARGE EARTHQUAKES.

35

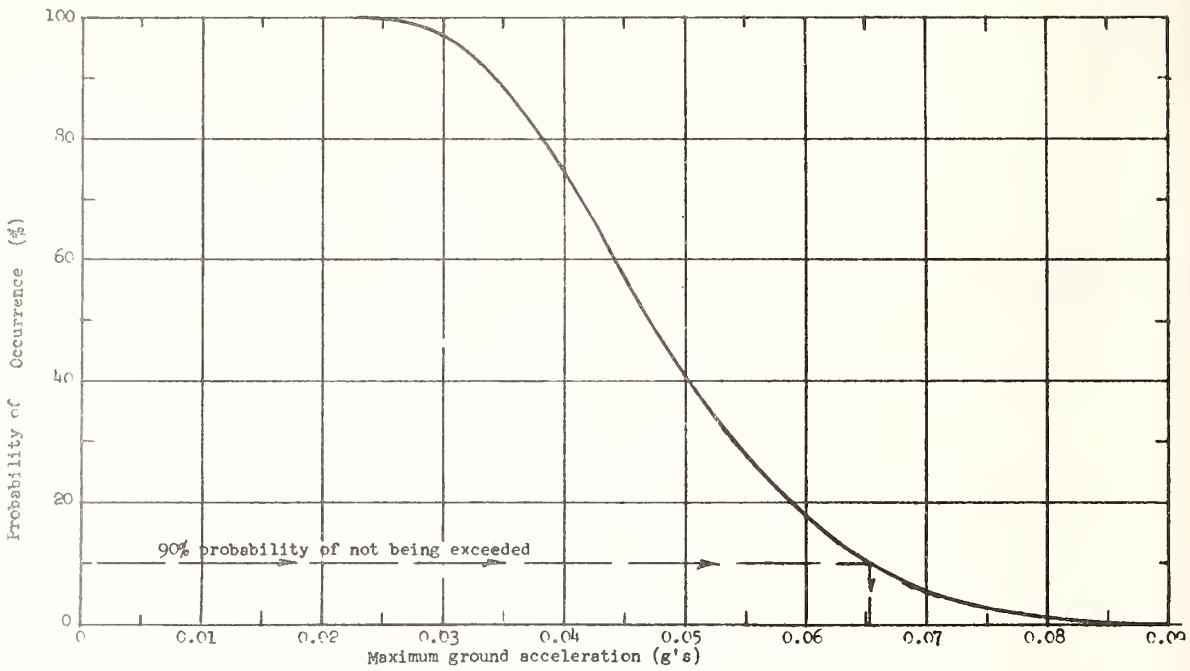

FIGURE 8. PROBABILITY VERSUS MAXIMUM GROUND ACCELERATION FOR 25 YEAR EARTHQUAKE, NAS, NORTH ISLAND, CALIFORNIA (SAN ANDREAS FAULT.

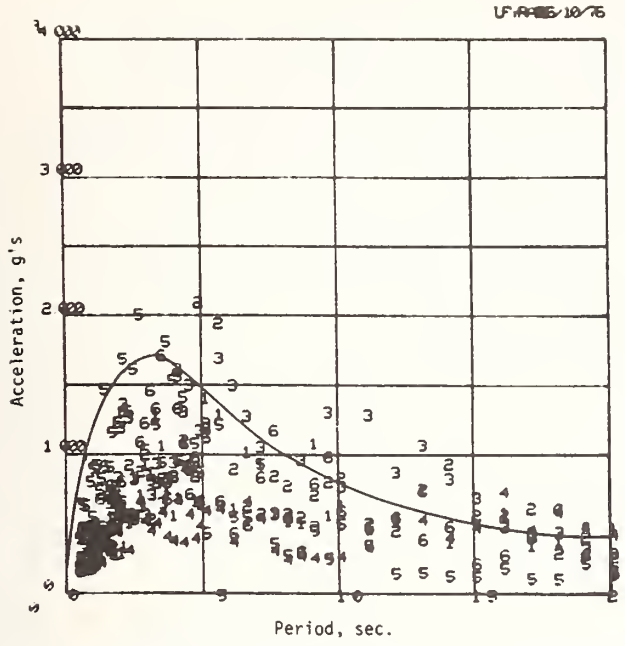

FIGURE 9. RESPONSE SPECTRUM PLOTS FOR 0% OF CRITICAL DAMPING FOR FAR FIELD EARTHQUAKE.

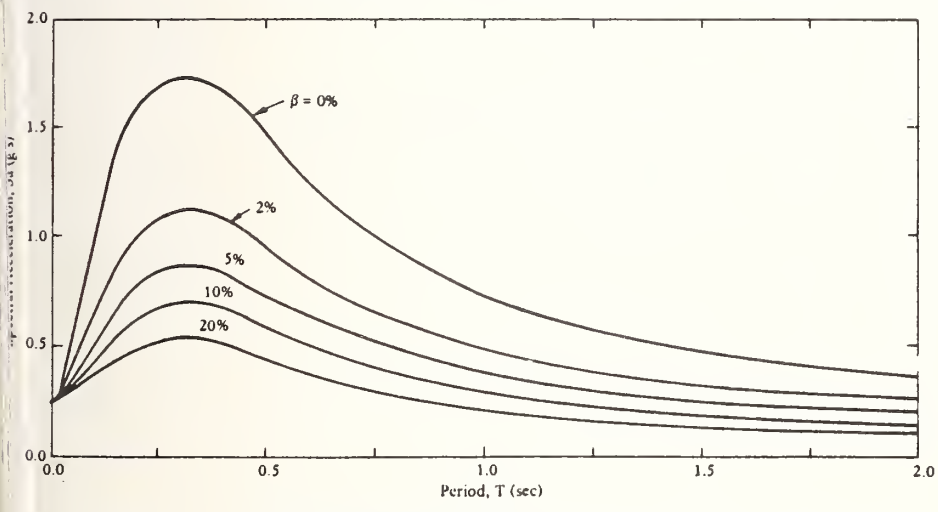

FIGURE 10. SITE RESPONSE SPECTRA FOR FACILITIES AT NAVAL AIR STATION, NORTH ISLAND.

35

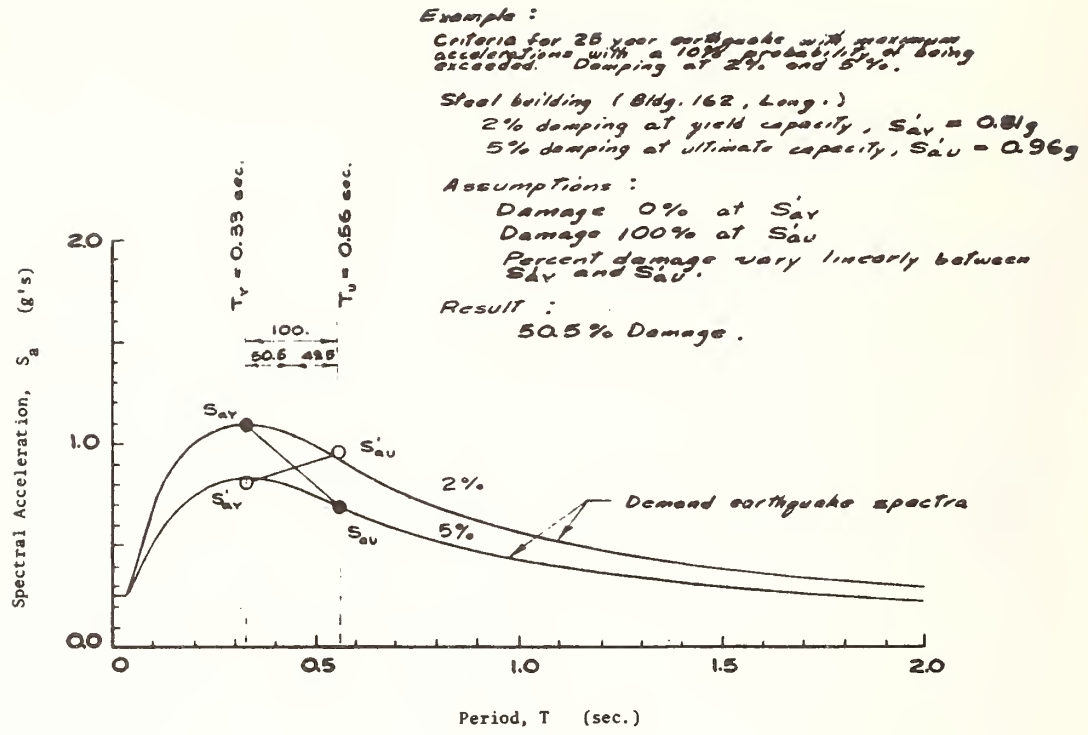

FIGURE 11. GRAPHICAL ILLUSTRATION OF DAMAGE ESTIMATES.

Table 2. DETAILED INVENTORY OF NAVAL SHORE FACILITIES

10 OCT 1975

SEQUENCE: (1) FIRST DIGIT CATEGORY CODE (2) REPLACEMENT COST (LARGEST)

AIR STATION, NORTH ISLAND NUMBER OF RUNWAYS... 2 (CLAIMANT..PACFLT)

CATEGORY CODE	DESCRIPTION																
15220	BERTHING WHARF	STRC	P	1945	19765.00SY	3325.00FB		3324	53	10		U100A	200026		1312	5697	2872[illegible]
11320	ACFT PRKG APRN	STRC	S	1945	1665446.00SY							U100S	201799	A35		2299	11284
11110	RUNWAY	STRC	P	1943	250000.00SY	7500.00LF		7500	300			U100A	201661			[illegible]38	[illegible]
12510	POL PIPELINE	STRC	P	1933		18.40MI						U100A	200010			705	[illegible]
11110	RUNWAY	STRC	P	1943	177778.00SY	8000.00LF		8000	200			U100A	201660			814	4717
11320	ACFT PRKG APRN	STRC	P	1944	398039.00SY							U100S	201767	A35		836	45[illegible]
11210	TAXIWAY	STRC	P	1952	374797.00SY	LF	X					U100A	201605			[illegible]	[illegible]
15120	GP BERTH PIER	STRC	P	1945	5955.55SY	800.00FB		800	67	9		U100A	201363		1310	630	[illegible]
13375	AIR RADAR BLDG	BLDG	P	1934	15174.00SF		X	222	56	35	1	U100A	200237		93'	492	3950
11320	ACFT PRKG APRN	STRC	S	1945	294895.00SY							U100S	201806	A35		579	[illegible]
17120	APPL INSTR BLDG	BLDG	P	1958	66310.00SF	MN	X	206	251	28	2	U100A	201403		678	1151	2651
11320	ACFT PRKG APRN	STRC	S	1945	195605.00SY							U100S	201808	A35		479	2350
13520	TELE LINES/OTHR	UTIL	P	1957		49.02MI						U100A	200003			934	2201
14179	TRANSIT SHED	BLDG	P	1945	127205.00SF		X	820	150	50	1	U100A	200474		651'	389	1903
13115	COMM CENTER	BLDG	P	1939	22074.00SF			122	82	27	3	U100A	200467		335	242	[illegible]07
12510	POL PIPELINE	STRC	P	1959		9.10MI						U100A	280026			740	1654
11320	ACFT PRKG APRN	STRC	S	1940	251587.00SY							U100S	201800	A35		232	1594
13630	RUNWAY LIGHTING	STRC	P	1944		20400.00LF						U100A	201758			290	1589

CONTINUED ON NEXT PAGE

35

Table 3. PROGRAM CEL 3, PREDICTION OF MAXIMUM ACCELERATION AT SITE USING MONTE CARLO PROCEDURES.

PREDICTION OF SEISMIC SEVERITY FOR MAP,SAN DIEGO SITE

ESTIMATION OF MAXIMUM GROUND ACCELERATION AT SITE WITH 90 PERCENT PROBABILITY OF OCCURRENCE USING MONTE CARLO PROCEDURES
EARTHQUAKES OCCURING WITH EPICENTERS ON SAN ANDREAS FAULT SYSTEM

RANGE OF MAGNITUDE 7.0- 7.5
RANGE OF DISTANCE TO FAULT 125.0- 90.0 MILES
RANGE OF FOCAL DEPTH 6.0- 10.0 MILES
CSD 1.00 CV= 0.00 PCL= .90

1	7.034	111,046	9,624	.033	7.089	96,624	9,506	.045	7,340	109,643	9,942	.052	7,258	109,567	9,177	.046
5	7.157	98,730	7,130	.047	7.130	120,631	9,531	.033	7,398	124,683	6,955	.046	7,411	106,885	6,989	.060
9	7.119	92,429	9,763	.049	7,223	110,869	8,280	.043	7,167	93,500	8,945	.052	7,429	112,111	9,600	.057
13	7.185	111,221	6,377	.041	7,398	119,921	6,202	.049	7,008	108,551	6,509	.033	7,176	105,434	6,051	.044
17	7.497	106,164	8,595	.068	7,322	113,557	8,289	.048	7,371	101,184	7,711	.061	7,278	102,852	9,690	.052
21	7.003	94,481	9,624	.046	7,478	111,529	7,112	.061	7,033	107,643	6,895	.035	7,482	116,146	9,538	.058
25	7.271	103,218	9,728	.052	7,331	113,875	9,389	.048	7,020	90,609	7,902	.049	7,194	106,753	7,363	.048
29	7.358	105,732	9,460	.056	7,106	102,323	9,578	.041	7,420	124,686	6,857	.048	7,173	97,728	6,667	.049
33	7.388	110,309	6,337	.055	7,358	96,593	9,625	.064	7,350	94,870	6,321	.066	7,018	108,391	8,509	.038
37	7.245	105,316	6,819	.051	7,211	102,851	8,913	.048	7,419	102,455	6,783	.064	7,457	111,994	7,197	.059
41	7.319	108,499	7,251	.051	7,009	119,112	7,992	.029	7,354	115,318	6,116	.049	7,059	112,067	6,485	.038
45	7.462	123,388	8,053	.051	7,307	121,810	7,632	.042	7,056	122,352	9,291	.029	7,048	118,770	6,377	.030
49	7.061	112,499	7,467	.030	7,197	95,212	6,982	.053	7,873	106,963	6,931	.065	7,266	104,990	6,436	.050
53	7.038	111,725	8,351	.033	7,197	110,636	7,424	.042	7,417	104,762	9,009	.062	7,224	116,993	6,581	.040
57	7.430	102,876	8,823	.065	7,380	124,789	6,532	.045	7,098	91,447	7,439	.050	7,412	111,644	9,719	.056
61	7.147	96,451	7,331	.048	7,448	124,074	7,884	.050	7,467	116,656	9,695	.056	7,343	103,621	7,557	.057
65	7.187	118,911	6,408	.037	7,220	91,558	8,831	.058	7,075	111,650	9,730	.035	7,094	95,263	7,185	.047
69	7.152	113,411	9,790	.038	7,395	91,818	7,993	.074	7,244	98,055	6,090	.054	7,217	103,885	8,965	.047
73	7.406	106,058	8,701	.060	7,157	96,452	9,746	.049	7,153	116,516	9,510	.036	7,199	93,321	7,751	.055
77	7.370	95,005	6,225	.068	7,231	114,693	7,080	.039	7,181	121,143	9,684	.035	7,145	96,419	9,026	.048
81	7.184	108,723	6,318	.043	7,079	98,502	9,482	.044	7,398	98,723	9,129	.070	7,448	112,995	8,213	.058
85	7.339	99,453	7,897	.060	7,176	91,333	6,848	.055	7,052	115,059	9,827	.032	7,407	114,970	7,840	.053
89	7.317	116,653	9,637	.046	7,377	111,792	8,391	.053	7,004	91,583	9,912	.048	7,128	109,796	7,006	.038
93	7.395	98,961	9,828	.070	7,153	107,915	9,834	.041	7,099	123,605	8,385	.031	7,039	124,621	9,143	.028
97	7.297	106,065	7,852	.051	7,481	117,560	7,706	.057	7,117	104,905	6,348	.041	7,206	97,878	6,849	.051
989	7.[illegible]	11[illegible].922	8,221	.047	7,[illegible].7	106,587	9,[illegible]82	.038	7,248	93,[illegible]2	7,652	.[illegible]8	7,498	91,969	7,071	.084
993	7.391	102,733	9,42[illegible]	.061	7,231	123,549	9,078	.037	7,[illegible]86	107,695	6,905	.066	7,[illegible]00	95,[illegible]18	7,748	.070
997	7.276	116,871	6,75[illegible]	.043	7,208	91,350	8,663	.057	7,048	103,926	7,703	.037	7,481	99,[illegible].5	9,738	.073

NUMBER OF TRIALS 1000
AVERAGE ACCELERATION AT SITE .049G
STANDARD DEVIATION .012G

Table 3. CONTINUED

PREDICTION OF SEISMIC SEVERITY FOR NAS,SAN DIEGO SITE

ESTIMATION OF MAXIMUM GROUND ACCELERATION AT SITE WITH 90 PERCENT PROBABILITY OF OCCURRENCE USING MONTE CARLO PROCEDURES
EARTHQUAKES OCCURING WITH EPICENTERS ON SAN ANDREAS FAULT SYSTEM

RANGE OF MAGNITUDE 7.0- 7.5
RANGE OF DISTANCE TO FAULT 125.0- 90.0 MILES
RANGE OF FOCAL DEPTH 6.0- 10.0 MILES
CS= 1.00 CV= 0.00 PCL= .90

1	0.00	1000	1.000
2	.01	1000	1.000
3	.02	1000	1.000
4	.03	974	.974
5	.04	747	.747
6	.05	417	.417
7	.06	178	.178
8	.07	56	.056
9	.08	12	.012
10	.09	0	0.000
11	.10	0	0.000
12	.11	0	0.000
13	.12	0	0.000
14	.13	0	0.000
15	.14	0	0.000
16	.15	0	0.000
17	.16	0	0.000
18	.17	0	0.000
19	.18	0	0.000
20	.19	0	0.000
21	.20	0	0.000
22	.21	0	0.000
23	.22	0	0.000
24	.23	0	0.000
25	.24	0	0.000
26	.25	0	0.000
27	.26	0	0.000
28	.27	0	0.000
29	.28	0	0.000
30	.29	0	0.000
31	.30	0	0.000
32	.31	0	0.000
33	.32	0	0.000
34	.33	0	0.000
35	.34	0	0.000
36	.35	0	0.000
37	.36	0	0.000
38	.37	0	0.000
39	.38	0	0.000
40	.39	0	0.000
41	.40	0	0.000
42	.41	0	0.000
43	.42	0	0.000
44	.43	0	0.000

← 10% probability of occurrence (0.065 or 0.07g)

35

Table 4. COMPUTATION OF EQUIVALENT STIFFNESS AND RIGIDITY CHARACTERISTICS OF WALLS WITH OPENINGS

COMPUTATION OF EQUIVALENT STIFFNESS AND DISPLACEMENT CHARACTERISTICS OF SHEAR WALLS

TOTAL PROB. = EQUIVALENT STIFFNESS OF SHEAR WALL WITH OPENINGS

MODULUS OF ELASTICITY, E = 2200.0 KSI

END CONDITIONS F IS PIERS

F = FIXED
C = CANTILEVERED

TYPE FOR COMBINING COMPONENT PIERS

P = PIERS IN PARALLEL
S = PIERS IN SERIES

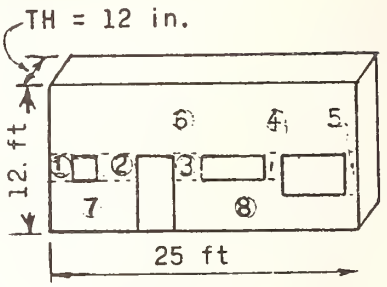

CHARACTERISTICS OF INDIVIDUAL PIER COMPONENTS

PIER	PIER NUMBER	END COND	HT FT	WIDTH FT	THICKNESS INCHES	AREA SQ IN	DELTA IN/KIP	RIGIDITY KIPS/IN	TOT RIG KIPS/IN
1	1	F	2.0	2.00	12.00	288.0	.0001515	6600.0	6600.0
2	1	F	2.0	3.00	12.00	432.0	.0000870	11494.2	11494.2
3	1	F	2.0	4.00	12.00	576.0	.0000616	16234.2	16234.2
4	1	F	2.0	5.00	12.00	720.0	.0000479	20886.1	20886.1
5	1	F	3.0	1.00	12.00	144.0	.0013536	733.3	733.3
6	1	C	4.0	25.00	12.00	3600.0	.0000294	34051.5	34051.5
7	1	C	4.0	7.00	12.00	1008.0	.0000932	10728.9	10728.9
8	1	C	4.0	15.00	12.00	2160.0	.0000332	30142.1	30142.1

TOTAL SHEAR AREA 8928.0 SQ INCHES

CHARACTERISTICS OF EQUIVALENT PIERS

PIER	NO IN GRP	TYPE	PIER NUMBERS IN GROUP								DELTA (IN/KIP)	STIFFNESS (KIPS/IN)
9	2	P	1	2	-0	-0	-0	-0	-0	-0	.0000553	18096.8
10	2	S	7	9	-0	-0	-0	-0	-0	-0	.0001485	6735.6
11	3	S	3	4	5	-0	-0	-0	-0	-0	.0000264	37865.6
12	2	S	8	11	-0	-0	-0	-0	-0	-0	.0000596	16782.6
13	2	P	10	12	-0	-0	-0	-0	-0	-0	.0000425	23518.2
14	2	S	6	13	-0	-0	-0	-0	-0	-0	.0000719	13910.6

Table 5. COMPUTATION OF FIRST MODE SHAPE, NATURAL PERIOD, SPECTRAL ACCELERATION CAPACITY. (CEL8)

NAS SAN DIEGO BLDG 783 BEQ TRANSVERSE

COMPUTATION OF FIRST NATURAL MODE AND FREQUENCY AND PARTICIPATION FACTOR

TRIAL NO. 1

WEIGHT	(KIP)	600	600	600	600	600	600	500	
MASS (IN KP UN)		1.553	1.553	1.553	1.553	1.553	1.553	1.294	
STIFFNESS (KP/IN)		121900	121900	121900	121900	80950	80950	48200	
XA	(A)	.112	.219	.318	.404	.544	.641	.700	
M*XA	(A*2)	1.715E-01	3.382E-01	4.875E-01	6.194E-01	8.343E-01	9.833E-01	9.058E-01	
F	(A*2)	4.338E+00	4.186E+00	3.830E+00	3.343E+00	2.723E+00	1.889E+00	9.058E-01	
FOR	(A*2)	3.559E-05	3.559E-05	3.559E-05	3.559E-05	3.559E-05	3.559E-05	3.559E-05	
XD	(A*2)	3.559E-05	6.977E-05	1.012E-04	1.286E-04	1.733E-04	2.043E-04	2.231E-04	
XDN	(A*2)	.112	.219	.318	.404	.544	.641	.700	3137.891

CIRCULAR FREQUENCY 56.02 RADIANS/SEC
NATURAL FREQUENCY 8.92 CYCLES/SEC
NATURAL PERIOD .11 SECONDS

NORMALIZED FIRST MODE SHAPE

INDEX	1	DISPLACEMENT	.075
INDEX	2	DISPLACEMENT	.146
INDEX	3	DISPLACEMENT	.212
INDEX	4	DISPLACEMENT	.270
INDEX	5	DISPLACEMENT	.304
INDEX	6	DISPLACEMENT	.429
INDEX	7	DISPLACEMENT	.466

TOTAL SHEAR AREA 20660.000 SQ IN

YIELD STRESS .070 KSI
ULTIMATE STRESS .100 KSI

FIRST FLOOR SHEAR CAPACITY AT YIELD (KIP) 1446.200
FIRST FLOOR SHEAR CAPACITY AT ULTIMATE (KIP) 2066.000

DUCTILITY FACTOR 2.0

PARTICIPATION FACTOR,FIRST MODE 2.929
TOTAL WEIGHT OF BUILDING 4100.0 KIPS
FIRST MODE BASE SHEAR FACTOR 1.248
SPECTRAL YIELD CAPACITY .440 GS PERIOD AT YIELD .11 SECONDS
SPECTRAL ULTIMATE CAPACITY .629 GS PERIOD AT ULTIMATE .13 SECONDS

35

Table 6. PROGRAM FOR ESTIMATING EARTHQUAKE DAMAGE. (CEL9)

DAMAGE ESTIMATES FOR VARIOUS LEVELS OF EARTHQUAKE

SITE NORTH ISLAND NAVAL AIR STATION SAN DIEGO

BLDG TA3 BACHELORS ENLISTED QUARTERS

BUILDING PROPERTIES AND DAMAGE ESTIMATE FOR A NOMINAL ACCELERATION OF .25 G

	PERIOD (SEC)	DAMPING	SA STR CAPACITY (G)	SA SITE DEMAND (G)
TRANSVERSE DIRECTION				
YIELD LEVEL	.110	.05	.640	.646
ULTIMATE LEVEL	.130	.10	.629	.584
LONGITUDINAL DIRECTION				
YIELD LEVEL	.130	.05	.399	.698
ULTIMATE LEVEL	.150	.10	.570	.620

BUILDING REPLACEMENT COST $ 4445000

ESTIMATED TOTAL DAMAGE TO BUILDING 94.0 PERCENT

ESTIMATED COST OF DAMAGE $ 4179363

DAMAGE ESTIMATES FOR VARIOUS LEVELS OF MAXIMUM GROUND ACCELERATIONS

MAX GRND ACCL. G	TRANSVERSE DIRECTION SPECTRAL ACCEL YIELD G	ULT. G	DAMAGE PCNT	LONGITUDINAL DIRECTION SPECTRAL ACCEL YIELD G	ULT. G	DAMAGE PCNT	COMBINED DAMAGE PCNT	DAMAGE EST 1000 $
.05	.129	.117	0.0	.140	.124	0.0	0.0	0
.10	.258	.234	0.0	.279	.248	0.0	0.0	0
.15	.388	.350	0.0	.419	.372	9.1	6.1	269
.20	.517	.467	32.2	.558	.496	68.3	56.3	2500
.25	.646	.584	82.1	.698	.620	100.0	94.0	4179
.30	.775	.701	100.0	.838	.744	100.0	100.0	4444
.35	.904	.818	100.0	.977	.868	100.0	100.0	4444
.40	1.034	.934	100.0	1.117	.992	100.0	100.0	4444
.45	1.163	1.051	100.0	1.256	1.116	100.0	100.0	4444
.50	1.292	1.168	100.0	1.396	1.240	100.0	100.0	4444

36

US-SOUTHEAST ASIA SYMPOSIUM ON ENGINEERING FOR NATURAL HAZARDS PROTECTION

A. H-S. Ang

Department of Civil Engineering
University of Illinois at Urbana-Champaign

Prepared for
National Science Foundation

US-Southeast Asia Symposium on Engineering for Natural Hazards Protection

The need for protection of man and manmade structures and facilities against the extreme forces of natural hazards is worldwide. This need is particularly pronounced in the region of Southeast Asia where typhoons, monsoons, severe thunderstorms, and earthquakes are yearly occurrences that regularly pose serious threats to lives and material properties. To mitigate these forces and provide adequate protection within the developing economies of the countries in the region are real challenges for the local engineering communities.

Some aspects of the approach to the engineering design of structures and systems to withstand the forces of natural hazards are common irrespective of geographic regions. In this regard, the recent developments in the United States, particularly in the areas of earthquake and wind engineering, would be of interest and benefit to the engineers and research of the Southeast Asian Countries. Nevertheless, each region in the world may have special problems peculiar to the region; moreover, because of the frequency and regularity of major hazards in Southeast Asia, the study of extreme natural hazards in this region would be of special interest to engineering researchers, particularly those working in the areas of earthquake and strong wind. Certain countries in this region lie directly within the circum-Pacific belt of active seismic activity. Also, this region is regularly subjected to severe typhoons and heavy rainstorms, the magnitude or intensity of which are some of the most severe in the world. There are also areas in this region that are exposed to tidal waves (which may be earthquake-induced) and volcanic hazards. Flooding, as well as landslides, are frequent results of these natural phenonema.

The Symposium provided a forum for delegates from the U.S. and the Southeast Asian countries to review the current state of technologies that have recently been developed for the design of facilities and structures to resist the extreme forces of natural hazards, with specific reference to earthquakes and strong wind. This Symposium also provided the opportunity to review the current research and development efforts, both in the United States and countries of Southeast Asia, as well as to identify those problems that are unique to the region.

The technical program consisted of two days of formal paper presentations, and one and one-half days of workshop discussions. It was the purpose of the workshop to define and identify specific topics related to natural hazards that are most promising for future collaborative efforts between the U.S. and countries in Southeast Asia, or among countries in Southeast Asia.

Aside from the U.S. and the Philippines, which had the largest delegations to the Symposium, there were delegations also from Japan, Australia, New Zealand, Hong Kong, Thailand, and Singapore. Invitations to participate in the symposium were sent to Indonesia, Malaysia, and South Korea; however, these countries were not able to send delegations to Manila, due largely to the short lead time available (between March and September 1977). In any future symposium of this type, every effort should be made to get representation from these other countries.

The participation of the U.S. delegation at the Manila Symposium was made possible through the support of the National Science Foundation under Grant No. INT 77-15418 to the Department of Civil

Engineering, University of Illinois at Urbana-Champaign. The initial incentive for a symposium in Southeast Asia was developed through discussions with Dr. S. C. Liu of NSF-RANN and Dr. A. Holt of NSF-International Programs Division. Their personal encouragement and support during the organizational phase of the symposium are gratefully acknowledged.

Much of the credit for the successful organization of the Symposium in Manila must go to the local organizers under the able leadership of Dr. E. Tabujara of the University of Philippines and R. Venturina of the National Science Development Board of the Philippines. Also, the co-sponsorship and financial support of the National Science Development Board and the University of the Philippines, as well as the contributions from other governmental and private agencies in the Philippines, all served to insure the success of the symposium in Manila. To our Philippine hosts and organizers, the foreign delegates are grateful for their kind hospitality, and for the magnificent and beautiful facilities provided for the conference.

The Symposium benefited immeasureably from the participation and personal support of the following Philippine dignitaries: Dr. M. S. Magno, Chairman of the National Science Development Board; Dr. O. D. Corpuz, President of the University of the Philippines System; and Hon. A. L. Juinio, Secretary of Public Works, Transportation and Communications, and Dean of the College of Engineering at the University of the Philippines.

The technical contents of a symposium of this type, of course, depend on the contributions of all the participants; the efforts of all the delegates, guests, and observers are greatly appreciated. In particular, the efforts of the chairmen of the various working groups deserve special acknowledgment; indeed, they deserve the credit for the successful conduct of the research workshop sessions and for their respective working group reports (reprinted here).

The Research Workshop

The Research Workshop consisted of one-and-a-half days of discussions by small groups of delegates. The objective was to identify and define specific topics for research that would be of mutual interest and potential benefit to the countries involved. Eventually, it is hoped that these will form the basis for future collaborative research programs between the countries represented at the Symposium. Indeed, the extent to which the topics defined at this Symposium can be developed to full research projects will eventually prove to be the real significance of the Symposium.

The discussions were divided into five working groups; the working groups and their reports are summarized in the following sections of this paper.

Working Group E1: Earthquake Response and Design

Chairmen:	Dr. William J. Hall
	Prof. Felisberto G. L. Reyes
Rapporteur:	Prof. Marino M. Mena

Report of Group E1

With recognition that the need for protection against the extreme forces and deformations of natural hazards, such as

earthquake, is worldwide, Working Group E1 undertook an examination of a set of study topics that we believe would help mitigate these effects in providing protection for the population and in reducing economic loss. In general this objective can be met through improved design and construction practices, especially as they lead to more costeffective structures. To this end, it should be noted that the primary purpose of the Symposium was "to identify and define specific study areas or topics for future collaborative research among the countries represented in this Symposium."

At the outset it is worth noting that the topics selected herein for specific comments are major areas of concern not only to Southeast Asian countries but to other parts of the world as well, including the United States and Japan. Within this context then the formulation of a comprehensive research and development study should involve the cooperative effort of all countries concerned and should have as its goal to develop improvements in technology for all.

After a brief review of the status of earthquake engineering design/analysis/construction practice as reflected in the papers presented at the Symposium and in the discussion at the working group meeting, it was agreed that the following ten topical headings incorporate the areas of research needed to improve our earthquake resistant design and construction practice:

(1) Design Philosophy, Codes and Standardization
(2) Material Quality, Control, and Construction Practices
(3) Non-Engineered Structures -- Low-Cost, Low-Rise
(4) Engineered Structures -- Building Framing Systems, Ductility, and Non-Structural Elements
(5) Evaluation of the Adequacy of Existing Buildings
(6) Information Base, Application and Interpretation
(7) Soil-Structure Interaction
(8) Bridges
(9) Utilities
(10) Dams and Reservoirs

The working group agreed that the first six topics deserved special interpretative description since they appear to be amenable to cooperative effort within a reasonable time. This was not meant to mean that the last four items were deemed to be unimportant, for indeed soil-structure interaction is intrinsically a part of almost all of the first five items; since it is under intensive investigation in several countries and the research involves large amounts of time and money, it suffices to introduce synthesis and review at the appropriate time rather than to undertake detailed studies at this time as a part of a cooperative study.

With regard to bridges, utilities and dams (Items 8, 9, and 10), it was noted that all of these areas are under study at the moment in such countries as Japan and the United States. In several years, it may be advantageous to examine these topics in further detail for possible cooperative effort. It was noted that in the case of bridges, for example, studies currently underway may suggest low-cost techniques for upgrading bridge resistance and such information should be brought to the attention of the cooperating countries when available in view of the importance of transportation systems to the economy and to recovery.

Design Philosophy, Codes and Standardization

In recent years many new national building codes and guides for resisting seismic effects have been developed. These codes commonly include provisions for estimating the seismic forces, techniques for providing seismic resistance, and specifications pertaining to material strength, allowable stress, and deformation. These codes differ in part as might be expected. In the interest of providing a base for review or upgrading such codes from time to time, it is believed that it would be desirable to prepare some position statements concerning the philosophy behind the development of such codes or design guides including, for example, such items as selection of the hazards, analysis and design techniques for loading and resistance, and assessment of the associated risk and margin of safety. It is believed that it would be desirable on a general basis (not in detailed form) to compare and summarize differences and similarities. It is believed that this effort would provide a valuable basis for code modifications in the future.

Another ambitious program that could be of value would be the preparation of a design guide that would include specific recommendations as to proportioning and detailing of structural elements.

Material Quality, Control, and Construction Practices

The state-of-the-art in local construction practices is usually based on past experience and rule of thumb. The majority of severe damage sustained by low-rise, low-income housing due to earthquakes could be mitigated by more explicit and simple design and construction guidelines.

Particular attention is drawn to material quality, control, and construction practices. Quality assurance programs and procedures in construction starting from the manufacture through the inspection, and up to the installation of the materials, should be established in a simple and systematic manner.

The development of indigenous construction materials that will perform well during an earthquake, such as the use of bamboo fiber, coconut coir, abaca fiber, etc., in roofing, wall and ceiling boards, should be undertaken with the end view of increased strength and reduced weight and cost.

Techniques of strengthening adobe and soil cement block houses against earthquake disturbance by providing tension reinforcement, banding or membrane continuity in the form of indigenous materials should be developed, with particular attention given to anchorage and connections. Connections and anchorage devices that increase the safety in critical joints and sections in structures that exhibit frequent failures during an earthquake should be studied and developed. It may be possible to develop simple guides to permit installation of some of these strengthening techniques in existing buildings and housing.

It is believed that studies of the type outlined specifically in Topic 2, but also Topic 5 generally, could be carried out in building research laboratories in the countries concerned or as a part of cooperative programs. The investigations should be carefully planned so as to expedite adoption in practice.

Non-Engineered Structures -- Low-Cost, Low-Rise

Many aspects of research required for improvement of the earthquake resistance of a non-engineering structure are contained in Topic 2. However, in addition to the specific detailed topics outlined in Topic 2, it is believed that there is a need for an examination of the structural system as a whole and the development and simplification of procedures for use by practitioners to expedite evaluation of the seismic resistance of such structural systems. In view of the large number of such structures throughout the world, it should be obvious that any adopted improvements should lead to major economic savings and increased public safety.

Engineered Structures -- Building Framing Systems, Ductility and Non-Structural Elements

In the interest of improving design practices for engineering structures throughout the world, it is recommended that intensive research be continued in the development of resistant framing systems (for all materials) with the aim of improving their capability of maintaining strength throughout deformation without degradation. Structural elements should be able to resist both in-plane or out-of-plane loadings.

As a part of these studies, there should be encouragement in all cooperative countries to investigate new materials, and combinations of new materials in conjunction with new types of framing systems. One goal is to develop techniques for evaluating and demonstrating the adequacy of new systems so that they can be accepted for use in practice.

Recent earthquake damage assessment studies have shown clearly the need for more attention to the design and attachment of non-structural and secondary elements in buildings. This subject needs intensive study and the development of guidelines to permit improvement in design and construction.

Evaluation of the Adequacy of Existing Buildings

The evaluation of the adequacy of existing buildings is composed of two general areas: (a) the evaluation of the structures following an earthquake, and (b) the evaluation of structures as part of the general assessment of adequacy at periodic intervals.

With regard to the former item, studies are need of the procedures for assessing physical adequacy of the structures as well as of legal responsibilities involved in assessing adequacy and/or repairability of the damaged buildings. At the same time there needs to be an assessment as to whether or not there should be a mandate that a building which externally does not appear damaged should be examined to confirm that its structural adequacy is not impaired.

With regard to the second subtopic there needs to be a study of methods that might be employed by engineering firms and governmental bodies to ascertain the adequacy of existing buildings within a given area to resist seismic loadings. It is envisioned that such investigation should be contemplated for structures that are, in general, old or possibly constructed at a time when different materials and techniques were employed and considered desirable. Among the techniques that might be considered are non-destructive testing and certain forms of analysis coupled with selective testing.

Information Base, Application and Interpretation

In Southeast Asia there is a general lack of comprehensive and centralized reference sources of technical information pertaining to engineering design for natural hazards, analysis procedures, construction techniques, and material properties. In contrast the United States and Japanese depositories are replete, but not necessarily complete, with such information. It is recommended that designated representatives of countries involved in cooperative programs of development make known generally to all participants major sources of information in order that they can procure those of most interest if they so desire. In addition to journals or proceedings, the names and addresses of cognizant organizations should be provided so that continual updating can be maintained.

It is conceivable that in some cases at the national level, it may be found expedient to collect and collate abstracts of significant existing information for purposes of review and evaluation by appropriate groups. A depository for such abstracts in the Philippines could be The Technology Resource Center. To save effort and resources, if certain countries undertake this effort they should make their collection known to other cognizant countries to prevent duplication of effort.

To disseminate information and concepts rapidly as a result of research and development activities, and to expidite information exchange generally between the co-perating groups, it is suggested that symposia be held in other cities throughout Southeast Asia. Such symposia, if structured carefully in advance, could prove to be highly desirable and beneficial in terms of synthesizing research and development information and in expediting technology transfer. To insure that these major symposia will be structured properly, it is suggested that certain investigators meet as appropriate at intermediate periods to compare and study results and to guide preparation of topics that would be presented in the symposia.

It is recommended that each Southeast Asia country involved in the cooperative effort urge their respective policy-making bodies to develop and systematize a plan to expedite research efforts and applications to practice.

To implement this plan, the information base described in sub-Item No. 1 above is necessary but there is also an implication of a more serious commitment of funds for qualified personnel and equipment to achieve the goals over some planned time period. It is recognized that a major portion of the technology transfer should be structured to be of use in accordance with specific engineering requirements of any particular country.

Another item that should not be overlooked pertains to the social aspect, such as disaster planning and rehabilitation following an earthquake. The efforts in this field need to be planned separately but coordinated with the technical studies.

Working Group E2: Ground Motion And Seismic Risk

Chairmen:	Dr. Joseph Penzien
	Dr. Salvador F. Reys
Rapporteur:	Ms. Perlita Morales

Report of Group E2

Working group E2, Ground Motion and Seismic Risk, identified six areas where cooperation is recommended. The first four of these areas -- (1) Seismic Zoning Map of the Philippines, Indonesia, and other Southeast Asian countries, (2) Intensity Attenuation Laws, (3) Prediction and Characteristics of Bedrock Ground Motions, and (4) Effects of Local Soil Conditions on Ground-Motion Characteristics -- are basic research studies of mutual value to all seismic regions of the world. The fifth area, Design Basic Earthquakes, would bring together the results of the first four to provide a basis for establishing design earthquakes that could be used in designing important structures such as nuclear power plants, high-rise buildings, and dams in the Southeast Asian countries. The sixth area, Institutional Approach to Reserach Information Dissemination, is directed towards stimulating research in the Southeast Asian countries and towards collecting and disseminating research results. The following is a brief outline of each of the six areas:

Seismic Zoning Map

Statement of Research: This research would concentrate on collecting, collating, and analyzing significant data on seismic events, such as location of epicenters, magnitudes, frequencies of occurrence, epicentral distances, focal depths, intensities, etc., and on correlating the results with geologic conditions.

Need for Research: There is a great need for seismic zoning maps in the Southeast Asian developing countries that will define seismic intensity levels for use in the design of important structures such as nuclear power plants, high-rise buildings, dams, etc.

Description of Research: Statistical analyses of basic seismological data would be made to establish seismic intensity levels in probabilistic form for the Southeast Asian countries, with special emphasis given to the metropolitan areas. Seismic intensity maps would be developed for use in engineering design.

Cooperative Efforts: Since the results of this research are basic in nature, they would be of value to all seismic regions of the world. Therefore, cooperation among the Southeast Asian countries, Japan, and the United States in the overall effort is recommended. The individual efforts should be coordinated with educational and research institutions and with professional organizations within the participating countries. This cooperative program could be carried out with a minimum of financial support and equipment.

Intensity Attenuation Laws

Statement of Research: This research would focus on the development of theoretical and empirical laws for the statistical prediction of ground motion intensities during an earthquake of known magnitude and location.

Need for Research: Once the probable locations of epicenters are known, attenuation laws are needed to predict intensities of motion at particular sites. Therefore, there is a need for (1) development of attenuation laws for regions where such laws are not available, and (2) improvement of exisiting attenuation laws for regions where they have been developed previously.

Description of Research: Basic research is needed in two directions, namely (1) collection and exchange of recorded and observed data from past earthquakes which are now available and documented in participating countries, and (2) development of equations relating ground motion intensity to earthquake magnitude, distance, and other significant parameters. Information on soil and geologic conditions at recording stations should be part of this study. Various intensity scales, such as the MM scale, the RF scale, and maximum ground motion scales should be explored depending on the avaiability of data and engineering needs. Relationships between the various intensity scales should be established to convert available data into a form most useful for engineering design purposes. The statistical scatter of data about the proposed attenuation laws should be established as it is significant in determining levels of seismic risk. Attention should also be given to: (1) the frequency dependency of attenuation rates, (2) defining the most appropriate distance parameter for use in attenuation laws, and (3) influence of source mechanism parameters on attenuation rates.

Cooperative Efforts: Cooperation of participating countries is essential in the compilation of statistical data that form the basis for attenuation law studies. Comparison of results and coordination of efforts are believed to be vital for the success of such a program.

Prediction and Characteristics of Bedrock Ground Motions

Statement of Research: This research is aimed at (1) establishing seismic risk maps in terms of ground motion parameters of engineering interest, (2) characterizing strong ground motions at bedrock level, and (3) developing appropriate stochastic models for bedrock ground motions.

Need for Research: This research will generate information much needed by engineers in establishing seismic load levels and characterizations of seismic ground motions.

Description of Research: There is a great need for a comprehensive study aimed at establishing seismic risk maps in terms of ground motion parameters of engineering interest. At present, all available information is in the form of qualitative intensities. There is a need to relate this information to such parameters as ground acceleration, ground velocity, duration, and other strong motion parameters. These relationships should be established for all major local seismic provinces and the similarities of data and results for these provinces should be compared with comparable information available in Japan, the United States, and other countries. In time, further information will become available from the strongmotion instrumentation now being installed. Such information will supplement existing data bases and should be incorporated into a more comprehensive study of seismic risk and characterization of strong earthquakes.

In characterizing strong ground motions for engineering purposes, three parameters, namely, intensity, dominant ground period, and duration are important as they greatly influence structural response. Duration is particularly important for non-elastic systems. Ideally, information about the joint likelihood of occurrence of these three parameters should be developed. In addition, information on the variations of ground motion intensity and its frequency content with time should be established. Such information is needed in developing appropriate stochastic models for three-dimensional ground motions.

Cooperative Efforts: Cooperative studies will be especially effective for regions where seismic zoning can be achieved only in terms of qualitative intensity scales. The results of studies for these regions can be compared with results worked out in terms of engineering parameters for other regions having similar geological conditions. Calibration between such regions will provide quantitative reasoning for other regions not having instrumental data and will provide a more uniform international basis for seismic zoning. Cooperative studies will also be highly desirable in the field of statistical analysis and data supply for characterizing earthquake ground motions and establishing appropriate models. Of greaest importance is the development of strong-motion seismograph networks on a uniform technical basis as well as the analysis of data obtained using a common methodology.

Effects of Local Soil Conditions on Ground Motion

Statement of Research: This research has two objectives: (1) to collect subsoil information; e.g., depths to bedrock and physical properties of soils, sufficient for establishing preliminary soil factors for design purposes in urbanized areas, and (2) to provide a data base which can be utilized for studying motions in alluvial ground overlying bedrock and for correlating the results of such studies with available recorded strong ground motions.

Need for Research: The effects of earthquakes on engineering structures in different locations may depend significantly on the conditions of the underlying foundations soils; therefore, the effect of local soils on the characteristics of ground motion greatly needs investigation. Unfortunately, in most regions of Southeast Asia, information on local soil conditions is severely lacking.

Description of Research: Information on local soil conditions throughout Southeast Asia should be collected and organized (work along this line is now being carried out in Metro-Manila). This information should include depths to bedrock, depths to the water table, and the physical properties of the overlying soils as obtained by various engineering and geophysical techniques. Since much controversy exists regarding the effects of local soil conditions on ground motion, correlation studies should be carried out comparing predicted ground motion characteristics with measured ground motion characteristics. Improved methods for assessing local soil effects should be developed.

Cooperative Efforts: Since this research is basic in nature, the results would be of value for all seismic regions of the world; therefore, cooperation in the overall effort is recommended among the Southeast Asian countries, Japan, and the United States.

Design Basis Earthquakes

Statement of Cooperative Effort: This effort is aimed at establishing design basis earthquakes to be used in the design of structures, such as industrial facilities, nuclear power plants, high-rise buildings, residential buildings, dams, etc., to be located in the Southeast Asian countries.

Need for Research: Design basis earthquakes are needed so that engineering designs are consistent with acceptable safety levels, economic constraints, professional practice, and other pertinent local factors.

Description of Research: The development of design basis earthquakes should follow two approaches, namely (1) establishing appropriate values for the design lateral force coefficient roughly comparable to the Z-factor in the Uniform Building Code, and (2) establishing appropriate response spectrum curves for modal analyses and accelerograms for use in time-history analyses.

The effect due to local soil conditions should be separated from the lateral force coefficient mentioned above and should be treated separately. Maps should be established showing the lateral force coefficient to be used for any site in Southeast Asia.

The design basis earthquake defined through response spectrum curves or an accelerogram, which would be used for more important structures, should be established after full consideration of plate techtonic theory, available geological and seismological data, attenuation laws, local soil conditions, etc.

Public policy factors applicable to local regions (social, economic, political, legal, etc.) should also be considered when setting the design basis earthquake, whether it be expressed in terms of the lateral force coefficient, response spectra, or an accelerogram of ground motion.

Cooperative Efforts: This work would be carried out primarily by individuals and groups in the Southeast Asian countries working cooperatively; however, assistance and cooperation from individuals and groups in Japan and the United States are highly desirable due to their previous experience in this area of activity. The overall effort would be of benefit to all participating countries.

Institutional Approach to Research and Information

Statement of Problem: Answers are needed to the following questions: (1) How can all information pertinent to natural hazards mitigation be effectively collected and disseminated throughout the Southeast Asia region?, (2) How can this information be effectively used in research and engineering practice?, (3) How can research be stimulated and engineering practice be improved in the Southeast Asian countries?, (4) How can engineers and scientists be given opportunities for continuing education related to natural hazards mitigation?, and (5) How can funding be obtained for programs in natural hazards mitigation?

Possible Solution: There appears to be little incentive to find answers to the above questions. To assist in solving this problem, it is suggested that consideration be given to the establishment of an institute in one of the Southeast Asian countries where high seismicity is present (Manila has been suggested as a logical location). This institute could serve as a natural hazards data and research center for the Southeast Asia region and as an educational center for engineers and scientists working in this field. It could possibly publish a journal (say, the Journal of Natural Hazards Protection in Southeast Asia), sponsor seminars, organize short courses, etc. Such an institute, if properly supported, might well provide some of the answers to the questions raised above.

If favorable consideration is eventually given to the establishment of an institute of this type, every effort should be made to make the activities of the institute complementary to activities of

other institutes, such as the Asian Institute of Technology (AIT) and the International Institute of Seismology and Earthquake Engineering (IISEE).

Cooperative Efforts: Clearly, an institutional approach to research and information dissemination in Southeast Asia can be successful only if all countries in the region cooperate fully, assistance and cooperation is received from countries such as Japan and the United States, and adequate funding is made available.

Working Group W1: Wind Response and Design

Chairmen: Dr. Richard D. Marshall
Prof. Angel A. Alejandrino
Rapporteur: Mr. Enrico G. Gregorio

Report of Group W1

Working group W1 reviewed the general area of wind response and design with the purpose of identifying those items or topics that are in need of additional research and that might offer an opportunity for international collaboration. While the discussions covered many topics, ranging from single-family dwellings to long-span flexible bridges and nuclear power plants, three topics emerged as having a significant potential for protection against natural hazards. In addition, these three topics are believed to represent achievable goals when the very real constraints of existing research capability and available funds are applied. The topics are listed in order of priority and are followed by comments describing the scope of the proposed effort and means of implementation.

An International Wind Engineering Extension Service

The objective is to disseminate existing information of the nature of wind forces, the design of buildings and other structures to resist these forces, and recent developments in the formulation of codes and standards. To make this dissemination effective and to ensure its use by the engineering profession, it is proposed that regional seminars or workshops be conducted from time to time in appropriate countries of Southeast Asia, the courses being presented by international experts and certain individuals from the engineering profession in the host country. These seminars or workshops would introduce the latest technology to the profession and would also provide an opportunity to document current practice and experience in the host country. Documents could be distributed and otherwise be made available by appropriate local agencies such as the Technology Resource Center (TRC), which has recently been established in the Philippines.

Post-Disaster Investigations

The objectives of this topic are: (1) to investigate and report on disasters caused by extreme winds, (2) relate observed damage and wind intensities to structural performance, and (3) to assess existing design criteria and provide feedback to the affected country or countries. It is important to understand that this topic involves far more than just the documentation of wind damage and that the real value lies in the second and third items above. To be effective, contacts would have to be established before the fact with participating countries so that investigative teams (to consist of international experts and members of the engineering profession in the affected country) could have timely and unlimited access to the disaster area.

It is believed that the International Association for Wind Engineering could provide the leadership and coordination for such an undertaking. Admittedly, this group is currently organized along very informal lines without an operating budget and would require financial assistance to carry out the objectives outlined above.

Establishment of a Boundary-Layer Wind Tunnel Facility

In addition to being an extremely useful research tool, a boundary-layer wind tunnel is an essential component in the design of structures having unusual geometric features or dynamic characteristics which may make them sensitive to wind forces. The work group believes that the establishment of such a facility, to be supported by and made available to the countries of Southeast Asia, is justified on the basis of current need by the engineering profession and on the basis of its potential for the reduction of wind hazards. It is believed that the major cost of establishing such a facility lies in the training of staff members who would carry out commercial work in response to the needs of the engineering community and who would also conduct research into the mechanisms of wind loading. To be successful, a regional facility such as this should be associated with an established research center or institution.

Working Group W2: Wind Hazards and Characteristics

Chairmen: Dr. R. Scanlan
Dir. Jesus F. Flores
Rapporteur: Prof. Evangel P. Quiwa

Report of Group W2

The work of the group was divided into four subsessions of approximately 1-1/2 hours each, having the following centers of focus:

- o Session 1: Objectives of the session and definition of technical problem areas
- o Session 2: A discussion of the present state of the engineering art relative to wind and the natural hazards caused by it in Southeast Asia.
- o Session 3: A broad discussion of possible research and study projects needed in the area.
- o Session 4: A focussing discussion in which a limited number of possible research and study projects needed in the area were identified.

In session 1 the general objectives of the National Science Foundation in this context were outlined as centering around the international cooperation in the natural hazards area in Southeast Asia. Particular willingness to supply travel funds to qualified U.S. nationals acting as co-investigators in cooperative study projects was indicated.

In the four working subsessions particular emphasis was given to information and viewpoints supplied by representatives from Australia, Hong Kong, Japan, New Zealand, Philippines, and the United States of America. The absence of representatives from other Southeast Asian countries was noted and the general hope expressed that these absences could be remedied at future meetings of similar type.

Principal Conclusions

A total of some 24 topics for research, and data-gathering were broadly discussed. These finally were reduced to some 5 areas, of which the following list is a highly condensed summary:

1. Needs for Continued Experimental Data-gathering relative to

   - o Large-scale cyclonic storms (typhoons, cyclones, hurricanes)
   - o tornadoes
   - o Boundary-layer properties of the wind at wind-chosen locations (velocity profile, spectra and spatial correlations of turbulence, etc.)
   - o Personal discomfort in tall buildings and plazas
   - o Wind-tunnel modeling of specific problems

2. Needs for Storm-Disaster Management, Damage Assessment, and Damage-Reduction

   - o Creation of a natural hazard data collection center and clearing house for Southeast Asia (possibly based on PAGASA).
   - o Development of highly engineered approaches to disaster warning and control.
   - o Establishment of qualified disaster evaluation teams to be sent rapidly into areas of storm damage after an event.
   - o Launching of a campaign of public education emphasing engineering measures that can improve the storm resistance of non-engineered structures and reduce storm casualties associated with them.

3. Needs for Wind-hazard Risk-assessment Studies Based on State-of-the-Art Probabilistic and Analogous Approaches

   - o Assessment of tornado and typhoon risks to cities, agricultural resources, sensitive installations such as nuclear plants, special laboratories, factories, etc.

   - o Needs to gather and compare wind codes from a wide range of sources for structural engineering

   - o Studies assessing the effect of particular code applications on representative designs.

4. Assessment of the Full Implications and Efficiency of Typhoon Modification and Reduction Efforts

A list of documents was submitted to Professor E. P. Quiwa, rapporteur of panel W2 by interested parties. These documents have been turned over to the documentation office of the Building Research Center, University of the Philippines.

The Director of Typhoon Research at the Philippine Atmospheric, Geophysical, and Astronomical Services Administration offered concluding remarks regarding his willingness to cooperate with structural engineers, in collecting and storing wind data.

Working Group H: Other Hazards

Chairmen: Dr. Severino L. Koh
Dr. John Y. Lai
Rapporteur: Mr. Ronoldo I. Borja

Report of Group H

The group identified five problem areas of importance to the Southeast Asia region in general and to the countries represented in the group in particular. These problem areas were:

- o Storm-generated Waves and Surges
- o Landslides and Related Hazards
- o Volcanic Hazards
- o Inland Flooding
- o Seismic-generated Waves (Tsunamis)

The group attempted a priority listing of the various research topics based on three criteria: urgency, organizational support, and availability of interested, qualified personnel to undertake the specific work. The group subsequently determined that all five problem areas were important to the region, and the participants at the Group discussions individually expressed interest in certain specific topics.

The group noted that some collaborative efforts existed between the Philippines and Japan on studies of inland flooding. However, collaboration on the other areas had not been initiated. Nevertheless, common interests were expressed by the participants, and possible collaboration appeared to be most promising in the areas of storm-generated waves and surges, and in landslides and related hazards. Possible collaboration among Hong Kong, the Philippines, and the United States in the area of landslips of filled slopes and mud avalanche was also expressed.

The group considered several questions relative to future collaborative activities. Specifically, the group discussed the need for continuing dialogues among the scientists and engineers of the participating countries, the need to discuss research progress, to establish research institutes for concentrated work in specified fields, and to create a data collection and information center and repository of research findings. Based on these deliberations, the group formalized three specific recomendations. These are presented below.

Mathemetical Models for Predicting Storm Surges

A number of countries in southeast Asia are visited annually by tropical cyclones which create substantial damage to property and loss of lives. In terms of damage wrought, the storm-generated waves and surges constitute the greatest hazard in the coastal areas around the Bay of Bengal, Hong Kong, Japan, and the Philippines. Mitigation of the damage and loss of lives from these hazards could be enhanced by the timely issuance of accurate warnings of their impending occurrence. This could be done through the development of suitable mathematical prediction models.

There are now some simplified models that seem to be adequate for coastal areas which have relatively straight coastal lines and well-behaved coastal bathymetry. At best, these models give only rough and preliminary estimates of potential surges in most Southeast Asian coastal areas due to the highly irregular coastal configurations and the steep bathymetry in many areas. Furthermore, unusually large surges occur in closed or semi-closed basins or bays.

To predict storm surges in the region more accurately, there is an urgent need for the development and formulation of more realistic mathematical models. Such models should predict flooding

azards resulting from the generation and the propagation of storm urges and waves in the Southeast Asian coastal complexes including pen coasts, bays, and rivers. They should: (a) include the ffects of irregularities in the coastal boundaries and the bathymtry of the continental shelves; (b) reflect time-dependent inundaion boundary conditions along the low-lying terrains; (c) provide n acceptable degree of numerical resolution of the non-linear dvection terms to improve the stability criteria as well as the onvergence capability of the model; (d) be applicable for storms ravelling parallel as well as perpendicular to the shoreline; and e) be reasonable in computational time.

Advances in mathematical modeling achieved by scientists from he United States and Japan would be helpful to the Southeast Asia egion. Specifically, the ongoing research efforts on storm surges n the Philippines supported by the NSDB* with primary activity in he PAGASA** could benefit from collaboration with workers from he United States and Japan.

Development of Risk Methodology for Storm Surges

Supplementing the work described above, a quantitative risk ethodology for predicting the hazards from storm surges could be eveloped. This effort would involve the development of a deducive probabilistic model for evaluating the annual probabilities (or eturn-periods) associated with specified surge levels at a given ite. For effective implementation, the model must necessarily epend on and make use of available data on the major factors hat influence storm surges as well as on the mechanics of surge evelopment.

The successful development of the model should serve to improve he risk mapping of specific regions of a country. Such a model ould also serve to identify the data required for improving risk ssessments.

Instrumentation and Remote Sensing for Monitoring Storm Surges

The advancement of the present state of knowledge on prediction f storm surges, waves, and currents suffers from a deficiency in dequate measurement of parameters under storm conditions. Wave nd storm surge research efforts in Southeast Asia can be boosted ignificantly with collaborative help from American scientists who ave been successful in developing suitable instrumentation and emote sensing techniques for storm conditions.

A special instrumentation system for obtaining surge history nd waves under hurricane conditions has been developed in Florida. uch a system can be deployed in the Philippines to supplement and upport their studies on storm surges. A possible area of collabration could be the installation and maintenance of the instrumenation system by Filipino participants at sites of their choice. he American participants can build and furnish the finished instruentation system, and can provide instructions and training for its se, while the Filipino participants could assist in the installation nd maintenance of the system at preselected sites. The analysis f data would then be conducted jointly in relation to storm surge odels available in the United States and in the Philippines.

36

NSDB - National Science Development Board of the Philippines.
* PAGASA - Philippine Atmospheric, Geophysical, and Astronomical Services Administration.

The United States is also launching the first oceanographic satellite in May 1978. The capabilities include the measurement of wind speed and direction, wave height and direction, ocean surface elevation, and ocean surface temperature. Information obtained from SEASAT-A in Southeast Asia can be provided to those countries that have an interest in receiving the data and are willing and able to furnish surface data measurements to calibrate the satellite data. The Philippine agnecy. PAGASA, has indicated a strong interest in such a collaborative undertaking.

Rain-induced Landslides and Mud Avalanches

While extensive studies have been done to understand the mechanics of earthquake-induced landslides, comparatively little effort has been spent on landslides cause by means other than seismic disturbances. In the Philippines, in Hong Kong, and other parts of the Southeast Asia region, landslides triggered by heavy rains cuased considerable damage and loss of life. The landslips of 1972 and 1976 in Hong Kong were particularly disastrous. In the Philippines, rockslides and landslides are common occurrences during typhoon passages as well as during the monsoon season. Yet little is known regarding the fundamental tie-up between the varying properties of soil and soil instability. No suitable prediction methods for the occurrence of these hazards are available.

Collaboration between American scientists and those from the Philippines, Hong Kong and other parts of Southeast Asia can prove useful in the development of new knowledge on the mechanics rain-induced landslides, where theoretical models can be tested in actual situations in the Southeast Asia region. Ultimately, the goal of such a collaborative project would be to develop methods for analyzing slope stability and design criteria for slope structures. Manuals on slope such as that being developed for Hong Kong would be useful to other parts of Southeast Asia.

Damage Evaluation Criteria for Soil Structures

Natural slopes and man-made cuts are subjected to such influences as earthquakes and heavy rains to the extent that the integrity of the soil structure is threatened, instability is induced, and landslides are caused. In some cases, only minor relative earth motions are experienced and the integrity of the soil structure remains intact. Nevertheless, it is necessary that a damage evaluation system be developed for soil structures so that the stability of the slope can be assessed and the threat of landslides be monitored and their occurrences predicted.

Collaborative studies can be undertaken with the specific aim of developing methods for assessing cumulative damage resulting from successive seismic loads or instances of heavy rainfall of different intensities and duration. Prediction models may be tested against properly instrumented experimental models.

Insitu Testing of Soils to Determine Liquefaction Potentials

The possibilities of submerged deposits of loose cohesionless soil liquefying during seismic loadings are always of concern to a designer in a country like the Philippines due to the frequency of seismic activities and the rather extensive damage that soil liquefaction causes. Because soils of this type are hard to sample for laboratory testing and because of the resulting poor correlation between laboratory test data and field data, it is desirable to extend new knowledge on field testing procedures developed in the

United States and other countries to the developing countries in Southeast Asia.

A Risk Methodology for the Prediction of Volcanic Eruption

A risk evaluation method should be developed for assessing and predicting the hazards from volcanic eruptions of an individual volcano and/or the hazards to a given site from surrounding volcanoes. The work should involve the development of suitable probabilistic models for calculating the probabilities of volcanic eruptions, depth of ash falls, lava flows, mud flows, and the areas affected.

The purpose of the model will include the determination of the likelihood of levels of volcanic hazards in specific regions of a country. The form of the required model must necessarily depend on available data of previous eruptions as well as the science and and mechanics of volcanology.

The improve and support the information base needed in the risk methodology, additional data on the probable type of volcanic activity have to be obtained in terms of seismic and geothermic and behavior and petrogenesis. For this purpose, further instrumentation and monitoring of specific volcanoes will be vital.

Inland Flooding

Inland flooding is a major problem in Southeast Asia. Heavy monsoon rains and typhoons annually tax the inadequate flood control and drainage system in the countries resulting in considerable damage to properties and loss of life. While some success has been experienced in the operation of a flood forecasting network for the Pampanga River Basin, existing models like the tank model give only gross information on the expected behavior of the natural drainage system in response to hydro-meteorological events. These models prove inadequate in that they fail to take into proper account the physical characteristics of the specific basin. Therefore, there is an urgent need for the development of realistic models as indicated below.

Development of Conceptual Models for River Basins

Fundamental studies on flows and river stages which take into consideration hydrologic models are needed to improve techniques for flood forecasting. Conceptual models may then be developed for specific river basins. The results of these efforts are urgently needed to provide inputs for the development of flood control systems and drainage designs for frequently flooded basins in the country. The urgency of the problem is understood by the fact that very vitual economic and developmental activities are either in progress or planned for major river basins and deltas in the Philippines as well as in other parts of Southeast Asia.

The PAGASA and the Bureau of Public works of the Philippines have started working on flood forecasting and control for the major river basins in the country. Very recently, the National Flood Forecasting Office was created under PAGASA to oversee this particular activity. Basic studies are here proposed together with specific applications to particular regions would prove useful in improving the flood warning capabilities of these agencies.

Seismic Generated Waves (Tsunamis)

The Intergovernmental Oceanographic Commission of the UNESCO through the Tsunami Warning System Coordinating Group is the coordinating body for the study of Tsunamis. The Philippines participates in this work, and the Internatinal Tsunami Information Center in Honolulu provides some assistance in training. Locally, several academic institutions and government agencies are involved in the different aspects of this natural hazard ranging from basic studies to the diseemination of information to the provision of assistance to damage areas. Three specific needs are indicated below.

Development of Risk Methodology

Research on the risk of Tsunamic occurrences should be undertaken for the various areas of the Philippines. A form of probability map could be developed to formulate some sort of measure for land-use planning and infrastructure construction in developing areas, particularly along the eastern coast of the Philippines.

Instrumentation and Remote Sensing for Monitoring Tsunamis

Instrumentation and remote sensing projects such as that discussed earlier could also be useful for improving the Tsunami warning system in the Pacific. Better warning systems should be developed to the extent tht the lead time is lengthened. An effort should also be made to educate the public about Tsunamis, to be able to react to such disaster, as well as for site planning and resettlement.

Development of Damage Evaluation System

A system for evaluating damage to both terrestrial and aquatic life and property should be the subject of investigation. This should consider as well the impact caused by Tsunamis on the environment.

Additional Recommendations

The group supports unanimously and recommends strongly the organization of future symposia similar to the Manila Symposium every two years at different locations in Southeast Asia. The possibility of having the next one in 1979 either in Thailand or in Singapore was accepted by the group.

The group is of the consensus that research institutes could be organized with specific charges in specified areas. It takes note of the fact that a Center for Volcanology Research is now under the consideration of UNESCO. However, the group feels that at this point in the creation of a Southeast Asia Committee to oversee this as well as to coordinate future symposia would be more easily achieved than to establish institutes.

Participants at the meetings of the group voiced a need for more technical and scientific information, journals, books, and other publications in the developing countries. The group feels that it would be useful to establish an efficient mechanism for quick interchange of information. A data information center could be organized; however, the group feels that such an endeavor should be approached with caution in that the organization of yet another center might duplicate needlessly the serivces available at other centers, e.g., the Asian Information Center for Geotechnical Engineering.

Summary and Conclusions

The Manila Symposium is the first of its kind in Southeast Asia on the subject of Engineering for Natural Hazards Protection. The theme of the symposium is clearly of great importance to the countries in this region; therefore, the convening of the symposium in Manila was timely and indeed was long overdue.

The conference part of the Symposium afforded an opportunity for local participants to get an overview of the current state-of-the-art of engineering research and developments related to engineering for natural hazards protection, with emphasis on earthquake and wind. It served also to provide a forum for the researchers from the different countries to review their recent research results and approaches.

During the research workshop phase of the Symposiu, a number of worhtwhile research topics were identified and defined as suitable for joint collaborative support between or among the countries represented at the Symposium. The specific topics have been well summarized in the report of the various working groups, as presented in Chapter 3. Besides these specific research topics, several recurring problems that are unique to the Southeast Asia region were emphasized by the different working groups; these are worthy of repeating, and may be summarized as follows:

(1) There are local and special requirements that are unique to Southeast Asia and thus specialized research studies are needed; however, one of the most urgent needs in the region is for the proper dissemination and adaptation of available information and research results already developed by other countires, especially in the U.S. and Japan. In particular, there is currently a general lack of comprehensive and up-to-date references on technology related to natural hazards protection in the region. Consequently, there is a critical need for an information center and repository of research findings for this region; the establishment of an information center for the entire Southeast Asia region was suggested.

(2) Concern was expressed also for an effective collection of data related to natural hazards, and for the systematic analysis and dissemination of this information aimed at stimulating the improvement of engineering practice. The idea of establishing an institute in one of the Southeast Asian countries for these purposes was suggested. Such an institute could serve as a natural hazards data and research center, and as an educational center to sponsor seminars, organize short courses, etc.

(3) The main problem in implementing the suggestions developed at this symposium would be the commitment of sufficient funds for qualified personnel and equipment necessary to achieve the goals of any joint program. It is the hope that symposia of this type will help to enhance the recognition of such needs by appropriate funding agencies, and expedite or encourage the future commitment of needed funds.

(4) The holding of additional future symposia on the subject of engineering for natural hazards in Southeast Asia was strongly endorsed by the various working groups. In this regard, there is an offer from the delegation of Thailand to organize and co-sponsor the second symposium on the same subject in Bangkok, Thailand, with a suggested (tentative) data of January 1980. In any future symposia on this subject, wider representation and participation

by the countries should be encouraged. Planning of future symposia may include a pre-conference meeting of the organizers, for the purpose of selecting conference topics and preparaton of avaialble research material.

37

STORM SURGE

Celso S. Barrientos

National Weather Service
National Oceanic and Atmospheric Administration
Department of Commerce

Storm Surge

When a tropical or intense extratropical cyclone approaches or crosses a coastline, sea level rises anywhere fron a fraction of a meter to as much as 9 m. above the normal tide. This rise of sea level due to the storm is called storm surge. It is defined as the difference between the observed actual sea level and the sea level that would have occurred without the storm; it is that portion of the rise of sea level due to the storm alone. Storm surge is usually estimated from tide record by subtracting the normal or astronomic tide from the observed tide. This is illustrated in Figure 1, a two-day record for Atlantic City.

Storm surge occurs worldwide. In the Western Pacific it is associated with typhoons. In the Indian Ocean and Bay of Bengal, storm surges are due to cyclones. Australia has been struck recently by two intense cyclones. The first, "Althea," struck the coast of Queensland on the morning of 24 December 1971 and gave a surge of 2.7 m. The second cyclone, "Tracy," hit Darwin in the early morning of Christmas Day 1974. Tracy had a maximum wind of 175 km^{-1} with gust of 200 km hr^{-1}, but the surge was only 4.6 m.

In Japan, many typhoons bring surges over 2.0 m. along the coastal areas. A typhoon that moved over Ise Bay on 26 September 1959 produced a peak surge of 3.6 m. near Nagoya. On August 21, 1970, a typhoon moved over Tosa Bay that gave a peak surge of 2.4 m.; the highest water level, 3.4 m., was recorded in Ashisuri. Table 1 shows some major surges in Japan.

The northern portions of the Bay of Bengal are susceptible and vulnerable to storm surges. A very intense cyclone passed over Bangladesh on 12-13 November 1970. It generated an extremely high surge, which was estimated to be more than 6 m. This cyclone caused much damaged and killed several hundred thousand inhabitants in the off-shore island and coastal districts of Bangladesh. Storm surges reaching up to 9 m. have been estimated in the Visayan Island of the Philippines.

Storm surges are generated by wind and atmospheric pressure gradients associated with the passage of storms. However, passage of storms alone does not mean they will be accompanied by surge. There are other significant factors in surge generation: path of storm, water transport by waves, the earth's rotation, coastal configuration, and off-shore depth field (bathymetry).

Figure 2 illustrates the direct wind effect in raising the water level. If the wind is blowing at an oblique angle to the coastline, parallel current will be generated, and because of the earth's rotation (Coriolis effect) this current will raise the surge. This is shown in Figure 3. Wave breaking also causes the water to pile up on the coastline as shown in Figure 4. This paper will discuss how the coastal configuration and bathymetry are important in surge generation later.

37

The remaining part of this paper will focus on the United States. I will review the forecast methods for storm surges used by the National Weather Service (NWS).

Climatology of storm surge is important in determining future probability of surges and in computing tidal frequency. We need to know the probability of surges for designing and constructing

coastal structures. Surge frequency is also necessary to estimate flood insurance rates. Further, accurate and timely forecasting of surges can save lives and prevent property damage.

On the Gulf and East coasts of the United States, there are two types of meteorological systems that can cause storm surge. These are the extratropical storms that occur on the east coast of the U.S. during the winter and the tropical storms (or hurricanes) that strike both the Gulf and East coasts from May to December. I will discuss here these two phenomena and the forecast techniques we use to predict surges connected with them.

Low water or negative storm surge (sea level below normal) can also cause problems. In the western end of Lake Erie and in the north end of Chesapeake Bay near Baltimore, negative surge can threaten navigation.

Extratropical Storm Surges

The damage caused by storm surges is most severe in the northeast and mid-Atlantic states. These storms generally move along the coast and may cause heavy snowfall in the eastern seaboard. The storm is generally referred to as a "northeaster."

Although extratropical storm surges are not as high as the hurricane surges, they linger for a considerable length of time (2 to 5 days), and can be superimposed on tidal maxima. The long duration of the surges also cause severe beach erosion, thus destroying the foundation of structures.

A typical sequence of weather maps for extratropical storms during 18-20 February 1972 is shown in Figure 5. This storm caused extremely high tides, plus extensive damage and beach erosion in the northern U.S. Atlantic coasts (Figures 6 and 7). Figure 8 is the storm track, observed tide curves, and storm surge curves for 17-21 February 1972 for stations on the east coast. Most of the extratropical storm surge data here are from a study by Pore, Richardson, and Perrotti [1974] on forecasting extratropical storm surges.

The series of slides I will be showing you will further illustrate the damage caused by extratropical storm surges. These slides are not in my paper because they will be quite expensive to reproduce. The slides are from the collection of Mr. Art Pore, who is the chief of our marine techniques branch.

Probably, the most devasting east coast storm in recent times is the one that occurred on 5-8 March 1962. This storm is commonly known in meteorological circles as the "Ash Wednesday" storm. Extensive damage and severe beach erosion were left behind by this "northeaster." This storm is a typical case similar to the 1972 storm. However, the difference was the intense pressure gradient causing a strong northeast wind blowing along an unusually long fetch. Figure 9 is the sequence map for this storm. Figure 10 is the storm surge during this storm, for some stations on the east coast.

Tropical Storm Surges

Tropical storms form in the warm tropical ocean and move generally toward the west. The storm is a warm core system with generally a pronounced "eye." It is most frequent during late summer, when the heating of the tropical oceans has peaked. When

the storms approach the land mass, they generally recurve northward. In the northern hemisphere, tropical storms are most frequent in the western Pacific, followed in frequency in the western Atlantic. The storm is known as a typhoon in the Pacific and a hurricane in the Atlantic. However, strictly speaking, typhoons or hurricanes are both defined as storms with a maximum wind speed of 120 km hr^{-1} or more.

Since tropical storms are low-pressure systems, water bulges up under the storm. This is referred to as the inverted barometer effect. With the strong circulating wind acting on the water surface, a complicated rotating mound of water forms under the storm. In the open ocean, this rotating mound of water is hardly noticeable under a chaotic sea. When the storm reaches the continental shelf, the rotating mound of water will start to "feel" the bottom and coastal boundary. The constrained water results in storm surges. That is to say, a small amount of vorticity is converted to divergence and manifested as a surge.

The Gulf of Mexico and the east coasts of the United States have relatively wide and shallow continental shelves; additionally, the coasts are concave in shape. These coastal characteristics are favorable factors to high surges.

One of the most devastating hurricanes was "Camille" in the Gulf of Mexico in 1969. Camille generated a surge of 7.4 m. near Pass Christian, Miss. It is one of the highest surges recorded in the U.S. More than 250 people lost their lives and several hundred million dollars in damage was left in the wake of Camille. Figure 11 is an illustration of the damage of Camille. The bottom picture shows what is left of some apartments after the passage of Camille. In this apartment building alone, over 30 people died during a "hurricane party".

Forecasting Techniques for Storm Surges

The empirical method was the earliest technique used for predicting storm surges. This is based on correlating variations in sea-level (surge) with the meteorological factors in surge generation. Those meteorological factors are sea-level pressure (or intensity of storm) and the strength and direction of the prevailing wind (wind forcing). The only problem with this kind of statistical study, is that a large number of observations is needed to attain a meaningful level of significance for prediction. Since surge episodes are caparatively rare, large numbers of observations to derive empirical equations are generally not available.

On the east coast of the United States, it is fortunate that we have enough extratropical strom surge cases to derive statistical forecast techniques. We used the surge data and the sea-level pressure at various points to compute statistical forecast equations. Figure 12 shows the station on the east coast where forecast equations were derived. Figure 13 shows the grid points where the sea-level pressure data were used in the derivation of the forecast equations. These forecast techniques are used routinely in the National Weather Service. Figure 14 is an example of a forecast teletypewriter message by this technique. Extratropical storm surge forecasts are issued by the NWS Forecast Offices.

The NWS National Hurricane Center is responsible for predicting storm surges associated with tropical storms and hurricanes. The forecast is generated by a numerical-dynamical model developed by Jelesnianski. The computer forecast model is called SPLASH (Special Program to List Amplitudes of Surges from Hurricanes).

SPLASH consists of a storm traveling across a rectangular coastal basin with variable depth. The storm surge driving forces-- wind and pressure gradient--are derived from the storm model. Figure 15 is an example of the output of SPLASH (for hurricane Camille).

Recently, the World Meteorological Organization (WMO), one of the specialized agencies of the United Nations, has published "Present Techniques of Tropical Storm Surge Predictions." The publication was authored by Dr. Miyazaki from Japan, Dr. Jelesnianski from the United States, and Dr. Das from India.

TABLE 1. MAJOR SURGES IN JAPAN (MIYAZAKI, 1957)

Date	Affected area	Peak surge (m)	Highest water level (m)	Pressure (mb)	Extreme Values Wind ($m\,s^{-1}$)	Lacatian
1.10.1917	Tokya Bay	2.3	3.1	950.4	SSE 40.0	Takya
18.7.1930	Ariake Sea	2.5	-	954.6	ENE 30.6	Tamie
21.9.1934	Osaka Bay	3.1	3.2	954.3	S 48.4	Osaka
1.9.1938	Tokya Bay	2.2	-	978.6	S 31.0	Takyo
3.9.1950	Osaka Bay	2.1	2.5	964.3	NE 33.4	Kabe
17.8.1956	Ariake Bay	2.4	4.2	968.4	SE 27.0	Saga
26.9.1959	Ise Bay	3.6	3.9	958.5	SSE 37.0	Nagaya
16.9.1961	Osaka Bay	2.5	2.9	937.3	SSE 33.3	Osaka
25.9.1964	Osaka Bay	2.1	2.6	983.5	S 27.1	Sumoto
10.9.1965	Osaka Bay	2.2	-	966.0	SSE 38.8	Sumato
21.8.1970	Tasa Bay	2.4	3.4	962.3	SW 35.8	Ashizuri

37

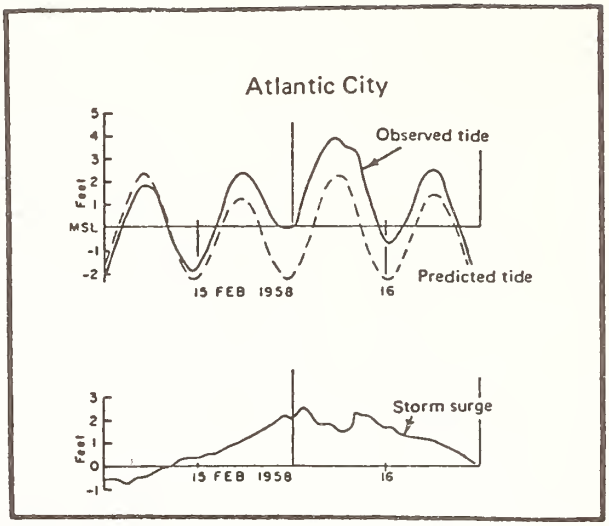

Source: Pore 1974

FIGURE 1. TIDE DATA

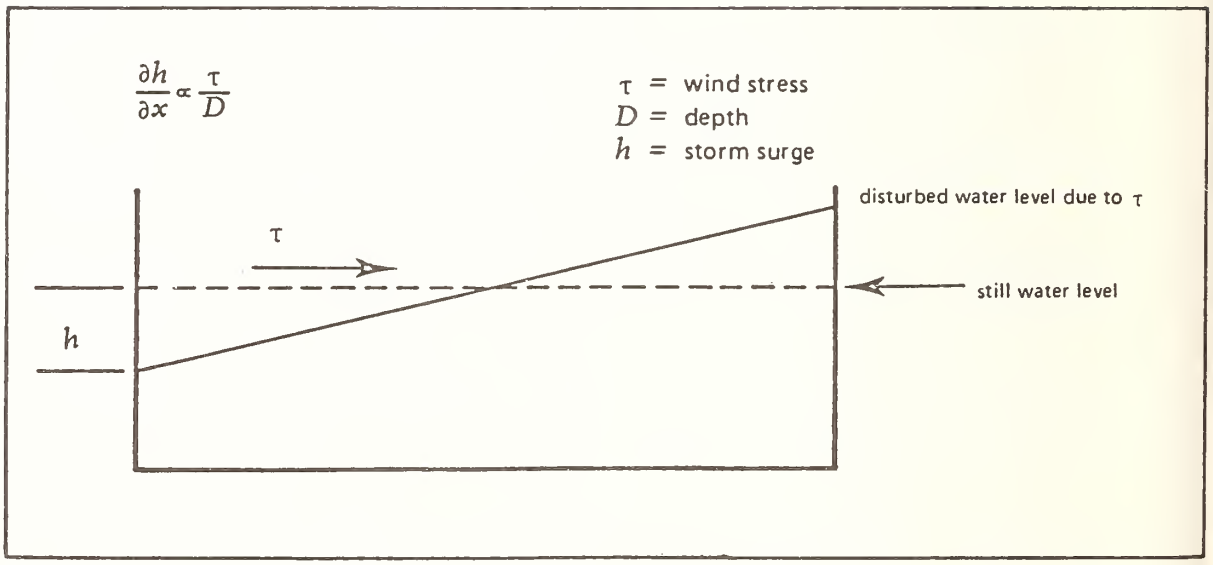

Source: Harris 1963a

FIGURE 2. EFFECT OF ONSHORE WIND ON WATER LEVEL

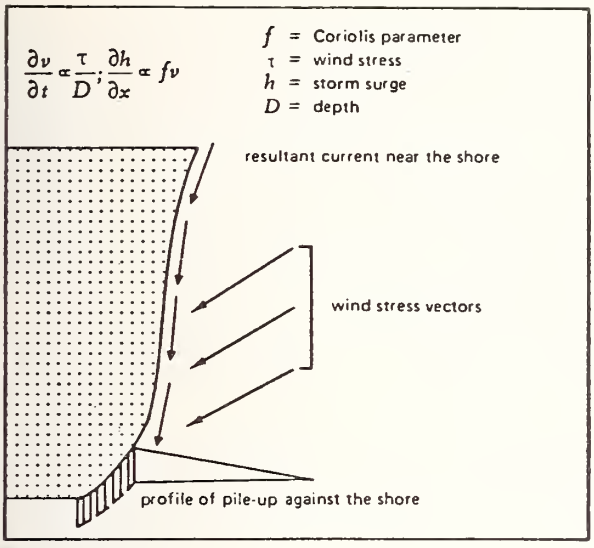

Source: Harris 1963*a*

FIGURE 3. EFFECT OF OBLIQUE WIND ON WATER LEVEL

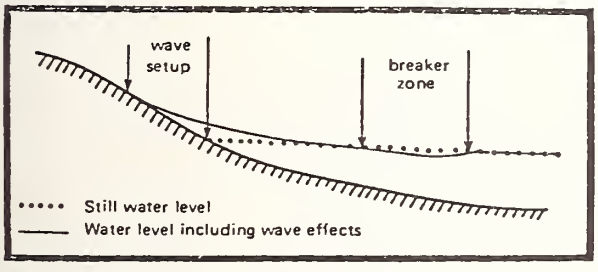

Source: Harris 1963*a*

FIGURE 4. WAVE SETUP IN VERTICAL PLANE

37

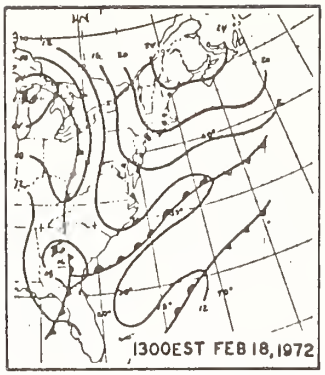

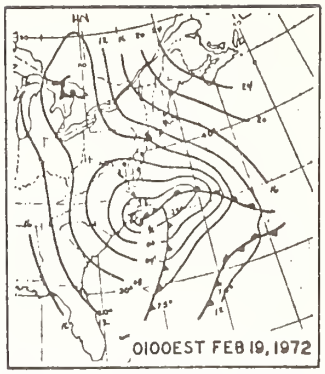

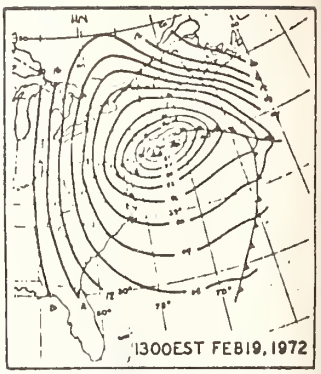

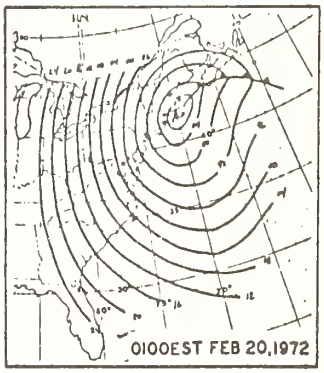

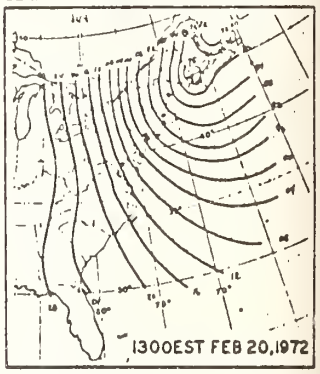

LEGEND

= cold front

= warm front

= low pressure center

= high pressure center

Source: Pore, Richardson, and Perrotti 1974

FIGURE 5. SURFACE WEATHER, 18-20 FEBRUARY 1972

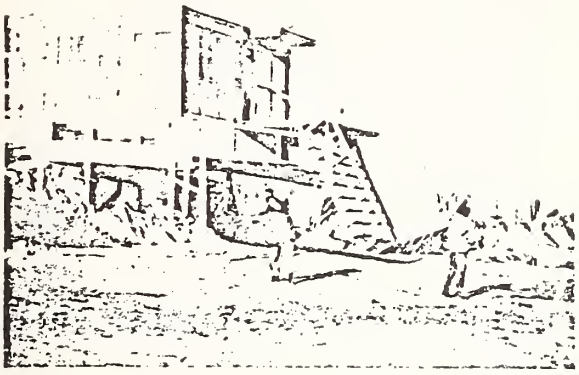

FIGURE 6. DAMAGE TO HOUSE AT WESTHAMPTON BEACH, NY, BY 18-20 FEBRUARY 1972 STORM. (COURTESY OF US ARMY CROPS OF ENGINEERS COASTAL ENGINEERING RESEARCH CENTER)

FIGURE 7. UNDERMINED CONCRETE SLAB PARKING LOT AT JONES BEACH NY, FROM 18-20 FEBRUARY 1972 STORM. (COURTESY OF US ARMY CROPS OF ENGINEERS COASTAL ENGINEERING RESEARCH CENTER)

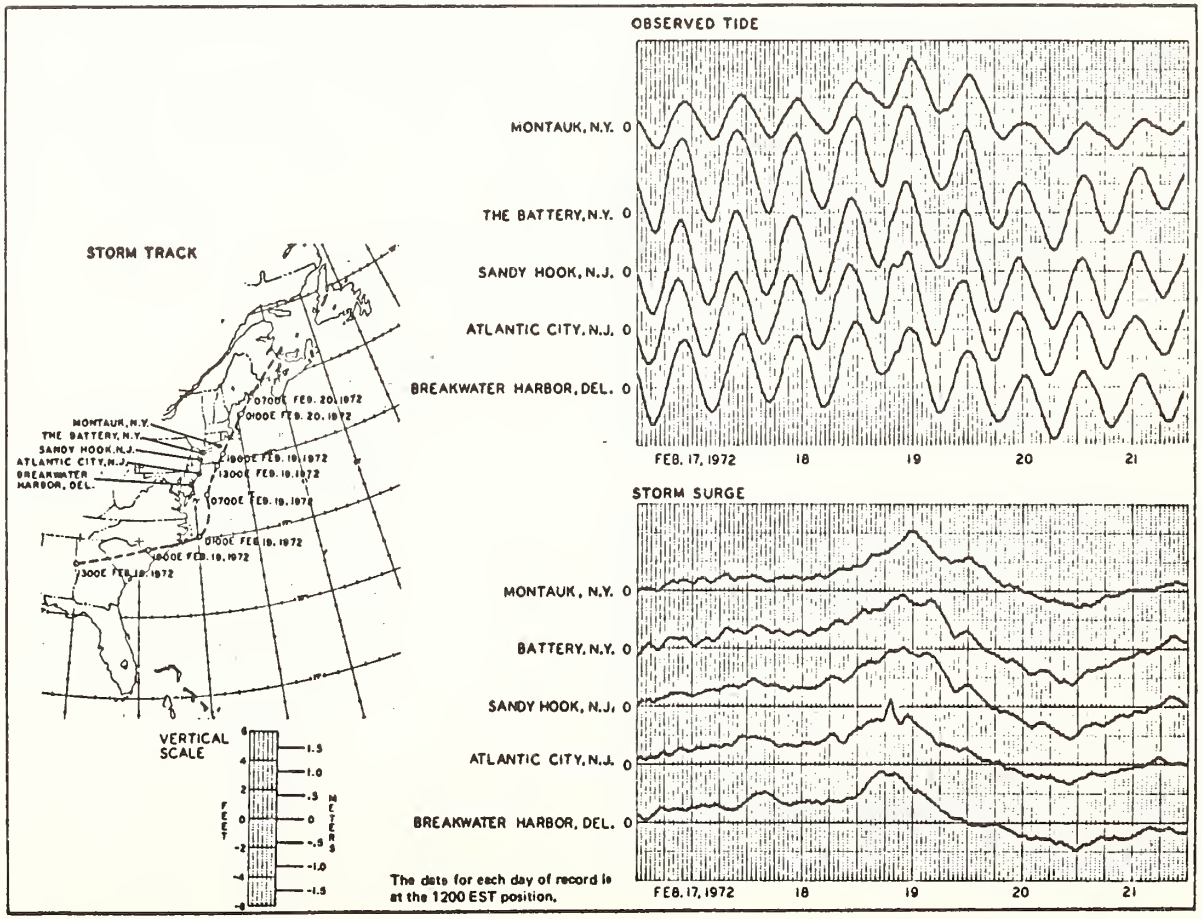

FIGURE 8. TRACK, OBSERVED TIDE CURVES, AND STORM SURGE CURVES FOR 17-21 FEBRUARY 1972. ZERO ON VERTICAL SCALE OF OBSERVED TIDE CURVE IS MEAN SEA LEVEL

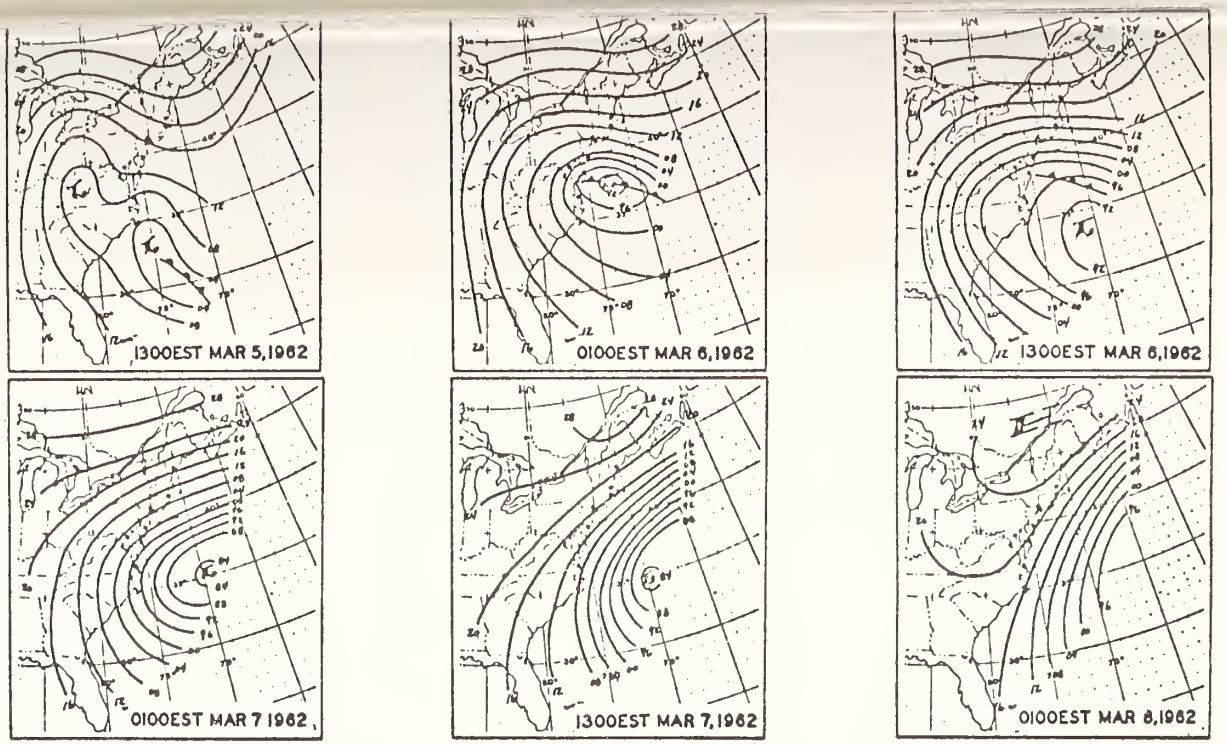

Source: Pore, Richardson, and Perrotti 1974

FIGURE 9. SURFACE WEATHER, 5-8 MARCH 1962

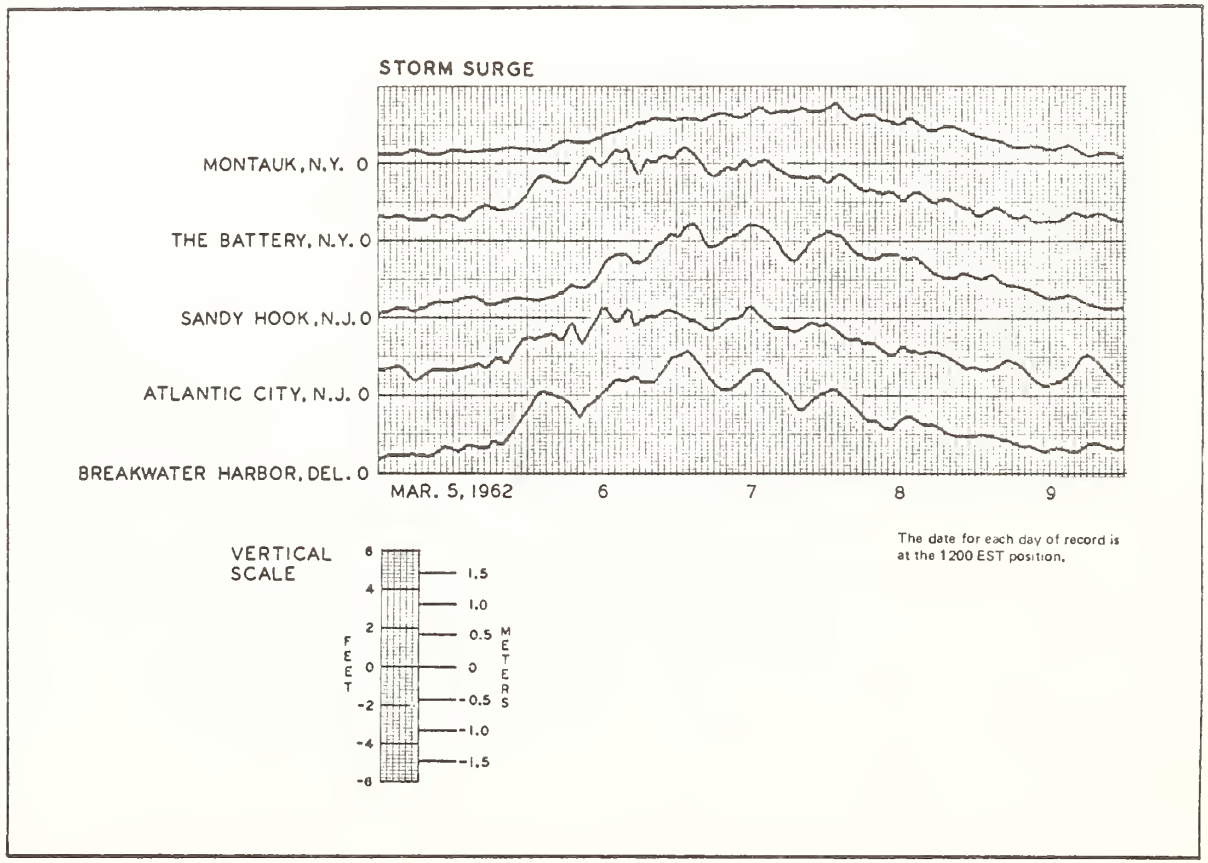

FIGURE 10. STORM SURGE CURVES FOR 5-8 MARCH 1962 STORM

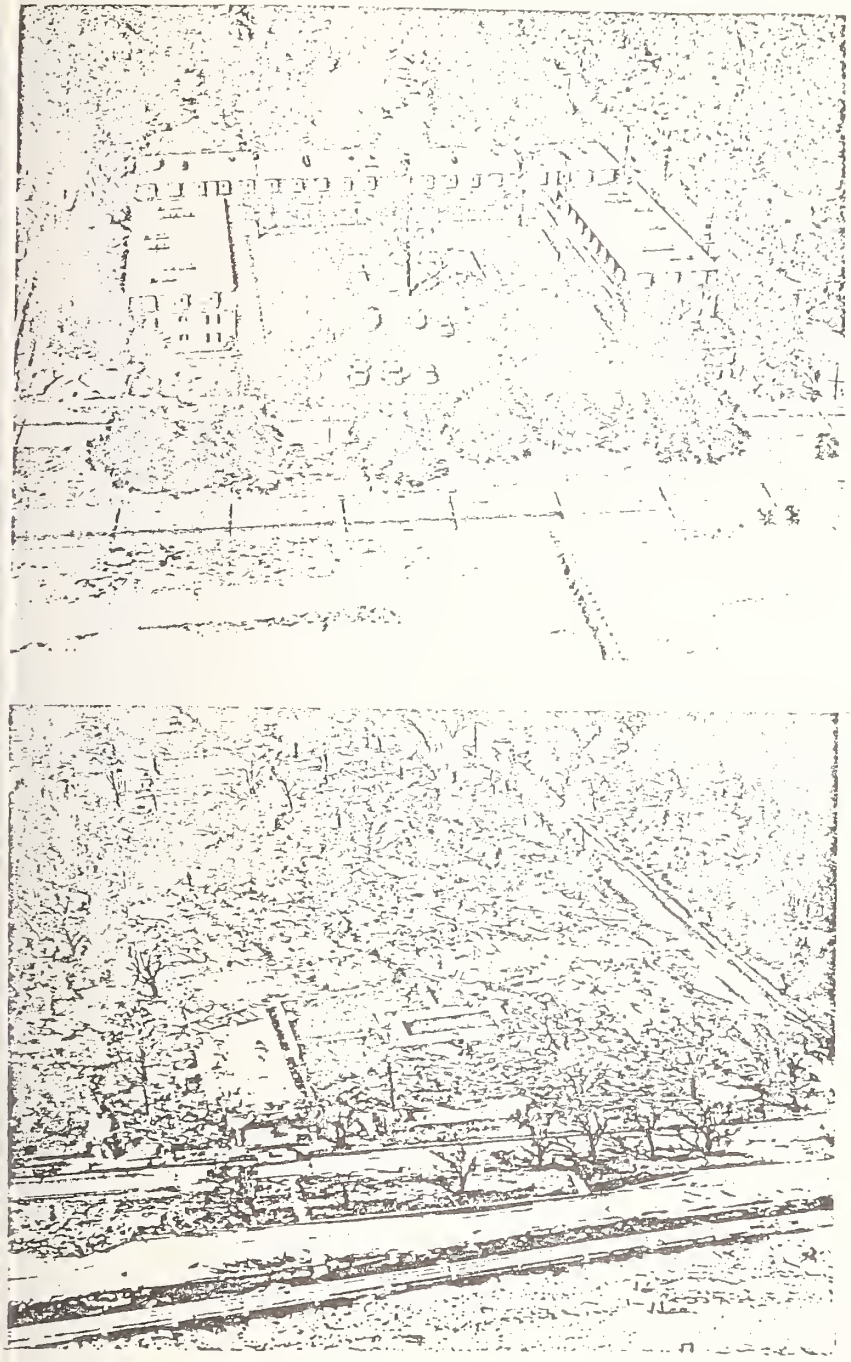

IGURE 11. RICHELIEU APARTMENTS; 1969. TWENTY-FIVE-FOOT STORM SURGE.

37

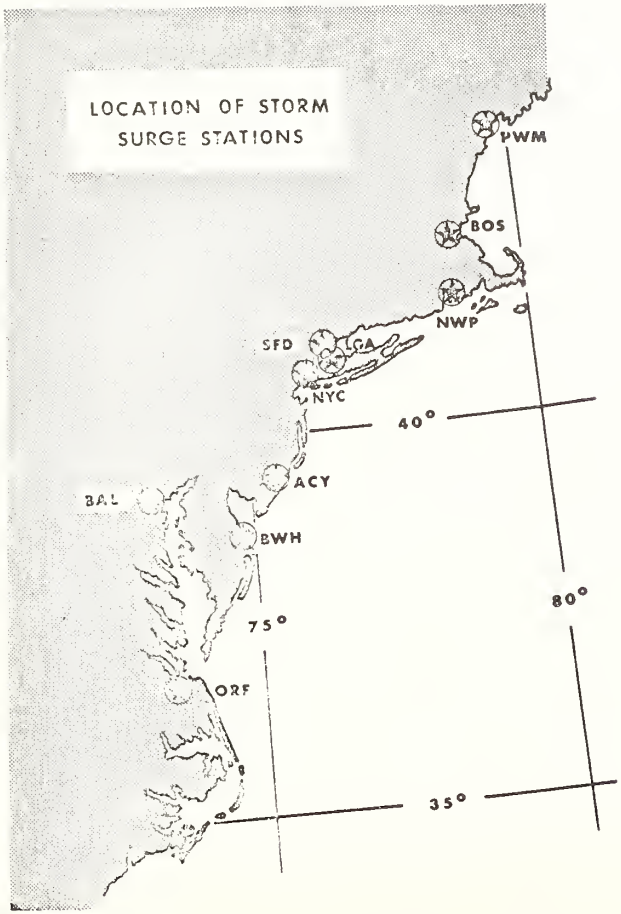

FIGURE 12. EAST COAST STATIONS WHERE EXTRATROPICAL STORM SURGES ARE FORECAST

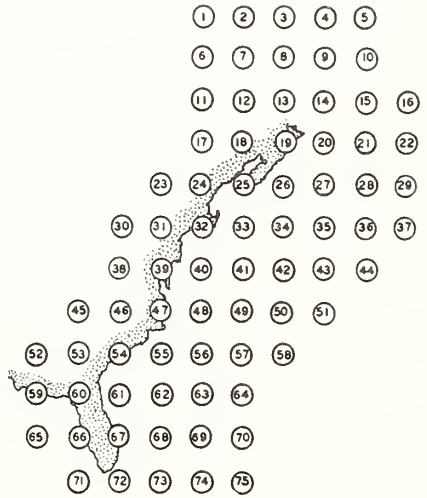

FIGURE 13. GRID POINTS WITH SEA-LEVEL PRESSURE DATA FOR DERIVING EXTRATROPICAL STORM SURGE FORECAST EQUATIONS

FZUS3 KWBC 021200
EAST COAST STORM SURGE FORECAST IN FEET

	12Z	18Z	00Z	06Z	12Z	18Z	00Z	06Z	12Z
PWM	0.1	0.4	0.5	0.7	0.7	0.9	0.8	0.9	0.7
BOS	0.1	0.2	0.3	0.4	0.4	0.5	0.4	0.6	0.3
NWP	0.8	1.0	1.1	1.2	1.2	1.3	1.1	1.1	0.9
SFD	1.0	1.1	1.2	1.2	0.9	0.7	0.6	0.1	0.0
LGA	1.0	1.0	1.0	1.3	1.2	1.0	1.0	0.8	0.7
NYC	1.2	1.3	1.4	1.4	1.3	1.2	1.0	0.9	0.7
ACY	0.8	0.9	1.0	0.9	0.9	0.9	0.8	0.8	0.7
BWH	1.1	1.1	1.2	1.0	0.9	0.9	0.7	0.7	0.6
BAL	2.4	2.5	2.6	2.8	2.8	2.6	2.4	2.0	1.9
ORF	0.9	0.8	0.9	0.8	0.8	0.8	0.7	0.6	0.9

PWM Portland, Maine
BOS Boston, Massachusetts
NWP Newport, Rhode Island
SFD Stamford, Connecticut
LGA Willets Point, New York
NYC Battery, New York
ACY Atlantic City, New Jersey
BWH Breakwater Harbor, Delaware
BAL Baltimore, Maryland
ORF Hampton Roads, Virginia

Source: Pore, Richardson, and Perrotti 1974

FIGURE 14. STORM SURGE FORECAST TELETYPE MESSAGE. VALID TIMES INDICATED ABOVE EACH COLUMN; STATION CALL SIGNS IDENTIFIED BELOW MESSAGE

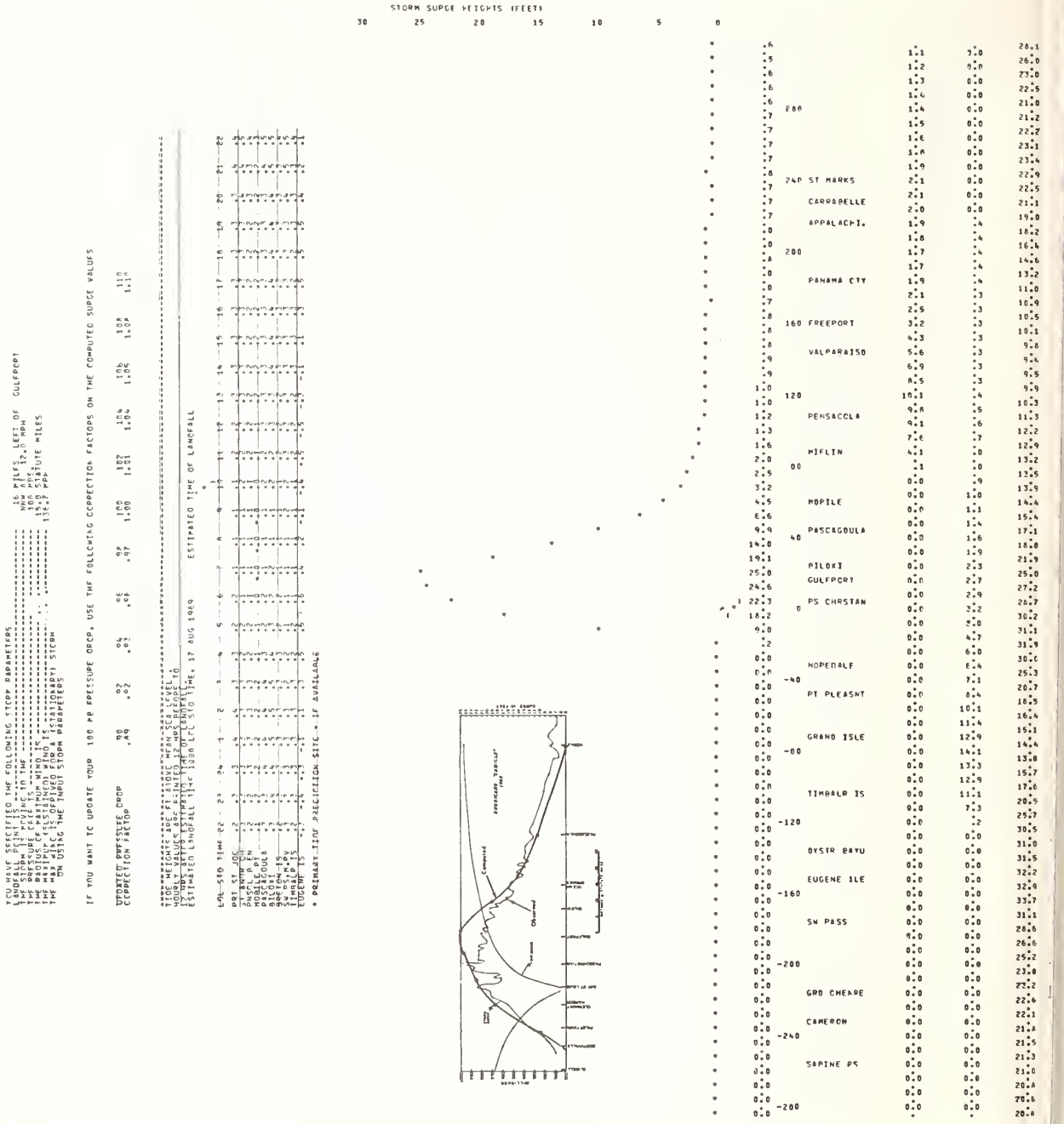

FIGURE 15. OUTPUT OF TROPICAL STORM SURGE MODEL, SPLASH, FOR HURRICANE "CAMILLE" 1969

38

OPERATION OF TSUNAMI WARNING SYSTEM IN THE PACIFIC

Mark G. Spaeth

National Weather Service
National Oceanic and Atmospheric Administration

Operation of the Tsunami Warning System in the Pacific

After the devastating Aleutian tsunami of April 1, 1946, military and civilian sources criticized the U.S. Coast and Geodetic Survey for the lack of warning in the Hawiian Islands. The critics correctly pointed out that seismic waves from this earthquake were recorded at Honolulu and other observatories within minutes after the occurrence of the earthquake; and consequently, the tsunami could have been predicted. The error in this criticism lay in the fact that seimograph records were changed only once each day, and until the film records were developed, no knowledge of an earthquake occurrence was normally available. In addition, the great majority of underwater earthquakes do not cause tsunamis, and no arrangements were then in effect to verify the existence of the tsunami through actual observation.

Another necessity for efficient operation of a warning system was the development of a method to determine quickly and accurately the amount of time between the occurrence of a tsunami-producing earthquake and the arrival of the waves in the Hawaiian Islands. Ths problem was solved by the preparation of seismic sea-wave travel time chart for Honolulu in early 1947. This chart consists of a series of more or less concentric lines overprinted on a chart of the Pacific Ocean. The lines represent distances from Honolulu for each half hour and hour of the wave's travel time. Travel time to Honolulu is obtained by plotting the epicenter of an earthquake on the chart and noting its position with respect to the time lines. Given the time of the disturbance, the arrival time of the first sea wave at the Honolulu tide station becomes immediately available. The need for traveltime charts based on the other tide stations became evident early in the operation of the Tsunami Warning System (TWS). This need was based on two factors: (1) The necessity of estimating when the existence or absence of a wave could be observed at a particular tide station, and (2) the necessity of providing accurate estimates of tsunami arrival times to additional countries and areas. Charts for all tide stations in the TWS were completed by 1950. Traveltime charts are prepared on a continuing basis for new tide stations that join the Warning System from time to time.

Because the manual preparation of traveltime charts is a tedious, time-consuming task, a computer program was developed to compute the charts. Estimated times of arrival are now determined by table look-up on a computer.

Personnel in the U.S. Coast and Geodetic Survey believed that the technical problems preventing the establishment of a workable seismic sea wave warning system could be overcome. Although the Coast Survey had no obligation under law to provide tsunami warning, it saw the need for such warnings and had the scientific know-how and part of the organization necessary for such an undertaking. Furthermore, responsible officials in the Coast Survey considered themselves morally obligated to create and organize such a system. Under the direction of Cdr. E. B. Roberts, Cdr. C. K. Green, and Mr. W. B. Zerbe, work began.

38

The acquisition of suitable seismographs and visible recording equipment was one problem that had to be solved. Photographic techniques were generally used by seismologists for recording earthquakes because they were simple, practical, and precise. Visible recording apparatus in existence in 1946 was generally unsatisfactory and of

poor accuracy due to electronic problems. Various instrumental sys-systems were tried, the most promising being that designed by Fred Keller, a New Kensington, Pa., scientist. In 1947 and 1948, equipment following his design was built and installed at Tucson, Ariz.; College, Alaska; and Honolulu, Hawaii. These installations were modified during the summer of 1950 by the addition of a highly stable, cathode-coupled, split-beam amplifier developed by R. M. Wilson and L. R. Burgess of the U.S. Coast and Geodetic Survey. Today, the TWS generally relies on helicorders driven by solid-state amplifiers. When a strong earthquake is recorded by these instruments, an alarm (audible, visible, or both), located where it is always noticeable, is tripped, thus insuring the prompt observation of all major earthquakes.

The collaboration of the Armed Forces and the Civil Aeronautics Administration (now the Federal Aviation Agency) was sought to establish a rapid, high-priority communications system. A meeting was held on August 12, 1948, to discuss a proposed communication plan for the warning system. Attending this meeting were representatives of the U.S. Army,Air Force, Navy, Civil Aeronautics Administration, and Coast and Geodetic Survey. As the various armed services and the CAA were well aware of the need for a tsunami warning system in the Pacific, the tentative plan was approved. Thus, the operation of the U.S. Coast and Geodetic Survey's Seismic Sea Wave Warning System in the Pacific began [Tsunami Warning System since March 15, 1967].

Initially, the Warning System consisted of the U.S. Coast and Geodetic Survey seismological observatories at College and Sitka, Alaska; Tucson, Ariz.; and Honolulu, Hawaii; and the following tide stations -- Attu, Adak, Dutch Harbor, and Sitka, Alaska; Palmyra Island; Midway Island; Johnston Atoll; and Hilo and Honolulu, Hawaii. However, the Warning System began to expand almost immediately. By November 15, 1949, when the first edition of the Communcation Plan for the Seismic Sea Wave Warning System was issued by the U.S. Coast and Geodetic Survey, seismological observatories at Berkeley and Pasadena, Calif., and Tokyo, Japan, and tide stations at Kodiak, Alaska; San Pedro and La Jolla, Calif.; Balboa, C.Z.; Canton Island; Apra Harbor, Guam; Koror Island; Kwajalein Atoll; Wake Island; and Pago Pago Harbor, American Samoa, had been added. Some seismological and tide stations have join ed the TWS and others have left it over the years. At present, 22 seismological observatories and 53 tide stations are participating. Some of the observatories report telemetered data from extensive seismic nets. Figure 1 shows the participating stations.

Initially, the TWS was to supply tsunami warning information to the civil authorities of the Hawaiian Islands and to the various military headquarters in the Hawaiian Islands for dissemination to military bases throughout the Pacific and to the U.S. Trust Territory of the Pacific Islands. Beginning on October 14, 1953, the warning information furnished to the civilian authorities of the Hawaiian Islands also was given to the Civil Defense Agencies of California, Oregon, and Washington. In June 1957, the Pacific Tsunami Warning Center (PTWC) began supplying estimated arrival times for seismic sea waves on the coasts of these three states. The great destruction caused by the May 1960 Chilean tsunami caused a large number of countries and territories to join the Warning System in order to be protected from future tsunamis. Beginning in November 1960, warnings were supplied to Canada, Alaska, and Tahiti. Additional warning information was supplied to Japan, beginning in February and March 1961. Taiwan started receiving warnings in November 1961, and the Republic of the Philippines and the Fiji

Islands in December 1961. During 1962, the PTWC began supplying warnings to Chile (March), Hong Kong (June), and New Zealand (July). Western Samoa began receiving warnings in January 1963, and American Samoa in November 1963.

The first test of the TWS came in connection with the Tonga Islands earthquake of September 8, 1948. Seismograph reports were obtained, and the epicenter of the earthquake was located. A travel time of 6 hours and 35 minutes for the wave from the epicenter to Honolulu was predicted from the traveltime chart, and military and civilian agencies were alerted to stand by for a possible tsunami warning. As wave reports came in, it became evident that the wave would be small, and the alert was cancelled. Later, as predicted, the Honolulu tide-gage record showed that a 6-inch seismic sea wave had arrived.

Several small tsunamis were registered in various parts of the Pacific during the years 1949, 1950, and 1951, but no warnings were issued to the public as a result of the action by the Tsunami Warning System. The extreme iregularity of earthquake occurrences was demonstrated in the years 1950 and 1951. In 1950 the Pacific Tsunami Warning Center requested tide reports in connection with 16 earthquakes, but in 1951, there were only 3 such occasions.

Regular monthly tests to keep operating personnel familiar with the communication methods and requirements were begun early in 1949. These communication tests have been instrumental (1) in eliminating flaws that showed up in the TWS from time to time, and (2) in determining the most rapid and reliable communication routes.

The first major tsunami in the Pacific after the formation of Warning System occurred in connection with November 4, 1952, Kamchatka earthquake. Advance warnings provided to communities in the path of this tsunami resulted in a reduction of damage and no casualties. The March 9, 1957 Aleutian Tsunami, the second major Pacific tsunami following the formation of the SSWWS, caused $3 million damage in the Hawaiian Islands, but once again, due to timely warning, there was no loss of life. The May 1960 Chilean tsunami pointed out a weakness in the Warning System. Although tsunami warnings were broadcast to the residents of the Hawaiian Islands well in advance of the arrival of the wave, 61 people were killed in Hilo, Hawaii, because they failed to heed the warnings.

The 1960 Chilean tsunami and the 1964 Alaskan tsunami stimulated a sizeable increase in the basic research on tsunamis, and also caused a number of countries to request tsunami warnings from the PTWC. These requests necessitated the addition of tide and seismic stations to secure the coverage necessary to provide timely warnings.

A reorganization in the U.S. Government on September 16, 1973, assigned operation of the TWS to the National Weather Service.

Operations

The operation of the Tsunami Warning begins with the detection of a major earthquake by one of the observatories in the System. Alarms are set so that any earthquake of magnitude 6.0 anywhere in the Pacific will trigger at least one. The Pacific Tsunami Warning Center (PTWC) collects and interprets the seismic data, locating the epicenter and determining the magnitude of the earthquake. If

the earthquake is of insufficient magnitude or is located in an area where a tsunami will not be generated, an information bulletin is issued and the investigation is closed.

When an earthquake of sufficient magnitude occurs in an area where the generation of a tusnami is possible, the PTWC issues a watch bulletin immediately to the dissemination agencies. This watch bulletin includes the location and magnitude of the earthquake and the estimated arrival time of the tsunami if one has been generated.

When the PTWC determines that the possibility of tsunami generation exists, they immediately begin requesting data from the tide stations nearest the epicenter. When confirmation of the existence of a tsunami is obtained, a warning is issued to the dissemination agencies. This warning contains the location of magnitude of the earthquake generating the tsunami and the estimated time of arrival of the disturbance at the locations for which the TWS provides warnings. The dissemination agencies are then responsible for warning the population in the areas likely to be impacted by the tsunami and telling them what to do to avoid danger. The dissemination agencies also have the responsibility for educating the public about tsunami dangers and preparing disaster plans.

Tsunami Warning System criteria call for the issuance of watch messages within one hour of the occurrence of an earthquake meeting magnitude and location criteria. The threshold calling for the issuance of a tsunami watch is the occurrence of an earthquake with a magnitude 7.0 in the Pacific. Generally, the TWS meets this objective although epicentral locations are occasionally in error by 2 or 3 degrees due to lack of proper distribution of seismic data.

The TWS attempts to issue necessary tsunami warnings within 2 hours of the earthquake occurrence. This criteria often cannot be met because of poor communication links to many of the tide stations and also because there may be no participating tide station within 2 hours travel time of the tsunami generating area.

Once a watch or warning has been issued by the TWS, supplementary bulletins are issued at intervals of one hour until the investigation is closed. The automation of message preparation and handling has greatly helped meeting this requirement.

Regional Tsunami Warning Systems

The National Weather Service operates regional tsunami warning systems in Alsaka and Hawaii. Because tsunamis generated in these regions can strike the shore almost immediately after the earthquake occurs, the systems were set up to provide immediate response on the basis of seismic data telemetered to the warning centers. While data from tide stations are telemetered to the centers, these data are used only for confirmation or cancellation of the warnings issued as a result of the interpretation of seismic data.

Procedures adopted at the warning centers have been selected so that tsunami warnings can be issued in 15 minutes or less. The Alaskan center limits the warning area depending on earthquake magnitude and location, but the Hawaiian center, reflecting the smaller area it serves, issues regional warnings for the entire state.

The Alaska Regional TWS issues an immediate tsunami watch for an area within a 200 mile radius of the epicenter of a coastal quake

with a magnitude of 6.75 to 7.0. A warning is issued for the rest of the Alaskan coast. If the magnitude of a coastal earthquake exceeds 7.75, a warning is issued for an area within 500 miles of the epicenter and a watch is issued for the rest of the coast. The Hawaii Regional TWS issues a warning for the state whenever a coastal earthquake of magnitude 7 or greater occurs in the region.

Planned TWS Improvements

For the past 3 years, the Pacific Tsunami Warning Center has been using a time-share computer for message generation and epicenter location. A program has been added to compute estimated time of arrival.

A new minicomputer was delivered to the PTWC this month (May 1978) and installation and programming are proceeding. This minicomputer will provide sufficient capacity for on-line processing of seismic data telemetered in from the Hawaii Regional TWS net. It is also planned to store data on past tsunamis in the computer memory to aid the Warning System personnel in making judgments on the necessity for issuance of watch and warning information.

The greatest weakness in the TWS is its inability to provide forecasts of tsunami wave heights for threatened coastlines. Current model studies of propagation and terminal effects have proceeded to their useful limits. Data from open ocean gages are necessary to provide relatively undistorted tsunami wave parameters for input to these models. With such data available in real time, tsunami height forecasts may eventually be included in warning messages.

To eliminate delays in data gathering occasioned by the necessity of contacting observers to interpret tide and seismic data and then transmitting the data over what are often slow or unreliable communication circuits, the National Weather Service has been developing, in conjunction with the U.S. Geological Survey, a method of telemetering tide and seismic data via geostationary satellite. The tide platforms consist of an interrogatable radio and a data register that accepts data from a tide gage and stores it until the data becomes obsolete. The first platform installed at La Jolla, California, takes data from a Bristol time-duration tide transmitter, storing one data point every 30 seconds and holding 40 data points in its register. A second platform, to be built by the University of Hawaii, will accept data from a pressure transducer to be installed off Wake Island at a depth of 311 meters.

The seimic platforms consist of an interrogatable radio and a data register that accepts data from microprocessor that in turn monitors the output of a standard seismometer and the arrival time of primary seismic waves. A variable combination of amplitude, period, and duration gates provides a reliability of better than 90% on the detection earthquakes of interest to the TWS. The platform uses time braodcast by the satellite, thus eliminating the possibility of error or drift in an external clock.

The ultimate in tsunami warning will come when we are able to reliably predict coastal and offshore earthquakes. Knowing in advance the expected magnitude and relative fault movement, the TWS should be able to forecast tsunami and their heights on exposed coasts.

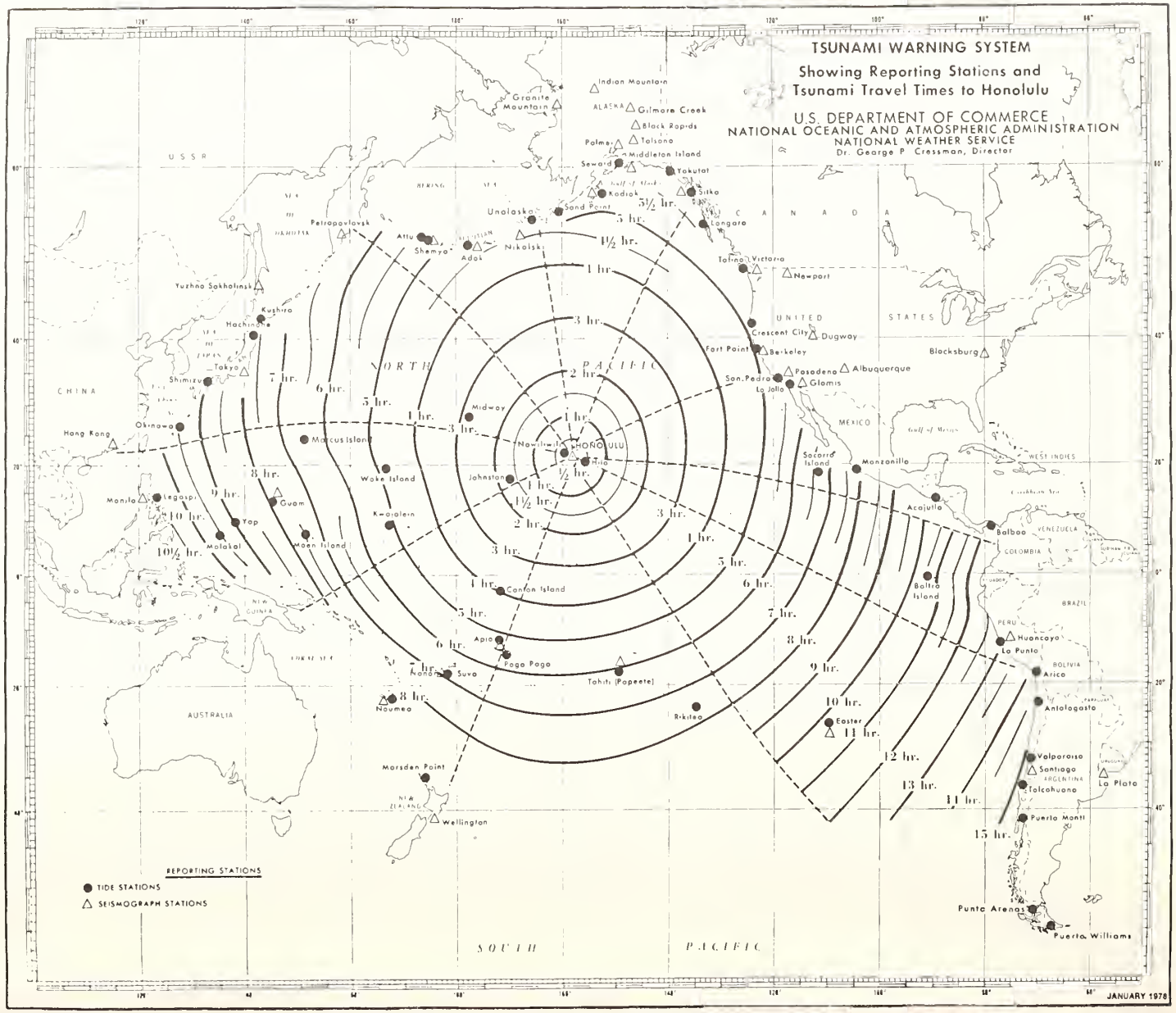

FIGURE 1. TSUNAMI WARNING SYSTEM

MEMBERS OF TASK COMMITTEES

TASK COMMITTEE	U.S. PANEL	JAPANESE PANEL
A. Strong Motion Instrumentation Arrays and Data	*Dr. Gerry Brady Mr. James Lander Mr. Jerry Dodd	*Mr. H. Tsuchida Mr. T. Iwasaki Mr. K. Ohtani Dr. M. Watabe Dr. M. Otsuka
B. Large Scale Testing Program	*Dr. E. V. Leyencecker Dr. S. C. Liu Dr. W. Shaw Dr. H. S. Lew Dr. R. McGuire	*Mr. K. Ohtani Mr. T. Murota Mr. N. Narita Mr. K. Sawada Dr. M. Watabe Mr. H. Tsuchida
C. Repair and Retrofit of Existing Structures	*Dr. John B. Scalzi Mr. James Cooper Mr. John J. Healy Dr. E. V. Leyendecker	*Dr. K. Nakano Mr. E. Kuribayashi Mr. T. Asama Mr. Y. Shioi
D. Structural Performance Evaluation	*Mr. Robert Fuller Mr. Jack Meehan Dr. John B. Scalzi Dr. W. F. Marcuson, III	*Dr. M. Watabe Dr. T. Kunihiro
E. Land Use Programs for Controlling Natural Hazard Effects	*Dr. S. T. Algermissen Dr. M. P. Gaus Mr. Jack Meehan	*Mr. E. Kuribayashi Dr. H. Sato Dr. S. Hattori
F. Life-Line Systems	*Mr. C. F. Scheffey Mr. Jack Meehan Mr. J. D. Cooper	*Dr. T. Okubo Mr. S. Fujiwhara Dr. S. Hayashi Mr. T. Iwasaki Mr. E. Kuribayashi Mr. T. Murota
G. High Speed Wind Data	*Dr. T. D. Potter Dr. R. Marshall Mr. M. Changery	*Mr. S. Fujiwhara Dr. K. Naito Mr. T. Murota Mr. N. Narita
H. Soil Behavior and Stability During Earthquakes	*Dr. W. F. Marcuson, III Mr. Jerry Dodd Mr. D. Tiedemann	*Dr. M. Ohashi Mr. T. Iwasaki Mr. K. Sawada Mr. H. Tsuchida Mr. Y. Shioi

TASK COMMITTEE REPORTS

A. TASK COMMITTEE ON STRONG-MOTION INSTRUMENTAL ARRAYS AND DATA

ATENDEES: U.S. Side - A. G. Brady, Co-Chairman
J. F. Lander
M. P. Gaus

Japan Side - K. Ohtani, Co-Chairman

I. The task Committee's plan to continue their respective efforts in the exchange of data is outline in the following six points.

a) After an earthquake which has caused damage to strucures or an earthquake during which maximum acceleration exceeding about 0.1 G has been recorded, the task committee of a country where the earthquake has taken place will provide a list of the strong-motion earthquake records for the counterparts of the task committee. The list contains maximum component acceleration of each record. If there is such a list compiled by any organization, the list mentioned above may be replaced by it.

b) Every year the task committees will exchange catalogs of the strong-motion earthquake records recovered in the last year. The catalog contains maximum component acceleration and wave forms of major records. If there is such a catalog compiled by any organization, the catalog mentioned above may be replaced by it.

c) The task committees make appropriate arrangements to provide digitizable copies of records when they are requested. In addition, arrangements will be made to provide information on the characteristics of the site and structures at the locations where such records are obtained.

d) When the organizations taking part in the panel's publish reports on the strong-motion earthquake records, the organizations will distribute copies of the reports to the organizations of the panels interested in them. The task committees exchange list of the organizations which wish to receive the reports.

e) Every year at the time of the joint meeting the task committees exchange lists of reports on the strong-motion earthquake records and on analysis of the records published in the last year. The list will cover all the reports on the above mentioned topics published by the organizations taking part in the panels and as many reports as possible published by other organizations and universities.

f) The task committees will continue to exchange lists of digitized data on all the major strong-motion earthquake records recovered in both countries. Besides the digitized records in form of lists, an exchange of digitized records in form of computer magnetic tapes, cards, and other media will be continued.

II. The task committees plan to assist and cooperate, where possible, in the following areas.

a) Assistance and cooperation with governmental organizations in other seismic areas, in order to promote high quality strong earthquake motion observations in all seismically active areas of the world.

b) Assistance and cooperation with any international effort to record strong ground motions close to the source of a large magnitude shock.

III. Furthermore, in view of the preceding paragraphs, the following item is appended.

The task committees applaud the efforts of the International Association for Earthquake Engineering and the International Association of Seismology and Physics of the Earth's Interior for instigating the International Workshop on Strong-Motion Earthquake Instrument Arrays May 2-5, 1978, in Honolulu, Hawaii, USA, and especially congratulates the workshop for the wording of their resolution. The exchange of complete information on all aspects of the program, as it develops particularly in Japan and the United States will be carried out in the manner of our standard exchanges when appropriate.

The task committees feel the Panel should play a major cooperative role in the implementation of relevant parts of the specific recommendations in that resolution.

B. TASK COMMITTEE ON LARGE-SCALE TESTING PROGRAMS

ATTENDEES: U.S. Side - E. V. Leyendecker, Co-Chairman
E. O. Pfrang
C. Culver
R. Fuller
C. Thiel
S. C. Liu
H. S. Lew
C. Scheffey
S. Takahashi

Japan Side - K. Ohtani, Co-Chairman

I. The status of the current NSF-funded project on planning large scale structural tests was discussed. Co-chairmen of this project are Dr. Penzien of the University of California at Berkeley and Dr. Unemura of the University of Tokyo. Membership from the U.S. and Japan sides includes member of the UJNR Panel on Wind and Seismic Effects, as well as others.

The first meeting of this NSF-funded planning group was held in Tokyo September 5-10, 1977. Topics discussed at that meeting included descriptions of some of the testing facilities in both the U.S. and Japan, various methods of testing, as well as the need for testing at large scale. As a result of that meeting the following building types were agreed to for study and ranking of importance at a later meeting.

a) Reinforced Concrete
b) Structural Steel
c) Mixed Construction (steel and reinforced concrete)
d) Precast and/or prestressed reinforced concrete
e) Masonry
f) Timber

Study groups were established for each of these construction types. The second meeting of this planning group was held in San Francisco May 15-19, 1978. At that meeting the construction types were categorized in order of importance into three groups.

Group A - Reinforced Concrete, Structural Steel
Group B - Mixed Construction (steel and reinforced concrete, precast and/or prestressed reinforced concrete)
Group C - Timber and Masonry

These construction types were ranked according to importance in both countries and do not necessarily reflect the major concerns in each country.

Topics discussed at the San Francisco meeting included details of specific designs, needed component tests, and needed analyses.

The third meeting of the NSF-funded planning group has been schedule to be held in Tokyo December 18-23, 1978. At that meeting detailed designs for a reinforced

concrete and a structural steel building, that is the structures in Group A, will be presented. These details will be for a building seven stories in height.

The fourth and final meeting of the NSF-funded planning group has not yet been schedule, but will include the final recommendations for a first full-scale test to be undertaken jointly by the U.S. and Japan, dependent upon the availability of funds.

The final details for conducting such an international program between the U.S. and Japan on large-scale testing have not yet been completed. Discussions between the U.S. and Japan thus far have resulted in agreements that the joint research program will be conducted under the framework of the UJNR agreement and that the UJNR Panel on Wind and Seismic Effects will be used as the implementation and coordination mechanism for the joint program.

II. The following resolution was agreed to:

The Task Committee on Large-Scale Testing Programs should keep the UJNR Panel on Wind and Seismic Effects informed of development in large-scale testing programs. Programs proposed by the current NSF-funded planning group should be circulated to UJNR for review and comments with appropriate recommendations returned to the planning group for consideration.

C. TASK COMMITTEE ON REPAIRS AND RETROFIT OF EXISTING STRUCTURES

(Report from Meeting of May 1978)

ATTENDEES: U.S. Side - Dr. J. Scalzi, Co-Chairman
Mr. J. D. Cooper
Dr. J. Wright

Japan Side - Dr. M. Watabe, Co-Chairman

I. SCOPE: Determine analytical and experimental methods for the repair and rehabilitation of buildings and bridges.

II. OBJECTIVES: To coordinate research activities, to exchange data and information, and to determine research needs.

III. POINTS OF DISCUSSION:

a) The chairman of Task Committees B, C and D should maintain close contact so that activities in the respective committees could be coordinated.

One of the first tasks should be the development of a glossary of technical terms in both languages.

Technical papers of interest to the Committee should be translated into both languages.

SCHEDULE OF ACTIVITIES:

a) U.S. to establish membership of the Task Committee as soon as possible.

b) U.S. to outline areas of interest for repair and retrofit of buildings and bridges.

c) Send items 1 and 2 to Japan Chairman of Task Committee for review and comment.

d) Japan will return data with their membership and confirmation of areas of interest and commonality, and suggestions for other areas of mutual interest.

e) U.S. will confirm areas of mutual interest with suggestions of priorities for specific topics to pursue.

f) Japan will review topics and confirm priorities for study.

g) At 11th Joint Meeting, respective Chairmen will discuss specifics of the projects selected for mutual activity and cooperation.

D. TASK COMMITTEE ON STRUCTURAL PERFORMANCE EVALUATION

ATTENDEES: U.S. Side - G. Robert Fuller, Co-Chairman
John F. Meehan
John B. Scalzi
Richard D. McConnell
S. K. Takahashi
James K. Wight
Roland L. Sharpe

Japan Side - M. Watabe, Co-Chairman
T. Kubota

I. DISCUSSION:

a) The Report of the Task Committee Meeting held in Tokyo on May 26, 1977, as prepared by Dr. John B. Scalzi and Dr. Makoto Watabe, was reviewed. The Task Committee concurred in the general proposals of the Report, and considered the Report useful as a base for discussion in order to establish specific recommendations.

b) It was proposed that a Scope for the Task Committee be formulated in order to establish priorities for future activities. Possible implementation procedures were also suggested.

c) General coordination of activities with the task committees was emphasized in agreement with discussions and reports of those Task Committees.

II. SCOPE OF TASK COMMITTEE (not prioritized):

a) Evaluation of Existing Structures - Analytical and experimental programs need to be initiated by both countries to determine resistance of existing structures to high wind and seismic forces. Present evaluation methodologies and techniques need to be compiled and analyzed.

b) Stochastic Risk Analysis and Probabilistic Hazard Determination - Further studies need to be initiated by both countries to develop an inventory of structures subject to possible failures and damage caused by high winds and earthquakes so that proper risk and hazard potential can be determined.

c) Coordination of Large-Scale Testing Program with Analytical Studies Necessary analytical studies are needed by each industry by each country for proper planning before the physical testing, and to correlate results of physical testing afterward. Closer coordination with the Large-Scale Testing Group should be maintained.

d) Non-Structural and Structural Component Interaction - Studies are needed and data compiled on the effect of nonstructural elements on the structural performance of buildings. It is possible that performance of buildings should be evaluated with respect to

non-structural elements as well as structural. The Task Committee could then be changed to "Evaluation of Performance of Structures."

e) Post-Earthquake and Post-Storm Evaluation of Performance of Structures - Investigative and eduational efforts need to be better coordinated, both internally within each country and between countries.

f) Analysis, Strengthening and Retrofit of Structures - In coordination with task committee (C), an earthquake and high wind information center should be established to compile data on present technology. Possibly the Interagency Discussion Group on Disaster Mitigation in Washington, DC and governmental institutions of Japan can assemble an annotated bibliography on this subject.

Benchmark Structures - A methodology is needed to establish "benchmark structures to which future proposed codes and standards can be compared. Structures need to be tested and analyzed to determine actual resistance to high winds and earthquakes. (The USGS-NOAA report on the 1971 San Fernando Earthquake, Buildings in Los Angeles was referenced).

III. PROPOSAL:

a) This suggested "scope" should be studied by other task committees for possible coordination.

b) The Task Committee will evaluate this "scope" plus any comments by other task committees, to prioritize the items prior to the 11th Joint Meeting.

c) Each side will endeavor to initiate discussion on the various topics in the "scope" so that preliminary planning may properly incorporate the suggested studies.

E. TASK COMMITTEE ON LAND USE PROGRAMS FOR CONTROLLING NATURAL HAZARD EFFECTS

ATTENDEES: U.S. Side - Dr. Robin McGuire, Co-Chairman

Japan Side - Dr. S. Hayashi, Co-Chairman

I. The Task Committee's efforts are summarized in the following:

a) The resolutions of the 8th and 9th Joint Panel Meetings are still in effect and will continue.

b) The exchange of papers and references on land use planning has been very useful and should continue.

c) The exchange of experts is useful both for the host country and for the visiting expert; for instance, the visit of Dr. McGuire to Japan in 1977 and the expected visit of Mr. Tazaki to the U.S. in 1978 and 1979. These exchanges should be promoted.

d) Research and methods of land use planning to reduce seismic hazards should be promoted more vigorously, in view of the importance and potential savings of life and property.

e) The lessons which can be learned about proper land use planning from post-earthquake investigations in all areas are great. Therefore, both countries will cooperate in investigation of effects of damaging earthquakes.

f) Research and methods of evaluating and mapping future potential damage to various types of structures should be promoted, as a method of understanding the hazard in terms of the types of constructed facilities at risk and their locations.

F. TASK COMMITTEE ON LIFELINE SYSTEMS

ATTENDEES: U.S. Side - C. F. Scheffey, Co-Chairman

Japan Side - T. Okubo, Co-Chairman

I. The members of the task group express satisfaction at the growing level of interest in both the U.S. and Japan for lifeline earthquake engineering activity and for the benefits of exchange of information accomplished in this past year. The meeting of the Task Group generated useful discussion of three issues:

a) Arrangements by which the work of the task group committee may obtain wider participation of both governmental and proffessional groups.

b) Coordination of our work with other task groups of the Panel on Wind and Seismic Effects established along functional lines rather than by the class of structure involved; and

c) Lifeline components and systems for which full-scale tests are necessary.

II. As a result of this discussion, the following resolutions were adopted:

a) The present areas of information exchange on design standards and criteria, research information and administrative regulations with regard to lifeline safety should continue, with increased effort to include non-govenrmental standards and research data.

b) Both co-chairmen will explore expansion of the work of the task committee by inviting additional agencies of their respective governments having lifeline responsibility to become involved and will exchange proposals within six months for matching counterpart agencies. A specific proposal will be presented to the Panel on Wind and Seismic Effects at its 11th joint session.

c) The task commiteee will examine and investigate the problems of lifeline earthquake engineering which may be appropriate for full-scale tests, particularly where analytical and component tests are inadequate. A list of candidate tests will be prepared for the 11th joint meeting, and a specific plan for one or more projects within twelve months of that date.

d) The Lifeline Disaster Prevention Methods Task Committee will suggest to the other Task Committees, which have responsibilities related to our work, appropriate limitations of our efforts to avoid duplication. It will make specific recommendations to such task committees as those responsible for Strong Motion Instrument Arrays, Full Scale Testing and Soil Behavior and Stability in Earthquakes for inclusion in their programs. In general, our group will confine itself to those problems peculiar and unique to lifelines systems, such as aeroelastic effects on bridges.

G. TASK COMMITTEE ON HIGH SPEED WIND DATA

ATTENDEES: U.S. Side - M. Changery, Co-Chairman (for T. Potter)
M. Gaus
C. Barrientos
R. Marshall

Japan Side - T. Okubo, Co-Chairman
M. Kanai

I. EXISTING ITEMS:

a) Exchange documentation types and periods of record of high wind data available from the respective nation meterological services and special observation sites.

b) Determine the requirements for actual wind observations (documented) in #1) in digitized form. If required, the Task Chairmen will establish procedures to facilitate the exchange of such data.

c) Exchange available specialized high wind data sets in digitized form to facilitate research on high winds on structures. The information may include both surface and higher meteorological data sets. Documentation on instrument characteristics, exposure and elevation above ground may be included.

d) Refine procedures to exchange on a timely basis records of future episodes of high speed wind which cause loss of life and extensive property damage.

e) Request U.S. and Japanese side to prepare summary reports, for future Joint Meetings, which contain information on high winds and associated loss of life and extensive property damage.

f) Promote research on the characterization of high winds on structures.

g) Exchange data on wind pressure on buildings and structures and on profiles of the free wind field.

h) Establish standard wind test methods for boundary layer wind tunnels.

II. NEW ITEMS:

a) Encourage the interaction between meteorologists and engineers to improve the specifications of wind data required in the future use: in establishing extreme wind distributions; in determining wind loadings on structures; in understanding the urban wind climate; and in considering wind energy usage and factor in structure design.

H. TASK COMMITTEE ON SOIL BEHAVIOR AND STABILITY DURING EARTHQUAKES

ATTENDEES: U.S. Side - W. F. Marcuson, III, Co-Chairman

Japan Side - Mr. M. Okahara, Co-Chairman
Dr. S. Hayashi

I. RESULTS OF DISCUSSIONS:

a) Activities and Principal Accomplishments to Date

The task committee (both U.S. and Japanese sides) has prepared and exchanged:

i) list of documents relating to soil liquefaction during earthquakes, and,

ii) list of soil dynamics laboratories.

At our last meeting, we also agreed to exchange existing codes and guidelines for assessing soil liquefaction. At present, we know of no such documents in the U.S. and the Japanese side transmitted an outline of some of the typical provisions used in Japan to the U.S. side.

b) Future Programs

Guidelines for assessing soil liquefaction are currently in preparation in the U.S. This work is being sponsored by the U.S., N.R.C., and will be transmitted to the Japan side when completed.

A discussion of the possibility for exchange of data and field crew and equipment to establish uniformity for penetration resistance testing as conducted in Japan and the U.S. produced the following:

i) we will attempt to organize, plan and initiate such a study, and,

ii) we will attempt to secure funding for such a study, and,

iii) we recognize that such a study is complex and therefore, may be difficult to execute; however, we will attempt to overcome these difficulties.

Discussions were held on:

i) Soil liquefaction potential for submerged foundations

ii) Foundation settlement due to earthquake motion, and

iii) Joint visits and exchange of information on embankment dams which have suffered damage or failure during earthquakes.

Items i) and ii) above were discussed and it appears that both the U.S. and Japan have limited data which is applicable. Therefore, future work in this area is postponed until more data becomes available.

Discussions of item 3 indicates that Mr. T. Uwabe of the Port and Harbour Research Institute plans to visit the Waterways Experiment Station for a period of about one year. During his stay he plans to conduct joint research on the response of earth embankments to dynamic loads. It was also proposed that site visits to case histories should be conducted at the next UJNR Plan meeting in Japan. The Japanese have one or maybe two case histories of embankments which have suffered damage during the Near Izu Oshima Earthquakes.

-114A (REV. 2-8C)

U.S. DEPT. OF COMM. BIBLIOGRAPHIC DATA SHEET (See instructions)	1. PUBLICATION OR REPORT NO. NBS SP 560	2. Performing Organ. Report No.	3. Publication Date October 1980

TITLE AND SUBTITLE

Wind and Seismic Effects
Proceedings of the Tenth Joint Panel Conference of the U.S.-Japan Cooperative Program in Natural Resources, May 23-26, 1978, Washington, D.C.

AUTHOR(S)

H.S. Lew, Editor

PERFORMING ORGANIZATION (If joint or other than NBS, see instructions)

NATIONAL BUREAU OF STANDARDS
DEPARTMENT OF COMMERCE
WASHINGTON, D.C. 20234

7. Contract/Grant No.

8. Type of Report & Period Covered

Final

SPONSORING ORGANIZATION NAME AND COMPLETE ADDRESS (Street, City, State, ZIP)

Same as above

SUPPLEMENTARY NOTES

Library of Congress Catalog Card Number: 79-600134

☐ Document describes a computer program; SF-185, FIPS Software Summary, is attached.

ABSTRACT (A 200-word or less factual summary of most significant information. If document includes a significant bibliography or literature survey, mention it here)

This volume includes thirty eight technical papers presented at the Tenth Joint Meeting of the U.S.-Japan Panel on Wind and Seismic Effects. It also includes the formal resolutions and the reports of the Panel's eight task committees. The subjects covered in the Joint Meeting include: (1) natural wind characterization and extreme wind records, (2) characterization of earthquake ground motions and strong-motion earthquake data, (3) engineering seismology, (4) response of hydraulic and earth structures to seismic forces, (5) structural responses to wind loading, (6) recent developments in seismic design criteria, (7) design and analysis of special structures, (8) damage evaluation, repair and retrofit, (9) earthquake hazard mitigation, and (10) storm surge and tsunami.

KEY WORDS (Six to twelve entries; alphabetical order; capitalize only proper names; and separate key words by semicolons)

Accelerograph; codes; design criteria; disaster; earthquakes; ground motion; seismology; standards; storm surge; structural engineering; structural response; tsunami; wind loads; winds

AVAILABILITY

☒ Unlimited

☐ For Official Distribution. Do Not Release to NTIS

☒ Order From Superintendent of Documents, U.S. Government Printing Office, Washington, D.C. 20402.

☐ Order From National Technical Information Service (NTIS), Springfield, VA. 22161

14. NO. OF PRINTED PAGES

644

15. Price

$11.00

USCOMM-DC 6043-P80

*U S GOVERNMENT PRINTING OFFICE: 1980 328-577/6553

There's a new look to...

DIMENSIONS/NBS

. . . the monthly magazine of the National Bureau of Standards. Still featured are special articles of general interest on current topics such as consumer product safety and building technology. In addition, new sections are designed to . . . PROVIDE SCIENTISTS with illustrated discussions of recent technical developments and work in progress . . . INFORM INDUSTRIAL MANAGERS of technology transfer activities in Federal and private labs. . . DESCRIBE TO MANUFACTURERS advances in the field of voluntary and mandatory standards. The new DIMENSIONS/NBS also carries complete listings of upcoming conferences to be held at NBS and reports on all the latest NBS publications, with information on how to order. Finally, each issue carries a page of News Briefs, aimed at keeping scientist and consumer alike up to date on major developments at the Nation's physical sciences and measurement laboratory.

(please detach here)

RIPTION ORDER FORM

y Subscription To DIMENSIONS/NBS at $11.00. Add $2.75 for foreign mailing. No additional is required for mailing within the United States or its possessions. Domestic remittances be made either by postal money order, express money order, or check. Foreign remittances be made either by international money order, draft on an American bank, or by UNESCO .

☐ Remittance Enclosed (Make checks payable to Superintendent of Documents)

☐ Charge to my Deposit Account No.

ubscription to:

NAME-FIRST, LAST

COMPANY NAME OR ADDITIONAL ADDRESS LINE

STREET ADDRESS

CITY | STATE | ZIP CODE

PRINT

MAIL ORDER FORM TO:
Superintendent of Documents
Government Printing Office
Washington, D.C. 20402

NBS TECHNICAL PUBLICATIONS

PERIODICALS

RNAL OF RESEARCH—The Journal of Research of the onal Bureau of Standards reports NBS research and develop- in those disciplines of the physical and engineering sciences in h the Bureau is active. These include physics, chemistry, neering, mathematics, and computer sciences. Papers cover a d range of subjects, with major emphasis on measurement hodology and the basic technology underlying standardization. included from time to time are survey articles on topics ly related to the Bureau's technical and scientific programs. special service to subscribers each issue contains complete ions to all recent Bureau publications in both NBS and non- media. Issued six times a year. Annual subscription: domestic foreign $16.25. Single copy, $3 domestic; $3.75 foreign.

TE: The Journal was formerly published in two sections: Sec- A "Physics and Chemistry" and Section B "Mathematical nces."

ENSIONS/NBS—This monthly magazine is published to in- scientists, engineers, business and industry leaders, teachers, nts, and consumers of the latest advances in science and nology, with primary emphasis on work at NBS. The magazine lights and reviews such issues as energy research, fire protec- building technology, metric conversion, pollution abatement, h and safety, and consumer product performance. In addi- it reports the results of Bureau programs in measurement dards and techniques, properties of matter and materials, neering standards and services, instrumentation, and matic data processing. Annual subscription: domestic $11; gn $13.75.

NONPERIODICALS

ographs—Major contributions to the technical literature on ous subjects related to the Bureau's scientific and technical ac- es.

dbooks—Recommended codes of engineering and industrial tice (including safety codes) developed in cooperation with in- ted industries, professional organizations, and regulatory es.

ial Publications—Include proceedings of conferences spon- d by NBS, NBS annual reports, and other special publications opriate to this grouping such as wall charts, pocket cards, and ographies.

ied Mathematics Series—Mathematical tables, manuals, and es of special interest to physicists, engineers, chemists, gists, mathematicians, computer programmers, and others ged in scientific and technical work.

onal Standard Reference Data Series—Provides quantitative on the physical and chemical properties of materials, com- from the world's literature and critically evaluated. loped under a worldwide program coordinated by NBS under uthority of the National Standard Data Act (Public Law 96).

NOTE: The principal publication outlet for the foregoing data is the Journal of Physical and Chemical Reference Data (JPCRD) published quarterly for NBS by the American Chemical Society (ACS) and the American Institute of Physics (AIP). Subscriptions, reprints, and supplements available from ACS, 1155 Sixteenth St., NW, Washington, DC 20056.

Building Science Series—Disseminates technical information developed at the Bureau on building materials, components, systems, and whole structures. The series presents research results, test methods, and performance criteria related to the structural and environmental functions and the durability and safety characteristics of building elements and systems.

Technical Notes—Studies or reports which are complete in themselves but restrictive in their treatment of a subject. Analogous to monographs but not so comprehensive in scope or definitive in treatment of the subject area. Often serve as a vehicle for final reports of work performed at NBS under the sponsorship of other government agencies.

Voluntary Product Standards—Developed under procedures published by the Department of Commerce in Part 10, Title 15, of the Code of Federal Regulations. The standards establish nationally recognized requirements for products, and provide all concerned interests with a basis for common understanding of the characteristics of the products. NBS administers this program as a supplement to the activities of the private sector standardizing organizations.

Consumer Information Series—Practical information, based on NBS research and experience, covering areas of interest to the consumer. Easily understandable language and illustrations provide useful background knowledge for shopping in today's technological marketplace.

Order the **above** *NBS publications from: Superintendent of Documents, Government Printing Office, Washington, DC 20402.*

Order the **following** *NBS publications—FIPS and NBSIR's—from the National Technical Information Services, Springfield, VA 22161.*

Federal Information Processing Standards Publications (FIPS PUB)—Publications in this series collectively constitute the Federal Information Processing Standards Register. The Register serves as the official source of information in the Federal Government regarding standards issued by NBS pursuant to the Federal Property and Administrative Services Act of 1949 as amended, Public Law 89-306 (79 Stat. 1127), and as implemented by Executive Order 11717 (38 FR 12315, dated May 11, 1973) and Part 6 of Title 15 CFR (Code of Federal Regulations).

NBS Interagency Reports (NBSIR)—A special series of interim or final reports on work performed by NBS for outside sponsors (both government and non-government). In general, initial distribution is handled by the sponsor; public distribution is by the National Technical Information Services, Springfield, VA 22161, in paper copy or microfiche form.

BIBLIOGRAPHIC SUBSCRIPTION SERVICES

T **ollowing current-awareness and literature-survey bibliographies a ssued periodically by the Bureau:**

C **genic Data Center Current Awareness Service.** A literature sur- ssued biweekly. Annual subscription: domestic $35; foreign

S

L **efied Natural Gas.** A literature survey issued quarterly. Annual sc cription: $30.

Superconducting Devices and Materials. A literature survey issued quarterly. Annual subscription: $45. Please send subscription orders and remittances for the preceding bibliographic services to the National Bureau of Standards, Cryogenic Data Center (736) Boulder, CO 80303.

U.S. DEPARTMENT OF COMMERCE
National Bureau of Standards
Washington, D.C. 20234

OFFICIAL BUSINESS

Penalty for Private Use, $300

POSTAGE AND FEES PAID
U.S. DEPARTMENT OF COMMERCE
COM-215

SPECIAL FOURTH-CLASS RATE
BOOK

1293